UNIVERSIDADE FEDERAL DO PARANÁ

VALÉRIA PEREIRA FERRER

Identificação e avaliação de uma isoforma de hialuronidase (*Dietrich´s Hyaluronidase*) do veneno de *Loxosceles intermedia* (aranha-marrom): da clonagem molecular à caracterização bioquímica e funcional

Curitiba
2014

UNIVERSIDADE FEDERAL DO PARANÁ

VALÉRIA PEREIRA FERRER

Identificação e avaliação de uma isoforma de hialuronidase (*Dietrich´s Hyaluronidase*) do veneno de *Loxosceles intermedia* (aranha-marrom): da clonagem molecular à caracterização bioquímica e funcional

Tese apresentada ao programa de Pós Graduação em Biologia Celular e Molecular, Departamento de Biologia Celular, Setor de Ciências Biológicas, Universidade Federal do Paraná, como parte das exigências para obtenção de título de Doutor em Biologia Celular e Molecular.

Orientador: Prof. Dr. Silvio Sanches Veiga
Co-orientadora: Profa. Dra. Andrea Senff Ribeiro

Curitiba
2014

Pereira Ferrer, Valéria.

Identificação e avaliação de uma isoforma de hialuronidase (*Dietrich´s Hyaluronidase*) do veneno de *Loxosceles intermedia* (aranha-marrom): da clonagem molecular à caracterização bioquímica e funcional/ Valéria Pereira Ferrer – Curitiba, 2014.

238 f.:il.(algumas color.)

Orientador: Silvio Sanches Veiga

Tese (Doutorado em Biologia Celular e Molecular) – Setor de Ciências Biológicas, Universidade Federal do Paraná

1. Hialuronidase 2. Veneno 3. Aranha-marrom

PROGRAMA DE PÓS-GRADUAÇÃO EM BIOLOGIA CELULAR E MOLECULAR

Departamento de Biologia Celular e Departamento de Fisiologia
Setor de Ciências Biológicas - Universidade Federal do Paraná
Instituto Carlos Chagas (ICC/FIOCRUZ)

PARECER

A banca examinadora, instituída pelo colegiado do Programa de Pós-Graduação em Biologia Celular e Molecular, do Setor de Ciências Biológicas, da Universidade Federal do Paraná, composta por:

Prof. Dr. Silvio Sanches Veiga
Orientador e presidente da banca
Universidade Federal do Paraná - UFPR

Profa. Dra. Maria Elena de Lima Perez Garcia
Universidade Federal de Minas Gerais - UFMG

Prof. Dr. Stenio Perdigão Fragoso
Instituto Carlos Chagas - ICC

Profa. Dra. Célia Regina Cavichiolo Franco
Universidade Federal do Paraná - UFPR

Prof. Dr. Francisco Filipak Neto
Universidade Federal do Paraná - UFPR

E tendo como suplente,

Prof. Dr. Silvio Marques Zanata
Universidade Federal do Paraná – UFPR

Após arguir a candidata ***Valéria Pereira Ferrer***, em relação ao seu trabalho intitulado: "Identificação e avaliação de uma isoforma de hialuronidase (*Dietrich's Hyaluronidase*) do veneno de *Loxosceles intermedia* (aranha-marrom): da clonagem molecular à caracterização bioquímica e funcional", são de parecer favorável à APROVAÇÃO da acadêmica, habilitando-a ao título de Doutora em Biologia Celular e Molecular, área de concentração em Biologia Celular e Molecular.
A obtenção do título está condicionada à implementação das correções sugeridas pelos membros da banca examinadora, bem como ao cumprimento integral das exigências estabelecidas no Regimento Interno deste Programa de Pós-Graduação.

Curitiba, 25 de Fevereiro de 2014

Prof. Dr. Edvaldo da Silva Trindade
Coordenador do Programa de Pós-Graduação em Biologia Celular e Molecular - UFPR
Matr. 185795

Aos **meus pais e irmãos** por sempre
terem acreditado no meu potencial e
não terem poupado esforços para que eu
chegasse até a esta tese!

AGRADECIMENTOS

Primeiramente gostaria de agradecer a Deus, por ter me fornecido saúde, disposição e intelectualidade para o desenvolvimento deste trabalho. Em alguns momentos difíceis que passei somente uma força Divina para fazer continuar e eu só tenho a agradecer.

Ao meu orientador desde a iniciação científica, Prof. Dr. Silvio Sanches Veiga, pela oportunidade de fazer parte da equipe do “Laboratório de Matriz Extracelular e Biotecnologia de Venenos”, a qual me orgulho tanto! Por ter me confiado este projeto e por meu crescimento científico adquirido durante esses anos.

À minha co-orientadora, Profa. Dra. Andrea Senff Ribeiro, pelas várias reuniões de discussão científica, por ter confiado esse projeto a mim e por toda ajuda prestada na burocracia da patente desse trabalho.

À minha co-orientadora, não no papel... mas de coração sempre, Profa. Dra. Olga Meiri Chaim! Por ter depositado toda a confiança em mim desde minha iniciação científica! A qualquer hora esteve disposta a ouvir e discutir assuntos relacionados ao laboratório fosse de origem científica ou organizacional. Muito obrigada! Levarei sua amizade sempre comigo!

À Dra. Dilza Trevisan Silva! Bem Dil, sem comentários, né?! Companheira e amiga de todas as horas desde que eu entrei no laboratório! Muito obrigada por tudo! Pelas discussões científicas, pelos experimentos, cursos, disciplinas e tarefas realizados juntos... E claro, por sua amizade magnífica!

À Profa. Dra. Luiza Helena Gremski! Lu, obrigada por ser este exemplo de cientista e pessoa! Eu só tenho a agradecer por toda a ajuda prestada durante todos esses anos nos experimentos, discussões científicas, correções de inglês, entre diversas outras tarefas! Muito obrigada por você sempre me escutar e ter acreditado no meu potencial!

Ao querido e quase mestre Thiago Lopes de Mari! Obrigada por ter me ajudado tanto durante esses anos e também por sua amizade! Tenho muito orgulho de ter contribuído para sua formação científica e torço por uma carreira de muito sucesso pra você!

Aos demais amigos do LME: MSc. Fernando H. Matsubara, MSc. Gabriel O. Meissner, MSc. Adriano M. Morgon, MSc. Aline V. Bednaski, à quase mestre

Marianna B. Ferreira, Alessandra Hamasaki, MSc. Ana Carolina Wille, Lucas Pedrosa, Brenda Marin, Bruna L. Dias, Verônica Cubas e Hanna Justa. Obrigada pela grande ajuda e amizade durante esses anos! Certamente essa tese não se desenvolveria sem vocês! Lembrarei sempre de vocês com muito carinho! Não existem palavras para agradecê-los pela ajuda e convivência diária... Mas fica aqui meu muito obrigada!

Aos amigos ex-integrantes do laboratório: MSc. Youssef B. Sade, Dra. Daniele C. Moreira, Prof. Dr. Rafael B. da Silveira, Profa. Dra. Kátia S. Paludo, Profa. Dra. Márcia Helena Appel, MSc. Jennifer Nowatski, MSc. Matheus R. Belisário, MSc. Daniela Buch, MSc. Rodrigo Schneider, Kiane S. Freitas, Eduardo S. Constantino e Isabela C. Rossato... Obrigada a vocês também por toda ajuda prestada quando requeridos e pela amizade que certamente contribuiu para a minha formação como profissional e pessoa!

Aos meus pais Nelson Alves Ferrer e Edinéia Ana Pereira Ferrer, por serem a base de minha pessoa! Muito obrigada por todo o esforço de vocês (e eu sei o quanto) para que eu conseguisse chegar até aqui! Obrigada por me escutarem nos meus momentos de estresse (aproveito e peço desculpas pelos dias em que exagerei), pelos conselhos e pela compreensão de sempre! Pra vocês eu realmente fico sem palavras... Mas fica aqui uma tentativa de agradecimento!

Aos meus irmãos queridos Pércio e Bruno, obrigada por toda torcida, compreensão, ajuda e admiração! Talvez vocês nem saibam o quanto me ajudaram a chegar até aqui!

Aos demais familiares, muito obrigada pela torcida e principalmente pela compreensão nos meus momentos de ausência. Em especial eu gostaria de agradecer à Tia Elza, Tia Edina, Tia Maria Eunice e ao Tio Antônio Pereira e aos meus primos: Maria Claudia, Camila, Hugo e Angelita! Vocês sempre foram grandes amigos e torceram constantemente pelo meu sucesso!

À minha pequena adorável afilhada Helena Fernanda, que sempre me enxergou como uma heroína... Obrigada pela confiança que deposita em mim e por me fazer sentir uma pessoa privilegiada!

Aos meus amigos Mariza G. Pondé, Andressa M. Moreira, Francine M. Aleixo, Viviane Sawanoi, Suély K. Weiss, Camila Z. Hermes, Allan Bourscheidt, Thiago Jacomasso, Gina Borghetti, Adriana Yamaguchi, Taísa Adamowicz, Daniele Pequito

e Isabela Coelho. Muito obrigada pela amizade! Vocês foram sempre grandes companheiros! Certamente essa tese não seria possível sem vocês!

Ao meu querido namorado Igor Guedes Farias, muito obrigada por me escutar, ajudar e incentivar sempre! Você foi meu suporte em vários momentos no decorrer do doutorado! Obrigada por me fazer sentir uma pessoa especial!

À banca desse trabalho: Profa. Dra. Helena Bonciani Nader, Profa. Dra. Maria Elena de Lima Perez Garcia, Prof. Dr. Stenio Perdigão Fragoso, Profa. Dra. Célia Regina Cavichiolo Franco, Prof. Dr. Francisco Filipak Neto e Prof. Dr. Silvio Marques Zanata pelo exemplo de dedicação à ciência e prontidão em que aceitaram avaliar esse trabalho! Muito obrigada!

Aos órgãos de fomento: CNPq, CAPES, SETI e Fundação Araucária por terem financiado esse trabalho. E por fim, quero agradecer à todos que contribuíram de uma forma ou outra e não foram citados, principalmente ao povo brasileiro, que de forma indireta financiou minha pesquisa! Muito obrigada!

"*Vejo a natureza como uma estrutura magnífica que podemos compreender apenas imperfeitamente, e que deveria inspirar em qualquer pessoa com capacidade de reflexão um sentimento de humildade*". *Albert Eistein*

"Talvez não tenha conseguido fazer o melhor, mas lutei para que o melhor fosse feito. Não sou o que deveria ser, mas Graças a Deus, não sou o que era antes". Marthin Luther King

Resumo

Loxoscelismo é o termo utilizado para os sintomas clínicos desencadeados após a picada de aranhas do gênero *Loxosceles*. As manifestações clínicas incluem necrose da pele com espalhamento gravitacional e complicações sistêmicas. O veneno loxoscélico contém várias enzimas, como por exemplo, fosfolipases-D, serinoproteases, metaloproteases e hialuronidases. As hialuronidases ao degradar glicosaminoglicanos de tecido conjuntivo potencializaria a ação de outros componentes do veneno facilitando a penetração e distribuição dos mesmos a diferentes tecidos. Este trabalho teve como objetivo a clonagem, expressão e caracterização bioquímica e biológica de uma isoforma de hialuronidase do veneno de *L. intermedia* (aranha-marrom). Através de uma biblioteca de cDNA da glândula de veneno, uma isoforma de hialuronidase (1200 pb) foi clonada e denominada *Dietrich´s Hyaluronidase* (DHAase). Após subclonagem da hialuronidase madura em vetor de expressão pET-14b, a construção resultante foi transformada em *Escherichia coli* BL21(DE3)pLysS e AD494(DE3). Fora testada a expressão em volume de 50 mL em diferentes concentrações de indutor IPTG (0,05-0,4 mM) e diferentes temperaturas (30º, 22º e 16ºC). Para obtenção da solubilidade da enzima recombinante, a sequência da hialuronidase madura foi também clonada em vetor de expressão pET-SUMO e expressa em *E. coli* SHuffle a 30ºC sob as mesmas condições de indutor descritas anteriormente. Em um maior volume de cultura (1L) nenhuma das cepas foi eficiente em expressar a DHAase solúvel. Sendo assim a alternativa escolhida para conseguir a hialuronidase recombinante de forma solúvel e ativa foi a técnica de redobramento *in vitro*. Vários tampões foram testados e a atividade só foi obtida com um tampão contendo glutationas, albumina bovina (BSA) e L-arginina. Depois do redobramento, DHAase foi capaz de degradar ácido hialurônico (HA) e condroitim-4-sulfato (C4S) em ensaios de cinética e zimografia. Por meio de análises de imunodetecção foi visto que anticorpos policlonais produzidos com a DHAase desnaturada e com o veneno reagiram de forma cruzada. Através de experimentos *in vivo* de dermonecrose em pele de coelho, foi demonstrado que DHAase aumentou a área de necrose produzida por uma isoforma de fosfolipase-D recombinante (toxina dermonecrótica) do veneno de *L. intermedia* (LiRecDT1). Dados macroscópicos e histológicos suportam a hipótese de que a hialuronidase é um "fator de espalhamento" do veneno de *L. intermedia*. Adicionalmente, estudando modelos *in vitro* de células endoteliais de aorta de coelho (RAEC) e células de melanoma murino (B16F1 e B16F10) onde essas células foram expostas por até 24 h com DHAase, foi visto que a hialuronidase recombinante não induziu alteração da morfologia ou desadesão das RAECs. Por outro lado ela alterou a proliferação e a morfologia das células de melanoma murino, sendo que a linhagem mais metastática (B16F10) teve os efeitos mais pronunciados sob a ação de DHAase. A viabilidade celular de B16F10 diminui significativamente com a exposição da hialuronidase recombinante por 16 h. *Dietrich´s Hyaluronidase* foi uma ferramenta útil para um estudo pioneiro no loxoscelismo e se mostrou eficiente em estudar o efeito do catabolismo de HA em linhagens cancerosas de melanoma, embora estudos adicionais se façam necessários. Em conclusão, o presente trabalho tornou evidente a possível utilização de DHAase como uma ferramenta de estudo em processos patológicos relacionados ao ácido hialurônico.

Palavras-chave: *Loxosceles*, aranha-marrom, veneno, ácido hialurônico, hialuronidases, proteínas recombinantes, redobramento *in vitro*, melanoma.

Abstract

Loxoscelism is the designation given to clinical symptoms evoked by *Loxosceles* spider's bites. Clinical manifestations include skin necrosis with gravitational spreading and systemic disturbs. The venom contains several enzymatic toxins such as phospholipase-D, serine proteases, metalloproteases and hyaluronidases. Hyaluronidases by degrading glycosaminoglycans from connective tissue may be able to enhance the action from other venom constituents by facilitating the diffusion from local bite to other tissues. This work aimed the cloning, expression and the biochemical and biological characterization of a hyaluronidase isoform from *L. intermedia* venom (brown spider). Employing a venom gland cDNA library, we cloned a hyaluronidase (1200 bp) which was named Dietrich´s Hyaluronidase (DHAase). The mature sequence was subcloned with a pET-14b plasmid and the expressed construction was inserted into *E. coli* BL21(DE3)pLysS and AD494(DE3). The induction of recombinant protein expression was tested in different IPTG concentrations (0.05-0.4 mM) and temperatures (30º, 22º and 16ºC). The DHAase mature sequence was also subcloned with pET-SUMO and it was expressed in *E. coli* SHuffle at 30ºC with the same IPTG concentrations. Neither of *E.coli* strains tested was able to express DHAase in a soluble form in large scale. The chosen alternative to achieve a soluble and active DHAase was the refolding *in vitro* technique. Several conditions were tested and the activity was only reached with a buffer containing glutathione, bovine serum albumin (BSA) and L-arginine. After the refolding, the recombinant hyaluronidase was able to degrade hyaluronic acid (HA) and chondroitin-4-sulfate (C4S) in a kinetic assay and zymography. Immunoblot analysis showed that antibodies which recognize the DHAase cross-reacted with native hyaluronidases from the whole venom as well as an anti- whole venom serum reacted with the recombinant protein. Through *in vivo* experiments of dermonecrosis using rabbit skin, DHAase was shown to increase the dermonecrotic effect produced by recombinant dermonecrotic toxin (phospholipase-D) from *L. intermedia* venom (LiRecDT1). Macroscopic and histologic findings sustain these data. Together, results support the hypothesis that hyaluronidase is a ‘‘spreading factor’’ from *L. intermedia* venom. In addition, studying *in vitro* culture model of rabbit aortic endhotelial cells (RAEC) and murine melanoma cells (B16F1 e B16F10), which the cells were exposed up to 24 h with DHAase, showed that recombinant hyaluronidase not induced RAEC´s morphologic changes neither cell detachment. On the other hand, it caused morphologic and cell proliferation changes in melanoma cells. B16F10, a more metastatic subtype, was more affected by hyaluronidase action than the B16F1. The B16F10 cell viability was significantly reduced by DHAase within 16 h. DHAase provided a useful tool for a pioneering study into loxoscelism and it was efficient in studying the HA metabolites effect in melanoma cancer cells, although further studies are necessary. In conclusion, this work provide evidences of the use of DHAase as a tool for studying HA pathological process.

Keywords: *Loxosceles*, brown spider, venom, hyaluronic acid, hyaluronidases, recombinant protein, refolding *in vitro*, melanoma

LISTA DE FIGURAS

ABREVIATURAS E SIGLAS

BOD: *Biological Oxygen Demand*
cDNA: DNA complementar
CD44: *Cluster of differentiation* 44
CS: Condroitim Sulfato
C4S: Condroitim-4-Sulfato
DHAase: *Dietrich´s Hyaluronidase*
DO: Densidade Óptica
DS: Dermatam Sulfato
DTT: *Dithiotreitol*
EDTA: Ácido Etilenodiaminotetra-Acético
GAG: glicosaminoglicano (s)
GSH: Glutationa reduzida
GSSG: Glutationa dissulfeto
HA: Ácido Hialurônico
HAase: Hialuronidase
HAS: Ácido Hialurônico Sintase
HTB: Hialuronidase Testicular Bovina
HS: Heparam Sulfato
IPTG : Isopropil-β-D-Tiogalactopiranosídeo
LiRecDT1: *Loxosceles intermedia Dermonecrotic Toxin*
MEC: Matriz Extracelular
PCR : Reação em Cadeia da Polimerase
pH: potencial Hidrogeniônico
pI: ponto Isoelétrico
RACE: *Rapid Amplification of cDNA End*
RAEC: *Rabbit Aortic Endothelial Cells*
RHAMM: *Hyaluronan-Mediated Motility Receptor*
rpm: rotações por minuto
RT-PCR: Transcrição Reversa Acoplada à Reação em Cadeia da Polimerase
TAE: Tampão Tris-Acetato-EDTA

SUMÁRIO

1 INTRODUÇÃO GERAL

As aranhas-marrons do gênero *Loxosceles* estão amplamente distribuídas em todo mundo, sendo encontradas em todos continentes, exceto na Antártica (DA SILVA et al., 2004). No Brasil já foram descritas 12 espécies (PLATNICK, 2013) e dessas, quatro são encontradas no Estado do Paraná (*L. intermedia, L. laeta, L. gaucho e L. hirsuta*). As três espécies de maior importância médica são *L. intermedia*, *L. laeta e L. gaucho*, sendo que *L. intermedia* é a espécie mais abundante no Estado e principalmente na cidade de Curitiba e Região Metropolitana (MÁLAQUE et al., 2002; GONÇALVES-DE-ANDRADE et al., 2012). Acidentes com aranhas-marrons caracterizam-se como um problema de saúde pública no Estado do Paraná, com um número médio de 5.417 acidentes por ano (SINAN, 2013).

O termo loxoscelismo é tipicamente utilizado para descrever os sinais e sintomas resultantes de acidentes envolvendo aranhas do gênero *Loxosceles* (DA SILVA et al., 2004). O loxoscelismo cutâneo é predominante nos acidentes e caracteriza-se por hemorragia local e lesão dermonecrótica com espalhamento gravitacional algumas horas após o acidente. O loxoscelismo sistêmico é observado em aproximadamente 3 a 16% dos casos, sendo que seus sintomas geralmente se iniciam 24 horas após a picada e são caracterizados, em sua maioria, por distúrbios hemostáticos e da função renal. Em casos mais raros os pacientes desenvolvem alergia, choque anafilático e/ou vão a óbito (LUNG e MALLORY, 2000; DA SILVA, et al., 2004; APPEL et al., 2005; CHAIM et al., 2006; PIPPIRS et al., 2009).

O veneno de *Loxosceles* é uma mistura essencialmente proteica, com presença abundante de enzimas em sua composição. Análises eletroforéticas revelam a presença, em sua maioria, de proteínas de baixa massa molecular (3-40 kDa) (MACHADO et al., 2005; GREMSKI et al., 2010). Toxinas, incluindo peptídeos inseticidas, fosfolipases-D (toxinas dermonecróticas), hialuronidases, metaloproteases (família de astacinas), proteínas tumorais controladas traducionalmente (TCTPs), alérgenos, serinoproteases e inibidores de serinoproteases, já foram identificadas nesse veneno (SENFF-RIBEIRO et al., 2008; GREMSKI et al., 2010; CHAIM et al., 2011a).

Hialuronidases (HAases) são descritas em diversos venenos animais como o “fator de espalhamento”. Essa toxina por degradar constituintes da matriz

extracelular e contribuir na desorganização do tecido, potencializaria a ação de outros componentes do veneno facilitando a penetração desses do tecido inoculado até a circulação sanguínea (KEMPARAJU e GIRISH, 2006; SENFF-RIBEIRO et al., 2008; FERRER et al., 2013).

Em 1973, Wright e colaboradores foram os primeiros a descrever a atividade hialuronidásica em veneno do gênero *Loxosceles*. O trabalho desse grupo foi realizado com *L. reclusa,* onde estimaram que as massas moleculares dessas glicosidases seriam de 33 e 63 kDa (WRIGHT et al., 1973). Para o veneno de *L.intermedia,* da Silveira e colaboradores (2007) propuseram que as hialuronidases presentes nesse veneno eram moléculas de 41 e 43 kDa e que essas enzimas degradavam ácido hialurônico (HA) em modelo *ex vivo* de derme de coelho (DA SILVEIRA, et al., 2007a).

O HA e HAases contribuem na regulação de diversos processos essenciais para as células como regulação do ciclo celular, proliferação, adesão e migração (GIRISH e KEMPARAJU, 2007). Portanto, a degradação do HA está relacionada a diversos processos fisiológicos e patológicos (BOUGA et al., 2010), como por exemplo, embriogênese, angiogênese, inflamação, cicatrização de feridas, patogênese microbiana, envenenamentos e tumorigênese (GIRISH e KEMPARAJU, 2007). O metabolismo do HA em patologias vem ganhando enfoque nos últimos anos (WHATCOTT et al., 2011; TIAN et al., 2013).

O intuito desse trabalho foi obter uma isoforma de hialuronidase recombinante do veneno de *L.intermedia*, a qual denominamos *Dietrich´s Hyaluronidase* (DHAase) em sua forma ativa. Em um primeiro plano, estudar um pouco mais sobre o papel das hialuronidases no loxoscelismo e, posteriormente, utilizá-la como uma ferramenta para análise do efeito de hialuronidases exógenas na patologia do câncer.

Capítulo I:

Obtenção de uma isoforma de hialuronidase (*Dietrich´s Hyaluronidase*) em modelo procarioto, seu redobramento *in vitro* e avaliação de sua atividade sobre glicosaminoglicanos *in vitro* e *in vivo*.

2 INTRODUÇÃO

A quantidade de veneno produzido por uma aranha-marrom é variável, são poucos microlitros que contém geralmente 65 a 100 µg de proteínas por extração (SAMS et al., 2001; DA SILVA et al., 2004). Portanto, uma das principais dificuldades no estudo dos venenos loxoscélicos é a obtenção de grandes quantidades do veneno total e, consequentemente, das toxinas nativas purificadas (GREMSKI et al., 2010).

Diversos estudos estão direcionados na caracterização de componentes isolados de venenos para um maior entendimento do loxoscelismo e desenvolvimento de metodologias terapêuticas mais eficazes no tratamento. A produção de proteínas recombinantes representa um grande avanço na determinação da atividade tóxica do veneno de aranha-marrom e diante da diversidade de toxinas presentes nesses venenos com variadas atividades bioquímicas, é evidente o potencial dessas moléculas para emprego como insumos biotecnológicos, ferramentas de estudo ou de diagnóstico (GIRISH e KEMPARAJU, 2006; SENFF-RIBEIRO et al., 2008; CHAIM et al., 2011a).

A sequência completa de uma isoforma de hialuronidase de *L.intermedia* foi obtida pelo nosso grupo utilizando técnicas específicas de biologia molecular. A isoforma completa clonada apresentou massa molecular teórica de aproximadamente 46 kDa. Já a hialuronidase madura (sem o peptídeo sinal) possuiria 45 kDa e ponto isoelétrico (pI) de 8,75 (FERRER, 2010). O nosso grupo se propôs então realizar a subclonagem da hialuronidase em vetor de expressão e padronizar sua expressão heteróloga até à obtenção de sua conformação ativa. A escolha do modelo heterólogo de expressão foi o bacteriano (*E. coli*), embora vários trabalhos relatem que a expressão de proteínas eucarióticas solúveis em modelo procarioto seja um evento raro (DECHAVANNE et al., 2011; KIRIAKE et al., 2014).

Quando há superprodução da proteína recombinante nas células bacterianas ocorre a exposição de regiões hidrofóbicas, formando agregados. Isso pode ocorrer devido à rapidez com que a proteína de interesse é sintetizada e/ou devido às modificações pós-traducionais que o sistema bacteriano não realiza, dessa forma, não permitindo o dobramento proteico correto (BURGESS, 2009). Porém, existem diversas estratégias para se tentar solucionar os problemas de solubilidade e atividade das proteínas recombinantes (BRONDYK et al., 2009; NG et al., 2005).

Nesse capítulo serão abordadas as estratégias utilizadas para se obter a atividade de DHAase, sua caracterização bioquímica e sua caracterização dentro do quadro do loxoscelismo. As construções da sequência referente à DHAase nos plasmídeos de expressão pET-14b ou pET-SUMO foram expressas em cepas específicas de *E.coli*. Porém, essa proteína recombinante foi expressa em sua forma insolúvel em todas as condições utilizadas. DHAase insolúvel foi purificada para a produção de anticorpos policlonais em coelhos e o soro anti-DHAase foi capaz de reconhecer as hialuronidases nativas do veneno. Com o intuito da obtenção de DHAase em sua conformação ativa foi utilizada a técnica de redobramento *in vitro*. Após o uso dessa técnica, DHAase foi capaz de degradar ácido hialurônico e condroitim-4-sulfato *in vitro*. Utilizando DHAase ativa foi também demonstrado pela primeira vez na literatura que as hialuronidases do veneno de *L.intermedia* são “fatores de espalhamento” desse veneno, sendo enzimas que contribuem para o aumento da toxicidade do mesmo.

3 REVISÃO BIBLIOGRÁFICA

3.1 ARANHAS DO GÊNERO *Loxosceles*

As aranhas do gênero *Loxosceles* são aranhas de pequeno porte, com tamanho corporal de 8 a 15 mm, sendo que suas pernas podem chegar a medir 30 mm (DA SILVA et al., 2004). São conhecidas popularmente como aranhas-marrons, pois as aranhas desse gênero apresentam cor uniforme que varia de marrom claro à marrom escuro. Principalmente em países da América do Norte e Europa são também designadas como aranhas-violino por possuírem um desenho no cefalotórax (Figura 1) que lembra o formato do instrumento (FUTRELL,1992; PETERSON, 2006). Possuem como outra característica marcante três pares de olhos reunidos em semicírculo sobre o cefalotórax e os machos possuem corpo menor e pernas relativamente mais longas do que as fêmeas, conforme demonstrado também na Figura 1 (SWANSON e VETTER, 2006; CABRERIZO et al., 2009).

Pertencem à família Loxoscelidae (Sicariidae), subordem Labidognatha, ordem Araneida, classe Arachnida e filo Arthropoda (PLATNICK, 2013). A variação de coloração entre as diferentes espécies do gênero *Loxosceles* auxilia na identificação das mesmas. Essas aranhas preferem a escuridão e possuem hábitos noturnos. Vivem geralmente sob pedras, troncos de árvores, restos vegetais, telhas e tijolos empilhados, mas podem adquirir hábitos intradomiciliares sob condições especiais, vivendo então atrás de quadros, no meio de roupas, livros e outros objetos (FISCHER, 1996; FISCHER, 2005). Elas constroem teias irregulares que lembram fios de algodão e são mais ativas em meses quentes (DA SILVA, et al., 2004).

A maioria dos acidentes ocorre quando as pessoas comprimem a aranha inadvertidamente no ato de vestir-se, calçar-se, enxugar-se ou durante o sono (FUTRELL, 1992; RIBUFFO et al., 2012). As aranhas-marrons são artrópodes sedentários, não agressivos, e carnívoros, que se alimentam de pequenos insetos, principalmente, traças, baratas, moscas, mosquitos e cupins. Alguns trabalhos relatam que elas possuem preferência por presas mortas (MARQUES-DA-SILVA e FISCHER, 2005; SANDIDGE, 2004). Essas aranhas possuem grande capacidade de adaptação, suportando amplas variações de temperatura (8 a 43°C), bem como

longos períodos sem comida (276 dias) e água (DA SILVA, et al., 2004; SENFF-RIBEIRO et al., 2008).

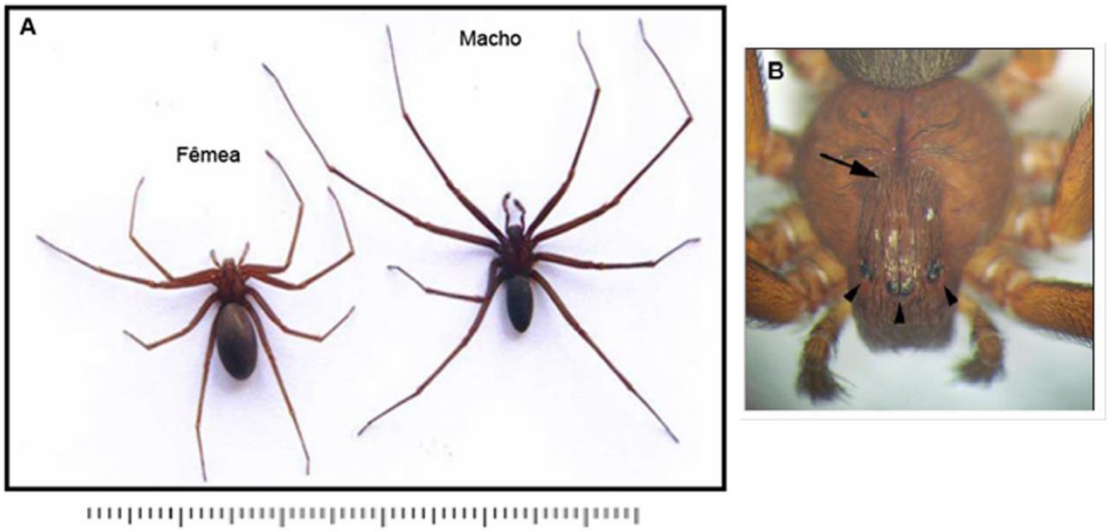

FIGURA 1: ASPECTOS MORFOLÓGICOS DA ARANHA-MARROM. (A) Diferença entre machos e fêmea (B) Na seta, desenho de violino no cefalotórax. Pontas de seta indicam os 3 pares de olhos formando semicírculo. ADAPTADO DE: CHAIM et al., 2011a.

As aranhas são animais peçonhentos comuns. Porém, uma morbidade clínica significativa decorre de um número pequeno de espécies e mesmo assim o índice de óbitos é baixo (WHITE, 2011). Por outro lado, alguns gêneros de aranha causam morbidade e mortalidade significativas e, portanto, podem ser considerados problemas de saúde pública, como é o caso das aranhas do gênero *Loxosceles* (SINAN, 2013).

Embora as aranhas sejam aracnídeos e não insetos, inseticidas são eficazes na redução da população de aranha-marrom. Muitas substâncias químicas podem não matar a aranha, mas perturbam o sistema nervoso e outras funções, como a locomoção das mesmas (SANDIDGE e HOPWOOD, 2005). Sandidge (2004) investigou o controle biológico de *L. reclusa* usando aranhas naturalmente encontradas na maioria das casas. Três destas, *Achaearanea tepidariorum*, *Steatoda triangulosa* e *Pholcus phalangioides,* prontamente se alimentam de aranhas-marrons e foram consideradas benéficas no controle da população de *L. reclusa*. O mais importante, é que essas três espécies são relativamente inofensivas aos seres humanos (RAMIRES et al*.,* 2007).

3.2 DISTRIBUIÇÃO GEOGRÁFICA E EPIDEMIOLOGIA

Representantes do gênero *Loxosceles* estão espalhadas pelos cinco continentes e há relatos de acidentes com seres humanos em diferentes regiões do planeta envolvendo essas aranhas. Espécimes foram encontrados no leste Europeu (PERNET et al., 2010; RIBUFFO et al., 2012), no Oriente Médio (TASKESEN et al., 2011), na África (DUNCAN et al., 2010), na Oceania (VETTER e ISBISTER, 2008), na América do Norte (SAUPE et al., 2011) e do Sul (BUCARETCHI et al., 2010; CHATZAKI et al., 2012).

No continente americano provavelmente se encontra a maior diversidade de espécies, sendo relatadas mais de 50 espécies apenas na América do Norte e mais de 30 espécies na América do Sul (PLATINICK, 2013). O número de casos de loxoscelismo em todo o mundo é provavelmente subestimado porque a maioria dos casos não é relatada (RIBUFFO et al., 2012). Mesmo assim, em algumas regiões do Brasil, Chile e Peru os acidentes provocados por aranhas do gênero *Loxosceles* constituem um significativo problema de saúde pública (HOGAN, 2004; DA SILVA, et al., 2004).

Sabe-se atualmente da existência de 12 espécies de aranha-marrom no Brasil (PLATINICK, 2013; GONÇALVES-DE-ANDRADE et al., 2012), sendo que quatro ocorrem no Estado do Paraná: *L. intermedia*, *L. gaucho*, *L.laeta* e *L. hirsuta* (MARQUES-DA-SILVA e FISHCER, 2005; FISCHER, 2008). A espécie *L. intermedia* é a predominante no município de Curitiba (FISCHER, 2008).

Na cidade de Curitiba e Região Metropolitana são registrados em média 2000 casos de loxoscelismo por ano. No ano de 2012 foram registrados 7.528 acidentes com aranhas *Loxosceles* no Brasil, sendo que aproximadamente 55% desses acidentes (4.139) ocorreram no estado do Paraná e cerca de 13% foram registrados em Curitiba (964). Se analisarmos uma média entre os anos de 2007 a 2011, o número de acidentes em Curitiba em relação ao restante do país sobe para 32,5% (SINAN, 2013).

3.3 LOXOSCELISMO

As picadas das aranhas do gênero *Loxosceles* provocam nos acidentados um conjunto de sinais e sintomas denominado loxoscelismo. O loxoscelismo pode estar relacionado a dois quadros clínicos distintos: na maioria dos acidentes ocorre o quadro cutâneo ou dermonecrótico (até 90% dos casos) e o quadro cutâneo-visceral

ou sistêmico com menor frequência (até 10% dos casos) (DA SILVA et al., 2004; APPEL et al., 2005; PIPPIRS et al., 2009; ISBISTER e FAN, 2011).

A evolução e severidade de um acidente loxoscélico e o desenvolvimento de um ou ambos os quadros clínicos dependem de inúmeros fatores, tais como a espécie de aranha-marrom, o sexo da aranha, o estágio de desenvolvimento da aranha, a quantidade e a composição do veneno inoculado. Há a influência também da susceptibilidade individual do acidentado ao veneno, do local da picada e do tempo que o acidentado leva para procurar diagnóstico e tratamentos adequados (BARBARO et al., 1994; SEZERINO et al., 1998; ISBISTER e FAN, 2011; PICHARDO-RODRIGUÉZ, 2013).

FIGURA 2: LESÃO DERMONECRÓTICA DE DIFÍCIL CICATRIZAÇÃO (A) Paciente de 6 anos com lesão cutânea típica de acidente loxoscélico. (B) Detalhe da placa marmórea após 36 horas do acidente. (C) Escara necrótica após 8 dias de evolução. (D) Cicatriz com quelóide após 3 meses do acidente. ADAPTADO DE: CABRERIZO et al. 2009.

O loxoscelismo cutâneo caracteriza-se classicamente por uma lesão dermonecrótica com espalhamento gravitacional e alto quadro inflamatório (Figura 2A e 2B). A picada da aranha-marrom é praticamente indolor e por isso muitas vezes

passa despercebida pelos indivíduos acidentados. Após 2 a 8 horas, surge dor local relatada como dor tipo “queimação”. Esses sintomas, inicialmente, podem estar associados a um pequeno ponto de eritema e edema. Entre 12 e 24 horas, há o rompimento dos vasos causando equimose. Uma área de tecido isquêmico é formada, circundada por um halo vermelho e zonas pálidas, denominada placa marmórea. Com o decorrer do tempo, a lesão necrótica adquire coloração violácea e um nítido espalhamento gravitacional aumenta ainda mais a área de necrose tecidual (Figura 2A e 2B). A agressão causada ao acidentado pode produzir ferimentos por longos períodos de tempo, com ulcerações cutâneas persistentes (Figura 2C e 2D) (FUTRELL, 1992; DA SILVA et al., 2004; MILLER et al., 2007; ISBISTER e FAN, 2011). Entre 3 e 7 dias, forma-se uma ferida rígida que, ao longo do tempo e em alguns casos, pode expor uma escara de difícil cicatrização necessitando, muitas vezes, de cirurgia plástica reparadora para remoção do tecido necrosado e substituição por enxerto (SEZERINO et al., 1998; DA SILVA et al., 2004; APPEL et al., 2005). Essa lesão pode ter como agente sinérgico, acentuando sua gravidade, a presença de microrganismos provenientes das quelíceras, que no momento da picada é injetado concomitantemente com o veneno (MONTEIRO et al., 2002).

Os dados clínicos e histopatológicos de biópsias de pele de pacientes que sofreram acidentes loxoscélicos mostram intenso infiltrado inflamatório, trombose, hemorragia, dermatite, endurecimento da região lesionada, eritema e necrose liquefativa da derme e epiderme (FUTRELL, 1992; YIANNIAS e WINKELMANN, 1992; DA SILVA et al., 2004; PAULI et al., 2009).

Achados histopatológicos do efeito do veneno de *L. intermedia* em coelhos já foram bem descritos. Nas primeiras horas já são observados efeitos como edema, grande presença de leucócitos e deposição intravascular de rede de fibrina com o surgimento de trombos. Em 12 horas constata-se a desorganização das células da derme e infiltrado leucocitário nas fibras de músculo esquelético. A partir de 24 horas ocorre desorganização das fibras de colágeno, destruição de vasos sanguíneos e necrose dérmica e muscular (OSPEDAL et al., 2002; CHATZAKI et al., 2012).

A ação do veneno como um ativador de células endoteliais, estimulando a liberação de moléculas pró-inflamatórias e a adesão de células polimorfonucleares, leva a uma resposta inflamatória descontrolada que contribui nas lesões

dermonecróticas (PATEL et al., 1994; PALUDO et al., 2009; BARBARO et al., 2010). É intrigante o estudo de Sunderkotter e colaboradores (2001), no qual camundongos expostos ao veneno de aranha-marrom (por injeção intradérmica) não desenvolvem lesão dermonecrótica macroscópica; embora, entre 4 e 6 horas após a inoculação apresentem alterações histológicas como infiltrado de células inflamatórias, edema na derme e alterações na integridade dos vasos sanguíneos (SUNDERKOTTER et al., 2001).

Algumas vítimas podem desenvolver a forma mais grave de loxoscelismo, que corresponde ao quadro cutâneo-visceral ou sistêmico. O loxoscelismo sistêmico severo é raro, no entanto, em alguns casos, o comprometimento sistêmico pode ser a causa de morte, geralmente quando associado à complicações hematológicas e renais (DA SILVA, et al., 2004; APPEL et al., 2005; SOUZA et al., 2008).

Os sintomas sugestivos desse quadro são episódios de vômitos, alterações sensoriais, cefaleias e febre baixa. Pode haver também *rash* cutâneo, prurido generalizado e petéquias (FUTRELL, 1992; BRAVO et al., 1993; PIPPIRS et al., 2009). Nos casos mais graves, as alterações no quadro hematológico incluem anemia hemolítica, trombocitopenia decorrente da agregação plaquetária e coagulação intravascular disseminada (DA SILVA et al., 2004; ISBISTER et al., 2005; CHAVES-MOREIRA et al., 2009).

A insuficiência renal aguda também é uma grave complicação do quadro sistêmico, caracterizada por hematúria e hemoglobinúria, muitas vezes refletindo as desordens hematológicas (LUNG e MALLORY et al., 2000; CHAIM et al., 2006; CHAVES-MOREIRA et al., 2009). É descrito que o quadro mais frequente no loxoscelismo sistêmico é a presença de hemólise intravascular, sendo a insuficiência renal aguda mais rara e associada ao quadro de hemólise (MALAQUE et al., 2011). O quadro de injúria renal foi descrito como sendo resultado dos distúrbios da hemostase e da reação inflamatória exacerbada em resposta ao veneno, porém, já é descrito que componentes do veneno podem ligar-se diretamente às estruturas renais (TAMBOURGI et al., 1998; CHAIM et al., 2006; KUSMA et al., 2008).

3.4 VENENO LOXOSCÉLICO

O veneno é produzido por um par de glândulas situadas no cefalotórax, ligadas a um par de quelíceras, as quais fazem a conexão entre o interior da

glândula e o meio externo. Esse par de glândulas possui epitélio secretor e são revestidas por membrana basal e duas camadas de músculo estriado: uma camada interna e outra externa. As células do epitélio secretório são ricas em vesículas próximas a um complexo de Golgi proeminente. A morfologia das glândulas e células indica que o tipo de secreção é principalmente holócrina, onde o produto secretado é liberado com toda a célula. O volume de veneno inoculado pela aranha é em torno de 4 µL e cerca de 20-200 µg de proteínas são inoculados no momento da picada, dependendo da espécie, tamanho, sexo e estado nutricional da aranha em questão (DOS SANTOS et al., 2000; DA SILVA et al., 2004).

O veneno de *Loxosceles* é um líquido cristalino e incolor, de natureza essencialmente proteica (DOS SANTOS et al., 2000), sendo composto basicamente por enzimas e proteínas não enzimáticas, biologicamente ativas. No veneno é encontrado um grande conteúdo de proteínas de baixa massa molecular (5-40 kDa), em detrimento de uma pouca expressão de proteínas acima de 40 kDa (Figura 3A e 3B). Os venenos das espécies *L. laeta*, *L. intermedia* e *L. reclusa* possuem perfil eletroforético semelhante em gel unidimensional, apresentando as principais bandas entre 7-35 kDa. Embora o perfil dos venenos seja semelhante, eles não são os mesmos. De Oliveira e colaboradores (2005) mostraram que há variações significativas entre o conteúdo dos venenos de *L. intermedia* e *L. laeta*. As variações da composição desses venenos foram extrapoladas para suas atividades biológicas, tais como a atividade dermonecrótica maior do veneno de *L. laeta* quando comparado com o de *L. intermedia*, observada em pele de coelhos pelo tamanho da lesão. Além disso, as lesões provocadas pelo veneno de fêmeas foram maiores em área do que as lesões provocadas pelo veneno de machos (DE OLIVEIRA et al., 2005).

O conteúdo total do veneno ainda não é totalmente conhecido, sabe-se que além da grande quantidade de proteínas, a mistura também é constituída por ácidos nucleicos, aminoácidos livres, histamina, poliaminas neurotóxicas e sais inorgânicos (ESCOUBAS et al., 2000). Os eventos inflamatórios iniciais provocados pelo veneno de aranha-marrom podem também estar relacionados com o conteúdo de histamina do veneno (RATTMANN et al., 2008; PALUDO et al., 2009). É consenso o fato da toxicidade do veneno da aranha-marrom ser decorrente do efeito sinérgico de seus constituintes (GEREN et al., 1976; BARBARO et al., 2005; GREMSKI et al., 2010).

Várias toxinas com atividade enzimática já foram descritas em venenos de diferentes espécies de *Loxosceles*, entre as quais se podem destacar as serinoproteases, metaloproteases, hialuronidases e fosfolipases-D (FEITOSA et al., 1998; FUTRELL, 1992, DA SILVA et al., 2004; DE CASTRO et al., 2004; VEIGA et al., 2000). Na última década, devido ao avanço das técnicas de biologia molecular e ao grande interesse em se identificar a complexa composição dos venenos loxoscélicos, trabalhos de transcriptomas da glândula produtora de veneno de espécies de aranha-marrom foram publicados (FERNANDES-PEDROSA et al., 2008; GREMSKI et al., 2010). Segundo Gremski e colaboradores (2010), considerando apenas o conteúdo de transcritos da glândula produtora do veneno de *L.intermedia* que codifica toxinas (Figura 3C), temos uma representação majoritária de peptídeos potencialmente inseticidas (55,9% dos transcritos), metaloproteases do tipo astacina (22,6%) e fosfolipases-D (20,2%). Por outro lado, há proteínas menos expressas, que em conjunto representam menos que 5% dos transcritos que codificam toxinas, como é o caso de serinoproteases, TCTP, alérgenos, hialuronidases e inibidores de serinoproteases (GREMSKI et al., 2010).

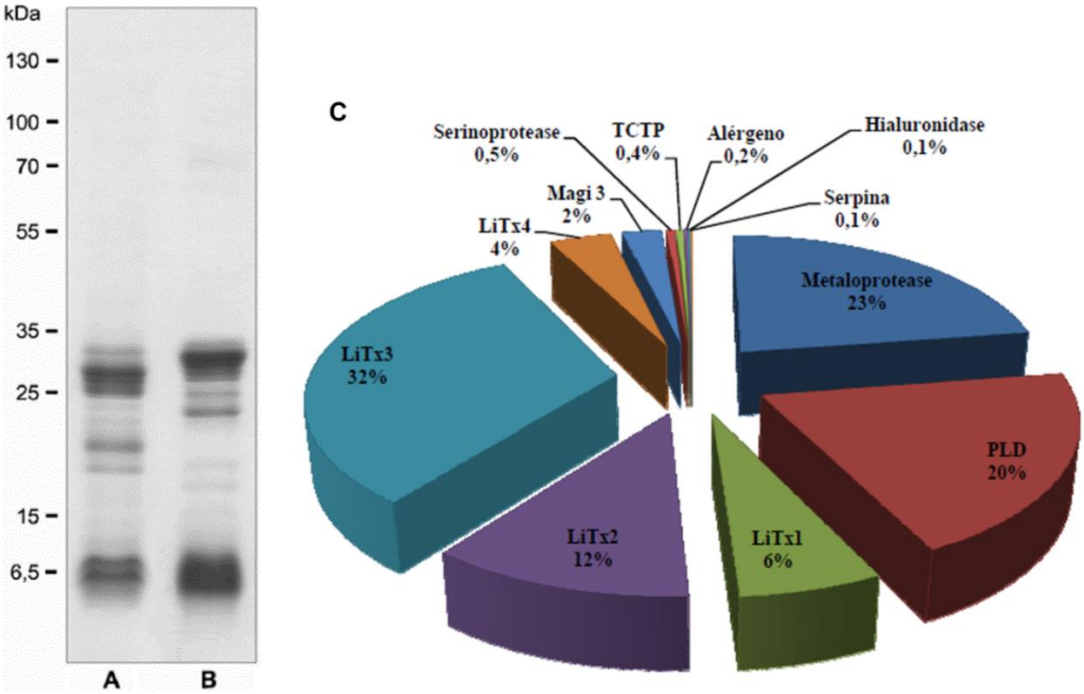

FIGURA 3: PERFIL DO VENENO DE *L. intermedia.* (A) Perfil eletroforético em SDS-PAGE de amostras reduzidas e (B) não reduzidas. As massas moleculares estão representadas à esquerda da figura. (C) Proporção relativa de cada toxina em relação ao total de transcritos que codificam para toxinas. ADAPTADO DE: GREMSKI et al., 2010; CHAVES-MOREIRA, 2011.

Dos componentes presentes no veneno de *L. intermedia*, as toxinas melhor caracterizadas são as pertencentes à família de toxinas dermonecróticas ou família *Loxtox*. São enzimas do tipo fosfolipase-D, e estão envolvidas com a maioria dos efeitos tóxicos do veneno. Sejam as nativas ou as isoformas recombinantes, estas toxinas parecem desempenhar um importante papel nos sinais e sintomas do loxoscelismo. As fosfolipases são capazes de induzir experimentalmente dermonecrose, resposta inflamatória, agregação plaquetária, hemólise, aumento da permeabilidade vascular, nefrotoxicidade, letalidade em camundongos e efeitos citotóxicos em diferentes linhagens celulares (FUTREL, 1992; DA SILVA et al., 2004; APPEL et al., 2005; CHAIM et al., 2006; DA SILVEIRA et al., 2006; DA SILVEIRA et al., 2007b; RIBEIRO et al., 2007; APPEL et al., 2008; CHAVES-MOREIRA et al., 2009; VUITIKA et al., 2013).

As fosfolipases-D possuem massa molecular variável entre 30-35 kDa e exibem sequências relativamente conservadas de aminoácidos (55% a 99%). Especialmente existe a conservação dos resíduos envolvidos na catálise do substrato (CHAIM et al., 2006; KALAPOTHAKIS et al., 2007). É consenso na literatura que existam mais de 10 isoformas dessas toxinas (GOMEZ et al., 2002; CHAIM et al., 2011b; WILLE et al., 2013). O mecanismo de ação das fosfolipases ainda não foi totalmente esclarecido, mas acredita-se que a hidrólise de lipídios, gerando mediadores como ceramida-1-fosfato e ácido lisofosfatídico, possam ativar determinadas vias de sinalização causando as alterações fisiopatológicas e os efeitos deletérios dessas toxinas (KUSMA et al., 2008; CHAVES-MOREIRA et al., 2009; VUITIKA et al., 2013).

Existem várias toxinas presentes no veneno que atuam sobre componentes de matriz extracelular. Serinoproteases foram identificadas pela primeira vez em veneno de *Loxosceles* sp. como zimogênios ativados por tripsina (VEIGA et al., 2000). Através de ensaios de zimograma, foram identificadas duas serinoproteases (85 e 95 kDa) com atividade gelatinolítica, possivelmente relacionadas com a atividade tóxica do veneno de *L. intermedia*. Essas proteases degradando proteínas da matriz extracelular de tecido conjuntivo ou de membranas basais podem estar envolvidas com distúrbios hemorrágicos, agravamento da lesão dermonecrótica e aumento da permeabilidade vascular (DA SILVA et al., 2004; CHAIM et al., 2011b). Em análise do transcriptoma da glândula de veneno de *L. intermedia* foram

encontrados cinco sequências de transcritos de serinoproteases (GREMSKI et al., 2010).

Quanto às metaloproteases, foram caracterizadas como sendo moléculas de baixa massa molecular com atividade fibronectinolítica e fibrinogenolítica (20-28 kDa) e gelatinolítica (32-35 kDa). Foram primeiramente descritas no veneno de *L. intermedia* e posteriormente nos venenos de *L. laeta*, *L. gaucho* e *L. rufescens*. A atividade dessas está possivelmente relacionada a distúrbios hemostáticos tais como hemorragia da derme e injúria dos vasos sanguíneos (DA SILVEIRA et al., 2007c; SENFF-RIBEIRO et al., 2008). A metaloprotease recombinante descrita no veneno de *L. intermedia* (LALP1, *Loxosceles astacin-like protease*) possui os domínios conservados da família das astacinas (HEXXHXXGXXHEXXRXDR e SXMHY) e não apresenta os domínios não catalíticos, típicos de metaloproteases, na porção C-terminal (DA SILVEIRA et al., 2007c; GOMIS-RUTH, 2003; BECKER-PAULY et al., 2009).

Recentemente, duas novas isoformas de proteases *astacin-like* foram identificadas no veneno de *L. intermedia* (nomeadas LALP2 e LALP3) e no veneno de *L. laeta* (LALP4) e *L. gaucho* (LALP5). Esses resultados demonstram que essas proteases são uma família de toxinas presentes no veneno de *Loxosceles sp* e que são componentes importantes desses venenos (TREVISAN-SILVA et al., 2010). Corroborando com essa ideia, nos trabalhos de transcriptomas de *L. laeta* e *L. intermedia* foi demonstrado que uma grande porcentagem dos transcritos codifica para metaloproteases (FERNANDES-PEDROSA et al., 2008; GREMSKI et al., 2010).

Outras enzimas caracterizadas nos venenos loxoscélicos que exibem ação sobre componentes da matriz extracelular são as hialuronidases. Acredita-se que essas enzimas atuem degradando glicosaminoglicanos e funcionem como um “fator de espalhamento” do veneno, contribuindo para sua toxicidade (BARBARO et al., 2005; DA SILVEIRA et al., 2007a).

3.5 HIALURONIDASES

A descoberta das hialuronidases foi através da observação de que extratos de testículos e outros tecidos continham um “fator de espalhamento” que facilitava a difusão de corantes e vacinas antivirais aplicadas subcutaneamente (DURAN-

REYNALS, 1928; CHAIN e DUTHIE, 1940). As hialuronidases são um grupo de enzimas que medeiam a degradação do ácido hialurônico (também chamado hialuronam, HA), aumentam a permeabilidade de tecidos conjuntivos e decrescem a viscosidade dos fluídos corporais. São distribuídas através de todo o reino animal e expressas tanto em procariotos quanto eucariotos. Karl Meyer (1971) foi quem primeiro utilizou o termo hialuronidase. Em seu estudo, Meyer classificou-as em três diferentes grupos baseados na análise bioquímica dos produtos finais gerados por essas enzimas (MEYER, 1971).

Hialuronidases de mamíferos são hialuronoglicosaminidases ou endo-β-N-acetilhexosaminidases que randomicamente clivam ligações glicosídicas β1-4 em HA, condroitim (Figura 4A e 4B) e condroitim sulfato (CS) produzindo majoritariamente tetra e hexassacarídeos com N-acetilhexosamina na porção redutora. Enzimas dessa classe têm atividade hidrolítica e transglicosidase e estão presentes em espermatozóides de mamíferos, lisossomos, venenos de serpentes, répteis e himenópteros (CRAMER et al., 1994; STAIR-NAWY et al., 1999; STERN-CSÓKA, 2000; GUSHULAK et al., 2012).

Por sua vez, hialuronoglucuronidases são endo-β-D-glucuronidases que clivam as ligações glucuronato (β1-3) no HA (Figura 4B) e são inertes a outros glicosaminoglicanos (GAGs). Da mesma forma, os principais produtos gerados são tetra e hexassacarídeos, porém, com ácido glucurônico na porção redutora do produto. Essa classe inclui enzimas presentes nas glândulas salivares de sanguessugas e ancilostomídeos (HOTEZ et al., 1992; STERN, 2004).

Têm-se também as hialuronidases microbianas que clivam o HA na ligação glicosídica β1-4 usando β-eliminação e produzindo oligossacarídeos Δ4-5 insaturados (Figura 4B). Diferente das outras duas classes, esse tipo de enzima não utiliza hidrólise em sua atividade. Incluem hialuronato liases, por exemplo, de *Streptococcus pneumoniae* e *S. agalactiae* (KREIL, 1995; GIRISH e KEMPARAJU, 2007).

Independente da classificação anterior, as hialuronidases podem ser classificadas em dois grupos baseados em seu perfil de atividade pH dependente. As hialuronidases com atividade em ambiente ácido são enzimas que são otimamente ativas em pH entre 3-4. Esse grupo inclui, por exemplo, enzimas lisossomais, séricas e do fígado humano. Hialuronidases com atividade em ambiente

neutro são as que possuem atividade ótima entre os pHs 5-8. Esse grupo tem como exemplo as enzimas de serpentes, de esperma de mamíferos e veneno de abelha (KREIL, 1995; STERN, 2004; KEMPARAJU e GIRISH, 2006).

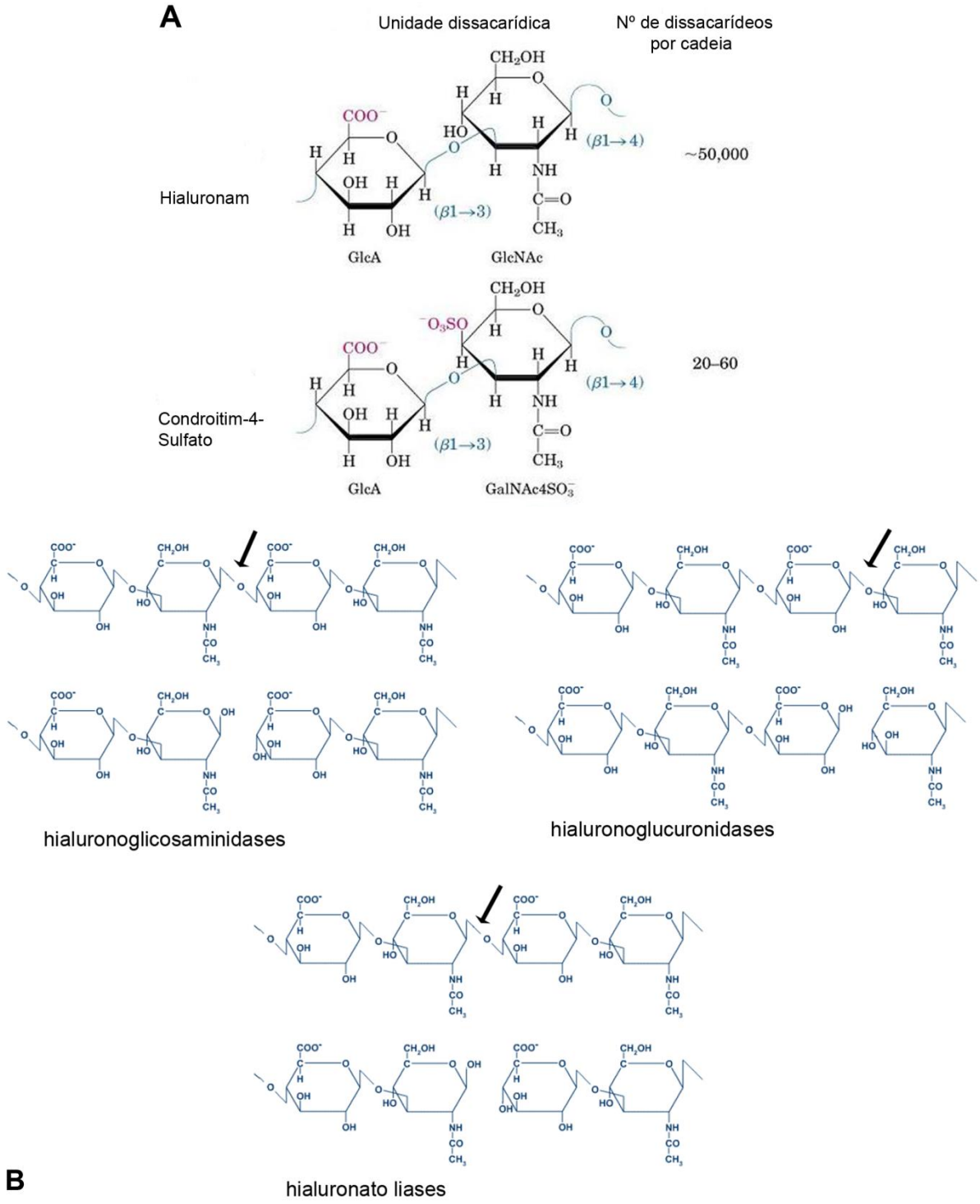

FIGURA 4: ATIVIDADE DE HIALURONIDASES EM GLICOSAMINOGLICANOS (A) Diferença estrutural entre HA e C4S ou CS tipo A. (B) Classificação das hialuronidases segundo a especificidade de catálise. ADAPTADO DE: (A) VERCRUYSSE et al., 1995 (B) HOVING e LINKER 1999.

As hialuronidases já foram encontradas desde organismos simples, como bactérias, fungos e vírus (SHIMIZU et al., 1995; HART et al., 2013; LEE et al., 2010) até mamíferos (BOOKBINDER et al., 2006). Estão presentes em vários órgãos humanos (testículo, olho, pele, baço, fígado, rins e útero) e fluidos (placenta, lágrimas, sangue e esperma) (STERN e JEDRZEJAS, 2006). A taxa de renovação do HA em mamíferos, onde as hialuronidases são essenciais, é surpreendentemente elevado para um componente de matriz extracelular. Um indivíduo de 70 kg possui cerca de 15 g de HA, um terço do qual se renova diariamente. O HA tem diferentes taxas de *turnover* dependendo do tecido: na pele a meia-vida é de um dia, na cartilagem de uma a três semanas e na corrente sanguínea de dois a cinco minutos (STERN e CSÓKA, 2000). A atividade hialuronidásica é modulada por vários ativadores, como por exemplo, adrenalina, histamina e fosfatases alcalinas; e inibidores - anti-histamínicos, salicilatos, heparina, dicumarina, vitamina C e flavonoides (MENZEL e FARR, 1998; GIRISH et al., 2009).

Hialuronidases são enzimas comuns em venenos animais, tendo sido encontradas em venenos de serpentes, lagartos, escorpiões, aranhas, lagartas, raias e vespas (KEMPARAJU e GIRISH, 2006; DA C. B. GOUVEIA et al., 2005, HADDAD et al., 2004). Em todos os venenos animais ela é referida como um “fator de espalhamento” das demais toxinas (GIRISH e KEMPARAJU, 2007).

A primeira hialuronidase eucariótica clonada via cDNA foi a partir do veneno de abelha (GMACHL et al., 1993). A proteína madura apresenta ~41 kDa, pontes dissulfetos e N-glicosilação. A atividade dessa enzima foi demonstrada ser do tipo endo-β-N-hexosaminidase. Já a primeira hialuronidase marinha foi isolada do peixe pedra *Synanceja horrida* sendo classificada, como a de abelha, como uma enzima que cliva ligações β1-4 por hidrólise (GIRISH e KEMPARAJU, 2007). Essa enzima de peixe é uma glicoproteína de 62 kDa e não é tóxica por natureza. Duas hialuronidases purificadas diretamente do veneno de *Naja naja* (uma delas apresentando ~70 kDa e outra ~52 kDa) demonstraram especificidade por HA e indiretamente potencializaram o efeito de uma miotoxina e de um complexo hemorrágico do mesmo veneno (GIRISH e KEMPARAJU, 2005a).

3.5.1 Hialuronidases em venenos loxoscélicos

No loxoscelismo cutâneo é comum a presença de edema, eritema, equimose e necrose, sintomas que sugerem alterações de matriz extracelular (BARBARO et al., 2005; PAULI et al., 2009). A primeira descrição de hialuronidases em veneno de aranha-marrom foi por SDS-PAGE em 1973, como toxinas de 33 kDa e 63 kDa no veneno de *L. reclusa* (WRIGHT et al., 1973). Essas enzimas exibiram atividade sobre HA e CS tipo A, B e C.

Semelhante a outros venenos, a hipótese era que as hialuronidases presentes nos venenos de aranha-marrom seriam um "fator de espalhamento" desses venenos. Além de contribuir para o quadro cutâneo, essas enzimas contribuiriam também para a forma clínica sistêmica e o agravamento dos acidentes (DA SILVEIRA et al., 2007a).

Esse tipo de glicosidase foi também descrita no veneno de *L. rufescens*, como uma toxina de 32,5 kDa (YOUNG; PINCUS, 2001) e nos venenos de *L. reclusa*, *L. deserta*, *L. gaucho*, *L. laeta* e *L. intermedia* (BARBARO et al., 2005).

Em estudos com o veneno de *L. intermedia* foi detectada a degradação de HA e CS. Experimentos de zimografia com o veneno de *L.intermedia* demonstraram atividade lítica frente a esses substratos em 41 e 43 kDa. Com o uso de reações colorimétricas foi observado que a hidrolase do veneno de *L. intermedia* era uma endo-β-N-acetil-D-hexosaminidase. Análises em microscopia de fluorescência (Figura 5) confirmaram a ação desse veneno sobre o HA em derme de coelho (DA SILVEIRA et al., 2007a).

A grande dificuldade no estudo das hialuronidases se deve ao fato de sua existência em pequenas quantidades nos venenos de aranhas, justificando a quase ausência de estudos de purificação e isolamento a partir dos venenos desses animais nas últimas décadas (NAGARAJU et al., 2007). Os transcriptomas de venenos de aranha-marrons corroboraram tal fato. No transcriptoma de *L.laeta* foi observado que transcritos de hialuronidase representam 0,13% dos transcritos totais da glândula produtora de veneno (FERNANDES-PEDROSA et al., 2008). Já no trabalho realizado com a espécie *L.intermedia,* levando em consideração os transcritos relacionados à toxinas, hialuronidases representam apenas 0,1%

desses. Em quantidade proteica, esse número pode ser ainda menor. No entanto a atividade dessas enzimas é pronunciada nos venenos (GREMSKI et al., 2010).

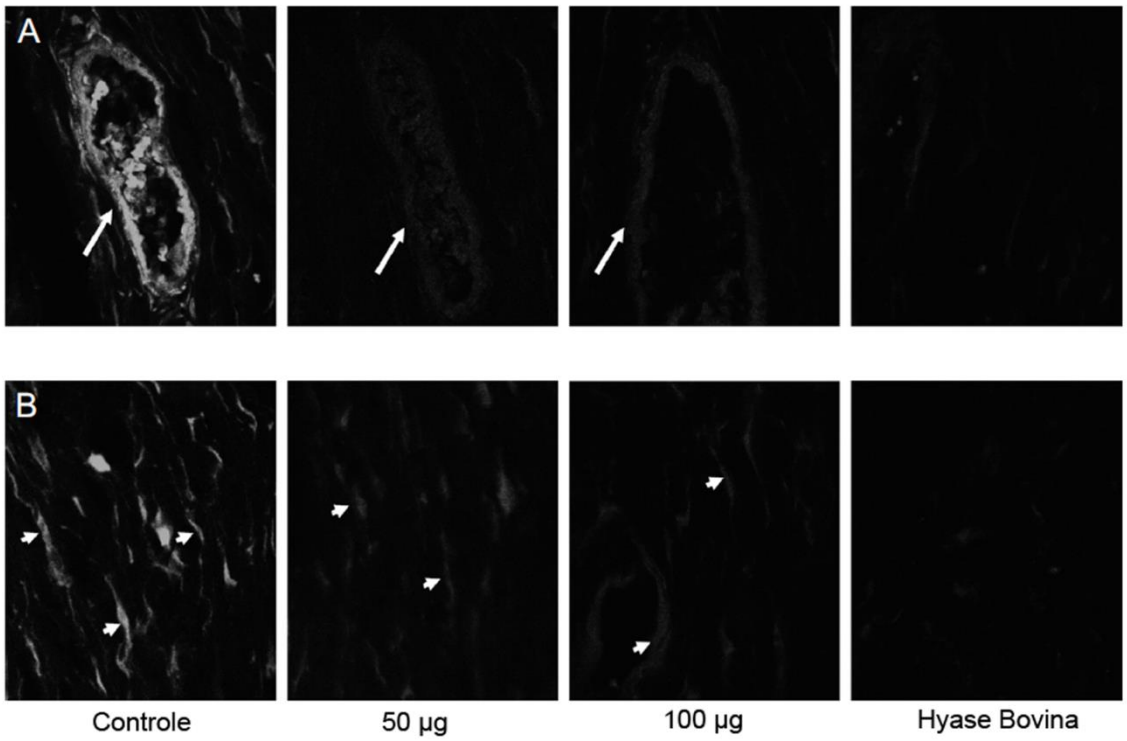

FIGURA 5: ANÁLISE DE FLUORESCÊNCIA CONFOCAL DO ÁCIDO HIALURÔNICO DE DERMES DE COELHOS INCUBADAS COM O VENENO DE *L. intermedia*. Corte histológico da derme onde está demonstrado (A) um vaso sanguíneo. (B) matriz extracelular de tecido conjuntivo. O controle representa a ausência de veneno. Cinquenta e 100 µg do veneno total de *L.intermedia* foram incubados com os cortes histológicos pré-fixados. Como controle positivo foram utilizados 4U de hialuronidase testicular bovina (HTB) comercial. ADAPTADO DE: DA SILVEIRA et al., 2007a.

Apesar do empecilho de uma pequena quantidade de transcritos para esta classe de enzima, foi obtida por técnicas de RACEs (*Rapid Amplification of cDNA End*) a sequência completa de uma isoforma de hialuronidase do veneno de *L. intermedia* (Figura 6), a qual foi denominada *Dietrich´s Hyaluronidase* (DHAase) em homenagem ao Professor Carl Peter von Dietrich, que dedicou sua vida científica em estudar glicosaminoglicanos e proteoglicanos (FERRER et al., 2013). O cDNA completo dessa enzima apresentou 1200 pb e uma sequência única de leitura, codificando para uma proteína de 400 aminoácidos (~46 kDa) (FERRER, 2010). Os primeiros 19 resíduos de aminoácidos é predito como um peptídeo sinal de endereçamento para o retículo endoplasmático, com o qual se originaria uma proteína madura de ~45 kDa com ponto isoelétrico de 8,75.

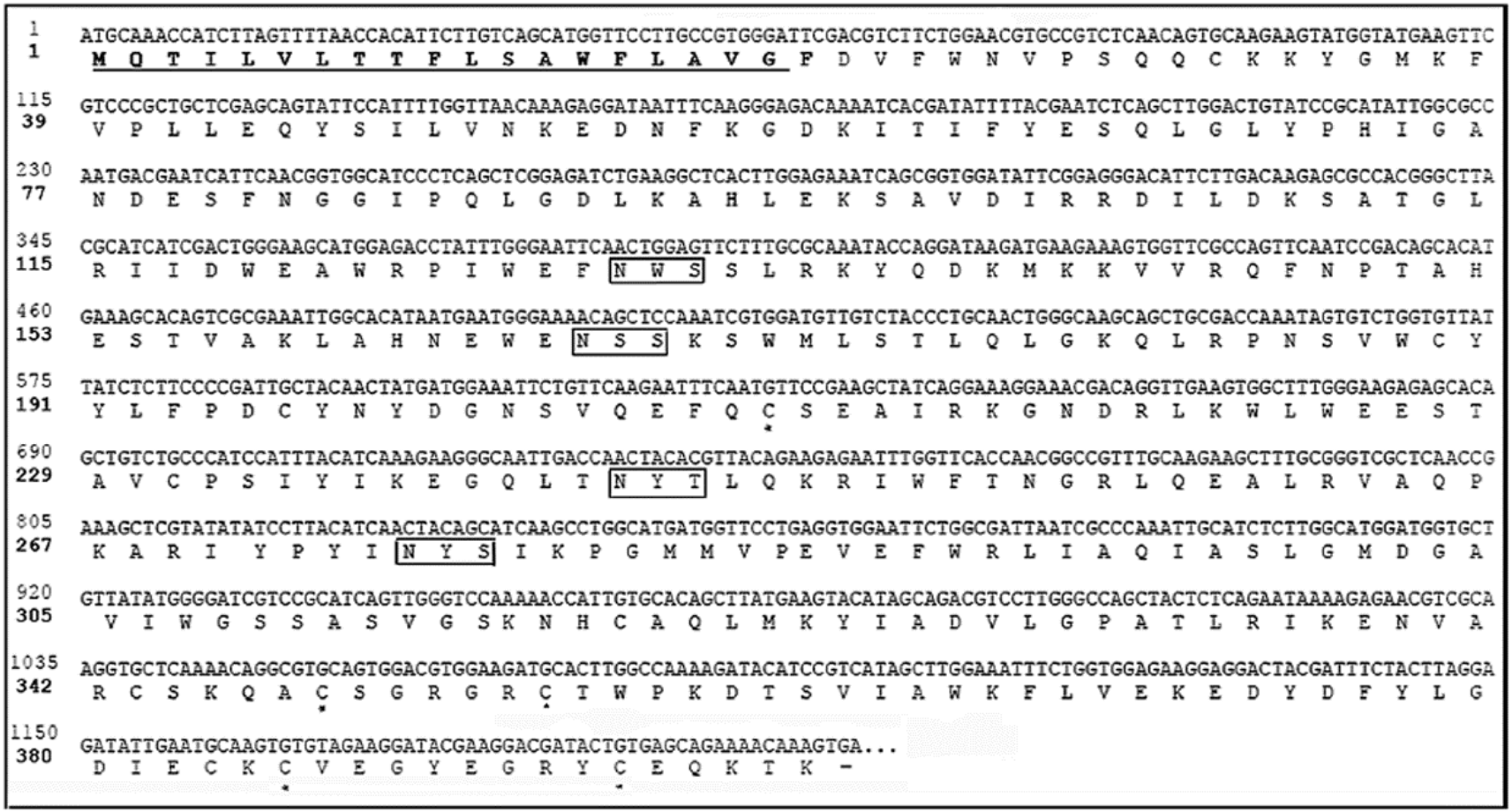

FIGURA 6: CLONAGEM MOLECULAR DE DHAase, UMA NOVA PROTEÍNA DO VENENO DE *L. intermedia*. Sequência nucleotídica e aminoacídica deduzida. A sequência de aminoácidos deduzida possui 400 resíduos de aminoácidos, onde o possível peptídeo sinal se encontra sublinhado. Nos retângulos estão os sítios de N-glicosilação preditos (*Expasy tool*). Os asteriscos indicam os resíduos de cisteínas que teoricamente podem formar pontes dissulfeto (DIANNA *web server*). ADAPTADO DE: FERRER et al., 2013.

3.5.2 Estrutura das hialuronidases

No Banco de Dados de Proteínas (PDB) existem até o momento 42 estruturas de hialuronidases resolvidas. A grande maioria delas é representada por hialuronidases de bactérias, sendo que apenas 5 estruturas são de enzimas provenientes de veneno (4 de *Apis melífera* e 1 de *Vespula vulgaris*).

A hialuronidase nativa de abelha possui 30% de identidade com a hialuronidase (PH-20) de humano. Markovic-Housley e colaboradores (2000) co-cristalizaram a hialuronidase de abelha com HA. Esse cristal revelou que o sítio de ligação ao HA é situado na porção C-terminal de um barril β e é composto de muitos resíduos de aminoácidos conservados (Figura 7A). A estrutura do complexo fortemente sugere um mecanismo catalítico ácido-base, com Ácido Glutâmico (Glu) agindo como doador de próton e grupos N-acetil-carboxil do HA agindo como bases nucleofílicas (Figura 8) (MARKOVIC-HOUSLEY et al., 2000). Uma fenda de aproximadamente 30 x 10 Å é observada na superfície da hialuronidase de abelha e é rica em aminoácidos aromáticos e hidrofóbicos que participam da ligação ao substrato e da catálise (STERN e CSÓKA, 2000; STERN e JEDRZEJAS, 2006).

As hialuronidases Hyal-1 (humana), de vespa (Figura 7B) e de abelha pertencem à família 56 das hidrolases. A estrutura da Hyal – 1 é estabilizada por 5 pontes dissulfetos (CHAO et al., 2007), enquanto que as de abelha e de vespa são estabilizadas por duas (MARKOVIC-HOUSLEY et al., 2000, SKOV et al., 2006). A hialuronidase de abelha possui 2 sítios de N-glicosilação (MARKOVIC-HOUSLEY et al., 2000) e de vespa possui 3 desses sítios (SKOV et al., 2006).

O mecanismo molecular da hidrólise das hialuronidases pertencentes à família 56 das hidrolases envolve o ácido glutâmico. Análise de bioinformática realizada com a sequência da DHAase classificou-a como pertencente a essa família e com 4 possíveis sítios de N-glicosilação (Figura 6) e 3 possíveis pontes dissulfeto (FERRER, 2010).

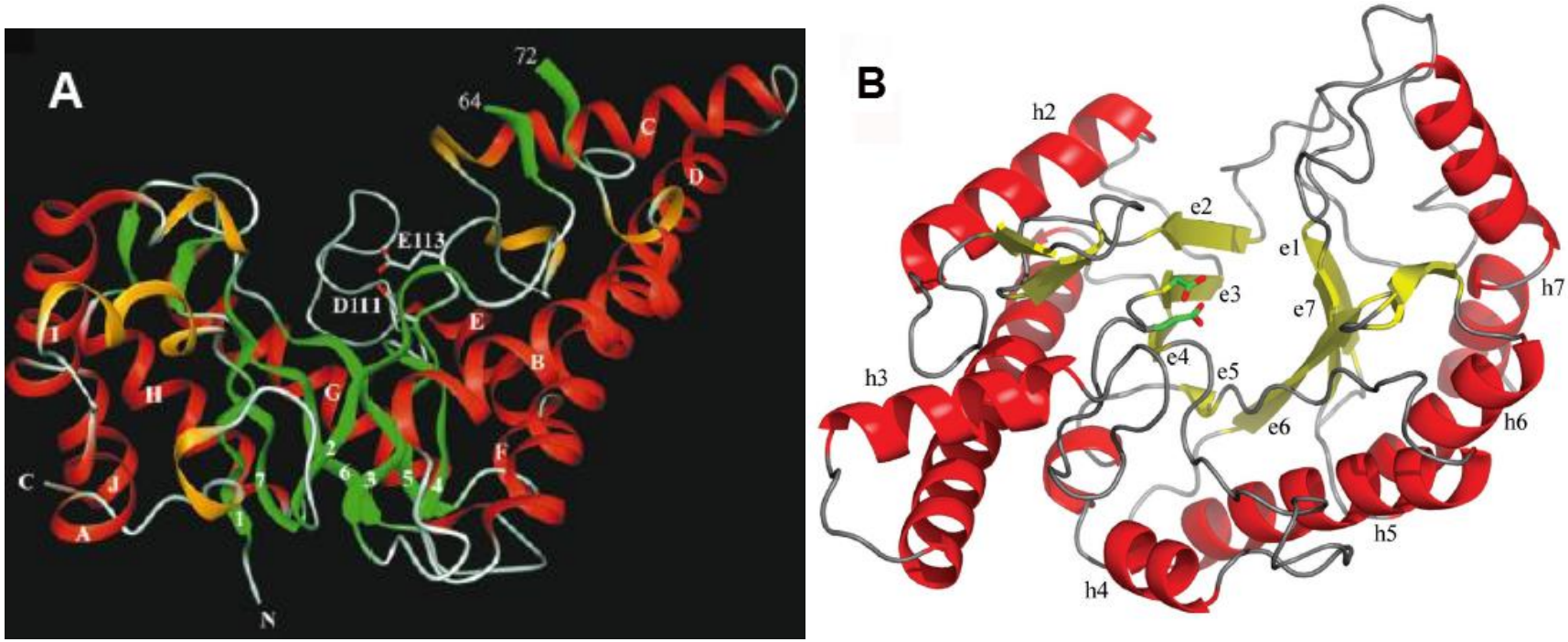

FIGURA 7: REPRESENTAÇÃO EM FITAS DOS CRISTAIS DE HIALURONIDASES DE VENENOS. (A) De abelha (*Apis mellifera*), com vista lateral. As 10 α hélices (A-J) estão representadas em vermelho, 3 hélices em laranja e em verde a representação das 7 folhas β. A fenda de ligação ao substrato está localizada no final da porção C-terminal dos barris β (parte superior). Ácido aspártico 111 e ácido glutâmico113 estão representados em modelo de bastão. (B) Vespa (*Vespula vulgaris*). Dobramento geral de rVes v 2, incluindo resíduos do sítio ativo ácido aspártico107 e ácido glutâmico109. Estão representadas as folhas β (e1-e7) e α hélices (h2-h7) do *core* do barril TIM$(\beta/\alpha)_7$. ADAPTADO DE: (A) MARKOVIC-HOUSLEY et al., 2000 e (B) SKOV et al., 2006.

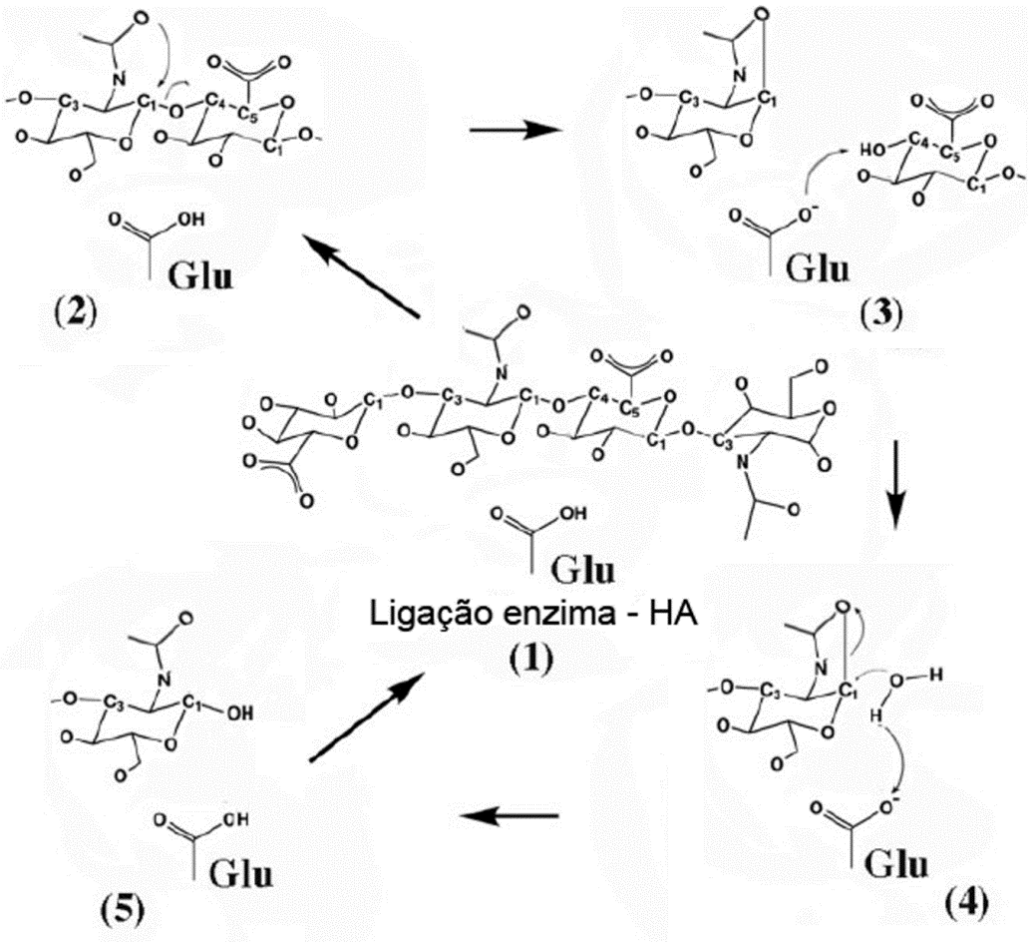

FIGURA 8: ESQUEMA DO MECANISMO DE HIDRÓLISE COMUM PARA AS HIALURONIDASES HUMANAS. A função catalítica ácida é desenvolvida por um resíduo de ácido glutâmico conservado entre as hialuronidases. A função nucleófila é atribuída ao oxigênio do carbono 2 (grupo acetamido) dos substratos: HA, condroitim e CS. ADAPTADO DE: STERN e JEDRZEJAS, 2006.

3.5.3 Aplicações médicas e biotecnológicas de hialuronidases

Hialuronidases aumentam a permeabilidade de membrana, reduzem a viscosidade e deixam os tecidos mais permeáveis e fluídos. Dessa maneira, esse tipo de enzima pode ser usada terapeuticamente para aumentar a velocidade de absorção de compostos e para promover a reabsorção de excesso de fluídos (FROST et al., 1996; FARR et al., 1997; HANRAHAN et al., 2013). Hialuronidases permitem a absorção mais rápida de medicamentos para o tecido-alvo em até vinte vezes (BOOKBINDER et al., 2006). O seu uso como adjuvante aumenta a efetividade de anestesias locais e diminui a destruição tecidual por injeções subcutâneas e

intramusculares, por exemplo, nos casos de nutrição parenteral e quimioterápicos (MENZEL e FARR, 1998; NEEVES et al., 2007; CHAIM et al., 2011b).

Essas enzimas têm sido amplamente utilizadas em várias áreas médicas, tais como ortopedia, cirurgia, oftalmologia, oncologia, ginecologia e dermatologia (BORRELLI et al., 1986; MENZEL e FARR, 1988; FROST et al., 1996; KLOCKER et al., 1995; NEEVES et al., 2007). Esse tipo de hidrolase proveniente de esperma desempenha um importante papel no sucesso das fertilizações de mamíferos, incluindo humanos (PRIMAKOFF et al., 1985; LIN et al., 1994; MORIN et al., 2010).

Hialuronidases são comercializadas legalmente nos Estados Unidos desde 1948. Elas foram aprovadas para serem comercializadas como adjuvante na absorção ou dispersão de medicamentos injetáveis. As primeiras enzimas utilizadas foram de origem testicular ovina (Vitrase) ou bovina (Hydase), porém esses extratos eram imunogênicos (BOOKBINDER et al., 2006). Devido às ocorrências de reações alérgicas foi proibido o uso da enzima bovina (EBO et al., 2005). Em 2005 a hialuronidase humana, conhecida como rHuPH20 ou Hylenex, foi purificada (BOOKBINDER et al., 2006).

Hialuronidases tem sido utilizadas para melhorar a absorção de agentes radiopacos na urografia (DUNN et al., 2010) e também tem sido usadas no tratamento da fimose em associação com betametasona (FAVORITO et al., 2008). A indústria brasileira Apsen comercializa para o tratamento de: fimose - Postec® (hialuronidase 150 UTR/g + valerato de betametasona 2,5 mg/g); para hemorroidas – Xilodase® (hialuronidase 50 UTR/g + lidocaína 50 mg/g + sulfato de neomicina 5 mg/g); para otite média – Otoxilodase® (hialuronidase 100 UTR/mL + lidocaína 50 mg/mL + sulfato de neomicina 5 mg/mL); para a difusão de anestésicos e reabsorção de exsudatos – Hyalozima® (400 UTR/mL e 4000 UTR/mL) e para edemas locais, a Hyalozima creme® (1330 UTR/g) (Apsen Industrias Farmacêuticas, Bulas, 2013).

Por outro lado, hialuronidases têm sido relacionadas a diversos processos fisiológicos e patológicos como embriogênese, angiogênese, inflamação, cicatrização de feridas, patogênese microbiana e difusão sistêmica de toxinas de venenos. Portanto, a identificação e caracterização de inibidores de hialuronidases pode ser útil para o desenvolvimento, por exemplo, de contraceptivos, agentes antitumorais,

antimicrobianos e antivenenos. (MIO e STERN, 2002; KHANUM et al., 2005; GIRISH e KEMPARAJU, 2005a,b; ISOYAMA et al., 2006; MACHIAH et al., 2006). Um trabalho realizado com veneno de serpente demonstrou que a inibição da hialuronidase em venenos pode aumentar a eficiência da terapia, retardando a difusão das toxinas e atenuando os efeitos adversos da terapia, pois uma menor dose de medicamentos seria necessária (GIRISH e KEMPARAJU, 2011).

3.6 OTIMIZAÇÃO DE EXPRESSÃO HETERÓLOGA DE PROTEÍNAS RECOMBINANTES EM *E.coli* E REDOBRAMENTO PROTEICO *in vitro*

É consenso na literatura que a produção de proteínas recombinantes é uma técnica fundamental na pesquisa e na biotecnologia. Porém, também se sabe que a obtenção de proteínas recombinantes solúveis e ativas não é uma tarefa fácil (BURGESS et al., 2009; BUCHFINK et al., 2010; YAMAGUCHI et al., 2010). Quando proteínas eucarióticas são expressas de maneira heteróloga em modelo procarioto, em sua grande maioria se encontram insolúveis, formando corpos de inclusão no citoplasma bacteriano. Existe uma grande busca de métodos e estratégias para que se consiga a produção de proteínas recombinantes em sua forma biologicamente ativa (SINGH e PANDA, 2005; DECHAVANNE et al., 2011).

Alguns trabalhos sugerem um investimento de tempo na variação e escolha correta da cepa de expressão (SORENSEN e MORTENSEN, 2005; SAHDEV et al., 2008). Somado a isso, variáveis como, por exemplo, temperatura e quantidade de indutor podem modificar consideravelmente o perfil de solubilidade da proteína recombinante expressa (KUBE et al., 2006; SAHDEV et al., 2008). Outros trabalhos demonstram que para a solubilidade de proteínas recombinantes pode se trabalhar com estratégias de clonagem fusionando peptídeos ou proteínas que favoreçam o dobramento adequado da proteína de interesse durante a expressão (KRALICEC et al., 2011; DAS et al., 2011). As “etiquetas de fusão” mais comumente utilizadas para se aumentar a solubilidade de proteínas recombinantes são Tioredoxina (TX), Proteína de Ligação a Maltose (MBP), Glutationa S-Transferase (GST), SUMO (*Small Ubiqutin like MOdifier*) e NusA (*N-utilization substance* A) (WALLS e LOUGHRAN, 2011). Vários trabalhos demonstram a eficácia do SUMO em aumentar a solubilidade de proteínas

recombinantes em sistema de *E. coli* (ZUO et al., 2005; MARBLESTONE et al., 2006; BUTT et al., 2005). Quando a “etiqueta SUMO” foi fusionada a uma glicoproteína da superfície do vírus da raiva, por exemplo, a expressão dessa glicoproteína quase dobrou e a sua quantidade solúvel foi aproximadamente três vezes maior quando comparada à expressão da glicoproteína não fusionada (SINGH et al., 2012).

Uma estratégia bastante utilizada também quando a proteína recombinante é expressa em corpos de inclusão e não se quer utilizar modelos eucarióticos, é o redobramento *in vitro* – método conhecido como *refolding* (SINGH e PANDA, 2005; BRONDYK et al., 2009). Essa técnica consiste basicamente do isolamento da proteína de interesse dos corpos de inclusão, solubilização da mesma em tampão desnaturante e retirada do agente desnaturante de tal forma que a proteína consiga se dobrar de maneira correta. Existem diferentes métodos em que esse redobramento pode ser realizado: por diluição rápida, lenta, por diferença de pressão ou em coluna cromatográfica, entre outros. Porém, a parte considerada crucial dessa técnica é a escolha do tampão em que se faz o redobramento. Para a escolha desse se deve levar em consideração características bioquímicas e físico-químicas da proteína recombinante, afinal, para que uma proteína adquira a sua estrutura ativa, sua conformação de menor energia livre deve ser encontrada e essa deve estar sob pH, força iônica e temperatura adequados (IGNATOVA e GIERASCH, 2006; HOFINGER et al., 2007; BURGESS et al., 2009; BELD et al., 2010).

A solubilidade e atividade de algumas hialuronidases recombinantes foram obtidas por meio da técnica do redobramento *in vitro*. Por exemplo, para a hialuronidase de abelha, os corpos de inclusão purificados foram solubilizados em tampão de guanidina 5M pH 8,0 contendo DTT (ditiotreitol) 1 mM e posteriormente dialisados com água a 4°C (GMACHL e KREIL, 1983). Já para a atividade da hialuronidase do veneno de vespa foi utilizado um tampão de redobramento em pH 7,0 contendo glutationa dissulfeto (GSSG) 15 mM e EDTA 3 mM (SKOV et al., 2006). Com o objetivo de obter a atividade da hialuronidase humana (Hyal-1) usando os corpos de inclusão obtidos em expressão com *E. coli,* o tampão de redobramento padronizado conteve o sistema redox de glutationas (1:3 mM) e arginina 1M (HOFINGER et al., 2007). No entanto, é também relatado que algumas hialuronidases recombinantes não

obtiveram atividade após o redobramento *in vitro,* mas somente quando foram expressas em sistemas eucarióticos de expressão (NG et al., 2005; CLEMENT et al., 2012; KIRIAKE et al., 2014).

Para se estudar melhor o papel das hialuronidases do veneno de *Loxosceles* nos envenenamentos ocorridos após a picada com esses animais, o presente trabalho teve como intuito a obtenção de uma isoforma de hialuronidase recombinante do veneno de *L. intermedia* (DHAase) em sua forma ativa, para sua posterior caracterização. Para tal, DHAase foi expressa em diferentes cepas de *E.coli*. Nas expressões heterólogas foram variadas a quantidade de indutor e temperatura. A técnica do redobramento *in vitro* foi também utilizada e, com o uso de um tampão de redobramento contendo arginina 0,4 M; BSA 0,2 mg/mL e GSH e GSSG na proporção 10:1 pôde se alcançar a atividade de DHAase tanto *in vitro* quanto *in vivo* (FERRER et al., 2013).

4 OBJETIVO GERAL

Obtenção de uma isoforma de hialuronidase recombinante do veneno de *Loxosceles intermedia* em sua conformação bioativa, caracterização do seu perfil bioquímico e caracterização de seu papel no loxoscelismo.

4.1 OBJETIVOS ESPECÍFICOS

- Obter a expressão heteróloga em grande escala, purificação e conformação ativa de uma hialuronidase recombinante do veneno de *L. intermedia* (DHAase);

- Verificar se DHAase possui perfil bioquímico *in vitro* similar às hialuronidases nativas presentes no veneno de *L. intermedia*;

- Avaliar se anticorpos policlonais produzidos com a DHAase reconhecem as relacionadas enzimas nativas do veneno;

- Avaliar se a hialuronidase recombinante reproduz o espalhamento gravitacional desenvolvido na dermonecrose dos acidentes loxoscélicos em modelo animal, sendo assim, um contribuinte para a toxicidade do veneno.

5 MATERIAIS E MÉTODOS

5.1 REAGENTES

Os sais, ácidos, bases, solventes orgânicos foram adquiridos da Merck (Darmstadt, Alemanha). Os marcadores de massa molecular para SDS-PAGE, o BSA, o ágar-ágar, o Ponceau-S, o OPD, os anticorpos secundários utilizados nos ensaios de imunodetecção (*Western Blotting*) e o ácido hialurônico purificado foram adquiridos da Sigma (St. Louis, MI, EUA). As enzimas de restrição e modificação, o marcador de números de pares de bases “Gene Ruler 100 pb DNA Ladder Plus” e o IPTG foram adquiridos da empresa Fermentas (Vilnius, Lituânia). O BCIP, o NBT, o brometo de etídio e o kit miniprep Plus SV Wizard foram adquiridos da Promega (Madison, WI, EUA). Os reagentes Dodecil Sulfato de Sódio, corante Azul de Coomassie, Tris e Glicina foram adquiridos da GibcoBRL (Grand Island, NY, EUA). A agarose, as cepas bacterianas e a resina Ni- NTA agarose e os reagentes para RT-PCRs foram adquiridos da Invitrogen (Carlsbad, CA, EUA). Os antibióticos foram adquiridos da USB (Cleaveland, OH, EUA). Os oligonucleotídeos empregados em PCR foram sintetizados pela IDT (Coralville, IA, EUA). Os reagentes para meio de cultura, tais como peptona, extrato de levedura e triptona foram adquiridos da Himedia (Mumbai, Índia). Compramos o plasmídeo de expressão pET-14b da Novagen (Novagen , Madison, EUA) o kit pET-SUMO (Champion™ pET SUMO Expression System) da Life Technologies (Grand Island, NY, EUA). Os padrões de glicosaminoglicanos utilizados foram heparam sulfato de pâncreas bovino (Dietrich et al., 1983), condroitim sulfato de cartilagem bovina e dermatam sulfato de pele de porco (Seikagaku , Kogyo Co., Tóquio, Japão).

5.2 EXPRESSÃO HETERÓLOGA DE DHAase EM CEPAS *E. coli*

5.2.1 Expressão e avaliação da solubilidade da construção em pET-14b nas cepas BL21(DE3)pLyS e AD494(DE3)

A preparação plasmidial da construção DHAase/pET-14b foi transformada em cepa bacteriana de expressão *E. coli* BL21(DE3)pLysS quimiocompetentes e foram

plaqueadas em meio LB-ágar contendo ampicilina (100 µg/mL) e cloranfenicol (34 µg/mL).

Um teste piloto de expressão foi realizado para determinar o tempo ótimo de expressão e a concentração ideal do indutor IPTG (*Isopropyl-β-D-thiogalactopyranoside*). O protocolo foi extraído de Sambrook e Russel (2001) com algumas alterações.

Uma colônia isolada foi inoculada em 5 mL de meio LB contendo os antibióticos adequados à 37°C durante 16 h. Essa cultura foi inoculada em diluição 1:100 em 50 mL de meio LB acrescido dos antibióticos e o crescimento monitorado pela determinação da densidade óptica (D.O.) em 550 nm. Quando as culturas atingiram a D.O.(550nm) entre 0,4 e 0,6 foi adicionado o indutor IPTG em diferentes concentrações (0,05 mM; 0,1 mM; 0,2 mM; 0,4 mM) e coletadas amostras em diferentes tempos (0 h; 0,5 h; 1 h; 2 h; 3 h; 4 h e 5 h) de expressão à 30ºC. As amostras foram analisadas por eletroforese em gel SDS-PAGE 12,5% em condições redutoras (5% de β-mercaptoetanol).

As culturas foram centrifugadas (3.000xg, 10 minutos) e ressuspendidas em 8 mL de tampão de ligação nativo (fosfato sódico 50 mM pH 8.0, NaCl 500 mM, imidazol 10 mM e lisozima 1 mg/mL). A suspensão bacteriana foi congelada a -20 °C por 16 h e lisadas por prensa mecânica ou ultrasom. O sobrenadante do lisado foi também analisado nas mesmas condições de SDS-PAGE.

Outra cepa testada foi a *E. coli* AD494(DE3), a qual foi transforamada por eletroporação (1 µL da construção em pET-14b sob 1.8kV, 25MF, 200 Ω, Gene Pulser X-Cell® BioRad) e plaqueada em meio LB-ágar contendo ampicilina (100 µg/mL) e kanamicina (15 µg/mL). O teste piloto de expressão foi realizado em iguais condições ao descrito para BL21(DE3)pLysS.

Tendo padronizado a quantidade de tempo de expressão e concentração do indutor, foi realizada a variação da temperatura da expressão. Para BL21(DE3)pLysS e AD494(DE3) foram utilizadas adicionalmente as temperaturas de 22ºC e 16ºC.

Para a cepa AD494(DE3) a expressão em maior escala foi também realizada. A expressão foi de maneira semelhante aos testes pilotos, proporcionalmente a 1 L de meio de cultura na concentração e tempo padronizados.

5.2.2 Subclonagem em vetor de expressão pET-SUMO

Para a subclonagem do cDNA correspondente à DHAase madura em pET-SUMO, as reações de PCR de alta fidelidade foram feitas utilizando *Pfu* DNA polimerase e como molde um clone em pGEM-T contendo a sequência completa da enzima. Como o plasmídeo pET-SUMO é um plasmídeo A-T, os oligonucleotídeos foram desenhados sem sítios de restrição. Como sense sintetizamos 5´- TTC GAC GTC TTC TGG AAC GTG C – 3´; como antisense: 5´- TCA CTT TGT TTT CTG CTC ACA GTA TC – 3´. Os produtos de PCR com *Pfu* DNA polimerase foram analisados em gel de agarose 1,5% preparado em tampão TAE contendo brometo de etídio 0,5 µg/mL e purificados com Ilustra GFX PCR DNA kit (GE Healthcare, Pittsburgh, PA, EUA). Os produtos de PCR purificados foram submetidos à adenilação da porção 3' com *Taq* DNA polimerase. Para tanto, as reações foram preparadas com tampão para *Taq* DNA polimerase (1 X); dATP (0,2 mM); $MgCl_2$ (1,5 mM); produto de PCR de interesse (volume total do PCR anterior) e *Taq* DNA polimerase (1,25 U/ 50 µL). Essa mistura foi colocada em termociclador a 72°C por 15 minutos. Esses produtos adenilados foram utilizados para ligação em pET-SUMO. A reação de ligação foi realizada com T4 DNA ligase na proporção 3:1 (inserto/50 ng de vetor) a 16°C por 16 h em volume de 10 µL. O produto da ligação (2 µL) foi transformado em *E. coli* MachI quimicamente competentes. A mistura foi mantida em gelo por 30 minutos e foi submetida a choque térmico por 90 segundos a 42°C e novamente em gelo por 2 minutos. Ao tubo foram adicionados 250 µL de meio SOC (Triptona 20 g/L, extrato de levedura 5 g/L; NaCl 0,5 g/L; KCl 2,5 mM; $MgCl_2$ 10 mM; $MgSO_4$ 10mM e glicose 0,2 M) e mantidos sob agitação por 1 h a 37°C para recuperação. As bactérias recuperadas foram plaqueadas em meio LB-ágar suplementado com kanamicina (50 µg/mL). O plaqueamento foi feito com auxílio de alça de Gauss estéril em duas placas, sendo que em uma delas foi plaqueado 100 µL da cultura de bactérias em meio SOC e a outra recebeu os 200 µL restantes. As placas foram incubadas a 37°C por 16 h em estufa BOD.

Para identificar os clones contendo o inserto orientado corretamente, realizou-se PCR de colônia com o *sense* utilizado para a clonagem e um oligonucleotídeo do vetor, *T7 reverse*. Nos microtubos de PCR contendo as bactérias foram adicionados tampão

para *Taq* DNA polimerase (1 X); dNTPs (0,2 mM); $MgCl_2$ (1,5 mM); oligonucleotídeo do inserto (0,2 µM); oligonucleotídeo *T7 reverse* (0,2 µM) e *Taq* DNA polimerase (1,25 U/ 50µL). Essa mistura foi colocada em termociclador e submetida aos seguintes ciclos: 1 ciclo a 95°C/5min; 35 ciclos a 95°C/30s – 58°C/30s – 72°C/1min; 1 ciclo a 72°C/10 min e um ciclo de espera a 4°C/∞. O produto foi analisado em gel de agarose 1,5% com brometo de etídio. Três clones positivos foram submetidos à extração por minipreparação com reagentes do *kit Wizard Plus SV Minipreps DNA purification Systems* (Promega) e as construções corretas foram confirmadas por sequenciamento de ambas as fitas, utilizando os iniciadores *T7 promoter* e *T7 reverse* com reagente *BigDye® Terminator v3.1 Cycle Sequencing Kit* (Life Technologies, Foster, CA, EUA). Foi utilizado o sequenciador automático *Genetic Analyser 3500* (Applied Biosystems TM, Foster, CA, EUA). Um desses plasmídeos, o qual continha a sequência confirmada pelo sequenciamento, foi utilizado (100 ng em 1µL) para a transformação de *E. coli* SHuffle por eletroporação sob as mesmas condições descritas anteriormente.

5.2.3 Expressão e avaliação da construção realizada em pET-SUMO em cepa SHuffle T7 Express pLYS Y

O teste de mini-expressão da hialuronidase recombinante para essa cepa foi realizado semelhante ao descrito no item 5.2.1. A diferença é que apenas a temperatura de 30°C foi utilizada para a expressão desse ensaio piloto.

5.3 SUPEREXPRESSÃO DE DHAase EM *E.coli* BL21(DE3)pLysS

A construção do cDNA correspondente à DHAase madura em pET-14b foi expressa como uma proteína fusionada a uma cauda 6x-His N-terminal. A cepa de expressão escolhida para a obtenção de grande quantidade de hialuronidase recombinante, mesmo que insolúvel, foi a *E. coli* BL21(DE3)pLysS. A cepa foi transformada com a referida construção e semeada em LB-ágar com 100 µg/mL ampicilina e 34 µg/ml cloranfenicol. Uma colônia escolhida ao acaso foi inoculada em meio LB (100 µg/mL ampicilina e 34 µg/mL cloranfenicol) e cultivada por 16 h a 37ºC. Essas culturas foram diluídas a 1:100 em 1 L de meio LB/ampicilina/cloranfenicol e

incubadas a 37ºC até que a $D.O._{550\ nm}$ = 0,4-0,6. A expressão da proteína recombinante foi induzida pela adição de 0,1 mM de IPTG e as células foram incubadas durante 3,5 h a 30ºC sob agitação. As células foram recolhidas por centrifugação (4.000xg, 7 minutos, 4 ºC), ressuspensas em 20 mL de tampão de ligação desnaturante (uréia 8M, NaH_2P0_4 100 mM e Tris 10 mM pH 8,0) ou tampão de ligação nativo (fosfato de sódio 50 mM pH 8,0, NaCl 500 mM, imidazol 10 mM, lisozima 1 mg/mL) e congelado a -20 ºC por pelo menos 16 h.

5.3.1 Purificação em condições desnaturantes por cromatografia de afinidade

As células bacterianas ressuspensas em tampão de ligação nativo (o mesmo descrito no intem anterior) foram submetidas à um disruptor de células de ultrassom (potência de 500-W) utilizando 4 ciclos com intensidade máxima durante 30 segundos. O extrato bacteriano obtido foi clareado por centrifugação (9.000xg por 20 minutos) e o sedimento ressuspendido em tampão de ligação desnaturante (descrito anteriormente). Essa solução foi submetida à cromatografia de afinidade a metal imobilizado (IMAC). As proteínas contendo a etiqueta de 6x-His ligariam preferencialmente à fase estacionária Ni-NTA (Invitrogen) através da coordenação ao cátion Ni^{2+} imobilizado. A resina foi transferida a uma coluna e lavada com tampão de lavagem desnaturante (Ureia 8M, NaH_2P0_4 100 mM e Tris 10 mM pH 6,0), para que proteínas fracamente ligadas por possuírem histidinas sequenciais se desligassem da coluna e diminuíssem a contaminação da proteína de interesse. As proteínas foram então eluídas com tampão desnaturante (Ureia 8M, NaH_2P0_4 100 mM e Tris 10 mM pH 4,0) e frações coletadas foram analisadas por SDS-PAGE. Alternativamente, a eluição foi também realizada mantendo todos os tampões em pH 8,0 e fazendo um gradiente de imidazol (10 mM para o tampão de ligação, 20 mM para o tampão de lavagem e 250 mM para o tampão de eluição).

Para analisar se o pH do tampão de ligação desnaturante influenciava na ligação da hialuronidase a resina, 1 mL desse tampão teve o seu pH modificado de 8 para 7; 9; 10; 11 ou 12 e esses foram submetidos à cromatografia de afinidade em microtubos utilizando 100 µL de resina Ni-NTA. Após centrifugação (3.000xg por 3 minutos) a

resina foi sedimentada e o que permaneceu no sobrenadante (ou seja, não ligou na resina) foi analisado por SDS-PAGE.

5.3.2 Purificação em condições desnaturantes por eletroeluição

Um método alternativo para a obtenção da DHAase desnaturada foi o da eletroeluição. A fração insolúvel da superexpressão solubilizada em tampão de ligação desnaturante (Uréia 8M, pH 8,0) foi diluída em tampão de amostra e aplicada em gel SDS-PAGE preparativo. Após a corrida, o gel foi precipitado com KCl 100 mM gelado e a banda referente à proteína de interesse foi removida com bisturi sobre um fundo escuro. Para retirar a proteína desejada da matriz do gel de acrilamida foi utilizado o processo de eletroeluição. A banda foi levemente fragmentada e colocada em uma membrana de diálise com poro de 12-14 kDa (Sigma-Aldrich) com 2 mL de tampão de corrida para SDS-PAGE. As membranas com as extremidades seladas foram colocadas dentro de uma cuba eletroforética contendo o mesmo tampão de corrida e submetidas a uma corrente de 50 mA por 2 h. Após esse período, o tampão de corrida presente dentro da membrana foi coletado e a concentração de proteína foi dosada por espectrofotometria em comprimento de onda de 280 nm. Esse último passo da eletroeluição foi repetido mais duas vezes, pois ainda se recuperou proteína. O protocolo foi adaptado a partir de Bongertz (1989).

5.3.3 Padronização do tampão de redobramento em microplaca

Para o teste das melhores condições de redobramento *in vitro* de DHAase, utilizamos em microplaca tampões Tris-HCl 100 mM em pH 8, 9, ou 10. Nesses tampões foram utilizadas diferentes proporções de DTT (0,1 mM; 0,5 mM e 1,0 mM); glutationas reduzida e dissulfeto (10:1, 1:1 e 1:10) e glicerol (5, 7 e 10%). No teste de redobramento foi utilizada a proteína purificada por eletroeluição e dos corpos de inclusão após lavagens (processo detalhado no item 5.3.4). As enzimas desnaturadas foram solubilizadas em Tris 100 mM pH 10,0 contendo Ureia 8 M e a concentração proteica ajustada para 5 mg/mL. Os diferentes tampões de redobramento em teste foram preparados e 190 µL de cada um foram pipetados em seus respectivos poços.

Depois foi adicionado 10 µL de DHAase em tampão uréia (foi realizado em triplicada cada condição) e homogeneizado. As placas foram mantidas à temperatura ambiente por 120 minutos e a absorbância foi lida em leitor de microplaca em 320 nm (TECAN, Mönnedorf, Zurique, Suíça). A leitura obtida de cada variável foi descontada de 0,2, que é a absorbância referente aos poços vazios. As menores absorbâncias correspondem aos tampões em que a solubilidade da proteína de interesse foi atingida, uma vez que a absorbância, nesse teste, indica a presença de agregados proteicos (Burgess, 2009). As três condições com as absorbâncias mais baixas foram utilizadas para o redobramento em maior escala e posteriormente para teste de atividade por turbidimetria (descrito no item 5.7.1).

5.3.4 Redobramento *in vitro* de DHAase

A cultura bacteriana congelada em tampão de lise nativo foi descongelada e lisada com 8 ciclos de ultrassom com intensidade média durante 20 segundos usando um sonicador 500-W. O material lisado foi centrifugado (20.000xg, 30 minutos, 4 ºC), e o sedimento foi lavado com tampão desnaturante (Tris-HCl 100 mM pH 10,0, ureia 2 M, Triton X-100 1%) e sonicado três vezes em baixa intensidade. Após centrifugação a 6.000xg durante 10 minutos o precipitado resultante foi solubilizado em Tris-HCl 100 mM pH 10,0 com ureia 8 M e DTT 50 mM. A solução contendo a proteína recombinante desnaturada e reduzida foi ajustada a uma concentração de 5 mg/mL (por dosagem em UV) e adicionada gota a gota ao tampão de redobramento (Tris-HCl 100 mM pH10, GSH 3 mM, GSSG 0,3 mM, L-arginina 0,4 M, BSA 0,2 mg/mL) por agitação durante 16 h a 4ºC. O protocolo utilizado foi baseado nos artigos de Burgess e Hofinger e colaboradores (BURGESS, 2009; HOFINGER et al., 2007). A diálise foi realizada com PBS e a hialuronidase solúvel foi concentrada por centrifugação (4.500xg) utilizando filtros com poros de 30 kDa (Millipore, Schwalbach, Alemanha) pelo tempo necessário para se obter a concentração proteica desejada.

5.4 ELETROFORESE EM GEL DESNATURANTE DE POLIACRILAMIDA (SDS-PAGE)

Eletroforeses de proteínas foram realizadas em géis de poliacrilamida com SDS (dodecil sulfato de sódio) em condições redutoras (5% β-mercaptoetanol). A corrida eletroforética foi realizada com amperagem constante de 25 mA. Para a detecção das proteínas, os géis foram corados com Azul Brilhante de Coomassie 0,02% (p/v) dissolvido em metanol 50% (v/v), ácido acético 10% (v/v) e água deionizada quantidade suficiente para completar 100% (v/v).

5.5 IMUNIZAÇÕES EM COELHOS

Foram utilizados coelhos adultos neo-zelandeses (~3 kg) para as imunizações com DHAase. Os coelhos foram mantidos sob os cuidados do Biotério da Pontíficia Universidade Católica do Paraná. Todos os procedimentos utilizados estavam de acordo com a Lei Federal Brasileira, seguindo as regras da Comissão de Ética de Uso de Animais da Universidade Federal do Paraná (CEUA/BIO-UFPR), certificado de aprovação 353 (em anexo). O protocolo seguido foi baseado em Harlow e Lane (1998) com algumas modificações. Foram feitas 4 imunizações com intervalos de 21 dias, utilizando adjuvante completo de Freund (Sigma) na primeira aplicação e nos reforços adjuvante incompleto de Freund (Sigma), ambos na proporção 1 toxina:1 adjuvante (v/v). A emulsão que foi injetada nos animais continha 100 µg de DHAase insolúvel (diluído em PBS para volume final de 300 µL). Após a formação da emulsão, o volume final foi distribuído em três pontos de aplicação, sendo dois intramusculares e um subcutâneo.

Para a obtenção do soro pré-imune e do soro hiperimune a coleta de sangue foi feita por punção venosa da veia auricular. Os coelhos foram anestesiados com cetamina (180 a 240 mg/kg do animal) e xilazina (24 a 45 mg/kg do animal) antes do procedimento. A coleta do soro pré-imune foi feita 7 dias antes das imunizações e para o soro hiperimune foi feita a coleta 10-12 dias após a quarta imunização, sendo coletado 15 mL de sangue de cada coelho. A retração do coágulo das amostras de sangue coletados, foi feita à 4°C por 16 h, o material foi centrifugado a 3.000xg por 5 minutos e o soro contido no sobrenadante foi armazenado em alíquotas de 500 µL em freezer -20°C.

5.6 ENSAIOS DE IMUNODETECÇÃO (“WESTERN BLOTTING”)

As amostras foram submetidas à corrida eletroforética (SDS-PAGE) e as proteínas foram transferidas para membrana de nitrocelulose por 2 h à voltagem constante de 100 V. Em seguida as membranas foram bloqueadas por 1 h com leite desnatado em pó (3% p/v) diluído em PBS e incubadas por 2 h à temperatura ambiente sob constante agitação com soro hiperimune anti-DHAase ou anti-veneno de *L.intermedia* (diluído na mesma solução de bloqueio) ou com IgG anti-6xHis (Qiagen). As membranas foram lavadas com o mesmo tampão na ausência de anticorpo e incubadas com anticorpos secundários anti-IgG de coelho ou anti-IgG de camundongo conjugados com fosfatase alcalina (Sigma) por 1 h à temperatura ambiente. Após lavagens, a reação foi revelada com o substrato BCIP e o cromógeno NBT (Promega) em tampão ótimo para atividade de fosfatase alcalina (Tris-HCl 100 mM pH 9,5; NaCl 100 mM e $MgCl_2$ 5 mM).

5.7 ESPECIFICIDADE DA ATIVIDADE DE DHAase SOBRE GLICOSAMINOGLICANOS

5.7.1 Ensaio de Turbidimetria

A atividade da enzima recombinante solúvel inicialmente foi testada por turbidimetria. O ensaio descrito por Poh e colaboradores (1992) foi utilizado com algumas modificações. Cinquenta microgramas de HA foi incubado na proporção 1:1 com DHAase ou veneno de *L. intermedia* a 37°C por 16 h. Como controle negativo foi utilizado o HA em PBS sob as mesmas condições. Após o tempo de incubação o HA não degradado (volume final de reação de 0,5 mL) foi precipitado com 1 mL de cetavlon 2,5% (brometo de N-cetil–N,N,N-trimetil amônio) em NaOH 2%. A absorbância de cada reação foi obtida em espectrofotômetro com o comprimento de onda de 400 nm. A absorbância do PBS com o cetavlon (branco) foi descontada dos valores obtidos. A cada novo redobramento *in vitro* realizado, o teste de turbidimetria foi feito para a confirmação da atividade daquele lote antes de se prosseguir com outros ensaios.

5.7.2 Géis de agarose

O método de microeletroforese em gel de agarose, modificado por Dietrich e Dietrich (1976) baseia-se no uso de lâminas de gel de agarose (0,55%) submetidas a uma corrida eletroforética em caixa refrigerada sob uma voltagem constante de 100 V. Ácido hialurônico purificado (15 µg) foi incubado com o veneno total ou hialuronidase recombinante em uma razão de 1:1 durante 3, 6 e 16 h a 37°C. A degradação foi analisada por eletroforese em gel de agarose em tampão Tris-acetato 50 mM pH 8,0. Para avaliação da atividade de glicosidase sobre C4S, dermatam sulfato (DS) e heparam sulfato (HS), a eletroforese foi realizada em 50 mM de acetato 1,3-diaminopropano pH 9,0 (Aldrich, Milwaukee, EUA). Condroitim sulfato, DS e HS (5 µg) foram incubados com veneno ou DHAase nas proporções 1:1 durante 16 h a 37°C.

Após a eletroforese, os compostos foram precipitados no gel utilizando 0,1% de Cetavlon durante 2 h à temperatura ambiente. Os géis foram secos e corados com Azul de Toluidina 0,1% em ácido acético 1% e etanol 50% (DIETRICH e DIETRICH, 1976; DA SILVEIRA et al., 2007). Os glicosaminoglicanos utilizados como padrão da corrida estão descritos nos reagentes.

5.7.3 Zimogramas

Cinco microgramas de hialuronidase recombinante de *L.intermedia* foi submetida à zimografia em SDS-PAGE 10% co-polimerizado com 0,17 mg/mL de ácido HA ou 0,34 mg/mL de C4S. A amostra em estudo, diluída em tampão Laemmli, em condições não redutora, foi submetida à eletroforese (15 mA) a 4ºC. Após a migração eletroforética, os géis foram incubados 3 vezes em Triton X-100 (Reagen, RJ, BR) 2,5% por 20 minutos cada e em seguida incubados a 37ºC em tampão ótimo para a atividade enzimática (Tris-HCl 50 mM pH 7,4; NaCl 200 mM) durante 16 h e o gel foi corado com Azul de Alcian e co-corado com Azul de Coomassie.

5.8 ENSAIO DE DERMONECROSE

Para avaliar o efeito de DHAase no espalhamento gravitacional, 10 µg da toxina recombinante dermonecrótica (LiRecDT1) diluída em PBS foram injetados por via intradérmica em uma área de pele depilada de coelhos com ou sem a hialuronidase recombinante. Com a mesma finalidade 10 µg de DHAase sozinha (diluída em PBS; 0,2 mg/mL BSA), também foram injetados. Utilizamos dois controles negativos: PBS-BSA 0,2 mg/mL, para assegurar que o BSA utilizado para redobrar a hialuronidase recombinante por si só não induziria alterações; e outro controle, uma toxina recombinante com massa molecular similar à hialuronidase (LALP 1, DA SILVEIRA et al., 2007c) e purificada sob as mesmas condições, porém sem atividade sobre glicosaminoglicanos. O uso desse controle nos garantiria que potenciais contaminantes bacterianos não teriam influência nos resultados. O veneno e a toxina dermonecrótica foram usados como controles positivos. Os coelhos foram escolhidos para esses experimentos porque reproduzem lesões dermonecróticas próximas às observadas nos acidentes com humanos (CHAIM et al., 2011b). Esse experimento foi repetido com 4 animais e o desenvolvimento da necrose experimental foi observado em 3 h, 6 h e 24 h após as injeções. Os procedimentos utilizados foram aprovados pela Comissão de Ética de Uso de Animais da Universidade Federal do Paraná (CEUA/BIO-UFPR), certificado 353 (anexo).

5.9 HISTOLOGIA PARA MICROSCOPIA DE LUZ

Amostras da pele dos animais que receberam os controles e as toxinas recombinantes foram coletadas após anestesia com cetamina (Agribands, Campinas, Brasil) e acepromazina (Univet, São Paulo, Brasil). Estas amostras de tecido foram fixadas em “Alfac” (etanol 85%, formaldeído 10%, ácido acético glacial 5%) durante 16 h à temperatura ambiente. Após a fixação, as amostras foram desidratadas numa série gradual de etanol antes de serem parafinizadas (por 2 h a 58ºC). Secções de 4 µm de espessura foram processadas para lâminas histológicas e coradas com Tricrômio de Masson (CHAIM et al., 2011a).

6 RESULTADOS

Tendo por objetivo a expressão de uma isoforma de hialuronidase do veneno de *L. intermedia* na sua conformação ativa e em quantidade suficiente para sua avaliação bioquímica e biológica, iniciamos o presente trabalho com expressões heterólogas em diferentes cepas de *E.coli*. Foi utilizado também o método de redobramento *in vitro*.

6.1 EXPRESSÃO E SOLUBILIDADE DA CONSTRUÇÃO DHAase/pET-14b EM *E. coli* BL21(DE3)PLYS*S* E *E. coli* AD494(DE3).

Trabalho anterior do grupo obteve por técnicas de biologia molecular a sequência completa de uma isoforma de hialuronidase de *L.intermedia*, bem como, a subclonagem dessa enzima em vetor de expressão pET-14b (FERRER, 2010). O teste de expressão foi realizado primeiramente em cepa *E. coli* BL21(DE3)pLysS em diferentes concentrações do indutor, conforme demonstrado na Figura 9.

Como pode ser observado nessa figura, foi obtida uma expressão significativa da enzima recombinante a partir de 2 h nas concentrações testes de 0,1; 0,2 e 0,4 mM de indutor. A expressão com 1,0 mM de IPTG teve perfil similar ao obtido nas outras três concentrações (dado não demonstrado).

Tendo a hialuronidase expressa de forma recombinante, foi-se então verificar a solubilidade da mesma no sistema procariótico escolhido. Uma vez na concentração de 0,1 mM ter-se obtido uma massa considerável de proteína, visando a solubilidade, testou-se uma concentração menor de IPTG (0,05mM) e o tempo de expressão estabelecido foi de 3 h e meia.

O resultado da mini-expressão com 0,05 mM de IPTG após 3 h e meia, bem como, a verificação da solubilidade de DHAase nessas condições pode ser visualizado na Figura 10. Como se pode observar na coluna 3 dessa figura, a hialuronidase recombinante foi expressa de forma insolúvel. Mesmo realizando expressões em temperaturas mais baixas (22°C e 16°C), os resultados não foram diferentes (dados não demonstrados).

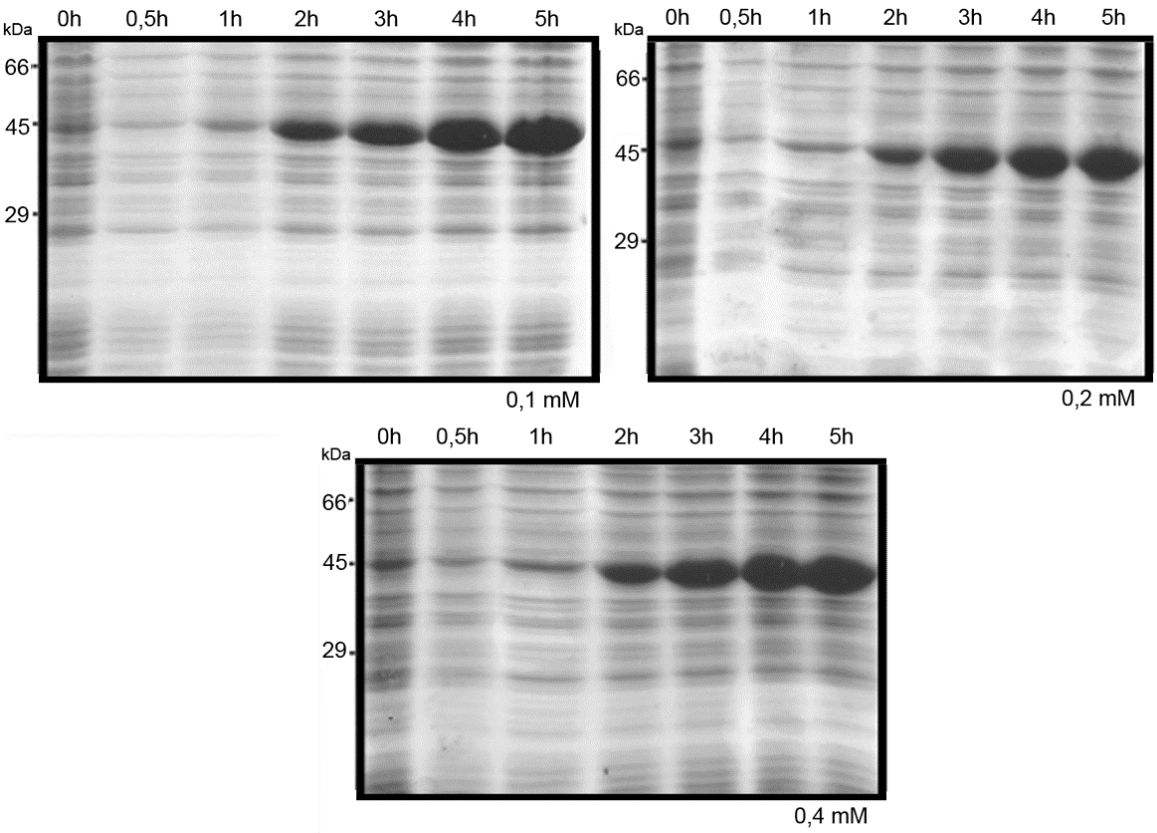

FIGURA 9**:** TESTE DE INDUÇÃO PARA EXPRESSÃO DE DHAase EM BL21(DE3)pLysS. A proteína foi expressa a 30 °C, em diferentes concentrações de IPTG (0,1; 0,2 e 0,4 mM) e tempos (0; 0,5; 1; 2; 3; 4 e 5 horas). A análise foi realizada por SDS-PAGE 12,5%. Em cada gel estão indicadas as massas moleculares, os tempos utilizados e a concentração de IPTG.

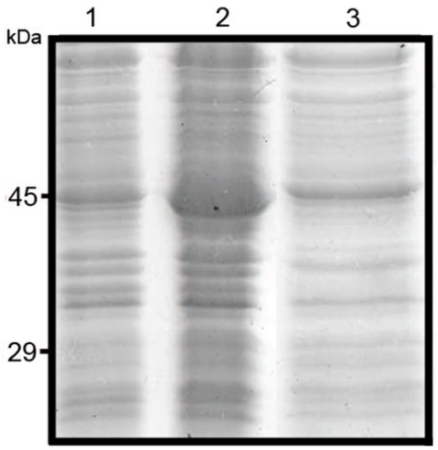

FIGURA 10**:** TESTE DE EXPRESSÃO E SOLUBILIDADE DE DHAase EM BL21(DE3) pLysS COM 0,05 mM DE IPTG. A proteína foi expressa a 30 °C por 3,5 h na concentração de 0,05 mM de indutor. A expressão foi analisada em SDS-PAGE 12,5%. Em 1 tem-se uma alíquota representativa da cultura antes da indução, em 2, três horas e meia depois da indução e em 3, o sobrenadante da cultura após a lise da cultura por prensa mecânica.

Visto a sequência de DHAase conter possíveis pontes dissulfeto, a alternativa escolhida para se obter a solubilidade dessa enzima foi a expressão da construção DHAase/pET-14b em um sistema bacteriano que possui um ambiente citosólico menos redutor, a cepa *E. coli* AD494(DE3). O resultado das mini-expressões em diferentes concentrações de indutor está demonstrado na Figura 11.

Como pode ser visualizado nos diferentes géis apresentados nessa figura, a hialuronidase recombinante foi expressa em todas as concentrações testes (0,05 mM - 0,4 mM) na cepa AD494(DE3), porém visualmente em uma menor quantidade que em BL21(DE3)pLysS. Foi-se então verificar a solubilidade da enzima recombinante nesse novo sistema de expressão.

Devido a uma alta concentração de proteínas na região de 45 kDa no SDS-PAGE, foi feito um *western-blotting* com anticorpos que reconhecem a cauda de histidina, para a confirmação de que a banda que se acreditava ser correspondente à enzima recombinante se encontrava realmente entre as proteínas solúveis.

Conforme demonstrado na Figura 12, com a cultura de AD494(DE3) induzida a 30ºC com 0,05 mM de IPTG, uma fração da proteína foi expressa em sua forma solúvel.

Dessa forma, a expressão em maior escala (1 L) utilizando a cepa AD494(DE3) foi realizada com 0,05 mM de IPTG a 30ºC por 4 h. Porém, o resultado obtido em mini-escala não foi reproduzido após várias tentativas. A proteína recombinante encontrava-se insolúvel. A temperatura de expressão foi reduzida para 22ºC e 16ºC por mais tempo na tentativa de se alcançar a solubilidade, porém, sem resultados favoráveis (dados não demonstrados).

6.2 EXPRESSÃO E SOLUBILIDADE DA CONSTRUÇÃO DHAase/pET-SUMO EM CEPA *E. coli* SHuffle.

Devido a tentativa de solubilidade da DHAase não ter tido sucesso em cepas de expressão compatíveis com pET-14b, tentou-se então a subclonagem dessa enzima em um plasmídeo que possui a estratégia de “etiqueta de solubilidade” (pET-SUMO).

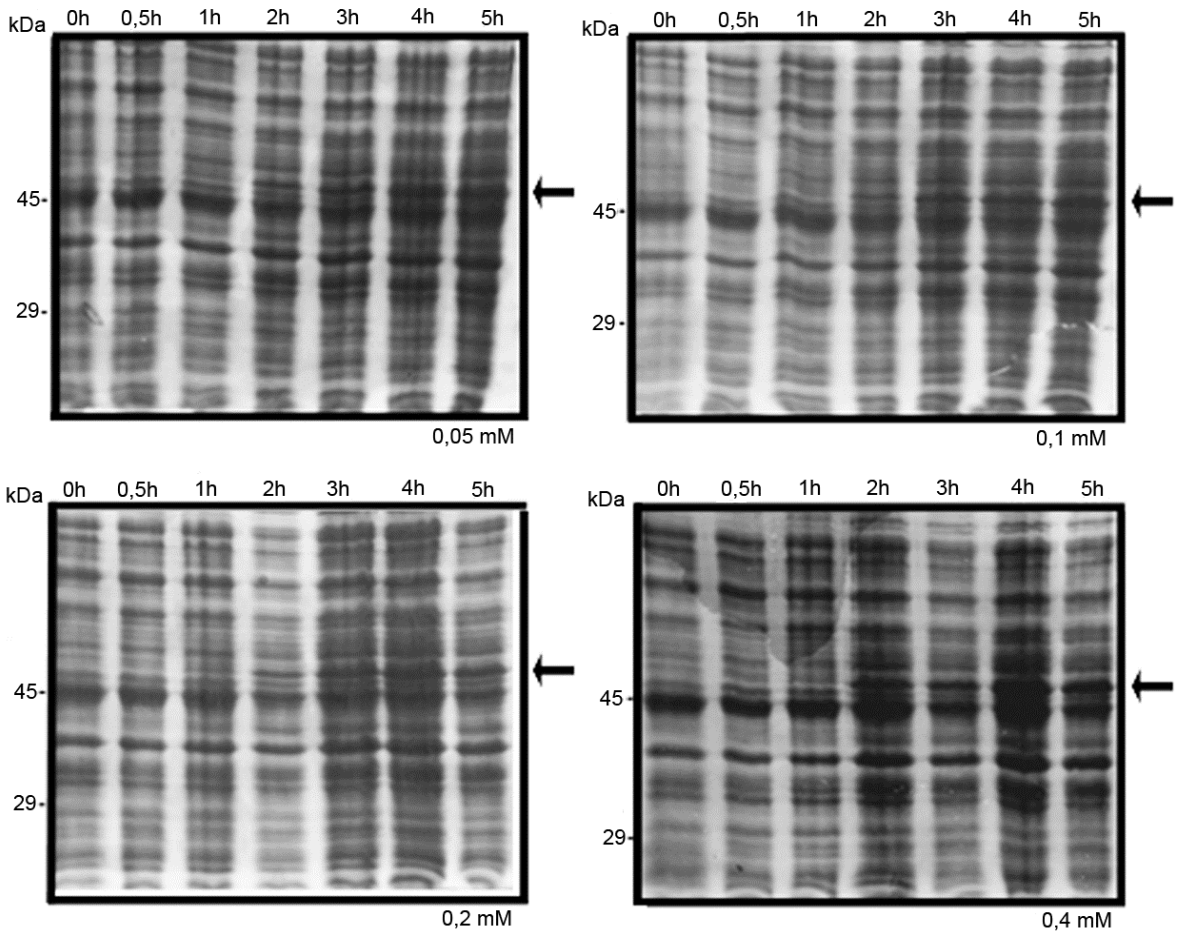

FIGURA 11: TESTE DE EXPRESSÃO DE DHAase EM AD494(DE3). A proteína foi expressa a 30 °C, em diferentes concentrações de IPTG (0,05; 0,1; 0,2 e 0,4 mM) e tempos (0; 0,5; 1; 2; 3; 4 e 5 horas). A análise foi realizada por SDS-PAGE 12,5%. Em cada gel estão indicadas as massas moleculares, os tempos e a concentração de IPTG. Na seta a altura correspondente à hialuronidase recombinante.

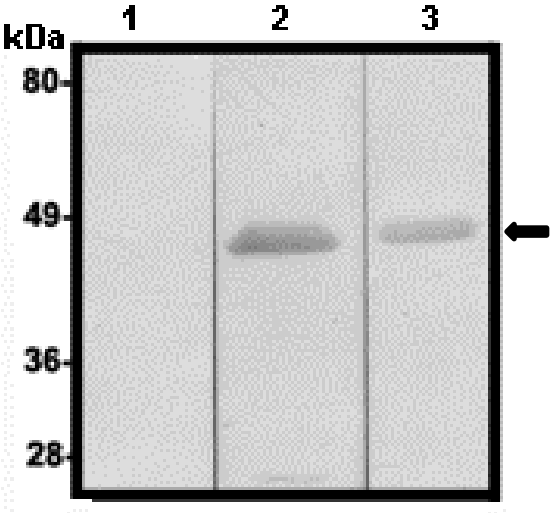

FIGURA 12: TESTE DE SOLUBILIDADE DE DHAase EM AD494(DE3) UTILIZANDO 0,05 mM de IPTG. A proteína foi expressa a 30°C com 0,05 mM de IPTG por 5 horas. A cultura foi ressuspendida em tampão de ligação nativo e após sonicação o sobrenadante do lisado foi avaliado. *Western-blotting* realizado com anticorpo primário anti-6xHis. A revelação foi realizada por fosfatase alcalina. Em 1 tem-se amostra representativa da cultura no tempo antes da indução, em 2, cinco horas depois da indução e em 3 o sobrenadante do lisado. Na seta a indicação da proteína recombinante entre as proteínas solúveis bacterianas.

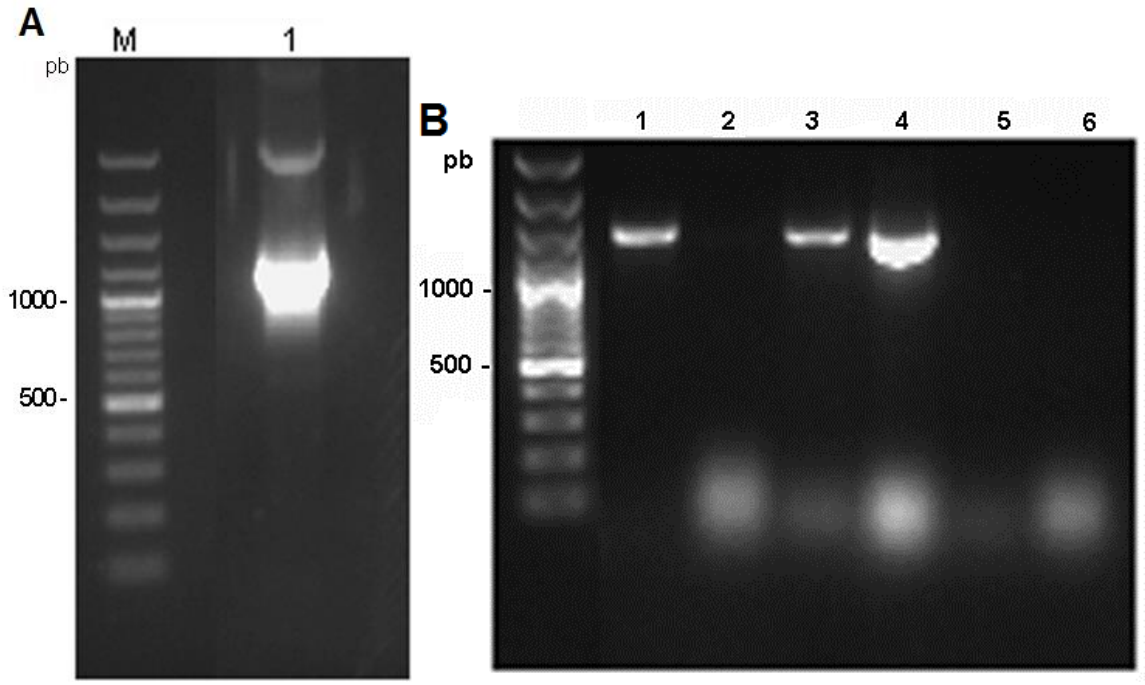

FIGURA 13: CLONAGEM DA DHAase EM pET-SUMO. Eletroforese em gel de agarose 1,5%. (A) inserto da DHAase com aproximadamente1200 pb. (B) PCR de colônia da construção DHAase/pET-SUMO em MachI, demonstrando insertos acimas de 1200 pb devido a etiqueta SUMO.

Como se pode observar na Figura 13A, com os primers sintetizados para DHAase compatíveis com o pET-SUMO, obteve-se quantidade suficiente de inserto específico para a ligação no plasmídeo. Após a ligação e transformação em cepa MachI, obtivemos clones positivos em fase de leitura, como demonstrado na Figura 13B, colunas 1, 3 e 4.

Os três clones positivos foram selecionados para sequenciamento. Foi confirmado por meio desse que nenhuma mutação havia ocorrido nas etapas de amplificação do inserto. Sendo assim, o clone 1 foi escolhido de maneira aleatória para transformação em cepa de expressão *E. coli* SHuffle.

Na Figura 14A, pode-se observar que a hialuronidase recombinante foi expressa em pET-SUMO (~54 kDa). Pode-se detectar visualmente sua expressão após 2 h tanto na expressão realizada com 0,05 mM de IPTG quanto na realizada com 0,1 mM do indutor.

Com a expressão utilizando pET-SUMO obteve-se a expressão de hialuronidase em todas as concentrações de indutor testadas, embora visualmente em menor

quantidade quando comparado com a expressão em BL21(DE3)pLysS. As expressões com 0,2 e 0,4 mM de IPTG (dado não demonstrado) tiveram perfil semelhante ao visto em 0,1 mM. Mesmo com a expressão de DHAase em um sistema que tem por objetivo aumentar a solubilidade (utilização da etiqueta SUMO e expressão em *E.coli* SHuffle), a hialuronidase foi expressa de forma insolúvel, como pode ser visualizado pela Figura 14B. Nas concentrações do indutor testadas não se observou uma banda na altura de DHAase/SUMO dentre as proteínas solúveis (coluna SND).

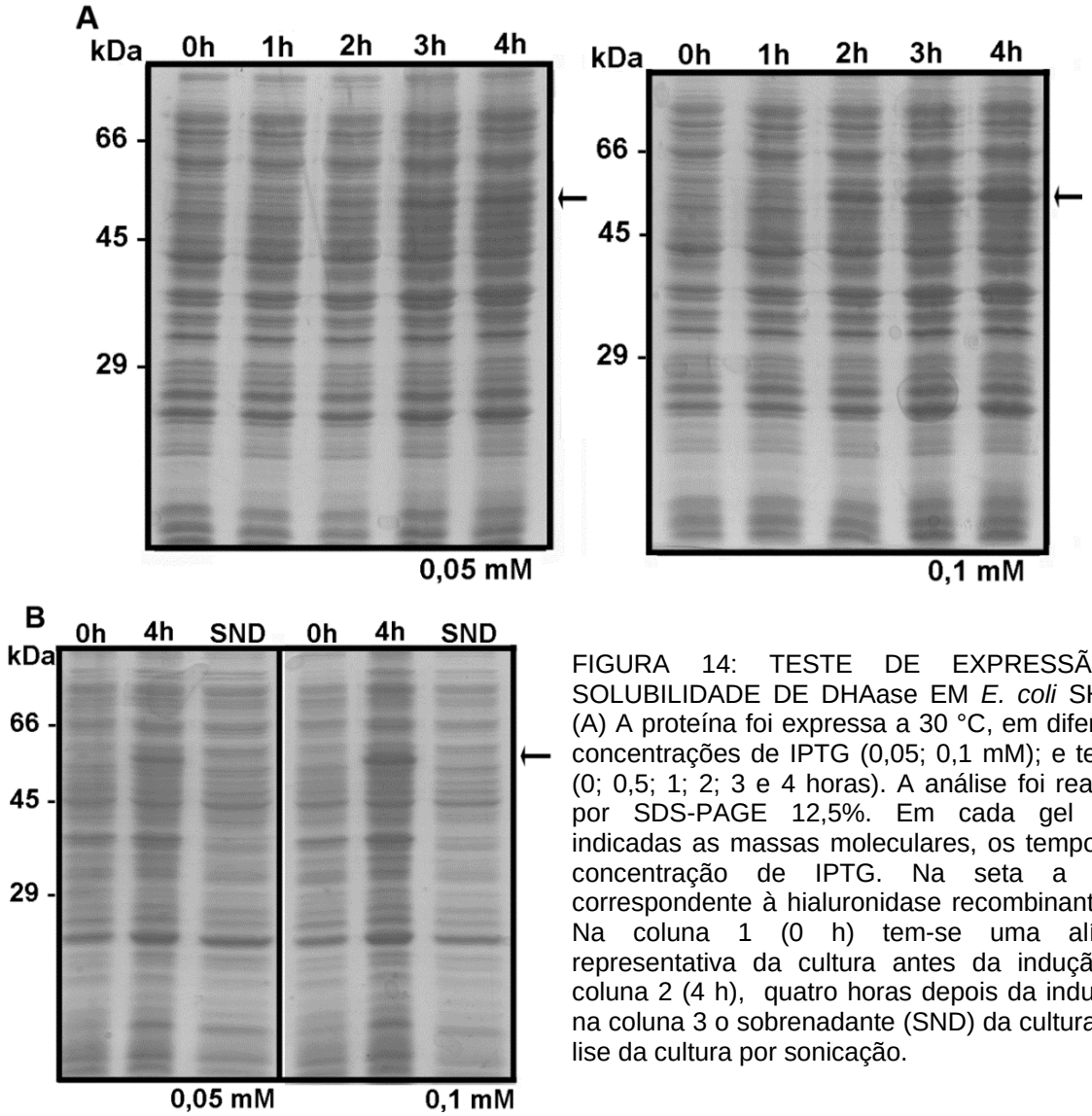

FIGURA 14: TESTE DE EXPRESSÃO E SOLUBILIDADE DE DHAase EM *E. coli* SHuffle. (A) A proteína foi expressa a 30 °C, em diferentes concentrações de IPTG (0,05; 0,1 mM); e tempos (0; 0,5; 1; 2; 3 e 4 horas). A análise foi realizada por SDS-PAGE 12,5%. Em cada gel estão indicadas as massas moleculares, os tempos e a concentração de IPTG. Na seta a altura correspondente à hialuronidase recombinante. (B) Na coluna 1 (0 h) tem-se uma alíquota representativa da cultura antes da indução, na coluna 2 (4 h), quatro horas depois da indução e na coluna 3 o sobrenadante (SND) da cultura após lise da cultura por sonicação.

Devido ao insucesso em se obter DHAase de forma solúvel e ativa, o foco do trabalho foi purificá-la desnaturada tanto para sua utilização como antígeno na produção de anticorpos em coelho, tanto para o processo de redobramento *in vitro*.

6.3 PURIFICAÇÃO EM CONDIÇÕES DESNATURANTES PARA PRODUÇÃO DE ANTICORPOS

Com o objetivo de produzir anticorpos policlonais que reconhecessem DHAase, a purificação da enzima foi realizada em condições desnaturantes utilizando cromatografia de afinidade em resina Ni-NTA agarose.

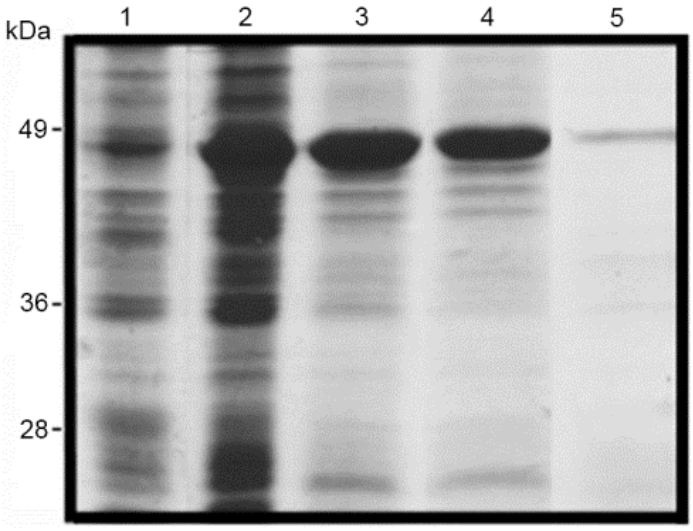

FIGURA 15: PURIFICAÇÃO DE DHAase EM CONDIÇÕES DESNATURANTES. Em 1 tem-se uma amostra representativa da cultura de BL21(DE3)pLysS antes da indução; em 2, depois de 5 h de indução a 30ºC com 0,1 mM de IPTG; em 3, o pellet ressuspendido com tampão de ligação desnaturante 8 M de uréia pH 8,0; em 4, amostra representativa do que não se ligou na resina Ni-NTA (*Void*); em 5, as proteínas purificadas com tampão de eluição desnaturante 8 M de uréia pH 4.0.

Como pode ser visualizado na Figura 15 (colunas 3 e 4) a ligação da proteína em resina Ni-NTA não foi eficiente mesmo em condições desnaturantes, pois o "pré-coluna" e o "*void"* possuem praticamente a mesma quantidade de proteína recombinante. Sendo assim, a quantidade de DHAase conseguida na purificação foi pequena, na escala de algumas centenas de microgramas (coluna 5).

Visto esse problema na ligação em condições desnaturantes, verificou-se que o pH do tampão de ligação desnaturante utilizado era o recomendado pelo manual. Buscou-se saber, então, se seria pela razão do pI (ponto isoelétrico, de valor de 8,75) da DHAase ser próximo ao valor do pH recomendado ao tampão, a dificuldade de ligação na resina. Para tal, foi realizado um teste de mini-purificação em diferentes pHs para o tampão de ligação.

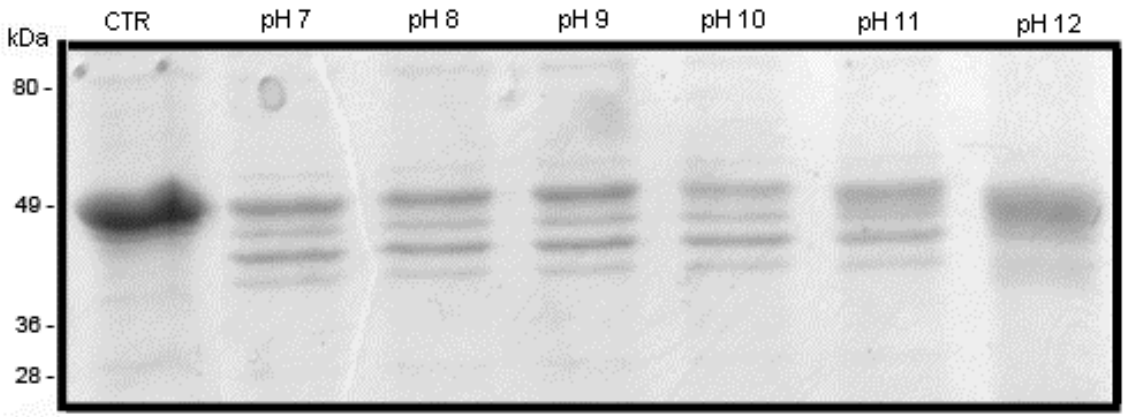

FIGURA 16: VARIAÇÃO NO pH DO TAMPÃO DE LIGAÇÃO DESNATURANTE EM PURIFICAÇÃO DE AFINIDADE. Determinada quantidade de DHAase (controle) foi submetida à ligação em 100 µL de resina Ni-NTA em diferentes pHs. As amostras foram centrifugadas à baixa rotação e os sobrenadantes (*void*) foram analisados por SDS-PAGE 12,5%. Na figura estão indicadas as massas moleculares à esquerda, e nas colunas o controle e o pH utilizado para cada amostra.

Como pode ser observado na Figura 16, tomando como base a quantidade inicial de proteína antes da incubação com a resina (controle), nos pHs de 7 a 10 houve a ligação de parte da proteína inicial, sendo a ligação mais eficiente no pH 10. Nos pHs 11 e 12 a ligação da proteína com a resina não foi tão eficiente como nos outros valores de pH testados. Em microensaios a proteína se ligava adequadamente a resina, mas isso não foi reproduzido em maiores volumes. Foi realizada a purificação desnaturante de DHAase utilizando gradiente de imidazol ao invés de gradiente de pH, porém, também não foi obtido sucesso.

Como alternativa ao método de purificação em cromatrografia de afinidade, realizou-se a extração de DHAase diretamente do SDS-PAGE, pelo método de eletroeluição, com intuito de utilizar a proteína para imunizações. Nesse método foi possível obter DHAase na escala de miligramas. Como demonstrado na Figura 17, a imunização foi satisfatória, pois houve resposta imune contra a hialuronidase recombinante (colunas 1 e 2). Além disso, os anticorpos produzidos com a DHAase conseguiram reconhecer as hialuronidases nativas do veneno (colunas 3 e 4) e, de forma semelhante, o soro antiveneno total de *L. intermedia* foi capaz de reconhecer a hialuronidase recombinante (colunas 5 e 6).

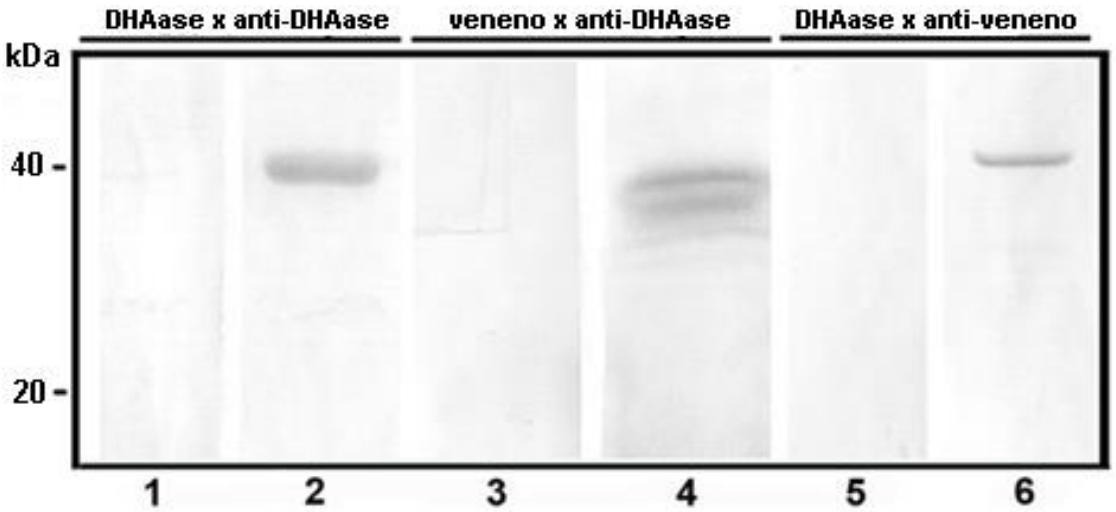

FIGURA 17: REATIVIDADE CRUZADA DO VENENO DE *L.intermedia* E DHAase. Aplicação de DHAase (2,0 µg; colunas 1, 2, 5 e 6) ou veneno total (40 µg; colunas 3 e 4) foram separados por 12,5% de SDS-PAGE sob condições redutoras, transferido para membranas de nitrocelulose e expostas a soros contra DHAase (colunas 2 e 4) ou contra toxinas do veneno total (coluna 6). As colunas 1, 3 e 5 indicam as reações na presença de soro pré-imune (controle para a especificidade do anticorpo). As posições dos marcadores de massa molecular estão mostradas à esquerda da figura.

6.4 REDOBRAMENTO *in vitro*

Alternativa de escolha para tentar obter a solubilidade e, por conseguinte, estudar a atividade de DHAase foi a utilização da técnica de redobramento *in vitro*.

Diferentes tampões de redobramento foram testados em microplaca com a leitura da agregação proteína-proteína realizada depois de 2 h (absorbância em 320 nm). O resultado desse teste é apresentado na Figura 18. Como pode ser observado no gráfico, os tampões que mais reduziram a formação de agregados e assim tiveram uma menor absorbância, foram as soluções que continham Tris-HCl 100 mM em pH 10,0 e a adição do par de glutationas (tampões 7-9). Para o teste em maior escala o tampão de escolha foi o número 7 (demonstrado na Figura 18), pois foi o que demonstrou menor absorbância.

Embora uma parte da hialuronidase tenha ficado solúvel no teste em maior escala, a enzima não apresentou atividade. A mesma só foi obtida quando a hialuronidase foi purificada por lavagens dos corpos de inclusão (e não por eletroeluição) e quando ao tampão de escolha (o número 7, Figura 18) foi adicionado 0,4 M de L-arginina e 0,2 mg/mL de BSA.

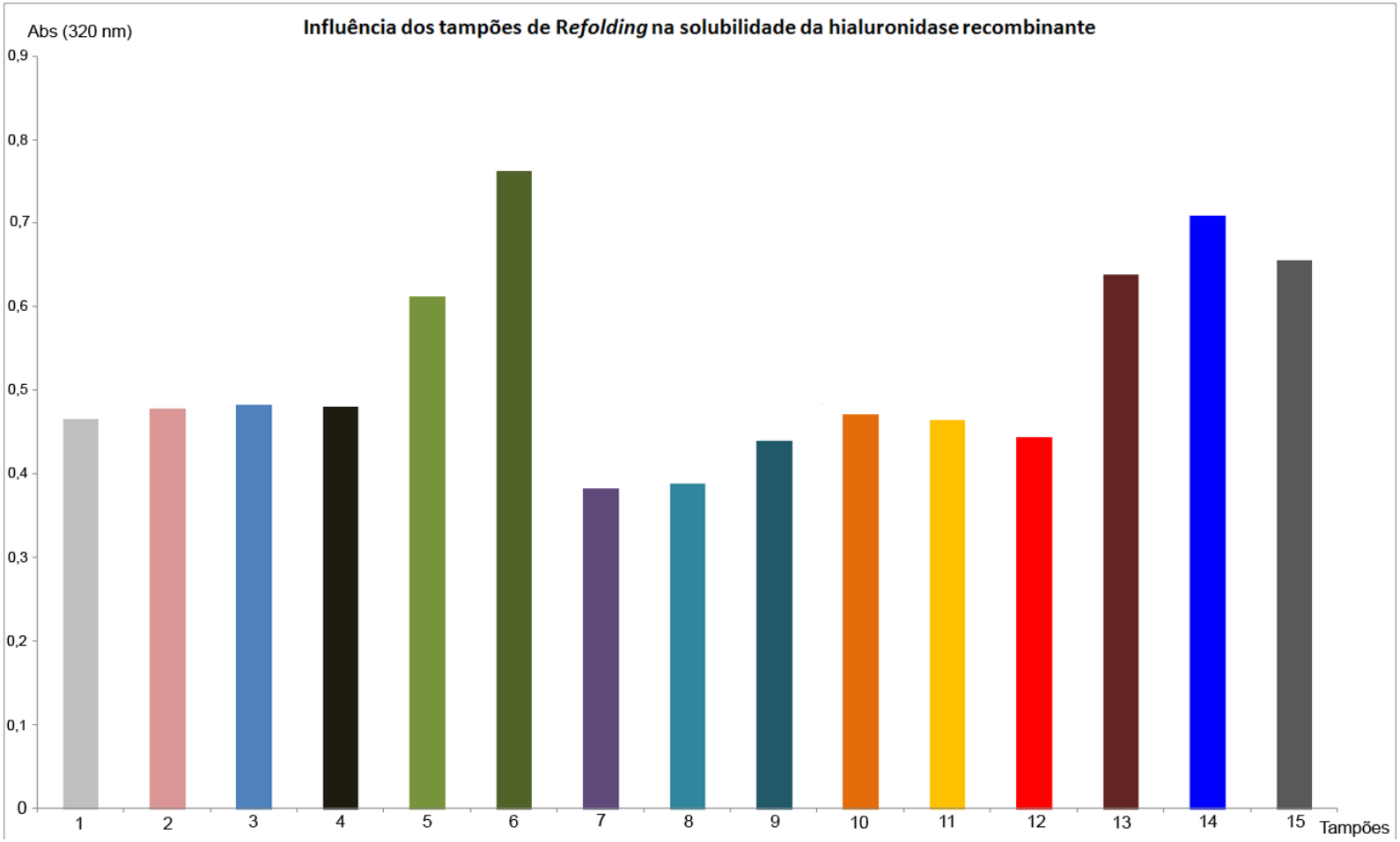

FIGURA 18: AVALIAÇÃO DA SOLUBILIDADE DE DHAase EM DIFERENTES TAMPÕES DE REDOBRAMENTO. A DHAase foi purificada em condições desnaturantes por eletroeluição. A concentração da toxina purificada foi ajustada a 5mg/mL e foi realizada uma diluição 1:20 em diversos tampões de redobramento (identificados de 1 a 15 conforme legenda). O teste foi realizado em microplaca e a leitura da absorbância foi realizada em 320 nm após incubação por 120 min à temperatura ambiente. **Tampão 1**: 100 mM Tris-HCl pH 8,0; **2**: 100 mM Tris-HCl pH 9,0; **3**: 100mM Tris-HCl pH 10,0; **4**: 100 mM Tris-HCl pH 10,0 + 0,1 mM DTT; **5**: 100 mM Tris-HCl pH 10,0+ 0,5 mM DTT; **6**: 100 mM Tris-HCl pH 10,0 + 1,0 DTT; **7**: 100 mM Tris-HCl pH 10,0 + 3,0 mM GSH + 0,3 mM GSSG; **8**: 100 mM Tris-HCl pH 10,0 + 3,0 mM GSH + 3,0 mM GSSG; **9**: 100 mM Tris-HCl pH 10,0 + 0,3 mM GSH + 3,0 mM GSSG; **10**: 100 mM Tris-HCl pH 10,0 + 5% glicerol; **11**: 100 mM Tris-HCl pH 10,0 + 7% glicerol; **12**: 100 mM Tris-HCl pH 10,0 + 10% glicerol; **13**: 100 mM Tris-HCl pH 10,0 + 0,5 mM DTT + 0,3 mM GSH + 3mM GSSG; **14**: 100 mM Tris-HCl pH 10,0 + 0,5 mM DTT + 3,0 mM GSH + 0,3mM GSSG; **15**: 100 mM Tris-HCl pH 10,0 + 0,5 mM DTT + 3,0 mM GSH + 3,0 mM GSSG

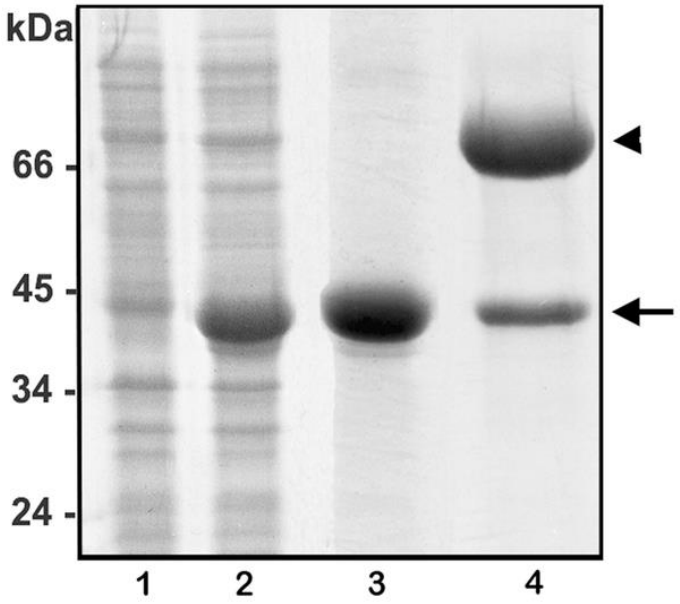

FIGURA 19: REDOBRAMENTO *in vitro* DE DHAase. A expressão da DHAase em maior escala foi feita em BL21(DE3)pLysS com 0,1 mM de IPTG por 5 h. A cultura foi concentrada e congelada em tampão de ligação nativo. As células foram rompidas por descongelamento e sonicação. O *pellet* foi lavado 2x com tampão de lavagem (Tris-HCl 100 mM pH 10, uréia 1M e 0,5% TritonX-100). O *pellet* resultante foi ressuspendido em tampão Tris-HCl 100 mM, uréia 8M pH 10 e DTT 50 mM. Essa solução protéica foi diluída gota a gota em tampão de redobramento (Tris-HCl 100 mM pH 10,0; GSH 3 mM: GSSG 0,3 mM; 0,2 mg/mL de BSA; L-arginina 0,4 M) e deixada 16 h a 4ºC sob agitação. Em 1 tem-se uma alíquota representativa da cultura antes da indução; em 2, cinco horas depois da indução; em 3, DHAase lavada dos corpos de inclusão; em 4, DHAase depois da diálise em PBS pH 7,2 (seta) e o BSA utilizado no tampão de redobramento (ponta de seta).

Na coluna 4 da Figura 19 é demonstrado que uma parte da hialuronidase purificada dos corpos de inclusão foi obtida em sua forma solúvel após o processo de redobramento *in vitro*. A atividade dessa fração solúvel foi testada por turbidimetria, precipitando o HA não degradado pela enzima. Com esse teste foi possível observar que DHAase após o redobramento no tampão contendo BSA e L-arginina havia adquirido sua forma ativa, pois a turbidez do controle (em 400 nm) foi ~4 vezes superior do que a obtida com DHAase.

6.5 ATIVIDADE DE DHAase

6.5.1 Avaliação *in vitro* do perfil de degradação

Após verificar que nas condições padronizadas a hialuronidase estava solúvel e ativa, foi realizada uma cinética de degradação com HA na proporção 1:1 substrato: hialuronidase ou substrato: veneno. Como pode ser demonstrado na Figura 20 colunas 2 e 3, tanto o veneno como a toxina recombinante foram hábeis em degradar totalmente o HA teste em apenas 3 h. Embora não se possa comparar a quantidade de enzima recombinante e a de enzima nativa no veneno, esse resultado demonstra que

mesmo DHAase não tendo as modificações pós-traducionais que provavelmente a nativa possui, a técnica padronizada para o redobramento *in vitro* foi suficiente para deixá-la em conformação ativa semelhante às presentes no veneno.

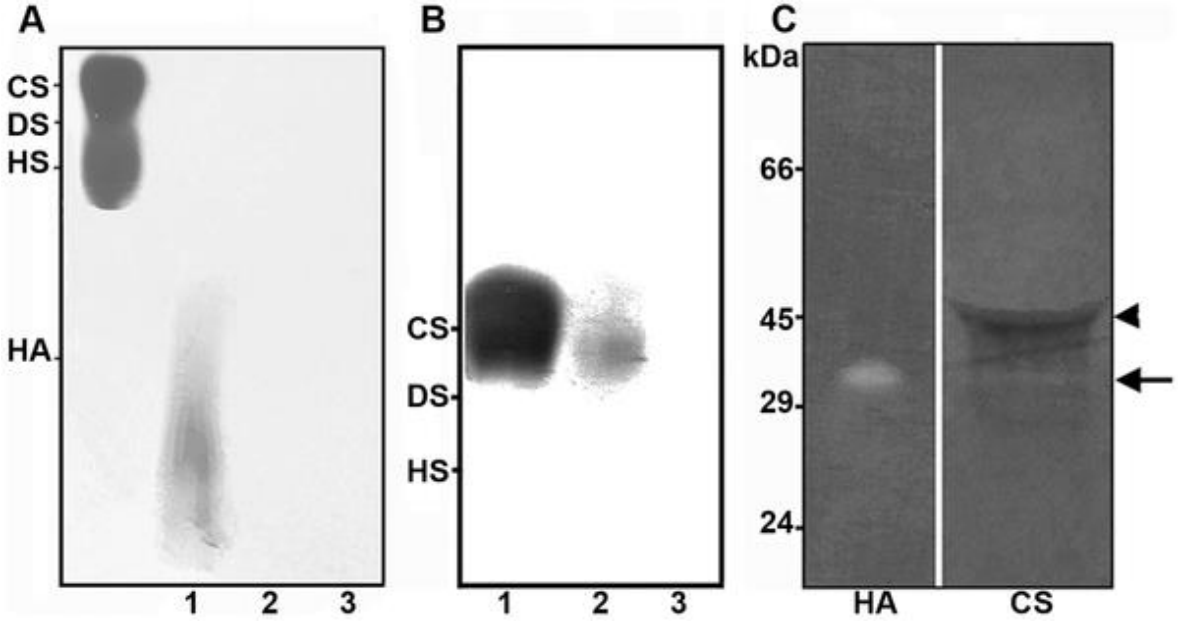

FIGURA 20: ATIVIDADE DE DHAase SOBRE ÁCIDO HIALURÔNICO E CONDROITIM SULFATO. (A) Ácido hialurônico (HA) purificado (15 µg) incubado com o veneno total ou DHAase (1:1) durante 3 h a 37°C. A degradação foi analisada por eletroforese em gel de agarose corado com azul de toluidina. O condroitim sulfato (CS), dermatam (DS) e heparam sulfato (HS) foram utilizados como marcadores de massa molecular. A coluna 1 representa o controle negativo e as colunas 2 e 3 mostram o HA incubado com o veneno e DHAase, respectivamente. (B) Cinco microgramas de C4S purificado (nesta figura representado por CS) incubado com veneno (coluna 2) ou DHAase (coluna 3) nas proporções 1:1 durante 16 h a 37°C. O controle do C4S é mostrado na coluna 1. (C) Cinco microgramas de DHAase foram submetidos à zimografia em SDS-PAGE 10% co-polimerizado com 0,17 mg/mL de HA ou 0,34 mg/mL de C4S, corado com Azul de Alcian e co-corado com Azul de Coomassie. A seta preta indica a atividade da hialuronidase recombinante. Na ponta de seta está demonstrado o BSA persistente após a proteólise realizada antes da coloração. As posições dos marcadores de massa molecular estão apresentadas à esquerda da figura.

Era sabido por trabalhos anteriores do grupo que as hialuronidases presentes no veneno de *L. intermedia* possuiam atividade de condroitinase (DA SILVEIRA et al., 2007a). Como demonstrado na Figura 20, DHAase degradou o C4S assim como o observado para as glicosidases nativas do veneno.

Sequencialmente, para se avaliar a estabilidade adquirida pela DHAase no redobramento, foi feito um ensaio de zimografia no qual a enzima foi exposta a uma

desnaturação em SDS-PAGE em condições não redutoras e depois submetida a um novo redobramento em tampão ótimo por 16 h. Conforme pode ser visto na Figura 20C a hialuronidase recombinante (coluna 2) se renaturou e teve atividade tanto em substrato de HA, quanto em C4S.

Depois de demonstrada por ensaios *in vitro* a atividade de DHAase, o propósito se tornou avaliar sua atividade *in vivo*.

6.5.2 Espalhamento Gravitacional

Para determinar a participação *in vivo* das hialuronidases do veneno de aranha-marrom no envenenamento foram desenvolvidos experimentos de dermonecrose usando coelhos neozelandeses. Para tal, foram feitas injeções intradérmicas de veneno bruto de *L. intermedia*, toxina recombinante dermonecrótica (controles positivos) e toxina dermonecrótica adicionada de DHAase (teste). A indução de dermonecrose macroscópica na pele do coelho foi observada por 3, 6 e 24 h e pode-se constatar que tanto os controles positivos quanto o teste desenvolveram dermonecrose (Figura 21A e B). Por outro lado, a injeção de DHAase sozinha (Figura 21B), PBS/BSA e uma proteína recombinante não relacionada com a hidrólise de HA (Figura 21A) - os controles negativos, não apresentaram macroscopicamente eritema, edema, equimose ou dermonecrose. O tamanho das lesões na pele de coelho da toxina dermonecrótica injetada concomitantemente com DHAase foi substancialmente maior do que para a toxina dermonecrótica sozinha (Figura 21B). Pode-se também observar que o espalhamento gravitacional e edema induzidos pelas enzimas recombinantes em conjunto foram muito semelhantes ao veneno total aplicado, o qual contém hialuronidases e fosfolipases nativas (Figura 21C).

6.5.3 Histologia da dermonecrose

A título de comparação, utilizando imagens panorâmicas sob as mesmas condições, nota-se que os efeitos deletérios induzidos pela toxina dermonecrótica sozinha (LiRecDT1) foram inferiores aos induzidos pela mistura LiRecDT1 e DHAase (Figura 22).

A análise das biópsias de pele de coelho por microscopia óptica 24 h após a dermonecrose experimental sugere que DHAase foi capaz de desorganizar a matriz extracelular da derme da pele de coelho (Figura 23-4). A toxina dermonecrótica sozinha provocou o acúmulo de células inflamatórias (setas pretas, Figura 23-2 e -5) e os sinais de edema típicos (Figura 22, 23-5), bem como a desorganização das fibras de colágeno (setas brancas, Figura 23-5) e presença de fibrina no tecido conjuntivo (pontas de seta, Figura 23-5). No entanto, percebemos que esses eventos inflamatórios desenvolvidos pela toxina dermonecrótica foram intensificados quando foi adicionado DHAase (Figura 22; Figura 23-3, -5 e -6), com um edema extenso e difusão da lesão.

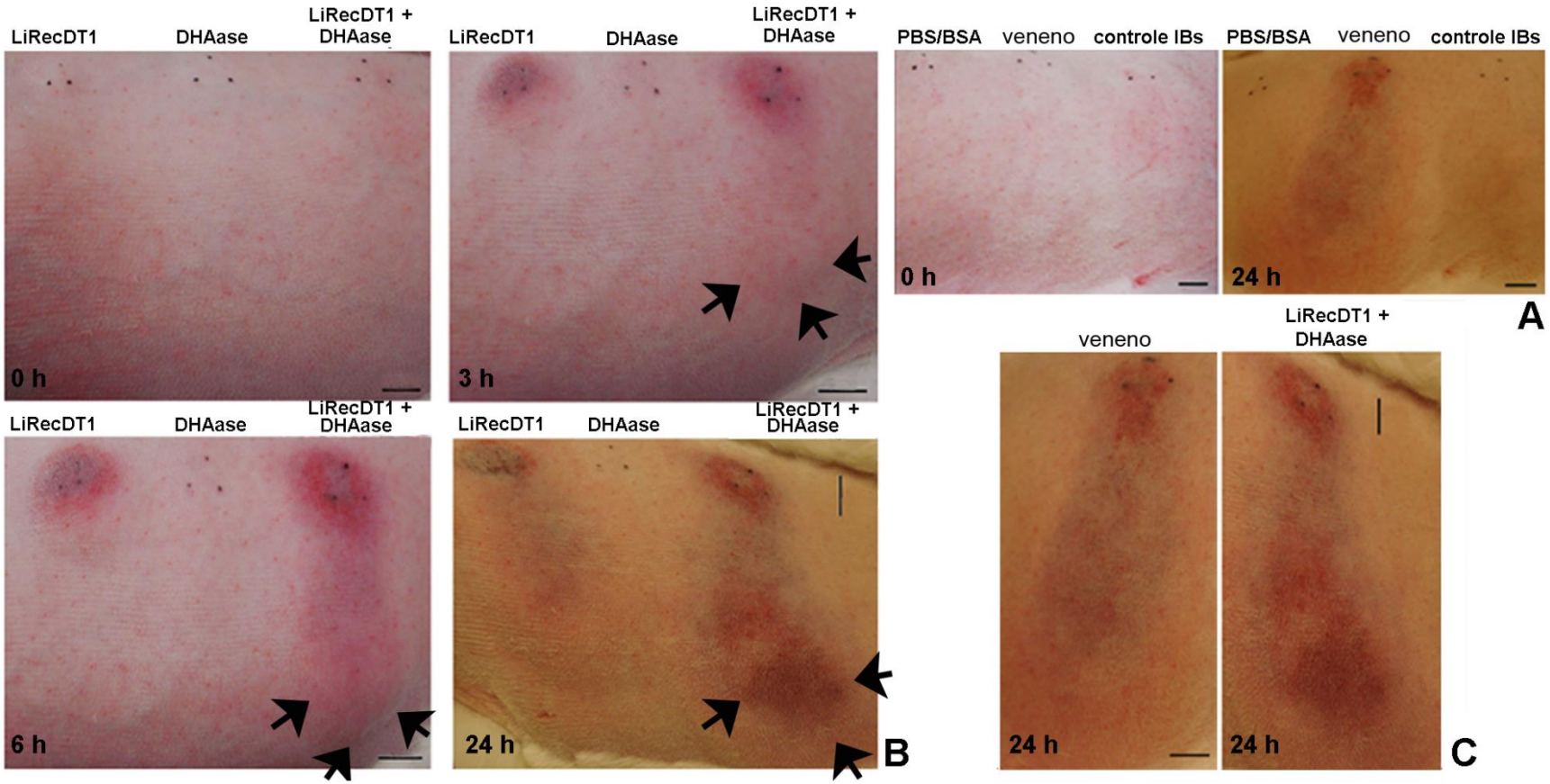

FIGURA 21: ALTERAÇÕES MACROSCÓPICAS EM PELE DE COELHO EXPOSTA AO VENENO, LiRecDT1 E DHAase. (A) visualização macroscópica de lesões da pele de coelhos com injeções intradérmicas de 10 µg de veneno total (veneno), 10 µg de uma metaloprotease recombinante inativa (LALP1) não relacionada com a hidrólise do HA ou dermonecrose (controle dos corpos de inclusão, controle IBs) e mesmo volume de PBS/BSA (controle negativo). As lesões foram observadas 0 e 24 h após a injeção. (B) visualização macroscópica das lesões da pele de coelhos desenvolvidas com a injeção intradérmica de 10 µg de toxina dermonecrótica (LiRecDT1), 10 µg de DHAase ou ambas toxinas (10 µg:10 µg). Foram observadas as lesões em 0, 3, 6 e 24 h após as injeções. As setas apontam para o maior desenvolvimento de espalhamento gravitacional das lesões necróticas após a injeção de LiRecDT1 e DHAase, em comparação com lesões desenvolvidas devido apenas à toxina dermonecrótica. (C) Em detalhe, a comparação das lesões dermonecróticas desenvolvidas pelo veneno ou uma mistura de DHAase e LiRecDT1. As injeções foram aplicadas no centro do triângulo indicado por três pontos. A escala é mostrada à direita de cada imagem e representa 1 cm.

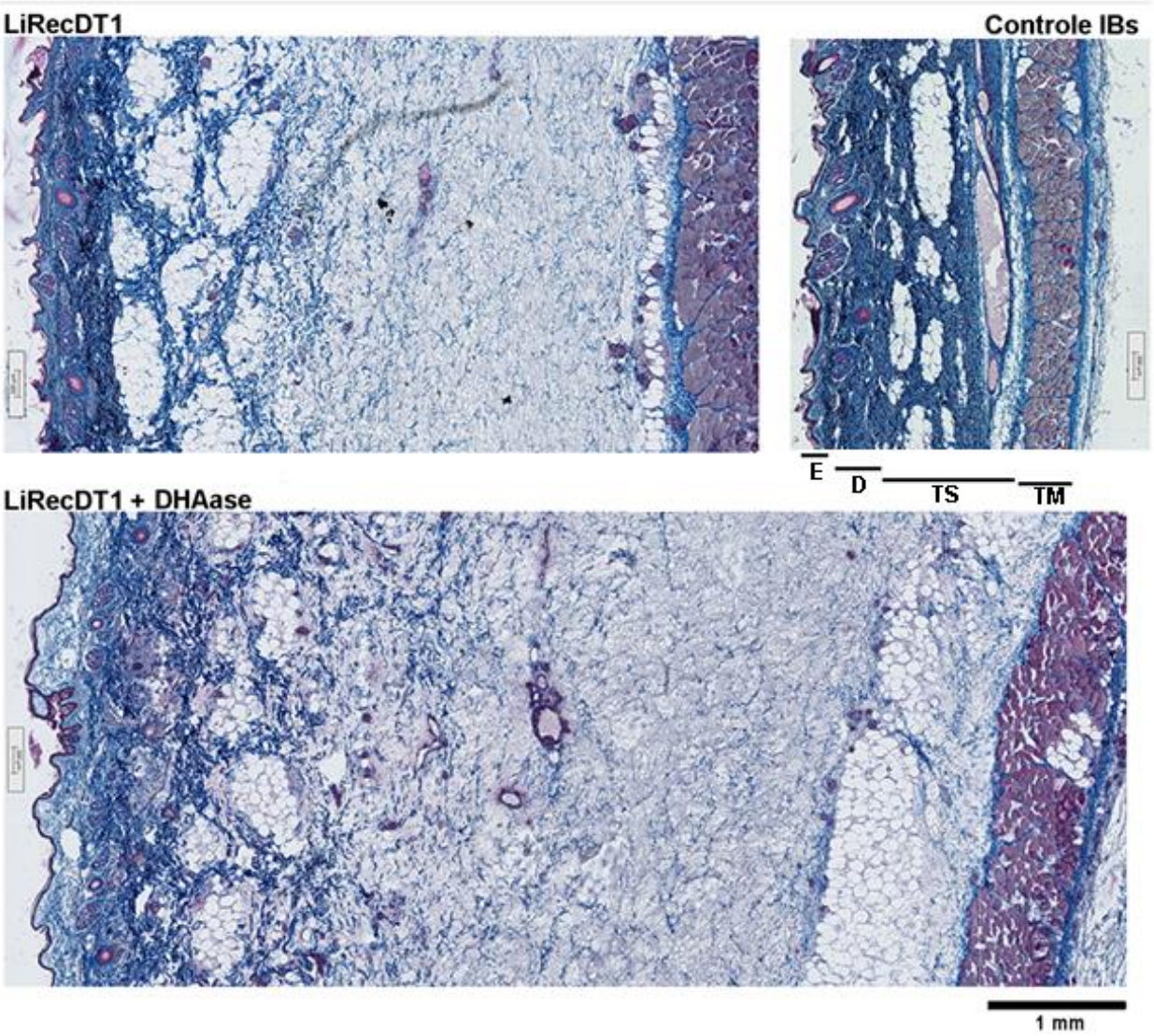

FIGURA 22: AVALIAÇÃO DE ALTERAÇÕES HISTOPATOLÓGICAS EM PELE DE COELHO EXPOSTA À LiRecDT1 e DHAase. A análise microscópica de secções de tecido de pele de coelho foi realizada 24 h após as injeções intradérmicas das enzimas recombinantes ou controle. Maior edema provocado na pele de coelho (desorganização das fibras de colágeno e espessamento do tecido) pela combinação da toxina dermonecrótica (LiRecDT1) e DHAase quando comparado à LiRecDT1 somente ou o controle. A comparação foi feita pelo espessamento do tecido que abrange desde a epiderme (do lado esquerdo da figura) até os tecidos musculares (lado direito da figura) por meio de captura de imagens sob as mesmas condições. E= Epiderme; D= Derme; TS= Tecido Subcutâneo; TM= Tecido Muscular. As secções de tecido foram coradas com Tricrômio de Masson. Ampliação de 15x. A barra abaixo da figura indica 1 mm.

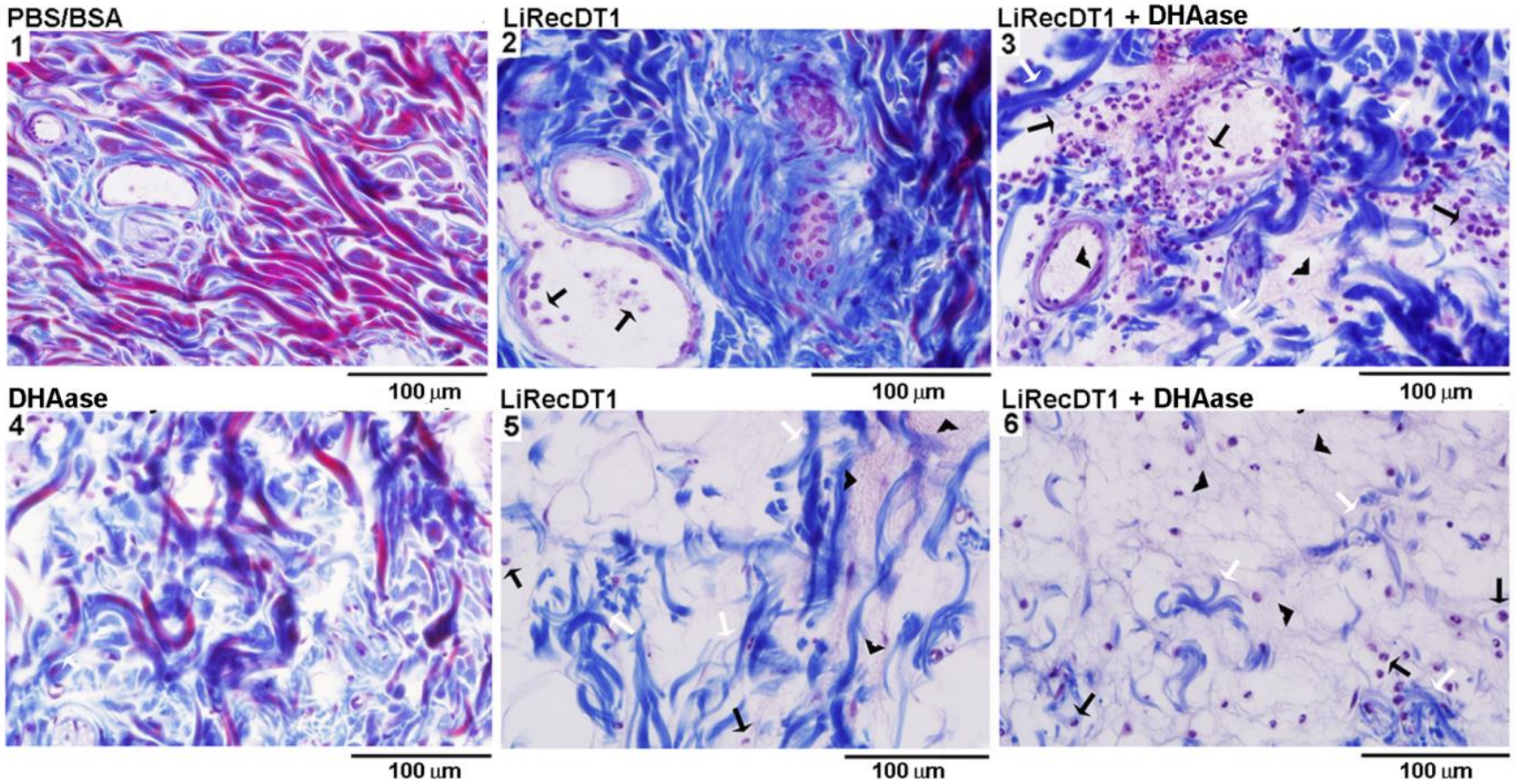

FIGURA 23: INFLAMAÇÃO EM PELE DE COELHO EXPOSTA À LiRecDT1 e DHAase. A pele exposta à toxina recombinante dermonecrótica, à hialuronidase recombinante ou as duas em conjunto modifica a matriz extracelular do tecido conjuntivo causando a desorganização das fibras de colágeno (quadro 3, 4, 5 e 6) (setas brancas); exsudado fibrinóide na derme (quadros 3, 5 e 6) (pontas de setas), e uma resposta inflamatória intensa com neutrófilos dentro dos vasos sanguíneos e difusamente nas estruturas da derme (quadros 2, 3, 5 e 6) (setas pretas). Ampliação de 400x. A barra abaixo da figura indica 100 µm. A coloração utilizada foi Tricrômio de Masson.

Capítulo II:

Efeito da adição de *Dietrich´s Hyaluronidase* sobre cultivo de linhagens celulares normais e cancerosas.

7 INTRODUÇÃO

O ácido hialurônico desempenha papel fundamental no comportamento celular mediando e regulando processos como adesão, diferenciação e proliferação. Esse GAG também está relacionado com processos patológicos como, por exemplo, progressão tumoral (BOUGA et al., 2010). Em diversos tipos de células tumorais enzimas que sintetizam (HAS) ou degradam (HAases) ácido hialurônico, já foram relacionadas com processos de crescimento, migração, invasão, metástase e angiogênese do tumor (LAURICH et al., 2004; WHATCOTT et al., 2011; WILLENBERG et al., 2011).

Existem alguns trabalhos na literatura que demonstram uma maior adesão de células cancerosas às superfícies recobertas com HA comparado com superfícies recobertas por outras moléculas de matriz. Adicionalmente, as células cancerosas parecem adquirir morfologia e comportamento mais próximos ao observado *in vivo*, quando cultivadas em superfícies de HA (DICKINSON et al., 2010; GURSKI et al., 2012).

Melanoma, um tumor maligno das células produtoras de pigmento, os melanócitos, é um dos tipos mais agressivos de câncer de pele (LEE et al., 2013). Em modelo de melanoma murino, a quantidade de HA está aumentada durante as fases iniciais do tumor e essa molécula foi localizada na interface entre as células tumorais e o seu estroma. Estudos *in vitro* mostram que o aumento da produção de HA e HAases está correlacionado com o aumento da motilidade dessas células, no entanto, a expressão de HA em melanomas invasivos profundos foi mostrada estar diminuída (SIISKONEN et al., 2013). O receptor celular de HA melhor estudado, CD44 (*Cluster of differentiation* 44), medeia a adesão dos melanomas ao HA e esse receptor parece ser essencial para a proliferação das mesmas (AHENS et al., 2001).

Contrariamente ao que é observado para as células cancerosas foi demonstrado que em cultura de fibroblastos a adição de HAases recombinantes não causa inibição de adesão, alterações morfológicas ou desadesão dessas células (VOGEL, 1978; BRUNS e GROSS, 1980; CHORILLI et al., 2005). Outros tipos celulares normais, como condrócitos e células cardíacas, também se aderem e proliferam preferencialmente em

superfícies recobertas com outras moléculas que não o HA (BARBUCCI et al., 2005; FUKUDA et al., 2006; KHADEMHOSSEINI et al., 2007).

Dada a importância do HA em processos patológicos e tendo em mãos uma hialuronidase recombinante biologicamente ativa (DHAase) com potencial biotecnológico diverso, o foco do trabalho foi avaliar o efeito que a ação de DHAase, uma hialuronidase não secretada pelas próprias células, teria em processos essenciais para células normais e cancerosas.

Foram utilizadas células endoteliais de aorta de coelho (RAEC) como modelo de célula normal. Trabalhos demonstram que esse tipo celular teve sua morfologia e comportamento alterado pelo veneno de *L.intermedia* e por uma metaloprotease recombinante desse, LALP1 (NOWATZKI et al., 2012; DA SILVEIRA et al., 2007c). Como modelo de célula tumoral, por sua vez, foram utilizadas duas linhagens bem estabelecidas de melanoma murino - B16F10, uma linhagem relativamente mais metastática e B16F1, menos metastática. Wille e colaboradores (2013) em estudos *in vitro* demonstraram que B16F10 aumentou sua proliferação dose e tempo dependentes sob a ação de fosfolipases-D do veneno de *L.intermedia* (LiRecDT1) e que LiRecDT1 manteve a viabilidade dessas células inalterada.

Diversos trabalhos demonstram que proteínas recombinantes do veneno de *L.intermedia* alteraram processos celulares em diferentes tipos de cultura de células (DA SILVEIRA et al., 2007c; KUSMA et al., 2008; CHAIM et al., 2011b; NOWATZKI et al., 2012). Nesse contexto, esse capítulo abordará a avaliação preliminar do que a atividade de DHAase causa na dinâmica celular das linhagens RAEC, B16F1 e B16F10.

8 REVISÃO BIBLIOGRÁFICA

8.1 ÁCIDO HIALURÔNICO, SEU METABOLISMO E O CÂNCER.

O glicosaminoglicano HA contribui diretamente para a homeostase, interagindo com proteínas e proteoglicanos de conexão, mantendo a integridade estrutural da matriz extracelular e pericelular. O HA interage também com receptores na superfície das células influenciando o seu comportamento (Figura 24). Devido a essas funções, HA desempenha um papel no comportamento básico das células como adesão, migração, reconhecimento e diferenciação, participando em importantes processos de morfogênese, remodelagem, inflamação e em diversos processos patológicos como no crescimento tumoral e aterosclerose (BOUGA et al., 2010).

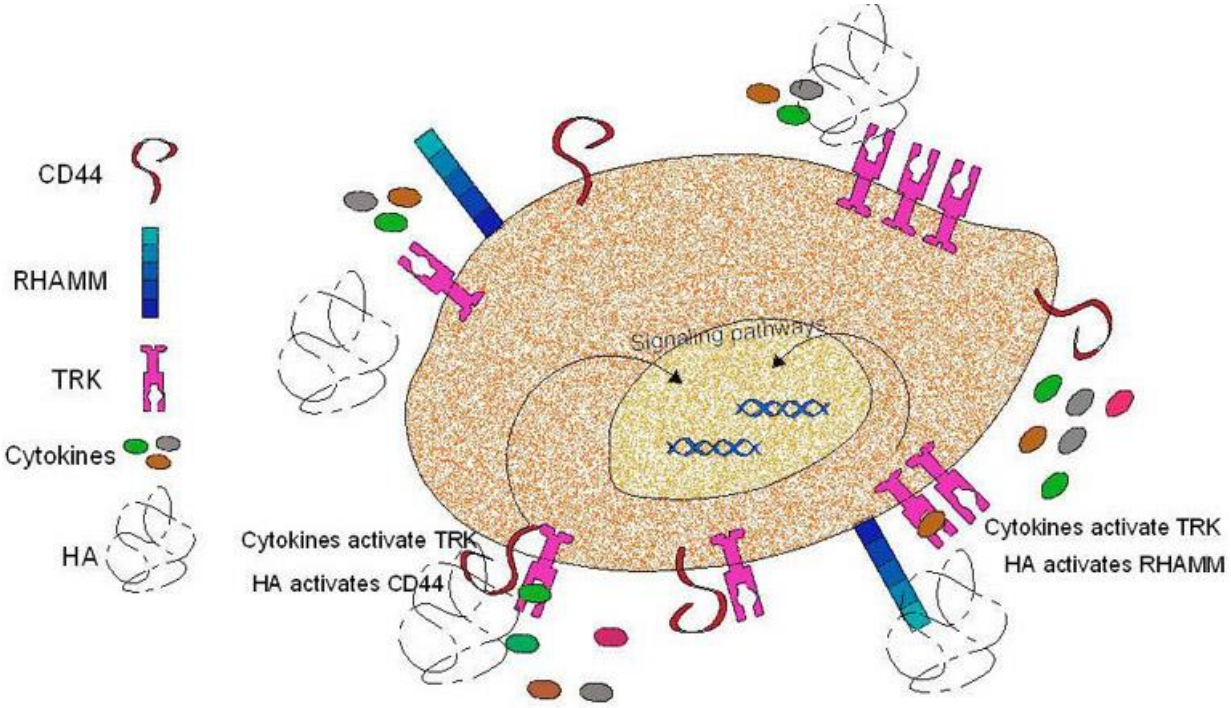

FIGURA 24: INTERAÇÃO DE ÁCIDO HIALURÔNICO COM A SUPERFÍCIE CELULAR. Representação esquemática da interação de HA e seus receptores celulares CD44 (*Cluster of differentiation* 44) e RHAMM (*Hyaluronan-Mediated Motility Receptor*). A sinalização celular induzida por HA acontece via CD44 e RHAMM e envolve a ativação de receptores tirosina quinase (TRKs) por citocinas e outras quinases (família Src). Os complexos de sinalização promovem transições de fenótipo, sobrevivência celular e diferenciação. Para que haja efetivamente a ativação de determinada via, muitos mecanismos devem ser acionados concomitantemente. ADAPTADO DE: ASTACHOV et al., 2011.

Níveis elevados de HA e seus fragmentos parcialmente catabolizados estão relacionados com várias potenciais malignidades devido à perda do controle entre a

síntese e a degradação dessa molécula (BOUGA et al., 2010). Na patogênese do câncer, o HA pode promover tanto o crescimento do tumor quanto metástases (Figura 25) (LAURICH et al., 2004).

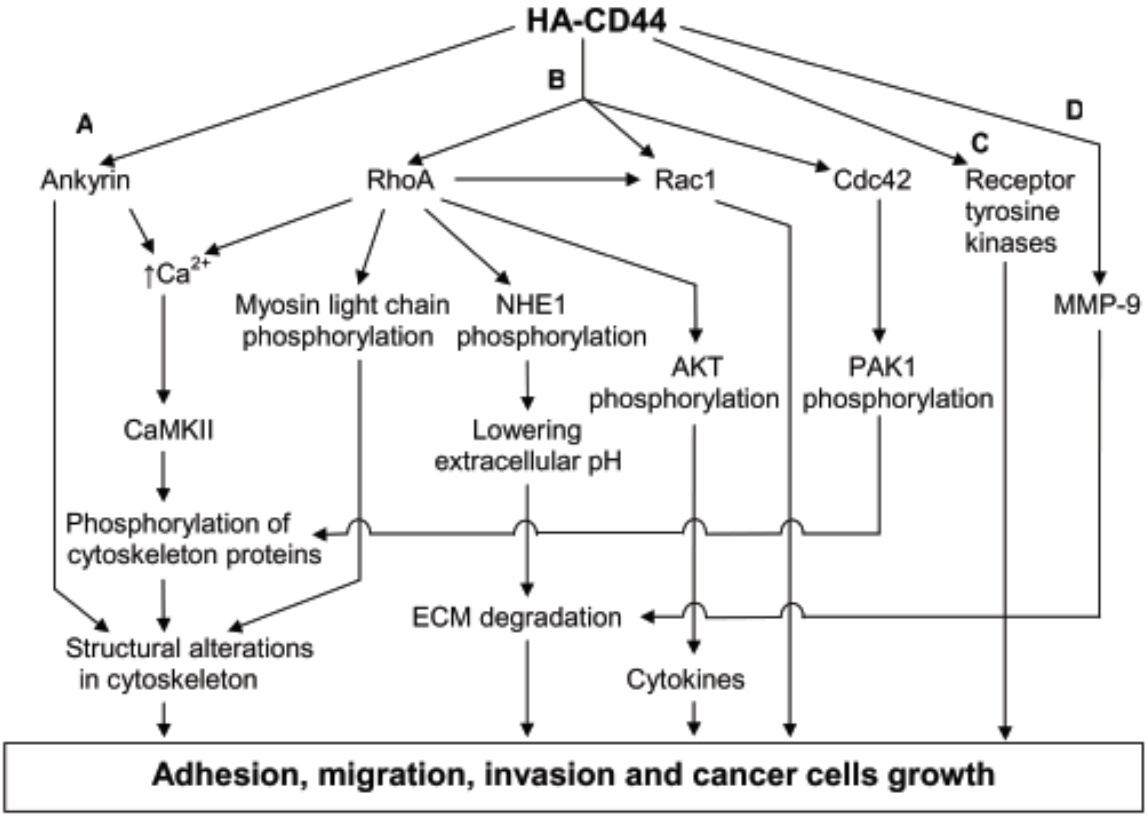

FIGURA 25: INTERAÇÃO HA-CD44 E O SEU IMPACTO NA SINALIZAÇÃO INTRACELULAR E NA PROGRESSÃO TUMORAL. Após a interação de CD44 com o HA há a sinalização de diversas cascatas intracelulares que culminam em adesão, migração, invasão e crescimento do tumor. ADAPTADO DE: KARBOWNIK e NOWAK, 2013.

Quanto à migração no estabelecimento de uma lesão metastática, HAases facilitam o extravasamento e deixa o tecido alvo livre de matriz extracelular (MEC). Os produtos de clivagem de HA são essenciais também na angiogênese (LI e COZZI, 2009).

Entre os receptores celulares de HA, os melhor estudados são CD44 (*Cluster of Differentiation 44*) e RHAMM (*Receptor for Hyaluronan-Mediated Motility*). O papel de CD44, e suas isoformas, na progressão do câncer ainda não é completamente compreendido, mas sabe-se que a sua interação com HA claramente induz a formação de *clusters* na membrana da célula e a ativação de cascatas de sinalização que

influenciam e determinam o comportamento celular (Figura 25). Da mesma forma, os mecanismos de ação de RHAMM não são totalmente elucidados. É sabido que quando RHAMM passa de uma localização citosólica ou nuclear para a membrana e interage com HA e/ou CD44, sua ativação promove vias de sinalização, principalmente, as que envolvem as quinases Src (Sarcoma) e Ras (Sarcoma de Rato) (Figura 24). RHAMM também pode ativar FAK (Quinase de Adesão Focal) e ERK1/2 (Quinase Regulada por sinal Extracelular), enzimas relacionadas aos processos de adesão e proliferação das células (KULTTI et al., 2012).

O processo de metástase envolve os eventos de proliferação celular, invasão através do estroma, migração até o sistema linfo-vascular e adesão ao endotélio e parênquima do tecido alvo. Adesão à MEC é um pré-requisito para esses processos. Por exemplo, células com um fenótipo mais agressivo de carcinoma de pulmão obrigatoriamente devem ser hábeis em aderir à proteínas de MEC para desenvolver metástase, e células de carcinoma de ovário que expressam altos níveis de moléculas de adesão à matriz foram associadas com pouca sobrevivência dos pacientes (DICKINSON et al., 2010).

Foi suposto recentemente a relação entre HA e adesão de células cancerosas (FUKUDA et al., 2006; KHADEMHOSSEINI et al., 2007). Ácido hialurônico medeia a adesão de câncer de próstata à medula óssea, o principal foco de metástase dessas células. HA também estimula a adesão e migração de câncer de mama *in vitro*. Esses dados sugerem que HA desempenha um papel crítico em facilitar a adesão celular necessária para a metástase de alguns tumores (Figura 26 e 27) (DICKINSON et al., 2010).

A quantidade de HA pericelular e do estroma pode ser uma predição negativa da sobrevivência do paciente. Em adenocarcinomas de mama, ovário, cólon e ventrículo, o aumento da quantidade de HA se correlaciona diretamente com o grau do tumor e mau prognóstico (TAMMI et al., 2008; KOSUNEN et al., 2004). Existe a relação de uma produção excessiva de HA em células malignas e o aumento de HAases no soro, com a progressão e prognóstico em alguns tipos de cânceres, como o gástrico, coloretal, de mama e ovário (BOUGA et al., 2010; WHATCOTT et al., 2011). Em contrapartida, em carcinomas de células escamosas (SCC) da pele, boca, laringe e pulmão, o conteúdo

de HA é diminuído em tumores de alto grau e, por exemplo, em câncer oral (SCC) isso é associado com mau prognóstico (LAURICH et al., 2004; TAMMI et al., 2008; KOSUNEN et al., 2004). Corroborando com os últimos dados mencionados, um trabalho recente descobriu que a causa da resistência ao câncer de uma espécie de roedor (*Heterocephalus glaber*) é justamente o acúmulo de HA. Quando esse glicosaminoglicano foi experimentalmente degradado ou não sintetizado, os ratos se tornaram susceptíveis ao desenvolvimento de tumores malígnos (TIAN et al., 2013).

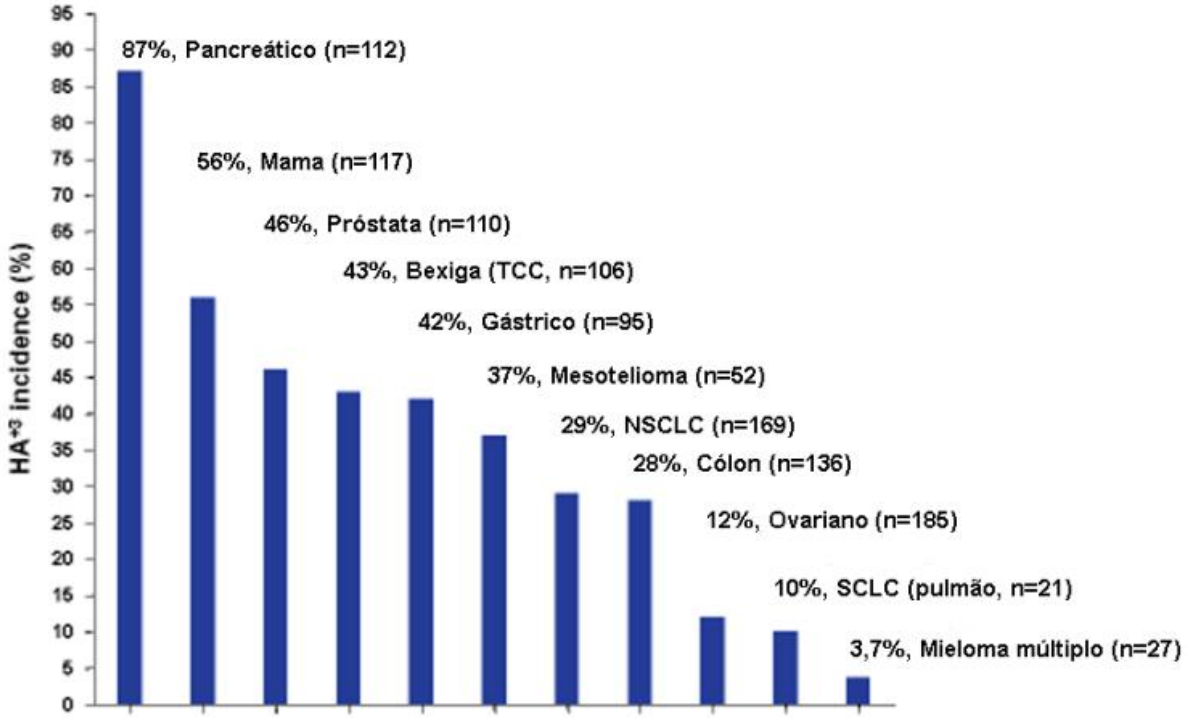

FIGURA 26: ACÚMULO DE ÁCIDO HIALURÔNICO EM DIFERENTES TIPOS DE CÂNCERES. O acúmulo de HA ocorre em 87% dos cânceres de pâncreas e 25-30% dos tumores sólidos em geral. TCC = *Transitional Cell Carcinoma*; SCLC = *Small Cell Lunger Carncer*, NSCLC = *Non Small Cell Lunger Carncer*. ADAPTADO DE: KULTTI et al., 2012.

Uma vez uma lesão metastática estabelecida, RHAMM pode cooperar com CD44 na angiogênese para promover a migração de células endoteliais próximas em direção ao tumor (OUHTIT et al., 2007). Somado a isso, fatores de crescimento e proteínas de MEC estão entre os sinais cruciais na regulação do ciclo celular (BHARADWAJ et al., 2011). O acúmulo de HA nos tumores pode armazenar fatores de

crescimento e citocinas pró-tumorigênicas, além de formar uma barreira para a migração de células do sistema imune até as células malignas (KULTTI et al., 2012).

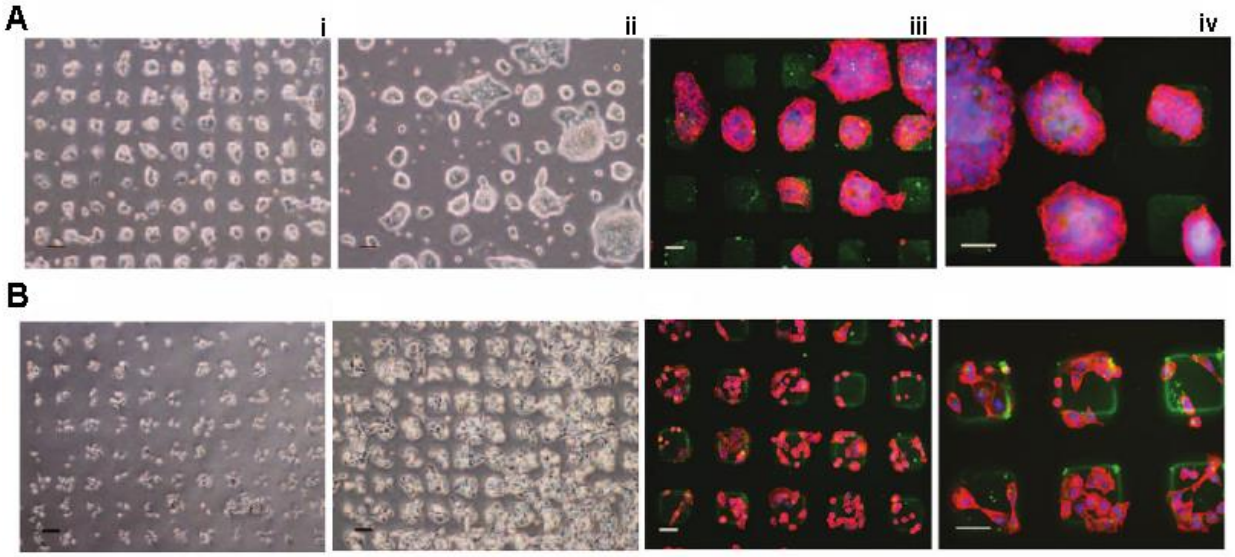

FIGURA 27: SUPERFÍCIES DE ÁCIDO HIALURÔNICO PARA CULTURA DE CÉLULAS CANCEROSAS (A) Células de câncer de cólon (B) células de câncer de mama incubadas em superfícies moldadas com HA (quadrados). (i) formação de colônias (ii) crescimento em tamanho. Análise de fluorescência de CD44+ em (iii) menor e (iv) maior aumento. ADAPTADO DE: DICKINSON et al., 2010.

Sabe-se que HA de alta massa molecular (HMWHA, > 1000 kDa) é um sinal para reprimir a mitogênese e tem ação antiinflamatória enquanto HA de baixa massa molecular (LMWHA, 50 a 1000 kDa) promove proliferação e inflamação (TIAN et al., 2013). Porém, um trabalho *in vitro* demonstrou que o efeito sobre a proliferação celular depende da concentração de HMWHA utilizado e do número de interações dessa molécula com o CD44 na superfície das células (AHRENS et al., 2001).

No genoma humano, atualmente, existem 6 genes conhecidos que codificam para sequências de hialuronidases, tendo um alto grau de homologia, mas com diferença em suas distribuições nos tecidos. São chamadas de Hyal-1 até Hyal-4, PH20/Spam-1 e um pseudogene Phyal1, a qual não é traduzida. Hyal-1 e Hyal-2 são as enzimas majoritárias para a degradação de HA em tecidos somáticos. Hyal-2 degrada HMWHA em produtos de aproximadamente 20 kDa, enquanto Hyal-1 pode degradá-lo em pequenos oligômeros, principalmente tetrassacarídeos. Estudos preliminares demonstram que Hyal-4 é também uma condroitinase com predominância de atividade sob condroitim e CS. Entre as 6 hialuronidases de mamíferos, Hyal-1 é a hialuronidase mais encontradas em tumores e é expressa por uma variedade de

células tumorais, fato confirmado por diversas técnicas como RT-PCR, clonagem, purificação proteica e ensaios de imunodetecção (LOKESHWAR et al., 2001; LI e COZZI, 2009).

Se HAases funcionam como promotoras ou supressoras do tumor parece ser um efeito concentração dependente. Níveis que excedem doses endógenas encontradas em tumores (100 mU/10^6 células) foram demonstrados reduzir o crescimento tumoral por indução de apoptose, enquanto baixos níveis de HAases promovem o crescimento tumoral (KULTTI et al., 2012).

Por sua vez, as HA sintases (HAS) são enzimas transmembranas responsáveis pela biossíntese de HA. Três isoformas humanas foram identificadas: HAS1, HAS2 e HAS3, sendo cada uma capaz de sintetizar HA. Expressão diferencial de isoformas de HAS tem sido também relacionada com progressão de câncer. Foi demonstrado que expressão de HAS e produção de HA pericelular são críticos para o crescimento ancoragem-independente e invasão de células cancerosas de carcinoma de cólon. É proposto que HA pericelular e isoformas de HAS podem oferecer novos marcadores para o diagnóstico e terapia nesse tipo de câncer (LAURICH et al., 2004).

8.2 MELANOMAS E ÁCIDO HIALURÔNICO

Melanoma é um tumor maligno que se origina nas células produtoras de melanina, os melanócitos. Embora represente menos de 5% de todos os cânceres de pele, é um dos tipos mais agressivos desses, sendo responsável pela maioria das mortes relacionadas à câncer de pele. É o quinto câncer mais comum em homens e o sexto mais comum em mulheres (LEE et al., 2013). A incidência de melanoma tem continuado a aumentar nos últimos 30 anos. O melanoma cutâneo é curável com cirurgia em seus estágios iniciais, mas o seu marcado potencial metastático e a sua resistência aos tratamentos atuais apresentam um desafio terapêutico para os médicos (SIEGEL et al., 2012).

Dados do Instituto Nacional de Câncer no Brasil (INCA) demonstram que a maior incidência de melanoma ocorre em indivíduos adultos brancos. No Brasil o câncer de pele é o tipo de câncer mais frequente (25%), sendo que desses 4%

correspondem à melanomas. Embora não tenha uma incidência alta, o melanoma é considerado o tipo mais grave de câncer de pele no país devido às metástases. Em 2012, houve a estimativa de mais de 6 mil novos casos no Brasil, com incidência semelhante entre homens e mulheres (INCA, 2014).

A taxa de sobrevida de 5 anos do melanoma é de apenas 15% para metástases e melhorou apenas ligeiramente na última década. Devido ao mau prognóstico e a falta de opções terapêuticas eficazes para pacientes com metástases, muito esforço tem sido feito para descobrir a etiologia e patogenia do melanoma. Ambos os fatores ambientais e suscetibilidade genética parecem ter um papel na progressão da doença (MILLER e MIHM, 2006; VEIEROD et al., 2013). Fatores de riscos para o desenvolvimento de melanoma incluem a exposição ao sol, presença de nevos (pintas comum) atípicos, pigmentação da pele e histórico familiar de melanoma. As pesquisas têm focado em informações substanciais sobre as vias moleculares envolvidas no melanoma (LEE et al., 2013).

A radiação ultravioleta, que é um dos fatores de risco mais importantes para o melanoma, foi demonstrada ser capaz de induzir acúmulo de HA. A exposição também se mostrou relacionada com o desenvolvimento de hiperplasia, displasia e câncer na epiderme de camundongos. Após uma exposição em longo prazo (três vezes por semana por 35 minutos em 10,5 meses) os animais desenvolveram câncer de pele, principalmente carcinoma das células escamosas (~20%). Tais dados sugerem um papel do HA nas primeiras fases de transformação maligna em pele expostas ao ultravioleta (SIISKONEN et al., 2011).

Em modelo de melanoma murino, a quantidade de HA aumentou durante as fases iniciais de tumorigênese. Esse aumento de HA foi localizado na interface entre as células de melanoma e o estroma (TURLEY e TRETIAK., 1985). Estudos *in vitro* têm mostrado que o aumento da produção de HA está correlacionado com aumento da motilidade das células de melanoma (ICHIKAWA et al., 1999; KUDO et al., 2004). A inibição da síntese de HA por 4-metilumbeliferona (4- MU) diminuiu a migração, adesão e invasão em culturas 3D de melanoma (SIISKONEN et al., 2013). Fibroblastos são a principal fonte de HA no estroma de melanoma, enquanto os melanócitos malígnos sintetizam menores quantidades do mesmo (Figura 28) (WILLENBERG et al., 2011).

O papel de HAS e HAases tem sido investigado em muitos adenocarcinomas, mas relativamente poucos trabalhos são encontrados com melanomas (JACOBSON et al., 2002; UDABAGE et al., 2005; SIMPSON et al., 2006). Cultura de células de melanoma na presença de HMWHA resultou num efeito dose dependente na proliferação dessas células. Uma solução de 0,1 mg/mL desse glicosaminoglicano de alta massa aplicada sobre a cultura induziu as células se proliferarem mais quando comparado à solução de concentração de 1 mg/mL (AHENS et al., 2001).

Um trabalho recente demonstrou que a expressão de HA e CD44 aumentou no tecido displásico e no tumor *in situ*, comparado ao tecido normal, mas foi reduzida em estádio I (tumor < 1 mm) e em melanomas malígnos invasivos. A marcação dessas moléculas teve uma correlação inversa com o aumento do tamanho, espessura e nível de invasão desses tumores. Nas lesões benignas nevomelanocíticas a expressão de HA e CD44 foi uniforme (Figura 29). Dessa maneira, os níveis de HA puderam ser associados com prognósticos de pacientes (SIISKONEN et al., 2013).

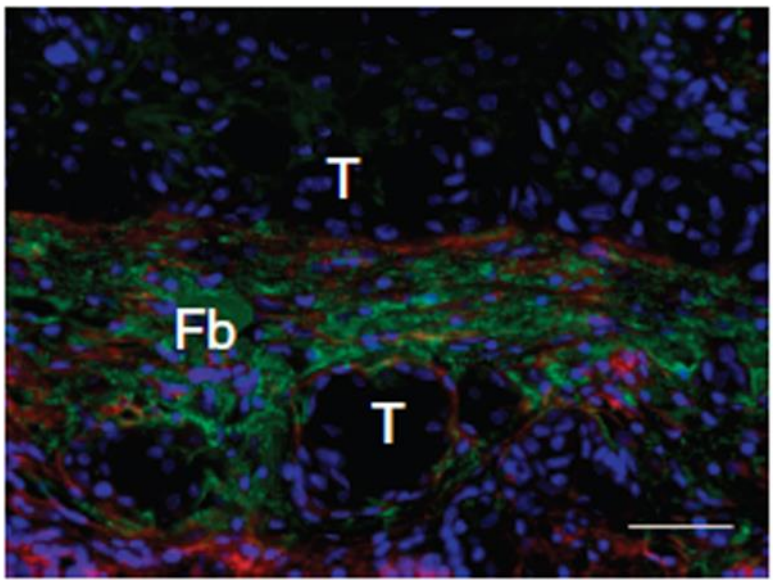

FIGURA 28: ÁCIDO HIALURÔNICO DE MELANOMA É PREDOMINANTEMENTE EXPRESSO POR CÉLULAS DO ESTROMA, *in vivo*. Ácido hialurônico em melanoma malígno é depositado principalmente no estroma rico em fibroblasto. Imagem de fluorescência de biopsia com HA *Binding Protein*-biotina detectada por estreptavidina-488 (em vermelho) e anti-CD90 como marcação dos fibroblastos por Cy3 (em verde). Fb = fibroblasto, T = tumor. ADAPTADO DE: WILLENBERG et al., 2012.

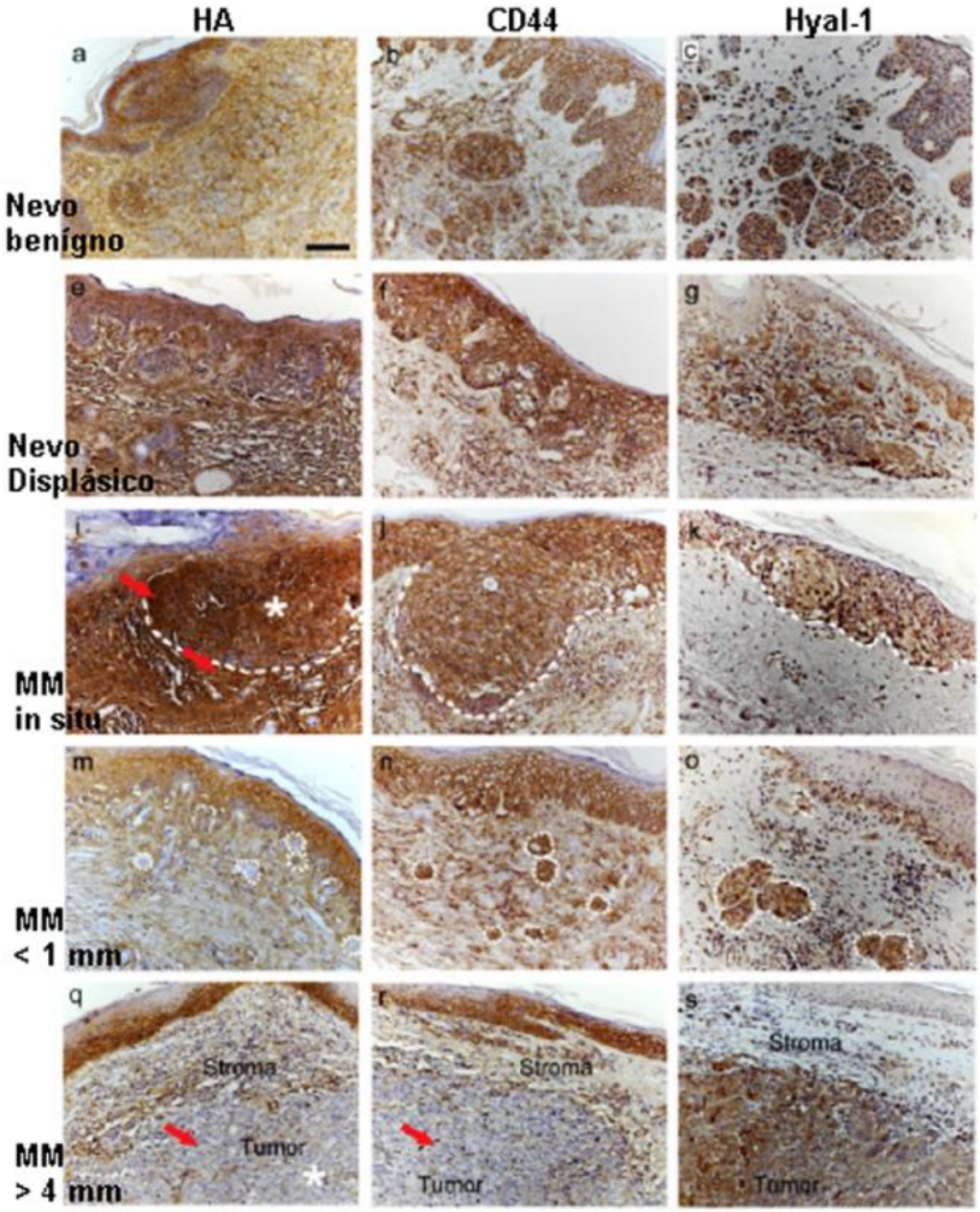

FIGURA 29: MARCAÇÕES DE ÁCIDO HIALURÔNICO, CD44 E HIALURONIDASE-1 DE NEVOS BENIGNOS (PINTAS COMUNS) À MELANOMAS PROFUNDOS. (a-c) nevos benignos (e-g) displasia (i-k) melanoma *in situ* (m-o) melanoma superficial (q-s) melanoma profundo. As flechas vermelhas indicam (i) o aumento de HA em melanócitos e estroma do tumor *in situ* (q) pontos de redução da marcação de HA e (r) a redução da marcação de CD44. Os asteriscos brancos indicam (i) marcação forte de HA nas células do melanoma *in situ*, enquanto em (q) demonstra a redução de HA em melanomas profundos. As linhas brancas (i-k) delimitam a fronteira entre as células tumorais e o estroma do tumor *in situ* e em (m-o) delimitam as células tumorais invasivas do tumor superficial. MM = melanoma malígno. A escala representa 100 µm. ADAPTADO DE: SIISKONEN et al., 2013.

8.3 ESTUDOS CLÍNICOS COM QUIMIOTERÁPICOS E HIALURONIDASES

Muitos tumores sólidos desenvolvem fibrose, resultado do que é chamado de reação desmoplásica, um aumento significativo na produção de proteínas da matriz extracelular, bem como uma grande proliferação de células do tipo miofibroblastos. O resultado é a formação de um tecido conjuntivo fibroso denso que é composto de vários componentes da matriz extracelular, incluindo colágeno dos tipos I, III, e IV, fibronectina, laminina, ácido hialurônico e osteonectina. Esse componente fibro-inflamatório do tumor (por vezes chamado de estroma) contribui para um aumento da pressão do fluido intersticial do tumor, bloqueando a perfusão de terapias para as células tumorais, contribuindo para a quimioresistência (WHATCOTT et al., 2011).

Em conjunto com agentes citotóxicos dirigidos contra as células tumorais, o alvo de componentes estromais vem ganhando destaque como uma potencial abordagem para o tratamento de pacientes e de superação da quimioresistência. As enzimas que degradam matriz extracelular têm sido propostas como agentes na degradação do estroma. No entanto, a sensibilidade a pHs e imunoreatividade de agentes que degradam a MEC, tais como as colagenases, tem sido um problema que tem limitado o estudo *in vivo*. Outro componente da MEC que tem sido alvo de degradação é o ácido hialurônico (OLIVE et al., 2010).

Como o HA atua como uma barreira molecular que impede a penetração de drogas a hipótese é que o tratamento com agentes que o degradam, tais como as HAases, pode ter o potencial de aumentar a penetração de fármacos através do estroma e, finalmente, até as células tumorais. Dado a importância do HA na MEC em tumores sólidos, é possível que a segmentação da matriz com HAases possa melhorar os resultados terapêuticos em pacientes com esse tipo de tumor (SIRONEN et al., 2011).

De fato, a adição de hialuronidases em quimioterápicos melhora o catabolismo de HA, e aumenta significativamente a eficácia dos medicamentos mesmo em tumores previamente considerados resistentes à quimioterapia. A eficácia de HAases para melhorar quimioterapias tem sido explorada para vários tipos de tumores incluindo de mama, cérebro, melanoma, e sarcomas. A hipótese do efeito sinérgico da adição desse

tipo de enzima em quimioterápicos é de que ela auxilie no tratamento do câncer através da redução da pressão intratumoral e/ou pela capacidade de quebrar a barreira molecular do HA em si (MINCHINTON et al., 2006).

Em modelos de cultura de células, a adição de HAase diminuiu a quimioresistência intrínseca de modelos de câncer que formam colônias (cólon, mama, e próstata, por exemplo), resultando em desagregação das células e aumento significante da penetração da droga e morte celular (KOHNO et al., 1994; WHATCOTT et al., 2011). O fato de que o pré-tratamento de HAase dentro do tumor pode aumentar a concentração da droga no mesmo (Figura 30) é particularmente interessante, uma vez que pode aumentar a eficácia de terapias já existentes (MINCHINTON et al., 2006; SIRONEN et al., 2011).

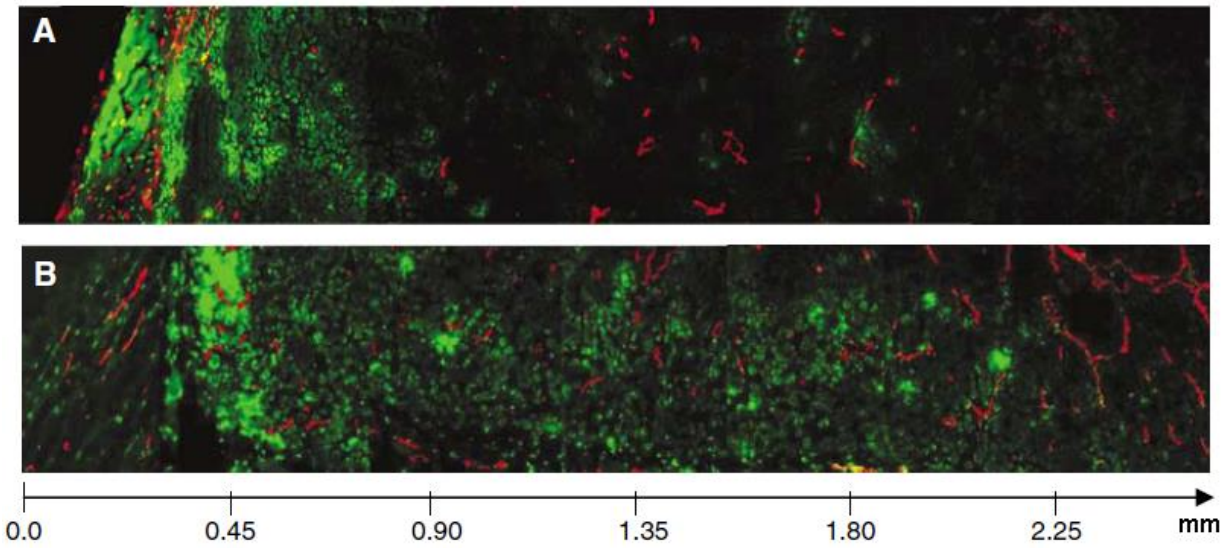

FIGURA 30: DISTRIBUIÇÃO DO QUIMIOTERÁPICO DOXORUBICINA (DOX) EM XENOTRANSPLANTES DE OSTEOSARCOMA. (A) Tratamento com lipossomos de Dox 16 mg/kg (B) Tratamento de Dox (16 mg/kg) com 1500 U de HAase. ADAPTADO de EIKENES et al., 2005.

Múltiplos estudos clínicos preliminares demonstraram um aumento da eficácia das terapias com o pré-tratamento de hialuronidase testicular bovina (HTB) em pacientes com câncer. Uma limitação dessa HAase como agente terapêutico foi o desenvolvimento de reações alérgicas para essa enzima, devido a sua origem bovina. A hialuronidase recombinante humana (Hylenex™) foi desenvolvida em anos recentes. O material recombinante humano eliminou também o risco de transmissão de doenças por meio de contaminantes encontrados nas enzimas derivadas de outros animais. O

FDA (*Food and Drug Administration*) aprovou o uso dela como adjuvante da dispersão e absorção de vários medicamentos injetados (YOCUM et al., 2007; KULTTI et al., 2012; SHPILBERG e JACKISCH, 2013).

Hialuronidases recombinantes estão sendo investigadas em diferentes formulações para o câncer superficial de bexiga (fase I / II, NCT00318643) e em pacientes com tumores sólidos (fase I, NCT00834704). Considerando o papel biológico do HA, os efeitos adversos do tratamento com HAases como parte de um regime prolongado anticâncer seria a indução de inflamação e dores nas articulações. Alguns desses efeitos colaterais foram controlados pela administração de corticosteróides ou pelo ajuste da dose utilizada (BAUMGARTNER et al., 1998; SIRONEN et al., 2011).

Devido à importância do ácido hialurônico e hialuronidases na progressão tumoral e tendo em mãos DHAase ativa, o intuito do trabalho foi verificar o efeito dessa enzima na dinâmica de células normais e cancerosas *in vitro*.

9 OBJETIVOS

9.1 OBJETIVO GERAL

Avaliar o efeito da ação de DHAase no comportamento de células de linhagem não maligna (RAEC) e de melanoma murino (B16F1 e B16F10).

9.2 OBJETIVOS ESPECÍFICOS

- Verificar o efeito que DHAase causa na dinâmica celular por meio de análise da morfologia em linhagem de célula endotelial de aorta de coelho (RAEC) e em linhagens celulares de melanoma murino B16F1 e B16F10;

- Avaliar se DHAase causa perda de viabilidade nas referidas linhagens tumorais de melanoma murino.

10 MATERIAIS E MÉTODOS

10.1 REAGENTES

As linhagens celulares de melanoma foram adquiridas da *American Type Culture Collection* (Rockville, MD). Os meios de cultura foram comprados pela Cultilab (Campinas, SP, Brasil) e o Soro Fetal Bovino pela LGC Biotecnologia (Cotia, SP, Brasil). Os sais de cristal violeta e MTT foram adquiridos da Merck (Darmstadt, Germany).

10.2 CONDIÇÕES DE CULTURA

RAEC (BUONASSISI e VENTER, 1976) foram cultivadas como cultura em monocamada com meio F12 contendo gentamicina (40 mg/L) suplementado com soro fetal bovino a 10% (SFB) . As culturas foram mantidas a 37°C numa atmosfera umidificada com 5% de CO_2. Após a contagem, as células foram ressuspensas em volume adequado de meio e 10^4 células foram plaqueadas por poço em placas de 96 poços e deixadas aderir e crescer durante 8 h sem soro. As células foram incubadas na presença de DHAase, veneno e controle negativo (enzima não relacionada com a hidrólise de HA e purificada sob as mesmas condições que DHAase). Os tratamentos foram realizados na concentração de 50 µg/mL. As alterações na morfologia celular foram avaliadas 4, 12, 16 e 24 h após a adição do tratamento e fotografadas (em 24 h) utilizando microscópio invertido (DMIL Leica, Wetzlar, Alemanha). B16F1 e B16F10 foram cultivadas em monocamada com meio DMEM contendo garamicina (40 mg/L) suplementado com SFB a 10%. As culturas foram mantidas em atmosfera apropriada e depois de contadas foram plaqueadas (10^4/poço) em microplaca (96 poços) e deixadas aderir antes do “tratamento”, por 24 h (para o ensaio de proliferação) e 8 h (para os demais ensaios). As células foram incubadas na presença de 25 ou 50 µg/mL de DHAase, 50 µg/mL do controle negativo (enzima purificada sob as mesmas condições) e 500 µg/mL de hialuronidase testicular bovina (HTB,Sigma) como controle positivo. Possíveis alterações morfológicas foram avaliadas em 4, 12, 16 e 24 h após o “tratamento”. As células foram fotografadas (em 16 ou 24 h) utilizando o microscópio

invertido. As concentrações utilizadas de DHAase foram escolhidas conforme a média de concentrações obtida após os redobramentos *in vitro*. Uma concentração dez vezes maior de HTB foi utilizada para que houvesse a extrapolação dos possíveis resultados observados com DHAase.

10.3 ENSAIO DE PROLIFERAÇÃO

O ensaio de cristal violeta é útil para obter informações quantitativas sobre a densidade relativa de células aderidas em placas de cultura. Ao final do período de incubação, e depois da remoção do meio de cultura, as microplacas foram lavadas com 100 µL de PBS por poço. Retirado o PBS, 100 µL de PFA 3% (paraformaldeído) foram colocados em cada poço e mantidos durante 10 minutos para que se iniciasse a fixação das células. Após, 100 µL de metanol 2% foi colocado em cada poço e incubado também por 10 minutos. Depois de fixadas, as células foram então coradas durante 10 minutos com 30 µL de Cristal Violeta 0,5% (em Metanol 20%). Os poços foram lavados exaustivamente com banho de água corrente em bandeja e o corante foi extraído com 100 µL de Citrato de Sódio 0,1 M (em Metanol 50%, pH 4,2). A leitura da absorbância foi realizada em 550 nm. O ensaio foi realizado em triplicata.

10.4 ENSAIO DE VIABILIDADE CELULAR

O ensaio com o brometo de 3-(4,5-dimetiltiazol-2-il)-2,5-difeniltetrazólio (MTT) é um ensaio colorimétrico que reflete a viabilidade celular. Este ensaio baseia-se na capacidade de células metabolicamente ativas reduzirem no meio intracelular o sal solúvel de tetrazólio dando origem à cristais de formazan, que é um produto de cor azul escura insolúvel em água (MOSMANN, 1983). Depois do tempo de tratamento com DHAase (50 µg/mL por 16 h) ou com os controles negativos (PBS/BSA ou 50 µg/mL de LALP1 inativa purificada sob as mesmas condições), o meio de cultura das células foi removido e as células foram incubadas com MTT em solução salina. As células foram incubadas com MTT 0,5 mg/mL durante 3-4 h a 37°C. Após o período de incubação a solução salina de MTT foi removida e os cristais insolúveis de formazan foram

dissolvidos em 100 µL de DMSO. A absorbância foi determinada em comprimento de onda de 550 nm. O ensaio foi feito em duplicata.

10.5 ANÁLISE ESTATÍSTICA

As análises estatísticas foram realizadas utilizando ANOVA (*One-way analyses of variance*) e o pós-teste Tukey. Elas estão representadas por médias, tendo o desvio padrão em barras. A significância estatística foi ajustada em $p<0,05$.

11 RESULTADOS

11.1 ENSAIO DE PROLIFERAÇÃO CELULAR EM CÉLULAS DE MELANOMA MURINO SOB A AÇÃO DE DHAase

O ensaio de cristal violeta foi escolhido para avaliar o efeito dos produtos gerados pela ação de DHAase na proliferação das células de melanoma murino B16F1 e B16F10.

Conforme pode ser visualizado na porção A da Figura 31, quando as células B16F1 foram expostas por 16 h com 50 µg/mL de DHAase, a proliferação dessas células aumentou significativamente em ~10% ($p<0,05$). Por sua vez, quando as células de B16F1 foram expostas a 500 µg/mL de HTB, a proliferação foi significativamente diminuída em ~42% ($p<0,001$).

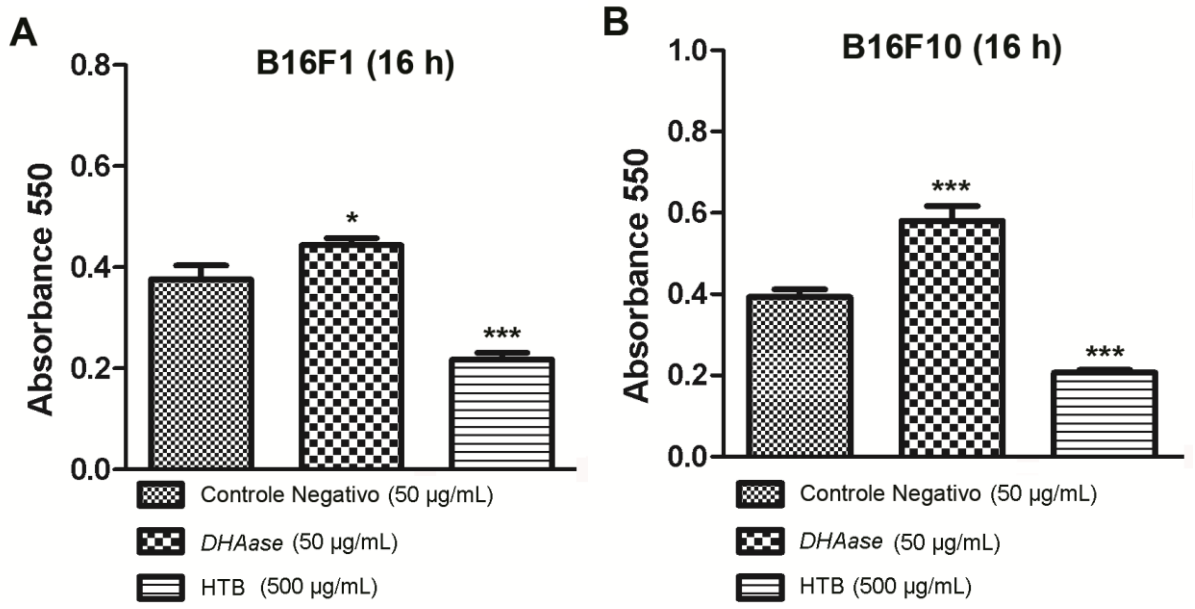

FIGURA 31: ENSAIO DE PROLIFERAÇÃO POR CRISTAL VIOLETA DE CÉLULAS DE MELANOMA MURINO EXPOSTAS À DHAase. (A) Células B16F1 plaqueadas em microplacas por 24 h sem soro e expostas com 50 µg/mL de DHAase por 16 h aumentaram significativamente sua proliferação quando comparado ao controle negativo. B16F1, sob as mesmas condições de cultivo, quando expostas a 500 µg/mL da HBT diminuíram significativamente sua proliferação quando comparado ao controle negativo.(B) B16F10 plaqueadas em microplacas por 24 h sem soro e expostas com 50 µg/mL de DHAase por 16 h, aumentou significativamente sua proliferação quando comparado ao controle. Nas mesmas condições de cultivo, quando B16F10 foi exposta com 500 µg/mL de HTB elas reduziram sua proliferação significativamente. *$p<0,05$; ***$p<0,001$.

De maneira semelhante, mas de forma mais pronunciada, quando a linhagem de melanoma murino B16F10 foi exposta por 16 h com 50 µg/mL de DHAase (Figura 31-

B), sua proliferação aumentou significativamente em ~45% ($p<0,001$). Quando as mesmas células foram expostas com 500 µg/mL da enzima bovina a proliferação diminui de maneira significativa em 47,5% ($p<0,001$).

11.2 MORFOLOGIA DE CÉLULAS CANCEROSAS E NÃO CANCEROSAS SOB A ATIVIDADE DE DHAase

Para a confirmação *in vitro* dos dados observados no ensaio macroscópico de dermonecrose e da histologia da derme de coelho (Capítulo I, Figuras 21 e 23), os quais demonstraram que o tratamento com DHAase sozinha não causou extravasamento do conteúdo intravascular, nem acúmulo de células inflamatórias; células de aorta de coelho (RAEC) foram incubadas com 50 µg/mL de DHAase. Como é demonstrado na Figura 32, as células de RAEC não sofreram nenhuma alteração morfológica quando foram tratadas com a hialuronidase recombinante (DHAase), comparado ao controle negativo. Por sua vez, quando as células foram tratadas com o veneno de *L.intermedia* sofreram desadesão e arredondamento após poucas horas de tratamento, como demonstrado na Figura 32-3 em 16 h.

Devido à impossibilidade técnica de aumentar a concentração utilizada de DHAase, a quantidade de horas de recuperação das células entre o plaqueamento e a exposição às enzimas foi reduzida de 24 para 8 h. Dessa maneira, proporcionalmente haveria menor quantidade de células de melanoma murino e de matriz extracelular quando comparado ao ensaio de proliferação. Na Figura 33 está demonstrada a alteração morfológica de células da linhagem B16F10 ao serem tratadas por hialuronidases. Conforme demonstrados no quadro A-2, com 25 µg/mL de DHAase depois de 16 h, as células estão sutilmente mais fusiformes. Nos quadros A-3 e B-2 correspondente a 50 µg/mL dessa enzima, pode ser visto que as células perderam sua morfologia normal, estando mais arredondadas ou fusiformes. Pode-se observar também que nessa concentração e tempo as células estão em menor quantidade quando comparado ao controle negativo. No quadro B-3 da mesma figura é visto que a HTB utilizada como controle positivo (500 µg/mL) causou um arredondamento proeminente e também a diminuição da quantidade de células de B16F10 observadas quando comparado ao controle.

Conforme demonstrado na Figura 34, DHAase e HTB após 24 h de tratamento modificaram a morfologia de B16F1, mas não houve diferença na morfologia quando a cultura foi observada em 16 h (dado não demonstrado). Conforme observasse na Figura 34-3, 500 µg/mL da enzima de origem bovina foi capaz de causar nesse horário, alteração morfológica e diminuição na quantidade celular observada quando comparado ao controle negativo.

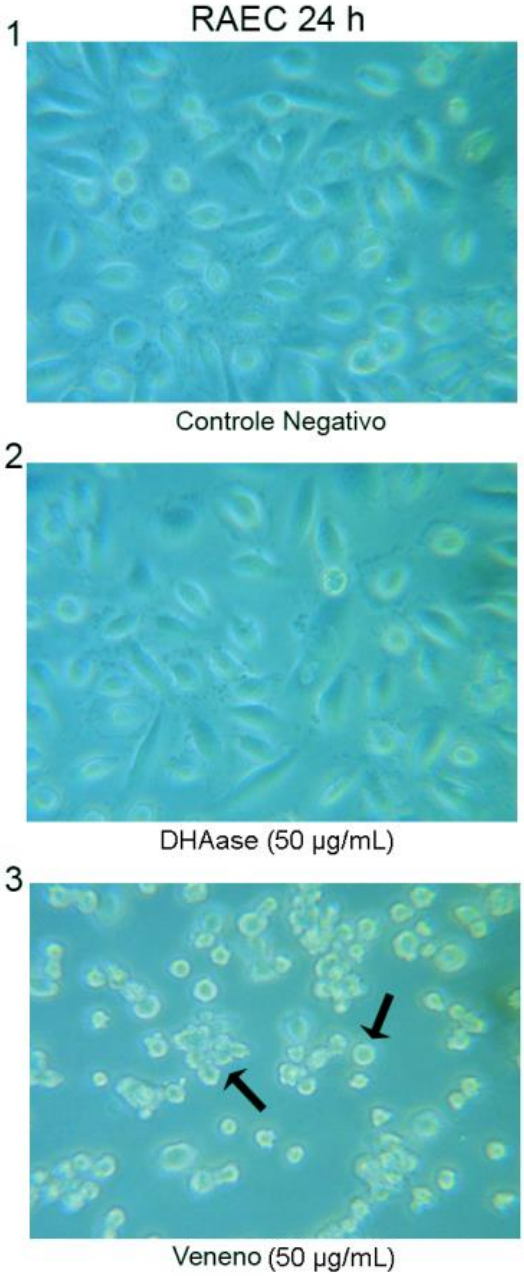

FIGURA 32: MORFOLOGIA DE CÉLULAS DE AORTA DE COELHO (RAEC) SOB A ATIVIDADE DE DHAase POR 24 HORAS. Oito horas depois de serem plaqueadas, o meio sem soro foi retirado e foram adicionados as enzimas e o veneno diluídos em meio de cultivo. Após 24 h de incubação a cultura foi fotografada em microscópio invertido. Em 1 temos o controle negativo no qual foi utilizado uma enzima sem atividade sobre HA (metaloprotease inativa, LALP1) e purificada nas mesmas condições que DHAase. Em 2 temos a incubação com 50 µg/mL de DHAase e em 3 com 50 µg/mL de veneno de *L. intermedia*. Somente o veneno causou o arredondamento e a desadesão da cultura (flechas) Aumento de 600x.

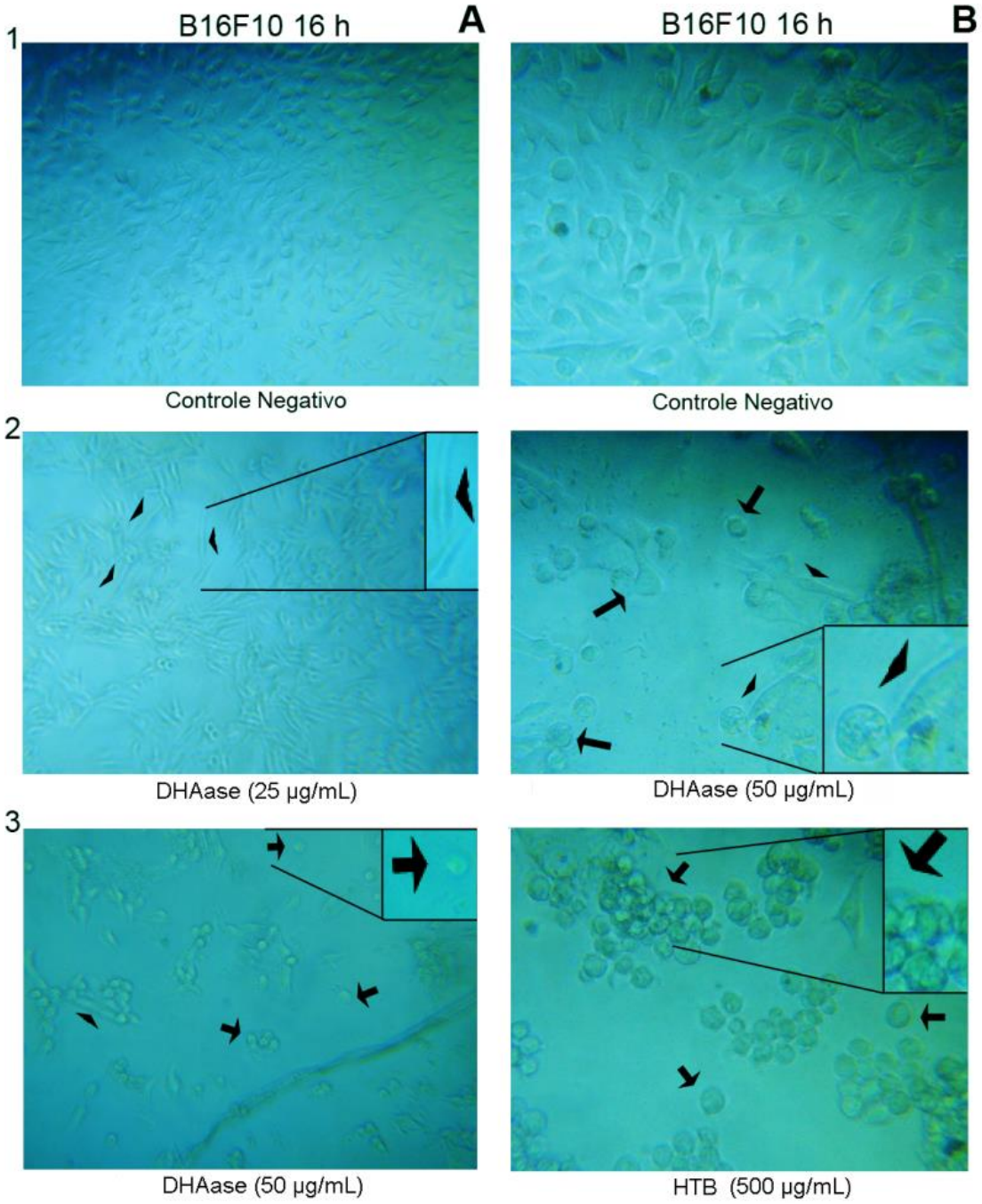

FIGURA 33: ALTERAÇÕES MORFOLÓGICAS DE CÉLULAS DE MELANOMA MURINO (B16F10) EXPOSTAS À DHAase POR 16 HORAS. Oito horas depois de serem plaqueadas, o meio sem soro foi retirado da cultura e foram adicionadas as enzimas diluídas em meio de cultivo. Após 16 h de tratamento a cultura foi fotografada em microscópio invertido. Controle negativo representa 50 µg/mL de uma enzima sem atividade sobre HA (LALP1 inativa) e purificada nas mesmas condições que a DHAase. Como controle positivo foi utilizado 500 µg/mL da HTB comercial. As enzimas DHAase e HBT ocasionaram a perda da morfologia normal (formato fusiforme apontado com ponta de seta, e com flechas, o arredondamento celular). Observa-se também a diminuição do número de células após 16 h, com o tratamento das hialuronidases quando comparado ao controle. Aumento de (A) 240x (B) 600x. Em destaque as alterações morfológicas com um aumento adicional de 4x.

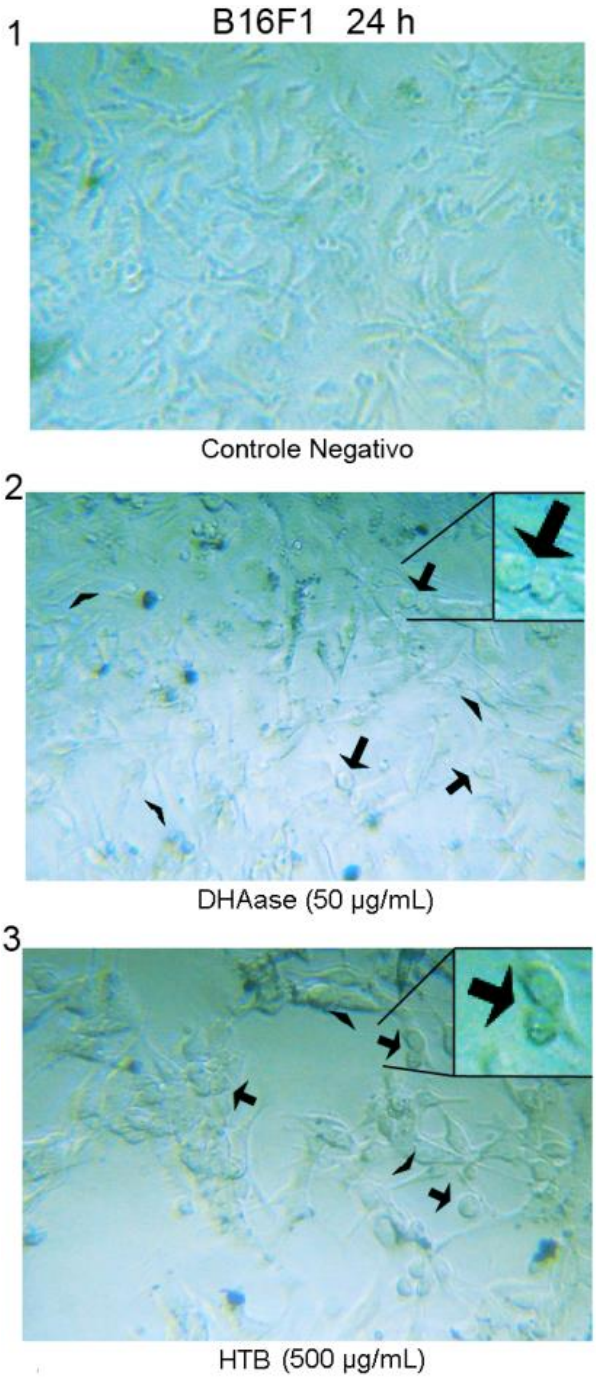

FIGURA 34: ALTERAÇÕES DE MORFOLOGIA DE CULTURA DE MELANOMA MURINO (B16F1) EXPOSTA Á DHAase POR 24 HORAS. Oito horas depois de serem plaqueadas, o meio sem soro foi retirado e foi adicionado o tratamento diluído em meio de cultivo. Após 24 h de tratamento a cultura foi fotografada em microscópio invertido. Em 1 temos o controle negativo no qual foi utilizado uma enzima sem atividade sobre HA (LALP1 inativa) e purificada sob as mesmas condições que a DHAase. Em 2 temos a incubação com 50 µg/mL de DHAase e em 3 com 500 µg/mL de hialuronidase testicular bovina. Somente após 24 h de tratamento foi possível constatar diferença morfológica em relação ao controle negativo. Nas flechas, o arredondamento celular e nas pontas de seta o formato fusiforme adquirido. Aumento de 600x. Em destaque, as alterações morfológicas com um aumento adicional de 4x.

11.3 ENSAIO DE VIABILIDADE CELULAR DE B16F10 SOB A AÇÃO DE DHAase

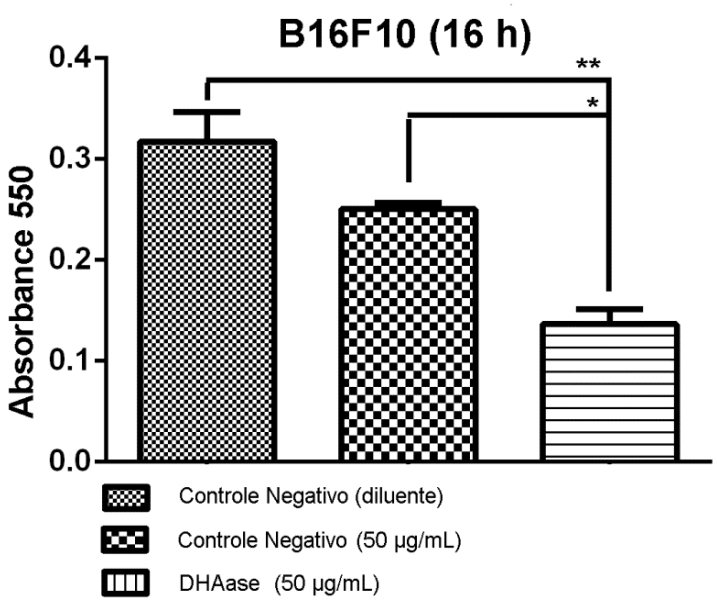

FIGURA 35: ENSAIO DE VIABILIDADE CELULAR POR MTT EM CULTURA DE B16F10 SOB A ATIVIDADE DE DHAase POR 16 HORAS. As células foram plaqueadas em microplacas e suplementadas com meio sem soro por 8 h. Após 16 h de incubação com DHAase ou controles, o ensaio de MTT foi desenvolvido. A absorbância foi lida em 550 nm. Como controle negativo da reação foi utilizado o diluente de DHAase (PBS/BSA) e LALP1 inativa purificada nas mesmas condições que DHAase (Controle Negativo). Houve diferença significativa entre a viabilidade das células tratadas com DHAase e os controles negativos. *$p<0,05$; **$p<0,01$.

Para avaliar a viabilidade das células de melanoma murino foi realizado o ensaio de MTT sob as mesmas condições do ensaio de morfologia. No ensaio de MTT, houve diferença significativa da viabilidade celular de B16F10 entre os controles negativos e DHAase (Figura 35). A viabilidade das células tratadas com DHAase comparada com o diluente foi significativa com $p<0,01$ e diminui cerca de 60%. A viabilidade das células tratadas com DHAase comparada com a proteína controle da purificação diminui em ~43% e foi também significativa, com $p<0,05$. Um maior número de replicatas será necessário para a confirmação desse dado e o mesmo ensaio deverá ser realizado em paralelo com a linhagem B16F1.

12 DISCUSSÃO

O estudo isolado das toxinas que compõem o veneno total das aranhas-marrons é um tanto limitado, uma vez que a quantidade de veneno obtido por aranha através de coleta por eletroestimulação é de poucos microlitros e geralmente contém de 65 µg a 100 µg de proteínas totais (FEITOSA et al., 1998; SAMS et al., 2001). Para a purificação das toxinas diretamente do veneno seriam necessários miligramas de veneno total para que fossem obtidos poucos microgramas da toxina de interesse. Tratando-se da fração acima de 40 kDa e mais especificamente de HAases, onde especula-se que a representatividade em massa dessa enzima dentre as toxinas é pequena, a purificação das enzimas nativas a partir do veneno seria ainda mais difícil (KALAPOTHAKIS et al., 2007; NAGARAJU et al., 2007; GREMSKI et al., 2010). Por essa razão optou-se por tentar estudar o papel das HAases do veneno de *L. intermedia* através de sua forma recombinante.

E. coli foi o primeiro sistema utilizado para expressão de proteínas recombinantes e, atualmente, continua sendo o sistema de expressão heteróloga mais utilizado (SAHDEV et al., 2008). Isso porque, os métodos utilizados para expressão em *E. coli* são simples, rápidos e não são caros. Quando essas bactérias são cultivadas em alta densidade, possibilita a produção em larga escala da proteína de interesse (SAHDEV et al., 2008; BRONDYK, 2009). As cepas de *E. coli* para expressão de proteínas recombinantes apresentam algumas características específicas, como, deficiência na produção de proteases e manutenção da estabilidade dos plasmídeos de expressão (SORENSEN e MORTENSEN, 2005). A cepa BL21(DE3) pLysS é uma das cepas mais comuns de *E. coli* e algumas toxinas de *Loxosceles* já foram expressas nessa cepa (CHAIM et al., 2006; DA SILVEIRA et al., 2006; DA SILVEIRA et al., 2007b; APPEL et al., 2008; KUSMA et al., 2008; SADE et al., 2012). Por esses motivos, foi a cepa escolhida para se iniciar a expressão de DHAase.

Outra cepa de *E. coli* utilizada foi a AD494(DE3). Essas bactérias apresentam deficiência em proteínas redutoras, como a tioredoxina trxB, tornando o ambiente citoplasmático menos redutor, o que favorece a formação de pontes dissulfeto. A cepa SHuffle T7 Express LysY foi também utilizada como modelo de expressão para

DHAase, visto que essa enzima possivelmente possui pontes dissulfeto. Essa cepa tem como característica o citoplasma menos redutor, por ser deficiente em glutaredoxina e tioredoxina, além de possuir uma dissulfeto isomerase que atua como uma chaperona no citoplasma, auxiliando no dobramento correto de proteínas recombinantes (LOBSTEIN et al., 2012).

Todas as cepas utilizadas foram hábeis em expressar a DHAase, mas falharam em expressá-la de maneira solúvel. É descrito um aumento na solubilidade de proteínas recombinantes quando essas são expressas em baixas temperaturas, pois interações hidrofóbicas para formação de corpos de inclusão são dependentes dessa grandeza física. Dessa forma, baixas temperaturas aumentariam a estabilidade e os padrões corretos de dobramento proteico (SAHDEV et al., 2008). Foram realizadas expressões da DHAase em temperaturas de 22°C e 16°C para as cepas BL21(DE3)pLysS e AD494(DE3), entretanto, as proteínas ainda foram expressas formando corpos de inclusão. No caso da expressão em SHuffle foi utilizado o plasmídeo pET-SUMO. Esse plasmídeo tem como característica uma pequena ubiquitina modificada (SUMO) para aumentar a solubilidade da proteína a ele fusionada. Porém, a hialuronidase recombinante não se encontrou solúvel também nesse modelo de expressão.

Até 2009, 10% das proteínas eucarióticas que já foram expressas em *E. coli* foram produzidas na forma solúvel (BURGUESS, 2009). Isso demonstra que a obtenção de proteínas recombinantes na forma solúvel e ativa é uma tarefa árdua. Nesse contexto, vale ressaltar que não existem muitos trabalhos na literatura sobre a atividade de HAases recombinantes de venenos (NG et al., 2005; SKOV et al., 2006), em especial de aranhas (CLEMENT et al., 2012; FERRER, et al., 2013). A atividade da hialuronidase recombinante do veneno de tarântula (BvHyal) foi obtida através da expressão em *Baculovirus*, um sistema de expressão em células de inseto (CLEMENT, et al., 2012).

Como as expressões em procariotos falharam em obter a DHAase em sua forma solúvel, optou-se pela alternativa do redobramento *in vitro*, antes de tentar a expressão em eucariotos. No que diz respeito à técnica de redobramento *in vitro*, a influência do pH e aditivos na solução em que a proteína insolúvel será redobrada é essencial para o

sucesso da técnica. O tampão no qual uma proteína consegue o redobramento de sua forma insolúvel para a solúvel é muito exato (DECHAVANNE et al., 2011; BURGESS et al., 2009), sendo que qualquer variação de concentração de algum aditivo pode ser crucial para a eficiência do método.

Para o redobramento químico, as proteínas de interesse são geralmente purificadas por cromatografia de afinidade em condições desnaturantes ou alternativamente o sedimento bacteriano é lavado utilizando desnaturantes fracos, conseguindo-se uma pureza da proteína de interesse de mais de 80% (BURGESS et al., 2009). É comum também, a purificação ser feita por cromatografia após o processo de redobramento, o que tem a vantagem de eliminar possíveis multímeros formados (BAI e GENG, 2011, HOFINGER et al., 2007; BURGESS et al., 2009; SINGH e PANDA, 2005). Como a DHAase apresentou dificuldades de ligação em resina Ni-NTA mesmo em condições desnaturantes e a enzima purificada por eletroeluição não foi redobrada de forma ativa; optou-se por fazer a lavagem dos corpos de inclusão com posterior solubilização em agente caotrópico forte e redobramento por diluição lenta. Como demonstrado nos resultados, as lavagens dos corpos de inclusão permitiram uma pureza de mais de 80%. O tampão de redobramento para DHAase foi padronizado contendo glutationas, L-arginina e BSA na sua composição. Não se sabe ao certo qual é o mecanismo pelo qual a arginina e o BSA atuam no redobramento proteico, mas acredita-se que a arginina forme estruturas supramoleculares negativas impedindo a agregação proteica e que a albumina, compete com as HAases para formar complexos eletrostáticos inativos com o HA. Essa competição induziria HAases livres o que resultaria em um aumento na taxa de hidrólise das mesmas (IGNATOVA e GIERASCH, 2006; LENORMAND et al., 2008). Ainda com relação à albumina, uma HAase recombinante de abelha foi expressa de maneira ativa fusionada à albumina de soro humano (HSA) em modelo de levedura *Picchia pastoris*. Esses autores também comentam que proteínas oriundas do soro têm sido fusionadas a diversas proteínas para uso biotecnológico, muitas vezes aumentando à meia-vida desses produtos (REITINGER et al., 2008).

A forma ativa de DHAase foi obtida após a técnica de redobramento *in vitro* e essa atividade foi demonstrada tanto sobre HA como C4S purificados. Esses

resultados estão de acordo com dados anteriores nos quais foi utilizado o veneno, ou seja, as HAases nativas (DA SILVEIRA et al., 2007a).

A atividade hidrolítica encontrada entre 29-45 kDa nos ensaios de zimograma copolimerizados com HA ou C4S corrobora com a atividade degradativa dos glicosaminoglicanos purificados visualizados em géis de agarose. A atividade nos zimogramas sugere estabilidade no dobramento da DHAase. Mais uma vez, os resultados mostram que a DHAase também pode ser considerada uma condroitinase, conforme relatado para as enzimas nativas (BARBARO et al., 2005; DA SILVEIRA et al., 2007a).

A caracterização da reatividade cruzada entre a DHAase e as HAases nativas do veneno de *L. intermedia* mostrou que o veneno contém proteínas que têm identidade antigênica (epítopos sequenciais) com DHAase, visto o soro produzido com essa ter sido capaz de reagir com o veneno. Duas bandas de proteínas no veneno foram reconhecidas pelo soro anti-DHAase, corroborando com resultados anteriores que mostram duas zonas líticas em experimentos de zimografia usando o veneno total. Essas bandas provavelmente correspondem a duas isoformas (no mínimo) de HAases presentes no veneno de *L. intermedia* (BARBARO et al., 2005, DA SILVEIRA et al., 2007a). Adicionalmente, o soro antiveneno reagiu de forma cruzada com a DHAase, sugerindo que a glicosidase recombinante mantém determinantes antigênicos lineares das enzimas nativas. Dessa forma, o antisoro da DHAase ou os anticorpos purificados a partir desse, podem ser uma ferramenta biológica na terapia do loxoscelismo ou para fins de investigação. Essa reação cruzada é observada também para outras enzimas do veneno, como fosfolipases-D e metaloproteases (DA SILVEIRA et al., 2007b; TREVISAN-SILVA et al, 2010).

Hialuronidases estão presentes em vários tecidos e estão envolvidas em importantes eventos biológicos, incluindo o desenvolvimento embrionário, inflamação, fertilização, metástase de células tumorais, patogênese bacteriana e envelhecimento. Hialuronidases têm sido descritas também em vários venenos (KEMENI et al., 1984, DECHAVANNE et al., 2011, KUMAR et al., 2011) atuando como "fator de espalhamento" por degradar HA e CS e tornar as regiões circundantes ao local da picada mais permeáveis, facilitando a difusão de outras toxinas dos venenos por todo o

corpo das vítimas (KREIL et al., 1995, KUMAR et al., 2011). Uma HAase isolada a partir do veneno da aranha “funnel web” foi capaz de aumentar a atividade de outras toxinas. Esse trabalho está de acordo com a hipótese de que HAases aumentam a toxicidade do envenenamento (GIRISH et al., 2005a).

Esse tipo de enzima foi descrito há muitos anos no veneno de várias espécies de *Loxosceles*, caracterizando um evento conservado e sugerindo significância biológica no ciclo de vida dessas aranhas (BARBARO et al., 2005). Depois de obtermos a DHAase solúvel e ativa, conforme demonstrado por experimentos *in vitro*, o objetivo se tornou avaliar o papel das HAases do veneno de aranha-marrom no desenvolvimento dos sintomas e sinais clínicos relatados após as picadas. Para tal, foi utilizado o ensaio de dermonecrose em derme de coelho.

No que diz respeito às HAases do veneno de aranha-marrom, extrapolando a propriedade de difusão, essas enzimas seriam as principais responsáveis pela propagação de toxinas do local da picada para a circulação sistêmica (FUTRELL, 1992; DA SILVA et al., 2004; DA SILVEIRA et al., 2007a). Dados da literatura relataram sinais de intoxicação sistêmica após as picadas de *Loxosceles*, incluindo vômitos, febre, anemia hemolítica, trombocitopenia, coagulação intravascular disseminada e nefrotoxicidade (FUTRELL, 1992; KUSMA et al., 2008; LUCATO et al., 2011). Além disso, a HAase do veneno de aranha-marrom é sugerida desempenhar um papel importante nas lesões cutâneas após as picadas, tal como descrito para as HAases de outros venenos (NAGARAJU et al., 2007; FENG et al., 2008).

A exposição experimental do veneno de *L.intermedia* na pele de coelhos mostrou que o veneno degrada tanto o HA de tecido conjuntivo quanto o HA periférico aos vasos sanguíneos da derme (DA SILVEIRA et al., 2007a). Por perturbar a estrutura da matriz extracelular, as HAases poderiam influenciar a estabilidade das paredes dos vasos sanguíneos no local da picada. Esses eventos aumentariam a disseminação das outras toxinas do veneno aumentando a área das lesões cutâneas após as picadas de aranha-marrom e contribuiria para a disseminação sistêmica. Corroborando com as idéias descritas acima, o nosso trabalho demonstrou que DHAase foi capaz de facilitar a propagação da fosfolipase-D a partir do local de injeção na pele de coelho. A sugestão é que essa enzima degrade HA e C4S também *in vivo.* A permeabilidade

capilar e o aumento da toxicidade sistêmica *in vivo* causada por DHAase em associação com outras toxinas são ainda tópicos a serem avaliados.

Outro sintoma típico do loxoscelismo é o espalhamento gravitacional das lesões na pele que aparecem algumas horas após a picada ou envenenamento experimental de modelos animais (FUTRELL, 1992; DA SILVA et al., 2004; CABRERIZO et al., 2009). O mecanismo pelo qual o veneno de *Loxosceles* causa essa propagação gravitacional da necrose não é totalmente compreendido. Inoculação experimental de toxina dermonecrótica recombinante (fosfolipase-D, com atividades não-proteolítica ou glicolítica), já provoca um espalhamento da lesão dermonecrótica na pele de coelhos (DA SILVEIRA et al., 2006; APPEL et al., 2008; VUITIKA et al., 2013). Porém, observamos que a DHAase aumentou a área lesionada quando comparado à lesão induzida pela fosfolipase-D recombinante sozinha. Nos resultados histopatológicos para as amostras do tecido exposto à toxina dermonecrótica recombinante, como esperado, observou-se a presença de infiltrado de células polimorfonucleares, desorganização das fibras de colágeno e sinais de edema, como por exemplo, o espessamento do tecido (APPEL et al., 2008, CHAIM et al., 2011b). No entanto, quando foram analisadas as amostras de tecidos tratados com LiRecDT1 e DHAase, observou-se que esses efeitos inflamatórios foram bem mais intensos. Sugerimos que DHAase tornou o tecido conjuntivo mais permeável e permitiu uma maior ação da fosfolipase-D. Pela primeira vez na literatura resultados experimentais mostram que as HAases do veneno de *Loxosceles* são, de fato, um "fator de espalhamento" desse veneno.

Além de contribuir para uma melhor compreensão da patogênese do loxoscelismo, DHAase pode ser uma ferramenta importante para fins biotecnológicos futuros (SENFF-RIBEIRO et al., 2008, CHAIM et al., 2011a). Uma vez que HAases estão envolvidas em processos fisiológicos e patológicos (GIRISH e KEMPARAJU, 2007) como patogênese de bactérias, propagação de toxinas e venenos, fertilização e progressão de tumores malígnos (MENZEL e FARR, 1998; SHUSTER et al., 2002, BOTZKI et al., 2004; CHAO et al., 2007). Curiosamente, uma HAase recombinante do veneno do escorpião *Buthus martensi* (BmHYA1) regulou para uma menor expressão de CD44 numa linhagem celular de câncer de mâma (MDA-MB). Esse resultado sugere

que variantes de células cancerosas podem ser moduladas por tratamento de HAases de veneno (FENG et al., 2008).

Além disso, essas enzimas podem promover o contato direto entre patógenos e a superfície das células hospedeiras. Despolimerização de HA também afeta a dinâmica da matriz extracelular e prejudica a sua atividade como um reservatório de fatores de crescimento, citocinas e enzimas envolvidas na transdução de sinal. A inibição da degradação de HA, por conseguinte, pode ser importante na redução da progressão de doenças inflamatórias e na redução de agentes patogênicos (SENFF-RIBEIRO et al., 2008; GREMSKI et al., 2010).

Inibidores de HAases são potentes agentes reguladores que estão envolvidos na manutenção do equilíbrio entre o anabolismo e catabolismo de HA. Inibidores de HAases podem servir como contraceptivo, uma vez que essas enzimas estão envolvidas na fertilização de ovócitos de mamíferos. Outra aplicação possível dos inibidores de HAases seria como agentes antitumorais (SHUSTER et al., 2002; GIRISH e KEMPARAJU, 2007; BENITEZ et al., 2011), antibacterianos (BOTZKI et al., 2004; YADAV et al., 2009) e antivenenos (DA SILVEIRA et al., 2007a, CHAIM et al., 2011).

Para melhor entender o efeito que uma HAase de veneno exógena teria no comportamento de células cancerosas, o nosso trabalho teve como propósito analisar a dinâmica de células de melanomas (B16F1 e B16F10) comparando-a à de uma linhagem de célula normal (RAEC) após exposição com DHAase.

Afinal, muito se tem estudado para aumentar a sobrevida e qualidade de vida de pacientes que possuem câncer (ABRAHAM e GIBBONS, 2007; GURSKI et al., 2009; SHINDOH et al., 2013) e um fator que contribui para a mortalidade de vários tipos de tumores é o espalhamento desses através do organismo do paciente, processo conhecido como metástase (BOGENRIEDER e HERLYN, 2003). O interesse sobre HA e HAases em câncer tem crescido consideravelmente nos últimos anos (LAURICH et al., 2004; DICKINSON et al., 2010; WHATCOTT et al., 2011; TIAN et al., 2013). Entender melhor os mecanismos de carcinogênese pode possibilitar tentativas de terapias mais eficientes (GURSKI et al., 2009; EDWARD et al., 2010).

De um modo geral para os tumores, quanto maior a quantidade de HA e maior a expressão de HAases e HAS, maior a agressividade do câncer (LAURICH et al., 2004;

BOUGA et al., 2010; EDWARD et al., 2010). Para os melanomas, a quantidade de HA está aumentada durante as fases iniciais de invasão e têm-se demonstrado que o aumento da produção dessa molécula está correlacionado com aumento da motilidade das células de melanoma. Por sua vez em tumores mais profundos e invasivos, a quantidade de HA e CD44 parece estar diminuída nos melanomas, enquanto que, a expressão de Hyal-1 sofre redistribuição no tecido e a de Hyal-2 está aumentada (SIISKONEN et al., 2013).

Embora haja indícios que a maior quantidade de HA do melanoma seja secretada por fibroblastos (WILLENBERG et al., 2011), o intuito foi primeiramente avaliar o comportamento de células de melanoma em cultura simples e não em co-cultura com fibroblastos. Duas linhagens de melanoma murino foram utilizadas: uma potencialmente mais metastática (B16F10) (FIDLER, 1975) e outra, menos metastática (B16F1).

Em termos gerais, a atividade aumentada de HAases está envolvida com uma maior motilidade de células metastáticas e em vários tipos celulares, fragmentos de HA de baixa massa molecular estão relacionados com uma maior proliferação celular (TIAN et al., 2013). No ensaio de proliferação desenvolvido verificou-se que quando as células foram tratadas com 50 µg/mL de DHAase a proliferação celular aumentou significativamente tanto na linhagem de B16F1, quanto na de B16F10. Sendo que o efeito mais pronunciado foi visto na linhagem mais metastática. Quando as células de melanoma murino, por sua vez, foram tratadas com uma concentração dez vezes maior de HAase recombinante (500 µg/mL de HTB) o efeito observado foi contrário, houve uma diminuição significativa da proliferação celular em ambas as linhagens. Pode se supor que em uma menor concentração de hialuronidase haja principalmente a formação de HA de baixa massa molecular e esse aumente a proliferação celular. Por outro lado, quando é usada uma concentração dez vezes maior de hialuronidase, haja a formação de oligossacarídeos e esses, por sua vez, diminuam a proliferação celular (GHATAK et al., 2002).

Esses resultados corroboram com um trabalho que demonstra que em concentrações altas (maiores que 320 µg/mL), oligômeros de HA inibiram a proliferação celular de B16F10 em 90%. Quando a concentração de oligômeros foi menor que 160

μg/mL a proliferação das células foi estimulada. Em modelo *in vivo* os oligômeros em alta concentração foram capazes de inibir o crescimento do tumor em 85% (ZENG et al., 1998; GHATAK et al., 2002).

Na observação da morfologia das células de melanoma realizada, em ambas as linhagens de melanoma na presença de DHAase houve a perda da morfologia normal, com as células tornando-se fusiformes ou arredondas. Para a linhagem B16F10 também se notou que após o tratamento com DHAase as culturas tinham menor quantidade de células, visualmente. Pôde-se observar que em B16F1 o efeito da ação de DHAase foi menor do que em B16F10, uma vez a alteração morfológica naquela linhagem só ter sido observada após 24 h de tratamento e de maneira menos acentuada.

O ensaio de proliferação e de morfologia sugerem uma maior dependência ao HA de células com maior potencial metastático. Dados da literatura vêm ao encontro dessa observação. Sabe-se que as células mais metastáticas possuem maior quantidade de HA na superfície celular (LAURICH et al., 2004). Em células de melanoma a quantidade de HA pericelular em B16F10 é maior do que em B16F1 (TURLEY e TRETIAK, 1975). Além disso, quando células de câncer de colón (de uma linhagem mais e outra menos metastática) foram incubadas previamente com HAase antes de um ensaio de adesão, as células mais metastáticas aderiram significativamente menos enquanto que a outra linhagem não alterou a sua aderência ao substrato (LAURICH et al., 2004).

Diversos trabalhos demonstram também que células normais são resistentes à adesão em superfícies contendo HA, ao passo que, células cancerosas se aderem preferencialmente nessas superfícies (BARBUCCI et al., 2005; KHADEMHOSSEINI et al., 2007; DICKINSON et al., 2010). Corroborando com esses trabalhos observou-se que células normais de aorta de coelho não sofreram qualquer alteração com o tratamento de DHAase. No entanto, quando o tratamento foi feito com o veneno houve o arredondamento e desadesão das mesmas. Tal fato demonstra que a adesão de RAECs é mais dependente de moléculas de matriz que são substratos de outras enzimas do veneno, como por exemplo, serinoproteases e metaloproteases (DA SILVEIRA et al., 2007c). Esse dado corrobora também com as observações *in vivo* do

ensaio de dermonecrose, no qual com a injeção de DHAase sozinha na derme dos coelhos não houveram alterações das células endoteliais dos vasos sanguíneos com sinais de inflamação e/ou hemorragia (FERRER et al., 2013).

No ensaio de proliferação o efeito sofrido pelas células de melanoma murino foi dependente da proporção quantidade de células:hialuronidase. Em uma menor concentração de hialuronidase observou-se o aumento da proliferação celular, ao passo que, em uma maior concentração de hialuronidase o efeito foi o oposto. Essas observações corroboram com os resultados obtidos na morfologia das células e no ensaio de MTT. Nesses últimos ensaios, as células foram deixadas aderir em microplaca por 8 h antes da ação de DHAase, e no ensaio de proliferação, 24 h. Consequentemente há uma menor quantidade de células e matriz extracelular em cada réplica nos ensaios de viabilidade e morfologia do que no ensaio de proliferação, mesmo que a quantidade inicial de células plaqueadas tenha sido a mesma. Como consequência foi observado que após o tratamento de 16 h, no ensaio de viabilidade e morfologia, 50 µg/mL de DHAase já foram suficientes para que as células tivessem sinais de sofrimento e perda da viabilidade. Enquanto que no ensaio de proliferação, nessa concentração de DHAase houve o aumento da proliferação celular. Conforme mencionado anteriormente, com uma menor concentração de hialuronidase haveria a formação de HA de baixa massa molecular e com uma maior concentração dessa enzima haveria a formação de oligossacarídeos, o que resultaria em efeitos opostos sobre a dinâmica celular. Sendo assim, torna-se necessário a padronização dos tempos prévios e após a incubação das enzimas entre os diferentes ensaios, bem como, a utilização da mesma concentração entre DHAase e HTB.

A obtenção de resultados paradoxos, nesse caso, sugere uma resposta dependente da quantidade e do tamanho dos fragmentos gerados de HA, além da influência do ambiente local (FUCHS et al., 2013). Ácido hialurônico de baixa massa molecular tem efeitos estimulantes sobre a angiogênese e proliferação de alguns tipos celulares, processos essenciais para o crescimento e progressão do tumor. No entanto, a administração de oligômeros para vários tipos de tumores inibem ao invés de estimular o crescimento tumoral. Há a hipótese de que os oligômeros de HA competem com o HMWHA na interação com CD44 e que diferentes tamanhos de HA tenham

afinidades diferentes por esse receptor (GHATAK et al., 2002). Portanto, o microambiente do tumor desempenha um papel importante no desenvolvimento e progressão do câncer. A interação entre as células cancerosas e esse microambiente parece ser essencial para o crescimento do tumor primário e sua progressão (FUCHS et al., 2013).

Neste trabalho, com a obtenção de DHAase solúvel e ativa se comprovou que HAases do veneno de *L.intermedia* são de fato “fatores de espalhamento” desse veneno. Porém, novos questionamentos dentro do loxoscelismo são possíveis a partir de tal fato. As HAases são essenciais para o aumento da toxicidade sistêmica no envenenamento de *Loxosceles*? A utilização do soro anti-DHAase pode atenuar o loxoscelismo cutâneo e/ou sistêmico? A resolução de estruturas tridimensionais de DHAase seria útil em desenvolver novos inibidores para essa classe de enzimas? Quantas isoformas de HAases o veneno de *L.intermedia* possui? E outros venenos loxoscélicos? Adicionalmente, o conjunto de resultados preliminares obtidos nesse trabalho sugere que DHAase foi útil em estudar o catabolismo do HA e o seu efeito em células de melanoma em cultura. Essa enzima teria os mesmos efeitos em melanoma *in vivo*? Ou ainda, em outros tipos de cânceres ou outras patologias que envolvam HA? Diversas abordagens experimentais deverão ser realizadas para a tentativa de respota desses questionamentos e assim, para um maior conhecimento molecular do veneno loxoscélico, do loxoscelismo e das possíveis aplicações biotecnológicas de DHAase.

13 CONCLUSÕES

O presente estudo permitiu a expressão de uma isoforma de hialuronidase do veneno de *L.intermedia* em diversas cepas de *E.coli*. *Dietrich´s Hyaluronidase* (DHAase), como foi chamada essa isoforma, foi expressa em todas as concentrações de indutor utilizadas e em todas as temperaturas testes em *E.coli* BL21(DE3)pLysS, AD494 (DE3) e Shuffle T7 Express Lys Y. Porém, nas cepas bacterianas utilizadas a enzima foi expressa de maneira insolúvel.

Somente após a purificação da mesma por meio de lavagem dos corpos de inclusão produzidos em BL21(DE3)pLysS e padronizando tampões para o *refolding* é que a enzima adquiriu sua forma solúvel e ativa. O tampão de escolha para o redobramento *in vitro* de DHAase teve em sua composição glutationas, L-arginina e BSA, sugerindo que a não agregação proteica e a formação de pontes dissulfeto são essenciais para sua atividade.

Dietrich´s Hyaluronidase demonstrou atividade sobre HA e C4S em ensaios de cinética e zimografia, perfil semelhante ao observado para as nativas do veneno. Durante esse trabalho também foi desenvolvido anticorpos policlonais que reconheceram tanto a DHAase, como as glicosidases nativas do veneno de *L.intermedia,* os quais poderão ser utilizados em estudos posteriores.

A DHAase foi capaz de aumentar os efeitos de edema, eritema, equimose, infiltração de células inflamatórias, deposição de fibrina e necrose desenvolvidos por uma toxina dermonecrótica recombinante (LiRecDT1) em pele de coelho *in vivo*. Dessa maneira, a hipótese de que as HAases do veneno de *L.intermedia* são “fatores de espalhamento” desse veneno, intensificando o efeito das demais toxinas, pôde ser comprovada.

Utilizando a DHAase ativa (50 µg/mL), como ferramenta de estudo do comportamento de células normais e cancerosas, foi demonstrado que essa enzima não alterou a morfologia e adesão de células endoteliais de aorta de coelho (RAEC). Por outro lado, essa HAase recombinante foi capaz de aumentar significativamente a proliferação celular e alterar a morfologia das linhagens de melanoma murino (B16F1 e B16F10). Essas células ficaram mais fusiformes e arredondadas e pôde-se observar

uma menor quantidade, visualmente, de células na cultura de B16F10. Essa linhagem potencialmente mais metastática teve os efeitos mais pronunciados com a exposição à DHAase. Foi visto ainda que as células de B16F10 perderam sua viabilidade de maneira significativa quando tratadas com essa enzima. Em conjunto esses dados sugereriram que quanto mais próximo um tipo celular é do normal, menores são os efeitos sofridos pela ação de DHAase.

Através da utilização de uma hialuronidase testicular bovina (HTB) em uma concentração dez vezes maior que DHAase, relacionando o tempo de incubação das células de melanoma antes da exposição às HAases com o efeito sofrido pela exposição às enzimas recombinantes inferiu-se também que a proporção célula:hialuronidase pode modificar o tipo de comportamento das células de melanoma murino. Sendo assim, a padronização das concentrações das enzimas e dos tempos entre os ensaios deverão ser realizados a fim de resultados mais conclusivos.

Por fim, nesse trabalho foi demonstrado que DHAase solúvel e ativa foi uma ferramenta para um melhor entendimento sobre a patologia do loxoscelismo e que essa enzima recombinante pode ser utilizada para se estudar outros processos patológicos que envolva o metabolismo de HA, como o câncer.

REFERÊNCIAS

ABRAHAM, R.T.; GIBBONS, J.J. The mammalian target of rapamycin signaling pathway: twists and turns in the road to cancer therapy. **Clin Cancer Res**, v. 13, n. 11, p. 3109–14, 2007.

AHRENS, T.; ASSMANN, V.; FIEBER, C.; TERMEER, C.; HERRLICH, P.; HOFMANN, M.; SIMON, J.C. CD44 is the principal mediator of hyaluronic-acid-induced melanoma cell proliferation. **J Invest Dermatol**. v. 116, n. 1, p. 93-101, 2001.

AMERICAN CANCER SOCIETY. **Cancer Facts & Figures 2009**. American Cancer Society. Disponível em < http://www.cancer.org/research/cancerfactsfigures>. Acesso em: 06 Out. 2013.

ANTTILA, M. A.; TAMMI R.H.; TAMMI M.I.; SYRJÄNEN K.J.; SAARIKOSKI, S.V.; KOSMA V.M. High Levels of Stromal Hyaluronan Predict Poor Disease Outcome in Epithelial Ovarian Cancer High Levels of Stromal Hyaluronan Predict Poor Disease Outcome in Epithelial Ovarian Cancer. **Cancer Res,** v. 60, n. 1, p. 150-5, 2000.

APPEL, M.H.; DA SILVEIRA, R.B.; CHAIM, O.M.; PALUDO, K.S.; TREVISAN-SILVA, D.; CHAVES-MOREIRA, D., DA SILVA, P.H.; MANGILI, O.C.; SENFF-RIBEIRO, A.; GREMSKI, W.; NADER, H.B.; VEIGA, S.S. Identification, cloning and functional characterization of a novel dermonecrotic toxin (phospholipase D) from brown spider (*Loxosceles intermedia*) venom. **Biochim Biophys Acta,** v. 1780, n. 2, p. 167-78, 2008.

APPEL, M. H.; DA SILVEIRA, R. B.; GREMSKI, W.; VEIGA, S. S. Insights into brown spider and loxoscelism. **ISJ,** v. 2, p. 152-8, 2005.

APSEN INDÚSTRIA FARMACÊUTICA. **Bulas, Brasil, 2013**. Disponível em: < http://www.apsen.com.br >. Acesso em: 18 Nov. 2013.

ASTACHOV, L.; VAGO, R.; AVIV, M.; NEVO, Z. Hyaluronan and mesenchymal stem cells: from germ layer to cartilage and bone. **Front Biosci (Landmark Ed)**, v. 1, n. 16, p. 261-76, 2011.

AUVINEN, P.; TAMMI, R.; PARKKINEN, J.; TAMMI, M.; AGREN, U.; JOHANSSON, R.; HIRVIKOSKI, P.; ESKELINEN, M.; KOSMA, V.M. Hyaluronan in peritumoral stroma and malignant cells associates with breast cancer spreading and predicts survival. **Am J Pathol**, v. 156, n. 2, p. 529–36, 2000.

BAI, Q.; GENG, X. Protein folding liquid chromatography. **Methods Mol Biol**, v. 705, p. 69-85, 2011.

BARBARO K.C.; LIRA, M.S.; ARAÚJO, C.A.; PAREJA-SANTOS, A., TÁVORA, B.C.; PREZOTTO-NETO, J.P., KIMURA, L.F., LIMA, C., LOPES-FERREIRA, M., SANTORO, M.L. Inflammatory mediators generated at the site of inoculation of *Loxosceles gaucho* spider venom. **Toxicon**, v. 56, n. 6, p. 972-9, 2010.

BARBARO, K. C.; EICKSTEDT, V. R. D.; MOTA, I. Antigenic cross-reactivity of venoms from medically important *Loxosceles* (araneae) species in Brazil. **Toxicon**, v. 32, n. 1, p. 113-120, 1994.

BARBARO, K. C.; KNYSAK, I.; MARTINS, R.; HOGAN, C.; WINKEL, K. Enzymatic characterization, antigenic cross-reactivity and neutralization of dermonecrotic activity of five *Loxosceles* spider venoms of medical importance in the Americas. **Toxicon**, v. 45, n. 4, p. 489–99, 2005.

BARBUCCI, R.; TORRICELLI, P.; FINI, M.; PASQUI, D.; FAVIA, P.; SARDELLA, E.; D'AGOSTINO, R.; GIARDINO, R. Proliferative and re-defferentiative effects of photo-immobilized micro-patterned hyaluronan surfaces on chondrocyte cells. **Biomaterials**, v. 26, n. 36, p. 7596-605, 2005.

BAUMGARTNER, G.; GOMAR-HÖSS, C., SAKR, L., ULSPERGER, E., WOGRITSCH, C. The impact of extracellular matrix on the chemoresistance of solid tumors-experimental and clinical results of hyaluronidase as additive to cytostatic chemotherapy. **Cancer letters**, v. 131, n. 1, p. 85–99, 1998.

BECKER-PAULY, C.; BRUNS, B.C.; DAMM, O.; SCHUTTE, A.; HAMMOUTI, K.; BURMESTER, T.; STOCKER, W. News from an ancient world: two novel astacin metalloproteases from the horseshoe crab. **J. Mol. Biol**., v. 385, p. 236-248, 2009.

BELD, J.; WOYCECHOWSKY, K.J.; HILVERT, D. Diselenides as universal oxidative folding catalysts of diverse proteins. **J Biotechnol**., v. 150, n. 4, p. 481-9, 2010.

BENITEZ, A., YATES, T.J., LOPEZ, L.E., CERWINKA, W.H., BAKKAR, A., LOKESHWAR, V.B. Targeting hyaluronidase for cancer therapy: antitumor activity of sulfated hyaluronic acid in prostate cancer cells. **Cancer Res**, v. 71, n. 12, p. 4085-95, 2011.

BHARADWAJ, A.G.; GOODRICH, N.P.; MCATEE, C.O.; HAFERBIER, K.; OAKLEY, G.G.; WAHL, J.K. 3rd, SIMPSON, M.A. Hyaluronan suppresses prostate tumor cell proliferation through diminished expression of N-cadherin and aberrant growth factor receptor signaling. **Exp Cell Res,** v. 317, n. 8, p. 1214-25, 2011.

BHARADWAJ, A. G.; KOVAR, J.L.; LOUGHMAN, E.; ELOWSKY, C.; OAKLEY, G.G.; SIMPSON, M.A. Spontaneous metastasis of prostate cancer is promoted by excess hyaluronan synthesis and processing. **Am J Pathol**, v. 174, n. 3, p. 1027–36, 2009.

BOGENRIEDER, T.; HERLYN, M. Axis of evil: molecular mechanisms of cancer metastasis. **Oncogene**, v. 22, n. 42, p. 6524–36, 2003.

BONGERTZ, V. Eluição de proteínas de gel de poliacrilamida: descrição de metodologia simples e econômica. **Rev. Inst. Med. Trop. São Paulo**, v. 31, n. 1, p.44-47, 1989.

BOOKBINDER, L.H.; HOFER, A.; HALLER, M.F.; ZEPEDA, M.L.; KELLER, G.A.; LIM, J.E.; EDGINGTON, T.S.; SHEPARD, H.M.; PATTON, J.S.; FROST, G.I. A recombinant human enzyme for enhanced interstitial transport of therapeutics. **J Control Release,** v. 114, p. 230–241, 2006.

BORRELLI, F.; ANTONETTI, F.; MARTELLI, F.; CAPRINO, L. The co-operative action of hyaluronidase and urokinase on the isoproterenol-induced myocardial infarction in rats. **Thromb Res**, v. 42, p. 153–164, 1986.

BOTZKI, A.; RIGDEN, D.J.; BRAUN, S.; NUKUI, M.; SALMEN, S.; HOECHSTETTER, J.; BERNHARDT, G.; DOVE, S.; JEDRZEJAS, M.J.; BUSCHAUER, A. L-ascorbic acid 6-hexadecanoate, a potent hyaluronidase inhibitor - X-ray structure and molecular modeling of enzyme-inhibitor complexes. **J Biol Chem**, v. 279, n. 44, p. 45990-997, 2004.

BOUGA, H.; TSOUROS, I.; BOUNIAS, D.; KYRIAKOPOULOU, D.; STAVROPOULOS, M.S.; PAPAGEORGAKOPOULOU, N.; THEOCHARIS, D.A.; VYNIOS, D.H. Involvement of hyaluronidases in colorectal cancer. **BMC cancer**, v. 10, p. 499, 2010.

BRAVO, L. M.; PURATIC, S.O.; BEHN, T.C.; FARDELLA, B.C.; CONTREPA, F.A. Estudio de la hemólisis inducida por veneno de *L. laeta*. Experiência *in vitro*. **Rev. Med. Chile**, v. 121, p.16-20,1993.

BRONDYK, W.H. Selecting an appropriate method for expressing a recombinant protein. **Methods Enzymol**, v. 463, p. 131-47, 2009.

BRUNS, R.R.; GROSS J. Collagen and glycosaminoglycans in cell adhesion. **Exp Cell Res**. v. 128, n. 1, p.1-7, 1980.

BUCARETCHI, F.; DE CAPITANI, E.M.; HYSLOP, S.; SUTTI, R.; ROCHA-E-SILVA, T.A.; BERTANI, R. Cutaneous loxoscelism caused by *Loxosceles anomala*. **Clin Toxicol,** v. 48, n. 7, p. 764-5, 2010.

BUCHFINK, R.; TISCHER, A.; PATIL, G.; RUDOLPH, R.; LANGE, C. Ionic liquids as refolding additives: variation of the anion. **J Biotechnol,** v. 150, n. 1, p.64-72, 2010.

Buonassisi, V.; Venter, J.C. Hormone and neurotransmitter receptors in an established vascular endothelial cell line. Proc Natl Acad Sci U S A. 1976 May;73(5):1612-6.

BURGESS, R. R. Refolding solubilized inclusion body proteins. **Methods Enzymol**, v. 463, p. 259-82, 2009.

BUTT, T. R.; EDAVETTAL, S. C.; HALL, J. P.; MATTERN, M. R. SUMO Fusion Technology for Difficult-to-Express Proteins. **Protein Expr. Purif**, v. 43, p. 1–9, 2005.

CABRERIZO, S.; DOCAMPO, P. C.; CARI, C.; ORTIZ DE ROZAS, M.; DIAZ, M.; DE ROODT, A.; CURCI, O. Loxoscelism: epidemiology and clinical aspects of an endemic patology in the country. **Arch Argent Pediatr**, v. 107, n. 2, p. 152-9, 2009.

CHAIM, O.M.; DA SILVEIRA, R.B.; TREVISAN-SILVA, D.; FERRER, V.P.; SADE, Y.B.; BÓIA-FERREIRA, M.; GREMSKI, L.H.; GREMSKI, W.; SENFF-RIBEIRO, A.; TAKAHASHI, H.K.; TOLEDO, M.S.; NADER, H.B.; VEIGA, S.S. Phospholipase-D activity and inflammatory response induced by brown spider dermonecrotic toxin: Endothelial cell membrane phospholipids as targets for toxicity. **Biochim Biophys Acta,** v. 1811, p. 84–96, 2011b.

CHAIM, O.M.; SADE, Y.B.; DA SILVEIRA, R.B.; TOMA, L., KALAPOTHAKIS, E.; CHÁVEZ-OLÓRTEGUI, C.; MANGILI, O.C.; GREMSKI, W.; VON DIETRICH, C.P.; NADER, H.B.; VEIGA, S.S. Brown spider dermonecrotic toxin directly induces nephrotoxicity. **Toxicol Appl Pharmacol**, v. 211, n. 1, p. 64–77, 2006.

CHAIM, O. M.; TREVISAN-SILVA, D.; CHAVES-MOREIRA, D.; WILLE, A.C.; FERRER, V.P.; MATSUBARA, F.H.; MANGILI, O.C.; DA SILVEIRA, R.B.; GREMSKI, L.H.; GREMSKI, W.; SENFF-RIBEIRO, A.; VEIGA, S.S. Brown spider (*Loxosceles* genus) venom toxins: tools for biological purposes. **Toxins**, v. 3, n. 3, p. 309–44, 2011a.

CHAIN, E.; DUTHIE, E.S. Identity of hyaluronidase and spreading factor. **Br J Exp Pathol**., v. 21, p.324–338, 1940.

CHAO, K. L.; MUTHUKUMAR, L.; HERZBERG, O. Structure of human hyaluronidase-1, a hyaluronan hydrolyzing enzyme involved in tumor growth and angiogenesis. **Biochemistry**, v. 46, n. 23, p. 6911-6920, Jun 12 2007.

CHATZAKI, M., HORTA, C.C., ALMEIDA, M.O., PEREIRA, N.B., MENDES, T.M., DIAS-LOPES, C., GUIMARÃES, G., MORO, L., CHÁVEZ-OLÓRTEGUI, C., HORTA, M.C., KALAPOTHAKIS, E. Cutaneous loxoscelism caused by *Loxosceles similis* venom and neutralization capacity of its specific antivenom. **Toxicon**. v. 60, n. 1, p. 21-30, 2012.

CHAVES-MOREIRA, D. **Caracterização bioquímica e biológica de fosfolipases presentes em veneno de *Loxosceles intermedia* e *Lonomia obliqua***. 300 f. Tese (Doutorado em Biologia Celular e Molecular), Departamento de Biologia Celular, Universidade Federal do Paraná, Curitiba, Paraná, 2011.

CHAVES-MOREIRA, D.; CHAIM, O. M.; SADE, Y. B.; PALUDO, K. S.; GREMSKI, L. H.; DONATTI, L.; DE MOURA, J.; MANGILI, O. C.; GREMSKI, W.; DA SILVEIRA, R. B.; SENFF-RIBEIRO, A.; VEIGA, S. S. Identification of a direct hemolytic effect

dependent on the catalytic activity induced by phospholipase-D (dermonecrotic toxin) from brown spider venom. **J Cell Biochem**, v. 107, n. 4, p. 655-66.2009.

CHORILLI, M.; DE SOUZA CARVALHO, L.; DE CAMPOS, M.S.M.P.; LEONARDI, G. R., RIBEIRO; M.C.A.P.; POLACOW, M.L.O. Avaliação Histológica da Hipoderme de Suínos Submetida a Tratamento Mesoterápico com Tiratricol, Cafeína e Hialuronidase. **Acta Farm. Bonaerense,** v. 24, n. 1, p. 14-8, 2005.

CLEMENT, H.; OLVERA, A.; RODRÍGUEZ, M.; ZAMUDIO, F.; PALOMARES, L.A.; POSSANI, L.D.; ODELL, G.V.; ALAGÓN, A.; SÁNCHEZ-LÓPEZ, R. Identification, cDNA cloning and heterologous expression of a hyaluronidase from the tarantula *Brachypelma vagans* venom. **Toxicon**. v. 60, n. 7, p. 1223-7, 2012

CRAMER, J. A.; BAILEY, L. C.; BAILEY, C. A.; MILLER, R. T. Kinetic and mechanistic studies with bovine testicular hyaluronidase. **Biochim Biophys Acta**, v. 1200, p. 315–321, 1994.

DA SILVEIRA, R.B.; CHAIM, O.M.; MANGILI, O.C.; GREMSKI, W.; DIETRICH, C.P.; NADER, H.B.; VEIGA, S.S. Hyaluronidases in *Loxosceles intermedia* (Brown spider) venom are endo-β-N-acetyl-D-hexosaminidases hydrolases. **Toxicon**, v. 49, p. 758–768, 2007a.

DA SILVEIRA, R.B.; WILLE, A.C.M.; CHAIM, O.M.; APPEL, M.H.; SILVA, D.T.; FRANCO, C.R.; TOMA, L.; MANGILI, O.C.; GREMSKI, W.; DIETRICH, C.P.; NADER, H.B.; VEIGA, S.S. Identification, cloning, expression and functional characterization of an astacin like metalloprotease toxin from *Loxosceles intermedia* (brown spider) venom. **Biochem J,** v. 406, p. 355–363, 2007c.

DA SILVEIRA, R.B.; PIGOZZO, R.B.; CHAIM, O.M.; APPEL, M.H.; SILVA, D.T.; DREYFUSS, J.L.; TOMA, L.; DIETRICH, C.P.; NADER, H.B.; VEIGA, S.S.; GREMSKI, W. Two novel dermonecrotic toxins LiRecDT4 and LiRecDT5 from brown spider

(*Loxosceles intermedia*) venom: from cloning to functional characterization. **Biochimie**, v. 89, n. 3, p. 289-300, 2007b.

DA SILVEIRA, R.B., PIGOZZO, R.B., CHAIM, O.M., APPEL, M.H., DREYFUSS, J.L., TOMA, L., MANGILI, O.C., GREMSKI, W., DIETRICH, C.P., NADER, H.B., VEIGA, S.S. Molecular cloning and functional characterization of two isoforms of dermonecrotic toxin from *Loxosceles intermedia* (brown spider) venom gland. **Biochimie**, v.88, n. 9, p. 1241-53, 2006.

DAS, K.M.; BANERJEE, S.; SHEKHAR, N.; DAMODARAN, K.; NAIR, R.; SOMANI, S.; RAIKER, V.P.; JAIN, S.; PADMANABHAN, S. Cloning, Soluble Expression and Purification of High Yield Recombinant hGMCSF in *Escherichia coli*. **Int J Mol Sci,** v. 12, n. 3, p. 2064-76, 2011.

DE CASTRO, C. S.; SILVESTRE, F. G.; ARAUJO, S. C.; GABRIEL DE, M. Y., MANGILI, O. C.; CRUZ, I.; CHAVEZ-OLORTEGUI, C.; KALAPOTHAKIS, E. Identification and molecular cloning of insecticidal toxins from the venom of the brown spider *Loxosceles intermedia*. **Toxicon**, v. 44, p. 273-280, 2004.

DECHAVANNE, V.; BARRILLAT, N.; BORLAT, F.; HERMANT, A.; MAGNENAT, L.; PAQUET, M.; ANTONSSON, B.; CHEVALET, L. A high-throughput protein refolding screen in 96-well format combined with design of experiments to optimize the refolding conditions. **Protein Expr Purif**, v. 75, n.2, p. 192-203, 2011.

DE OLIVEIRA, C. DE; GONC, R. M.; FERREIRA, J. M. C.; BERG, C. W. VAN DEN; TAMBOURGI, D. V. Variations in Loxosceles spider venom composition and toxicity contribute to the severity of envenomation. **Toxicon**, v. 45, p. 421–429, 2005.

DICKINSON, L.E.; HO, C.C.; WANG, G.M.; STEBE, K.J.; GERECHT, S. Functional surfaces for high-resolution analysis of cancer cell interactions on exogenous hyaluronic acid. **Biomaterials**, v. 31, n. 20, p.5472-8, 2010.

DIETRICH, C.P.; DIETRICH, S.M. Electrophoretic Behavior of Acidic Mucopolysaccharides in Diamine Buffers. **Anal Biochem,** v. 70, p. 645–647, 1976.

DIETRICH, C.P.; NADER, H.B.; STRAUS, A.H. Structural differences of heparan sulfates according to the tissue and species of origin. **Biochem Biophys Res Commun,** v. 111, p. 865–871, 1983.

DOS SANTOS, V.L.; FRANCO, C.R.; VIGGIANO, R.L.; DA SILVEIRA, R.B.; CANTÃO, M.P.; MANGILI, O.C.; VEIGA, S.S.; GREMSKI, W. Structural and ultrastructural description of the venom gland of *Loxosceles intermedia* (brown spider). **Toxicon**, v. 38, p. 265-285, 2000.

DUNCAN, R. P.; RYNERSON, M. R.; RIBERA, C.; BINFORD, G. J. Molecular Phylogenetics and Evolution Diversity of *Loxosceles* spiders in Northwestern Africa and molecular support for cryptic species in the *Loxosceles rufescens* lineage. **Mol Phylogenet Evol.**, v. 55, n. 1, p. 234–248, 2010.

DUNN, A.L.; HEAVNER, J.E.; RACZ, G., DAY, M. Hyaluronidase: a review of approved formulations, indications and off-label use in chronic pain management. **Expert Opin Biol Ther**, v. 10, n. 1, p.127-131, 2010.

DURAN-REYNALS, F. Exaltation de l'activité du virus vaccinal par lês extraits de certains organs. **Comptes Rendus des Séances de la Société de Biologie et de Ses Filiales**, v. 99, p. 6–7, 1928.

EBO, D.; GOOSSENS, S.; OPSOMER, F.; BRIDTS, C.H.; STEVENS, W.J. Flow-assited diagnosis of anaphylaxis to hyaluronidase. **Allergy**, v. 60, n. 10, p. 1333-1334, 2005.

EDWARD, M.; Quinn, J.A.; PASONEN-SEPPÄNEN, S.M.; MCCANN, B.A.; TAMMI, R.H. 4-Methylumbelliferone inhibits tumour cell growth and the activation of stromal

hyaluronan synthesis by melanoma cell-derived factors. **Br J Dermatol**, v. 162, n. 6, p. 1224–32, 2010.

EIKENES, L.; TARI, M.; TUFTO, I.; BRULAND, Ø.S.; DE LANGE DAVIES, C. Hyaluronidase induces a transcapillary pressure gradient and improves the distribution and uptake of liposomal doxorubicin (Caelyx™) in human osteosarcoma xenografts. **Br J Cancer**, v. 93, n. 1, p. 81–88, 2005.

EKICI, S.; CERWINKA, W.H.; DUNCAN, R.; GOMEZ, P.; CIVANTOS, F.; SOLOWAY, M.S.; LOKESHWAR, V.B. Comparison of the prognostic potential of hyaluronic acid, hyaluronidase (HYAL-1), CD44v6 and microvessel density for prostate cancer. **Int J Cancer**, v. 112, n. 1, p. 121–9.

ESCOUBAS, P.; DIOCHOT, S.; CORZO, G. Structure and pharmacology of spider venom neurotoxins, **Biochimie**, v. 82, 2000.

FARR, C.; MENZEL, J.; SEEBERGER, J.; SCHWEIGLE, B. Clinical pharmacology and possible applications of hyaluronidase with reference to Hylase “Dessau”. **Wien Med Wochenschr**, v. 147, p. 347–355, 1997.

FAVORITO, L. A.; BALASSIANO, C. M.; COSTA, W. S.; SAMPAIO, F.J.B. Treatment of phimosis: structural analysis of prepuce in patients submitted to topical treatment with betamethasone in association with hyaluronidase. **Eur Urol Suppl**, v. 7, p. 247, 2008.

FEITOSA, L.; GREMSKI, W.; VEIGA, S. S.; ELIAS, M. C. Q. B.; GRANER, E. Detection and characterization of metalloproteinases with gelatinolytic, fibronectinolytic and fibrinogenolytic activities in brown spider (*Loxosceles intermedia*) venom. **Toxicon**, v. 36, n. 7, p. 1039–1051, 1998.

FENG, L.; GAO, R.; GOPALAKRISHNAKONE, P. Isolation and characterization of a hyaluronidase from the venom of Chinese red scorpion *Buthus martensi*. **Comp Biochem Physiol C Toxicol Pharmacol**. v. 148, n.3, p. 250-7, 2008.

FERNANDES-PEDROSA, M. D. F.; JUNQUEIRA-DE-AZEVEDO, I. D. L. M.; GONÇALVES-DE-ANDRADE, R. M.; KOBASHI, L.S.; ALMEIDA, D.D.; HO, P.L.; TAMBOURGI, D.V. Transcriptome analysis of *Loxosceles laeta* (Araneae, Sicariidae) spider venomous gland using expressed sequence tags. **BMC Genomics**, v. 12, p. 1–12, 2008.

FERRER, V. P. **Clonagem e expressão heteróloga de hialuronidase e alérgeno presentes no veneno de aranha marrom (*Loxosceles intermedia*)**. 102 f. Dissertação (Mestrado em Biologia Celular e Molecular) - Departamento de Biologia Celular, Universidade Federal do Paraná, Curitiba, Paraná, 2010.

FERRER, V. P.; MARI, T. L. DE; GREMSKI, L. H.; TREVISAN SILVA, D.; DA SILVEIRA, R.B.; GREMSKI, W.; CHAIM, O.M.; SENFF-RIBEIRO, A.; NADER, H.B.; VEIGA, S.S. A novel hyaluronidase from brown spider (*Loxosceles intermedia*) venom (Dietrich's Hyaluronidase): from cloning to functional characterization. PLoS neglected tropical diseases, v. 7, n. 5, p. e2206, 2013.

FIDLER, I.J. Biological behavior of malignant melanoma cells correlated to their survival *in vivo*. **Cancer Res,** v. 35, p. 218-24, 1975.

FISCHER, M.L.; VASCONCELLOS-NETO, J. Microhabitats occupied by *Loxosceles intermedia* and *Loxosceles laeta* (Araneae: Sicariidae) in Curitiba, Paraná, Brazil. **J Med Entomol**, v. 42, n. 5, p. 756-65, 2005.

FISCHER, M. L. Descrição do comportamento agonístico de *Loxosceles laeta*, *L. hirsuta* e *L. intermedia* (Araneae: Sicariidae). **Rev. Bras. Zool**, v. 25, n. 4, p. 579-586, 2008.

FISCHER, M. L. **Biologia e Ecologia de Loxosceles intermedia Mello- Leitão, 1934 (Araneae, Sicariidae), no Município de Curitiba, Paraná**. Tese (Doutorado em Zoologia) - Departamento de Zoologia, Universidade Federal do Paraná, Curitiba, Paraná. 1996.

FROST, G.I.; CSOKA, T.; STERN, R. The hyaluronidases: a chemical, biological and clinical overview. **Trends Glycosci Glycotech**, v. 8, p. 419–434, 1996.

FUKUDA, J.; KHADEMHOSSEINI, A.; YEH, J.; ENG, G.; CHENG, J.; FAROKHZAD, O.C.; LANGER, R. Micropatterned cell co-cultures using layer-by-layer deposition of extracellular matrix components. **Biomaterials**. v. 27, n. 8, p.1479-86, 2006.

FUTRELL, J. M. Loxoscelism. **Am J Med Sci**, v. 304, n. 4, p. 261-7, 1992.

FUCHS, K.; HIPPE, A.; SCHMAUS, A.; HOMEY, B.; SLEEMAN, J.P.; ORIAN-ROUSSEAU, V. Opposing effects of high- and low-molecular weight hyaluronan on CXCL12-induced CXCR4 signaling depend on CD44. **Cell Death Dis**. v. 4, e819, 2013.

GEREN, C. R.; CHAN, T. K.; HOWELL, D. E.; ODELL, G. V. Isolation and characterization of toxins from brown recluse spider venom (*Loxosceles reclusa*). **Arch Biochem Biophys**, v. 174, p. 90-99,1976.

GHATAK, S.; MISRA, S.; TOOLE, B. P. Hyaluronan oligosaccharides inhibit anchorage-independent growth of tumor cells by suppressing the phosphoinositide 3-kinase/Akt cell survival pathway. **J Biol Chem**, v. 277, n. 41, p. 38013–20, 2002.

GIRISH, K.S.; KEMPARAJU, K.; NAGARAJU, S.; VISHWANATH, B.S. Hyaluronidase inhibitors: a biological and therapeutic perspective. **Curr Med Chem**. v. 16, n. 18, p. 2261-88, 2009.

GIRISH, K. S.; KEMPARAJU, K. Inhibition of *Naja naja* venom hyaluronidase: role in the management of poisonous bite. **Life sciences**, v. 78, n. 13, p. 1433–40, 2006.

GIRISH, K. S.; KEMPARAJU, K. The magic glue hyaluronan and its eraser hyaluronidase : A biological overview. **Life Sci**, v. 80, p. 1921–1943, 2007.

GIRISH, K.S.; KEMPARAJU, K. A low molecular weight isoform of hyaluronidase: purification from Indian cobra (*Naja naja*) venom and partial characterization. **Biochemistry (Mosc)**, v. 70, p. 708–712, 2005a.

GIRISH, K.S.; KEMPARAJU, K. Inhibition of *Naja naja* venom hyaluronidase by plant-derived bioactive components and polysaccharides. **Biochemistry (Mosc)**, v. 70, p. 948–952, 2005b.

GIRISH, K.S.; KEMPARAJU, K. Overlooked issues of snakebite management: time for strataegic approach. **Curr Top Med Chem**, v. 11, n. 20, p. 2494-2508, 2011.

GMACHL, M.; SAGAN, S.; KETTER, S.; KREIL, G. The human sperm protein PH-20 has hyaluronidase activity. **FEBS Lett**, v. 336, n. 3, p. 545–548, 1993.

GOMEZ, H.F.; KRYWKO, D.M.; STOECKER, W.V. A new assay for the detection of Loxosceles species (brown recluse) spider venom. **Ann. Emerg. Med**. v. 39, p. 469-474, 2002.

GOMIS-RUTH, F. X. Structural aspects of the metzincin clan of metalloendopeptidases. **Mol Biotechnol**. v. 24, n. 2, p.157-202, 2003.

GONÇALVES-DE-ANDRADE, R. M.; BERTANI, R.; NAGAHAMA, R. H.; BARBOSA, M. F. R. *Loxosceles niedeguidonae* (Araneae, Sicariidae) a new species of brown spider from Brazilian semi-arid region. **ZooKeys**, v. 36, n. 175, p. 27–36, 2012.

GONÇALVES-DE-ANDRADE, R.M.; DE OLIVEIRA, K.C.; GIUSTI, A.L.; DIAS DA SILVA, W.; TAMBOURGI, D.V. Ontogenetic development of *Loxosceles intermedia* spider venom. **Toxicon**. v. 37, n. 4, p. 627-32, 1999.

DA C. B. GOUVEIA, A.I.; DA SILVEIRA, R.B.; NADER, H.B.; DIETRICH, C.P.; GREMSKI, W., VEIGA, S.S. Identification and partial characterisation of hyaluronidases in *Lonomia obliqua* venom. **Toxicon**. v. 45, n. 4, p. 403-10, 2005.

GREMSKI, L. H.; DA SILVEIRA, R. B.; CHAIM, O. M.; PROBST, C.M.; FERRER, V.P.; NOWATZKI, J.; WEINSCHUTZ, H.C.; MADEIRA, H. M.; GREMSKI, W.; NADER, H.B.; SENFF-RIBEIRO, A.; VEIGA, S.S. A novel expression profile of the *Loxosceles intermedia* spider venomous gland revealed by transcriptome analysis. **Mol Biosyst**, v. 6, n. 12, p. 2403–16, 2010.

GURSKI, L.A.; JHA, A.K.; ZHANG, C.; JIA, X.; FARACH-CARSON, M.C. Hyaluronic acid-based hydrogels as 3D matrices for in vitro evaluation of chemotherapeutic drugs using poorly adherent prostate cancer cells. **Biomaterials**, v. 30, n. 30, p. 6076-85, 2009.

GURSKI, L.A.; XU, X.; LABRADA, L.N.; NGUYEN, N.T.; XIAO, L.; VAN GOLEN, K.L.; JIA, X.; FARACH-CARSON, M.C. Hyaluronan (HA) interacting proteins RHAMM and hyaluronidase impact prostate cancer cell behavior and invadopodia formation in 3D HA-based hydrogels. **PLoS One**, v. 7, n. 11, e50075, 2012.

GUSHULAK, L.; HEMMING, R.; MARTIN, D.; SEYRANTEPE, V.; PSHEZHETSKY, A.; TRIGGS-RAINE, B. Hyaluronidase 1 and β-hexosaminidase have redundant functions in hyaluronan and chondroitin sulfate degradation. **J Biol Chem**. v. 287, n. 20, p. 16689-97, 2012.

HADDAD, V. JR.; NETO, D.G.; DE PAULA NETO, J.B.; DE LUNA MARQUES, F.P.; BARBARO, K.C. Freshwater stingrays: study of epidemiologic, clinic and therapeutic

aspects based on 84 envenomings in humans and some enzymatic activities of the venom. **Toxicon**. v. 43, n. 3, p. 287-94, 2004.

HANRAHAN, K. Hyaluronidase for treatment of intravenous extravasations: implementation of an evidence-based guideline in a pediatric population. **J Spec Pediatr Nurs**, v. 18, n. 3, p. 253-62, 2013.

HARLOW, E.; LANE, D. **Antibodies: a Laboratory Manual**. New York, USA: Cold Spring Harbor Laboratory, 1988.

HART, M.E.; TSANG, L.H.; DECK, J.; DAILY, S.T.; JONES, R.C.; LIU, H.; HU, H.; HART, M.J.; SMELTZER, M.S. Hyaluronidase expression and biofilm involvement in *Staphylococcus aureus* UAMS-1 and its sarA, agr and sarA agr regulatory mutants. **Microbiology**, v. 159, Pt 4, p. 782-91, 2013.

HOFINGER, E.S.; SPICKENREITHER, M.; OSCHMANN, J.; BERNHARDT, G.; RUDOLPH, R.; BUSCHAUER, A. Recombinant human hyaluronidase Hyal-1: insect cells versus *Escherichia coli* as expression system and identification of low molecular weight inhibitors. **Glycobiology**. v. 17, n. 4, p.444-53, 2007.

HOGAN, C. J. Loxoscelism: Old Obstacles, New Directions. **Ann Emerg Med**, v. 44, n. 6, p. 608-24, 2004.

HOTEZ, P.J.; NARASIMHAN, S.; HAGGERTY, J.; MILSTONE, L.; BHOPALE, V.; SCHAD, G.A.; RICHARDS, F.F. Hyaluronidase from infective Ancylostoma hookworm larva and its possible function as a virulence factor in tissue invasion and in cutaneous larva miigrans. **Infect Immun**, v. 60, p.1018–1023, 1992.

ICHIKAWA, T.; ITANO, N.; SAWAI, T.; KIMATA, K.; KOGANEHIRA, Y.; SAIDA, T.; TANIGUCHI, S. Increased synthesis of hyaluronate enhances motility of human melanoma cells. **J Invest Dermatol**, v. 113, n. 6, p. 935–9, 1999.

IGNATOVA, Z.; GIERASCH, L.M. Inhibition of protein aggregation *in vitro* and *in vivo* by a natural osmoprotectant. **Proc Natl Acad Sci USA,** v. 103, n. 36, p. 13357-61, 2006.

INSTITUTO NACIONAL DO CÂNCER, **Câncer de pele, melanoma**, INCA < http://www2.inca.gov.br/wps/wcm/connect/tiposdecancer>. Acesso em: 13 Jan. 2014.

ISBISTER, G.K.; FAN, H.W. Spider bite. **Lancet**, v. 378, n. 9808, p. 2039-47, 2011.

ISBISTER, G.K.; VETTER, R.S. Loxoscelism and necrotic arachnidism: more myths and minor corrections. **Ann Emerg Med**, v. 46, n. 2, p. 205-6, 2005.

ISOYAMA, T.; THWAITES, D.; SELZER, M.G.; CAREY, R.I.; BARBUCCI, R.; LOKESHWAR, V.B. Differential selectivity of hyaluronidase inhibitors toward acidic and basic hyaluronidases. **Glycobiology**, v. 16, p. 11–21, 2006.

ITANO,N.; SAWAI, T.; ATSUMI, F.; MIYAISHI, O.; TANIGUCHI, S.; KANNAGI, R.; HAMAGUCHI, M.; KIMATA, K. Selective expression and functional characteristics of three mammalian hyaluronan synthases in oncogenic malignant transformation. **J Biol Chem**, v. 279, n. 18, p. 18679–87, 2004.

JACOBSON, A.; RAHMANIAN, M.; RUBIN, K.; HELDIN, P. Expression of hyaluronan synthase 2 or hyaluronidase 1 differentially affect the growth rate of transplantable colon carcinoma cell tumors. **Int J Cancer**, v. 102, n. 3, p. 212–9, 2002.

KALAPOTHAKIS, E.; CHATZAKI, M.; GONÇALVES-DORNELAS, H.; DE CASTRO, C.S.; SILVESTRE, F.G.; LABORNE, F.V.; DE MOURA, J.F.; VEIGA, S.S.; CHÁVEZ-OLÓRTEGUI, C.; GRANIER, C.; BARBARO, K.C. The Loxtox protein family in *Loxosceles intermedia* (Mello-Leitão) venom. **Toxicon**, v. 50, n. 7, p. 938-46, 2007.

KARBOWNIK, M.S.; NOWAK, J.Z. Hyaluronan: Towards novel anti-cancer therapeutics. **Pharmacol Rep** v. 65, n. 5, p. 1056-74, 2013.

KEMENY, D.M.; DALTON, N.; LAWRENCE, A.J.; PEARCE, F.L.; VERNON, C.A. The purification and characterisation of hyaluronidase from the venom of the honey bee, *Apis mellifera*. **Eur J Biochem**, v. 139, p. 217–223, 1984.

KEMPARAJU, K.; GIRISH, K. S. Snake venom hyaluronidase: a therapeutic target. **Cell Biochem Funct**, v. 24, n. 1, p. 7–12, 2006.

KHADEMHOSSEINI, A.; ENG, G.; YEH, J.; KUCHARCZYK, P.A.; LANGER, R., VUNJAK-NOVAKOVIC, G.; RADISIC, M. Microfluidic patterning for fabrication of contractile cardiac organoids. **Biomed Microdevices**, v. 9, n. 2, p. 149-57, 2007.

KHANUM, S.A.; MURARI, S.K.; VISHWANATH, B.S.; SHASHIKANTH, S. Synthesis of benzoyl phenyl benzoates as effective inhibitors for phospholipase A2 and hyaluronidase enzymes. **Bioorg Med Chem Lett**, v. 15, p. 4100–4104, 2005.

KIRIAKE, A.; MADOKORO, M.; SHIOMI, K. Enzymatic properties and primary structures of hyaluronidases from two species of lionfish (*Pterois antennata* and *Pterois volitans*). **Fish Physiol Biochem**, [Epub ahead of print], 2014.

KLOCKER, J.; SABITZER, H.; RAUNIK, W.; WIESER, S.; SCHUMER, J. Combined application of cisplatin, vindesine, hyaluronidase and radiation for treatment of advanced squamous cell carcinoma of the head and neck. **Am J Clin Oncol**, v. 8, p. 425–428, 1995.

KOHNO, N.; OHNUMA, T.; TRUOG, P. Effects of hyaluronidase on doxorubicin penetration into squamous carcinoma multicellular tumor spheroids and its cell lethality. **J Cancer Res Clin Oncol**, v. 120, n. 5, p. 293-7, 1994.

KOSUNEN, A.; ROPPONEN, K.; KELLOKOSKI, J.; PUKKILA, M.; VIRTANIEMI, J.; VALTONEN, H.; KUMPULAINEN, E.; JOHANSSON, R.; TAMMI, R.; TAMMI, M.; NUUTINEN, J.; KOSMA, V.M. Reduced expression of hyaluronan is a strong indicator

of poor survival in oral squamous cell carcinoma. **Oral Oncol**, v. 40, n. 3, p. 257–263, 2004.

KRALICEK, A.V.; RADJAINIA, M.; MOHAMAD, A.L.I., N.A.; CARRAHER, C.; NEWCOMB, R.D.; MITRA, A.K. A PCR-directed cell-free approach to optimize protein expression using diverse fusion tags. **Protein Expr Purif**, v. 80, n. 1, p. 117-24, 2011.

KREIL, G. Hyaluronidases - A group of neglected enzymes. **Protein Sci**, v. 4, n. 9, p. 1666-9, 1995.

KUBE, J.; BROKAMP, C.; MACHIELSEN, R.; VAN DER OOST, J.; MÄRKL, H. Influence of temperature on the production of an archaeal thermoactive alcohol dehydrogenase from *Pyrococcus furiosus* with recombinant *Escherichia coli*. **Extremophiles**, v. 10, n. 3, p. 221-7, 2006.

KUDO, D.; KON, A.; YOSHIHARA, S.; KAKIZAKI, I.; SASAKI, M.; ENDO, M.; TAKAGAKI, K. Effect of a hyaluronan synthase suppressor, 4-methylumbelliferone, on B16F-10 melanoma cell adhesion and locomotion. **Biochem Biophys Res Commun**, v. 321, n. 4, p.783-7, 2004.

KULTTI, A.; LI, X.; JIANG, P., THOMPSON, C.B.; FROST, G.I.; SHEPARD, H.M. Therapeutic targeting of hyaluronan in the tumor stroma. **Cancers (Basel)**, v. 4, n. 3, p. 873-903, 2012.

KUMAR, K.; BHARGAVA, P.; ROY, U. *In Vitro* Refolding of Triosephosphate Isomerase from *L. donovani*. **Appl Biochem Biotechnol,** v. 164, p. 1207–1214, 2011

KUSMA, J.; CHAIM, O. M.; WILLE, A. C. M.; FERRER, V. P.; SADE, Y. B.; DONATTI, L.; GREMSKI, W.; MANGILI, O.C.; VEIGA, S.S. Nephrotoxicity caused by brown spider venom phospholipase-D (dermonecrotic toxin) depends on catalytic activity. **Biochimie**, v. 90, n. 11-12, p. 1722–1736, 2008.

LAURICH, C.; WHEELER, M.A.; IIDA, J.; NEUDAUER, C.L.; MCCARTHY, J.B.; BULLARD, K.M. Hyaluronan mediates adhesion of metastatic colon carcinoma cells. J **Surg Res**, v. 122, n. 1, p. 70–4, 2004.

LEE, J.H.; MOORE, L.D.; KUMAR, S.; PRITCHARD, D.G.; PONNAZHAGAN, S.; DEIVANAYAGAM, C. Bacteriophage hyaluronidase effectively inhibits growth, migration and invasion by disrupting hyaluronan-mediated Erk1/2 activation and RhoA expression in human breast carcinoma cells. **Cancer Lett**, v. 298, n. 2, p. 238-49, 2010.

LEE, N.; BARTHEL, S. R.; SCHATTON, T. Melanoma stem cells and metastasis: mimicking hematopoietic cell trafficking? **Lab Invest**, v. 94, n. 1, p. 13–30, 2013.

LENORMAND, H.; DESCHREVEL, B.; TRANCHEPAIN, F.; VINCENT, J.C. Electrostatic interactions between hyaluronan and proteins at pH 4: how do they modulate hyaluronidase activity. **Biopolymers,** v. 89, n. 12, p. 1088-103, 2008.

LI, Y.; COZZI, P.J. Angiogenesis as a strategic target for prostate cancer therapy. **Med Res Rev**, v. 30, p. 23 – 66, 2009.

LIN, Y.; MAHAN, K.; LATHROP, W.F.; MYLES, D.G.; PRIMAKOFF, P. A hyaluronidase activity of the sperm plasma membrane protein PH-20 enables sperm to penetrate the cumulus cell layer surrounding the egg. **J Cell Biol**, v. 125, p.1157–1163, 1994.

LOBSTEIN, J.; EMRICH, C.A.; JEANS, C.; FAULKNER, M.; RIGGS, P.; BERKMEN, M. SHuffle, a novel *Escherichia coli* protein expression strain capable of correctly folding disulfide bonded proteins in its cytoplasm. **Microb Cell Fact**, v. 11, p. 56, 2012.

LOKESHWAR, V. B.; RUBINOWICZ, D.; SCHROEDER, G.L.; FORGACS, E.; MINNA, J.D.; BLOCK, N.L.; NADJI, M.; LOKESHWAR, B.L. Stromal and epithelial expression of tumor markers hyaluronic acid and HYAL1 hyaluronidase in prostate cancer. **J Biol Chem**, v. 276, n. 15, p. 11922–32, 2001.

LOKESHWAR, V.B. Differential selectivity of hyaluronidase inhibitors toward acidic and basic hyaluronidases. **Glycobiology**, v.16, p.11–21, 2006.

LUCATO, R.V. JR.; ABDULKADER, R.C.; BARBARO, K.C.; MENDES, G.E.; CASTRO, I.; BAPTISTA, M.A.; CURY, P.M.; MALHEIROS, D.M.; SCHOR, N.; YU, L.; BURDMANN, E.A. *Loxosceles gaucho* venom-induced acute kidney injury - *in vivo* and *in vitro* studies. PLoS Negl Trop Dis, v. 5, n. 5, e1182, 2011.

LUNG, J. M.; MALLORY, S. B. Cameo A child with spider bite and glomerulonephritis : a diagnostic challenge. **Int J Dermatol**, p. 287–289, 2000.

MACHADO, L. F.; LAUGESEN, S.; BOTELHO, E. D.; RICART, C.A.; FONTES, W.; BARBARO, K.C.; ROEPSTORFF, P.; SOUSA, M.V. Proteome analysis of brown spider venom: identification of loxnecrogin isoforms in *Loxosceles gaucho* venom. **Proteomics**, v. 5, n. 8, p. 2167–76, 2005.

MACHIAH, K.D.; GIRISH, K.S.; GOWDA, T.V. A glycoprotein from a folk medicinal plant, *Withania somnifera*, inhibits hyaluronidase activity of snake venoms. **Comp Biochem Physiol C Toxicol Pharmacol,** v. 143, n. 2, p.158-61, 2006.

MÁLAQUE, C.M.S.; CASTRO-VALENCIA, J.E.; CARDOSO, J.L.C.; FRANÇCA, F.O.; BARBARO, K.C.; FAN, H.W. Clinical and epidemiological features of definitive and presumed loxoscelism in São Paulo, Brazil. **Rev Inst Med Trop Sao Paulo**, v. 44, n. 3, p. 139–43, 2002.

MALAQUE, C. M. S.; SANTORO, M. L.; CARDOSO, J.L.; CONDE, M.R., NOVAES, C.T.; RISK, J.Y.; FRANÇA, F.O.; DE MEDEIROS, C.R.; FAN, H.W. Toxicon Clinical picture and laboratorial evaluation in human loxoscelism. **Toxicon**, v. 58, n. 8, p. 664–671, 2011.

MARBLESTONE, J. G.; EDAVETTAL, S. C.; LIM, Y.; LIM, P.; ZUO, X.; BUTT, T. R. Comparison of SUMO Fusion Technology with Traditional Gene Fusion Systems: Enhanced Expression and Solubility with SUMO. **Protein Sci**, v.1 5, p. 182–189, 2006.

MARKOVIC-HOUSLEY, Z.; MIGLIERINI, G.; SOLDATOVA, L.; RIZKALLAH, P.J.; MULLER, U.; SCHIRMER, T. Crystal structure of hyaluronidase, a major allergen of bee venom. **Structure**, v. 8, p.1025–1035, 2000.

MARQUES-DA-SILVA, E.; FISCHER, M. L. Loxosceles Heinecken & Lowe, 1835 (Araneae; Sicariidae) species distribution in the State of Parana. **Rev Soc Bras Med Trop**, v. 38, n. 4, p. 331-5, 2005.

MENZEL, E. J.; FARR, C. Hyaluronidase and its substrate hyaluronan : biochemistry, biological activities and therapeutic uses. **Cancer Lett**, v. 131, p. 3–11, 1998.

MEYER, K. Hyaluronidases. In: Boyer, P.D. (Ed.), **The Enzymes**. 3ed, Academic press, New York, 1971. p. 307-320.

MILLER, A.J.; MIHM, M.C. Melanoma. **N Engl J Med**, v. 355, p. 51–65, 2006.

MILLER, M. S.; ORTEGON, M.; MCDANIEL, C. Negative pressure wound therapy: treating a venomous insect bite. **Int Wound J**, v. 4, n. 1, p. 88-92, 2007.

MINCHINTON, A. I.; TANNOCK, I. F. Drug penetration in solid tumours. **Nat Rev Cancer**, v. 6, n. 8, p. 583–92, 2006.

MIO, K.; STERN, R. Inhibitors of the hyaluronidases. **Matrix Biol**, v. 21, p. 31–37, 2002.

MONTEIRO, C.L.; RUBEL, R.; COGO, L.L.; MANGILI, O.C.; GREMSKI, W.; VEIGA, S.S. Isolation and identification of *Clostridium perfringens* in the venom and fangs of

Loxosceles intermedia (brown spider): enhancement of the dermonecrotic lesion in loxoscelism. **Toxicon**, v. 40, n. 4, p. 409-18, 2002.

MORIN, G.; SULLIVAN, R.; LAFLAMME, I.; ROBERT, C.; LECLERC, P. SPAM1 isoforms from two tissue origins are differentially localized within ejaculated bull sperm membranes and have different roles during fertilization. **Biol Reprod**, v. 82, n. 2, p. 271-81, 2010.

MOSMANN, T. Rapid colorimetric assay for cellular growth and survival: application to proliferation and cytotoxicity assays. **J Immunol Methods**, v. 65, n. 1-2, p. 55–63, 1983.

NAGARAJU, S.; DEVARAJA, S.; KEMPARAJU, K. Purification and properties of hyaluronidase from *Hippasa partita* (funnel web spider) venom gland extract. **Toxicon**, v. 50, n. 3, p. 383-93, 2007.

NEEVES, K.B.; SAWYER, A.J.; FOLEY, C.P.; SALTZMAN, W.M.; OLBRICHT, W.L. Dilation and degradation of the brain extracellular matrix enhances penetration of infused polymer nanoparticles. **Brain Res**, v. 14, n. 1180, p. 121-32.

NG, H.C.; RANGANATHAN, S.; CHUA, K.L.; KHOO, H.E. Cloning and molecular characterization of the first aquatic hyaluronidase, SFHYA1, from the venom of stonefish (*Synanceja horrida*). **Gene,** v. 14, n. 346, p. 71-81, 2005.

NOWATZKI, J.; SENE, R.V.; PALUDO, K.S.; RIZZO, L.E.; SOUZA-FONSECA-GUIMARÃES, F.; VEIGA, S.S.; NADER, H.B.; FRANCO, C.R.; TRINDADE, E.S. Brown spider (*Loxosceles intermedia*) venom triggers endothelial cells death by anoikis. **Toxicon**, v. 60, n. 3, p. 396-405, 2012.

OLIVE, K. P.; JACOBETZ, M.A.; DAVIDSON, C.J.; GOPINATHAN, A.; MCINTYRE, D.; HONESS, D.; MADHU, B.; GOLDGRABEN, M.A.; CALDWELL, M.E.; ALLARD, D.; FRESE, K.K.; DENICOLA, G.; FEIG, C.; COMBS, C.; WINTER, S.P.; IRELAND-

ZECCHINI, H.; REICHELT, S.; HOWAT, W.J.; CHANG, A.; DHARA, M.; WANG, L.; RÜCKERT, F.; GRÜTZMANN, R.; PILARSKY, C.; IZERADJENE, K.; HINGORANI, S.R.; HUANG, P.; DAVIES, S.E.; PLUNKETT, W.; EGORIN, M.; HRUBAN, R.H.; WHITEBREAD, N.; MCGOVERN, K.; ADAMS, J.; IACOBUZIO-DONAHUE, C.; GRIFFITHS, J.; TUVESON, D.A. Chemotherapy in a Mouse Model of Pancreatic Cancer. **Science**, v. 324, n. 5933, p. 1457–1461, 2010.

OSPEDAL, K. Z.; APPEL, M. H.; NETO, Â. F.; MANGILI, O. C.; SANCHES VEIGA, S., GREMSKI, W. Histopathological findings in rabbits after experimental acute exposure to the *Loxosceles intermedia* (brown spider) venom. **Int J Exp Pathol**. v. 83, n. 6, p. 287-94, 2002.

OUHTIT, A.; ABD ELMAGEED, Z.Y.; ABDRABOH, M.E.; LIOE, T.F.; RAJ, M.H. *In vivo* evidence for the role of CD44s in promoting breast cancer metastasis to the liver. **Am J Pathol**, v. 171, n. 6, p. 2033–9, 2007.

PATEL, K. D.; MODUR, V.; ZIMMERMAN, G.A.; PRESCOTT, S.M.; MCINTYRE, T.M. The necrotic venom of the brown recluse spider induces dysregulated endothelial cell-dependent neutrophil activation. Differential induction of GM-CSF, IL-8, and E-selectin expression. **J Clin Invest**, v. 94, n. 2, p. 631-42, 1994.

PAULI, I.; MINOZZO, J.C.; DA SILVA, P.H.; CHAIM, O.M.; VEIGA, S.S. Analysis of therapeutic benefits of antivenin at different time intervals after experimental envenomation in rabbits by venom of the brown spider (*Loxosceles intermedia*). **Toxicon**. v.53, n.6, p. 660-71, 2009.

PERNET, C.; DANDURAND, M.; MEUNIER, L.; STOEBNER, P. Necrotic arachnidism in the south of France : Two clinical cases of loxoscelism. **Ann Dermatol Venereol**. v. 137, n. 12, p. 808-12, 2010.

PETERSON, M. E. Brown spider envenomation. **Clin Tech Small Anim Pract**., v. 21, n. 4, p. 191–3, 2006.

PICHARDO-RODRÍGUEZ R. Possible clinical-epidemiological criteria for the diagnosis of loxoscelism cutaneous and visceral cutaneous. **Rev Chilena Infectol**. v. 30, n. 4, p. 453, 2013.

PIPPIRS, U.; MEHLHORN, H.; ANTAL, A. S.; SCHULTE, K. W.; HOMEY, B. Acute generalized exanthematous pustulosis following a *Loxosceles* spider bite in Great Britain. **Br J Dermatol**, v. 161, n. 1, p. 208–9, 2009.

PLATNICK, N. I. *The World Spider Catalog, Version* 14.5; The American Museum of Natural History: New York, NY, USA, 2013.

POH, C.H.; YUEN, R.; CHUNG, M.C.; KHOO, H.E. Purification and partial characterization of hyaluronidase from stonefish (*Synanceja horrida*) venom. **Comp Biochem Physiol**, v. 101, 159–163, 1992.

PRIMAKOFF, P.; HYATT, H.; MYLES, D. G. A Role for the Migrating Sperm Surface Antigen PH-20 in Guinea Pig Sperm Binding to the Egg Zona Pellucida. **J Cell Biol**. v. 101, n. 6, p. 2239–2244, 1985.

RAMIRES, E. N.; RETZLAFF, A. V. L.; DECONTO, L. R.; FONTANA, J. D.; MARQUES, F. A.; MARQUES-DA-SILVA, E. Evaluation of the efficacy of vacuum cleaners for the integrated control of brown spider *Loxosceles intermedia*. **J Venom Anim Toxins Incl Trop Dis**, v. 13, n. 3, p. 607, 2007.

RATTMANN, Y. D.; PEREIRA, C. R.; CURY, Y.; GREMSKI, W.; MARQUES, M.C.; DA SILVA-SANTOS, J.E. Vascular permeability and vasodilation induced by the *Loxosceles intermedia* venom in rats : Involvement of mast cell degranulation, histamine and 5-HT receptors. **Toxicon**, v. 51, p. 363–372, 2008.

REITINGER, S.; BOROVIAK, T.; LASCHOBER, G.T.; FEHRER, C.; MÜLLEGGER, J.; LINDNER, H.; LEPPERDINGER, G. High-yield recombinant expression of the extremophile enzyme, bee hyaluronidase in *Pichia pastoris*. **Protein Expr Purif**, v. 57, n. 2, p. 226-33, 2007.

RIBEIRO, R.O.; CHAIM, O.M.; DA SILVEIRA, R.B.; GREMSKI, L.H.; SADE, Y.B.; PALUDO, K.S.; SENFF-RIBEIRO, A.; DE MOURA, J.; CHÁVEZ-OLÓRTEGUI, C.; GREMSKI, W.; NADER, H.B.; VEIGA, S.S. Biological and structural comparison of recombinant phospholipase-D toxins from *Loxosceles intermedia* (brown spider) venom. Toxicon. v. 50, n. 8, p. 1162-74, 2007.

RIBUFFO, D.; ATZORI, L.; PAU, M.; ASTE, N. Upper eyelid necrosis and reconstruction after spider bite : case report and. **Eur Rev Med Pharmacol Sci**, v. 16, n. 3, p. 414-7, 2012.

ROPPONEN, K.; TAMMI, M.; PARKKINEN, J.; ESKELINEN, M.; TAMMI, R.; LIPPONEN, P.; AGREN, U.; ALHAVA, E.; KOSMA, V.M. Tumor cell-associated hyaluronan as an unfavorable prognostic factor in colorectal cancer. **Cancer Res**. v. 58, n. 2, p. 342-7, 1998.

SADE, Y.B.; BÓIA-FERREIRA, M.; GREMSKI, L.H.; DA SILVEIRA, R.B.; GREMSKI, W.; SENFF-RIBEIRO, A.; CHAIM, O.M.; VEIGA, S.S. Molecular cloning, heterologous expression and functional characterization of a novel translationally-controlled tumor protein (TCTP) family member from *Loxosceles intermedia* (brown spider) venom. **Int J Biochem Cell Biol**. v. 44, n. 1, p. 170-7, 2012.

SAHDEV, S.; KHATTAR, S.K.; SAINI, K.S. Production of active eukaryotic proteins through bacterial expression systems: a review of the existing biotechnology strategies. **Mol Cell Biochem**. v. 307, n.1-2, p. 249-64, 2008.

SAMBROOK, J.; RUSSELL, D.W. **Molecular Cloning: A Laboratory Manual**, 3rd ed. Cold Spring Harbor Laboratory Press, Cold Spring Harbor, N.Y., 2001

SAMS, H. H.; DUNNICK, C. A.; SMITH, M. L.; KING, L. E., JR. Necrotic arachnidism. **J Am Acad Dermatol**, v. 44, n. 4, p. 561-73, quiz 573-6, 2001.

SANDIDGE, J. Predation by cosmopolitan spiders upon the medically significant pest species *Loxosceles reclusa* (Araneae: Sicariidae): limited possibilities for biological control. **J Econ Entomol**, v. 97, n. 2, p. 230–234, 2004.

SANDIDGE, J. S.; HOPWOOD, J. L. Brown recluse spiders : A review of biology, life history and pest management Brown recluse spiders : A review of biology , life history and pest management. **Kansas Academy of Science**, v. 108, n. 3, p. 99–108, 2005.

SAUPE, E. E.; PAPES, M.; SELDEN, P. A.; VETTER, R. S. Tracking a Medically Important Spider : Climate Change, Ecological Niche Modeling, and the Brown Recluse (*Loxosceles reclusa*). **PLoS One**, v. 6, n. 3, p. 1–10, 2011.

SENFF-RIBEIRO, A.; HENRIQUE DA SILVA, P.; CHAIM, O. M.; GREMSKI, L.H.; PALUDO, K.S.; BERTONI DA SILVEIRA, R.; GREMSKI, W.; MANGILI, O.C.; VEIGA, S.S. Biotechnological applications of brown spider (*Loxosceles genus*) venom toxins. **Biotechnol Adv**, v. 26, n. 3, p. 210–8, 2008.

SETÄLÄ, L. P.; TAMMI, M.I.; TAMMI, R.H.; ESKELINEN, M.J.; LIPPONEN, P.K.; AGREN, U.M.; PARKKINEN, J.; ALHAVA, E.M.; KOSMA, V.M. Hyaluronan expression in gastric cancer cells is associated with local and nodal spread and reduced survival rate. **Br J Cancer**, v. 79, n. 7-8, p. 1133–8, 1999.

SEZERINO, U. M.; ZANNIN, M.; COELHO, L.K.; GONÇALVES JÚNIOR, J.; GRANDO, M.; MATTOSINHO, S.G.; CARDOSO, J.L.; VON EICKSTEDT, V.R.; FRANÇA, F.O.; BARBARO, K.C.; FAN, H.W. A clinical and epidemiological study of Loxosceles spider

envenoming in Santa Catarina, Brazil. **Trans R Soc Trop Med Hyg**, v. 92, n. 5, p. 546-548, 1998.

SHIMIZU, M.T.; JORGE, A.O.; UNTERKIRCHER, C.S.; FANTINATO, V.; PAULA, C.R. Hyaluronidase and chondroitin sulphatase production by different species of Candida. **J Med Vet Mycol**, v. 33, n. 1, p. 27-31, 1995.

SHINDOH, J.; KASEB, A.; VAUTHEY, J.N. Surgical Strategy for Liver Cancers in the Era of Effective Chemotherapy. **Liver Cancer**, v. 2, n. 1, p. 47-54. Review.

SHUSTER, S.; FROST, G.I.; CSOKA, A.B.; FORMBY, B.; STERN, R. Hyaluronidase reduces human breast cancer xenografts in scid mice. **Int J Cancer**, v. 102, n. 2, p. 192-197, 2002.

SIEGEL, R.; NAISHADHAM, D.; JEMAL, A. Cancer statistics, 2012. **CA Cancer J Clin**, v. 62, n. 1, p. 10-29, 2012.

SIISKONEN, H.; TÖRRÖNEN, K.; KUMLIN, T.; RILLA, K.; TAMMI, M.I.; TAMMI, R.H. Chronic UVR causes increased immunostaining of CD44 and accumulation of hyaluronan in mouse epidermis. **J Histochem Cytochem**, v. 59, n. 10, p. 908–17, 2011.

SIISKONEN, H.; POUKKA, M.; TYYNELÄ-KORHONEN, K.; SIRONEN, R.; PASONEN-SEPPÄNEN, S. Inverse expression of hyaluronidase 2 and hyaluronan synthases 1-3 is associated with reduced hyaluronan content in malignant cutaneous melanoma. **BMC cancer**, v. 13, p. 181, 2013.

SIMPSON, M. A. Concurrent expression of hyaluronan biosynthetic and processing enzymes promotes growth and vascularization of prostate tumors in mice. **Am J Pathol**, v. 169, n. 1, p. 247–57, 2006.

SISTEMA NACIONAL DE NOTIFICAÇÃO E AGRAVOS – SINAN, *Acidentes por Animais Peçonhentos no período de 2012*, Ministério da Saúde, Sistema de Informação de Agravos de Notificação, Brasil, 2013.

SINGH, A.; YADAV, D.; RAI, K.M.; SRIVASTAVA, M.; VERMA, P.C.; SINGH, P.K.; TULI, R. Enhanced expression of rabies virus surface G-protein in *Escherichia coli* using SUMO fusion. **Protein J.**, v. 31, n. 1, p. 68-74, 2012.

SINGH SM, PANDA AK. Solubilization and refolding of bacterial inclusion body proteins. **J Biosci Bioeng**, v. 99, n. 4, p. 303-10, 2005.

SIRONEN, R.K.; TAMMI, M.; TAMMI, R.; AUVINEN, P.K.; ANTTILA, M.; KOSMA, V.M. Hyaluronan in human malignancies. **Exp Cell Res**, v. 317, n. 4, p. 383-91, 2011.

SKOV, L.K.; SEPPÄLÄ, U.; COEN, J.J.; CRICKMORE, N.; KING, T.P.; MONSALVE, R.; KASTRUP, J.S.; SPANGFORT, M.D.; GAJHEDE, M. Structure of recombinant Ves v 2 at 2.0 Angstrom resolution: structural analysis of an allergenic hyaluronidase from wasp venom. **Acta Crystallogr D Biol Crystallogr,** v. 62, Pt 6, p. 595-604, 2006.

SORENSEN, H.P.; MORTENSEN, K.K. Soluble expression of recombinant proteins in the cytoplasm of *Escherichia coli*. **Microb Cell Fact**, v. 4, n. 1, p. 1, 2005.

SOUZA, A. L.; DE MALAQUE, C. M.; SZTAJNBOK, J.; ROMANO, C. C.; Duarte, A.J.; SEGURO, A.C. *Loxosceles* venom-induced cytokine activation, hemolysis, and acute kidney injury. **Toxicon**, v. 51, p. 151–156, 2008.

STAIR-NAWY, S.; CSOKA, A. B.; STERN, R. Hyaluronidase Expression in Human Skin Fibroblasts. **Biochem Biophys Res Commun**, v. 273, p. 268–273, 1999.

STERN, R. Hyaluronan catabolism : a new metabolic pathway. **Eur J Cell Biol**, v. 83, p. 317–325, 2004.

STERN, R. Hyaluronan metabolism: a major paradox in cancer biology. **Pathol Biol (Paris)**, v. 53, n. 7, p. 372–82, 2005.

STERN, R.; CSÓKA, A.B. **Mammalian hyaluronidases (HA 15)**. Glycoforum. Disponível em:<http://www.glycoforum.gr.jp/science/hyaluronan/hapdf/HA15.pdf> Acesso em 26 Nov. 2013.

STERN, R.; JEDRZEJAS, M.J. Hyaluronidases: their genomics, structures, and mechanism of action. **Chem Rev**, v. 106, n. 3, p. 818-839, 2006.

SUNDERKOTTER, C.; SEELIGER, S.; SCHÖNLAU, F.; ROTH, J.; HALLMANN, R.; LUGER, T.A.; SORG, C.; KOLDE, G. Different pathways leading to cutaneous leukocytoclastic vasculitis in mice. **Exp Dermatol**, v. 10, n. 6, p. 391-404, 2001.

SWANSON, D. L.; VETTER, R. S. Loxoscelism. Clinics in dermatology, v. 24, n. 3, p. 213–21, 2006.

TAMBOURGI, D.V.; MAGNOLI, F.C.; VAN DEN BERG, C.W.; MORGAN, B.P.; DE ARAUJO, P.S.; ALVES, E.W.; DA SILVA, W.D. Sphingomyelinases in the Venom of the Spider *Loxosceles intermedia* Are Responsible for both Dermonecrosis and Complement-Dependent Hemolysis. **Biochem Biophys Res Commun**, v. 373, p. 366–373, 1998.

TAMMI, R. H.; KULTTI, A.; KOSMA, V.M.; PIRINEN, R.; AUVINEN, P.; TAMMI, M.I. Hyaluronan in human tumors: pathobiological and prognostic messages from cell-associated and stromal hyaluronan. **Semin Cancer Biol**, v. 18, n. 4, p. 288–95, 2008.

TAŞKESEN, M.; AKDENIZ, S.; TAŞ, T.; KEKLIKÇI, U.; TAŞ, M.A. A rare cause of severe periorbital edema and dermonecrotic ulcer of the eyelid in a child: brown recluse spider bite. **Turk J Pediatr,** v. 53, n. 1, p. 87-90.

TIAN, X.; AZPURUA, J.; HINE, C.; VAIDYA, A.; MYAKISHEV-REMPEL, M.; ABLAEVA, J.; MAO, Z.; NEVO, E.; GORBUNOVA, V.; SELUANOV, A. High-molecular-mass hyaluronan mediates the cancer resistance of the naked mole rat. **Nature**, v. 499, n. 7458, p. 346–9, 2013.

TREVISAN-SILVA, D.; GREMSKI, L.H.; CHAIM, O.M.; DA SILVEIRA, R.B.; MEISSNER, G.O.; MANGILI, O.C.; BARBARO, K.C.; GREMSKI, W.; VEIGA, S.S; SENFF-RIBEIRO, A. Astacin-like metalloproteases are a gene family of toxins present in the venom of different species of the brown spider (genus *Loxosceles*). **Biochimie**, v. 92, n. 1, p. 21-32, 2010.

TURLEY, E. A.; TRETIAK, M. Glycosaminoglycan Production by Murine Melanoma Variants *in vivo* and *in vitro*. **Cancer Res**, v. 45, n. 10, p. 5098-105, 1985.

UDABAGE, L.; BROWNLEE, G.R.; NILSSON, S.K.; BROWN, T.J. The over-expression of HAS2, Hyal-2 and CD44 is implicated in the invasiveness of breast cancer. **Exp Cell Res**, v. 310, n. 1, p. 205–17, 2005.

VEIERØD, M.B.; COUTO, E.; LUND, E.; ADAMI, H.O.; WEIDERPASS, E. Host characteristics, sun exposure, indoor tanning and risk of squamous cell carcinoma of the skin. **Int J Cancer**, Epub ahead of print. 2013.

VEIGA, S.S.; DA SILVEIRA, R.B.; DREYFUS, J.L.; HAOACH, J.; PEREIRA, A.M.; MANGILI, O.C.; GREMSKI, W. Identification of high molecular weight serine-proteases in *Loxosceles intermedia* (brown spider) venom. **Toxicon**, v. 38, n. 6, p. 825-39, 2000.

VETTER, R. S.; ISBISTER, G. K. Medical Aspects of Spider Bites. **Annu Rev Entomol**. v. 53, p. 409-29, 2008.

VOGEL, K.G. Effects of hyaluronidase, trypsin, and EDTA on surface composition and topography during detachment of cells in culture. **Exp Cell Res**, v.113, n. 2, p. 345-57, 1978.

VUITIKA, L.; GREMSKI, L.H.; BELISÁRIO-FERRARI, M.R.; CHAVES-MOREIRA, D.; FERRER, V.P.; SENFF-RIBEIRO, A.; CHAIM, O.M.; VEIGA, S.S. Brown spider phospholipase-D containing a conservative mutation (D233E) in the catalytic site: identification and functional characterization. **J Cell Biochem**, v. 114, n. 11, p. 2479-92, 2013.

WALLS, D.; LOUGHRAN, S.T. Tagging recombinant proteins to enhance solubility and aid purification. **Methods Mol Biol**, v. 681, p.151-75, 2011.

WHATCOTT, C.J.; HAN, H.; POSNER, R.G.; HOSTETTER, G.; VON HOFF, D.D. Targeting the tumor microenvironment in cancer: why hyaluronidase deserves a second look. **Cancer Discov**, v. 1, n. 4, p. 291-6, 2011.

WHITE, J. Clinical toxinology. **Curr Infect Dis Rep**, v. 13, n. 3, p. 236–42, 2011.

WILLE, A.C.; CHAVES-MOREIRA, D.; TREVISAN-SILVA, D.; MAGNONI, M.G.; BOIA-FERREIRA, M.; GREMSKI, L.H.; GREMSKI, W.; CHAIM, O.M.; SENFF-RIBEIRO, A.; VEIGA SS. Modulation of membrane phospholipids, the cytosolic calcium influx and cell proliferation following treatment of B16-F10 cells with recombinant phospholipase-D from *Loxosceles intermedia* (brown spider) venom. **Toxicon**, v. 1; n. 67, p. 17-30, 2013.

WILLENBERG, A.; SAALBACH, A.; SIMON, J.C.; ANDEREGG, U. Melanoma cells control HA synthesis in peritumoral fibroblasts via PDGF-AA and PDGF-CC: impact on melanoma cell proliferation. **J Invest Dermatol**, v. 132, n. 2, p. 385–93, 2012.

WRIGHT, R.P.; ELGERT, K.D.; CAMPBELL, B.J.; BARRETT, J.T. Hyaluronidase and esterase activities of the venom of the poisonous brown recluse spider. **Arch Biochem Biophys**, v.159, n. 1, p. 415-26, 1973.

YADAV, G.; PRASAD, R.L.; JHA, B.K.; RAI, V.; BHAKUNI, V.; DATTA, K. Evidence for inhibitory interaction of hyaluronan-binding protein 1 (HABP1/p32/gC1qR) with *Streptococcus pneumoniae* hyaluronidase. **J Biol Chem**, v. 284, n. 6, p. 3897-905, 2009.

YAMAGUCHI, H., MIYAZAKI, M.; BRIONES-NAGATA, M.P.; MAEDA, H. Refolding of difficult-to-fold proteins by a gradual decrease of denaturant using microfluidic chips. **J Biochem**, v. 147, n. 6, p. 895-903, 2010.

YIANNIAS, J. A.; WINKELMANN, R. K. Persistent painful plaque due to a brown recluse spider bite. **Cutis**, v. 50, p. 273-275, 1992.

YOCUM, R.C.; KENNARD, D.; HEINER, L.S. Assessment and implication of the allergic sensitivity to a single dose of recombinant human hyaluronidase injection: a double-blind, placebo-controlled clinical trial. **J Infus Nurs**, v. 30, p. 293–299, 2007.

YOUNG, A R.; PINCUS, S. J. Comparison of enzymatic activity from three species of necrotising arachnids in Australia: *Loxosceles rufescens*, *Badumna insignis* and *Lampona cylindrata*. **Toxicon**, v. 39, n. 2-3, p. 391–400, 2001.

ZANETTI, V. C.; DA SILVEIRA, R.B.; DREYFUSS, J.L.; HAOACH, J.; MANGILI, O.C.; VEIGA, S.S; GREMSKI, W. Morphological and biochemical evidence of blood vessel damage and fibrinogenolysis triggered by brown spider venom. **Blood Coagul Fibrinolysis**, v. 13, n. 2, p. 135-148, 2002.

ZENG, C.; TOOLE, B.P.; KINNEY, S.D.; KUO, J.W.; STAMENKOVIC, I. Inhibition of tumor growth in vivo by hyaluronan oligomers. International journal of cancer. **Int J Cancer**, v. 77, n. 3, p. 396–401, 1998.

ZUO, X.; LI, S.; HALL, J.; MATTERN, M. R.; TRAN, H.; SHOO, J.; TAN, R.; WEISS, S.; R.; BUTT, T. R. Enhanced Expression and Purification of Membrane Proteins by SUMO Fusion in *Escherichia coli.* **J Struct Funct Genomics**, v. 6, p. 103–111, 2005.

ANEXOS

1 ARTIGOS PUBLICADOS DURANTE O PERÍODO DE DOUTORADO

1.1 GREMSKI, L.H.; DA SILVEIRA, R.B.; CHAIM, O.M.; PROBST, C.M.; FERRER, V.P. NOWATZKI, J.; WEINSCHUTZ, H.C.; MADEIRA, H.M.; GREMSKI, W.; NADER, H.B.; SENFF-RIBEIRO, A.; VEIGA, S.S. A novel expression profile of the *Loxosceles intermedia* spider venomous gland revealed by transcriptome analysis. **Mol Biosyst**, v. 6, n. 12, p. 2403-16, 2010. doi: 10.1039/c004118a

1.2 CHAIM, O.M.; DA SILVEIRA, R.B.; TREVISAN-SILVA, D.; FERRER, V.P.; SADE, Y.B.; BÓIA-FERREIRA, M.; GREMSKI, L.H.; GREMSKI, W.; SENFF-RIBEIRO, A.; TAKAHASHI, H.K.; TOLEDO, M.S.; NADER, H.B.; VEIGA, S.S. Phospholipase-D activity and inflammatory response induced by brown spider dermonecrotic toxin: endothelial cell membrane phospholipids as targets for toxicity. **Biochim Biophys Acta**. v. 1811, n. 2, p. 84-96, 2011. doi: 10.1016/j.bbalip.2010.11.005

1.3 CHAIM, O.M.; TREVISAN-SILVA, D.; CHAVES-MOREIRA, D.; WILLE, A.C.; FERRER, V.P.; MATSUBARA, F.H.; MANGILI, O.C.; DA SILVEIRA, R.B.; GREMSKI, L.H.; GREMSKI, W.; SENFF-RIBEIRO, A.; VEIGA, S.S. Brown spider (*Loxosceles* genus) venom toxins: tools for biological purposes. **Toxins (Basel)**, v. 3, n. 3, p. 309-44, 2011. Review. doi: 10.3390/toxins3030309.

1.4 FERRER, V.P.; DE MARI, T.L.; GREMSKI, L.H.; TREVISAN SILVA, D.; DA SILVEIRA, R.B.; GREMSKI, W.; CHAIM, O.M.; SENFF-RIBEIRO, A.; NADER, H.B.; VEIGA, S.S. A novel hyaluronidase from brown spider (Loxosceles intermedia) venom (Dietrich's Hyaluronidase): from cloning to functional characterization. **PLoS Negl Trop Dis**, v. 7, n. 5, e2206, 2013. doi: 10.1371/journal.pntd.0002206.

1.5 VUITIKA, L.; GREMSKI, L.H.; BELISÁRIO-FERRARI, M.R.; CHAVES-MOREIRA, D.; FERRER, V.P.; SENFF-RIBEIRO, A.; CHAIM, O.M.; VEIGA, S.S. Brown spider

phospholipase-D containing a conservative mutation (D233E) in the catalytic site: identification and functional characterization. **J Cell Biochem**, v.114, n. 11, p. 2479-92, 2013. doi: 10.1002/jcb.24594.

2 ARTIGO ACEITO PARA PUBLICAÇÃO DURANTE O PERÍODO DE DOUTORADO

2.1 Luiza Helena Gremski[a,b]; Dilza Trevisan-Silva[a]; Valéria Pereira Ferrer[a]; Fernando Hitomi Matsubara[a]; Gabriel Otto Meissner[a]; Ana Carolina Martins Wille[a,c]; Larissa Vuitika[a]; Camila Dias-Lopes[d]; Anwar Ullah[e]; Fábio Moraes[e]; Carlos Delfin Chávez-Olortegui[d]; Kátia Cristina Barbaro[f]; Mario Tyago Murakami[g]; Raghuvir Krishnaswamy Arni[e]; Andrea Senff-Ribeiro[a]; Olga Meiri Chaim[a]; Silvio Sanches Veiga[a*] Recent advances in the brown spider venoms: from biology of spiders to molecular understanding of toxins. **Toxicon**, accept for publication.

3 PARECER TÉCNICO DA CTN-Bio

4 PARECER DE APROVAÇÃO PELA COMISSÃO DE ÉTICA PARA O USO DE ANIMAIS

Molecular BioSystems

www.molecularbiosystems.org

Volume 6 | Number 12 | December 2010 | Pages 2341–2576

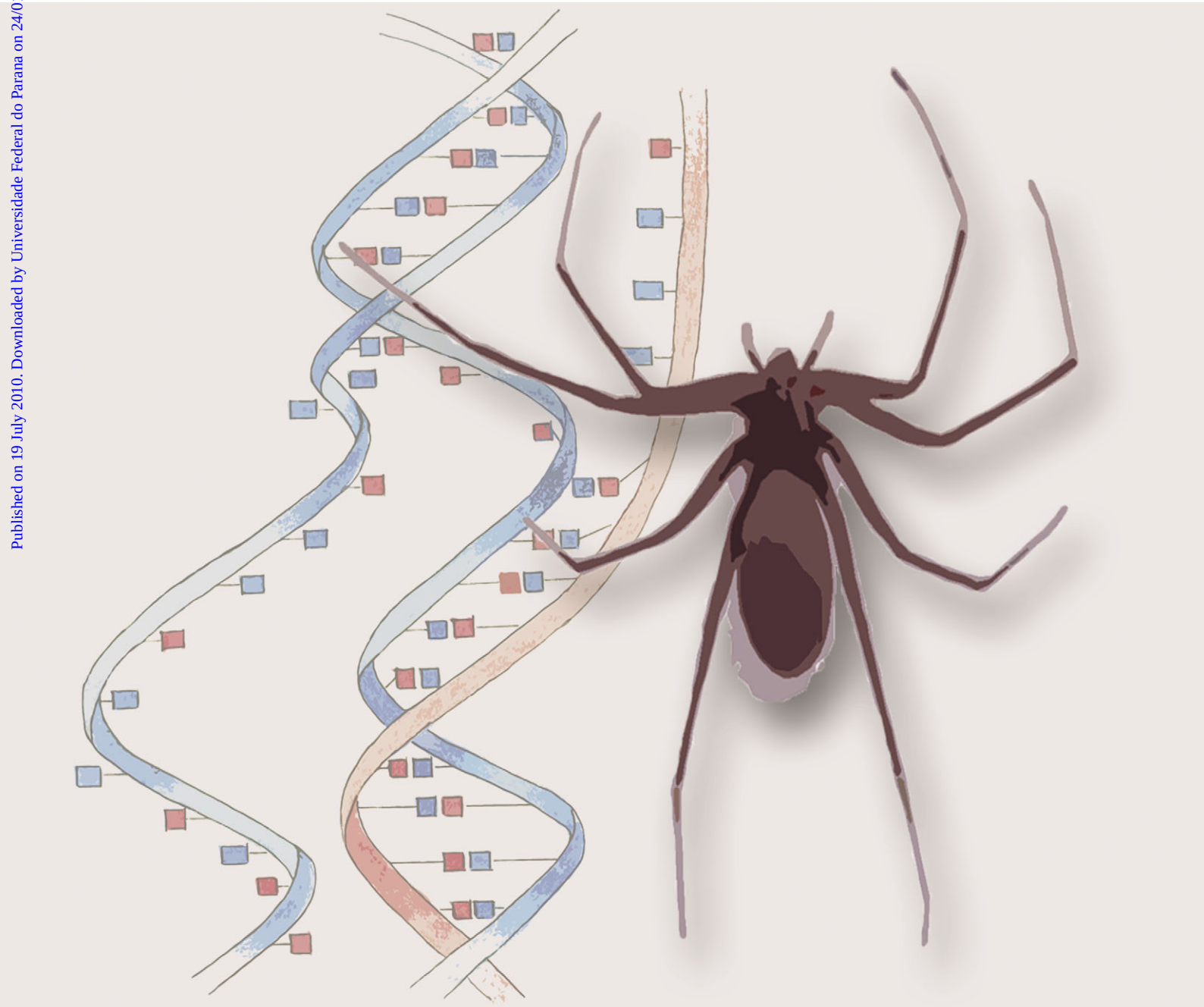

ISSN 1742-206X

RSC Publishing

PAPER

Veiga *et al.*

A novel expression profile of the *Loxosceles intermedia* spider venomous gland revealed by transcriptome analysis

A novel expression profile of the *Loxosceles intermedia* spider venomous gland revealed by transcriptome analysis

Luiza Helena Gremski,[a] Rafael Bertoni da Silveira,[b] Olga Meiri Chaim,[ac] Christian Macagnan Probst,[d] Valéria Pereira Ferrer,[c] Jenifer Nowatzki,[c] Hellen Chris Weinschutz,[e] Humberto Maciel Madeira,[e] Waldemiro Gremski,[e] Helena Bonciani Nader,[a] Andrea Senff-Ribeiro[c] and Silvio Sanches Veiga[ac]

Received 10th March 2010, Accepted 15th April 2010
DOI: 10.1039/c004118a

Spiders of the *Loxosceles* genus are cosmopolitan, and their venom components possess remarkable biological properties associated with their ability to act upon different molecules and receptors. Accidents with *Loxosceles intermedia* specimens are recognized as a public health problem in the south of Brazil. To describe the transcriptional profile of the *L. intermedia* venom gland, we generated a wide cDNA library, and its transcripts were functionally and structurally analyzed. After initial analyses, 1843 expressed sequence tags (ESTs) produced readable sequences that were grouped into 538 clusters, 281 of which were singletons. 985 reads (53% of total ESTs) matched to known proteins. Similarity searches showed that toxin-encoding transcripts account for 43% of the total library and comprise a great number of ESTs. The most frequent toxins were from the LiTx family, which are known for their insecticidal activity. Both phospholipase D and astacin-like metalloproteases toxins account for approximately 9% of total transcripts. Toxins components such as serine proteases, hyaluronidases and venom allergens were also found but with minor representation. Almost 10% of the ESTs encode for proteins involved in cellular processes. These data provide an important overview of the *L. intermedia* venom gland expression scenario and revealed significant differences from profiles of other spiders from the *Loxosceles* genus. Furthermore, our results also confirm that this venom constitutes an amazing source of novel compounds with potential agrochemical, industrial and pharmacological applications.

Introduction

The *Loxosceles* genus is one of four groups of spiders capable of causing human fatality.[1] They are distributed worldwide, and specifically in Brazil, only three species have been implicated in envenoming: *L. intermedia*, *L. gaucho* and *L. laeta*. The bites of brown spiders (*Loxosceles* genus) led to several clinical manifestations such as necrotic skin degeneration and gravitational spread at the bite site, renal failure and hematological disturbances. [2] Loxoscelism is the term used to describe the set of symptoms that commonly appear after accidents with brown spiders. The molecular and physiological mechanisms of loxoscelism are currently under investigation.

Several studies conducted over the past 30 years concerning the structural and biological roles of various venom components have shown the complex nature of these secretions.[3] Likewise, the venom of *Loxosceles* spiders is a complex mixture of protein toxins with a molecular mass profile ranging from 5 to 40 kDa.[4]

Today, it is evident that venom constituents are endowed with remarkable biological properties associated with their ability to act upon a number of specific and non-specific molecules and receptors in order to incapacitate their target organisms.[3] Spider venom has received less attention than the venom produced by other animals due to their minimal impact on human health.[5] Alternatively, spider venom constitutes an amazing putative source of novel compounds with potential agrochemical, industrial and pharmacological applications. Spiders are highly successful and one of the most diversified groups of arthropods, but only a few species have had their venom investigated.[6]

In *Loxosceles* venom, many proteins have been identified and biochemically characterized. Some of the components are not involved in the noxious activities of the venom, and others, such as members of the phospolipase D family (also known as dermonecrotic toxins) can produce deleterious effects that contribute significantly to the typical response after envenoming.[7] Despite this accumulated knowledge, it is essential to conduct a wider study concerning the nature of venom components and their proportion in the mixture. Today, modern molecular biology techniques for DNA and RNA manipulation allow the construction of vast transcript libraries that further the

[a] *Department of Biochemistry, Federal University of São Paulo, São Paulo, Brazil*
[b] *Department of Structural, Molecular Biology and Genetics, State University of Ponta Grossa, Paraná, Brazil*
[c] *Department of Cell Biology, Federal University of Paraná, Paraná, Brazil*
[d] *Instituto Carlos Chagas, Fiocruz, Paraná, Brazil*
[e] *Catholic University of Paraná, Health and Biological Sciences Institute, Paraná, Brazil*

understanding of the behavior of complex biological processes by identifying their molecular constituents. Also, a library will create an overview of the venom and may enable the discovery of new molecules of biotechnological interest.

Various studies of the repertoire of transcripts expressed in venom glands of diverse animals have been published recently.[8–12] The majority of these studies refer to the venom glands of snakes, whereas only a few studies were conducted concerning the transcripts present in spider venom glands.[13–16] As mentioned earlier, spider venom has become a valuable resource for the isolation of potentially useful molecules. Also, an expressed sequence tag (EST) analysis approach provides a rapid and reliable method for identifying new components as well as a resource for the analysis of the expression of known and unknown genes.

L. intermedia venom is a focus of different studies performed by our group for the last decade. Various components of the venom were identified and characterized, and some components were produced as active recombinant molecules for isolated studies and biological characterizations.[2,7,17–22] Up to now, two proteomic analyses of *L. intermedia* venom were performed: one focused on dermonecrotic proteins[23] and one more diverse that identified 39 proteins.[24] Therefore, in order to expand the knowledge about *L. intermedia* venom, a cDNA library was generated from venom glands and partial sequencing of cDNAs was performed, which resulted in thousands of ESTs that were subsequently analyzed.

Results and discussion

cDNA library and EST clustering

The length of cloned cDNAs was estimated by agarose gel electrophoresis analysis of PCR amplified products. The results showed a distribution between 200 and 2300 bp, with an average of 700 bp (data not shown). After sequencing and analysis, 1843 ESTs produced readable sequences. Subsequently, all ESTs were submitted to clustering, and 538 clusters were generated, of which 281 were singletons. Clusters including two or more sequences were named "LIC" followed by the number of the cluster (LIC179–LIC438). Analyses resulted in two classes of singletons: some with similar sequences when compared to other clusters (LIS1–LIS178) and others with no similarity with other clusters (LIS179–LIS282).

Cluster identification

Resulting clusters were analyzed against the GenBank database (blastx, blastn and tblastx) and submitted to GenBank dbEST under accession numbers HO002618–HO004460. Of 538 clusters, 246 (45.7%) resulted in significant hits to known sequences. The other 292 clusters, of which 153 were singletons, were similar to proteins with no associated function (hypothetical proteins), were not matched (no hits) or matched against deposited *L. laeta* mRNA sequences that presented no similarity to database sequences (*L. laeta* cDNA). Identified sequences were classified into two main classes according to their general attribution: toxic function (toxins) and proteins involved in cellular processes.

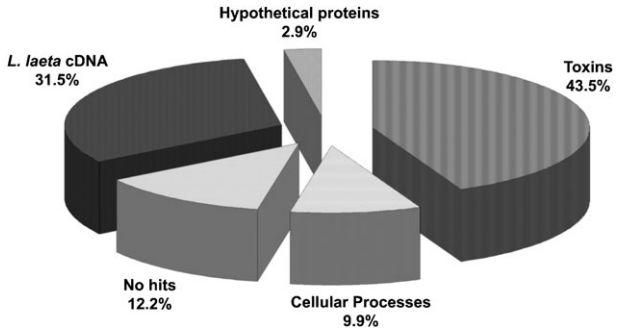

Fig. 1 The annotated *L. intermedia* venom gland transcriptome: relative proportions of toxin-encoding, hypothetical proteins, cellular processes, similar to *L. laeta* cDNA and non-significant hit ESTs.

The overview of the annotated *L. intermedia* venom gland transcriptome is presented in Fig. 1 and in more detail in Table 1. Based on data analysis, the majority of ESTs annotated as toxins are transcripts that were included in contigs (90%). These ratios are similar to other venom gland transcriptome studies[11,13] and reflect the tissue speciality, particularly during the phase of venom replacement.

The number of transcripts with no known function is significant (47%). As accounted by Fernandes-Pedrosa,[14] this number is understandable as *Loxosceles* genus sequences deposited in the public databases are still restricted. Furthermore, the complete function and components of the venom gland of *Loxosceles* are not yet fully characterized. Data also reveal that 68% of *L. intermedia* transcripts with no attributed function are similar to *L. laeta* ESTs sequences that do not match with known proteins. This ratio reveals that, as observed with already characterized proteins, unknown venom proteins produced by the two species are very similar. Furthermore, this finding demonstrates that a close evolutionary relationship exists between these species.

Transcripts assigned as toxins represent 43.4% of the total library and comprise the majority of ESTs. There are 801 toxin sequences grouped into 88 clusters and 80 singletons. The redundancy of clustering is in agreement with previous data and is due to the peculiar function of venom gland tissue in producing proteins that function in capturing prey and as a defense mechanism. Toxin clusters were grouped according to the structural and functional features of the protein: phospholipases; knottins LiTx1, 2, 3 or 4 (insecticidal peptides);[27] astacin-like metalloproteases; neurotoxins, and others. Fig. 2 shows the proportion of each group of toxins over the total of toxin-encoding transcripts. Table 2 describes the absolute numbers of each group of toxin-encoding messengers and their proportion among all transcriptome ESTs. A list of the putative identities of representative toxin-related clusters is provided in Table 3.

Data reveal that insecticidal peptides, structurally associated to knottins, comprise the majority of expressed toxins in *L. intermedia* venom glands. The proportion of transcripts encoding for phospholipases and astacin-like metalloproteases are next in size and are followed by lower expressed but not less important toxins, like neurotoxins and serine-proteases.

Table 1 Summary statistics after clustering of 1843 EST sequences

	No. of clusters	No. of ESTs	Percentage over total ESTs	Percentage over identified ESTs
Total no. of clusters (reads >1)	257	1562	84.75	87
Similar to toxins	88	721	39.12	73.2
Similar to cellular processes proteins	30	136	7.38	13.8
No hits	36	135	7.32	—
Similar to *L. laeta* cDNA	97	530	28.76	—
Hypothetical proteins	6	40	2.17	—
Total no. of singletons	281	281	15.25	13
Similar to toxins	—	80	4.34	8.1
Similar to cellular processes proteins	—	48	2.60	4.9
No hits	—	89	4.83	—
Similar to *L. laeta* cDNA	—	51	2.78	—
Hypothetical proteins	—	13	0.70	—
Total	538	1843	100	100

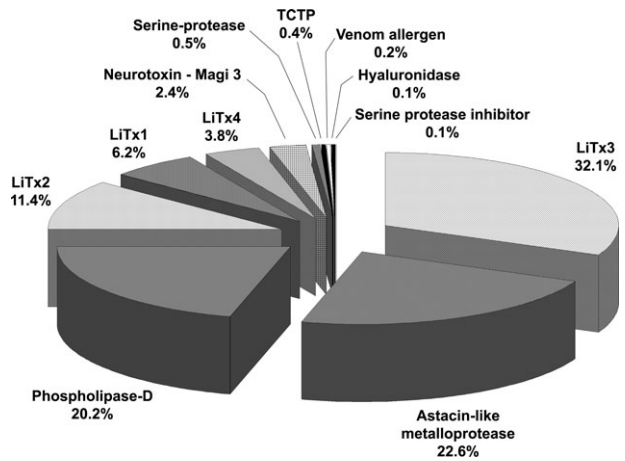

Fig. 2 Relative proportions of each group of toxins over the total toxin-encoding transcripts.

Knottins—insecticidal peptides

Insecticidal peptides isoforms LiTx1, LiTx2 and LiTx3 were initially described in the venom of *L. intermedia* and functionally characterized by de Castro.[27] The sequence of a new isoform of this class, LiTx4, was deposited in 2006 under the accession numbers DQ388598 (nucleotide) and Q27Q53 (amino acid).

Briefly, after submitting *L. intermedia* venom to various chromatography steps, the authors isolated three peptides with insecticidal activity, which were then sequenced by the Edman degradation method. Based on the peptide sequences, degenerated probes were used to screen a cDNA library of *L. intermedia* venom glands and positive clones had their plasmids sequenced. Similarity analysis revealed three isoforms of insecticidal peptides: LiTx1, LiTx2 and LiTx3. These three peptides, and the fourth isoform later described, are small disulfide-rich proteins that have a "disulfide through disulfide knot" that structurally defines the peptides as knottins.[27,28]

The biologically characterized components are polypeptides with molecular weights ranging from 5.6 to 7.9 kDa, and they presented insecticidal activity against highly destructive pests such as *Spodoptera frugiperda* and *Spodoptera cosmioides*. Sequence similarity analyses indicate that these molecules act on specific ion channels.[27]

The LiTx1 peptide has a calculated molecular weight of 7431.63 Da and may present *N*-myristoylation, protein kinase C phosphorylation, amidation and casein kinase II phosphorylation sites. Based on sequence similarity, it was not possible to

Table 2 Putative toxin transcripts classes identified in *L. intermedia* venom gland transcriptome

Toxins	No. of clusters	No. of ESTs	% of total
LiTx3[a]	70	257	13.9
Astacin-like metalloprotease	39	181	9.8
Phospholipase D	27	162	8.8
LiTx2[a]	1	91	4.9
LiTx1[a]	11	50	2.7
LiTx4[a]	5	30	1.6
Neurotoxin[b]	9	19	1
Serine proteinase	2	4	0.3
TCTP[c]	1	3	0.2
Venom allergen	1	2	0.1
Hyaluronidase	1	1	0.05
Serine proteinase inhibitor	1	1	0.05
Total	168	801	43.4

[a] LiTx—Knottins/Similar to insecticidal toxins of *L. intermedia*. [b] Neurotoxin—Similar to Neurotoxin Magi 3.[46]. [c] TCTP—Similar to Translationally controlled tumor protein.

Table 3 Catalogue of most representative toxin-encoding transcripts from *L. intermedia* cDNA library

Cluster	No. of ESTs	Bit score (*e*-value)	BLAST annotation
Knottin/Insecticidal toxin LiTx3			
LIC341	4	730 (0.0)	gb|AY681977.1| Loxosceles intermedia toxin 3 mRNA, complete cds
LIC430	29	739 (0.0)	gb|AY681977.1| Loxosceles intermedia toxin 3 mRNA, complete cds
LIC402	10	243 (2e-60)	gb|AY681977.1| Loxosceles intermedia toxin 3 mRNA, complete cds
LIC431	30	211 (5e-51)	gb|AY681977.1| Loxosceles intermedia toxin 3 mRNA, complete cds
LIC298	3	69.7 (1e-10)	sp|Q6B4T3.1|TX3_LOXIN Toxin 3 (LiTx3) precursor
LIC257	2	73.7 (6e-12)	sp|Q6B4T3.1|TX3_LOXIN Toxin 3 (LiTx3) precursor
LIS161	1	68.6 (8e-10)	sp|Q6B4T3.1|TX3_LOXIN Toxin 3 (LiTx3) precursor
Phospholipase D			
LIC434	62	2074 (0.0)	gb|DQ218155.1| Loxosceles intermedia dermonecrotic toxin isoform 1 mRNA, complete cds
LIC419	15	1978 (0.0)	gb|EF535250.1| Loxosceles intermedia loxtox i1 mRNA, complete cds
LIC420	16	1757 (0.0)	gb|DQ267927.1| Loxosceles intermedia dermonecrotic toxin isoform 3 mRNA, complete cds
LIC395	9	2241 (0.0)	gb|DQ431848.1| Loxosceles intermedia dermonecrotic toxin isoform 4 mRNA, complete cds
LIC336	4	1877 (0.0)	gb|DQ431849.1| Loxosceles intermedia dermonecrotic toxin isoform 5 mRNA, complete cds
LIC182	2	765 (0.0)	gb|EF474482.1| Loxosceles intermedia dermonecrotic toxin isoform 6 mRNA, complete cds
LIC365	5	1624 (0.0)	gb|EF535254.1| Loxosceles intermedia loxtox i5 mRNA, complete cds
LIC423	17	1092 (0.0)	gb|FJ171452.1| Loxosceles hirsuta isolate alphaIV2 sphingomyelinase D-like mRNA, partial cds
LIC316	3	365 (5e-99)	gb|ACN49022.1| sphingomyelinase D-like protein [Sicarius albospinosus]
LIC203	2	184 (9e-45)	gb|ABD91847.1| dermonecrotic toxin isoform 5 [Loxosceles intermedia]
LIS80	1	64.3 (1e-18)	gb|AAM21156.1| sphingomyelinase-like protein [Loxosceles laeta]
LIS279	1	265 (2e-69)	sp|Q8I914.1|SMD1_LOXLA Sphingomyelin phosphodiesterase D 1 (SMD1) precursor
Astacin-like metalloprotease			
LIC359	5	1580 (0.0)	gb|EF028089.1| Loxosceles intermedia astacin-like metalloprotease toxin precursor, mRNA, complete cds
LIC412	12	1463 (0.0)	gb|GQ227490.1| Loxosceles intermedia astacin-like metalloprotease toxin 2 precursor, mRNA, complete cds
LIC415	14	1559 (0.0)	gb|GQ227491.1| Loxosceles intermedia astacin-like metalloprotease toxin 3 precursor, mRNA, complete cds
LIC369	6	628 (1e-176)	gb|GQ227491.1| Loxosceles intermedia astacin-like metalloprotease toxin 3 precursor, mRNA, complete cds
Knottin/Insecticidal toxin LiTx2			
LIC436	91	809 (0.0)	gb|AY681976.1| Loxosceles intermedia toxin 2 mRNA, complete cds
Knottin/Insecticidal toxin LiTx1			
LIC425	18	780 (0.0)	gb|AY681975.1| Loxosceles intermedia toxin 1 mRNA, complete cds
LIC385	7	612 (1e-171)	gb|AY681975.1| Loxosceles intermedia toxin 1 mRNA, complete cds
Knottin/Insecticidal toxin LiTx4			
LIC427	20	580 (4e-162)	gb|DQ388598.1| Loxosceles intermedia toxin 4 mRNA, partial cds
Neurotoxin			
LIC327	4	294 (9e-76)	gb|EY188583.1| LLAE0211C Loxosceles laeta cDNA 5′ similar to Neurotoxin magi-3, mRNA sequence
LIC381	6	267 (1e-67)	gb|EY188583.1| LLAE0211C Loxosceles laeta cDNA 5′ similar to Neurotoxin magi-3, mRNA sequence
Serine-proteases			
LIC305	4	60.8 (2e-07)	ref|XP_001653721.1| serine protease [Aedes aegypti]
TCTP			
LIC317	3	253 (2e-65)	gb|AAY66972.1| translationally controlled tumor protein [Ixodes scapularis]
Venom allergen			
LIC179	2	108 (1e-21)	gb|ABX75373.1| venom allergen [Lycosa singoriensis]
Hyaluronidase			
LIS222	1	142 (2e-32)	gb|EDL77243.1| hyaluronoglucosaminidase 1 [Rattus norvegicus]
Serine-protease inhibitor			
LIS209	1	143 (2e-32)	gb|AAH06776.1| Serine (or cysteine) peptidase inhibitor, clade I, member 1 [Mus musculus]

conclude if LiTx1 interacts specifically with Na^+ or Ca^{2+} channels, like ω-toxins.[27] In the *L. intermedia* transcriptome, 50 sequences that grouped together in 11 clusters showed similarity with LiTx1, comprising 2.7% of total transcripts and 6% of toxin-encoding ESTs. By similarity analysis, 31 sequences appear to be LiTx1 itself. The remaining 19 ESTs annotated as LiTx1 are slightly different, with two important amino acid substitutions (data not shown). These substitutions are not located at the post-translational modification sites but still may reflect a distinct isoform of this toxin.

LiTx2 has the same possible post-translational modification regions of LiTx1, except the casein kinase II phosphorylation site. This peptide has a calculated molecular weight of 7920.11 Da, and, like LiTx1, the type of ion channel that LiTx2 interacts with is still unknown.[27] Almost 5% of the messengers produced by the *L. intermedia* venom gland correspond to LiTx2, and 11% among toxin-encoding transcripts are similar to this peptide. Interestingly, all 91 ESTs annotated as LiTx2 were grouped in the same cluster and appear to be LiTx2 itself. These data demonstrate with high reliability that LiTx2 is a highly conserved isoform.

The results of our study also reveal a minor expressed peptide annotated as LiTx4. This peptide has not yet been characterized by the authors who deposited the sequence at GenBank (DQ388598). However, there is an important similarity between LiTx2 and LiTx4 sequences (77%) that leads us to conclude that they are structurally and functionally related. It is possible to hypothesize that LiTx4 is also a member of the family of knottins and most likely possesses an ability to interact with ion channels. In the *L. intermedia* transcriptome, 30 transcripts annotated as LiTx4 were grouped in 5 clusters, and, like LiTx2, LiTx4 does not have sequence variability. The current sequence deposited at GenBank (DQ388598) is a partial coding sequence. The sequences clustered by similarity generated a consensus sequence that apparently completes the previous sequence of LiTx4 (data not shown); however, it is important to state that we are dealing with ESTs that are known to be low confidence sequences. Therefore, a more accurate analysis must be done to ensure this information.

The last insecticidal peptide characterized by de Castro[27] was named LiTx3. This component has a calculated molecular weight of 5648.49 Da and some post-translationally modified regions: *N*-myristoylation and protein kinase C phosphorylation sites. Based on sequence similarity analyses, the authors hypothesized that LiTx3 may interact with Na^+ channels. Structurally, LiTx3 can also be defined as a member of the knottin family. Different to the other three characterized peptides, LiTx3 presented significant similarity with metallothioneins, which are a family of small cysteine-rich proteins with the ability to bind heavy metals. According to de Castro,[27] metallothioneins in spider venom may act to regulate the toxicity of the venom because several toxic activities of venom proteins depend on divalent metals.

According to our data, transcripts annotated as LiTx3 were the most abundant sequences in the *L. intermedia* transcriptome: 13.9% of all ESTs showed similarity with this peptide. 257 sequences grouped in 70 clusters presented some grade of similarity with LiTx3, comprising 32% of toxin-encoding messengers. A more accurate analysis revealed that the *L. intermedia* venom gland may produce various isoforms of this toxin. Fig. 3 displays seven possible isoforms that differ in varying degrees from LiTx3. Represented by clusters LIC341 and LIC279, 57 transcripts grouped in 12 clusters appear to be LiTx3 itself and are described in Fig. 3 as group 1. Group 2 has only one amino acid substitution compared to LiTx3 (position 29), but it is a significant replacement and may be located in an important site of the peptide; we consider this version to be an isoform. According to our data, group 4 contains the most expressed transcripts: 74 sequences (clustered in 12 series) formed this group, while group 1 (LiTx3 itself) comprises 57 sequences. Groups 5, 6 and 7 contain sequences with more amino acid substitutions that modify the post-translational modification sites of LiTx3, and the sequences belonging to these groups are less numerous. Nevertheless, cysteine residues are highly conserved in all displayed sequences, as indicated by the asterisks in Fig. 3. The function of these molecules is not well understood; therefore, we cannot hypothesize how these differences in the primary structure of these peptides can modify the conformation and subsequently their activity and affinity. However, the number of isoforms certainly explains the abundance of transcripts annotated as the LiTx3 peptide.

Our data reveal a prevalence of peptides with insecticidal activities among the transcripts produced by the *L. intermedia* venom gland. The electrophoretic protein profile of *L. intermedia* venom (Fig. 4) agrees with this aspect of the transcriptome, as the intensity of bands located at the expected size of the peptides are clearly superior to the intensity of other bands (5–8 kDa). Also, the abundance of these neurotoxic components is not surprising because the primary role of brown spider venom, as in all arachnids, is to paralyze or kill envenomed prey.

Previous studies analyzed the protein electrophoretical separation of the venom of *L. intermedia* and *L. laeta*.[29] As demonstrated here, low molecular mass polypeptides (<14 kDa) appear in *L. intermedia*, as well as in the *L. laeta* profile, although in a minor concentration. It is intriguing that none of the peptides described in the *L. intermedia* venom were described in the *L. laeta* venom gland transcriptome.[14]

Arachnids, together with cone snails, are particularly remarkable because of the incredible diversity of toxic peptides produced by their venom glands. Some types of venom contain more than 1000 unique peptides.[30] The knowledge about the structural and pharmacological diversity of these peptides is limited despite the enormous number of these peptides. This diversification appears to be based on subtle variations on their conformational shapes and resultant surfaces, which may be caused by single residue modifications. These variations lead not only to different selectivity but also to diverse modes of interaction between the peptides and their receptors.[5] Here, we describe not only the high abundance of this class of molecules but also a great diversity of isoforms, confirming the tendency observed in other spider venom. However, our knowledge about these toxic peptides in *L. intermedia* venom is very limited, and this subject undoubtedly creates a lot of questions to be further investigated.

Most of these toxic peptides appear to target very specific subtypes of ion channels, receptors and transporters in the peripheral or central nervous system.[31] This activity justifies the increasing interest regarding the potential of some venom as sources of novel compounds with potential agrochemical or pharmacological applications. For example, insect ion channels are significantly different from their vertebrate counterparts, but the development of specific pharmacological reagents for studying these channels has not occurred.[30] Also, the higher specificity of spider peptides for insect receptors has led to the

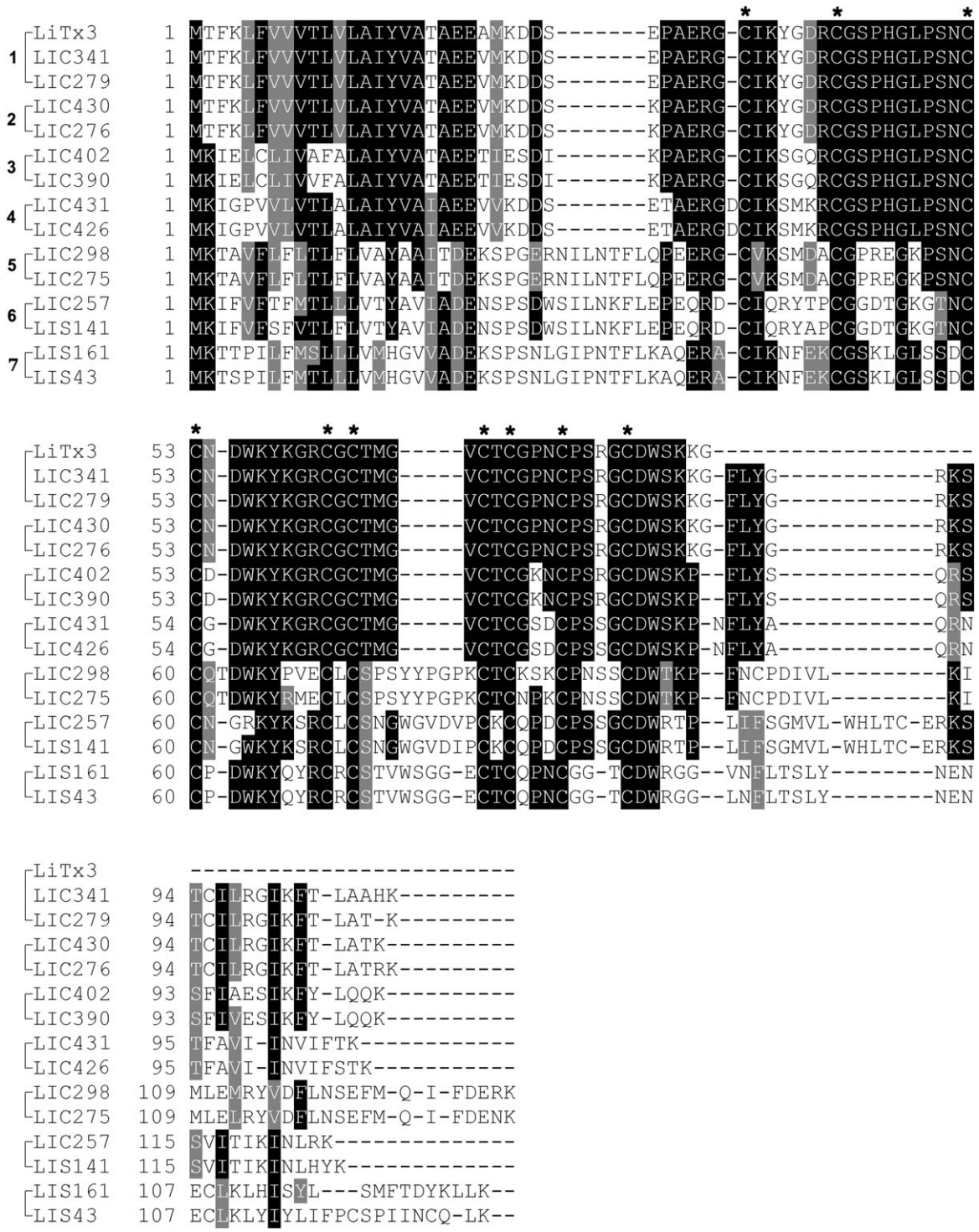

Fig. 3 Multiple alignment analysis of predicted amino acid sequences of LiTx3 and its novel presumable isoforms. Residues are numbered according to the aligned peptide sequences. Amino acid identities are shaded in black and conservative substitutions are in gray. The conserved cysteine residues are indicated by asterisks. The GenBank accession number for LiTx3 sequence is Q6B4T3.

proposal of using the peptides for defining novel insecticidal targets or for pioneering new biopesticides.[31]

Phospholipase D

Among all the toxins found in *Loxosceles* spider venom, dermonecrotic toxin is undoubtedly the most investigated and characterized component. A dermonecrotic toxin is able to reproduce the major biological effects triggered by whole venom such as dermonecrosis, massive inflammatory response, lysis of red blood cells, acute renal failure, among other effects. Currently, the term phospholipase D (PLD) is more accurate than sphingomyelinase D, having a broader spectrum

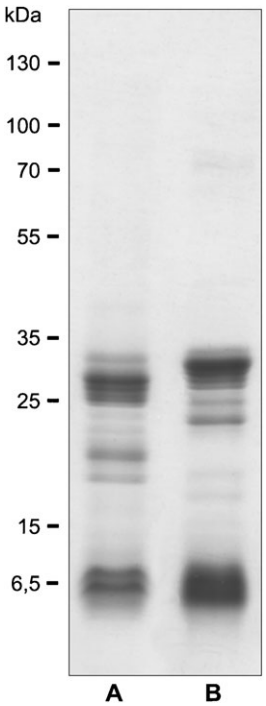

Fig. 4 SDS-polyacrylamide gel electrophoretic separation of *L. intermedia* venom. (A) Non-reduced sample. (B) Reduced sample. Numbers on the left correspond to positions of molecular weight markers.

of targets as it hydrolyzes sphingophospholipids and lysoglycerophospholipids.[32]

Our work revealed that 9% of all analyzed transcripts correspond to phospholipase D, comprising 162 sequences grouped in 27 clusters. These phospholipase D messenger RNAs are 20.2% of all toxin-encoding ESTs, which is a very significant proportion of the majority of toxins.

Dermonecrotic toxin comprises a family of toxins with different related isoforms that have biological, amino acid and immunological similarities, and which are found in diverse *Loxosceles* species. Various isoforms of phospholipase D were already reported for different species.[33] For example, Machado and colleagues[23] described eleven isoforms of phospholipase D toxins in the venom of *L. gaucho*. Many isoforms of dermonecrotic toxin were also characterized in the venom of other species such as *L. reclusa* and *L. laeta*.[34,35] In *L. intermedia* venom, several isoforms were described, and nine isoforms were already expressed as recombinant proteins.[33,34–36]

In light of this, we performed a more accurate analysis of phospholipase D sequences to study the profile of the different isoforms of this molecule in the *L. intermedia* venom gland. Gunning and colleagues[37] consider protein isoforms to be highly similar at the level of amino acids sequence and to perform highly related functions. Functional diversity in higher organisms is due to the description of several numbers isoforms families. In addition, the presence of protein families that retain sufficient similarity among members may compensate for the elimination of one isoform. A great number of isoforms can be created by single nucleotide polymorphisms.[38,39] In the case of the *Loxosceles* genus phospholipase D isoforms, it has been proposed that multiple paralogous genes and alleles may explain this phenomenon. For example, the cDNA sequences of the LiRecDT2, Loxtox i1 and i3 isoforms are identical, except for a few nucleotides located in the 3′ untranslated region (3′UTR) of the mRNA, and are, therefore, most likely, alleles.[36] Based on a phylogenetic analysis of putative mature PLD toxins, Kalapothakis and colleagues[36] proposed six possible major groups of this family of toxins in *L. intermedia* venom. Herein, we employed these categories to describe the profile of PLD isoforms expression in the *L. intermedia* venom gland.

Our results confirmed the presence of dermonecrotic toxin variants (Table 4). 69 clones were characterized as LiRecDT1 itself,[18] LiD1,[40] Loxtox i4[36] or P1,[35] proteins that share 99% of identity and were placed in the Loxtox group 2. These sequences add up to 41.3% of phospholipase D-encoding transcripts of the *L. intermedia* venom gland, which may explain why this phospholipase D isoform was the first to be described in *L. intermedia* venom.

Transcripts annotated as Loxtox groups 1 and 6 also presented an important proportion among phospolipase D-encoding ESTs: 14.2%. Loxtox group 6 includes LiRecDT3, which does not show dermonecrotic activity and has low sphingomyelinase activity.[41] This toxin has a different profile concerning its secondary structure when compared to other dermonecrotic phospholipase D proteins, which may explain its different biological and biochemical behavior. Nevertheless, different isoforms of the same toxins can account for the natural properties of whole venom and its activities.[21]

All other Loxtox groups were identified among *L. intermedia* venom gland transcripts, each one in its particular proportion. Dermonecrotic LiRecDT6 toxin was recently identified and characterized by Appel[22] and was also recognized among messengers (Table 4).

Five clusters annotated as phospholipase D proteins were also submitted to similarity analyses against all characterized *L. intermedia* phospholipase D molecules. However, despite having the amino acid residues typical of the catalytic domain of phospholipase D toxins, these sequences exhibit significant differences in the remaining residues. For example, LIC423 and LIS9 clusters could not be identified as any of the characterized *L. intermedia* phospholipase D toxins because the highest similarity level—observed with LiRecDT6—was 70%. These two clusters represent approximately 11% of all phospholipase D transcripts and may be considered as an important new isoform of this family of toxins produced by *L. intermedia*. Other clusters (LIC316, LIC203, LIS80 and LIS279) have the same profile and may also be different isoforms of phospholipase D not yet characterized (Table 4).

A minor proportion of phospholipase D-encoding transcripts were observed in our work when compared to the *L. laeta* venom gland transcriptome.[14] It is already known that *L. intermedia* female venom has higher concentrations of phospholipase D toxins compared to male.[42] *L. laeta* venom gland EST analysis was performed using only female specimens, whereas the *L. intermedia* venom gland transcriptome used specimens of both sexes. This finding may in part explain the significant difference between the proportions of the transcripts analyzed.

Table 4 Representation of phospholipase D ESTs in the venom gland of *L. intermedia*

Phospholipase-like toxins	No. of clusters	No. of ESTs	% Over total phospholipases
Loxtox group1[a]	4	23	14.2
Loxtox group 2[a]	2	67	41.3
Loxtox group 3[a]	2	9	5.6
Loxtox group 4[a]	1	5	3.1
Loxtox group 5[a]	1	4	2.5
Loxtox group 6[a]	4	23	14.2
LiRecDT6[b]	3	5	3.1
LIC423/LIS9	2	17	10.5
LIC316	1	3	1.8
LIC203	1	2	1.2
LIS80	1	1	0.6
LIS279	1	1	0.6

[a] Phospholipase D protein families proposed by Kalapothakis.[36] [b] GenBank accession number gb|EF474482.1.

Astacin-like metalloproteases

Astacin-like molecules were first described as a component of animal venom in a study that identified, cloned and characterized a metalloprotease from the *L. intermedia* venom gland.[19] This toxin was named LALP (*Loxosceles* astacin-like proteinase). Recently, Trevisan-Silva and co-workers[43] identified two different isoforms of this molecule in *L. intermedia* venom, designating the three isoforms LALP1 (previously named LALP), LALP2 and LALP3. This work also identified astacin-like metalloproteases in the venom of *L. laeta* and *L. gaucho*, named LALP4 and LALP5, respectively.

The astacin family of metalloproteases is formed by zinc endopeptidases. The family members are multifunctional proteases that present a consensus sequence, HEXXHXXGXXHE (zinc-binding motif) and a Met-turn (MXY), both essential elements for these molecules.[44]

In our study, astacin-like metalloproteases (LALPs) encoding transcripts represent 9.8% of all ESTs, *i.e.*, 181 messengers grouped in 39 clusters. Among toxin-encoding transcripts, LALP messengers comprise more than 22% of ESTs, which is a very significant ratio.

These molecules are homologous to digestive astacin-like metalloproteases from *Astacus astacus*. This fact may indicate that LALPs possess a digestive function used to initiate the degradation of prey molecules, facilitating the posterior ingestion process.[43] Furthermore, LALPs in *L. intermedia* venom may play an important role in the pathogenesis observed in loxoscelism, particularly at the local hemorrhage sites and difficulties during wound healing. Likewise, these metalloproteases can also render tissue structures more permeable, facilitating other noxious toxins to spread throughout the body of victims.[19] The putative functions attributed to this class of toxins legitimize the abundance of LALP-encoding transcripts in *L. intermedia* venom may.

As described earlier, three isoforms of LALPs were already described in *L. intermedia* venom. In the present work, transcripts encoding for LALP1, 2 and 3 were identified. Our data suggest that they are produced in different proportions and point to the predominance of LALP2-encoding transcripts, followed by LALP3 and then LALP1 (data not shown). These apparent proportions cannot be justified because the possible differences concerning biological activities of the three isoforms are still not elucidated.

A more accurate analysis showed that some clusters cannot be identified as any of the three characterized astacin-like metalloproteases because amino acid residues differ significantly from other LALPs residues. As shown in Fig. 5, these clusters (represented by LIC 313, LIC369 and LIC421) are more similar to LALP3, but it is possible to observe some important substitutions. For example, a phenylalanine replaces a leucine or a methionine at the third residue of the consensus sequence of astacin family members, which contains the zinc-binding motif. Interestingly the sequence of LIC421 shows significant differences from the sequences of LIC313 and LIC369, particularly in the initial and final regions. These findings support the hypothesis that two new isoforms of astacin-like metalloproteases are present in *L. intermedia* venom.

Neurotoxins similar to Magi 3

Over time, venomous animals were gradually equipped with a complex arsenal of neurotoxins that act against cellular receptors with a singular selectivity and sensibility. Among all venomous animals, spiders are poorly explored in this respect, despite their particular potential concerning the discovery of new ligands. The spiders' venom contains diverse polypeptide toxins that are highly reticulated by disulfide bridges.[45]

Previously in this work, peptides that selectively bind to ion channels were described as components of *L. intermedia* venom (LiTx peptides). However, our data revealed that some transcripts present some grade of similarity with another class of ion channel binding peptides. In total, 19 ESTs grouped in 9 clusters were annotated as similar to Neurotoxin Magi 3. In 2003, this toxin was isolated from the venom of the *Macrothele gigas* spider by Corzo and colleagues.[46] They characterized Magi 3 as a peptide with a molecular mass of 5222.8 Da that shows specific inhibitory effects on site 3 of the insect sodium channel. This property is associated with its ability to cause paralytic effects to insects, although it is not possible to confirm whether Magi 3 is specific only for insect sodium channels or if it can also act upon calcium channels.[46]

Fig. 6 shows an alignment of representative clusters that were annotated as Neurotoxin Magi 3 and the peptide sequence itself. As observed, there is a particular region (KCVVCYCH) with amino acid residues extremely conserved among all sequences. Moreover, this analysis suggests that two

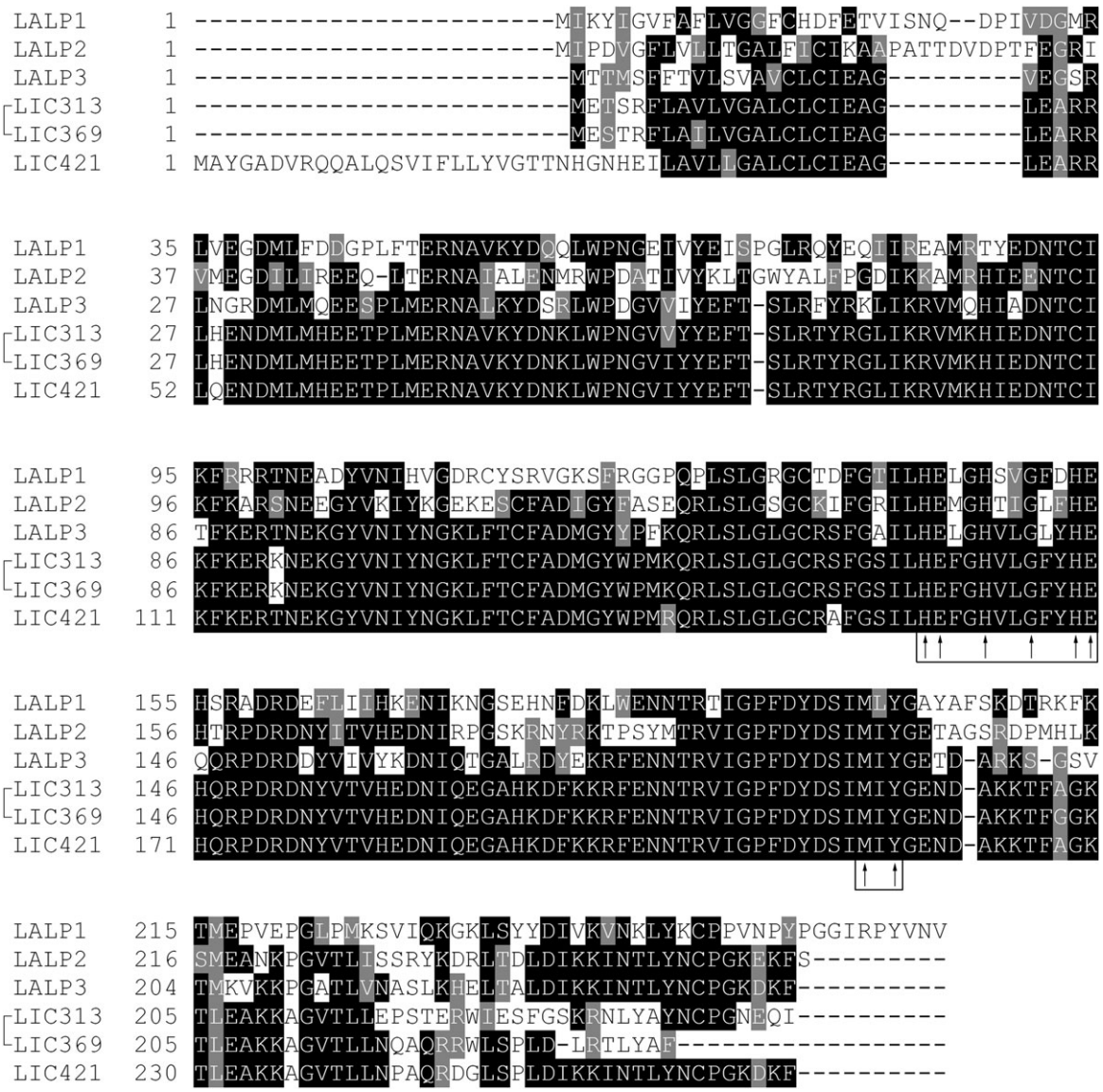

Fig. 5 Multiple alignment analysis of predicted amino acid sequences of *L. intermedia* astacin-like metalloproteases (LALPs) and the novel presumable isoforms of the toxin. Residues are numbered according to the aligned peptide sequences. Amino acid identities are shaded in black and conservative substitutions are in gray. Arrows in the box point to the astacin signature sequence and Met-turn. The GenBank accession numbers for the LALP1, 2 and 3 sequences are A0FKN6, ACV52010, ACV52011, respectively.

isoforms of these peptides may be present in *L. intermedia* venom, which increases the diversity of this class of toxins in the venom. Nevertheless, all cysteine residues present in the sequence of Neurotoxin Magi 3 are highly conserved in all *L. intermedia* sequences displayed in Fig. 6.

Magi 3, like all other *L. intermedia* peptides described here, is most likely a knottin due to the presence of various disulfide bonds in its structure.[46] Although it shares some important characteristics with the LiTx class of toxins, it is more likely that Magi 3 presents a different specificity when interacting with certain sites of cellular receptors. Thus, as observed in all spider venoms studied in this respect, we believe that *L. intermedia* venom also possesses a complex arsenal of neurotoxins that interact with different cellular targets. This diversity extends the variability of prey susceptible to the toxins, representing a great evolutionary process for a predator. Furthermore, this diversity represents an incredibly rich source of novel molecular tools with potential pharmacological and biotechnological applications.[45]

Serine proteases

Previous work from our group has already described two gelatinolytic proteases characterized as serine-type proteases.[47] This study also featured the gelatinolytic proteases as high molecular weight serine proteases (85 and 95 kDa), which are synthesized as zymogens and depend on the proteolytic cleavage of the pro-peptide domain by other proteases such as trypsin. Venom serine proteases, in addition to their contribution to the digestion of the prey, can play an important role in local tissue destruction and interfere in blood coagulation and fibrinolysis.[47–49]

Veiga[47] noted that characterized serine proteases from *L. intermedia* venom are apparently poorly expressed. Analyses

Fig. 6 Multiple alignment analysis of predicted amino acid sequences of Neurotoxin Magi 3 (GenBank accession number P83559) and its novel presumable isoforms. Residues are numbered according to the aligned peptide sequences. Amino acid identities are shaded in black and conservative substitutions are in gray. The conserved cysteine residues are indicated by asterisks.

of the *L. intermedia* venom gland transcriptome revealed five transcripts (0.3% of total ESTs) that displayed similarity with members of the serine protease database. These messengers were grouped into two clusters (LIC321 and LIS237) with no sequence similarity among each other. LIC321 significantly aligned with a serine protease reference sequence from *Aedes aegypti*, a trypsin-like serine protease probably synthesized as an inactive precursor zymogen because a cleavage site was identified.[50] Also, LIS237 presented similarity with a serine protease sequence from the recently published *Lycosa sigoriensis* venom gland transcriptome.[16]

Serine protease molecules are quite diverse molecules concerning their structures, targets, functions and modes of action.[51] Furthermore, as previously described, *L. intermedia* venom presented serine proteolytic activity in two high molecular weights, suggesting that two or more molecules in the venom exhibit these particular characteristics.[47] Thus, in our study, the presence of two different serine proteases corroborates these findings. The presence of different types of molecules from the same class leads to a highly efficient synergism of toxins acting in tissues of the prey or predator.

Venom allergen

Arthropod allergens are potent molecules capable of causing sensitization, and they provoke anaphylaxis. Several allergens have been described in various animals, and these molecules induce similar immune responses at the cellular level. The clinical signs vary depending on whether the allergens enter the body through mucus membranes, skin, or other ways.[52]

Data from our work show that some messengers encode for venom allergens that are cysteine-rich molecules. These messengers are poorly expressed, and two ESTs are grouped in one cluster. They make 0.2% of toxin-encoding transcripts. These transcripts encode for allergens that showed major similarity with this class of molecules described in another spider genus (*Lycosa sigoriensis*) and with a scorpion species (*Opisthacanthus cayaporum*). Significant similarities were also found with some mite allergens (*Ixodes scapularis* and *Argas monolakensis*). A *L. intermedia* venom proteomic study have also reported the possible occurrence of an allergenic protein similar to a mite allergen.[24] Fernandes-Pedrosa[14] described a venom allergen in the *L. laeta* venom gland transcriptome, which presents an important similarity with the *L. intermedia* venom allergen.

Allergic symptoms such as tissue swelling, hypotension, itching and dermatitis have been reported in a few cases of incidents involving spiders of the *Loxosceles* genus.[53] However, venom allergens like the allergen described in this work are likely to contribute to the development of these specific responses.

We also identified transcripts (LIC207) that presented significant similarity with troponin C. These transcripts were included in the group "cellular processes genes" due to the function of troponin C in muscle contraction. However, the annotation of this messenger comprises a troponin C sequence described in the *Blattella germanica* cockroach where it was featured as an allergen with a calcium dependent IgE reactivity, named Bla g 6.0101.[54] Another transcript (LIS263) coding for a myosin light chain protein also presented significant similarity with a *B. germanica* calcium binding allergen (Bla g 8) not yet fully characterized (GI|88657350). It is known that excreted materials, cast-overs from skin-molting and dead debris are sources of allergens that can sensitize genetically predisposed individuals and elicit allergic disorders.[55] Homologous allergens may occur among all arthropods and cause co-sensitization or allergenic cross-reactivity.[54]

Translationally controlled tumor protein

The translationally controlled tumor protein (TCTP) was first identified approximately 25 years ago by some groups interested in translationally regulated genes. Over time, the understanding of TCTP biological functions is a growing issue because it possesses diverse properties and its role in different processes is not yet clear.[56,57]

The TCTP protein is highly conserved in the animal kingdom: nearly 50% of all amino acid residues are preserved. Among species from the same genus, TCTPs are completely conserved. This fact can be clearly seen when comparing the TCTP sequence found in the *L. intermedia* venom gland transcriptome with the one described in the venom gland of *L. laeta*:[14] 97% of positivity is observed among predicted amino acid sequences (the low quality of ESTs should be considered to justify the subtle differences). *L. intermedia* TCTP also presented important similarities with the same protein from

other arthropods such as mites (*Ixodes scapularis*, *Amblyomma americanum*, *etc*.).[58,59]

It is already known that TCTP is essential for embryonic development and cell proliferation in mice and *Drosophila*. Moreover, the protein has calcium-binding activity and is capable of stabilizing microtubules, a property that may be related to a possible role of TCTP in cell cycle control.[56]

Extracellular activities of TCTP were also described,[56] and based on these data, we considered this transcript as a toxin-coding messenger. Studies demonstrate that the protein triggers histamine release in basophile leukocytes by means that may be dependent on or independent of the presence of IgE.[56] It is believed that a specific TCTP receptor may participate in the process, leading to mast cell activation. Mulenga and colleagues[60] showed that TCTP is expressed in diverse tissues from the *Dermacentor variabilis* tick, including its salivary gland. TCTP from the salivary gland was cloned and expressed as a recombinant protein and was able to release histamine from a basophilic cell lineage. *D. variabilis* TCTP is very similar to the *L. intermedia* TCTP described here. Thus, based on these data, it is possible that *L. intermedia* TCTP may also act as a histamine release factor. This hypothesis is reinforced by recent results from Paludo and colleagues[61] that revealed a component present in *L. intermedia* venom related to the histaminergic activity of venom.

However, TCTP mRNAs, including the transcript expressed in the *L. intermedia* venom gland, do not code for a signal sequence. Thus, TCTP may be secreted by a non-classical secretory pathway based on exosomes or, in the case of the *Loxosceles* venom gland, *via* holocrine secretion.

Hyaluronidases

Hyaluronidases are a class of enzymes that degrade hyaluronic acid, which is a major component of the extracellular matrix of vertebrates. In *L. intermedia* venom, two hyaluronidases (41 and 43 kDa) were already identified and characterized as *endo*-β-*N*-acetyl-D-hexosaminidases hydrolases.[20] Hyaluronidase precursor-like proteins were also described in a proteomic analysis of *L. intermedia* venom.[24] In accidents involving spiders of *Loxosceles* genus, hyaluronidases may act as spreading factors that increase the diffusion of other toxins and the gravitational spreading of the dermonecrotic lesion.[2]

Hyaluronidases were also described in the venom of other spiders of the *Loxosceles* genus.[62–64] A transcript with similarity to hyaluronoglucosaminidase 1 from *Rattus norvegicus* (gb|EDL77243.1) was found in the *L. intermedia* transcriptome. In the *L. laeta* transcriptome, only 0.1% of transcripts encode for hyaluronidases,[14] a proportion that matches our results showing the very low expression level of this enzyme. This fact may explain why we were able to describe only one of the hyaluronidases previously described in *L. intermedia* venom.

The identified hyaluronidase-coding sequence exhibits a significant alignment (e-Value of 4e-^{32}) with a hyaluronidase from *Bos Taurus* (NP_001008413.2), a known sperm adhesion molecule that binds to the pellucid zone. This property explains the role of hyaluronidases in the fertilization of eggs by mammalian sperm and suggests one of the potential biotechnological applications of these enzymes as tools for *in vitro* fertilization. Biotechnological applications of hyaluronidases are quite diverse as exposed by Senff-Ribeiro and co-workers.[7]

Serine protease inhibitors

Serine protease inhibitors are the largest and most broadly distributed superfamily of protease inhibitors. These molecules were already described in various venomous animals such as snakes, cone snails, ticks and spiders.[65–68] The reasons for the presence of protease inhibitors in animal venom and the physiological targets of these molecules are still not fully understood. It has been proposed that one of the putative roles of these protease inhibitors is to protect their venom protein toxins from prey proteases.[69] We identified one transcript expressed by the *L. intermedia* venom gland that presented significant similarity with serine proteases from mammals such as *Mus musculus* and *Pan troglodytes*. Important similarities were also found with a serine protease identified in the *Ambliomma americanum* tick.

Textilin-1 is a serine protease inhibitor isolated from the venom of the *Pseudonaja textilis* snake.[70] This molecule binds to and blocks the activity of serine proteases such as plasmin and trypsin. Textilin-1 is an experimental drug that is being investigated as an alternative intravenous treatment to aprotinin (Trasylol®), which has been used to reduce blood loss during cardiopulmonary surgery.[70] This fact demonstrates the biotechnological potential that venom serine proteases inhibitors present.

ESTs relevant to cellular functions

Transcripts encoding for proteins involved in cellular processes and ribosomal RNA account for almost 10% of the total sequences. This relative low proportion is due to the fact that RNA extraction was made when the venom gland was mobilized to restore its toxin content. Thus, except for certain cellular transcripts, most of the ESTs classified as housekeeping sequences were grouped in singletons or clusters with 2 or 3 sequences.

As shown in Fig. 7, the majority of housekeeping messengers were classified as membrane transporters, particularly NaPi co-transporters. This class of transporters imports a phosphate ion coupled with the internalization of a sodium ion.[71] The transporters are common in epithelial cells from the human digestive tract and the kidney. Furthermore, these transporters are mainly responsible for absorption and re-absorption of the phosphate ion. Although this transporter appears to be primordial for *L. intermedia* venom gland machinery, we cannot attribute any specific function to the protein in this context, and more information is needed to underlie this hypothesis.

Transcripts related to structural functions of cells were also found to encode proteins such as actin, tubulin and histones. The motor protein myosin and troponin coding messengers were the most abundant of the class (15 and 11 ESTs, respectively), which could be due to the contraction ability of the gland in order to release the venom to the fangs.

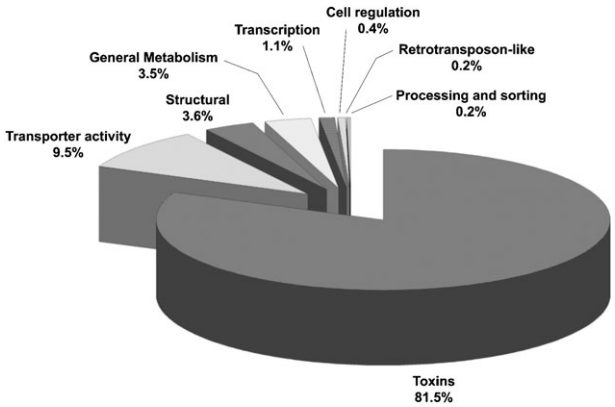

Fig. 7 Graphic showing toxin and cellular processes transcripts proportions in the *L. intermedia* venom gland.

General metabolism transcripts account for 3.5% of cellular processes encoding ESTs and include messengers such as NADH dehydrogenase and cytochrome C oxidase enzymes. ESTs related to transcription and translation functions, like ribosomal proteins, account for 1.1% of housekeeping messengers.

Sequences showing homology with retrotransposable elements were also detected by our analyses. Retrotransposable elements are mobile DNA sequences that can induce genomic rearrangements, such as gene duplication, acting as driving forces of genome evolution.[72] It is reasonable to assume that the finding of retrotransposable elements sequences in *L. intermedia* library is due to insights which hypothesized that gene families encoding spider venom toxins are evolving *via* mechanisms of rapid duplication. Those studies also suggest that the rapid duplication rates in these gene families can be assumed based on large numbers of paralogs expressed in animal venoms.[5,13,33,73,74]

As observed in the *L. laeta* transcriptome,[14] the *L. intermedia* venom gland also produces the processing enzyme, protein disulfide isomerase. Gowd and colleagues[75] have described protein disulfide isomerase in a protein extract from the venom duct of the marine snail *Conus amadis*. Conotoxins are the major components of the mixture of peptides contained in the Conus venom. These molecules are short peptides containing multiple disulfide bonds and are heavily post-translationally modified. Thus, disulfide isomerases would be essential in the formation of the native state cross-links. In the same logic, the presence of disulfide isomerases in the *L. intermedia* venom gland extract might be justified, since a large number of sequences encoding for peptides containing multiple disulfide bonds were also described in this work.

Transcripts related to *L. laeta* ESTs

As described above, 68% of *L. intermedia* transcripts with no attributed function are similar to *L. laeta* ESTs sequences that also have no match with known proteins.[14] Studies in cross-neutralization of lethal activity of different *Loxosceles* venom using immunized rabbit serum revealed that the anti-*L. laeta* serum was almost completely efficient against *L. intermedia* venom. Anti-*L. intermedia* serum was very efficient at neutralizing the lethal activity of *L. laeta* venom.[76] These data revealed many common antigenic components, suggesting a similar composition of the two venoms. Then, it is not surprising that a great part of functionally characterized and non-characterized ESTs from our work are similar to the ESTs from the *L. laeta* transcriptome (data not shown).

However, important differences among *Loxosceles* spider venom were also found in some studies. Machado and co-workers,[23] by means of proteomics analysis, reported some variations in the distribution of phospholipase D isoforms focused along the isoelectric point gradient, describing a larger number of basic isoforms in *L. intermedia* venom and a rather acidic major group of isoforms in *L. laeta* venom. This study also showed that the *L. intermedia* proteome exhibited more low molecular mass proteins (14–25 kDa) than observed in *L. laeta* and *L. gaucho*.

Furthermore, studies of LD50 using mice show that *L. intermedia* venom is more lethal than the venom of *L. laeta* and *L. gaucho*, although no difference in the dermonecrotic activity was reported.[29] Thus, it is possible that venom components that are not involved only in dermonecrotic activity may be present, probably in higher concentrations, in *L. intermedia* venom.

Important differences among the proportions of similar transcripts or even the presence of distinct molecules were observed between the *L. intermedia* and *L. laeta* transcriptomes; therefore, these inferences are in agreement with results presented in this work.

Finally, this work enabled us to have an overview of the *L. intermedia* venom gland expression scenario but, as we generated a non-normalized cDNA library, it is likely that some rare transcripts may have escaped from our analysis. According to Bogdanova and colleagues,[77] sequencing of a complete eukaryotic transcriptome may require the analysis of about $\sim 10^8$ clones from cDNA library to identify rare sequences, whereas transcripts of medium and high abundance are sequenced several times. The same authors describe an interesting normalization procedure, named DSN-normalization. The efficiency of this method has been confirmed in many EST sequencing projects. Thus, further studies using this kind of procedure extract must be done to find rare messages present in *L. intermedia* venom gland. Indeed, our work described some low expressed messengers RNAs. This work also enabled an overview of the expression profile of *L. intermedia* venom gland, and clarified some aspects concerning the mechanisms of envenoming, toxins' function and expression pattern.

Experimental

cDNA library construction

Venom glands of 350 *L. intermedia* spider specimens (male and female) were collected 5 days after venom extraction because transcription is highly intense at this time. After dissection, venom glands were immediately frozen in dry ice and kept in a −80 °C ultra low temperature (ULT) freezer until used. Total RNA was extracted with TRIzol reagent (Invitrogen, Carlsbad, CA, USA), and quality and quantity were checked by denaturing agarose gel electrophoresis and spectrophotometrically using the ratio of absorbances at 260 and 280 nm. mRNA was purified from total RNA using the magnetic separation kit,

PolyATtract® mRNA Isolation System III (Promega Corporation, Madison, WI, USA). A directional *L. intermedia* venom gland cDNA library was constructed using the Creator SMART cDNA Library Construction Kit (BD Biosciences Clontech, Mountain View, CA, USA). The first strand of cDNA was synthesized from purified mRNA, and the second strand was obtained by long distance PCR (LD-PCR), following the manufacturer's instructions. The cDNA was size fractionated *via* chromatography to avoid contaminating the library with short length sequences. Competent *Escherichia coli* DH5α cells were transformed with the cDNA library plasmids to amplify the cDNA. Transformants were selected on LB (Luria-Bertani) agar plates containing 34 μg mL^{-1} chloramphenicol, and more than 20 000 colonies were obtained.

DNA sequencing and bioinformatics analysis

From the resulting colonies, 2400 clones were randomly picked and placed in permanent culture plates with 96 wells and grown for 20 h in LB medium (34 μg mL^{-1} chloramphenicol). Next, the DNA was extracted by alkaline lysis. The DNA was sequenced with MegaBace™ 1000 DNA Analyzing Systems (Amersham Biosciences, Pittsburg, PA, USA), with the DYEnamic ET terminator Cycle Sequencing Kit (GE Healthcare, Piscataway, NJ, EUA). The forward primer was designed to anneal in the insert flanking region of the vector pDNR-LIB (TCGACGGTACCGGACATA). Base-calling was performed using PHRED. CrossMatch software was used to process the sequences to remove the vector and *E. coli* sequences. ESTs were assembled in clusters of contiguous sequences using the CAP3 program. Processed sequences were compared to GenBank sequences using blastx, blastn (E values $<$ 1e−05) and tblastx (E values $<$ 1e−10) algorithms. Afterwards, ESTs were manually inspected for functional classification. Selected sequences were submitted for further alignment analyses using CLUSTAL W2 Software (http://www.ebi.ac.uk/clustal).[25] Protein isoforms are highly similar at the level of amino acid sequence and perform highly related functions; therefore, we identified potential isoforms among the toxin-coding messengers of transcriptome.

SDS-polyacrylamide gel electrophoresis (SDS-PAGE)

Loxosceles intermedia venom was analyzed by SDS-PAGE (8–18% acrylamide resolution gels) under reducing and non-reducing conditions using the Laemmli method.[26] Prior to electrophoresis, venom samples (10 μg) were mixed with sample buffer. Aprotinin from bovine lung (6511 Da) (Sigma-Aldrich, St. Louis, MO, USA) and the PageRuler™ Plus Prestained Protein Ladder (Fermentas, Burlington, Canada) were used as molecular weight markers.

Conclusion

Different components of *Loxosceles intermedia* venom were already identified, characterized and even produced as recombinant toxins. However, it is known that this venom is a complex mixture of protein toxins and only a few of these proteins were already featured. Herein, by using the Expressed Sequence Tag strategy, it was possible to obtain an overview of the expression profile of the *L. intermedia* venom gland. Furthermore, we identified components not yet described in the venom. Data confirmed the highly specialized nature of the spider venom gland on producing toxins and allowed a broad description of these components. Results revealed that the most abundant transcripts code for insecticidal peptides, which agree with the fact that the primary role of the venom is to paralyze or kill envenomed prey. Components with notorious activity in mammal envenoming such as phospholipase D proteins and metalloproteases were also found as highly expressed toxins. Fewer expressed, but not less important toxins were also described; they include components like serine-proteases and hyaluronidases that were already identified in *L. intermedia* venom, and they may have a putative role in envenoming. In addition, molecules not yet identified in this venom were described here, such as a serine protease inhibitor, venom allergen, certain neurotoxins and the translationally controlled tumor protein (TCTP). More accurate analyses allowed the identification of probable new isoforms of some components. Data presented here revealed significant differences from the profiles of other *Loxosceles* spiders, such as *L. laeta* and *L. gaucho*, reinforcing previous data that denoted distinct behaviors among venoms from distinct *Loxosceles* species. Finally, the results obtained and presented here are an initial approach to the characterization of promissory biotechnologically relevant agents.

Acknowledgements

This work was supported by CAPES, CNPq, Fundação Araucária, Secretaria de Estado de Ciência, Tecnologia e Ensino Superior do Paraná and FAPESP.

References

1 G. K. Isbister and J. White, *Toxicon*, 2004, **43**, 477–492.
2 P. H. da Silva, R. B. da Silveira, M. H. Appel, O. C. Mangili, W. Gremski and S. S. Veiga, *Toxicon*, 2004, **44**, 693–709.
3 P. Escoubas, L. Quinton and G. M. Nicholson, *J. Mass Spectrom.*, 2008, **43**, 279–295.
4 J. Kusma, O. M. Chaim, A. C. Wille, V. P. Ferrer, Y. B. Sade, L. Donatti, W. Gremski, O. C. Mangili and S. S. Veiga, *Biochimie*, 2008, **90**, 1722–1736.
5 P. Escoubas, *Mol. Diversity*, 2006, **10**, 545–554.
6 P. Escoubas and G. F. King, *Expert Rev. Proteomics*, 2009, **6**, 221–224.
7 A. Senff-Ribeiro, P. Henrique da Silva, O. M. Chaim, L. H. Gremski, K. S. Paludo, R. Bertoni da Silveira, W. Gremski, O. C. Mangili and S. S. Veiga, *Biotechnol. Adv.*, 2008, **26**, 210–218.
8 M. Neiva, F. B. Arraes, J. V. de Souza, G. Radis-Baptista, A. R. Prieto da Silva, M. E. Walter, M. Brigido Mde, T. Yamane, J. L. Lopez-Lozano and S. Astolfi-Filho, *Toxicon*, 2009, **53**, 427–436.
9 J. Boldrini-França, R. S. Rodrigues, F. P. Fonseca, D. L. Menaldo, F. B. Ferreira, F. Henrique-Silva, A. M. Soares, A. Hamaguchi, V. M. Rodrigues, A. R. Otaviano and M. I. Homsi-Brandeburgo, *Biochimie*, 2009, **91**, 586–595.
10 C. M. Whittington, J. M. Koh, W. C. Warren, A. T. Papenfuss, A. M. Torres, P. W. Kuchel and K. Belov, *J. Proteomics*, 2009, **72**, 155–164.
11 S. Pahari, S. P. Mackessy and R. M. Kini, *BMC Mol. Biol.*, 2007, **8**, 115.
12 E. F. Schwartz, E. Diego-Garcia, R. C. Rodriguez de la Vega and L. D. Possani, *BMC Genomics*, 2007, **8**, 119.
13 L. Jiang, L. Peng, J. Chen, Y. Zhang, X. Xiong and S. Liang, *Toxicon*, 2008, **51**, 1479–1489.
14 F. M. de Fernandes-Pedrosa, I. de L. M. Junqueira-de-Azevedo, R. M. Goncalves-de-Andrade, L. S. Kobashi, D. D. Almeida, P. L. Ho and D. V. Tambourgi, *BMC Genomics*, 2008, **9**, 279.

15 J. Chen, L. Zhao, L. Jiang, E. Meng, Y. Zhang, X. Xiong and S. Liang, *Toxicon*, 2008, **52**, 794–806.
16 Y. Zhang, J. Chen, X. Tang, F. Wang, L. Jiang, X. Xiong, M. Wang, M. Rong, Z. Liu and S. Liang, *Zoology (Jena)*, 2010, **113**, 10–18.
17 L. Feitosa, W. Gremski, S. S. Veiga, M. C. Elias, E. Graner, O. C. Mangili and R. R. Brentani, *Toxicon*, 1998, **36**, 1039–1051.
18 O. M. Chaim, Y. B. Sade, R. B. da Silveira, L. Toma, E. Kalapothakis, C. Chavez-Olortegui, O. C. Mangili, W. Gremski, C. P. von Dietrich, H. B. Nader and S. Sanches Veiga, *Toxicol. Appl. Pharmacol.*, 2006, **211**, 64–77.
19 R. B. da Silveira, A. C. Wille, O. M. Chaim, M. H. Appel, D. T. Silva, C. R. Franco, L. Toma, O. C. Mangili, W. Gremski, C. P. Dietrich, H. B. Nader and S. S. Veiga, *Biochem. J.*, 2007, **406**, 355–363.
20 R. B. da Silveira, O. M. Chaim, O. C. Mangili, W. Gremski, C. P. Dietrich, H. B. Nader and S. S. Veiga, *Toxicon*, 2007, **49**, 758–768.
21 R. O. Ribeiro, O. M. Chaim, R. B. da Silveira, L. H. Gremski, Y. B. Sade, K. S. Paludo, A. Senff-Ribeiro, J. de Moura, C. Chavez-Olortegui, W. Gremski, H. B. Nader and S. S. Veiga, *Toxicon*, 2007, **50**, 1162–1174.
22 M. H. Appel, R. B. da Silveira, O. M. Chaim, K. S. Paludo, D. T. Silva, D. M. Chaves, P. H. da Silva, O. C. Mangili, A. Senff-Ribeiro, W. Gremski, H. B. Nader and S. S. Veiga, *Biochim. Biophys. Acta, Gen. Subj.*, 2008, **1780**, 167–178.
23 L. F. Machado, S. Laugesen, E. D. Botelho, C. A. Ricart, W. Fontes, K. C. Barbaro, P. Roepstorff and M. V. Sousa, *Proteomics*, 2005, **5**, 2167–2176.
24 L. D. dos Santos, N. B. Dias, J. R. A. S. Pinto and M. S. Palma, *Protein Pept. Lett.*, 2009, **16**, 933–943.
25 J. D. Thompson, D. G. Higgins and T. J. Gibson, *Nucleic Acids Res.*, 1994, **22**, 4673–4680.
26 U. K. Laemmli, *Nature*, 1970, **227**, 680–685.
27 C. S. de Castro, F. G. Silvestre, S. C. Araujo, M. Y. Gabriel de, O. C. Mangili, I. Cruz, C. Chavez-Olortegui and E. Kalapothakis, *Toxicon*, 2004, **44**, 273–280.
28 S. Cheek, S. S. Krishna and N. V. Grishin, *J. Mol. Biol.*, 2006, **359**, 215–237.
29 K. C. Barbaro, M. L. Ferreira, D. F. Cardoso, V. R. Eickstedt and I. Mota, *Braz. J. Med. Biol. Res.*, 1996, **29**, 1491–1497.
30 G. F. King, P. Escoubas and G. M. Nicholson, *Channels (Austin)*, 2008, **2**, 110–116.
31 G. Estrada, E. Villegas and G. Corzo, *Nat. Prod. Rep.*, 2007, **24**, 145–161.
32 D. Chaves-Moreira, O. M. Chaim, Y. B. Sade, K. S. Paludo, L. H. Gremski, L. Donatti, J. de Moura, O. C. Mangili, W. Gremski, R. B. da Silveira, A. Senff-Ribeiro and S. S. Veiga, *J. Cell. Biochem.*, 2009, **107**, 655–666.
33 G. J. Binford, M. R. Bodner, M. H. Cordes, K. L. Baldwin, M. R. Rynerson, S. N. Burns and P. A. Zobel-Thropp, *Mol. Biol. Evol.*, 2009, **26**, 547–566.
34 B. Ramos-Cerrillo, A. Olvera, G. V. Odell, F. Zamudio, J. Paniagua-Solis, A. Alagon and R. P. Stock, *Toxicon*, 2004, **44**, 507–514.
35 D. V. Tambourgi, F. F. P. M. de, C. W. van den Berg, R. M. Goncalves-de-Andrade, M. Ferracini, D. Paixao-Cavalcante, B. P. Morgan and N. K. Rushmere, *Mol. Immunol.*, 2004, **41**, 831–840.
36 E. Kalapothakis, M. Chatzaki, H. Goncalves-Dornelas, C. S. de Castro, F. G. Silvestre, F. V. Laborne, J. F. de Moura, S. S. Veiga, C. Chavez-Olortegui, C. Granier and K. C. Barbaro, *Toxicon*, 2007, **50**, 938–946.
37 P. Gunning, R. Weinberger, P. Jeffrey and E. Hardeman, *Annu. Rev. Cell Dev. Biol.*, 1998, **14**, 339–372.
38 T. Kobayakawa, S. Yamada, A. Mizuno, Y. Ohara-Nemoto, T. T. Baba and T. K. Nemoto, *Protein J.*, 2009, **28**, 24–28.
39 N. Ueffing, K. K. Singh, A. Christians, C. Thorns, A. C. Feller, F. Nagl, F. Fend, S. Heikaus, A. Marx, R. B. Zotz, J. Brade, W. A. Schulz, K. Schulze-Osthoff, I. Schmitz and C. Schwerk, *Blood*, 2009, **114**, 572–579.
40 E. Kalapothakis, S. C. Araujo, C. S. de Castro, T. M. Mendes, M. V. Gomez, O. C. Mangili, I. C. Gubert and C. Chavez-Olortegui, *Toxicon*, 2002, **40**, 1691–1699.
41 R. B. da Silveira, R. B. Pigozzo, O. M. Chaim, M. H. Appel, J. L. Dreyfuss, L. Toma, O. C. Mangili, W. Gremski, C. P. Dietrich, H. B. Nader and S. S. Veiga, *Biochimie*, 2006, **88**, 1241–1253.
42 K. C. de Oliveira, R. M. Goncalves de Andrade, A. L. Giusti, W. Dias da Silva and D. V. Tambourgi, *Toxicon*, 1999, **37**, 217–221.
43 D. Trevisan-Silva, L. H. Gremski, O. M. Chaim, R. B. da Silveira, G. O. Meissner, O. C. Mangili, K. C. Barbaro, W. Gremski, S. S. Veiga and A. Senff-Ribeiro, *Biochimie*, 2010, **92**, 21–32.
44 W. Bode, F. X. Gomis-Ruth and W. Stockler, *FEBS Lett.*, 1993, **331**, 134–140.
45 P. Escoubas, S. Diochot and G. Corzo, *Biochimie*, 2000, **82**, 893–907.
46 G. Corzo, N. Gilles, H. Satake, E. Villegas, L. Dai, T. Nakajima and J. Haupt, *FEBS Lett.*, 2003, **547**, 43–50.
47 S. S. Veiga, R. B. da Silveira, J. L. Dreyfus, J. Haoach, A. M. Pereira, O. C. Mangili and W. Gremski, *Toxicon*, 2000, **38**, 825–839.
48 R. M. Kini, *Pathophysiol. Haemostasis Thromb.*, 2005, **34**, 200–204.
49 S. Devaraja, S. Nagaraju, Y. H. Mahadeswaraswamy, K. S. Girish and K. Kemparaju, *Toxicon*, 2008, **52**, 130–138.
50 V. Nene, J. R. Wortman, D. Lawson, B. Haas, C. Kodira, Z. J. Tu, B. Loftus, Z. Xi, K. Megy, M. Grabherr, Q. Ren, E. M. Zdobnov, N. F. Lobo, K. S. Campbell and S. E. Brown, *et al.*, *Science*, 2007, **316**, 1718–1723.
51 E. Di Cera, *IUBMB Life*, 2009, **61**, 510–515.
52 L. G. Arlian, *Annu. Rev. Entomol.*, 2002, **47**, 395–433.
53 U. Pippirs, H. Mehlhorn, A. S. Antal, K. W. Schulte and B. Homey, *Br. J. Dermatol.*, 2009, **161**, 208–209.
54 J. Hindley, S. Wunschmann, S. M. Satinover, J. A. Woodfolk, F. T. Chew, M. D. Chapman and A. Pomes, *J. Allergy Clin. Immunol.*, 2006, **117**, 1389–1395.
55 K. Y. Jeong, C. S. Hong and T. S. Yong, *Protein Pept. Lett.*, 2007, **14**, 934–942.
56 U. A. Bommer and B. J. Thiele, *Int. J. Biochem. Cell Biol.*, 2004, **36**, 379–385.
57 K. W. Choi and Y. C. Hsu, *Cell Adhes. Migr.*, 2007, **1**, 129–130.
58 J. M. Ribeiro, F. Alarcon-Chaidez, I. M. Francischetti, B. J. Mans, T. N. Mather, J. G. Valenzuela and S. K. Wikel, *Insect Biochem. Mol. Biol.*, 2006, **36**, 111–129.
59 A. Mulenga and A. F. Azad, *Exp. Appl. Acarol*, 2005, **37**, 215–229.
60 A. Mulenga, K. R. Macaluso, J. A. Simser and A. F. Azad, *Insect Biochem. Mol. Biol.*, 2003, **33**, 911–919.
61 K. S. Paludo, S. M. Biscaia, O. M. Chaim, M. F. Otuki, K. Naliwaiko, P. A. Dombrowski, C. R. Franco and S. S. Veiga, *Comp. Biochem. Physiol., Part C: Toxicol. Pharmacol.*, 2009, **149**, 323–333.
62 R. P. Wright, K. D. Elgert, B. J. Campbell and J. T. Barrett, *Arch. Biochem. Biophys.*, 1973, **159**, 415–426.
63 A. R. Young and S. J. Pincus, *Toxicon*, 2001, **39**, 391–400.
64 K. C. Barbaro, I. Knysak, R. Martins, C. Hogan and K. Winkel, *Toxicon*, 2005, **45**, 489–499.
65 D. J. Strydom, *Nat. New Biol.*, 1973, **243**, 88–89.
66 C. Y. Dy, P. Buczek, J. S. Imperial, G. Bulaj and M. P. Horvath, *Acta Crystallogr., Sect. D: Biol. Crystallogr.*, 2006, **62**, 980–990.
67 A. Mulenga, R. Khumthong and M. A. Blandon, *J. Exp. Biol.*, 2007, **210**, 3188–3198.
68 C. H. Yuan, Q. Y. He, K. Peng, J. B. Diao, L. P. Jiang, X. Tang and S. P. Liang, *PLoS One*, 2008, **3**, e3414.
69 V. Župunski, D. Kordis and F. Gubensek, *FEBS Lett.*, 2003, **547**, 131–136.
70 E. K. Millers, M. Trabi, P. P. Masci, M. F. Lavin, J. de Jersey and L. W. Guddat, *FEBS J.*, 2009, **276**, 3163–3175.
71 I. C. Forster, N. Hernando, J. Biber and H. Murer, *Kidney Int.*, 2006, **70**, 1548–1559.
72 A. Böhne, F. Brunet, D. Galiana-Arnoux, C. Schultheis and J. N. Volff, *Chromosome Res.*, 2008, **16**, 203–215.
73 G. F. King, H. W. Teford and F. Maggio, *J. Toxicol., Toxin Rev.*, 2002, **21**, 359–389.
74 B. L. Sollod, D. Wilson, O. Zhaxybayeva, J. P. Gogarten, R. Drinkwater and G. F. King, *Peptides*, 2005, **26**, 131–139.
75 K. H. Gowd, K. S. Krishnan and P. Balaram, *Mol. BioSyst.*, 2007, **3**, 554–566.
76 K. C. Barbaro, V. R. Eickstedt and I. Mota, *Toxicon*, 1994, **32**, 113–120.
77 E. A. Bogdanova, D. A. Shagin and S. A. Lukyanov, *Mol. BioSyst.*, 2008, **4**, 205–212.

Biochimica et Biophysica Acta 1811 (2011) 84–96

Contents lists available at ScienceDirect

Biochimica et Biophysica Acta

journal homepage: www.elsevier.com/locate/bbalip

Phospholipase-D activity and inflammatory response induced by brown spider dermonecrotic toxin: Endothelial cell membrane phospholipids as targets for toxicity

Olga M. Chaim [a,b], Rafael B. da Silveira [c], Dilza Trevisan-Silva [b], Valéria P. Ferrer [b], Youssef B. Sade [b], Mariana Bóia-Ferreira [b], Luiza H. Gremski [a], Waldemiro Gremski [b,d], Andrea Senff-Ribeiro [b], Hélio K. Takahashi [a], Marcos S. Toledo [a], Helena B. Nader [a], Silvio S. Veiga [b,*]

[a] Department of Biochemistry, Federal University of São Paulo, São Paulo, Brazil
[b] Department of Cell Biology, Federal University of Paraná, Curitiba, Brazil
[c] Department of Structural, Molecular Biology and Genetics, State University of Ponta Grossa, Ponta Grossa, Brazil
[d] Catholic University of Paraná, Health and Biological Sciences Institute, Curitiba, Brazil

ARTICLE INFO

Article history:
Received 16 August 2010
Received in revised form 10 November 2010
Accepted 11 November 2010
Available online 20 November 2010

Keywords:
Venom
Loxosceles intermedia
Dermonecrotic toxin
Phospholipase-D
Endothelial cell
Inflammatory response

ABSTRACT

Brown spider dermonecrotic toxins (phospholipases-D) are the most well-characterized biochemical constituents of *Loxosceles* spp. venom. Recombinant forms are capable of reproducing most cutaneous and systemic manifestations such as dermonecrotic lesions, hematological disorders, and renal failure. There is currently no direct confirmation for a relationship between dermonecrosis and inflammation induced by dermonecrotic toxins and their enzymatic activity. We modified a toxin isoform by site-directed mutagenesis to determine if phospholipase-D activity is directly related to these biological effects. The mutated toxin contains an alanine substitution for a histidine residue at position 12 (in the conserved catalytic domain of *Loxosceles intermedia* Recombinant Dermonecrotic Toxin — LiRecDT1). LiRecDT1H12A sphingomyelinase activity was drastically reduced, despite the fact that circular dichroism analysis demonstrated similar spectra for both toxin isoforms, confirming that the mutation did not change general secondary structures of the molecule or its stability. Antisera against whole venom and LiRecDT1 showed cross-reactivity to both recombinant toxins by ELISA and immunoblotting. Dermonecrosis was abolished by the mutation, and rabbit skin revealed a decreased inflammatory response to LiRecDT1H12A compared to LiRecDT1. Residual phospholipase activity was observed with increasing concentrations of LiRecDT1H12A by dermonecrosis and fluorometric measurement *in vitro*. Lipid arrays showed that the mutated toxin has an affinity for the same lipids LiRecDT1, and both toxins were detected on RAEC cell surfaces. Data from *in vitro* choline release and HPTLC analyses of LiRecDT1-treated purified phospholipids and RAEC membrane detergent-extracts corroborate with the morphological changes. These data suggest a phospholipase-D dependent mechanism of toxicity, which has no substrate specificity and thus utilizes a broad range of bioactive lipids.

1. Introduction

Dermonecrotic toxins are biologically and biochemically well-characterized constituents of the Brown spider (genus *Loxosceles*) venom complex mixture. Most of the described toxic effects associated with brown spiders, such as an intense inflammatory response at the bite site, hemostasis disorders, renal injury, platelet aggregation, and the typical necrotic lesion of the skin, can be experimentally reproduced using dermonecrotic toxins [1–5].

Histological findings for animals exposed to whole venom have shown subendothelial blebs, vacuoles, endothelial cell membrane degeneration of the blood vessel walls, and fibrin and thrombus formation [6,7]. Moreover, Paludo et al. [8] demonstrated morphological alterations in an endothelial cell line derived from the rabbit aorta (RAEC) treated with whole venom such as cell retraction, homophilic disadhesion, and an increase in filopodia projections. In addition, venom was observed to bind to the cell surface and extracellular matrix. These direct cytotoxic effects on blood vessel cells could be responsible for triggering intense infiltration of inflammatory cells. In addition, they could indirectly lead to leukocyte and platelet activation, disseminated intravascular coagulation, and an increase in vessel permeability.

Dermonecrotic toxins are very characteristic and conserved molecules among *Loxosceles* species. Currently, more than ten complete mRNA sequences for *Loxosceles* spp. dermonecrotic toxins have been deposited in the nucleotide databases [3,9]. These toxins were biochemically reported as sphingomyelinase-D (or sphingomyelin phosphodiesterase D; E.C. 3.1.4.41) family members due to their

* Corresponding author. Department of Cell Biology, Federal University of Paraná, Jardim das Américas, 81531-990, Curitiba, Paraná, Brazil. Fax: +55 41 3266 2042.
E-mail address: veigass@ufpr.br (S.S. Veiga).

1388-1981/$ – see front matter © 2010 Elsevier B.V. All rights reserved.
doi:10.1016/j.bbalip.2010.11.005

ability to catalyze the hydrolysis of sphingomyelin [1,2]. Recently, Lee and Lynch [10] suggested that the dermonecrotic toxin family should be more accurately named phospholipases-D due to their additional hydrolytic activity upon glycerophospholipids.

Six isoforms of phospholipase-D were cloned from a cDNA library of *L. intermedia* gland venom and then expressed; they were shown to have similar toxic effects to those of native venom toxins [11–15]. Appel et al. [11] performed an alignment analysis of the cDNA-deduced amino acid sequences for LiRecDT1 (ABA62021), LiRecDT2 (ABB69098), LiRecDT3 (ABB71184), LiRecDT4 (ABD91846), LiRecDT5 (ABD91847), and LiRecDT6 (ABO87656). The results of this alignment corroborated the crystal structure analysis of a dermonecrotic toxin described by Murakami et al. [16] that suggested conserved residues at the proposed catalytic site.

Two histidine residues (H12 and H47) are postulated to be responsible for an acid–base reaction stabilized by Mg^{+2} ion coordination at the catalytic site. In the intermediate steps of the hypothetical mechanism, the His12 residue must be deprotonated for the subsequent nucleophilic attack of a water molecule to succeed. This mechanism can be followed by the final release of ceramide 1-phosphate (C1P) from the sphingomyelin substrate or lysophosphatidic acid (LPA) from a lysophospholipid [16,17].

Studies on lipid metabolism have shown that glycerophospholipids and sphingolipids are not simply structural constituents of cell membranes. Bioactive lipid mediators have been shown to play a major role in complex signaling pathways that control several cellular dynamics such as cell growth, survival, differentiation, and motility. They have also been shown to play roles in various pathophysiologic processes, all of which involve several G-protein-coupled receptors (GPCRs) and kinase cascades [18–20].

Pettus et al. [21] showed that C1P, rather than ceramide, functions as the proximal mediator of arachidonic acid release. Exogenous C1P alone can stimulate arachidonic acid release and prostaglandin E2 formation. Treatment of cells with spider venom sphingomyelinase-D to produce C1P from membrane sphingomyelin can elicit the arachidonic acid response [22]. Likewise, phospholipase-D can induce LPA formation by catalyzing the hydrolysis of a *lyso*-phospholipid precursor. In quiescent fibroblasts, exogenous PLD (from *Streptomyces chromofuscus*) generated bioactive LPA from pre-existing lysophosphatidylcholine in the outer membrane leaflet, resulting in the activation of G-protein-coupled LPA receptors and subsequent activation of the Ras, Rho, and Ca^{2+} signaling pathways [23]. Similarly, recombinant SMaseD from *L. laeta* was able to hydrolyze lysophosphatidylcholine to produce LPA and choline. Recombinant PLD from *L. recluse* also degraded several purified lysophospholipids and sphingomyelin substrates [10,24]. Gene expression profiles of human fibroblasts treated with *L. recluse* isoform I recombinant toxin (SMD) showed the upregulation of genes related to human cytokines and genes involved in the glycosphingolipid metabolism pathway. Furthermore, they speculated that sphingomyelinase activity on cell membranes, which results in ceramide 1-phosphate (C1P) production, induces the pro-inflammatory molecules NF-kB and IL-8 [25].

In the literature, there are several proteins with enzymatic activities (as well as catalytic domain structures) that are not responsible for the toxicity observed in experimental systems. Snake venom phospholipases A2 (PLA2) present remarkable diversity in their biological effects in addition to their catalytic activity. Sequence alignment analyses of functionally related PLA2 are frequently used to predict the structural determinants of these effects, and the predictions are subsequently evaluated by site-directed mutagenesis experiments and functional assays [26]. In this way, Sakamoto et al. [27] demonstrated that modified CyaAs (calmodulin-dependent adenylate cyclases from *Bordetella pertussis*) display hemolytic activity identical to the original toxin.

The absence of a clear correlation between catalysis and pharmacological activity and the diversity of biological effects raises questions regarding the structural basis of these biological functions. Nephrotoxicity and hemolysis directly induced by phospholipase-D activity were already reported in literature [10,28,29]. However, dermonecrosis *in vivo* and inflammatory response triggered by brown spider phospholipase-D toxin were not yet described as directly dependent on its catalytic activity. In this report, we used a site-directed mutagenesis strategy to clone and express a mutated form of the previously reported dermonecrotic toxin known as LiRecDT1 (ABA62021) [12]. The substitution of a histidine residue at position 12 in the amino acid sequence with an alanine was performed to modify the organization of the active site and interfere with the catalytic reaction of the enzyme.

We investigate the correlation between the toxicity reported in loxoscelism (mainly characterized by dermonecrosis and inflammatory disturbance) and the biochemical and catalytic mechanism of phospholipase-D. We report evidence demonstrating the dependence of the biological effects on phospholipase-D activity of dermonecrotic toxin *in vivo* and *in vitro*, bringing new insights to the molecular mechanism of phospholipase-D activity.

2. Materials and methods

2.1. Reagents

Whole venom from *L. intermedia* obtained by electrostimulation (15 V) of the cephalothorax of spiders captured in the wild was solubilized in PBS and maintained frozen until used, as described by Feitosa et al. [30]. Polyclonal antibodies to *L. intermedia* phospholipase-D toxin and whole venom were produced in rabbits as described by Chaim et al. [12]. Hyperimmune IgGs were purified from sera using a mixture of Protein-A and Protein-G Sepharose beads (GE Healthcare, Chalfont St Giles, England), as recommended by the manufacturer. Fluorescein-conjugated anti-rabbit IgG and alkaline phosphatase-conjugated or peroxidase-conjugated anti-rabbit IgG were purchased from Sigma (St. Louis, USA).

2.2. Site-directed mutagenesis of LiRecDT1

Cloning from the venom gland cDNA library was performed following the methods of Chaim et al. [12]. GenBank data deposition information for *L. intermedia* cloned cDNA can be found under LiRecDT1 (DQ218155). The cDNA corresponding to the mature phospholipase-D original protein was amplified by PCR. The sense primer used was 30Rec (5′-CTCGAGGCAGGTAATCGTCGGCCTATA-3′), which was designed to contain a XhoI restriction site (underlined) plus the sequence for the first seven amino acids of the mature protein. The antisense primer used was 30Rec (5′-CGGGATCC**TA**TTTCTTGAATGTCACCCA-3′), which contains a BamHI restriction site (underlined) and a stop codon (bold). The PCR product was cloned into the pGEM-T vector (Promega, Madison, USA), subcloned into pET-14b (Novagen, Madison, USA) and digested with XhoI and BamHI. The mutated toxin was obtained using the Megaprimer PCR method adapted from Sambrook and Russell [31]. This protocol was performed using three rounds of PCR to carry out site-directed mutagenesis in the LiRecDT1 sequence, and the resulting mutated toxin was named LiRecDT1 H12A. Briefly, the first round of PCR included site-directed mutagenesis of the first histidine amino acid residue using the forward primer T7, which anneals to the pSPORT vector 5′ portion, and the special reverse primer P1H12A (5′-ATTTACCATG**GC**CCCCATGATC-3′), which contains the codon substitute for alanine plus the sequence for the other original amino acids. The "megaprimer" for the next round was obtained by agarose gel electrophoresis of the first PCR product (~200 bp) and purified using the QIAquick Gel Extraction Kit (QIAGEN, Hilden, Germany). In the second step, PCR was performed to obtain the mutated product using the "megaprimer" as the sense primer and 30Rec as the antisense

primer (3′ BamHI restriction site). The second PCR product was subjected to the same protocol of agarose gel purification. In the final step of mutagenesis, a third PCR reaction was performed to insert the 5′ XhoI restriction site from the second PCR product by using 30Rec as the sense primer and 30Rec as the antisense primer. Finally, this last PCR product was digested with restriction enzymes and purified by agarose gel electrophoresis. The mutated product was then cloned into the pGEM-T vector (Promega) and subcloned into pET-14b (Novagen). The correct construct was confirmed by miniprep sequencing.

2.3. Original (LiRecDT1) and mutated LiRecDT1 (LiRecDT1 H12A) recombinant toxin expression and purification

Both recombinant constructs were expressed as fusion proteins with a poly-(6X) His tag at the N-terminus as previously described by Chaim et al. [12]. Briefly, pET-14b/*L. intermedia* cDNA constructs were transformed into One Shot *E. coli* BL21(DE3)pLysS competent cells (Invitrogen). Expression conditions were standardized for induction with IPTG (isopropyl β-D-thiogalactoside) for 3.5 h at 30 °C in 1 L of LB broth cultures. Cell suspensions were sonicated with six 10-second cycles at low intensity, and lysed materials were centrifuged (20,000×*g*, 20 min). The recovered supernatants were incubated for affinity chromatography with 1 ml of Ni^{2+}-NTA agarose beads for 1 h at 4 °C. Recombinant protein/beads suspensions were loaded into a column and exhaustively washed until the OD at 280 nm reached 0.01 (washing buffer: 50 mM sodium phosphate pH 8.0, 500 mM NaCl, 20 mM imidazole). Recombinant proteins were eluted with 10 ml of elution buffer (washing buffer, but 250 mM imidazole). Protein expression analysis on 12.5% SDS-PAGE was performed for purity and was stained with Coomassie Blue dye. For experimental negative controls, a recombinant toxin with similar molecular mass and obtained from the same cDNA library was used. This control toxin was characterized as an "astacin-like metalloprotease" [32] and caused no dermonecrosis, as evidenced by the dermonecrotic assay following injection into rabbit skin (data not shown).

2.4. Circular dichroism spectra measurements

Recombinant original and mutated toxins were dialyzed at 4 °C against 10 mM sodium phosphate buffer, pH 7.4, and their spectra were recorded in a Jasco J-810 spectropolarimeter (Jasco Corporation, Tokyo, Japan) using a 1-mm gap cuvette. Each reported spectrum (0.5 nm interval) is the average of eight measurements performed at a rate of 50 nm/min using a response time of 8 s and a bandwidth of 1 nm. The temperature was kept constant at 25 °C.

2.5. Phospholipase activity assay

Phospholipase-D activity was measured using the Amplex Red Assay Kit (Molecular Probes, Eugene, USA). In this assay, phospholipase-D activity was monitored using 10-acetyl-3,7-dihydroxyphenoxazine (Amplex Red reagent), a sensitive fluorogenic probe for H_2O_2. First, phospholipase hydrolyzes sphingomyelin to yield C1P and choline. Choline is oxidized by choline oxidase to betaine and H_2O_2. Finally, H_2O_2 in the presence of horseradish peroxidase reacts with Amplex reagent in a 1:1 stoichiometry to generate the highly fluorescent product resorufin. Recombinant toxins (10 μg each to start, in three trials; later 100, 250 and 500 μg of LiRecDT1 H12A) were added to the Amplex Red reagent mixture to a final volume of 500 μl. The reaction tubes were incubated at 37 °C in a water bath for 30 min and fluorescence was measured in a fluorometer (Shimadzu Model RF-5301 PC Fluorescence Spectrophotometer) using excitation at 560 nm and emission detection at 590 nm. The controls were LALP (loxosceles astacin-like protease) [32] for a negative control and whole venom for a positive control. Sphingomyelinase (0.004 U) from *Bacillus cereus* (1 U = 1 μmol min^{-1}) was co-tested, and fluorescence intensity was used as standard for comparing ends. Fluorescence intensity values were converted to units of phospholipase activity, which were expressed as μmol min^{-1} (amount of substrate hydrolyzed per minute).

2.6. Animals

Adult rabbits weighing approximately 3 kg obtained from the Central Animal House of the Federal University of Paraná were used for *in vivo* experiments with recombinant toxins. All experimental protocols using animals were performed according to the "Principles of laboratory animal care" (NIH Publication no. 85-23, revised 1985) and the "Brazilian Federal Laws" as well as the ethical committee agreement number 246 of the Federal University of Paraná.

2.7. Dermonecrosis in vivo

For the evaluation of dermonecrotic effects, 10 μg of each toxin was injected intradermally into a shaved area of the rabbit skin for the first experiments. Animals were observed over the course of dermonecrotic lesion evolution. The LiRecDT1 H12A residual activity experiment was performed under the same conditions, except that doses were increased to 100, 250, and 500 μg of mutated toxin. Acquisition of macroscopic pictures was performed after 4 h and 24 h of toxin application, and skin samples were collected at the end of the experiment for microscopic analysis and myeloperoxidase (MPO) activity assay.

2.8. Tissue MPO activity assay

The activity of tissue MPO was also assessed 24 h after injection of toxins into the rabbit skin, according to a technique modified from Bradley et al. [33,34]. Briefly, samples were placed in 0.75 ml of 80 mM phosphate-buffered saline (PBS), pH 5.4, containing 0.5% hexadecyltrimethylammonium bromide, and then homogenized (45 s at 0 °C) in a motor-driven homogenizer. The homogenate was decanted into a microfuge tube, and the vessel was washed with 0.75 ml of hexadecyltrimethylammonium bromide in buffer. The wash was added to the tube, and the 1.5-ml sample was centrifuged at 12,000×*g* at 4 °C for 15 min. Triplicate 30 μl samples of the resulting supernatant was added to 96-well microtiter plates. For the assay, 200 μl of a mixture containing 100 μl of 80 mM PBS, pH 5.4, 85 μl of 0.22 M PBS, pH 5.4, and 30 μl of 0.017% hydrogen peroxide was added to the wells. The reaction was started with the addition of 20 μl 18.4 mM tetramethylbenzidine HCl in dimethylformamide. Plates were incubated at 37 °C for 10 min, and then the reaction was stopped by the addition of 30 μl of 1.46 M sodium acetate, pH 3.0. Enzyme activity was determined colorimetrically using a plate reader (EL808, BioTech Instruments, Inc.) set to measure absorbance at 630 nm and was expressed as mOD/mg tissue.

2.9. Histological procedure for light microscopy

Skin samples were collected from rabbits anesthetized with ketamine (Agribands, Paulinia, Brazil) and acepromazine (Univet, São Paulo, Brazil) and then fixed in Bouin's fixative solution (picric acid saturated solution, 750 ml; formaldehyde 36–40%, 250 ml; acetic acid, 50 ml) for 16 h at room temperature. After fixation, samples were dehydrated in a graded series of ethanol before being paraffin embedded (for 2 h at 58 °C). Then, thin tissue sections (4 μm) were processed and stained with hematoxylin and eosin (H&E).

2.10. Immunological cross-reactivity of original and mutated toxin

The protein content of experimental samples was determined by the Coomassie Blue method (BioRad, Hercules, USA). For immunoblotting, 5 μg of each toxin was subjected to 12.5% SDS-PAGE under reducing conditions, transferred onto nitrocellulose filters overnight and immunostained with hyperimmune sera (either against phospholipase-D toxin or whole venom). Secondary alkaline phosphatase-coupled anti-IgG were detected and visualized using the BCIP/NBT substrate reaction. For the antibody capture assay (ELISA), tests were performed in pentaplicate with 10 μg/ml of venom and LiRecDTs toxins as antigens. Purified hyperimmune IgGs, anti-LiRecDT1, and anti-whole venom were tested (0.1–1 μg/ml), followed by detection with secondary peroxidase-coupled anti-IgG and reading of the absorbance at 450 nm for the OPD substrate reaction [35].

2.11. Protein–lipid overlay assay (fat blot)

The affinity of toxins for specific lipids was tested using the SphingoStrips recommended method (Molecular Probes, Eugene, USA). In summary, nitrocellulose membranes containing 100 pmol samples of 15 different lipids and a blank sample were blocked using Tris-buffered saline plus 0.02% Tween-20 (TBS-T) with 3% fatty acid-free bovine serum albumin (BSA) and gently agitated for 1 h at room temperature. Then, the membranes were incubated with 0.5 μg/ml of the toxins (whole venom, LiRecDT1, or LiRecDT1 H12A) in TBS-T plus 3% BSA at 4 °C overnight. Membranes were then washed with TBS-T plus 3% BSA three times for 10 min using gentle agitation. Toxin binding was detected using anti-venom or anti-LiRecDT1 purified IgGs and revealed by alkaline phosphatase-labeled secondary antibodies and BCIP/NBT substrate.

2.12. Cell culture conditions

RAEC (rabbit aorta endothelial cells) were grown as monolayer cultures in F12 medium containing gentamicin (40 mg/L) supplemented with 10% fetal calf serum (FCS). The cultures were kept at 37 °C in a humidified atmosphere with 5% CO_2. For inverted light microscopy observation and confocal immunofluorescence analysis, release of cells was performed by treatment with 0.25% viokase/HBSS for a few minutes. After counting, the cells were resuspended in an adequate volume of medium supplemented with FCS, and 5×10^3 cells were replated on glass coverslips (13 mm diameter) and allowed to adhere and grow for 48 h. The cells were then incubated in the presence of the recombinant toxins (10 μg/ml). Changes in cell morphology were evaluated and photographed using an inverted microscope (Leica-DMIL, Wetzlar, Germany) at 1 h and 4 h after recombinant toxin addition. The same experimental conditions were used with control cells, except that the medium contained appropriate amounts of vehicle (PBS) instead of recombinant toxins.

2.13. RAEC immunofluorescence assay

For immunofluorescence microscopy, after recombinant toxins exposure for 4 h at 37 °C, RAEC cells were rapidly washed with PBS, fixed with 2% paraformaldehyde in PBS for 30 min at 4 °C, incubated with 0.1 M glycine for 3 min, and blocked with PBS containing 1% BSA for 1 h at room temperature. Coverslips were incubated for 1 h with polyclonal antibodies raised against phospholipase-D (2 μg/ml) as described in the Reagents section. Cells were washed three times with PBS, blocked with PBS containing 1% BSA for 30 min at room temperature, and then incubated with Alexa® 488-conjugated anti-rabbit IgG secondary antibodies (Molecular Probes) at room temperature for 40 min. After washing, samples were mounted using Fluormont-G (Sigma) and observed under a fluorescence confocal microscope (Confocal Radiance 2100, BioRad) coupled to a Nikon-Eclipse E800 with Plan-Apochromatic objectives (Sciences and Technologies Group Instruments Division, Melville, USA).

2.14. Choline release detection from RAEC cell extract

Extracts of RAEC cell membranes were obtained from approximately 5×10^6 cells (150 cm^3 culture bottle). Cells were scraped and resuspended in 1 ml of cold extraction buffer (Tris–HCl 50 mM, NaCl 150 mM, Triton X-100 0.5%). After gently homogenizing for 10 min at 4 °C, cells were centrifuged at $20{,}000\times g$ for 20 min at 4 °C and supernatants were collected for later use. RAEC cells extracts (100 μl) were utilized as a substrate for LiRecDT1 and LiRecDT1 H12A (both in two concentrations, 50 μg and 100 μg) in a total final volume of 250 μl for 1 h at 37 °C and gently mixed using a rotational shaker in a BOD incubator. Treated extracts were then added to a 250 μl reaction mixture adapted from the Amplex Red Sphingomyelinase Assay Kit (Molecular Probes) containing choline oxidase (4 U), alkaline phosphatase (80 U), horseradish peroxidase (20 U), and Amplex Red reagent (100 μM), excluding sphingomyelin substrate. After incubation in a water bath for 1 h at 37 °C, fluorescence development was measured in a fluorometer (Shimadzu Model RF-5301 PC Fluorescence Spectrophotometer) using excitation set at 560 nm and emission detection at 590 nm.

2.15. Lipid analysis by high-performance thin-layer chromatography

For analysis of hydrolysis, recombinant toxins (50 μg) were incubated with RAEC cell extracts (50 μl or 100 μl) for 3, 8 or 16 h, and purified phospholipids for 3 h at 20 °C. Lipids present in these detergent-soluble samples were recovered directly by partition with 2 ml of water-saturated 1-butanol; the butanol fraction was dried, resuspended in chloroform, and analyzed by high-performance thin-layer chromatography (HPTLC). Analytical HPTLC was performed on silica gel 60 plates (E. Merck, Darmstadt, Germany) using chloroform–methanol–methylamine 40% (65:35:10 v/v/v) as the mobile phase. Lipid samples were dissolved in chloroform and 20 μl were applied by micropipetting, and then visualized under ultraviolet light after spraying with 0.01% primulin in 90% aqueous acetone [36]. Differences in lipid content were quantified by densitometry of digital images from HPTLC plates acquired by GeneSnap Software for G:Box Chemi XL (Syngene, Cambridge, England) and quantified by Quantity One Software for Chemic Doc XRS (BioRad, Hercules, USA). The standard mixture contained 1 mg/ml each of five phospholipids (Sigma): phosphatidylinositol (PI), phosphatidylcholine (PC), phosphatidylethanolamine (PE), and phosphatidylserine (PS). Toxins were also incubated with 10 μg of purified phospholipids: asymmetric PC or 16:0–18:0 PC (1-palmitoyl-2-stearoyl-*sn*-glycero-3-phosphocholine), and PAF *platelet-activating factor* or C16-2:0 PC (1-O-hexadecyl-2-acetoyl-*sn*-glycero-3-phosphocholine), and synthetic alkyl-phospholipids such as *lyso*PC or 16:0 Lyso PC (1-palmitoyl-2-hydroxy-*sn*-glycero-3-phosphocholine) and *lyso*PAF or C16 Lyso PAF (1-O-hexadecyl-2-hydroxy-*sn*-glycero-3-phosphocholine). Purified egg chicken sphingomyelin (egg SM) and other phospholipids tested were purchased from Avanti Polar Lipids, Inc. (Alabaster, USA).

2.16. Statistical analysis

Statistical analysis of phospholipase activity and choline release data were performed using analysis of variance (ANOVA) and the Tukey test for average comparisons GraphPad InStat program version 3.00 for Windows. Mean ± SEM. values were used. Significance was determined as $p \leq 0.05$.

3. Results

3.1. Cloning and expression of a mutated dermonecrotic toxin from LiRecDT1: drastic decrease of phospholipase-D activity by a single amino acid mutation

In order to obtain a mutated form of *L. intermedia* dermonecrotic toxin, an adapted "Megaprimer" PCR approach for site-specific mutation was used to clone a mutated dermonecrotic toxin based on the LiRecDT1 (GenBank accession number ABA62021) amino acid sequence [12]. This recombinant toxin contained an amino acid sequence that was substituted with alanine at the first histidine residue (His12), which plays a role in the catalytic reaction. Alteration of the active site was confirmed by sequencing analysis, and the resulting LiRecDT1 H12A mutated recombinant toxin was successfully expressed in the pET-14b system and purified in soluble form by Ni^{2+}-NTA affinity chromatography (Fig. 1A). To insure the correct folding of the mutated toxin occurred despite the changed nucleotide sequence, which codes for a different protein sequence, conformational circular dichroism spectra measurements were performed. Indeed, we observed a secondary structure spectrum for the mutated form that was very similar to the LiRecDT1 CD profile as depicted in Fig. 1B. To investigate the enzymatic behavior of the mutated LiRecDT1 H12A phospholipase-D toxin *in vitro*, a fluorometric assay using sphingomyelin as the reaction substrate was performed (see Materials and methods section for details). LiRecDT1 and whole venom showed the expected high phospholipase-D activity [12], but the mutated toxin had almost no sphingomyelin hydrolysis activity under the same conditions. Fig. 1C shows that the activity of 10 μg of recombinant original toxin was about 85-fold higher than that of the mutated toxin.

3.2. LiRecDT1 H12A did not induce dermonecrosis in rabbit skin and caused only a small inflammatory reaction

Dermonecrotic macroscopic development was observed in rabbit skin after 4 h and 8 h of exposure to 10 μg of whole venom (as a positive control) and original recombinant dermonecrotic toxin. However, treatment with the mutated form did not cause obvious dermonecrotic development, and the reaction was similar to the negative control (see Experimental). In addition, no edema or erythema was observed at the injection site in response to the mutated form (Fig. 2A). Light microscopic analysis of rabbit skin biopsies after 24 h of toxin treatment (Fig. 2B) demonstrated typical intense inflammatory cell accumulation and collagen fiber disorganization in the dermis with LiRecDT1 treatment. However, biopsy analysis of LiRecDT1 H12A exposed skin demonstrated a less intense inflammatory response. The neutrophil migration into the dermis was indirectly determined by means of MPO activity of tissue biopsies (Fig. 2C), and the differences in these values correlate with the microscopic analysis of inflammatory reaction.

3.3. The residual activity of LiRecDT1 H12A is concentration-dependent

As the microscopic analysis revealed an inflammatory reaction in rabbit skin treated with mutated recombinant toxin, it is possible that very low phospholipase-D activity persists despite modification of His12A in the catalytic site. This residual activity could be responsible for the observed biological effects. For this reason, phospholipase-D activity and dermonecrosis analysis of LiRecDT1 H12A were examined again at much higher concentrations. Higher amounts of LiRecDT1 H12A (100 μg, 250 μg, and 500 μg) were used in both experiments with the previously described conditions (Fig. 3). A 2.4-fold increase in phospholipase activity was observed between 100 and 500 μg protein. The phospholipase-D activity of the highest concentration tested (500 μg) compared to 10 μg of original recombinant toxin was still 7-fold less intense (Figs. 1C and 3A). Moreover, Fig. 3B depicts *in vivo* experiments showing formation of edema and erythema at the injection site that were much less intense compared to those observed with LiRecDT1 after 4 h. At 24 h post LiRecDT1 H12A exposure, rabbit skin showed more edema, and an initial white eschar, known as a marble plate in loxoscelism (that commonly evolves into necrotic lesion) could be seen. Microscopic analyses (Fig. 3C) of biopsies from

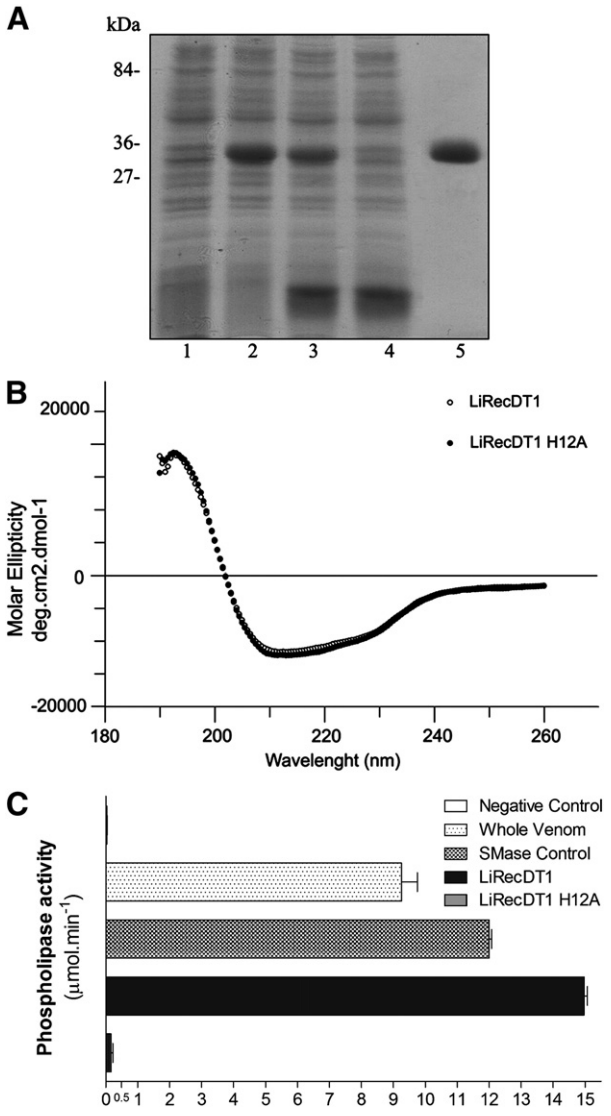

Fig. 1. Expression of a functional recombinant site-directed mutated dermonecrotic protein (LiRecDT1 H12A). (A) SDS-PAGE analysis of recombinant dermonecrotic toxin expression stained with Coomassie blue dye (12.5% gel under reducing conditions). Lanes 1 and 2 show *E. coli* BL21(DE3)pLysS cells collected by centrifugation and resuspended in gel loading buffer before and 3.5 h after induction with 0.05 mM IPTG, respectively. Lanes 3 and 4 depict the supernatant of cell lysates obtained by freeze thawing in extraction buffer before and after (*void*) incubation with Ni-NTA agarose beads, respectively. Lane 5 shows eluted recombinant protein. Molecular masses are shown on the left. (B) Circular dichroism spectra for the purified recombinant original and mutated toxins. Spectra were obtained using toxins in 10 mM sodium phosphate buffer, pH 7.4, at 25 °C. Molar ellipticity was analyzed in a wavelength range between 180 and 260 nm. (C) Phospholipase-D activity of recombinant toxins. Sphingomyelinase activities of LiRecDT1, LiRecDT1 H12A recombinant toxins, and whole venom were evaluated with the Amplex Red Assay Kit at 37 °C for 1 h; the product of the reaction was spectrofluorimetrically measured at 560 nm excitation and 590 nm emission wavelengths. A purified recombinant toxin without dermonecrotic and inflammatory activities was used as a negative control. Reactions were performed with 10 μg of whole venom or recombinant toxins ($n = 6$). Values given are the average ± SEM.

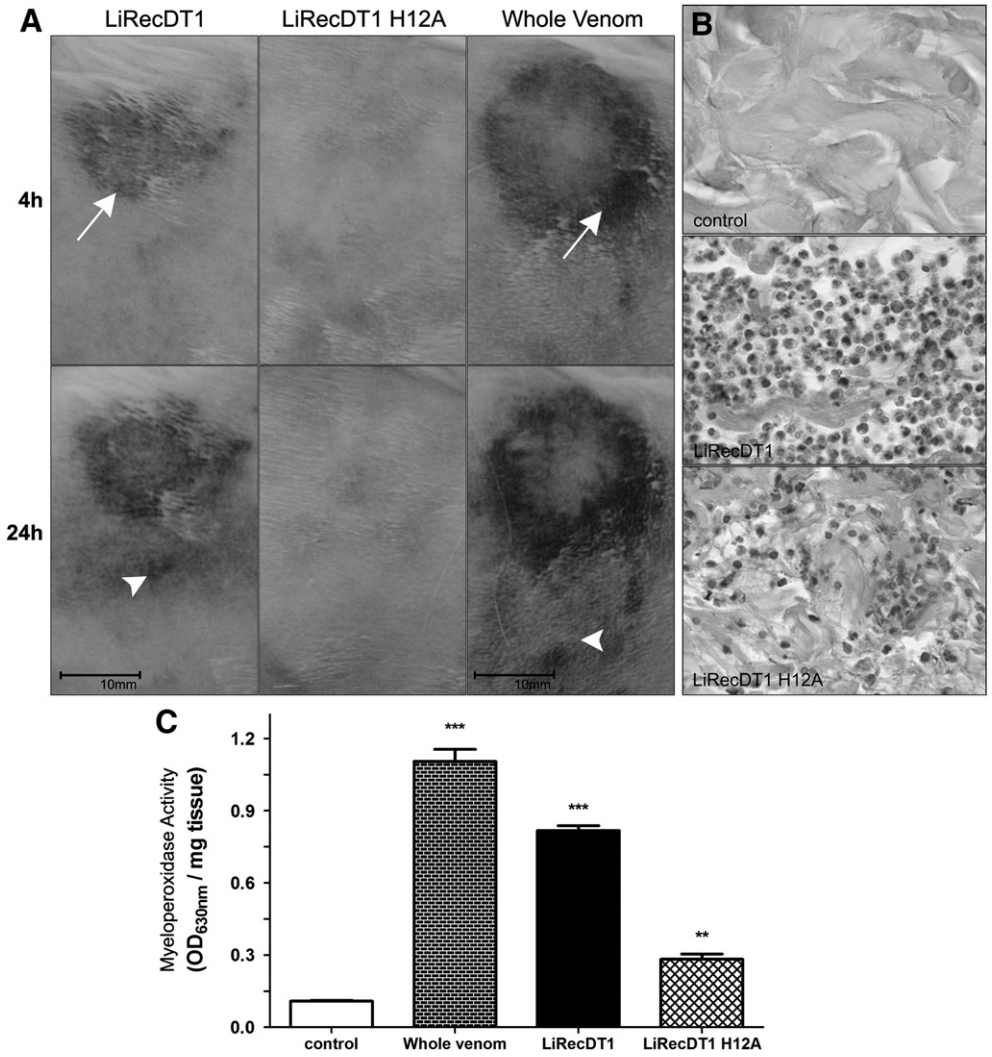

Fig. 2. Dermonecrosis and inflammatory response of rabbit skin exposed to recombinant toxins. (A) Macroscopic visualization of dermonecrosis of rabbits intradermally injected with 10 μg of whole venom (as positive control) or both recombinant toxins. Lesions were observed 4 and 24 h following venom and recombinant toxin injections. Arrows point to development of gravitational spreading of necrotic lesion post LiRecDT1 and whole venom injections. The scale bar is shown on the left. (B) Histopathological findings for rabbit skin were performed 24 h after recombinant toxin exposure. Light microscopic analysis of tissue sections were assessed by staining with hematoxylin and eosin (H&E). An intense inflammatory response with the presence of neutrophils and disorganization of collagen fibers in connective tissue is shown for the original toxin compared to a lower inflammatory reaction observed following mutated recombinant dermonecrotic toxin exposure. A recombinant toxin without phospholipase-D activity but obtained under identical conditions was used as a negative control (magnification 630×). (C) Inflammatory reactions induced by toxins and controls were estimated by measurement of myeloperoxidase activity from neutrophil infiltrate at the dermis. Values are expressed as mean ± SEM of absorbance at 630 nm. Each bar represents the mean of fifteen replicates (five from each of three tissue samples) of inoculation site at rabbit skin post 24 h. The asterisk denotes the significance levels when compared with negative control (*** $p<0.001$; ** $p<0.01$).

rabbit skin treated with LiRecDT1 H12A at the higher concentrations showed an abundant neutrophil perivascular infiltrate and collapse of blood vessel walls into the dermis.

3.4. Immunological cross-reactivity of original and mutated LiRecDTs

In order to determine whether antigens of our antibodies are conserved in the recombinant LiRecDT1 and LiRecDT1 H12A, we produced polyclonal antisera against whole venom and LiRecDT1. Whole venom served as the positive control for native phospholipase-D toxins, which were also recognized by both antisera. Experiments were performed by Western blot (antibodies recognize epitopes on denatured antigens) and ELISA (antibodies recognize non-denatured epitopes on antigens). The cross-immunoreaction of antisera for both recombinant toxins showed that site-directed mutation did not alter immunological recognition by polyclonal antibodies; therefore, these antibodies can be used for further experiments (Fig. 4).

3.5. Binding of both recombinant toxins to immobilized lipids in an overlapping assay

Fat blot assays are used for the identification of proteins possessing lipid recognition domains and for analysis of their lipid-binding specificities. Several different toxin interactions were detected via the protein–lipid overlay assay with a standard Western blot. These interactions have been shown to be involved in physiological and pathological processes including signal transduction mediated by GPCRs and induction of apoptosis [18–20,37,38]. With the goal of determining whether dermonecrotic toxin possesses some lipid affinity, we exposed the original and mutated isoform to immobilized lipids (Fig. 5). Additionally, we tested whole venom as a control to test native dermonecrotic toxins. Both recombinant isoforms bound to the same molecules: sphingomyelin and sphingosine 1-phosphate, phosphatidylcholine and *lyso*phosphatidylcholine, and cholesterol. As a negative control, the membrane containing immobilized lipids was exposed to antibodies in the absence of toxins (data not shown).

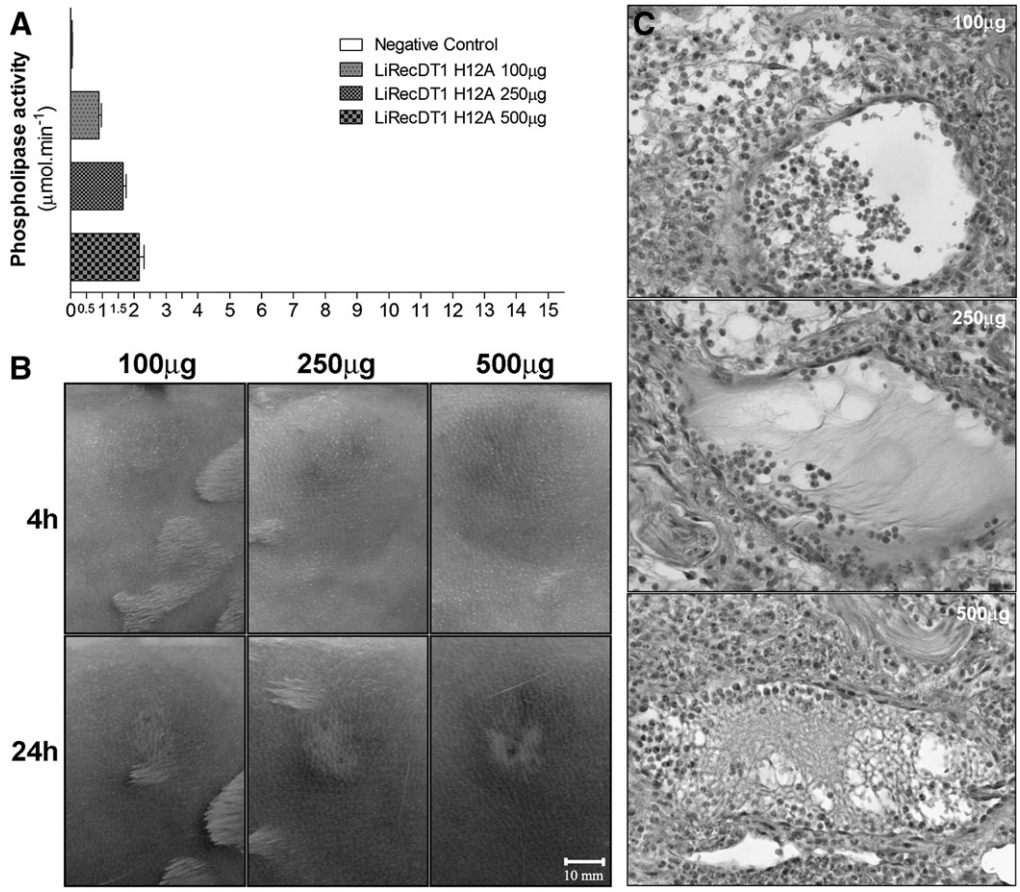

Fig. 3. Residual phospholipase-D and inflammatory activities of LiRecDT1 H12A. (A) Mutated recombinant toxin was tested for persistent sphingomyelinase activity with increasing doses of 100, 250, and 500 μg. Then, the Amplex Red Sphingomyelinase Assay Kit assay was performed using the same conditions and incubating at 37 °C for 1 h. Reactions were measured in a spectrofluorometer (wavelengths of 560 nm for excitation and 590 nm for emission). As a negative control, 10 μg of enzymatic non-related recombinant toxin was also tested to assess background fluorescence. Increasing concentration-dependent phospholipase-D activity was observed ($n=6$). Values given are the average ± SEM. (B) Macroscopic analysis of rabbit skin exposed to higher concentrations of LiRecDT1 H12A. In a dose-dependent reaction, we observed a punctate and transient erythema at the injection site 4 h post exposure to mutated toxin exposure (100, 250, and 500 μg). After 24 h, development of an ischemic halo surrounding the injection site indicates typical and initial formation of dermonecrosis described as a marble plate, and (C) microscopic analysis of tissue sections by H&E show a large inflammatory response with massive neutrophil diapedesis and fibrin deposition at disrupted blood vessels for all three concentrations tested (magnification 630×).

The H12A substitution in the catalytic domain did not alter LiRecDT1 binding-affinity to the lipids.

3.6. Recombinant dermonecrotic toxins bind to the RAEC cell surface as "planted antigens"

We next examined the cell membrane interaction of the dermonecrotic toxin phospholipase-D family specifically, as whole venom is a complex mixture of biochemically and biologically different toxins. To do this, we evaluated recombinant dermonecrotic toxin binding to the endothelial cell surface using hyperimmune IgGs against LiRecDT1 by confocal immunofluorescence analysis (Fig. 6). Cells treated with both recombinant toxins showed an intense positive reaction on the cell surface. Untreated cells (negative control) were treated to confirm that there was no non-specific binding of the hyperimmune antibodies. The interaction of toxins with RAEC cell membranes had a homogeneous distribution pattern. Again, LiRecDT1 H12A was also able to bind to the plasma membrane (an environment enriched in lipids) despite the mutation in the catalytic site.

3.7. Choline release from RAEC cell membrane extracts with LiRecDT1 treatment

Since the appearance of cluster-like aggregates were observed on RAEC cell membranes only after LiRecDT1 but not mutated toxin treatment, we examined whether cell membrane RAEC extracts could act as an enzymatic substrate for phospholipid hydrolysis. The original substrate used for the sphingomyelinase activity kit test (a purified sphingomyelin) was substituted with cell membrane detergent extract obtained from RAEC cells in culture (see Materials and methods for details). Therefore, not only sphingomyelin, but also other phospholipids from RAEC cell extracts could be the target of phospholipase-D. Incubation of recombinant toxins with extracts triggered significant formation of choline in response to LiRecDT1 in a concentration- and time-dependent manner (Fig. 7A). Changes in cell morphology triggered by LiRecDT1, such as cytoplasmic vacuolization and the presence of debris resulting from cell lysis were observed (Fig. 7B). These results suggested that phospholipase-D activity on membrane phospholipids correlates directly with cytotoxicity.

3.8. LiRecDT1 degrades lipids from RAEC cell membrane extracts and purified phospholipids

In addition to the phospholipase-D activity indirectly shown by choline release, hydrolysis of RAEC cell membrane extracts can be observed through high-performance thin-layer chromatography (HPTLC). Fig. 8A and B shows that after incubation with both LiRecDT1 and LiRecDT1 H12A, the intensity of primuline-positive bands decreased compared to non-treated extract control. With 50 μl of extracts, the band for phosphatidylethanolamine was gradually reduced to a final relative quantity of 37% after 16 h with active phospholipase-D. However, the mutated isoform was able to degrade

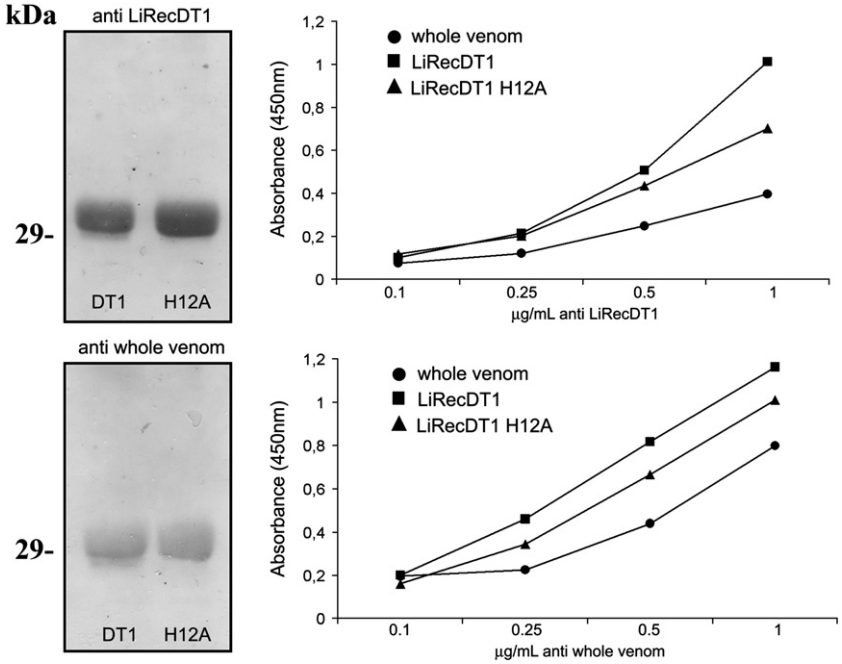

Fig. 4. Immunological cross-reactivity of the recombinant toxins LiRecDT1 and LiRecDT1 H12A. Original (DT1) and mutated (H12A) toxins at a concentration of 10 µg were electrophoresed by 12.5% SDS-PAGE under reducing conditions, transferred to nitrocellulose membranes, and incubated with purified IgGs from sera recognizing whole venom or LiRecDT1. Immunoblotting was performed with secondary antibodies coupled to alkaline phosphatase and BCIP/NBT substrate. Additionally, antibody capture assays (ELISA) were carried out using whole venom and recombinant toxins LiRecDT1 and LiRecDT1 H12A (10 µg/ml) immobilized on a solid phase. Again, purified antibodies against whole venom or LiRecDT1 (abscissa) were incubated for 2 h at room temperature and the immunoreaction was performed using secondary antibodies coupled to peroxidase and OPD substrate. Colorimetric measurement was performed by absorbance at 450 nm. Values given are average of pentuplicates.

only 5% of initial content. With two-fold greater volume (100 µl) of extracts but the same concentrations of recombinant toxins, bands for other lipids such as sphingomyelin and phosphatidylcholine are visible and show drastic intensity decreases. Specifically, SM was reduced to 5.6% and PC to 13.0% of the control. Interestingly, the mutated isoform of phospholipase-D was able to significantly degrade SM after 16 h to less than a half of initial content (41.1%), but the same was not observed for PC, which was only reduced to approximately 87.2% of control. The bands for phosphatidylserine were also reduced by both toxins, to 58.9% and 63.2% of control for LiRecDT1 and LiRecDT1 H12A, respectively. Next, we tested purified phospholipids individually (Fig. 8C and D) and found that 3 h after incubation, egg sphingomyelin and *lyso*PC were most susceptible to hydrolysis by recombinant toxins from *L. intermedia* with a reduction to 6.2% and 4.9% of control, respectively. The H12A mutation did not completely abolish its enzymatic ability, as the mutated toxin hydrolyzed both phospholipids but with lower effectiveness (77.0% and 59.2%, respectively). In addition, PC asymmetric, PAF and lysoPAF were also degraded by the toxins, but more significantly by the original than the mutated isoform. These results suggest that brown spider phospholipase-D has no specificity for one single type of lipid as a substrate/target. Lipid-derived products can be visualized at the top of those lanes with intense decrease of initial lipid content (*). Purified sphingomyelin and lysophospholipids were the best substrates of this enzyme, but after only 3 h of incubation other non-lysophospholipids were also significantly degraded. These were also observed in HPTLC with cell membrane extracts.

4. Discussion

Loxoscelism is characterized as a group of severe clinical symptoms triggered by brown spider (*Loxosceles* genus) bites. Brown spider bites can induce dermonecrotic lesions, hematological disorders, and renal failure [1,2]. Histopathological findings for rabbit skin experimentally

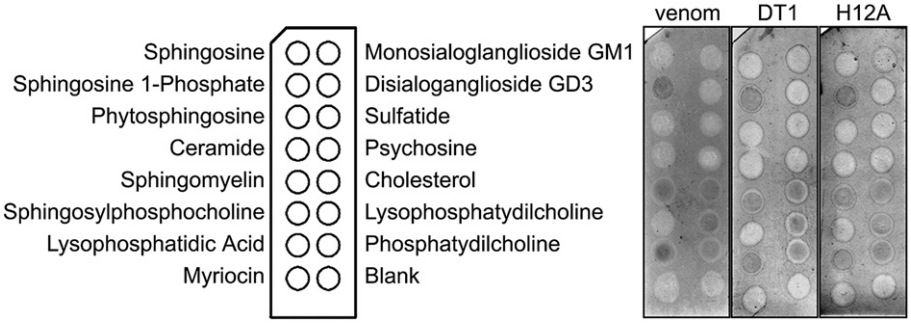

Fig. 5. Lipid binding of venom toxins in fat blot assays. Each spot contains 100 pmol of the indicated lipid in the layout of strips used to test the affinity of whole venom and recombinant toxins, which were incubated at a concentration of 0.5 µg/ml with the membranes. Samples of whole venom, LiRecDT1, and LiRecDT1 H12A show overlapping with the same spotted lipids: sphingosine 1-phosphate and sphingomyelin, lysophosphatidic acid, cholesterol, and both *lyso*phosphatidylcholine and phosphatidylcholine. Lipid binding of the toxins was detected using purified IgGs against whole venom or against LiRecDT1, and revealed with secondary antibodies coupled to alkaline phosphatase and BCIP/NBT substrate.

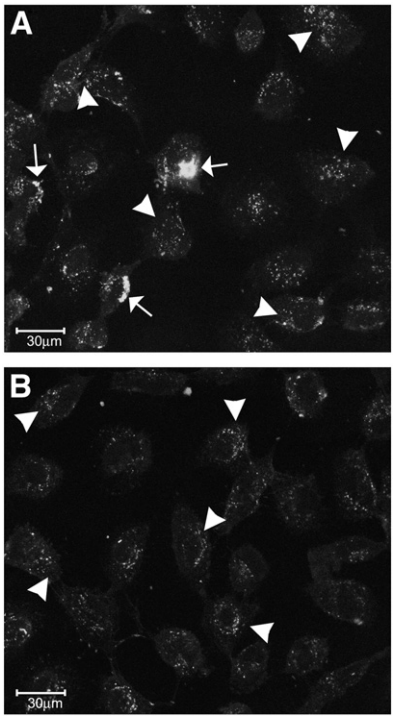

Fig. 6. Recombinant dermonecrotic toxin binding to RAEC cell membranes. Confocal immunofluorescence microscopy analysis was performed for both LiRecDT1 and LiRecDT1 H12A-treated endothelial cells incubated with antibodies anti-LiRecDT1 and a specific secondary fluorescent conjugate. (A) Four hours post-incubation of Original toxin (40 μg/ml), the cell surface showed punctate binding of LiRecDT1 (arrowheads) and deposition as aggregated clusters (arrows). (B) LiRecDT1 H12A treatment (40 μg/ml) also caused non-homogeneous binding of the mutated toxin (arrowheads), but no cell membrane aggregation was visualized. The scale bar is visualized on the left.

exposed to whole venom have shown the degeneration of blood vessel walls, endothelial cytotoxicity, and fibrin and thrombus formation [6,7]. Likewise, capillary hyperpermeability and intense infiltration of polymorphonuclear leukocytes around blood vessels cause a massive inflammatory response to the venom toxins [2,11].

Brown spider venom is a complex mixture of biochemically and biologically varied toxins reported by proteomic analysis to have molecular masses predominantly in the range of 3–40 kDa [39–41]. Most reported biological effects can be reproduced by dermonecrotic toxin family members (phospholipases-D). Previous reports have shown that a recombinant dermonecrotic toxin from the *L. intermedia* venom gland (LiRecDT1) was capable of stimulating dermonecrosis, hemolysis, platelet aggregation, renal disturbance, increased vascular permeability, and a deregulated inflammatory activation [11–13,15,41].

Futrell [2] has characterized dermonecrotic toxin as a sphingomyelinase-D enzyme because of its ability to hydrolyze sphingomyelin into choline and acylsphingosine phosphate. Recently, Lee and Lynch [10] suggested the term sphingomyelinase-D should be replaced by phospholipase-D to better classify brown spider dermonecrotic toxins based on their additional ability to hydrolyze glycerophospholipids. As such, the formation of lipid metabolites (also known as potent bioactive molecules) such as C1P or LPA could be responsible for the toxicity by activating signaling pathways related to a variety of pathophysiologic changes [10,18,20].

In this work, we investigated the dependence of the enzymatic activity of phospholipase-D to evoke the toxicity displayed in response to the biological effects of brown spider dermonecrotic toxin. To this end, we produced a mutated form of the dermonecrotic toxin from *L. intermedia* venom. The previously described LiRecDT1 was modified at the catalytic site with a single amino acid change using a site-directed mutagenesis strategy. In the literature, several studies have used the mutation of specific amino acid residues to evaluate the structure and function of toxins [42,43]. Kukreja et al. [44] examined the molecular action of botulinum neurotoxin endopeptidase by substituting Glu262 with Asp and showed a 3-fold decrease in catalytic efficiency. This mutation did not induce any significant structural alterations in the active site and did not interfere with substrate binding.

Based on a study of the crystal structure of *L. laeta* dermonecrotic toxin (SMaseI) [17], the proposed acid base catalytic mechanism postulated residues His12 and His47 as playing key roles and being supported by a network of hydrogen bonds between Asp34, Asp52, Trp230, Asp233, and Asn252. We chose the first histidine residue (His12) in the catalytic site as a mutation target, intending to abolish phospholipase-D activity of the resulting toxin.

Recombinant expression of the mutated toxin as a fusion protein was successfully achieved (Fig. 1A and B) and we named it LiRecDT1 H12A (*Loxosceles intermedia* dermonecrotic toxin 1, mutation at His12 to Ala residue). To confirm the effectiveness of the site-directed mutation in extinguishing phospholipase-D activity, we performed classic tests for characterizing dermonecrotic toxin: sphingomyelin hydrolysis *in vitro* and dermonecrosis *in vivo* [1,2]. Compared to 10 μg of the original toxin and whole venom, LiRecDT1 H12A presented insignificant phospholipase-D activity and no macroscopic effect on rabbit skin (Fig. 1C). Meanwhile, histopathological findings for the LiRecDT1 H12A tissue samples showed the presence of a neutrophil infiltrate and collagen fiber disorganization in the treated rabbit skin (Fig. 2B). Despite this controversial finding, we presume that LiRecDT1 H12A did not lose phospholipase-D activity completely. Indeed, residual enzymatic activity was observed by testing higher concentrations of the mutated toxin (Fig. 3). The phospholipase-D activity of 500 μg of the mutated toxin increased compared to 10, 50, and 100 μg, but was considerably lower than 10 μg of the original toxin, suggesting some residual catalytic activity of the protein.

Cross-reactivity experiments demonstrated that antibodies against venom or LiRecDT1 can also recognize linear (Fig. 4) and conformational epitopes (Fig. 4) of LiRecDT1 H12A. As a result, the mutated toxin could be used as a biological tool for comparing identical proteins with almost insignificant enzymatic activity that is a structural analogue for dermonecrotic toxin. First, anti-toxin hyperimmune IgGs were used to reveal the binding of LiRecDT1 to specific lipids immobilized in nitrocellulose (Fig. 5). Protein–lipid overlapping experiments are *in vitro* reproductions of biological events triggered by protein interactions with lipid domains on the plasma cell membrane. Recombinant original and mutated toxins bound to the same lipids, including sphingomyelin and phosphatidylcholine.

The His12Ala modification in the amino acid sequence of recombinant dermonecrotic toxin did not interfere with its lipid-binding property. LiRecDT1 may be interacting by a linear or conformational region in the molecule independently of catalytic activity or even the active site domain. It has been well described that proteins expose hydrophobic surfaces of their molecular structures, allowing them to bind phospholipids on the cell membrane and trigger various biological effects [45,46]. LiRecDT1 contains 42.6% hydrophobic residues in its amino acid sequence. Several short sequences show conserved hydrophobicity in LiRecDT1 (AILMFPWYV) and *L. laeta* SMase I (AY093599) based on amino acid sequence alignment. Structural analysis of recombinant dermonecrotic toxin from SMase I [16,17] has shown that hydrophobic loops participate in the interfacial region of the enzyme where the active site is located in a shallow cleft.

Hydrophobic domains in the secondary and tertiary structure of brown spider dermonecrotic toxin probably play a role in its ability to bind lipids on the cell membrane independent of enzymatic activity but not necessarily unrelated to the active site of LiRecDT1. Metal-coordination and charged residues in the catalytic domain must be important for targeting phospholipids in a hydrophilic environment

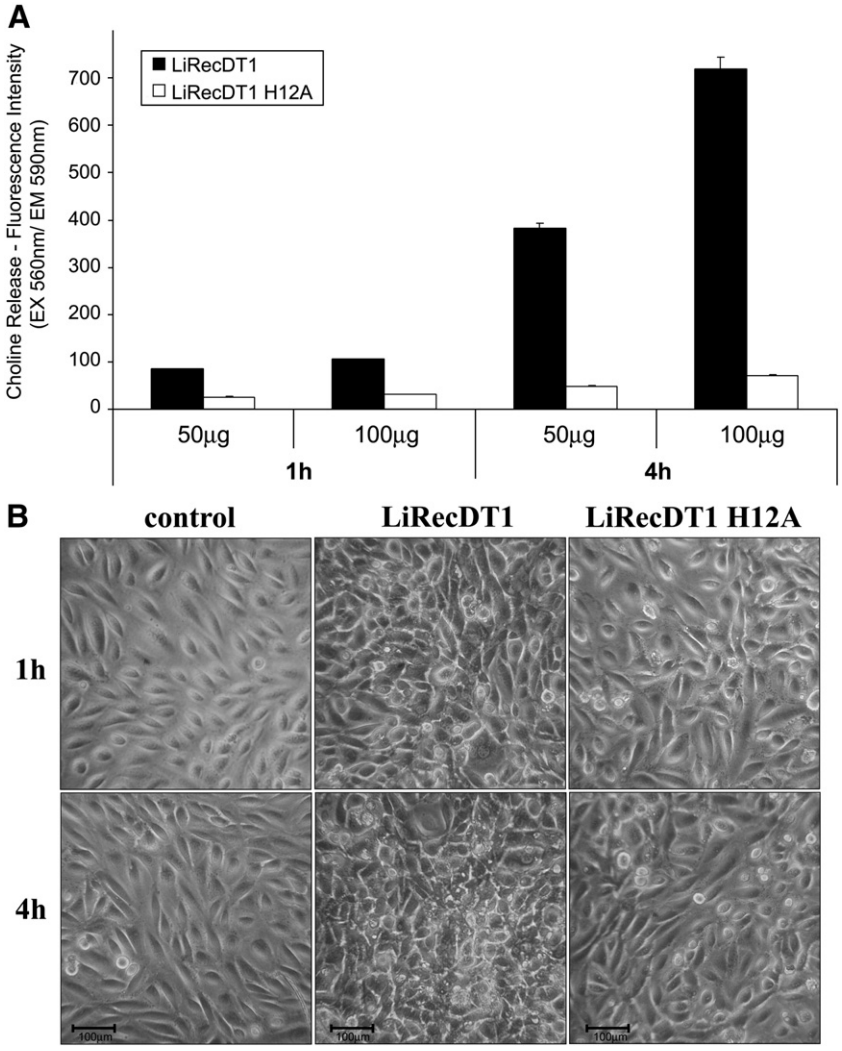

Fig. 7. Choline release induced by recombinant toxins from hydrolysis of membrane extracts as well as cytotoxic effects on endothelial cell cultures. (A) Detergent-extracts of RAEC cell membranes (100 µl) were incubated with LiRecDT1 or LiRecDT1 H12A (abscissa depicts both toxins used at concentrations of 50 µg or 100 µg) for 1 h and 4 h in a 37 °C water bath. Choline formation was detected using a reaction mixture adapted from the Amplex Red Sphingomyelinase Assay Kit (see Materials and methods). Degradation of cell membrane extracts by toxins results in indirect detection of a fluorescent product that was measured in a spectrofluorometer using an excitation at 560 nm with emission detection at 590 nm. (B) Using inverted light microscopy, morphological changes in RAEC cells were observed following incubation of recombinant toxins (10 µg/ml) and images were captured at 1 h and 4 h after exposure. First, LiRecDT1 triggered vacuolization of the cell cytoplasm, which is accompanied by cell lysis and alteration of cellular adhesion to other neighboring cells and substrate. Despite this, LiRecDT1 H12A does not seem to induce a significant change in treated-cells. Control cells, which received adequate amounts of vehicle (PBS) instead of recombinant toxins, displayed typical RAEC cell morphology throughout the experimental procedure.

and are indispensable for hydrolysis of membrane lipids. For example, a prediction for the interaction of alpha-toxin (a phospholipase C from *Clostridium perfringens*) with cell membranes has revealed two different domains: calcium mediated recognition of phospholipids head groups at the active site (amino-terminal region) and interaction of hydrophobic amino acids with the phospholipid tail group. These domains are structurally similar to phospholipid-binding domains in eukaryotic proteins (carboxy-terminal region) [47].

Structure function analysis of LiRecDT1 H12A supports this hypothesis because the same lipid affinity was observed via the fat blot assay despite almost insignificant enzymatic activity. The binding of both toxins was also maintained as demonstrated in treated RAEC cells (as "planted antigens") and immunofluorescence experiments. Recently, in biological approaches with recombinant toxin treated mice, Kusma et al. [28] showed that a mutated isoform binds to intrinsic renal structures as well as the LiRecDT1.

The anti-toxin antibody assays showed the same non-homogeneous pattern for the interaction of both toxins with the RAEC cell surface (Fig. 6). Both recombinant toxins seem to be aggregated throughout the RAEC surface, binding to specific microdomains in the cell membrane. A number of toxins such as bacterial and viral pathogens are able to exploit cholesterol and/or lipid rafts to gain a "foot hold" on their target hosts [48]. Leukotoxin (Ltx) is a bacterial protein toxin from *Actinobacillus actinomycetemcomitans* that induces Ca^{2+} fluxes, mobilizing clusters of LFA-1 (surface antigen of innate and adaptive immune cells) to lipid rafts. Ltx utilizes the raft to stimulate an integrin signaling pathway that results in target cell responses that mimic 'outside-in' activation signals, leading to apoptosis of target cells [49] but no change in lipid raft content.

Moreover, direct cytotoxicity was observed after LiRecDT1 exposure by changes in morphology of RAEC cell cultures (Fig. 7A). Vacuolization of the cytoplasm, cell lysis debris, and alteration of cell–cell and cell–substrate adhesion were induced in a time-dependent manner by LiRecDT1 toxin treatment. The response of RAEC cells to LiRecDT1 H12A was very similar to untreated cells (negative control). The direct cell membrane interaction with dermonecrotic toxins does not presuppose cytotoxic effects, as this only occurs when significant enzymatic activity is present. Likewise, morphological changes in MDCK cells and proteinuria and renal tissue damage in mice were only triggered by recombinant phospholipase-D with intact enzymatic activity [28].

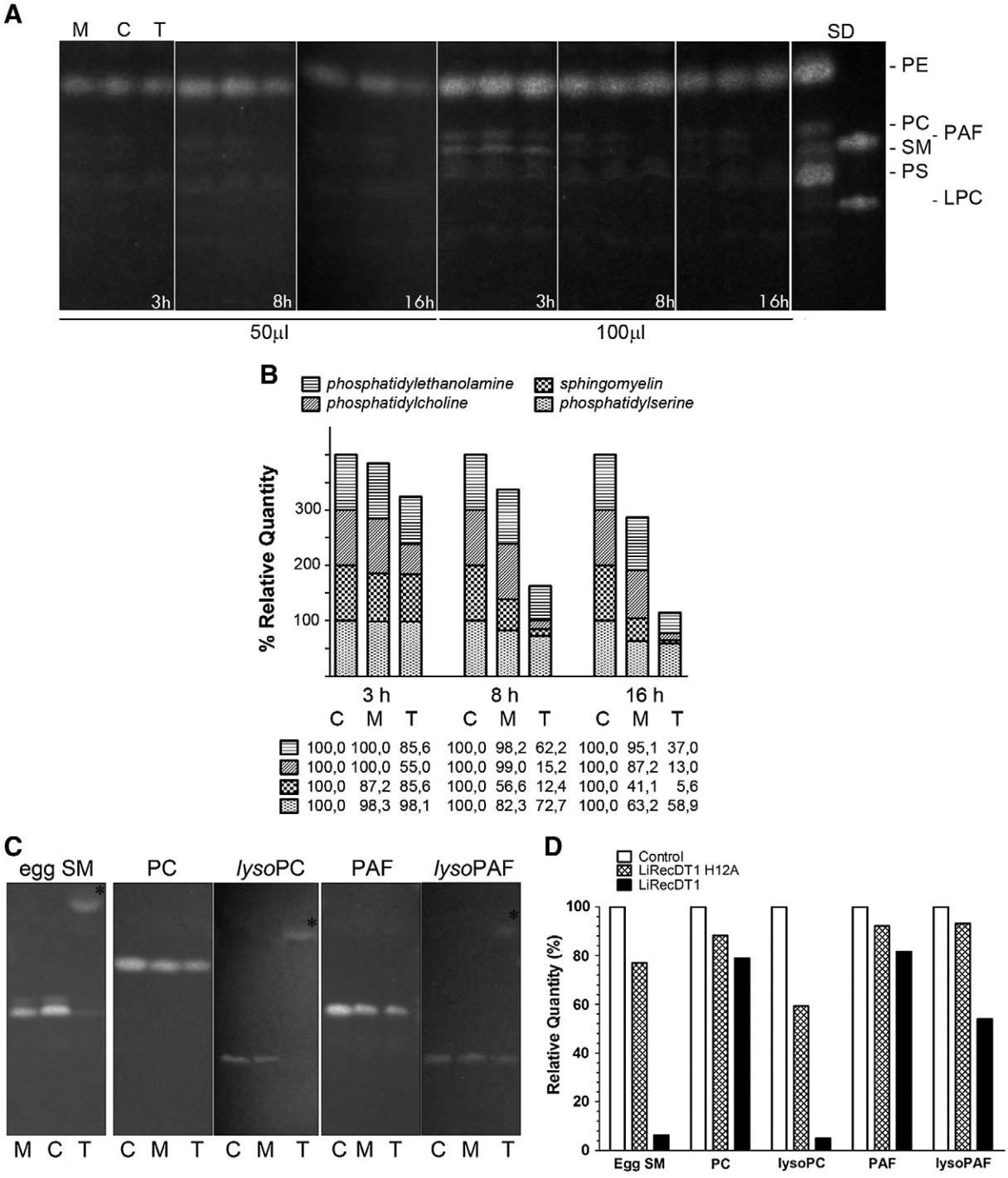

Fig. 8. HPTLC analysis of hydrolysis of RAEC cell membrane extracts and purified phospholipids by recombinant toxins. Triton X-100 extracts from endothelial cell cultures were incubated with 50 µg of either LiRecDT1 (T) or its mutated isoform, LiRecDT1 H12A (M), and non-treated extracts were used as control (C), for 3, 8, and 16 h. (A) Recovered lipids post-butanol extraction were visualized by primuline reagent in HPTLC plates, as described in Materials and methods. (C) After 3 h of incubation with toxins, purified lipids were also submitted to HPLC; egg chicken sphingomyelin (egg SM), asymmetric phosphatidylcholine C16:0–18:0 (PC), lysophosphatidylcholine (lysoPC), C16-2:0 PC (PAF), C16 Lyso PAF (lysoPAF). (B and D) Band intensities were estimated densitometrically and were plotted as percentage of relative quantity, comparing with respective control samples (100%). Percentage values are shown in the table (B), HPTLC bands of cell extracts lipid content were compared with migration patterns of phospholipids in the standard mixture (PE: phosphatidylethanolamine, PC: phosphatidylcholine, SM: sphingomyelin, PS: phosphatidylserine).

Phospholipase-D hydrolysis of the phosphodiester bond of glycerophospholipids generates (*lyso*)phosphatidic acid, and the degradation of sphingolipids forms ceramide. This reaction frees a headgroup, such as choline (resulting, for example, from sphingomyelin and (*lyso*)phosphatidylcholine [10,50]), which can act as a substrate for brown spider phospholipase-D. Choline release assays demonstrated direct hydrolysis of membrane extracts in a time- and concentration-dependent manner only with LiRecDT1 treatment (Fig. 8B), supporting the idea of catalytic-dependent cytotoxicity and suggesting that products of phospholipases-D degradation induce formation of bioactive mediators such as C1P or LPA [22,23].

In Fig. 8 (see *), the formation of subproducts induced by hydrolysis can be observed in HPTLC images, mainly in the top of those lanes where samples were exposed to active phospholipase-D and original lipid

content was almost degraded. Many lipids or lipid-derived products generated by phospholipases acting on phospholipids in membranes are implicated as mediators and second messengers in signal transduction [51]. For example, autotaxin (ATX) is an exo-enzyme originally identified as a tumor cell autocrine and paracrine motility factor. ATX is a multifunctional phosphodiesterase that primarily acts as a lysophospholipase D [52,53], converting lysophosphatidylcholine into LPA. LPA mediates multiple biological functions, including the cytoskeletal reorganization and chemotaxis observed in melanoma cells. Likewise, endothelial cell plasma membranes could be targeted by phospholipase-D activity, for which the regulation of lipid-derived second messenger levels intra- and intercellularly is not well understood [54]. Morphological alterations induced by phospholipase-D activity in RAEC cells could be explained by this hypothesis (Fig. 8B). Furthermore, the hallmark of brown spider dermonecrotic toxins is both dermonecrosis and hydrolysis of sphingomyelin, which in tissue context has been shown to be related to an inflammatory overreaction. This event is triggered by intense an neutrophil migration, which is dependent on the activation of fibroblast and endothelial cells by generating lipid mediators (such as C1P, an interconvertible molecule [22]) that cause a cascade of signaling events as pro-inflammatory cytokines upregulation and leukocytes recruitment [25].

As expected, LiRecDT1 and recombinant toxins obtained from *Loxosceles* genus venom glands have the ability to hydrolyze sphingomyelin and *lyso*phospholipids [10,55]. Interestingly, *L. intermedia* toxins also hydrolyze phospholipids such as phosphatidylcholine or PAF (platelet-activating factor), which are non alkyl-phospholipids (Fig. 8). The resulting lipid metabolite is phosphatic acid (PA), another bioactive metabolite related to LPA that has already been reported to play a role in stimulating several signaling pathways [56]. A juxtacrine mechanism for neutrophil adhesion on platelets involves platelet-activating factor and a selectin-dependent activation process, which are critical in cell–cell interactions in inflammatory and thrombotic responses of endothelial cells [54,57,58]. In the same way, hemostatic disturbances such as blood coagulation problems have been reported in with some brown spider bites [59]. In addition, platelet hyperaggregation was experimentally observed in human blood platelets exposed to a dermonecrotic toxin from *L. recluse* [60] and also thrombus formation and hemorrhage in rabbits tested with *L. gaucho* venom [61]. All phospholipids tested as substrates in HPTLC analysis with LiRecDT1 are important components/targets of plasma membranes of erythrocytes and platelets, for which phospholipase-D activity could be triggering several well known biological effects in brown spider accidents.

5. Conclusion

We present experimental data and literature supporting the direct involvement of dermonecrotic toxin in the biological effects evoked by brown spider venom. These data demonstrate phospholipase-D enzymatic activity on the endothelial cell membrane, suggesting a non-specific formation of different lipid mediators from cell membrane phospholipids. Our results bring new insights to the pathologic processes associated with a lipid role in pathways of the inflammatory response and dermonecrosis in Loxoscelism.

Acknowledgments

This work was supported by grants from Secretaria de Estado de Ciência, Tecnologia e Ensino Superior (SETI) do Paraná, Fundação Araucária-PR, FAPESP, CNPq and CAPES, Brazil.

References

[1] P.H. da Silva, R.B. da Silveira, M.H. Appel, O.C. Mangili, W. Gremski, S.S. Veiga, Brown spiders and loxoscelism, Toxicon 44 (2004) 693–709.
[2] J.M. Futrell, Loxoscelism, Am. J. Med. Sci. 304 (1992) 261–267.
[3] E. Kalapothakis, M. Chatzaki, H. Goncalves-Dornelas, C.S. de Castro, F.G. Silvestre, F.V. Laborne, J.F. de Moura, S.S. Veiga, C. Chavez-Olortegui, C. Granier, K.C. Barbaro, The Loxtox protein family in *Loxosceles intermedia* (Mello-Leitao) venom, Toxicon 50 (2007) 938–946.
[4] D.L. Swanson, R.S. Vetter, Loxoscelism, Clin. Dermatol. 24 (2006) 213–221.
[5] M.H. Appel, R.B. da Silveira, W. Gremski, S.S. Veiga, Insights into brown spider and loxoscelism, Invertebr. Surviv. J. 2 (2005) 152–158.
[6] S.S. Veiga, V.C. Zanetti, C.R. Franco, E.S. Trindade, M.A. Porcionatto, O.C. Mangili, W. Gremski, C.P. Dietrich, H.B. Nader, In vivo and in vitro cytotoxicity of brown spider venom for blood vessel endothelial cells, Thromb. Res. 102 (2001) 229–237.
[7] V.C. Zanetti, R.B. da Silveira, J.L. Dreyfuss, J. Haoach, O.C. Mangili, S.S. Veiga, W. Gremski, Morphological and biochemical evidence of blood vessel damage and fibrinogenolysis triggered by brown spider venom, Blood Coagul. Fibrinolysis 13 (2002) 135–148.
[8] K.S. Paludo, L.H. Gremski, S.S. Veiga, O.M. Chaim, W. Gremski, D. de Freitas Buchi, H.B. Nader, C.P. Dietrich, C.R. Franco, The effect of brown spider venom on endothelial cell morphology and adhesive structures, Toxicon 47 (2006) 844–853.
[9] A. Senff-Ribeiro, P. Henrique da Silva, O.M. Chaim, L.H. Gremski, K.S. Paludo, R. Bertoni da Silveira, W. Gremski, O.C. Mangili, S.S. Veiga, Biotechnological applications of brown spider (*Loxosceles* genus) venom toxins, Biotechnol. Adv. 26 (2008) 210–218.
[10] S. Lee, K.R. Lynch, Brown recluse spider (*Loxosceles reclusa*) venom phospholipase D (PLD) generates lysophosphatidic acid (LPA), Biochem. J. 391 (2005) 317–323.
[11] M.H. Appel, R.B. da Silveira, O.M. Chaim, K.S. Paludo, D.T. Silva, D.M. Chaves, P.H. da Silva, O.C. Mangili, A. Senff-Ribeiro, W. Gremski, H.B. Nader, S.S. Veiga, Identification, cloning and functional characterization of a novel dermonecrotic toxin (phospholipase D) from brown spider (*Loxosceles intermedia*) venom, Biochim. Biophys. Acta 1780 (2008) 167–178.
[12] O.M. Chaim, Y.B. Sade, R.B. da Silveira, L. Toma, E. Kalapothakis, C. Chavez-Olortegui, O.C. Mangili, W. Gremski, C.P. von Dietrich, H.B. Nader, S. Sanches Veiga, Brown spider dermonecrotic toxin directly induces nephrotoxicity, Toxicol. Appl. Pharmacol. 211 (2006) 64–77.
[13] R.B. da Silveira, O.M. Chaim, O.C. Mangili, W. Gremski, C.P. Dietrich, H.B. Nader, S.S. Veiga, Hyaluronidases in *Loxosceles intermedia* (Brown spider) venom are endo-beta-N-acetyl-D-hexosaminidases hydrolases, Toxicon 49 (2007) 758–768.
[14] R.B. da Silveira, R.B. Pigozzo, O.M. Chaim, M.H. Appel, D.T. Silva, J.L. Dreyfuss, L. Toma, C.P. Dietrich, H.B. Nader, S.S. Veiga, W. Gremski, Two novel dermonecrotic toxins LiRecDT4 and LiRecDT5 from brown spider (*Loxosceles intermedia*) venom: from cloning to functional characterization, Biochimie 89 (2007) 289–300.
[15] R.O. Ribeiro, O.M. Chaim, R.B. da Silveira, L.H. Gremski, Y.B. Sade, K.S. Paludo, A. Senff-Ribeiro, J. de Moura, C. Chavez-Olortegui, W. Gremski, H.B. Nader, S.S. Veiga, Biological and structural comparison of recombinant phospholipase D toxins from *Loxosceles intermedia* (brown spider) venom, Toxicon 50 (2007) 1162–1174.
[16] M.T. Murakami, M.F. Fernandes-Pedrosa, S.A. de Andrade, A. Gabdoulkhakov, C. Betzel, D.V. Tambourgi, R.K. Arni, Structural insights into the catalytic mechanism of sphingomyelinases D and evolutionary relationship to glycerophosphodiester phosphodiesterases, Biochem. Biophys. Res. Commun. 342 (2006) 323–329.
[17] M.T. Murakami, M.F. Fernandes-Pedrosa, D.V. Tambourgi, R.K. Arni, Structural basis for metal ion coordination and the catalytic mechanism of sphingomyelinases D, J. Biol. Chem. 280 (2005) 13658–13664.
[18] B. Anliker, J. Chun, Lysophospholipid G protein-coupled receptors, J. Biol. Chem. 279 (2004) 20555–20558.
[19] Y.A. Hannun, The sphingomyelin cycle and the second messenger function of ceramide, J. Biol. Chem. 269 (1994) 3125–3128.
[20] W.H. Moolenaar, L.A. van Meeteren, B.N. Giepmans, The ins and outs of lysophosphatidic acid signaling, Bioessays 26 (2004) 870–881.
[21] B.J. Pettus, A. Bielawska, S. Spiegel, P. Roddy, Y.A. Hannun, C.E. Chalfant, Ceramide kinase mediates cytokine- and calcium ionophore-induced arachidonic acid release, J. Biol. Chem. 278 (2003) 38206–38213.
[22] C.E. Chalfant, S. Spiegel, Sphingosine 1-phosphate and ceramide 1-phosphate: expanding roles in cell signaling, J. Cell Sci. 118 (2005) 4605–4612.
[23] M.C. van Dijk, F. Postma, H. Hilkmann, K. Jalink, W.J. van Blitterswijk, W.H. Moolenaar, Exogenous phospholipase D generates lysophosphatidic acid and activates Ras, Rho and Ca^{2+} signaling pathways, Curr. Biol. 8 (1998) 386–392.
[24] L.A. van Meeteren, F. Frederiks, B.N. Giepmans, M.F. Pedrosa, S.J. Billington, B.H. Jost, D.V. Tambourgi, W.H. Moolenaar, Spider and bacterial sphingomyelinases D target cellular lysophosphatidic acid receptors by hydrolyzing lysophosphatidylcholine, J. Biol. Chem. 279 (2004) 10833–10836.
[25] B. Dragulev, Y. Bao, B. Ramos-Cerrillo, H. Vazquez, A. Olvera, R. Stock, A. Algaron, J.W. Fox, Upregulation of IL-6, IL-8, CXCL1, and CXCL2 dominates gene expression in human fibroblast cells exposed to *Loxosceles reclusa* sphingomyelinase D: insights into spider venom dermonecrosis, J. Invest. Dermatol. 127 (2007) 1264–1266.
[26] L. Chioato, R.J. Ward, Mapping structural determinants of biological activities in snake venom phospholipases A2 by sequence analysis and site directed mutagenesis, Toxicon 42 (2003) 869–883.
[27] H. Sakamoto, J. Bellalou, P. Sebo, D. Ladant, Bordetella pertussis adenylate cyclase toxin. Structural and functional independence of the catalytic and hemolytic activities. J. Biol. Chem. 267 (1992) 13598–13602.
[28] J. Kusma, O.M. Chaim, A.C. Wille, V.P. Ferrer, Y.B. Sade, L. Donatti, W. Gremski, O.C. Mangili, S.S. Veiga, Nephrotoxicity caused by brown spider venom phospholipase-D (dermonecrotic toxin) depends on catalytic activity, Biochimie 90 (2008) 1722–1736.
[29] D. Chaves-Moreira, O.M. Chaim, Y.B. Sade, K.S. Paludo, L.H. Gremski, L. Donatti, J. de Moura, O.C. Mangili, W. Gremski, R.B. da Silveira, A. Senff-Ribeiro, S.S. Veiga, Identification of a direct hemolytic effect dependent on the catalytic activity

induced by phospholipase-D (dermonecrotic toxin) from brown spider venom, J. Cell. Biochem. 107 (2009) 655–666.
[30] L. Feitosa, W. Gremski, S.S. Veiga, M.C. Elias, E. Graner, O.C. Mangili, R.R. Brentani, Detection and characterization of metalloproteinases with gelatinolytic, fibronectinolytic and fibrinogenolytic activities in brown spider (*Loxosceles intermedia*) venom, Toxicon 36 (1998) 1039–1051.
[31] J. Sambrook, D.W. Russell, Molecular Cloning: A Laboratory Manual, 3rd ed. Cold Spring Harbor Laboratory Press, Cold Spring Harbor, N.Y., 2001
[32] R.B. da Silveira, A.C. Wille, O.M. Chaim, M.H. Appel, D.T. Silva, C.R. Franco, L. Toma, O.C. Mangili, W. Gremski, C.P. Dietrich, H.B. Nader, S.S. Veiga, Identification, cloning, expression and functional characterization of an astacin-like metalloprotease toxin from *Loxosceles intermedia* (brown spider) venom, Biochem. J. 406 (2007) 355–363.
[33] P.P. Bradley, D.A. Priebat, R.D. Christensen, G. Rothstein, Measurement of cutaneous inflammation: estimation of neutrophil content with an enzyme marker, J. Invest. Dermatol. 78 (1982) 206–209.
[34] J.C. Castardo, A.S. Prudente, J. Ferreira, C.L. Guimarães, F.D. Monache, V.C. Filho, M.F. Otuki, D.A. Cabrini, Anti-inflammatory effects of hydroalcoholic extract and two biflavonoids from *Garcinia gardneriana* leaves in mouse paw oedema, J. Ethnopharmacol. 118 (2008) 405–411.
[35] E. Harlow, D. Lane, Antibodies: A Laboratory Manual, Cold Spring Harbor Laboratory, Cold Spring Harbor, NY, 1988.
[36] K.A. Yoneyama, A.K. Tanaka, T.G. Silveira, H.K. Takahashi, A.H. Straus, Characterization of *Leishmania* (Viannia) *braziliensis* membrane microdomains, and their role in macrophage infectivity, J. Lipid Res. 47 (2006) 2171–2178.
[37] D. He, V. Natarajan, R. Stern, I.A. Gorshkova, J. Solway, E.W. Spannhake, Y. Zhao, Lysophosphatidic acid-induced transactivation of epidermal growth factor receptor regulates cyclo-oxygenase-2 expression and prostaglandin E(2) release via C/EBPbeta in human bronchial epithelial cells, Biochem. J. 412 (2008) 153–162.
[38] C. Luquain, V.A. Sciorra, A.J. Morris, Lysophosphatidic acid signaling: how a small lipid does big things, Trends Biochem. Sci. 28 (2003) 377–383.
[39] C.S. de Castro, F.G. Silvestre, S.C. Araujo, M.Y. Gabriel de, O.C. Mangili, I. Cruz, C. Chavez-Olortegui, E. Kalapothakis, Identification and molecular cloning of insecticidal toxins from the venom of the brown spider *Loxosceles intermedia*, Toxicon 44 (2004) 273–280.
[40] L.F. Machado, S. Laugesen, E.D. Botelho, C.A. Ricart, W. Fontes, K.C. Barbaro, P. Roepstorff, M.V. Sousa, Proteome analysis of brown spider venom: identification of loxnecrogin isoforms in *Loxosceles gaucho* venom, Proteomics 5 (2005) 2167–2176.
[41] R.B. da Silveira, R.B. Pigozzo, O.M. Chaim, M.H. Appel, J.L. Dreyfuss, L. Toma, O.C. Mangili, W. Gremski, C.P. Dietrich, H.B. Nader, S.S. Veiga, Molecular cloning and functional characterization of two isoforms of dermonecrotic toxin from *Loxosceles intermedia* (brown spider) venom gland, Biochimie 88 (2006) 1241–1253.
[42] M. Miyamoto, N. Onozato, D. Selvakumar, T. Kimura, Y. Furuichi, T. Komiyama, The role of the histidine-35 residue in the cytocidal action of HM-1 killer toxin, Microbiology 152 (2006) 2951–2958.
[43] B. Promdonkoy, D.J. Ellar, Structure–function relationships of a membrane pore forming toxin revealed by reversion mutagenesis, Mol. Membr. Biol. 22 (2005) 327–337.
[44] R.V. Kukreja, S. Sharma, S. Cai, B.R. Singh, Role of two active site Glu residues in the molecular action of botulinum neurotoxin endopeptidase, Biochim. Biophys. Acta 1774 (2007) 213–222.
[45] A. Mulgrew-Nesbitt, K. Diraviyam, J. Wang, S. Singh, P. Murray, Z. Li, L. Rogers, N. Mirkovic, D. Murray, The role of electrostatics in protein–membrane interactions, Biochim. Biophys. Acta 1761 (2006) 812–826.
[46] J.L. Pellequer, A.J. Gale, E.D. Getzoff, Blood coagulation: the outstanding hydrophobic residues, Curr. Biol. 10 (2000) R237–R240.
[47] R.W. Titball, C.E. Naylor, J. Miller, D.S. Moss, A.K. Basak, Opening of the active site of *Clostridium perfringens* alpha-toxin may be triggered by membrane binding, Int. J. Med. Microbiol. 290 (2000) 357–361.
[48] D.J. Hawkes, J. Mak, Lipid membrane; a novel target for viral and bacterial pathogens, Curr. Drug Targets 7 (2006) 1615–1621.
[49] K.P. Fong, C.M. Pacheco, L.L. Otis, S. Baranwal, I.R. Kieba, G. Harrison, E.V. Hersh, K. Boesze-Battaglia, E.T. Lally, *Actinobacillus actinomycetemcomitans* leukotoxin requires lipid microdomains for target cell cytotoxicity, Cell. Microbiol. 8 (2006) 1753–1767.
[50] M. McDermott, M.J. Wakelam, A.J. Morris, Phospholipase D, Biochem. Cell Biol. 82 (2004) 225–253.
[51] E.A. Dennis, S.G. Rhee, M.M. Billah, Y.A. Hannun, Role of phospholipase in generating lipid second messengers in signal transduction, FASEB J. 5 (1991) 2068–2077.
[52] M. Umezu-Goto, Y. Kishi, A. Taira, K. Hama, N. Dohmae, K. Takio, T. Yamori, G.B. Mills, K. Inoue, J. Aoki, H. Arai, Autotaxin has lysophospholipase D activity leading to tumor cell growth and motility by lysophosphatidic acid production, J. Cell Biol. 158 (2002) 227–233.
[53] L.A. van Meeteren, W.H. Moolenaar, Regulation and biological activities of the autotaxin-LPA axis, Prog. Lipid Res. 46 (2007) 145–160.
[54] R.E. Whatley, G.A. Zimmerman, T.M. McIntyre, S.M. Prescott, Lipid metabolism and signal transduction in endothelial cells, Prog. Lipid Res. 29 (1990) 45–63.
[55] S.A. de Andrade, M.T. Murakami, D.P. Cavalcante, R.K. Arni, D.V. Tambourgi, Kinetic and mechanistic characterization of the Sphingomyelinases D from *Loxosceles intermedia* spider venom, Toxicon 47 (2006) 380–386.
[56] X. Wang, S.P. Devaiah, W. Zhang, R. Welti, Signaling functions of phosphatidic acid, Prog. Lipid Res. 45 (2006) 250–278.
[57] L. Ostrovsky, A.J. King, S. Bond, D. Mitchell, D.E. Lorant, G.A. Zimmerman, R. Larsen, X.F. Niu, P. Kubes, A juxtacrine mechanism for neutrophil adhesion on platelets involves platelet-activating factor and a selectin-dependent activation process, Blood 91 (1998) 3028–3036.
[58] S.M. Prescott, G.A. Zimmerman, D.M. Stafforini, T.M. McIntyre, Platelet-activating factor and related lipid mediators, Annu. Rev. Biochem. 69 (2000) 419–445.
[59] R.S. Rees, C. Gates, S. Timmons, R.M. Des Prez, L.E. King Jr., Plasma components are required for platelet activation by the toxin of *Loxosceles reclusa*, Toxicon 26 (1988) 1035–1045.
[60] G. Kurpiewski, L.J. Forrester, J.T. Barrett, B.J. Campbell, Platelet aggregation and sphingomyelinase D activity of a purified toxin from the venom of *Loxosceles reclusa*, Biochim. Biophys. Acta 678 (1981) 467–476.
[61] F.L. Tavares, M.C. Sousa-e-Silva, M.L. Santoro, K.C. Barbaro, I.M. Rebecchi, I.S. Sano-Martins, Changes in hematological, hemostatic and biochemical parameters induced experimentally in rabbits by *Loxosceles gaucho* spider venom, Hum. Exp. Toxicol. 23 (2004) 477–486.

Toxins **2011**, *3*, 309-344; doi:10.3390/toxins3030309

OPEN ACCESS

toxins

ISSN 2072-6651

www.mdpi.com/journal/toxins

Review

Brown Spider (*Loxosceles* genus) Venom Toxins: Tools for Biological Purposes

Olga Meiri Chaim [1], Dilza Trevisan-Silva [1], Daniele Chaves-Moreira [1], Ana Carolina M. Wille [1,2], Valéria Pereira Ferrer [1], Fernando Hitomi Matsubara [1], Oldemir Carlos Mangili [3], Rafael Bertoni da Silveira [2], Luiza Helena Gremski [1], Waldemiro Gremski [1,4], Andrea Senff-Ribeiro [1] and Silvio Sanches Veiga [1,*]

[1] Department of Cell Biology, Federal University of Paraná, CEP 81531-980 Curitiba, Paraná, Brazil; E-Mails: olgachaim@ufpr.br (O.M.C.); dilzatrevisan@gmail.com (D.T.-S); dani_chaves@ufpr.br (D.C.-M); anacarolina.wille@yahoo.com.br (A.C.M.W.); valpf@ufpr.br (V.P.F.); fernando_matsubara@hotmail.com (F.H.M.); luiza_hg@yahoo.com.br (L.H.G.); senffribeiro@ufpr.br (A.S.-R)

[2] Department of Structural, Molecular Biology and Genetics, State University of Ponta Grossa, CEP 84030-900 Ponta Grossa, Paraná, Brazil; E-Mail: rafaelbertoni@uepg.br

[3] Pelé Pequeno Príncipe Research Institute, CEP 80250-060 Curitiba, Paraná, Brazil; E-Mail: oldcar25@yahoo.com.br

[4] Catholic University of Paraná, Health and Biological Sciences Institute, CEP 80215-901 Curitiba, Paraná, Brazil; E-Mail: w.gremski@pucpr.br

* Author to whom correspondence should be addressed; E-Mail: veigass@ufpr.br; Tel.: +55-41-33611776; Fax: +55-41-3266-2042.

Received: 21 December 2010; in revised form: 26 February 2011 / Accepted: 17 March 2011 / Published: 22 March 2011

Abstract: Venomous animals use their venoms as tools for defense or predation. These venoms are complex mixtures, mainly enriched of proteic toxins or peptides with several, and different, biological activities. In general, spider venom is rich in biologically active molecules that are useful in experimental protocols for pharmacology, biochemistry, cell biology and immunology, as well as putative tools for biotechnology and industries. Spider venoms have recently garnered much attention from several research groups worldwide. Brown spider (*Loxosceles* genus) venom is enriched in low molecular mass proteins (5–40 kDa). Although their venom is produced in minute volumes (a few microliters), and contain only tens of micrograms of protein, the use of techniques based on molecular biology and proteomic analysis has afforded rational projects in the area and permitted the

discovery and identification of a great number of novel toxins. The brown spider phospholipase-D family is undoubtedly the most investigated and characterized, although other important toxins, such as low molecular mass insecticidal peptides, metalloproteases and hyaluronidases have also been identified and featured in literature. The molecular pathways of the action of these toxins have been reported and brought new insights in the field of biotechnology. Herein, we shall see how recent reports describing discoveries in the area of brown spider venom have expanded biotechnological uses of molecules identified in these venoms, with special emphasis on the construction of a cDNA library for venom glands, transcriptome analysis, proteomic projects, recombinant expression of different proteic toxins, and finally structural descriptions based on crystallography of toxins.

Keywords: *Loxosceles*; brown spider; venom; recombinant toxins; biotechnological applications

1. The Spiders of Genus *Loxosceles* and Loxoscelism

The spiders of the *Loxosceles* genus, commonly denoted as brown spiders, belong to the family *Sicariidae*, sub-order *Labidognatha*, order *Araneida*, class *Arachnida,* and phylo *Arthropoda* [1,2]. The Sicariidae family also comprises the spiders of *Sicarius* genus. Strong evidences show that the genera *Loxosceles* and *Sicarius* are old, having originated from a common sicariid ancestor and diversified on Western Gondwana, before the separation of the African and South American continents. Both sicariid genera are diverse in Africa and South/Central America. *Loxosceles* spiders are also distributed in North America and the West Indies, and have species described from Mediterranean Europe and China. Apparently African and South American *Sicarius* have a common ancestor and South African *Loxosceles* are derived from this group. New World *Loxosceles* also have a common ancestor and fossil data is consistent with the hypothesis of North America colonization by South American *Loxosceles via* a land bridge predating the modern Isthmus of Panama [3].

The color of spiders of this genus ranges from a fawn to dark brown (Figure 1A). *Loxosceles* spiders have a violin-shaped pattern on the dorsal surface of their cephalothorax, vary in length from 1 cm to 5 cm, including legs, and have six eyes arranged in non-touching pairs in a U-shaped pattern (Figure 1B). This positioning of eyes has been described as the best means of identifying these brown spiders [4–8]. The brown spiders are sedentary, non-aggressive, have nocturnal habits and prefer to inhabit dark areas. In human habitats, brown spiders are often found behind furniture, pictures and associated with clothes.

Accidents involving *Loxosceles* genus spiders occur mainly in the warmest months of the year, predominantly during spring and summer [4,6]. The condition caused by brown spiders, categorized as Loxoscelism, is associated with a series of clinical symptoms including cutaneous lesions, which spread gravitationally from the spider bite. The lesions are characterized by necrotizing wounds that are dark blue-violet in color and become indurated, leading to the formation of scar tissue. Surrounding the lesion, there is also erythema and edema. At the systemic level (less frequent than the appearance of skin lesions), patients may experience fever, weakness, vomiting, pruritic reactions, renal failure,

and hematologic disturbances that may include thrombocytopenia, disseminated intravascular coagulation and hemolytic anemia [5,6,8,9].

Figure 1. Brown spider aspects. (**A**) *Loxosceles intermedia* adult specimens—female and male. (**B**) Violin-shaped pattern (arrow) on the dorsal surface of cephalothorax from *Loxosceles intermedia* adult spider, and its six eyes arranged in pairs as a semi-circle (arrowheads). (**C**) Venom harvesting by electric shock applied to the cephalothorax. Arrow points for a drop of *Loxosceles intermedia* venom. Briefly, venom is extracted using an electric shock of 15 V applied to the cephalothorax of the spider and the venom from the tips of the fang is collected and diluted in phosphate buffered saline (PBS) or dried and stored at -80 º C until use. (**D**) Brown spider venom glands of *Loxosceles intermedia* observed by stereo dissecting microscope (40X). Venom can be harvested directly from venom glands: the removed glands are washed in PBS and the venom is obtained by gentle compression of the glands.

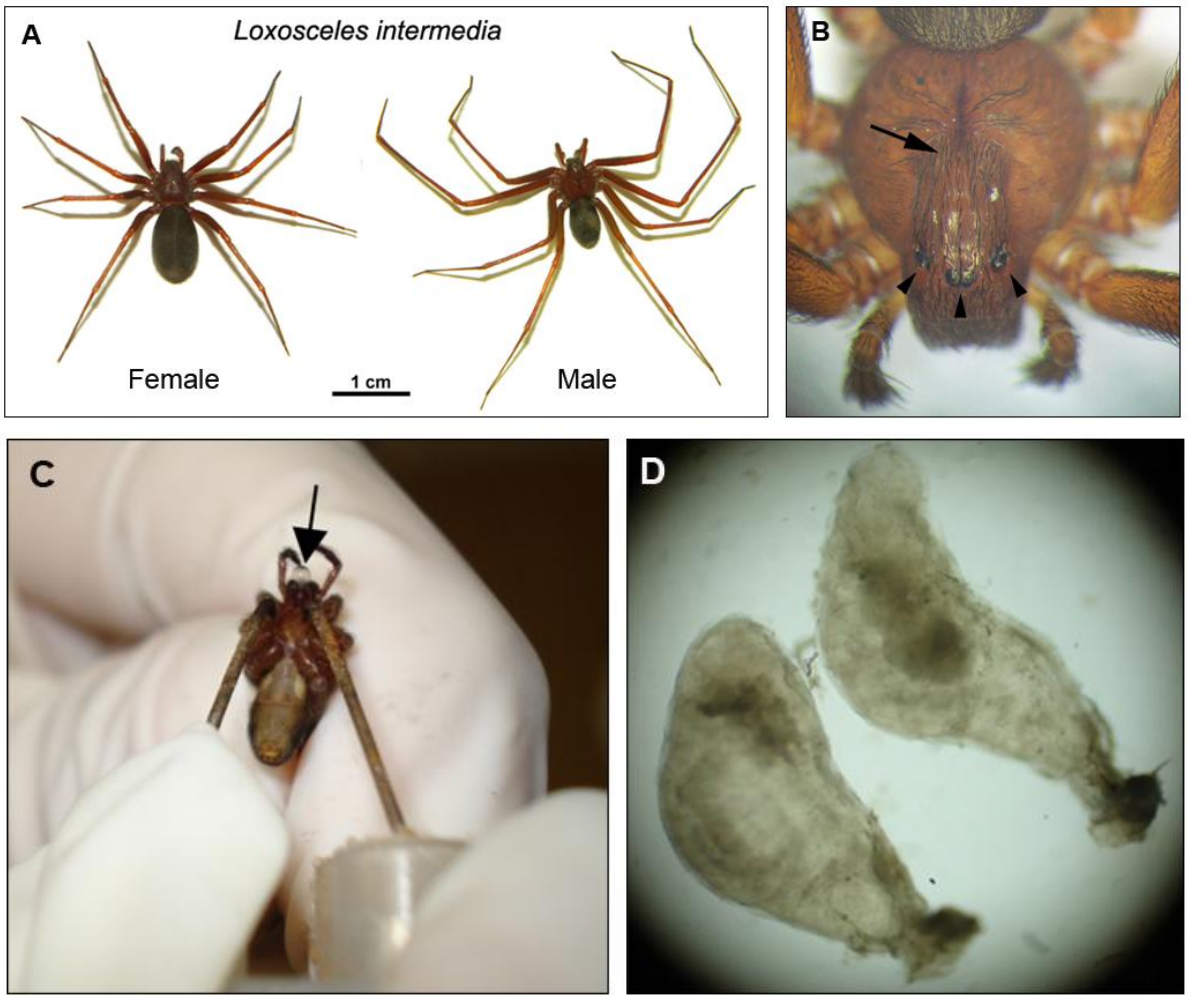

2. The *Loxosceles* Venoms

Over recent years, *Loxosceles* genus spider venoms have been studied by several scientific research groups worldwide, and many different toxins have been identified in the venoms. The corresponding biological and biochemical properties of these toxins have been reported, yielding insights into the pathophysiology of envenomation [4,5,7]. The venom of *Loxosceles* spiders is a complex mixture of protein and peptide toxins with a molecular mass profile ranging from 1 to 40 kDa [5]. To date, several molecules in the *Loxosceles* spider crude venoms have been described, including alkaline phosphatase [5,10], 5'-ribonucleotide phosphohydrolase [5], sulfated nucleosides [11], hyaluronidase [5,12–14], fosfolipases-D [5,15–17], metalloproteases, serine proteases [12,13,18–22] and insecticide toxins [23]. Table 1 contains a brief collection of main features from proteic toxins described in *Loxosceles* genus.

Low molecular weight components, such as neurotoxic and non-neurotoxic peptides, polyamines and other components are poorly studied in *Loxosceles* venom. Using NMR-spectroscopy, Schroeder and colleagues (2008) showed that sulfated guanosine derivatives comprise the major small-mollecule components of the brown recluse spider. They detected cross-peaks corresponding to 2,5-disulfated guanosine and 2-sulfated guanosine. It appears that sulfated nucleosides occur in several spider superfamilies, such as Agelenoidea and Amaurobioidea. The physiological properties of the sulfated nucleosides remain largely unexplored [11].

Serine proteases were already described in *Loxosceles* venom as high molecular weight enzymes (85–95 kDa) with gelatinolytic activity activated by trypsin [19]. Proteome and transcriptome analyses of *Loxosceles* venom also described this family of proteases [24,25]. Serine proteases generally are among the best characterized venom enzymes affecting the hemostatic system. However, the exact role of serine proteases in envenomation still remains to be clarified.

Recently, by using a cDNA library and transcriptome analysis, a novel expression profile has been elaborated for *Loxosceles intermedia* gland venom. This recently developed profile has allowed the identification of additional toxins as components of the venom, including insecticidal peptides similar to knottins (molecules that form an inhibitor cystin knot), astacin-like metalloproteases, venom allergen, a translationally controlled tumor protein family member (TCTP), serine protease inhibitors, and neurotoxins similar to Magi 3 [26,27]. Brown spider venoms display a broad diversity of toxin isoforms, including members of the phospholipase-D family and astacin-like toxins, even in the same sample [17,27–29]. Such features, which represent an adaptation to increase the survival of the spiders and the effectiveness of venoms, confer advantages to the spider predator. To confirm the existence of a new family of toxin isoforms, it is necessary to further characterize their biological properties. Recently, a spider toxin database called Arachnoserver which was manually curated [30], has cataloged 54 toxins from Sicariidae spiders family. It was elaborated, based on information gleaned through studies on complex venom mixtures, and has resulted in an exponential increase in the identification of peptide-toxins. King *et al.* [31] recommend a rational nomenclature for naming toxins from spiders and other venomous animals to avoid the continued use of *ad hoc* naming schemes that introduce confusion and make it difficult to compare toxins among species and establish evolutionary relationships.

Table 1. An overview of toxin families in *Loxosceles* genus.

Toxins	MW (kDa)	Characteristics and actions described	No. Seq *
Phospholipases-D (SicTox family members, such as LiRecDTs)	30–35	Several isoforms with variant features such as: - Dermonecrosis [12,13,16,32–38] - Lipids hydrolysis [33,39–42] - Hemolysis [38,43–45] - *In vitro* platelet aggregation [34,36,37] - Infiltration of inflammatory cells [35–37,42] - Edema [34,38] - Renal disturbances [35,46] - Lethality [34,38,46,47] - *In vitro* cytotoxicity [35,42,46] - Cytokine activation [41,48–50]	335
Insecticidal peptides	5–8	- LiTx family members [23,27] and Magi 3-related peptides [23,27,51] - LiTx: Lethal to *S. frugiperda* (flaccid paralysis) [23] - LiTx3: appears to act upon Na^+ channels [23]	8
Metalloproteases	28–35	- Astacin-like Metalloprotease (LALPs) [29,52] - Present in the venom of different species of *Loxosceles* genus [12,13,27,51,53] - Activity upon gelatin, fibronectin, fibrinogen and entactin [18,52–54]	4
Hyaluronidases	41–43	- Classified as endo-beta-N-acetyl-d-hexosaminidases hydrolases [14] - Activity upon hyaluronic acid and chondroitin sulphate [13,14] - Present in the venom of different species of *Loxosceles* genus[12–14,24,27,51,55]	-
Serine-proteases	85–95	- Gelatinolytic activity [19] - Activated *in vitro* by trypsin [19] - Present in the venom of *L. intermedia* and *L. laeta* [27,51]	-
Serine/Cysteine protease inhibitors	N.D.	- Belongs to Serpin superfamily [27] - Identified in *Loxosceles* spp. transcriptomes and proteome [24,27,51] - May be related to coagulation processes, fibrinolysis and inflammation [51]	-

Table 1. *Cont.*

TCTP (translationally controlled tumour protein)	~46	- Identified in *Loxosceles* spp. transcriptomes [27,51] - Putative functions: Histamine releasing factor in extracellular environment; several intracellular roles such as embryonic development, cell proliferation, stabilization of microtubules [56]	-
Lectin-like	N.D.	- Putative features: carbohydrate-binding molecules; involved in extracellular matrix organization, endocytosis, complement activation, *etc*. [51]	-
Alkaline-phosphatase	N.D.	- Degrades the synthetic substrate *p-nitrophenyl phosphate*[10]	-
ATPase	N.D	- ATP hydrolysis [10]	-

N.D.: not determined. *Number of sequences deposited in PUBMED protein database.

3. The Rational Use of Venom Toxins as Biotechnological Tools

The idea of using venom toxins as tools for biological purposes is currently gaining acceptance worldwide, as researchers incorporate the use of novel technologies to overcome old obstacles such as low venom volumes. Technological advancement has led to better techniques for protein purification; different models for synthesis of recombinant toxins; structural views of molecular domains, binding sites or catalytic sites of molecules of interest; design of synthetic inhibitors or agonists; and finally, cellular and animal models for testing the products obtained. The use of toxins directly as a source of materials to produce medicines or similar products has been receiving much attention from the pharmaceutical industry and experts in the field of applied research. Examples of toxin-derived biomedicines derived from venoms of different animals are abundant. Venoms from snakes, perhaps the best studied example of biotechnological applications among animal venoms, with biologically active toxins in the cardiovascular system, central nervous system, membrane lipids and proteins, hemostatic system, and muscular system, have led to the discovering of several products used in the treatment of various diseases. These drugs include Captopril (blood pressure), Integrilin (acute coronary syndrome), Aggrastat (myocardial infarct and ischemia), Ancrod (stroke), Defibrase (acute cerebral infarction and angina pectoris), Hemocoagulase (hemorrhage), and Exanta (anti-coagulant). Toxin-derived products from snake venoms have also been used for diagnosis. This group of compounds includes Protac (protein C activator, diagnosis of hemostatic disorders), Reptilase (diagnosis of blood coagulation disorder) and Ecarin (diagnostic of hemostatic disorder) (for review, see [57,58]).

Other toxin-derived medicines have been prepared from components of marine cone snail venoms, called conotoxins, which are potent ion channel modulators, and have facilitated the discovery of a novel analgesic agent named ziconide, used in the treatment of pain syndromes [59,60]. The honeybee venom toxin, called tertiapin (TPN), is an inhibitor of potassium channels, has generated TPNLQ, a variant and a potential novel model for the treatment of hypertension [61]. Exenatide (synthetic exendin-4) is a toxin-derived medicine from the venom of Gila monster lizard that stimulates the

production of insulin by pancreatic cells and has the potential to treat type 2 diabetes [62,63]. Scorpion venom toxins have been studied as well, and a large number of molecules with biological activities as pain-killers, agents that control the spread of cancer, and natural insecticides can be generated. Scorpion venom, such as kurtoxin and anuroctoxin, can target specific mammalian cell ion channels and their isolation has opened possibilities for drug design in the context of neurologic and autoimmune diseases [64,65]. Other scorpion venom toxins (beta-toxins) can selectively interact with insect voltage-gated sodium channels and can be used as toxin-based pesticides [66]. Sea anemone venom toxins have been reported as potential agents for the treatment of autoimmune diseases such as multiple sclerosis, rheumatoid arthritis and type I diabetes [67]. These toxins, such as Shk, a 35-residue polypeptide toxin that is a potassium channel blocker, have proven to be very useful sources of pharmacological tools. Furthemore, the molecule's analogs have been evaluated with regard to the development of new biopharmaceuticals for autoimmune disorders [68,69].

With regard to spider venoms, researchers are involved in the study of insecticidal toxins, which can be used as tools in the elaboration of environmentally safe pesticides. Notably, the venom of the Australian funnel web spider has been analyzed, with emphasis on the toxin omega-atracotoxin (ALTX) HV1, a 37-residue peptide molecule. One model proposes the use of baculoviruses to express spider toxin to act as a pesticide [59,70]. Additionally, spider venom toxins can be used as models for the development of transgenic plants expressing insecticidal toxins. One example of this situation is the case of omega-ACTH-Hvt1 toxin from the venom of *Hadronyche versuta*, which protects the tobacco plant against insects. Another rational use of spider venom toxin as a model for design of therapeutic agents involves use of the toxin from *Phoneutria nigriventer* venom as a tool for the treatment of erectile dysfunction. The toxin Tx2–6 causes an improvement in the level of nitric oxide in penile tissue in rats [71,72]. Additionally, antibacterial peptides were identified in the venom of the *Cupiennius salei* spider. These peptides appear to act as channel-forming toxins within the bacteria wall. Analogous synthetic molecules would be expected to have great potential, especially in the age of multiple-antibiotic-resistant bacteria and related threats to human health [59,73].

The biotechnological uses of *Loxosceles* spider venoms have received increased attention over recent years. Notably, a spider toxin-derived product (ARACHnase) was proposed for the diagnosis of lupus anticoagulant. Also, antisera produced with *Loxosceles* venom has been used as bioproducts for serum therapy after spider accidents (for more information, see [74]). Recently, several recombinant toxins from *L. intermedia, L. laeta*, *L. boneti*, *L .gaucho,* and *L. reclusa* have been described. These include members of the phospholipase-D family [32–37,39,43], members of metalloprotease/astacin family [29,52], a member of translationally controlled tumor protein family (TCTP), a hyaluronidase, a serine protease inhibitor, a venom allergen, an insecticide toxin, member of neurotoxin/Magi 3 family , and an insecticidal toxin [75]. Recombinant molecules will not only expand our knowledge of spider biology and the pathophysiology of Loxoscelism, but as we shall discuss in the next chapters, they will also provide additional molecules for biotechnological purposes [74].

4. Phospholipase-D

Phospholipase-D is the most studied type of molecule present in the venom from *Loxosceles* species. In the general literature, these toxins are referred to as sphingomyelinase-D, due to their first

biochemical description as enzymes capable to hydrolyze sphingomyelin substrate. Based on the IUBMB recommendations, these molecules are biochemically classified as sphingomyelin phosphodiesterases D (E.C. 3.1.4.41) [5,6] Dermonecrotic toxin is a biological term widely applied by toxinologists to *Loxosceles* phospholipase-D, due to the hallmark of brown spider bites, which trigger dermonecrosis *in vivo.* Kalapothakis *et al.* [17] have organized dermonecrotic toxins of *L. intermedia* into a protein family, denoted LoxTox, by using cDNA coding sequences of several dermonecrotic/sphingomyelinase proteins from *Loxosceles intermedia*. The authors present at least six distinct groups (LoxTox 1 to 6) based on similarities among the molecules. At the present moment, Arachnoserver [30] includes 49 toxins from the *Loxosceles* genus with biological activity patterns characterized by dermonecrosis; these toxins were denoted as brown spider phospholipase-D proteins or partial sequences following the phylogenetic analyses of sicariid SMases by Bindford *et al.* [1].

The *Loxosceles* and *Sicarius* genera uniquely share the dermonecrotic venom toxin phospholipase D within the Haplogyne lineage. The most prospective evolutionary scenario for the origin of this enzyme is a single origin in the most recent ancestor of the Sicariidae family [76]. Phospholipases-D vary in molecular mass between species of North American *Loxosceles* (31–32 kDa), Old World species (32–33.5 kDa) and South American *Loxosceles* (32–35 kDa) [76]. Sphingomyelinase-D activity can be detected in all (36) *Loxosceles* and *Sicarius* species already tested. Binford and colleagues (2008) proposed to call this specific gene family *SicTox* towards a rational nomenclature. Based on Bayesian analyses they also resolved two clades of SMD genes, labeled α and β. Sequences in the α clade are exclusively from New World *Loxosceles* and *Loxosceles rufescens* and include published genes for which expression products have SMase D and dermonecrotic activity. The β clade includes paralogs from New World *Loxosceles* that have no, or reduced, SMase D and no dermonecrotic activity and also paralogs from *Sicarius*. In the context of structural position and proposed active sites [40], α and β clades differ only in conservation of key residues surrounding the apparent substrate binding pocket [3].

The pathological mechanisms of brown spider phospholipase-D have been continuously investigated, Van Meeteran [48] and Lee and Lynch [41] observed that recombinant *Loxosceles* SMaseD isoforms are able to hydrolyze lysophospholipids, generating bioactive lipid mediators such as lysophosphatidic acid (LPA). These researches extended the boundary of knowledge, which had depended upon sphingomyelin as a well-known substrate molecule. Furthermore, Lee and Lynch [41] also postulate that the term **phospholipase-D** (**PLD**) would more effectively represent the broad range of hydrolysable phospholipids than previously supposed to be applied for dermonecrotic toxins from *Loxosceles* genus [48]. Nomenclature of these toxins should be updated to account for the recent accumulation of knowledge regarding the biological and biochemical properties of these compounds.

The great interest of toxinologists in PLD proteins, to the neglect of other toxins present in the venom (most of them also enzymes or bioactive peptides), is due to the ability of these proteins to reproduce many effects of necrotic arachnidism or Loxoscelism. The PLDs from the *Loxosceles* genus are described as being responsible for several biological properties ascribed to whole venom, including the following: dermonecrosis, massive inflammatory response with neutrophil infiltration and complement activation, platelet aggregation, immunogenicity, edema and increased blood vessel wall permeability, hemolysis, renal failure, toxicity for several cultured cell types, and animal lethality [4,38,74,77].

Clinical investigations by Futrell [5] indicated that a dermonecrotic factor was responsible for histopathological observations resembling those of the cutaneous Arthus reaction, as observed in victims of accidents with brown spiders. Futrell [5] also reported the native toxin from *L. reclusa* (32 kDa) was an enzyme that hydrolyzes sphingomyelin and releases choline and N-acylsphingosine phosphate (or ceramide 1-phosphate). Various isoforms of phospholipase D were already reported for different species. Using SDS-PAGE analysis and chromatography methods, a range of molecular mass between 30–35 kDa was determined for PLD toxins that have hemolytic, necrotic and platelet aggregation activity, from *L. reclusa*, *L. rufescens*, *L. gaucho*, *L. laeta* and *L. intermedia* venoms [5,15,16,44,47,78,79]. Advances in proteomic studies have facilitated the description of many more PLD-related proteins in whole venom. Luciano *et al.* [80] performed two-dimensional electrophoresis and observed enriched levels of a 30-kDa molecule as well as cationic properties in *L. intermedia* whole venom, indicating the presence of several PLD-related protein spots. Furthermore, proteomic analysis of *L. gaucho* whole venom led to the identification of at least eleven PLD proteins (30–32 kDa 'loxnecrogin' isoforms) by Edman chemical sequencing and capillary liquid chromatography-mass spectrometry [25]. In summary, PLDs are dermonecrotic toxins that comprise a family of toxins with different related isoforms that have biological, amino acid and immunological similarities and which are found in diverse *Loxosceles* species [4,27,38,74]. This variation in phospholipase-D molecules may be due to post-translational modification and the expression of paralogous genes, since recent data demonstrate that gene duplications are frequent and that PLD genes lie in a region with high recombination within the genome [3].

Nowadays, heterologous systems based on cDNA sequences encoding mRNA transcripts from the brown spiders are a very useful tool for the production of recombinant PLD proteins (mainly in prokaryotic models). Using extracts of the venom gland, which is the tissue that is specialized for the production and secretion of venom toxins, molecular biology techniques were optimized to obtain several sequences as template for the identification, characterization and recombinant expression of PLD proteins [74].

At present, a new generation of molecules developed through cloning techniques still remains under investigation by researchers aiming to determine molecular and cell mechanisms of PLDs by biological approaches. *L. intermedia* LiD1 recombinant protein (31.4 kDa) is a sphingomyelinase D family molecule without dermonecrotic activity but with antigenic activity [32]. *L. laeta* recombinant protein (33 kDa) is a sphingomyelinase isoform able to degrade sphingomyelin [43]. *L. laeta* recombinant phospholipase-D generates lysophosphatidic acid and induces lysis of red blood cells [41]. Keratinocyte apoptosis was induced by recombinant PLD (SMaseD P2) from *L. intermedia* [81]. Global gene expression changes in fibroblast cells induced by PLD recombinant protein from *L. recluse* (SMD) are related to components of inflammatory response, such as human cytokines, genes involved in the glycosphingolipid metabolism pathway, and proteins known to impact transcriptional regulation [49]. Six isoforms of phospholipase-D were cloned from a cDNA library of *L. intermedia* gland venom and then expressed; they were shown to have similar toxic effects to those of native venom toxins [34–38]. *L. intermedia* recombinant protein (LiRecDT1, 34 kDa) displays dermonecrotic activity and was able to directly induce nephrotoxicity in mice and cultured tubular epithelial cells [42,46]. It could also induce non-complement-dependent hemolysis *in vitro* and inflammatory response using endothelial cell membrane as target [42,45]. Nephrotoxicity and hemolysis are both toxic effects

that depend directly on catalytic enzyme activity. In the same way, LiRecDT2 (ABB69098), LiRecDT3 (ABB71184), LiRecDT4 (ABD91846), LiRecDT5 (ABD91847), and LiRecDT6 (ABO87656) were identified, cloned and characterized as PLD proteins with high similarity to each other based on sequence alignment; this similarity is due primarily to conserved amino acids at the catalytic site [34–37]. The results of this alignment corroborated with the crystal structure analysis of a dermonecrotic toxin [40] from *L. laeta*, which suggested there were conserved residues at the proposed catalytic site for SMase D. The recent transcriptome analysis of *L. intermedia* venom gland identified at least two clusters (annotated as PLD-related ESTs) as new possibilities for a novel PLD isoform in *L. intermedia* venom, adding a new group to the LoxTox family classification [17,27].

The knowledge of structural, biochemical and biological properties of PLD toxins could be employed in design studies for the development of new drugs, biopharmaceuticals, diagnostic tests and other biotechnological and industrial applications. Immunoassays using brown spider PLDs as probes have been tested [50,82] because differential diagnosis of brown spider bites can often lead to misdiagnosis [83,84]. Moreover, therapeutic serum development and vaccination have been studied to ascertain the benefits of antivenom [85,86]. Synthetic peptides designed based on PLDs toxins with specific biological/protective effects have also been utilized [87,88]. Additionally, brown spider PLDs could be employed in the development of a vaccine derived from the phospholipase-D-mutated toxin from *L. intermedia* (substitution of the Histidine12 for Alanine in the catalytic site—LiRecDT1H12A) for the immunization of people living in regions that are endemic for accidents involving *Loxosceles* spiders. This method may be useful because enzyme activity of LiRecDT1H12A is dramatically decreased and has neither hemolytic activity nor nephrotoxicity [45,46]. Another possible application for PLD is as reagent of immunodiagnostic assays for identification and quantification of phospholipase-D in the sera of patients bitten by *Loxosceles* spider because diagnosis of Loxoscelism is very controversial and is commonly based on clinical signs and symptoms [89]. Brown spider venom may be detected in hair, wound aspirates, and skin biopsy for at least seven days after inoculation [90].

PLD enzyme activity triggers the degradation of the cell membrane phospholipids, loss of membrane asymmetry, phosphatidylserine exposure and membrane reorganization [91–93]. Sphingomyelin degradation changes membrane properties, such as lipid raft organization and membrane fluidity, triggering intracellular pathways [94,95]. Phospholipid metabolites induce the release of prostaglandins, activate the complement cascade, stimulate platelet aggregation, and enhance neutrophil chemotaxis and inflammation. Brown spider PLD toxins could be used in lipid protocols for cell membrane studies related to biological effects of lipid metabolites, with emphasis on sphingolipid-derived bioactive molecules and their signaling pathways. The activity and expression of some phospholipases are increased in several human cancers, suggesting that these enzymes may have central roles in tumor development and progression [96,97]. This involvement raises the possibility of considering phospholipid metabolism as a potential target for the development of new antitumoral agents by using brown spider PLDs as a novel model for tumor cell studies.

Further studies improving the understanding of PLD catalysis are relevant not only for comprehension of phospholipases mechanisms in basic sciences, but also for related pharmaceutical and biotechnological applications [98]. The catalytic activity of brown spider PLD plays a role in the pathological activity of this toxin and therefore cannot be dismissed as a rational target for new

strategies to treat Loxoscelism. Degradation of the phospholipid head-groups by brown spider PLDs changes membrane surface potential and affects the functional properties of some cation channels. Brown spider PLDs can offer an effective pharmacological way to activate voltage-gated channels that could be useful for "channelopathy" studies [99]. Certainly, elucidation of the roles of PLDs in a variety of molecular and cell biology mechanisms might be the greatest value of brown spider PLDs as a biotechnological product, which depends on their continuous characterization with regard to the details of pathogenesis and biochemistry.

5. Hyaluronidase

Hyaluronidases are enzymes that mainly degrade hialuronic acid (HA), and which may have activity upon chondroitin, chondroitin sulfate (CS) and, to a limited extent, dermatan sulfate (DS) [14,100,101]. The hyaluronidases are a group of enzymes that are distributed widely throughout the animal kingdom. They were discovered through the observation that extracts of some tissues contained a "spreading factor", which facilitated the diffusion of dyes and subcutaneous antiviral vaccines [102]. These enzymes are present in the venoms of multiple organisms, such as lizards, scorpions, spiders, bees, wasps, snakes and stingrays [103–105].

Hyaluronidases in venoms have been described as "spreading factors" due to their ability to degrade extracellular matrix components and to increase the diffusion of other toxins in tissues adjacent to the inoculation site [103]. Data from crystallography and X-ray diffraction suggested the evolutionary conservation of many poison hyaluronidases in a comparative study of several animal venoms [106,107]. Tan and Ponnudurai [108] reported that all venoms exhibit a wide range of hyaluronidase and protease activities. With regard to spider venoms, Kaiser [109] was the first to report hyaluronidase activity, from Brazilian *Lycosa raptoral* spiders, now known as *Phoneutria nigriventer* [110]. Shortly after that report, hyaluronidase activity was detected in the venom of European window spider *L. tredecimguttatus* and of the tarantula *D. hentzi* venom. This enzyme was isolated from the funnel web *A. robustus* and the tarantula *E. californicum venom* [111]. Spider venom hyaluronidases have been described more recently in *Lycosa godeffroy*, *Lympona cylindrata/murina* [110] and *Cupiennius salei*[112]. The *Hipassa* genus showed similar hyaluronidase activity to that of *H. agelenoides, H. lycosina* and *H. partita* species [110,113]. Moreover, venom obtained from *Vitalius dubius*, a spider found in southeastern Brazil, showed high levels of hyaluronidase activity [114]. With regard to necrotizing Australian spiders, hyaluronidase activity was demonstrated in *Badumna insignis*, *Loxosceles rufescens*, and *Lampona cylindrata* [12].

In 1973, Wright *et al.* were the first to describe hyaluronidase activity in venom of the genus *Loxosceles* [55]. This work was performed with *L. recluse* venom, and the purified enzymes, which were estimated to have molecular weights of 33 and 63 kDa by SDS-PAGE [115], exhibited activity against HA and CS types A, B, and C. The authors also showed that rabbit anti-venom inhibited the spreading effect exhibited by whole venom *in vivo* and completely inhibited hyaluronidase activity *in vitro* [55]. Young and Pincus [12], analyzing *L. recluse* venom, described hyaluronidase activity for a protein determined to be 32.5 kDa by HA-substrate SDS-PAGE [12,115]. Barbaro *et al.* [13] studied venoms from five *Loxosceles* species of medical importance in the Americas (*L. deserta, L. gaucho, L intermedia, L. laeta and L. recluse*).

Hyaluronidase activity was detected in all species of *Loxosceles* spider venom tested by HA zymogram. All venom samples contained an enzyme with molecular weight of approximately 44 kDa, which was able to digest HA and which may contribute to the characteristic gravitational spread of the dermonecrotic lesion in patients suffering from the effects of these venoms [13,115]. da Silveira *et al.* [14] reported that zymography showed *L. intermedia* venom included hyaluronidase molecules of 41 and 43 kDa molecular weight. The activity of these enzymes is pH-dependent, with optimal activity between 6 and 8, and was able to degrade HA in rabbit skin. Pedrosa *et al.* [51] studying *L. laeta* transcriptome found transcripts with similarity to *Bos Taurus* 'hyaluronidase' (gb|AAP55713.1): 4 clones and 1 cluster (LLAE0048C), representing 0.13% of the total sequence. In addition, hyaluronidase represents only 0.1% of all total toxin-encoding transcripts in the venom gland of *L. intermedia* [27]. This result may explain the difficulty associated with purification this enzyme from *Loxosceles* venoms. To obtain the recombinant hyaluronidase from *L. intermedia* venom, through the use of appropriate molecular biology techniques, an isoform was cloned and showed to have a theoretical molecular mass of about 46.1 kDa [75].

Hyaluronidase-mediated degradation of HA increases membrane permeability, reduces viscosity and renders tissues highly permeable to injected fluids. This degradation process is involved in bacterial pathogenesis, the spread of toxins and venoms, fertilization, and cancer progression [102]. Therefore, brown spider hyaluronidase could be used therapeutically in many fields, including orthopedics, surgery, ophthalmology, internal medicine, oncology, dermatology and gynecology [74]. There are several studies showing that hyaluronidases can be used to promote resorption of excess fluids, to increase the effectiveness of local anesthesia and to diminish tissue destruction by subcutaneous and intramuscular injection of fluids [100,102]. For example, hyaluronidase has been used to reduce the extent of tissue damage following extravasation of parental nutrition solution, electrolyte infusions, antibiotics, aminophyline, mannitol and chemotherapeutic agents, including Vinca alkaloids [116].

Additionally, recombinant human hyaluronidase (rHuPH20) has been used in chronic pain management, to improve systemic absorption and bioavailability of drugs [117–120]. In the context of cancer therapy, testicular hyaluronidase (HAase) has been added to drug regimens to improve drug penetration. In limited clinical studies, HAase has been used to enhance the efficacy of vinblastin in the treatment of malignant melanoma and Kaposi's sarcoma, among other cancers [121]. Furthermore, when the level of HA decreases under conditions in which hyaluronidase activity increases, the moisture and tension of the skin are reduced, and histamine is released from mast cells [122]. Therefore, the identification and characterization of hyaluronidase inhibitors could be relevant to the development of contraceptives, as well as anti-tumor, anti-microbial, and anti-venom, anti-wrinkle, and anti-aging agents, and allergy and inflammation suppressors [14,122–124]. Therefore, *Loxosceles* recombinant hyaluronidases are associated with numerous potential applications [27,74,125,126].

6. Translationally Controlled Tumor Protein (TCTP)

Loxosceles intermedia TCTP protein was identified during an *L. intermedia* venom gland transcriptome study [27], although another spider TCTP had already been described from the venom gland of *Loxosceles laeta* by transcriptome analysis [51]. Proteins of the TCTP superfamily were first

identified in the late eighties by research groups studying translationally regulated genes. These proteins were named *translationally controlled tumor proteins* when the discovery of human cDNA was published [127]. This name was based on the protein's tumoral origin, a human mammary carcinoma, and on the observation that TCTP is regulated at the translational level. The translationally controlled tumor protein (TCTP), which was initially named P21, Q23 and P23 by three different groups and is also called HRF (histamine-releasing factor), represents a large family of proteins that are highly conserved and ubiquitous in eukaryotes [56,128].

Sequence alignment studies of TCTP sequences revealed that nearly 50% of all amino acid residues are preserved. Among species from the same genus, TCTPs are completely conserved [56]. When the TCTP sequence found in the *L. intermedia* venom gland transcriptome was compared with the one described in the venom gland of *L. laeta*, 97% similarity was observed. *L. intermedia* TCTP also presented important similarities with the other arthropod TCTPs, such as *Ixodes scapularis* and *Amblyomma americanum* from mites [27]. The scientific community's understanding of TCTP's biological function is growing. The compound possesses a wide range of functions, and different biochemical roles are currently being established [56,129].

Although TCTP participates in various biological functions, the primary physiological roles of this protein are still unknown [130]. TCTP is widely expressed in many tissues and cell types, and its protein levels are highly regulated in response to a wide range of extracellular signals and cellular conditions [56]. Interactions between TCTP and other cellular proteins have already been reported for tubulin [131], actin-F [132], the mammalian Plk [133], translation elongation factors eEF1A and eEF1Bbeta [134], Mcl-1 [135,136], TSAP6 [137], Na,K-ATPase [138], Bcl-XL [139] and Chrf [140]. Studies have already shown that TCTP is essential for embryonic development and cell proliferation in mice and *Drosophila* [141,142]. Moreover, the protein has calcium-binding activity and is capable of stabilizing microtubules, a property that may be related to a possible role of TCTP in cell cycle control, as it was also shown that TCTP interacts with a checkpoint protein (Chrf) [56,140].

Loxosceles intermedia transcriptome analysis highlighted TCTP transcript as a toxin-coding messenger due to TCTP extracellular activities already described above [27]. TCTP was described as a protein that triggers histamine release in basophil leukocytes and was therefore called 'histamine release factor' (HRF) [128]. Then, other studies reported that TCTP presents more general 'cytokine-like' activity, as it also induces the production of interleukins from basophils and eosinophils [143]. TCTP itself is induced by certain cytokines and acts as a growth factor for B-cells [144]. Studies demonstrate that TCTP triggers histamine release in basophile leukocytes by mechanisms that may be dependent on or independent of the presence of IgE. It is believed that a specific TCTP receptor may participate in the process, leading to mast cell activation [56]. Although TCTP protein was found in biological fluid of asthmatic or parasitized patients and in saliva from ticks, TCTP mRNAs do not code for a signal sequence and no precursor protein has been described [56,145]. TCTP secretion from cells proceeds via an endoplasmic reticulum/Golgi-independent or non-classical pathway, probably mediated by secreted vesicles called exosomes, which have been suggested as possible pathways for non-classical secretion [137,145]. In the case of the *Loxosceles* venom gland, TCTP is secreted via holocrine secretion [27]. TCTPs have been described in gland secretions of many arthropods, such as ixodid ticks and in the venom gland of the wolf spider [146–148].

L. intermedia TCTP is very similar to *Dermacentor variabilis* TCTP, which is expressed in diverse tissues from the tick, including its salivary gland. When this TCTP was cloned and expressed as a recombinant protein, it was able to release histamine from a basophilic cell line [27,146]. Based on these data, it is possible to suggest that *L. intermedia* TCTP may act as a histamine release factor. The presence of a component in *L. intermedia* venom related to the histaminergic activity of venom supports with this hypothesis [149]. Recently, some authors have called attention to the role of histamine and its receptors in the development of edema, involving increased vascular permeability and vasodilatation [150], which occurs in Loxoscelism. Histamine had been described as the principal pharmacological component in the venom of the wolf spider (*Lycosa godeffroyi*) [148,151]. Proteins of the TCTP family were described to be expressed in human parasites suggesting that could be related to the survival mechanisms of parasites in the host and to the onset of pathological processes [152–154]. The antimalarial drug artemisin [155], probably acts on *Plasmodium* TCTP, confirming its important function in the development of pathology [153,154].

Recently, an increasing number of researchers have focused their attention on the cellular and extracellular activities of TCTP, as it has been implicated in the promotion of cell growth and tumorigenesis as well as in protection against apoptosis and other consequences of cell stress [56,156–158]. TCTP protein levels are upregulated in cancer cells and in human tumors [159–161]. Downregulation of TCTP has been implicated in biological models of tumor reversion [159,162], and the protein is the target of various anticancer drugs [159,163]. TCTP has been proposed as a potential cancer biomarker [160,164,165] and therapeutic target [166].

TCTP has enormous biotechnological potential; this toxin presents a wide range of putative applications: from a biological tool at research laboratories to clinical oncology, as a biomarker and/or a model for drug design to cancer treatment. Drugs that cause inhibition of TCTP activity resulted in tumor growth inhibition both *in vitro* and *in vivo* [159]. TCTP and its biological tools (e.g., antibodies against TCTP) can also be used in experimental oncology to study tumor cell behavior and metabolism, as well as in the screening of anticancer drugs. Still in the field of cell proliferation, TCTP and its related biological tools could also be used to study cell cycle regulation and the microtubule cytoskeleton, as well as its role in cell physiology and organelle transport.

Calcium metabolism and signaling are other issues that could be explored using TCTP and its derived biological tools. Antiapoptotic activities were also described for TCTP: this protein potentiates MCL1 and BCL-X_L inhibits BAX [158]. These effects highlight TCTP as a candidate for apoptosis studies, as an apoptotic drug and as a model for anti-apoptotic reagents. Another possible application of this toxin could be its employment in allergic screening tests, due to TCTP's histaminergic activity. Inhibitors of TCTP are putative anti-histaminic drugs and other TCTP-derived biological tools could be useful at research laboratories that study histamine release, mast cell metabolism and activation, immediate hypersensitivity reactions and the allergy process in general. Protocols that involve proliferation of B cells represent other potential applications for TCTP. TCTP secretion to the extracellular milieu is mediated by a non-classical pathway involving exosomes [137]; therefore, it is a good reagent with which to study this type of cellular secretion. TCTP has a surprising number of different functions as described here, but how these different functions might be interrelated remains to be determined [167]. Therefore the putative applications suggested herein are just the first insights into the potential uses and applications of TCTP in the field of biotechnology.

7. Astacin-Like Metalloproteases

Metalloproteases in *Loxosceles* venom were first characterized in *L. intermedia* venom. Feitosa *et al.* [18] described two metalloproteases, Loxolisin A (20–28 kDa, with fibronectinolytic and fibrinogenolytic activity) and Loxolisin B (32–35 kDa, with gelatinolytic activity). Zanetti *et al.* [168] purified a 30 kDa molecule with fibrinogenolytic activity from *L. intermedia* crude venom. Furthermore, da Silveira *et al.* [53] showed that venom gland extracts from brown spiders possess proteolytic activity, and this activity could be inhibited by bivalent chelators. This study proved that metalloproteases are components of *L. intermedia* and *L. laeta* venoms, and eliminated the possibility that electrostimulated venom could have been contaminated with digestive hydrolytic enzymes during extraction [53].

Metalloproteases were also identified as components of different *Loxosceles* species venoms, such as *L. rufescens, L. gaucho, L. laeta, L. deserta* and *L. reclusa* [12,13,51,168]. Recently, a recombinant metalloprotease from the *L. intermedia* venom gland, named LALP (*Loxosceles* astacin-like metalloprotease), was characterized as an astacin-like enzyme. This functional characterization supported previous data describing metalloproteases in *Loxosceles* venom [52]. The identification of LALP in *L. intermedia* venom was the first report in the literature of the presence of an astacin family member as an animal venom constituent. Trevisan-Silva *et al.* [29] described two new astacin-like toxin isoforms from *L. intermedia* venom (LALP2 and LALP3) and found that metalloproteases in *L. laeta* and *L. gaucho* venoms are also members of the astacin family. This study described the presence of a gene family of astacin-like toxins in three *Loxosceles* species suggesting that these molecules will be found in all South America *Loxosceles* species [29]. Astacin-like proteases are the second most commonly expressed class of toxins in the *L. intermedia* venom gland, comprising 9% of all transcripts [27].

The astacin family enzymes are zinc-dependent metalloproteases, which are considered as part of the metzincin superfamily [54,169]. Members from the astacin family are ubiquitous, existing more than 200 described astacins, which are found in some bacteria species and in all animal kingdoms [169–173]. Astacins are characterized by the zinc-binding motif (**H**EXX**H**XX**G**XX**H**EXXRXDR), which contains three histidine residues that are responsible for the complexation of zinc. Below the active site, all astacins have a methionine residue within a typical Met-turn (SX**M**X**Y),** with a tyrosine residue that might be involved in substrate fixation [54,169,174–176]. This protease family was named after the identification of astacin from freshwater crayfish, *Astacus astacus*. Astacin is the prototypical digestive collagenolytic enzyme of the astacin family [177,178]. Astacin family members are reported to have a wide range of functions, playing roles in digestion, in peptide and matrix molecules processing, in the activation of growth factors and in the degradation of distinct proteins [169,174,175].

We have little information about the biochemical and biological function of *Loxosceles* venom astacins because astacin members have distinct functions and the study of astacins from *Loxosceles* venoms is just beginning. Previous studies of *Loxosceles* metalloproteases have shown that they degrade some matrix proteins (fibronectin, fibrinogen, gelatin and entactin), but the mechanism involved in the noxious effect of the venom is until unclear [18,20,21,52]. It has been suggested that astacin toxins could be involved in gravitational spreading of dermonecrosis, in hemorrhagic

disturbances observed in accidents, imperfect platelet adhesion and increased vascular permeability, which can occur near bite sites after brown spider accidents [13,29,52]. Also, astacin proteases could act as a spreading factor for other venom toxins and could serve as important agents, in the processing of other venom toxins, by cleaving inactive proteins and generating active peptides that may be involved in Loxoscelism effects [29,52].

Astacin-like proteases are biologically active enzymes that have potential applications in pharmaceutical studies and could be used as tools for research protocols [74]. The enzymatic activities of astacins upon different proteins highlight these molecules as useful tools in studies involving protein degradation, especially the degradation of extracellular matrix (ECM) components. Considering the physiological and pathological events related with ECM degradation, astacins can be used in protocols for medical and pharmaceutical research, such as ECM assembly and remodeling (including collagen processing and the healing process). Drug administration (as a co-adjuvant), cell membrane metabolism, embryogenesis, cellular differentiation (including stem cells), tumorigenesis and metastasis, enzymatic activation (latency and activation of zymogens), cell signaling based on proteolysis, inflammatory response and vascular permeability are other potential applications for these molecules.

Astacins from *L. intermedia* could also be used as starting materials to design new drugs/molecules, as agonists and/or inhibitors. One possible therapeutic use of astacins from *L. intermedia* is the context of vascular diseases (acute myocardial infarction, acute ischemic stroke, thrombosed aortic aneurysms, pulmonary embolism, etc.) and as thrombolytic agents. At present, intravenously administered tissue plasminogen activator (IV-TPA) remains the only FDA-approved therapeutic agent for the treatment of ischemic stroke within three hours of symptom onset. Although intra-arterial delivery of the thrombolytic agent seems effective, various logistic constraints limit its routine use and, as yet, no lytic agent has received full regulatory approval for intra-arterial therapy [179]. Moreover, astacin inhibitors may be therapeutically useful in atherosclerosis prevention. Meprins, which are members of the astacin family, hydrolyze and inactivate several endogenous vasoactive peptides, some of which could alter various functions of cells in the arterial wall. Recent studies have shown that a meprin inhibitor suppresses the formation of atherosclerotic plaques [180]. The recombinant astacins could also be used as reagents for laboratorial tests to diagnose Loxoscelism, as well as anti-loxosceles serum production, in the treatment of envenomation.

8. Insecticidal Peptides

Spider venoms are functionally related to defense against predators and primarily used to paralyze and capture natural prey, especially insects [89,181–183]. To execute these functions, spiders developed an arsenal of insecticidal molecules in their venoms, resulting in a combinatorial peptide library of insecticidal peptides that has been improved over the course of evolution [184]. Such peptides consist of single-chain, low molecular weight molecules of 3–10 kDa, with a high number of cysteine residues that form intramolecular disulfide bridges [185,186]. Over the last decade, these peptides have been investigated extensively through identification, purification, characterization and cloning studies [23].

The insecticidal peptides act in the nervous system of prey or predator, causing paralysis or even death, by interacting with specific neuronal ion channels of the excitable membranes [183]. These peptides can be classified depending on their mode of action, such as effects on sodium (Na^+), calcium (Ca^{2+}), potassium (K^+) and chloride (Cl^-) ion channels [111,187]. Many of these peptides present a structural motif designated as an inhibitory cystine knot (ICK), and therefore these molecules are named *knottins*. The ICK motif is composed of a triple-stranded, anti-parallel β-sheet, stabilized by a cystine knot containing three disulphide bridges [188,189], which confer rigidity to the molecules in addition to a stabilization of their secondary structures and relative resistance to denaturation [190].

Although there are a great number of insecticidal peptides characterized in several spider species, little is known about insecticidal molecules in *Loxosceles* spiders. By studying *L. intermedia* venom, de Castro *et al.* [23] first described and characterized three isoforms of insecticidal peptides named LiTx1, LiTx2 and LiTx3 which contain ICK motif and act on specific ion channels. The chromatographic fraction containing these peptides showed potent insecticidal activity against the agricultural pests *Spodoptera* species. LiTx1 (7.4 kDa) presents some sites to possible post-translational modifications, such as N-myristoylation, protein kinase C phosphorylation, amidation and casein kinase II phosphorylation. With regard to its specificity, the study was not able to determine whether LiTx1 interacts with Na^+ or Ca^{2+} channels. LiTx2 (7.9 kDa) and may present N-myristoylation, protein kinase C phosphorylation and amidation sites. Its specificity to ion channels was not determined. LiTx3 peptide (5.6 kDa) has also sites for N-myristoylation and protein kinase C phosphorylation. Based on bioinformatic analyses, de Castro, *et al.* hypothesized that LiTx3 may interact with Na^+ channels. In 2006, a new isoform, LiTx4, was identified (GenBank n ºDQ388598.1).

Transcriptome analysis of the *L. intermedia* venomous gland revealed ESTs with similarity to LiTx peptides described by de Castro *et al.* [23]. LiTx3 was the most abundant sequence in the *L. intermedia* transcriptome, comprising 32% of toxin-encoding messengers. LiTx2 had a representativeness of 11% in relation to the toxin-encoding transcripts. [27]. The transcriptome analysis of *L. intermedia* venomous gland additionally revealed the presence of another class of ion channel-binding peptides. These peptides present similarity to neurotoxin Magi 3, a peptide isolated by Corzo *et al.* [26] from the venom of the *Macrothele gigas* spider. Magi 3 peptide is able to paralyze insects, although the authors did not confirm whether Magi 3 is specific for insect sodium channels or also acts on calcium channels [191].

The specificity of insecticidal peptides for ion channels provides an important tool to understand their dynamic activity. Ion channels are transmembrane proteins involved in the control of ion fluxes across the membrane, regulating membrane potential and ion balance. Their activity is also related to the coordination of diverse cellular functions such as excitation-contraction coupling, hormone and neurotransmitter secretion and gene expression. Thus, the comprehension of the interaction between peptide-ionic channels allows a more refined investigation of the physiological role of ion channels, as well as the determination of possible therapeutic applications [192].

The ability to discriminate insect ion channels confers to insecticidal peptides with considerable potential in the development of an efficient bioinsecticide for the control of economically disadvantageous pests or insect vectors of new or re-emerging disease [182,193]. Recombinant baculovirus containing the gene encoding an insecticidal peptide has been studied and tested against many insect pests, such as *Heliothis virescens* (cotton bollworm), *Laspeyresia pomonella*

(codlingmoth) and *Neodiprion sertifer* (European sawfly) [183,194]. This biotechnological development could lead to alternative methods for chemical control, resulting in many benefits to the agricultural sector that will ultimately reduce economic losses.

9. Serine Protease Inhibitors

The control of proteases is normally achieved by the regulation of expression, secretion, activation of proenzymes and degradation. A second level of control is based on specific inhibition of activity. Despite microorganisms that produce non-proteinaceous compounds that block host proteases, the remaining all known natural protease inhibitors are proteins [195–197]. Among these natural protease inhibitors, the most extensively studied and described protein inhibitors of proteases are the group of serine protease inhibitors.

Serine protease inhibitors can be classified into one of three different types, according to their structures and the mechanism of inhibition: the canonical inhibitors, the non-canonical inhibitors and the serpins. The largest group is the canonical inhibitors, which are small proteins (14 to ~200 amino acid residues) represented mainly by the Kazal, BPTI (bovine pancreatic trypsin inhibitor), potato I and STI (soybean trypsin inhibitor) families [198,199]. Non-canonical are usually found in blood-sucking organisms and are responsible for blocking the blood-clotting cascade [196]. Serpins (*ser*ine *p*rotease *in*hibitors) are large proteins (typically 350 to 500 amino acids in size), also widely distributed in nature, and are abundant in human plasma. Similar to the canonical inhibitors, serpins exhibit binding loops and interact with the target enzyme in a substrate-like manner. However, cleavage of the serpin loop by the protease leads to dramatic conformational changes in the global structure of the inhibitor [196,200,201].

In brown spider venom, protease inhibitors were first reported in *L. laeta* [51]. The transcriptome analysis approach, which detected 0.6% of sequences with identity to intracellular coagulation inhibitor from *Tachypleus tridentatus* and sequences with identity to serine (or cysteine) proteinase inhibitors from *Mus musculus*, *Aedes aegypti*, *Branchiostoma lanceolatum*, *Gallus gallus*, and *Boophilus microplus* . Similar results were obtained for *L. intermedia* [27], in which one transcript presented significant similarity with a serine (or cysteine) peptidase inhibitor, clade I, member 1 from *Mus musculus*. In both cases (*L. laeta* and *L. intermedia*), the sequences analyzed were similar to serine proteinase inhibitors belonging to the Serpin superfamily.

Playing roles as potential toxins, serine protease inhibitors have been intensively described in several snake venoms, especially for those of the *Elapidae* and *Viperidae* families [202]. In these venoms, the majority of inhibitors characterized belong to the canonical type, particularly the Kunitz/BPTI inhibitors of trypsin and chymotrypsin. The peptides were typically 6–7 kDa in size and were isolated from crude venoms and studied by different methods [203–210]. The identification of this type of molecule allowed future isolation and further characterization of putative protease inhibitors, suggesting the possibility of a biotechnological application. The best example for this purpose is Textilinin-1, which is a well-known 6.7 kDa Kunitz-type serine protease inhibitor from the venom of the snake *Pseudonaja textilis* which binds and blocks certain proteases, including plasmin and trypsin [211]. The ability to reversibly inhibit plasmin has raised the possibility of using this drug as an alternative to aprotinin (Trasylol®), as a systemic antibleeding agent in cardiac surgery. Like

aprotinin, Textilinin-1 (in equimolar concentrations) almost completely inhibits tissue plasminogenactivator-induced fibrinolysis of whole blood clots. In mouse bleeding models, Textilin-1 shows shorter time of hemostasis compared to aprotinin and appears to be a more specific plasmin inhibitor than aprotinin [210–212].

Despite their presence in the majority of snake venoms, serine protease inhibitors have also been described and characterized in other organisms. Zhao *et al.* [213] isolated and characterized a 60 kDa serpin from skin secretions of *Bufo andrewsi*, which was denoted as Baserpin. This protein was able to irreversibly inhibit trypsin, chymotrypsin and elastase. Serine protease inhibitors are also present in spider venoms, particularly in the venom of tarantulas (*Ornithoctonus huwena* and *Ornithoctonus hainana*). The prototypic molecule in tarantula venom is HWTX-XI, 6.1 kDa peptide from *Ornithoctonus huwena* venom, which belongs to the Kunitz-type family of serine protease inhibitors. Just like Kunitz-type toxins in snake venoms, HWTX-XI is considered to be a bi-functional toxin because it is a strong trypsin inhibitor as well as a weak Kv1.1 potassium channel blocker [214].

Zhao *et al.* [213] isolated and characterized a 60 kDa serpin from skin secretions of *Bufo andrewsi*, which was denoted as Baserpin. This protein was able to irreversibly inhibit trypsin, chymotrypsin and elastase. The considerations above represent just a few insights concerning serine protease inhibitors uses and applications. The great importance of proteases in numerous different biological processes and the large number of protease inhibitors described suggest their strong biotechnological potential.

10. Conclusion

Research in brown spider venom toxins has increased over recent years, but the challenges and opportunities are enormous. To move the field forward, scientists must have access to the biodiversity of spiders within their countries. Different *Loxosceles* genus spider species are reported to inhabit every continent [5,6,8], and bureaucracy related to the capture of spiders should not be a hindrance to researchers on toxinology area. Official collaborations with groups based where brown spiders are endemic will facilitate access to their venom.

Another difficulty in working with *Loxosceles* venoms is the fact that the volume of venom is minute (just microliters, containing a few micrograms of protein, as previously discussed). This makes work difficult for researchers that use crude venom in their experiments. To overcome this difficulty, works can collect venom from hundreds, or even, thousands, of spiders during specific periods of the year when there is an abundance of spiders and store the venom under appropriate conditions (*i.e.*, lyophilized or in solutions at −80 ℃) [18]. Alternatively, brown spiders could be captured from the wild and kept individually (because they kill one another) under laboratory conditions, using insect larvae as food and with periodic hydration via water-soaked cotton balls, with venom collected as necessary.

Another technical solution for venom production is the standardization of long-term primary culture of secretory cells from the venom gland and the production of venom *in vitro*. The culture of secretory cells from different venomous animals has shown promising results, and represents a good system with which to obtain toxins without capturing animals from the wild and without the related ecological disturbances. To date, several groups have reported expertise on this topic, and have established protocols for the primary culture of secretory cells. Examples include those from the venom glands of

Crotalus durissus terrificus and *Bothrops jararaca* snakes [215,216], as well as those from the venom glands of the *Phoneutria nigriventer* spider [217]. Such protocols ensure that sufficient amounts of native toxins are produced and secreted for culture medium and used for technical purposes after purification. Unfortunately, for *Loxosceles* venom gland cells, there are no reports to date of successful primary cultures of secretory cells. This situation represents a rational challenge for the future regarding the acquisition of sufficient amounts of native molecules. Finally, the venom of *Loxosceles* species is commercially available, as is the case for *L. deserta* (Sigma, St. Louis, USA).

The cDNA library construction of *L. intermedia* venom gland [35], transcriptome analysis [27,51] and the cloning and synthesis of several recombinant toxins [29,32–37,39,43,52] is helping to elucidate the biology of *Loxosceles* genus and opening possibilities for biotechnology applications. Recombinant toxins have been expressed in bacteria, simple organisms that are easy to manipulate and cheap to work with; unfortunately these do not generate co- and post-translational modifications such as disulphide bonds and protein glycosylations. Certain recombinant molecules are expressed in their unfolded form, have incorrected conformations, are water insoluble, and have no biological function.

With regard to phospholipase-D family members, these recombinant toxins purified from bacteria have biological functions compatible with those described for native toxins. For native toxins, it was already very well demonstrated that inflammatory response with cytokines release is induced at the bite site, and lipid content might be relevant for tissue damage [218,219]. These recombinant toxins induce dermonecrosis, platelet aggregation, increased vessel permeability, deep inflammatory responses, and phospholipase-D activity [34–37]. On the other hand, a great number of brown spider venom recombinant toxins synthesized by bacteria are water-insoluble and have no biological function. To surpass this technical obstacle, insoluble toxins can be refolded by methods of protein refolding [220], but the final concentration of refolded toxins obtained is generally not enough for biotechnological uses.

Alternatively, toxins can be synthesized using other expression models, such as the yeast *Pichia pastoris* [221], an organism that has subcellular organelles as endoplasmic reticulum and Golgi apparatus. This yeast is able to perform co- and post-translational modifications of proteins. For *Loxosceles* toxins, preliminary experiments are underway [75], but a frequent problem to be overcome is the hyperglycosylation of secreted proteins, which alters the biological functions of the toxins. Expression in systems of insect cells, such as *Drosophila* Schneider cells, is a possible alternative method [222] because it is a eukaryotic expression system, in which proteins undergo post-translational modifications.

For *Loxosceles* toxins, again, experiments are just beginning and results are preliminary [75], but they can provide secreted toxins that are correctly folded and, in the near future, may be used as tools for biological evaluations. Baculovirus vector for protein expression in insect and mammalian system is also feasible [223], but we do not have information on *Loxosceles* molecules produced using this technique. Finally, the mammalian expression system is a rational alternative for expression of correctly folded recombinant proteins. Mammalian cells have the capacity for proper protein folding and assembly, as well as co- and post-translational modifications [224]. Currently, there are no data on *Loxosceles* venom toxins obtained using this system. However, because this model is a viable method for recombinant proteins of therapeutic use, scientists are expected to explore this system in the future.

The advancement of *Loxosceles* venom toxin research will also involve techniques from proteomic analysis. These techniques generally have high sensitivity and accuracy and normally use low venom concentration for analysis. To date, at least two works have been completed addressing this topic. By using proteomics methodologies, such as bi-dimensional electrophoresis, N-terminal amino acid sequencing and mass spectrometry, eleven isoforms for phospholipase-D toxin were identified in *L. gaucho* venom [25]. In addition, through mass spectrometry analysis using *L. intermedia* crude venom, 39 proteins were identified, and putative effects for envenomation were discussed [24]. The use of combinatorial data from proteomic and molecular biology techniques, such as mass spectrometry, transcriptome analysis and cDNA library constructions, will open possibilities for the discovery of novel toxins in complex venoms [225].

Additionally, in the near future, the biotechnological use of *Loxosceles* toxins could provide information related to the tridimensional structure of identified toxins, through crystallography and X-ray diffraction and/or nuclear magnetic resonance for soluble toxins [59]. Findings in these areas will bring insight related to the molecular structure of toxins and will be very important for the discovery of catalytic sites, sites that interact with natural substrates or ligands, and from such data, synthetic ligands, analogs, or inhibitors could be designed for biotechnological purposes.

Regarding *Loxosceles* spider venom toxins, a recombinant phospholipase-D from *L. laeta* was analyzed by crystallography and X-ray diffraction. The data collected allowed description of the amino acid residues involved in catalysis and metal ion coordination important for sphingomyelinase activity [226]. Experiments using other isoforms of phospholipase-D from *L. intermedia* venom (LiRecDT1, LiRecDT2, LiRecDT6, GFP-LiRecDT1, and LiRecDT1H12A, with a mutation on the catalytic site, [46]) are currently being conducted using crystallography and X-ray diffraction. Additionally, other *Loxosceles* recombinant toxins (enzymes and peptides) could be evaluated and represent potential biological tools in a wide range of fields.

Acknowledgements

This work was supported by grants from CNPq, CAPES, Fundação Araucária-Paraná and Secretaria de Estado de Ciência, Tecnologia e Ensino Superior do Paraná, SETI-PR, Brasil.

References

1. Binford, G.J.; Bodner, M.R.; Cordes, M.H.; Baldwin, K.L.; Rynerson, M.R.; Burns, S.N.; Zobel-Thropp, P.A. Molecular evolution, functional variation, and proposed nomenclature of the gene family that includes sphingomyelinase D in sicariid spider venoms. *Mol. Biol. Evol.* **2009**, *26*, 547–566.
2. Platnick, N.I. *The World Spider Catalog*, Version. 9.0.; American Museum of Natural History: New York, NY, USA, 2008,
3. Binford, G.J.; Callahan, M.S.; Bodner, M.R.; Rynerson, M.R.; Nunez, P.B.; Ellison, C.E.; Duncan, R.P. Phylogenetic relationships of Loxosceles and Sicarius spiders are consistent with Western Gondwanan vicariance. *Mol. Phylogenet. Evol.* **2008**, *49*, 538–553.
4. Appel, M.H.; Bertoni da Silveira, R.; Gremski, W.; Veiga, S.S. Insights into brown spider and loxoscelism. *Invertebr. Surviv. J.* **2005**, *2*, 152–158.

5. Futrell, J.M. Loxoscelism. *Am. J. Med. Sci.* **1992**, *304*, 261–267.
6. da Silva, P.H.; da Silveira, R.B.; Appel, M.H.; Mangili, O.C.; Gremski, W.; Veiga, S.S. Brown spiders and loxoscelism. *Toxicon* **2004**, *44*, 693–709.
7. Hogan, C.J.; Barbaro, K.C.; Winkel, K. Loxoscelism: old obstacles, new directions. *Ann. Emerg. Med.* **2004**, *44*, 608–624.
8. Swanson, D.L.; Vetter, R.S. Loxoscelism. *Clinics. Dermatol.* **2006**, *24*, 213–221.
9. Lung, J.M.; Mallory, S.B. A child with spider bite and glomerulonephritis: A diagnostic challenge. *Int. J. Dermatol.* **2000**, *39*, 287–289.
10. Sales, P.B.; Santoro, M.L. Nucleotidase and DNase activities in Brazilian snake venoms. *Comp. Biochem. Physiol. C Toxicol. Pharmacol.* **2008**, *147*, 85–95.
11. Schroeder, F.C.; Taggi, A.E.; Gronquist, M.; Malik, R.U.; Grant, J.B.; Eisner, T.; Meinwald, J. NMR spectroscopic screening of spider venom reveals sulfated nucleosides as major components for the brown recluse and related species. *Proc. Natl. Acad. Sci. USA* **2008**, *105*, 14283–14287.
12. Young, A.R.; Pincus, S.J., Comparison of enzymatic activity from three species of necrotising arachnids in Australia: Loxosceles rufescens, Badumna insignis and Lampona cylindrata. *Toxicon* **2001**, *39*, 391–400.
13. Barbaro, K.C.; Knysak, I.; Martins, R.; Hogan, C.; Winkel, K. Enzymatic characterization, antigenic cross-reactivity and neutralization of dermonecrotic activity of five Loxosceles spider venoms of medical importance in the Americas. *Toxicon* **2005**, *45*, 489–499.
14. da Silveira, R.B.; Chaim, O.M.; Mangili, O.C.; Gremski, W.; Dietrich, C.P.; Nader, H.B.; Veiga, S.S. Hyaluronidases in Loxosceles intermedia (Brown spider) venom are endo-beta-N-acetyl-d-hexosaminidases hydrolases. *Toxicon* **2007**, *49*, 758–768.
15. Barbaro, K.C.; Ferreira, M.L.; Cardoso, D.F.; Eickstedt, V.R.; Mota, I. Identification and neutralization of biological activities in the venoms of Loxosceles spiders. *Braz. J. Med. Biol. Res.* **1996**, *29*, 1491–1497.
16. Cunha, R.B.; Barbaro, K.C.; Muramatsu, D.; Portaro, F.C.; Fontes, W.; de Sousa, M.V. Purification and characterization of loxnecrogin, a dermonecrotic toxin from Loxosceles gaucho brown spider venom. *J. Protein Chem.* **2003**, *22*, 135–146.
17. Kalapothakis, E.; Chatzaki, M.; Goncalves-Dornelas, H.; de Castro, C.S.; Silvestre, F.G.; Laborne, F.V.; de Moura, J.F.; Veiga, S.S.; Chavez-Olortegui, C.; Granier, C.; Barbaro, K.C. The Loxtox protein family in Loxosceles intermedia (Mello-Leitao) venom. *Toxicon* **2007**, *50*, 938–946.
18. Feitosa, L.; Gremski, W.; Veiga, S.S.; Elias, M.C.; Graner, E.; Mangili, O.C.; Brentani, R.R. Detection and characterization of metalloproteinases with gelatinolytic, fibronectinolytic and fibrinogenolytic activities in brown spider (Loxosceles intermedia) venom. *Toxicon* **1998**, *36*, 1039–1051.
19. Veiga, S.S.; da Silveira, R.B.; Dreyfus, J.L.; Haoach, J.; Pereira, A.M.; Mangili, O.C.; Gremski, W. Identification of high molecular weight serine-proteases in Loxosceles intermedia (brown spider) venom. *Toxicon* **2000**, *38*, 825–839.
20. Veiga, S.S.; Feitosa, L.; dos Santos, V.L.; de Souza, G.A.; Ribeiro, A.S.; Mangili, O.C.; Porcionatto, M.A.; Nader, H.B.; Dietrich, C.P.; Brentani, R.R.; Gremski, W. Effect of brown spider venom on basement membrane structures. *Histochem. J.* **2000**, *32*, 397–408.

21. Veiga, S.S.; Zanetti, V.C.; Braz, A.; Mangili, O.C.; Gremski, W. Extracellular matrix molecules as targets for brown spider venom toxins. *Braz. J. Med. Biol. Res.* **2001**, *34*, 843–850.
22. Veiga, S.S.; Zanetti, V.C.; Franco, C.R.; Trindade, E.S.; Porcionatto, M.A.; Mangili, O.C.; Gremski, W.; Dietrich, C.P.; Nader, H.B. *In vivo* and *in vitro* cytotoxicity of brown spider venom for blood vessel endothelial cells. *Thromb. Res.* **2001**, *102*, 229–237.
23. de Castro, C.S.; Silvestre, F.G.; Araujo, S.C.; Gabriel de, M.Y.; Mangili, O.C.; Cruz, I.; Chavez-Olortegui, C.; Kalapothakis, E. Identification and molecular cloning of insecticidal toxins from the venom of the brown spider Loxosceles intermedia. *Toxicon* **2004**, *44*, 273–280.
24. dos Santos, L.D.; Dias, N.B.; Roberto, J.; Pinto, A.S.; Palma, M.S. Brown recluse spider venom: proteomic analysis and proposal of a putative mechanism of action. *Protein Pept. Lett.* **2009**, *16*, 933–943.
25. Machado, L.F.; Laugesen, S.; Botelho, E.D.; Ricart, C.A.; Fontes, W.; Barbaro, K.C.; Roepstorff, P.; Sousa, M.V. Proteome analysis of brown spider venom: identification of loxnecrogin isoforms in Loxosceles gaucho venom. *Proteomics* **2005**, *5*, 2167–2176.
26. Corzo, G.; Gilles, N.; Satake, H.; Villegas, E.; Dai, L.; Nakajima, T.; Haupt, J. Distinct primary structures of the major peptide toxins from the venom of the spider Macrothele gigas that bind to sites 3 and 4 in the sodium channel. *FEBS Lett.* **2003**, *547*, 43–50.
27. Gremski, L.H.; da Silveira, R.B.; Chaim, O.M.; Probst, C.M.; Ferrer, V.P.; Nowatzki, J.; Weinschutz, H.C.; Madeira, H.M.; Gremski, W.; Nader, H.B.; Senff-Ribeiro, A.; Veiga, S.S. A novel expression profile of the Loxosceles intermedia spider venomous gland revealed by transcriptome analysis. *Mol. Biosyst.* **2010**, *6*, 2403–2416.
28. Binford, G.J.; Cordes, M.H.; Wells, M.A. Sphingomyelinase D from venoms of Loxosceles spiders: evolutionary insights from cDNA sequences and gene structure. *Toxicon* **2005**, *45*, 547–560.
29. Trevisan-Silva, D.; Gremski, L.H.; Chaim, O.M.; da Silveira, R.B.; Meissner, G.O.; Mangili, O.C.; Barbaro, K.C.; Gremski, W.; Veiga, S.S.; Senff-Ribeiro, A. Astacin-like metalloproteases are a gene family of toxins present in the venom of different species of the brown spider (genus Loxosceles). *Biochimie* **2010**, *92*, 21–32.
30. Wood, D.L.; Miljenovic, T.; Cai, S.; Raven, R.J.; Kaas, Q.; Escoubas, P.; Herzig, V.; Wilson, D.; King, G.F., ArachnoServer: A database of protein toxins from spiders. *BMC Genomics* **2009**, *10*, 375.
31. King, G.F.; Gentz, M.C.; Escoubas, P.; Nicholson, G.M. A rational nomenclature for naming peptide toxins from spiders and other venomous animals. *Toxicon* **2008**, *52*, 264–276.
32. Kalapothakis, E.; Araujo, S.C.; de Castro, C.S.; Mendes, T.M.; Gomez, M.V.; Mangili, O.C.; Gubert, I.C.; Chavez-Olortegui, C. Molecular cloning, expression and immunological properties of LiD1, a protein from the dermonecrotic family of Loxosceles intermedia spider venom. *Toxicon* **2002**, *40*, 1691–1699.
33. Tambourgi, D.V.; Fernandes-Pedrosa, M.F.; van den Berg, C.W.; Goncalves-de-Andrade, R.M.; Ferracini, M.; Paixao-Cavalcante, D.; Morgan, B.P.; Rushmere, N.K. Molecular cloning, expression, function and immunoreactivities of members of a gene family of sphingomyelinases from Loxosceles venom glands. *Mol. Immunol.* **2004**, *41*, 831–840.

34. Appel, M.H.; da Silveira, R.B.; Chaim, O.M.; Paludo, K.S.; Silva, D.T.; Chaves, D.M.; da Silva, P.H.; Mangili, O.C.; Senff-Ribeiro, A.; Gremski, W.; Nader, H.B.; Veiga, S.S. Identification, cloning and functional characterization of a novel dermonecrotic toxin (phospholipase D) from brown spider (Loxosceles intermedia) venom. *Biochim. Biophys. Acta* **2008**, *1780*, 167–178.
35. Chaim, O.M.; Sade, Y.B.; da Silveira, R.B.; Toma, L.; Kalapothakis, E.; Chavez-Olortegui, C.; Mangili, O.C.; Gremski, W.; von Dietrich, C.P.; Nader, H.B.; Veiga, S.S. Brown spider dermonecrotic toxin directly induces nephrotoxicity. *Toxicol. Appl. Pharmacol.* **2006**, *211*, 64–77.
36. da Silveira, R.B.; Pigozzo, R.B.; Chaim, O.M.; Appel, M.H.; Dreyfuss, J.L.; Toma, L.; Mangili, O.C.; Gremski, W.; Dietrich, C.P.; Nader, H.B.; Veiga, S.S. Molecular cloning and functional characterization of two isoforms of dermonecrotic toxin from Loxosceles intermedia (brown spider) venom gland. *Biochimie* **2006**, *88*, 1241–1253.
37. da Silveira, R.B.; Pigozzo, R.B.; Chaim, O.M.; Appel, M.H.; Silva, D.T.; Dreyfuss, J.L.; Toma, L.; Dietrich, C.P.; Nader, H.B.; Veiga, S.S.; Gremski, W. Two novel dermonecrotic toxins LiRecDT4 and LiRecDT5 from brown spider (Loxosceles intermedia) venom: From cloning to functional characterization. *Biochimie* **2007**, *89*, 289–300.
38. Ribeiro, R.O.; Chaim, O.M.; da Silveira, R.B.; Gremski, L.H.; Sade, Y.B.; Paludo, K.S.; Senff-Ribeiro, A.; de Moura, J.; Chavez-Olortegui, C.; Gremski, W.; Nader, H.B.; Veiga, S.S. Biological and structural comparison of recombinant phospholipase D toxins from Loxosceles intermedia (brown spider) venom. *Toxicon* **2007**, *50*, 1162–1174.
39. Ramos-Cerrillo, B.; Olvera, A.; Odell, G.V.; Zamudio, F.; Paniagua-Solis, J.; Alagon, A.; Stock, R.P. Genetic and enzymatic characterization of sphingomyelinase D isoforms from the North American fiddleback spiders Loxosceles boneti and Loxosceles reclusa. *Toxicon* **2004**, *44*, 507–514.
40. Murakami, M.T.; Fernandes-Pedrosa, M.F.; de Andrade, S.A.; Gabdoulkhakov, A.; Betzel, C.; Tambourgi, D.V.; Arni, R.K. Structural insights into the catalytic mechanism of sphingomyelinases D and evolutionary relationship to glycerophosphodiester phosphodiesterases. *Biochem. Biophys. Res. Commun.* **2006**, *342*, 323–329.
41. Lee, S.; Lynch, K.R. Brown recluse spider (Loxosceles reclusa) venom phospholipase D (PLD) generates lysophosphatidic acid (LPA). *Biochem. J.* **2005**, *391*, 317–323.
42. Chaim, O.M.; da Silveira, R.B.; Trevisan-Silva, D.; Ferrer, V.P.; Sade, Y.B.; Bóia-Ferreira, M.; Gremski, L.H.; Gremski, W.; Senff-Ribeiro, A.; Takahashi, H.K.; Toledo, M.S.; Nader, H.B.; Veiga, S.S. Phospholipase-D activity and inflammatory response induced by brown spider dermonecrotic toxin: Endothelial cell membrane phospholipids as targets for toxicity. *BBA Mol. Cell Biol. Lipids* **2010**, *1811*, 84–96.
43. Fernandes Pedrosa, M.F.; Junqueira de Azevedo I. de, L.; Goncalves-de-Andrade, R.M.; van den Berg, C.W.; Ramos, C.R.; Ho, P.L.; Tambourgi, D.V. Molecular cloning and expression of a functional dermonecrotic and haemolytic factor from Loxosceles laeta venom. *Biochem. Biophys. Res. Commun.* **2002**, *298*, 638–645.
44. Tambourgi, D.V.; Magnoli, F.C.; Von Eickstedt, V.R.; Benedetti, Z.C.; Petricevich, V.L.; da Silva, W.D. Incorporation of a. 35-kilodalton purified protein from Loxosceles intermedia spider

venom transforms human erythrocytes into activators of autologous complement alternative pathway. *J. Immunol.* **1995**, *155*, 4459–4466.

45. Chaves-Moreira, D.; Chaim, O.M.; Sade, Y.B.; Paludo, K.S.; Gremski, L.H.; Donatti, L.; de Moura, J.; Mangili, O.C.; Gremski, W.; da Silveira, R.B.; Senff-Ribeiro, A.; Veiga, S.S. Identification of a direct hemolytic effect dependent on the catalytic activity induced by phospholipase-D (dermonecrotic toxin) from brown spider venom. *J. Cell. Biochem.* **2009**, *107*, 655–666.
46. Kusma, J.; Chaim, O.M.; Wille, A.C.; Ferrer, V.P.; Sade, Y.B.; Donatti, L.; Gremski, W.; Mangili, O.C.; Veiga, S.S. Nephrotoxicity caused by brown spider venom phospholipase-D (dermonecrotic toxin) depends on catalytic activity. *Biochimie* **2008**, *90*, 1722–1736.
47. Barbaro, K.C.; Sousa, M.V.; Morhy, L.; Eickstedt, V.R.; Mota, I. Compared chemical properties of dermonecrotic and lethal toxins from spiders of the genus Loxosceles (Araneae). *J. Protein Chem.* **1996**, *15*, 337–343.
48. van Meeteren, L.A.; Frederiks, F.; Giepmans, B.N.; Pedrosa, M.F.; Billington, S.J.; Jost, B.H.; Tambourgi, D.V.; Moolenaar, W.H. Spider and bacterial sphingomyelinases D target cellular lysophosphatidic acid receptors by hydrolyzing lysophosphatidylcholine. *J. Biol. Chem.* **2004**, *279*, 10833–10836.
49. Dragulev, B.; Bao, Y.; Ramos-Cerrillo, B.; Vazquez, H.; Olvera, A.; Stock, R.; Algaron, A.; Fox, J.W. Upregulation of IL-6, IL-8, CXCL1, and CXCL2 dominates gene expression in human fibroblast cells exposed to Loxosceles reclusa sphingomyelinase D: Insights into spider venom dermonecrosis. *J. Invest. Dermatol.* **2007**, *127*, 1264–1266.
50. Barrett, S.M.; Romine-Jenkins, M.; Blick, K.E. Passive hemagglutination inhibition test for diagnosis of brown recluse spider bite envenomation. *Clin. Chem.* **1993**, *39*, 2104–2107.
51. Fernandes-Pedrosa, F.; Junqueira-de-Azevedo, L.; Goncalves-de-Andrade, R.M.; Kobashi, L.S.; Almeida, D.D.; Ho, P.L.; Tambourgi, D.V. Transcriptome analysis of Loxosceles laeta (Araneae, Sicariidae) spider venomous gland using expressed sequence tags. *BMC Genomics* **2008**, *9*, 279.
52. da Silveira, R.B.; Wille, A.C.; Chaim, O.M.; Appel, M.H.; Silva, D.T.; Franco, C.R.; Toma, L.; Mangili, O.C.; Gremski, W.; Dietrich, C.P.; Nader, H.B.; Veiga, S.S. Identification, cloning, expression and functional characterization of an astacin-like metalloprotease toxin from Loxosceles intermedia (brown spider) venom. *Biochem. J.* **2007**, *406*, 355–363.
53. da Silveira, R.B.; dos Santos Filho, J.F.; Mangili, O.C.; Veiga, S.S.; Gremski, W.; Nader, H.B.; von Dietrich, C.P. Identification of proteases in the extract of venom glands from brown spiders. *Toxicon* **2002**, *40*, 815–822.
54. Stocker, W.; Grams, F.; Baumann, U.; Reinemer, P.; Gomis-Ruth, F.X.; McKay, D.B.; Bode, W. The metzincins--topological and sequential relations between the astacins, adamalysins, serralysins, and matrixins (collagenases) define a superfamily of zinc-peptidases. *Protein Sci.* **1995**, *4*, 823–840.
55. Wright, R.P.; Elgert, K.D.; Campbell, B.J.; Barrett, J.T. Hyaluronidase and esterase activities of the venom of the poisonous brown recluse spider. *Arch. Biochem. Biophys.* **1973**, *159*, 415–426.
56. Bommer, U.A.; Thiele, B.J. The translationally controlled tumour protein (TCTP). *Int. J. Biochem. Cell Biol.* **2004**, *36*, 379–385.

57. Marsh, N.; Williams, V. Practical applications of snake venom toxins in haemostasis. *Toxicon* **2005**, *45*, 1171–1181.
58. Koh, D.C.; Armugam, A.; Jeyaseelan, K. Snake venom components and their applications in biomedicine. *Cell Mol. Life Sci.* **2006**, *63*, 3030–3041.
59. Bailey, P.; Wilce, J. Venom as a source of useful biologically active molecules. *Emerg. Med. (Fremantle)* **2001**, *13*, 28–36.
60. Schmidtko, A.; Lotsch, J.; Freynhagen, R.; Geisslinger, G. Ziconotide for treatment of severe chronic pain. *Lancet* **2010**, *375*, 1569–1577.
61. Ramu, Y.; Xu, Y.; Lu, Z. Engineered specific and high-affinity inhibitor for a subtype of inward-rectifier K+ channels. *Proc. Natl. Acad. Sci. USA* **2008**, *105*, 10774–10778.
62. Gedulin, B.R.; Smith, P.; Prickett, K.S.; Tryon, M.; Barnhill, S.; Reynolds, J.; Nielsen, L.L.; Parkes, D.G.; Young, A.A. Dose-response for glycaemic and metabolic changes. 28 days after single injection of long-acting release exenatide in diabetic fatty Zucker rats. *Diabetologia* **2005**, *48*, 1380–1385.
63. Heine, R.J.; Van Gaal, L.F.; Johns, D.; Mihm, M.J.; Widel, M.H.; Brodows, R.G. Exenatide versus insulin glargine in patients with suboptimally controlled type. 2 diabetes: A randomized trial. *Ann. Intern. Med.* **2005**, *143*, 559–569.
64. Chuang, R.S.; Jaffe, H.; Cribbs, L.; Perez-Reyes, E.; Swartz, K.J. Inhibition of T-type voltage-gated calcium channels by a new scorpion toxin. *Nat. Neurosci.* **1998**, *1*, 668–674.
65. Bagdany, M.; Batista, C.V.; Valdez-Cruz, N.A.; Somodi, S.; Rodriguez de la Vega, R.C.; Licea, A.F.; Varga, Z.; Gaspar, R.; Possani, L.D.; Panyi, G. Anuroctoxin, a new scorpion toxin of the alpha-KTx. 6 subfamily, is highly selective for Kv1.3 over IKCa1 ion channels of human T lymphocytes. *Mol. Pharmacol.* **2005**, *67*, 1034–1044.
66. Gurevitz, M.; Karbat, I.; Cohen, L.; Ilan, N.; Kahn, R.; Turkov, M.; Stankiewicz, M.; Stuhmer, W.; Dong, K.; Gordon, D. The insecticidal potential of scorpion beta-toxins. *Toxicon* **2007**, *49*, 473–489.
67. Diochot, S.; Lazdunski, M. Sea anemone toxins affecting potassium channels. *Prog. Mol. Subcell. Biol.* **2009**, *46*, 99–122.
68. Mirshafiey, A. Venom therapy in multiple sclerosis. *Neuropharmacology* **2007**, *53*, 353–361.
69. Norton, R.S.; Pennington, M.W.; Wulff, H. Potassium channel blockade by the sea anemone toxin ShK for the treatment of multiple sclerosis and other autoimmune diseases. *Curr. Med. Chem.* **2004**, *11*, 3041–3052.
70. Fletcher, J.I.; Smith, R.; O'Donoghue, S.I.; Nilges, M.; Connor, M.; Howden, M.E.; Christie, M.J.; King, G.F. The structure of a novel insecticidal neurotoxin, omega-atracotoxin-HV1, from the venom of an Australian funnel web spider. *Nat. Struct. Biol.* **1997**, *4*, 559–566.
71. Villanova, F.E.; Andrade, E.; Leal, E.; Andrade, P.M.; Borra, R.C.; Troncone, L.R.; Magalhaes, L.; Leite, K.R.; Paranhos, M.; Claro, J.; Srougi, M. Erection induced by Tx2–6 toxin of Phoneutria nigriventer spider: expression profile of genes in the nitric oxide pathway of penile tissue of mice. *Toxicon* **2009**, *54*, 793–801.
72. Andrade, E.; Villanova, F.; Borra, P.; Leite, K.; Troncone, L.; Cortez, I.; Messina, L.; Paranhos, M.; Claro, J.; Srougi, M. Penile erection induced *in vivo* by a purified toxin from the Brazilian spider Phoneutria nigriventer. *BJU Int.* **2008**, *102*, 835–837.

73. Haeberli, S.; Kuhn-Nentwig, L.; Schaller, J.; Nentwig, W. Characterisation of antibacterial activity of peptides isolated from the venom of the spider Cupiennius salei (Araneae: Ctenidae). *Toxicon* **2000**, *38*, 373–380.
74. Senff-Ribeiro, A.; Henrique da Silva, P.; Chaim, O.M.; Gremski, L.H.; Paludo, K.S.; Bertoni da Silveira, R.; Gremski, W.; Mangili, O.C.; Veiga, S.S. Biotechnological applications of brown spider (Loxosceles genus) venom toxins. *Biotechnol. Adv.* **2008**, *26*, 210–218.
75. Veiga, S.S. Federal University of Paran á, Paran á, Brazil, Personal communication, 2011.
76. Binford, G.J.; Wells, M.A. The phylogenetic distribution of sphingomyelinase D activity in venoms of Haplogyne spiders. *Comp. Biochem. Physiol. B Biochem. Mol. Biol.* **2003**, *135*, 25–33.
77. Tambourgi, D.V.; Goncalves-de-Andrade, R.M.; van den Berg, C.W. Loxoscelism: From basic research to the proposal of new therapies. *Toxicon* **2010**, *56*, 1113–1119.
78. Barbaro, K.C.; Eickstedt, V.R.; Mota, I. Antigenic cross-reactivity of venoms from medically important Loxosceles (Araneae) species in Brazil. *Toxicon* **1994**, *32*, 113–120.
79. Mota, I.; Barbaro, K.C. Biological and biochemical properties of venoms from medically important Loxosceles (Araneae) species in Brazil. *Toxin Rev.* **1995**, *14*, 401–421.
80. Luciano, M.N.; da Silva, P.H.; Chaim, O.M.; dos Santos, V.L.; Franco, C.R.; Soares, M.F.; Zanata, S.M.; Mangili, O.C.; Gremski, W.; Veiga, S.S. Experimental evidence for a direct cytotoxicity of Loxosceles intermedia (brown spider) venom in renal tissue. *J. Histochem. Cytochem.* **2004**, *52*, 455–467.
81. Paixao-Cavalcante, D.; van den Berg, C.W.; de Freitas Fernandes-Pedrosa, M.; Goncalves de Andrade, R.M.; Tambourgi, D.V. Role of matrix metalloproteinases in HaCaT keratinocytes apoptosis induced by loxosceles venom sphingomyelinase D. *J. Invest. Dermatol.* **2006**, *126*, 61–68.
82. McGlasson, D.L.; Green, J.A.; Stoecker, W.V.; Babcock, J.L.; Calcara, D.A. Duration of Loxosceles reclusa venom detection by ELISA from swabs. *Clin. Lab. Sci.* **2009**, *22*, 216–222.
83. Vetter, R.S. Arachnids misidentified as brown recluse spiders by medical personnel and other authorities in North America. *Toxicon* **2009**, *54*, 545–547.
84. Reitz, M. Diagnosis of brown recluse spider bites is overused. *Am. Fam. Physician* **2007**, *76*, 943–944.
85. Pauli, I.; Minozzo, J.C.; da Silva, P.H.; Chaim, O.M.; Veiga, S.S. Analysis of therapeutic benefits of antivenin at different time intervals after experimental envenomation in rabbits by venom of the Brown spider (Loxosceles intermedia). *Toxicon* **2009**, *53*, 660–671.
86. Pauli, I.; Puka, J.; Gubert, I.C.; Minozzo, J.C. The efficacy of antivenom in loxoscelism treatment. *Toxicon* **2006**, *48*, 123–137.
87. Dias-Lopes, C.; Guimaraes, G.; Felicori, L.; Fernandes, P.; Emery, L.; Kalapothakis, E.; Nguyen, C.; Molina, F.; Granier, C.; Chavez-Olortegui, C. A protective immune response against lethal, dermonecrotic and hemorrhagic effects of Loxosceles intermedia venom elicited by a. 27-residue peptide. *Toxicon* **2010**, *55*, 481–487.
88. Felicori, L.; Fernandes, P.B.; Giusta, M.S.; Duarte, C.G.; Kalapothakis, E.; Nguyen, C.; Molina, F.; Granier, C.; Chavez-Olortegui, C. An *in. vivo* protective response against toxic effects of the

dermonecrotic protein from Loxosceles intermedia spider venom elicited by synthetic epitopes. *Vaccine* **2009**, *27*, 4201–4208.
89. Gomez, H.F.; Krywko, D.M.; Stoecker, W.V. A new assay for the detection of Loxosceles species (brown recluse) spider venom. *Ann. Emerg. Med.* **2002**, *39*, 469–474.
90. Krywko, D.M.; Gomez, H.F. Detection of Loxosceles species venom in dermal lesions: A comparison of 4 venom recovery methods. *Ann. Emerg. Med.* **2002**, *39*, 475–480.
91. McDermott, M.; Wakelam, M.J.; Morris, A.J. Phospholipase D. *Biochem. Cell. Biol.* **2004**, *82*, 225–253.
92. Gomez-Cambronero, J. New concepts in phospholipase D signaling in inflammation and cancer. *Sci. World J.* **2010**, *10*, 1356–1369.
93. Roth, M.G. Molecular mechanisms of PLD function in membrane traffic. *Traffic* **2008**, *9*, 1233–1239.
94. Huwiler, A.; Kolter, T.; Pfeilschifter, J.; Sandhoff, K. Physiology and pathophysiology of sphingolipid metabolism and signaling. *Biochim. Biophys. Acta* **2000**, *1485*, 63–99.
95. Mitsutake, S.; Igarashi, Y. Transbilayer movement of ceramide in the plasma membrane of live cells. *Biochem. Biophys. Res. Commun.* **2007**, *359*, 622–627.
96. Rodrigues, R.S.; Izidoro, L.F.; de Oliveira, R.J., Jr.; Sampaio, S.V.; Soares, A.M.; Rodrigues, V.M. Snake venom phospholipases A2: A new class of antitumor agents. *Protein Pept. Lett.* **2009**, *16*, 894–898.
97. Su, W.; Chen, Q.; Frohman, M.A. Targeting phospholipase D with small-molecule inhibitors as a potential therapeutic approach for cancer metastasis. *Future Oncol.* **2009**, *5*, 1477–1486.
98. Majd, S.; Yusko, E.C.; MacBriar, A.D.; Yang, J.; Mayer, M. Gramicidin pores report the activity of membrane-active enzymes. *J. Am. Chem. Soc.* **2009**, *131*, 16119–16126.
99. Ramu, Y.; Xu, Y.; Lu, Z. Enzymatic activation of voltage-gated potassium channels. *Nature* **2006**, *442*, 696–699.
100. Menzel, E.J.; Farr, C. Hyaluronidase and its substrate hyaluronan: Biochemistry, biological activities and therapeutic uses. *Cancer Lett.* **1998**, *131*, 3–11.
101. Cramer, J.A.; Bailey, L.C.; Bailey, C.A.; Miller, R.T. Kinetic and mechanistic studies with bovine testicular hyaluronidase. *Biochim. Biophys. Acta* **1994**, *1200*, 315–321.
102. Girish, K.S.; Kemparaju, K. The magic glue hyaluronan and its eraser hyaluronidase: A biological overview. *Life Sci.* **2007**, *80*, 1921–1943.
103. Kemparaju, K.; Girish, K.S. Snake venom hyaluronidase: a therapeutic target. *Cell Biochem. Funct.* **2006**, *24*, 7–12.
104. Magalhaes, M.R.; da Silva, N.J., Jr.; Ulhoa, C.J. A hyaluronidase from Potamotrygon motoro (freshwater stingrays) venom: Isolation and characterization. *Toxicon* **2008**, *51*, 1060–1067.
105. Girish, K.S.; Kemparaju, K. A low molecular weight isoform of hyaluronidase: purification from Indian cobra (Naja naja) venom and partial characterization. *Biochemistry (Mosc)* **2005**, *70*, 708–712.
106. Markovic-Housley, Z.; Miglierini, G.; Soldatova, L.; Rizkallah, P.J.; Muller, U.; Schirmer, T. Crystal structure of hyaluronidase, a major allergen of bee venom. *Structure* **2000**, *8*, 1025–1035.
107. Skov, L.K.; Seppala, U.; Coen, J.J.; Crickmore, N.; King, T.P.; Monsalve, R.; Kastrup, J.S.; Spangfort, M.D.; Gajhede, M. Structure of recombinant Ves v. 2 at 2.0 Angstrom resolution:

structural analysis of an allergenic hyaluronidase from wasp venom. *Acta Crystallogr. D Biol. Crystallogr.* **2006**, *62*, 595–604.

108. Tan, N.H.; Ponnudurai, G. Comparative study of the enzymatic, hemorrhagic, procoagulant and anticoagulant activities of some animal venoms. *Comp. Biochem. Physiol. C* **1992**, *103*, 299–302.
109. Kaiser, E. Trypsin and hyaluronidase inhibitor of human serum; the inhibition of the proteolytic and hyaluronic acid cleavage enzymes of snake and spider venoms by human serum. *Biochem. J.* **1953**, *324*, 344–350.
110. Nagaraju, S.; Devaraja, S.; Kemparaju, K. Purification and properties of hyaluronidase from Hippasa partita (funnel web spider) venom gland extract. *Toxicon* **2007**, *50*, 383–393.
111. Rash, L.D.; Hodgson, W.C. Pharmacology and biochemistry of spider venoms. *Toxicon* **2002**, *40*, 225–254.
112. Kuhn-Nentwig, L.; Schaller, J.; Nentwig, W. Biochemistry, toxicology and ecology of the venom of the spider Cupiennius salei (Ctenidae). *Toxicon* **2004**, *43*, 543–553.
113. Nagaraju, S.; Mahadeswaraswamy, Y.H.; Girish, K.S.; Kemparaju, K. Venom from spiders of the genus Hippasa: Biochemical and pharmacological studies. *Comp. Biochem. Physiol. C Toxicol. Pharmacol.* **2006**, *144*, 1–9.
114. Rocha-e-Silva, T.A.A.; Sutti, R.; Hyslop, S. Milking and partial characterization of venom from the Brazilian spider Vitalius dubius (Theraphosidae). *Toxicon* **2009**, *53*, 153–161.
115. Zobel-Thropp, P.A.; Bodner, M.R.; Binford, G.J. Comparative analyses of venoms from American and African Sicarius spiders that differ in sphingomyelinase D activity. *Toxicon* **2010**, *55*, 1274–1282.
116. Goolsby, T.V.; Lombardo, F.A. Extravasation of Chemotherapeutic Agents: Prevention and Treatment. *Semin. Oncol.* **2006**, *33*, 139–143.
117. Dunn, A.L.; Heavner, J.E.; Racz, G.; Day, M. Hyaluronidase: A review of approved formulations, indications and off-label use in chronic pain management. *Expert Opin. Biol. Ther.* **2010**, *10*, 127–131.
118. Muchmore, D.B.; Vaughn, D.E. Review of the mechanism of action and clinical efficacy of recombinant human hyaluronidase coadministration with current prandial insulin formulations. *J. Diabetes Sci. Technol.* **2010**, *4*, 419–428.
119. Etesse, B.; Beaudroit, L.; Deleuze, M.; Nouvellon, E.; Ripart, J. Hyaluronidase: Here we go again. *Ann. Fr. Anesth. Reanim.* **2009**, *28*, 658–665.
120. Misbah, S.; Sturzenegger, M.H.; Borte, M.; Shapiro, R.S.; Wasserman, R.L.; Berger, M.; Ochs, H.D. Subcutaneous immunoglobulin: opportunities and outlook. *Clin. Exp. Immunol.* **2009**, *158*, 51–59.
121. Lokeshwar, V.B.; Selzer, M.G. Hyalurondiase: Both a tumor promoter and suppressor. *Semin. Cancer Biol.* **2008**, *18*, 281–287.
122. Barla, F.; Higashijima, H.; Funai, S.; Sugimoto, K.; Harada, N.; Yamaji, R.; Fujita, T.; Nakano, Y.; Inui, H., Inhibitive effects of alkyl gallates on hyaluronidase and collagenase. *Biosci. Biotechnol. Biochem.* **2009**, *73*, 2335–2337.
123. Shuster, S.; Frost, G.I.; Csoka, A.B.; Formby, B.; Stern, R. Hyaluronidase reduces human breast cancer xenografts in SCID mice. *Int. J. Cancer* **2002**, *102*, 192–197.

124. Botzki, A.; Rigden, D.J.; Braun, S.; Nukui, M.; Salmen, S.; Hoechstetter, J.; Bernhardt, G.; Dove, S.; Jedrzejas, M.J.; Buschauer, A. L-Ascorbic acid. 6-hexadecanoate, a potent hyaluronidase inhibitor. X-ray structure and molecular modeling of enzyme-inhibitor complexes. *J. Biol. Chem.* **2004**, *279*, 45990–45997.
125. Calvete, J.J. Venomics: Digging into the evolution of venomous systems and learning to twist nature to fight pathology. *J. Proteomics* **2009**, *72*, 121–126.
126. Escoubas, P.; King, G.F. Venomics as a drug discovery platform. *Expert Rev. Proteomics* **2009**, *6*, 221–224.
127. Gross, B.; Gaestel, M.; Bohm, H.; Bielka, H. cDNA sequence coding for a translationally controlled human tumor. *Protein Nucleic Acids Res.* **1989**, *17*, 8367.
128. MacDonald, S.M.; Rafnar, T.; Langdon, J.; Lichtenstein, L.M. Molecular identification of an IgE-dependent histamine-releasing factor. *Science* **1995**, *269*, 688–690.
129. Choi, K.W.; Hsu, Y.C. To cease or to proliferate: New insights into TCTP function from a Drosophila study. *Cell Adh. Migr.* **2007**, *1*, 129–130.
130. Sun, J.; Wu, Y.; Wang, J.; Ma, F.; Liu, X.; Li, Q. Novel translationally controlled tumor protein homologue in the buccal gland secretion of Lampetra japonica. *Biochimie* **2008**, *90*, 1760–1768.
131. Gachet, Y.; Tournier, S.; Lee, M.; Lazaris-Karatzas, A.; Poulton, T.; Bommer, U.A. The growth-related, translationally controlled protein P23 has properties of a tubulin binding protein and associates transiently with microtubules during the cell cycle. *J. Cell. Sci.* **1999**, *112*, 1257–1271.
132. Bazile, F.; Pascal, A.; Arnal, I.; Le Clainche, C.; Chesnel, F.; Kubiak, J.Z. Complex relationship between TCTP, microtubules and actin microfilaments regulates cell shape in normal and cancer cells. *Carcinogenesis* **2009**, *30*, 555–565.
133. Yarm, F.R. Plk phosphorylation regulates the microtubule-stabilizing protein TCTP. *Mol. Cell. Biol.* **2002**, *22*, 6209–6221.
134. Cans, C.; Passer, B.J.; Shalak, V.; Nancy-Portebois, V.; Crible, V.; Amzallag, N.; Allanic, D.; Tufino, R.; Argentini, M.; Moras, D.; Fiucci, G.; Goud, B.; Mirande, M.; Amson, R.; Telerman, A. Translationally controlled tumor protein acts as a guanine nucleotide dissociation inhibitor on the translation elongation factor eEF1A. *Pro. Natl. Acad. Sci. USA* **2003**, *100*, 13892–13897.
135. Liu, H.; Peng, H.W.; Cheng, Y.S.; Yuan, H.S.; Yang-Yen, H.F. Stabilization and enhancement of the antiapoptotic activity of mcl-1 by TCTP. *Mol. Cell. Biol.* **2005**, *25*, 3117–3126.
136. Li, F.; Zhang, D.; Fujise, K. Characterization of fortilin, a novel antiapoptotic. *Protein J. Biol. Chem.* **2001**, *276*, 47542–47549.
137. Amzallag, N.; Passer, B.J.; Allanic, D.; Segura, E.; Thery, C.; Goud, B.; Amson, R.; Telerman, A. TSAP6 facilitates the secretion of translationally controlled tumor protein-histamine-releasing factor via a nonclassical pathway. *J. Biol. Chem.* **2004**, *279*, 46104–46112.
138. Jung, J.; Kim, M.; Kim, M.J.; Kim, J.; Moon, J.; Lim, J.S.; Kim, M.; Lee, K. Translationally controlled tumor protein interacts with the third cytoplasmic domain of Na,K-ATPase alpha subunit and inhibits the pump activity in HeLa cells. *J. Biol. Chem.* **2004**, *279*, 49868–49875.
139. Yang, Y.; Yang, F.; Xiong, Z.; Yan, Y.; Wang, X.; Nishino, M.; Mirkovic, D.; Nguyen, J.; Wang, H.; Yang, X.F. An N-terminal region of translationally controlled tumor protein is required for its antiapoptotic activity. *Oncogene* **2005**, *24*, 4778–4788.

140. Burgess, A.; Labbe, J.C.; Vigneron, S.; Bonneaud, N.; Strub, J.M.; Van Dorsselaer, A.; Lorca, T.; Castro, A. Chfr interacts and colocalizes with TCTP to the mitotic spindle. *Oncogene* **2008**, *27*, 5554–5566.
141. Chen, S.H.; Wu, P.S.; Chou, C.H.; Yan, Y.T.; Liu, H.; Weng, S.Y.; Yang-Yen, H.F. A knockout mouse approach reveals that TCTP functions as an essential factor for cell proliferation and survival in a tissue- or cell type-specific manner. *Mol. Biol. Cell* **2007**, *18*, 2525–2532.
142. Hsu, Y.; Chern, J.J.; Cai, Y.; Liu, M.; Choi, K.W. Drosophila TCTP is essential for growth and proliferation through regulation of dRheb GTPase. *Nature* **2007**, *445*, 785–788.
143. Bheekha-Escura, R.; MacGlashan Jr, D.W.; Langdon, J.M.; MacDonald, S.M. Human recombinant histamine-releasing factor activates human eosinophils and the eosinophilic cell line, AML14–3D10. *Blood* **2000**, *96*, 2191.
144. Kang, H.S.; Lee, M.J.; Song, H.; Han, S.H.; Kim, Y. M.; Im, J.Y.; Choi, I. Molecular Identification of IgE-Dependent Histamine-Releasing Factor as a B Cell Growth Factor. 1. *J. Immunol.* **2001**, *166*, 6545–6554.
145. Hinojosa-Moya, J.; Xoconostle-Cazares, B.; Piedra-Ibarra, E.; Mendez-Tenorio, A.; Lucas, W.J.; Ruiz-Medrano, R. Phylogenetic and structural analysis of translationally controlled tumor proteins. *J. Mol. Evol.* **2008**, *66*, 472–483.
146. Mulenga, A.; Azad, A.F. The molecular and biological analysis of ixodid ticks histamine release factors. *Exp. Appl. Acarology* **2005**, *37*, 215–229.
147. Rattmann, Y.D.; Pereira, C.R.; Cury, Y.; Gremski, W.; Marques, M.C.A.; da Silva-Santos, J.E. Vascular permeability and vasodilation induced by the Loxosceles intermedia venom in rats: Involvement of mast cell degranulation, histamine and. 5-HT receptors. *Toxicon* **2008**, *51*, 363–372.
148. Rash, L.D.; King, R.G.; Hodgson, W.C. Evidence that histamine is the principal pharmacological component of venom from an Australian wolf spider (Lycosa godeffroyi). *Toxicon* **1998**, *36*, 367–375.
149. Paludo, K.S.; Biscaia, S.M.; Chaim, O.M.; Otuki, M.F.; Naliwaiko, K.; Dombrowski, P.A.; Franco, C.R.; Veiga, S.S. Inflammatory events induced by brown spider venom and its recombinant dermonecrotic toxin: A pharmacological investigation. *Comp. Biochem. Physiol. C Toxicol. Pharmacol.* **2009**, *149*, 323–333.
150. Weisel-Eichler, A.; Libersat, F. Venom effects on monoaminergic systems. *J. Comp. Physiol. A Neuroethology Sens. Neural Behav. Physiol.* **2004**, *190*, 683–690.
151. Rattmann, Y.D.; Pereira, C.R.; Cury, Y.; Gremski, W.; Marques, M.C.; da Silva-Santos, J.E. Vascular permeability and vasodilation induced by the Loxosceles intermedia venom in rats: involvement of mast cell degranulation, histamine and. 5-HT receptors. *Toxicon* **2008**, *51*, 363–372.
152. Gnanasekar, M.; Rao, K.V.; Chen, L.; Narayanan, R.B.; Geetha, M.; Scott, A.L.; Ramaswamy, K.; Kaliraj, P. Molecular characterization of a calcium binding translationally controlled tumor protein homologue from the filarial parasites Brugia malayi and Wuchereria bancrofti. *Mol. Biochem. Parasitol.* **2002**, *121*, 107–118.
153. MacDonald, S.M.; Bhisutthibhan, J.; Shapiro, T.A.; Rogerson, S.J.; Taylor, T.E.; Tembo, M.; Langdon, J.M.; Meshnick, S.R. Immune mimicry in malaria: Plasmodium falciparum secretes a

functional histamine-releasing factor homolog in vitro and in vivo. *Proc. Natl. Acad. Sci. USA* **2001**, *98*, 10829–10832.

154. Rao, K.V.; Chen, L.; Gnanasekar, M.; Ramaswamy, K. Cloning and characterization of a calcium-binding, histamine-releasing protein from Schistosoma mansoni. *J. Biol. Chem.* **2002**, *277*, 31207–31213.
155. Efferth, T. Antiplasmodial and antitumor activity of artemisinin—From bench to bedside. *Planta Med.* **2007**, *73*, 299.
156. Susini, L.; Besse, S.; Duflaut, D.; Lespagnol, A.; Beekman, C.; Fiucci, G.; Atkinson, A.R.; Busso, D.; Poussin, P.; Marine, J.C.; Martinou, J.C.; Cavarelli, J.; Moras, D.; Amson, R.; Telerman, A. TCTP protects from apoptotic cell death by antagonizing bax function. *Cell Death Differ.* **2008**, *15*, 1211–1220.
157. Gnanasekar, M.; Thirugnanam, S.; Zheng, G.; Chen, A.; Ramaswamy, K. Gene silencing of translationally controlled tumor protein (TCTP) by siRNA inhibits cell growth and induces apoptosis of human prostate cancer cells. *Int. J. Oncol.* **2009**, *34*, 1241–1246.
158. Telerman, A.; Amson, R. The molecular programme of tumour reversion: the steps beyond malignant transformation. *Nat. Rev. Cancer* **2009**, *9*, 206–216.
159. Tuynder, M.; Fiucci, G.; Prieur, S.; Lespagnol, A.; Geant, A.; Beaucourt, S.; Duflaut, D.; Besse, S.; Susini, L.; Cavarelli, J.; Moras, D.; Amson, R.; Telerman, A. Translationally controlled tumor protein is a target of tumor reversion. *Proc. Natl. Acad. Sci. USA* **2004**, *101*, 15364–15369.
160. Slaby, O.; Sobkova, K.; Svoboda, M.; Garajova, I.; Fabian, P.; Hrstka, R.; Nenutil, R.; Sachlova, M.; Kocakova, I.; Michalek, J.; Smerdova, T.; Knoflickova, D.; Vyzula, R. Significant overexpression of Hsp110 gene during colorectal cancer progression. *Oncol. Rep.* **2009**, *21*, 1235–1241.
161. Ma, Q.; Geng, Y.; Xu, W.; Wu, Y.; He, F.; Shu, W.; Huang, M.; Du, H.; Li, M. The Role of Translationally Controlled Tumor Protein in Tumor Growth and Metastasis of Colon Adenocarcinoma Cells. *J. Proteome. Res.* **2009**, *9*, 40–49.
162. Tuynder, M.; Susini, L.; Prieur, S.; Besse, S.; Fiucci, G.; Amson, R.; Telerman, A. Biological models and genes of tumor reversion: Cellular reprogramming through tpt1/TCTP and SIAH-1. *Proc. Natl. Acad. Sci. USA* **2002**, *99*, 14976–14981.
163. Efferth, T. Mechanistic perspectives for. 1,2,4-trioxanes in anti-cancer therapy. *Drug Resist. Updat.* **2005**, *8*, 85–97.
164. Kim, J.E.; Koo, K.H.; Kim, Y.H.; Sohn, J.; Park, Y.G. Identification of potential lung cancer biomarkers using an in vitro carcinogenesis model. *Exp. Mol. Med.* **2008**, *40*, 709–720.
165. van de Sande, W.W.; Janse, D.J.; Hira, V.; Goedhart, H.; van der Zee, R.; Ahmed, A.O.; Ott, A.; Verbrugh, H.; van Belkum, A. Translationally controlled tumor protein from Madurella mycetomatis, a marker for tumorous mycetoma progression. *J. Immunol.* **2006**, *177*, 1997–2005.
166. Zhu, W.L.; Cheng, H.X.; Han, N.; Liu, D.L.; Zhu, W.X.; Fan, B.L.; Duan, F.L. Messenger RNA expression of translationally controlled tumor protein (TCTP) in liver regeneration and cancer. *Anticancer Res.* **2008**, *28*, 1575–1580.
167. Rinnerthaler, M.; Jarolim, S.; Heeren, G.; Palle, E.; Perju, S.; Klinger, H.; Bogengruber, E.; Madeo, F.; Braun, R.J.; Breitenbach-Koller, L.; Breitenbach, M.; Laun, P. MMI1 (YKL056c, TMA19), the yeast orthologue of the translationally controlled tumor protein (TCTP) has

apoptotic functions and interacts with both microtubules and mitochondria. *Biochim. Biophys. Acta* **2006**, *1757*, 631–638.

168. Zanetti, V.C.; da Silveira, R.B.; Dreyfuss, J.L.; Haoach, J.; Mangili, O.C.; Veiga, S.S.; Gremski, W. Morphological and biochemical evidence of blood vessel damage and fibrinogenolysis triggered by brown spider venom. *Blood Coagul. Fibrinolysis* **2002**, *13*, 135–148.
169. Gomis-Rüth, F. Structural aspects of the metzincin clan of metalloendopeptidases. *Mol. Biotechnol.* **2003**, *24*, 157–202.
170. Sterchi, E.E. Special issue: Metzincin metalloproteinases. *Mol. Aspects Med.* **2008**, *29*, 255–257.
171. Becker-Pauly, C.; Bruns, B.C.; Damm, O.; Schutte, A.; Hammouti, K.; Burmester, T.; Stocker, W. News from an ancient world: two novel astacin metalloproteases from the horseshoe crab. *J. Mol. Biol.* **2009**, *385*, 236–248.
172. Sarras, M.P., Jr., BMP-1 and the astacin family of metalloproteinases: A potential link between the extracellular matrix, growth factors and pattern formation. *Bioessays* **1996**, *18*, 439–442.
173. Mohrlen, F.; Hutter, H.; Zwilling, R. The astacin protein family in Caenorhabditis elegans. *Eur. J. Biochem.* **2003**, *270*, 4909–4920.
174. Bode, W.; Gomis-Ruth, F.X.; Stockler, W. Astacins, serralysins, snake venom and matrix metalloproteinases exhibit identical zinc-binding environments (HEXXHXXGXXH and Met-turn) and topologies and should be grouped into a common family, the 'metzincins'. *FEBS Lett.* **1993**, *331*, 134–140.
175. Bond, J.S.; Beynon, R.J. The astacin family of metalloendopeptidases. *Protein Sci.* **1995**, *4*, 1247–1261.
176. Stocker, W.; Zwilling, R. Astacin. *Methods Enzymol.* **1995**, *248*, 305–325.
177. Stocker, W.; Bode, W. Structural features of a superfamily of zinc-endopeptidases: The metzincins. *Curr. Opin. Struct. Biol.* **1995**, *5*, 383–390.
178. Dumermuth, E.; Sterchi, E.E.; Jiang, W.P.; Wolz, R.L.; Bond, J.S.; Flannery, A.V.; Beynon, R.J. The astacin family of metalloendopeptidases. *J. Biol. Chem.* **1991**, *266*, 21381–21385.
179. Sharma, V.K.; Teoh, H.L.; Wong, L.Y.; Su, J.; Ong, B.K.; Chan, B.P. Recanalization therapies in acute ischemic stroke: pharmacological agents, devices, and combinations. *Stroke Res. Treat.* **2010**, in press.
180. Gao, F.; Kiesewetter, D.; Chang, L.; Ma, K.; Rapoport, S.I.; Igarashi, M. Whole-body synthesis secretion of docosahexaenoic acid from circulating eicosapentaenoic acid in unanesthetized rats. *J. Lipid Res.* **2009**, *50*, 2463–2470.
181. Rash, L.D.; Hodgson, W.C. Pharmacology and biochemistry of spider venoms. *Toxicon* **2002**, *40*, 225–254.
182. Nicholson, G.M. Insect-selective spider toxins targeting voltage-gated sodium channels. *Toxicon* **2007**, *49*, 490–512.
183. De Lima, M.E.; Figueiredo, S.G.; Pimenta, A.M.; Santos, D.M.; Borges, M.H.; Cordeiro, M.N.; Richardson, M.; Oliveira, L.C.; Stankiewicz, M.; Pelhate, M. Peptides of arachnid venoms with insecticidal activity targeting sodium channels. *Comp. Biochem. Physiol. C Toxicol. Pharmacol.* **2007**, *146*, 264–279.
184. Sollod, B.L.; Wilson, D.; Zhaxybayeva, O.; Gogarten, J.P.; Drinkwater, R.; King, G.F. Were arachnids the first to use combinatorial peptide libraries? *Peptides* **2005**, *26*, 131–139.

185. Grishin, E. Polypeptide neurotoxins from spider venoms. *Eur. J. Biochem.* **1999**, *264*, 276–280.
186. Escoubas, P.; Diochot, S.; Corzo, G. Structure and pharmacology of spider venom neurotoxins. *Biochimie* **2000**, *82*, 893–907.
187. Dutra, A.A.; Sousa, L.O.; Resende, R.R.; Brandao, R.L.; Kalapothakis, E.; Castro, I.M. Expression and characterization of LTx2, a neurotoxin from Lasiodora sp. effecting on calcium channels. *Peptides* **2008**, *29*, 1505–1513.
188. Norton, R.S.; Pallaghy, P.K. The cystine knot structure of ion channel toxins and related polypeptides. *Toxicon* **1998**, *36*, 1573–1583.
189. Schalle, J.; Kampfer, U.; Schurch, S.; Kuhn-Nentwig, L.; Haeberli, S.; Nentwig, W. CSTX-9, a toxic peptide from the spider Cupiennius salei: amino acid sequence, disulphide bridge pattern and comparison with other spider toxins containing the cystine knot structure. *Cell Mol. Life Sci.* **2001**, *58*, 1538–1545.
190. Mouhat, S.; Jouirou, B.; Mosbah, A.; De Waard, M.; Sabatier, J.M. Diversity of folds in animal toxins acting on ion channels. *Biochem. J.* **2004**, *378*, 717–726.
191. Corzo, G.; Escoubas, P. Pharmacologically active spider peptide toxins. *Cell Mol. Life Sci.* **2003**, *60*, 2409–2426.
192. Corzo, G.; Escoubas, P.; Stankiewicz, M.; Pelhate, M.; Kristensen, C.P.; Nakajima, T. Isolation, synthesis and pharmacological characterization of δ-palutoxins IT, novel insecticidal toxins from the spider Paracoelotes luctuosus (Amaurobiidae). *Eur. J. Biochem.* **2000**, *267*, 5783–5795.
193. Tedford, H.W.; Sollod, B.L.; Maggio, F.; King, G.F. Australian funnel-web spiders: master insecticide chemists. *Toxicon* **2004**, *43*, 601–618.
194. Black, B.C.; Brennam, L.A.; Dierks, P.M.; Gard, I.E. Commercialization of baculoviral insecticides. In The Baculoviruses (Miller, Lois). In *The Viruses*; Plenum Press: New York, NY, USA, 1997; pp. 341–347.
195. Neurath, H. Proteolytic processing and physiological regulation. *Trends Biochem. Sci.* **1989**, *14*, 268–271.
196. Otlewski, J.; Krowarsch, D.; Apostoluk, W. Protein inhibitors of serine proteinases. *Acta Biochim. Pol.* **1999**, *46*, 531–565.
197. Rimphanitchayakit, V.; Tassanakajon, A. Structure and function of invertebrate Kazal-type serine proteinase inhibitors. *Dev. Comp. Immunol.* **2010**, *34*, 377–386.
198. Laskowski, M., Jr.; Kato, I. Protein inhibitors of proteinases. *Annu. Rev. Biochem.* **1980**, *49*, 593–626.
199. Krowarsch, D.; Cierpicki, T.; Jelen, F.; Otlewski, J. Canonical protein inhibitors of serine proteases. *Cell Mol. Life Sci.* **2003**, *60*, 2427–2444.
200. Irving, J.A.; Pike, R.N.; Lesk, A.M.; Whisstock, J.C. Phylogeny of the serpin superfamily: implications of patterns of amino acid conservation for structure and function. *Genome Res.* **2000**, *10*, 1845–1864.
201. Law, R.H.; Zhang, Q.; McGowan, S.; Buckle, A.M.; Silverman, G.A.; Wong, W.; Rosado, C.J.; Langendorf, C.G.; Pike, R.N.; Bird, P.I.; Whisstock, J.C. An overview of the serpin superfamily. *Genome Biol.* **2006**, *7*, 216.
202. Takahashi, H.; Iwanaga, S.; Suzuki, T. Distribution of proteinase inhibitors in snake venoms. *Toxicon* **1974**, *12*, 193–197.

203. Shafqat, J.; Beg, O.U.; Yin, S.J.; Zaidi, Z.H.; Jornvall, H. Primary structure and functional properties of cobra (Naja naja naja) venom Kunitz-type trypsin inhibitor. *Eur. J. Biochem.* **1990**, *194*, 337–341.
204. Shafqat, J.; Zaidi, Z.H.; Jornvall, H. Purification and characterization of a chymotrypsin Kunitz inhibitor type of polypeptide from the venom of cobra (Naja naja naja). *FEBS Lett.* **1990**, *275*, 6–8.
205. Chang, L.; Chung, C.; Huang, H.B.; Lin, S. Purification and characterization of a chymotrypsin inhibitor from the venom of Ophiophagus hannah (King Cobra). *Biochem. Biophys. Res. Commun.* **2001**, *283*, 862–867.
206. Chen, C.; Hsu, C.H.; Su, N.Y.; Lin, Y.C.; Chiou, S.H.; Wu, S.H. Solution structure of a Kunitz-type chymotrypsin inhibitor isolated from the elapid snake Bungarus fasciatus. *J. Biol. Chem.* **2001**, *276*, 45079–45087.
207. Lu, X.Z.; Zou, Y.G.; Yin, X.M.; Chen, W.T.; Zhang, C.P. Expression of MMP1 mRNA in oral squamous cell carcinoma and paired normal tissues. *Nan Fang Yi Ke Da Xue Xue Bao* **2008**, *28*, 1362–1364.
208. Zhou, X.D.; Jin, Y.; Lu, Q.M.; Li, D.S.; Zhu, S.W.; Wang, W.Y.; Xiong, Y.L. Purification, characterization and primary structure of a chymotrypsin inhibitor from Naja atra venom. *Comp. Biochem. Physiol. B. Biochem. Mol. Biol.* **2004**, *137*, 219–224.
209. He, D.; Natarajan, V.; Stern, R.; Gorshkova, I.A.; Solway, J.; Spannhake, E.W.; Zhao, Y. Lysophosphatidic acid-induced transactivation of epidermal growth factor receptor regulates cyclo-oxygenase-2 expression and prostaglandin E(2) release via C/EBPbeta in human bronchial epithelial cells. *Biochem. J.* **2008**, *412*, 153–162.
210. Millers, E.K.; Trabi, M.; Masci, P.P.; Lavin, M.F.; de Jersey, J.; Guddat, L.W., Crystal structure of textilinin-1, a Kunitz-type serine protease inhibitor from the venom of the Australian common brown snake (Pseudonaja textilis). *FEBS J.* **2009**, *276*, 3163–3175.
211. Flight, S.M.; Johnson, L.A.; Trabi, M.; Gaffney, P.; Lavin, M.; de Jersey, J.; Masci, P. Comparison of textilinin-1 with aprotinin as serine protease inhibitors and as antifibrinolytic agents. *Pathophysiol. Haemost. Thromb.* **2005**, *34*, 188–193.
212. Flight, S.M.; Johnson, L.A.; Du, Q.S.; Warner, R.L.; Trabi, M.; Gaffney, P.J.; Lavin, M.F.; de Jersey, J.; Masci, P.P. Textilinin-1, an alternative anti-bleeding agent to aprotinin: Importance of plasmin inhibition in controlling blood loss. *Br. J. Haematol.* **2009**, *145*, 207–211.
213. Zhao, Y.; Jin, Y.; Wei, S.S.; Lee, W.H.; Zhang, Y. Purification and characterization of an irreversible serine protease inhibitor from skin secretions of Bufo andrewsi. *Toxicon* **2005**, *46*, 635–640.
214. Yuan, C.H.; He, Q.Y.; Peng, K.; Diao, J.B.; Jiang, L.P.; Tang, X.; Liang, S.P. Discovery of a distinct superfamily of Kunitz-type toxin (KTT) from tarantulas. *PLoS One* **2008**, *3*, e3414.
215. Duarte, M.M.; Montes De Oca, H.; Diniz, C.R.; Fortes-Dias, C.L. Primary culture of venom gland cells from the South American rattlesnake (Crotalus durissus terrificus). *Toxicon* **1999**, *37*, 1673–1682.
216. Yamanouye, N.; Kerchove, C.M.; Moura-da-Silva, A.M.; Carneiro, S.M.; Markus, R.P. Long-term primary culture of secretory cells of Bothrops jararaca venom gland for venom production in vitro. *Nat. Protocols* **2007**, *1*, 2763–2766.

217. Silva, L.M.; Lages, C.P.; Venuto, T.; Lima, R.M.; Diniz, M.V.; Valentim, C.L.L.; Baba, E.H.; Pimenta, P.F.P.; Fortes-Dias, C.L. Primary culture of venom glands from the Brazilian armed spider, Phoneutria nigriventer (Araneae, Ctenidae). *Toxicon* **2008**, *51*, 428–434.
218. Domingos, M.O.; Barbaro, K.C.; Tynan, W.; Penny, J.; Lewis, D.J.; New, R.R. Influence of sphingomyelin and TNF-alpha release on lethality and local inflammatory reaction induced by Loxosceles gaucho spider venom in mice. *Toxicon* **2003**, *42*, 471–479.
219. Barbaro, K.C.; Lira, M.S.; Araujo, C.A.; Pareja-Santos, A.; Tavora, B.C.; Prezotto-Neto, J.P.; Kimura, L.F.; Lima, C.; Lopes-Ferreira, M.; Santoro, M.L. Inflammatory mediators generated at the site of inoculation of Loxosceles gaucho spider venom. *Toxicon* **2010**, *56*, 972–979.
220. Burgess, R.R.; Richard, R.B.; Murray, P.D. Refolding Solubilized Inclusion Body Proteins. In *Methods in Enzymology*; Academic Press: Salt Lake City, UT, USA, 2009; Volume 463, Chapter. 17, pp. 259–282.
221. Daly, R.; Hearn, M.T. Expression of heterologous proteins in Pichia pastoris: a useful experimental tool in protein engineering and production. *J. Mol. Recognit.* **2005**, *18*, 119–138.
222. Benting, J.; Lecat, S.; Zacchetti, D.; Simons, K. Protein Expression in Drosophila Schneider Cells. *Anal. Biochem.* **2000**, *278*, 59–68.
223. Rohrmann, G.F. *Baculovirus Molecular Biology*; European Molecular Biology Organization: Corvallis, OR, USA, 2008.
224. Wurm, F.M. Production of recombinant protein therapeutics in cultivated mammalian cells. *Nat. Biotech.* **2004**, *22*, 1393–1398.
225. Escoubas, P.; Sollod, B.; King, G.F. Venom landscapes: Mining the complexity of spider venoms via a combined cDNA and mass spectrometric approach. *Toxicon* **2006**, *47*, 650–663.
226. Murakami, M.T.; Fernandes-Pedrosa, M.F.; Tambourgi, D. V.; Arni, R.K. Structural basis for metal ion coordination and the catalytic mechanism of sphingomyelinases D. *J. Biol. Chem.* **2005**, *280*, 13658–13664.

OPEN ACCESS Freely available online

PLOS | NEGLECTED TROPICAL DISEASES

A Novel Hyaluronidase from Brown Spider (*Loxosceles intermedia*) Venom (Dietrich's Hyaluronidase): From Cloning to Functional Characterization

Valéria Pereira Ferrer[1], Thiago Lopes de Mari[1], Luiza Helena Gremski[1,2], Dilza Trevisan Silva[1], Rafael Bertoni da Silveira[1,3], Waldemiro Gremski[4], Olga Meiri Chaim[1], Andrea Senff-Ribeiro[1], Helena Bonciani Nader[5], Silvio Sanches Veiga[1]*

1 Department of Cell Biology, Federal University of Parana, Curitiba, Parana, Brazil, **2** Department of Clinical Pathology, Clinical Hospital, Federal University of Parana, Curitiba, Parana, Brazil, **3** Department of Structural, Molecular Biology and Genetics, State University of Ponta Grossa, Ponta Grossa, Brazil, **4** Catholic University of Parana, Health and Biological Sciences Institute, Curitiba, Parana, Brazil, **5** Department of Biochemistry, Federal University of São Paulo, São Paulo, Brazil

Abstract

Loxoscelism is the designation given to clinical symptoms evoked by *Loxosceles* spider's bites. Clinical manifestations include skin necrosis with gravitational spreading and systemic disturbs. The venom contains several enzymatic toxins. Herein, we describe the cloning, expression, refolding and biological evaluation of a novel brown spider protein characterized as a hyaluronidase. Employing a venom gland cDNA library, we cloned a hyaluronidase (1200 bp cDNA) that encodes for a signal peptide and a mature protein. Amino acid alignment revealed a structural relationship with members of hyaluronidase family, such as scorpion and snake species. Recombinant hyaluronidase was expressed as N-terminal His-tag fusion protein (~45 kDa) in inclusion bodies and activity was achieved using refolding. Immunoblot analysis showed that antibodies that recognize the recombinant protein cross-reacted with hyaluronidase from whole venom as well as an anti-venom serum reacted with recombinant protein. Recombinant hyaluronidase was able to degrade purified hyaluronic acid (HA) and chondroitin sulfate (CS), while dermatan sulfate (DS) and heparan sulfate (HS) were not affected. Zymograph experiments resulted in ~45 kDa lytic zones in hyaluronic acid (HA) and chondroitin sulfate (CS) substrates. Through *in vivo* experiments of dermonecrosis using rabbit skin, the recombinant hyaluronidase was shown to increase the dermonecrotic effect produced by recombinant dermonecrotic toxin from *L. intermedia* venom (LiRecDT1). These data support the hypothesis that hyaluronidase is a ''spreading factor''. Recombinant hyaluronidase provides a useful tool for biotechnological ends. We propose the name Dietrich's Hyaluronidase for this enzyme, in honor of Professor Carl Peter von Dietrich, who dedicated his life to studying proteoglycans and glycosaminoglycans.

Citation: Ferrer VP, de Mari TL, Gremski LH, Trevisan Silva D, da Silveira RB, et al. (2013) A Novel Hyaluronidase from Brown Spider (*Loxosceles intermedia*) Venom (Dietrich's Hyaluronidase): From Cloning to Functional Characterization. PLoS Negl Trop Dis 7(5): e2206. doi:10.1371/journal.pntd.0002206

Editor: Evanguedes Kalapothakis, Federal University of Minas Gerais, Brazil

Received October 16, 2012; **Accepted** March 25, 2013; **Published** May 2, 2013

Funding: This work was supported by grants from Conselho Nacional de Desenvolvimento Científico e Tecnológico (CNPq; www.cnpq.br), Coordenação de Aperfeiçoamento de Pessoal de Nível Superior (CAPES; http://www.capes.gov.br/), Fundação Araucária-PR (FAP; http://www.fundacaoaraucaria.org.br/), Secretaria de Estado de Ciência, Tecnologia e Ensino Superior do Paraná (SETI; http://www.seti.pr.gov.br/), and Fundação de Apoio à Pesquisa do Estado de São Paulo (FAPESP;www.fapesp.br/), Brazil. The funders had no role in study design, data collection and analysis, decision to publish, or preparation of the manuscript.

Competing Interests: The authors have declared that no competing interests exist.

* E-mail: veigass@ufpr.br

Introduction

Bites involving brown spiders are characterized by skin injuries at the venom inoculation site, including swelling, erythema, hemorrhage, dermonecrosis, and the hallmark of loxoscelism: gravitational spreading of cutaneous lesions [1,2]. Systemic involvement has also been reported including fever, malaise, weakness, nausea, vomiting and in severe cases, intravascular coagulation, hemolysis and acute renal disturbance [1,2,3,4,5].

The gravitational spread of skin lesions is a distinct characteristic of loxoscelism, described after experimental venom exposure in the skin of rabbits and in real cases. It appears hours or days after venom inoculation. Macroscopically, the development of lesions disperses in a gravitational direction with erythema, swelling, dark blue-violet color, and an eschar. Histologically, the lesion is reported as a collection of inflammatory cells in and around the blood vessels and diffusely distributed in the dermis. It is also possible to observe degeneration of blood vessel walls, disorganization of collagen fibers with edema, hemorrhage into the dermis, necrosis of cells, and destruction of tissue structures. Pathologically, the wound is described as aseptic coagulative necrosis [1,2,6,7,8].

The molecular mechanism by which brown spider venom induces gravitational spreading of skin lesions and systemic involvement is not fully understood. A fundamental requirement for venom to induce local spreading of lesions and systemic involvement is the presence of venom components that are able to degrade tissue barriers. The delivery of venom toxins to neighboring bite sites and into systemic circulation is assisted by molecules that degrade extracellular matrix constituents such as proteases and hyaluronidases [9,10,11,12].

Author Summary

Accidents involving brown spiders (*Loxosceles* genus) are reported throughout the world. South and Southeast of Brazil are endemic areas for this spider. *Loxosceles* bites commonly trigger local signs as swelling, erythema, hemorrhage and the hallmark symptom: a dermonecrotic lesion with gravitational spreading. Systemic effects are less common; however, are implicated in more severe cases. Hyaluronidases are referred in several venoms as "spreading factors" due to their enzymatic activity upon extracellular components. This activity facilitates the permeation of other toxins through the victim's body. In fact, a previous study identified the activity of *L. intermedia* venom upon glycosaminoglycans which are abundant components in the extracellular matrix of many tissues. Disclosing a little more about the role of hyaluronidases within this venom, we investigated the activities of a recombinant hyaluronidase from *L. intermedia* venom. Dietrich's hyaluronidase, as it was designated, was produced as a recombinant protein. By performing a rabbit skin dermonecrosis assay using Dietrich's Hyaluronidase and a dermonecrotic toxin, we showed that Dietrich's Hyaluronidase increased the dermonecrotic area induced by the dermonecrotic toxin. Our results confirm that hyaluronidases are a "spreading factor" of *L. intermedia* venom.

The venom is a mixture of proteins enriched in molecules with low molecular mass in the range of 5–40 kDa. Toxins including hyaluronidase, proteases, low molecular mass insecticidal peptides, Translationally Controlled Tumor Protein (TCTP) and phospholipases-D have been identified [1,2,13,14,15,16,17].

The existence of hyaluronidases in *Loxosceles* venoms comes from a previous report by Wright et al. (1973) [18], which reported hyaluronidase activity in the venom of *L. reclusa*. Additionally, hyaluronidase activity was described in the venom of *L. rufescens* [19] and several other *Loxosceles* venoms, including *L. deserta*, *L. gaucho*, *L. intermedia*, and *L. laeta* [11], suggesting biological conservation and significance of these enzymes. Da Silveira and colleagues (2007) [20] identified the hyaluronidases in *Loxosceles intermedia* venom as endo-β-N-acetyl-D-hexosaminidases that degrade hyaluronic acid and chondroitin sulfate. The idea that brown spider venom hyaluronidases play a role in the gravitational spreading of dermonecrosis and/or systemic diffusion of venom toxins, and then act as "spreading factors" comes from its degradative activity on hyaluronic acid and other glycosaminoglycans that mediate tissue integrity and stability. By degrading glycosaminoglycans, the hyaluronidase reduces the viscosity of hyaluronic acid and renders the extracellular matrix less rigid. This change makes the matrix more permeable to other toxins and facilitates the spread of other venom constituents and inflammatory cell mediators [21,22].

Although hyaluronidase activity has been described in several venoms including that of snakes [10,23], scorpions [24] spiders [22], bees [25], caterpillars [26], wasps [27], cone snails [28] and fish [29], the biochemical and biological characterization of these enzymes is restricted to a few examples [10,21,30]. In the case of the brown spider, the major technical problem is the minute volume of venom obtained per animal. The total volume harvested after an electric shock on the cephalothorax of the spider is limited to one or two microliters, and contains a few tens of micrograms of protein [31]. Purification of this native glycosidase to homogeneity for additional biochemical determination has not yet described for brown spider venom, and would be a very difficult task.

In recent years, using molecular biology techniques, scientists have obtained sufficient amounts of various recombinant toxins from brown spider venom to bring deeper insight into the molecular action of these toxins. Various venom phospholipase D isoforms and an Astacin-like metalloprotease have been reported for various species of spider venom [20,32,33,34,35,36].

Here, by using a cDNA library of *L. intermedia* venom glands [15], we described the cloning, heterologous expression and functional evaluation of a novel hyaluronidase. The results bring insight into loxoscelism, opening up possibilities for biotechnological applications for this recombinant enzyme as a research tool. This recombinant hyaluronidase would also be useful in future structural and functional studies of this class of enzymes.

Methods

Reagents

Salts and organic acids were purchased from Merck (Darmstadt, Germany). Agar, β mercaptoethanol, molecular mass markers and purified hyaluronic acid were purchased from Sigma (St. Louis, USA). Ethidium bromide, a Wizard Plus SV miniprep kit and pGEM-T vector were acquired from Promega (Madison, USA). Agarose, IPTG and Trizol were purchased from Invitrogen (Carlsbad, USA). We acquired DNA molecular mass standards, X-Gal, Taq DNA polymerase, Pfu DNA polymerase, T4 DNA ligase, restriction enzymes, dNTPs and CIAP from Fermentas (Burlington, Canada). For bacterial culture, we used tryptone, yeast extract and agar purchased from HiMedia (Mumbai, India). The antibiotics were purchased from USB (Cleveland, USA). The bacterial strains used in this study and the ImPromII Reverse Transcription System kit were acquired from Invitrogen. We purchased the pET-14b expression plasmid from Novagen (Novagen, Madison, USA). The glycosaminoglycan standards used were heparan sulfate from bovine pancreas [37], chondroitin sulfate from bovine cartilage and dermatan sulfate from pig skin (Seikagaku, Kogyo Co., Tokyo, Japan).

cDNA library construction and screening

The venom gland cDNA library construction was performed as described by Gremski et al. (2010) [15]. Briefly, processed sequences were compared to GenBank sequences using the *Basic Local Alignment Search Tools blastx*, *blastn* (E values<1e-05) and *tblastx* (E values<1e-10) algorithms. Afterwards, ESTs were manually inspected for functional classification. One toxin-coding messenger similar to a hyaluronidase from *Rattus novergicus* (gb|EDL77243.1) was found in this cDNA library and was used as a base sequence.

Amplification of the cDNA 5′ end

To obtain the complete 5′ end of hyaluronidase cDNA, a 5′RACE (Rapid Amplification of 5′cDNA Ends) protocol was performed following Sambrook and Russel (2001) [38] with minor modifications. Briefly, 1 µg total RNA from *L. intermedia* venom glands was used as a template. The first-strand cDNA was synthesized using the gene-specific reverse primer R1 (5′-GTTGCAGGGTAGACAACATCCACG-3′) and the Improm-II Reverse Transcriptase (Promega), according to the manufacturer's instructions. The cDNA was recovered by ethanol precipitation in the presence of ammonium acetate. The cDNA was poly(A) tailed with terminal deoxynucleotidyl transferase (Fermentas), as recommended by the supplier. The modified cDNA was amplified using PCR with a $(dT)_{17}$ adaptor primer (5′-CGGTACCATGGATCCTCGAGTTTTTTTTTTTTTTT-

TTV-3′) and the nested gene-specific reverse primer R2 (5′-CTCCATGCTTCCCAGTCGATGATGC-3′) using a Pfu DNA polymerase (Fermentas). Finally, the PCR product was purified from the gel using Illustra GFX PCR DNA and a Gel Band Purification kit (GE) following the manufacturer's instructions and sequenced on both strands using MegaBace DNA Analysis Systems (Amersham Bioscience).

Amplification of the cDNA 3′end

To achieve the complete sequence, a 3′RACE (Rapid Amplification of 3′cDNA End) protocol was modified from Sambrook and Russel [38]. Briefly, 1 μg total RNA from *L. intermedia* venom glands was used to synthesize the first-strand cDNA using the gene-specific forward primer F1 (5′-CGAATCAATCAACGGTGGCATCCCTC-3′) and the Improm-II Reverse Transcriptase (Promega). The cDNA was recovered as previously described. The cDNA was amplified with F2 (5′ -CCGCATTGGTTTTAGCCGCATTC-3′), $(dT)_{17}$ adaptor primer (5′ -CGGTACCATGGATCCTCGAGTTTTTTTTTTTTTTTTV-3′) and Pfu DNA polymerase (Fermentas). Purification from the gel with a Gel Band Purification kit (GE) was performed according to manufacturer's instructions, and the amplicon was sequenced on both strands.

Recombinant protein expression

The cDNAs encoding the putative mature hyaluronidase, which we named Dietrich's Hyaluronidase, were amplified with PCR using primers designed to contain *Nde* I restriction sites at the 5′ ends (5′-GGAATTCCATATGGACGTCTTCTGGAACG-3′) and *BamH* I sites (5′-CGGGATCCCTCACTTTGTTTTCTGCTC-3′). The PCR product was digested with *Nde* I and *BamH* I restriction enzymes. Subcloning was performed with a pET-14b plasmid (Novagen) digested with the same enzymes. The recombinant construct for mature protein was expressed as a fusion protein with a 6× His-Tag at the N-terminus. The expression construct was inserted into *E. coli* BL21(DE3)pLysS cells and plated on LB-agar plates containing 100 μg/mL ampicillin and 34 μg/mL chloramphenicol. Single colonies of the construct were inoculated into LB broth (100 μg/mL ampicillin and 34 μg/mL chloramphenicol) and grown overnight at 37°C. These cultures were diluted 1:100 into 1 L fresh LB broth/ampicillin/chloramphenicol and incubated at 37°C until the $OD_{550\ nm} = 0.4–0.6$. Recombinant protein expression was induced by the addition of 0.1 mM IPTG (isopropyl β-D-thiogalactoside) and cells were incubated for 3.5 h at 30°C in a shaker. Cells were harvested by centrifugation (4,000×g, 7 minutes, 4°C), suspended in 20 mL of extraction buffer (50 mM sodium phosphate pH 8.0, 500 mM NaCl, 10 mM imidazole, 1 mg/mL lysozyme) and frozen at −20°C overnight.

In vitro refolding of Dietrich's Hyaluronidase

Cells were thawed and disrupted with 8 cycles of sonication at medium intensity for 20 seconds using a 500-W ultrasonic cell disruptor. Lysed materials were centrifuged (20,000×g, 30 minutes, 4°C), and the pellet was washed with a denaturing buffer (100 mM Tris-HCl pH 10.0, 2 M urea, 1% Triton X-100) and sonication at low intensity. After centrifugation at 6,000×g for 10 minutes the resulting pellet was solubilized in 100 mM Tris-HCl pH 10.0 with 8 M urea and 100 mM DTT. The solution containing denatured and reduced recombinant protein was adjusted to a concentration of ~5 mg/mL and was added dropwise (1:10 ratio) to a refolding buffer (100 mM Tris-HCl pH 10.0, 3 mM reduced glutathione, 0.3 mM oxidized glutathione, 0.4 M L-arginine, 0.2 mg bovine serum albumin) by stirring over 16 h at 4°C. The protocol used was based on the works of Burgess et al. and Hofinger and co-workers [39,40]. Dialysis was against phosphate buffered saline, and recombinant hyaluronidase was concentrated using filter devices (MWCO 30,000 Millipore, Schwalbach, Germany).

SDS-PAGE and immunoblotting

Polyclonal antibodies against *L. intermedia* whole venom and against recombinant hyaluronidase were produced in rabbits as described by Harlow and Lane (1988) [41], with minor modifications [42]. Protein concentration was determined using the Coomassie Blue method [43] or ultraviolet measurement (280 nm). For protein analysis, 12.5% SDS-PAGE was performed under reducing conditions and gels were stained with Coomassie Blue. For immunoblotting, proteins were transferred onto a nitrocellulose membrane following Towbin et al. (1979) [44] and immunodetected using hyperimmune antisera, which reacts with hyaluronidase or venom.

Specificity of Dietrich's Hyaluronidase activity upon glycosaminoglycan substrates

Agarose gel electrophoresis was developed in 50 mM Tris–acetate buffer at pH 8.0 to evaluate hyaluronic acid degradation. Electrophoresis was performed in 50 mM 1,3-diaminopropane acetate buffer, pH 9.0 (Aldrich, Milwaukee, USA) to evaluate the cleavage activity of glycosidase on chondroitin sulfate, dermatan sulfate and heparan sulfate. After electrophoresis, compounds were precipitated in the gel using 0.1% cetavlon (cetylammonium bromide) for 2 h at room temperature. The gels were dried and stained with Toluidine Blue. The glycosaminoglycan standards used were as previously described [20,45]

Ethics statement

The Ethics Animal Experiment Commitee of the Setor de Ciências Biológicas of the Federal University of Parana, established by the decree 787/03-BL from May 9th 2003, and upon the internal regiment, certifies that the procedures using animal in this work are in agreement with the Ethical Principals established by Experimental Animal Brazilian Council (COBEA), and with the requirement of the "Guide for the Care and Use of Experimental Animals (Canadian Council on Animal Care)". Processes numbers: 23075.052088/2008-32 Approved: April 7, 2009 and 23075.087106/2011-01 Approved: August 9, 2011.

Animals

Adult rabbits (~3 kg) from the Central Animal House of the Catholic University of Parana were used for *in vivo* experiments with whole venom and recombinant enzymes (the product of antibodies and dermonecrosis studies). All procedures involving animals were carried out in accordance with Brazilian Federal Law, following the Ethical Subcommittee on Research Animal Care from the Federal University of Parana.

Dermonecrosis and gravitational spreading

To evaluate the potential gravitational spreading effect of brown spider hyaluronidase, 10 μg of a recombinant dermonecrotic toxin (LiRecDT1) diluted in PBS was injected intradermally into a shaved area of rabbit skin with or without recombinant hyaluronidase (10 μg). For the same purpose 10 μg of Dietrich's Hyaluronidase alone (diluted in PBS with 0.2 mg/mL BSA) was also injected. We used two negative controls: one was PBS with 0.2 mg/mL BSA, to assure that BSA used to refold recombinant hyaluronidase did not induce changes. The other was a

recombinant protein with similar molecular mass obtained under the same conditions as hyaluronidase, but without hyaluronidase activity. The last assay guarantees that potential bacterial contaminants did not influence the results. Ten micrograms of venom and dermonecrotic toxin were used as positive controls. Rabbits were used in dermonecrosis experiments because this model reproduces skin lesions very close to those observed in accidents with humans [46]. Experiments were repeated with 4 animals and the development of experimentally induced dermonecrosis was observed 3 h, 6 h and 24 h after the injection.

Histological methods for light microscopy

Rabbit skin pieces from animals that intradermally received recombinant proteins were collected following anesthetization with ketamine (Agribands, Campinas, Brazil) and acepromazine (Univet, São Paulo, Brazil). Collected tissue samples were fixed in "ALFAC" (ethanol 85%, formaldehyde 10% and glacial acetic acid 5%) for 16 h at room temperature. After fixation, samples were dehydrated in a graded series of ethanol before paraffin embedding (for 2 h at 58°C). Thin sections of 4 µm thickness were processed for histological procedures [42]. Tissue sections were stained with Masson's trichrome (TM) as described [47].

Bioinformatics tools

To compare new sequences generated against the GenBank database, we used the BLAST site (http://blast.ncbi.nlm.nih.gov/Blast.cgi). The parameters for blastn were refined by selecting the "others" search set with E values <1e-05. For blastx, we chose standard genetic code 1 and non-redundant protein sequences with E values <1e-05 parameter. Deduced amino acid sequence was found using the Open Reading Frame Finder site (http://www.ncbi.nlm.nih.gov/projects/gorf/) and an analysis of protein parameters and glycosylation modifications was conducted using the ExPASy Bioinformatics Research Portal (http://web.expasy.org/protparam/). Disulfide bond prediction was made using the DiANNA 1.1 web server http://clavius.bc.edu/~clotelab/DiANNA/. CLUSTAL W (http://www.ebi.ac.uk/Tools/msa/clustalw2/) was used for alignment and cladogram production. Finally, to search any possible signature recognition within Dietrich's Hyaluronidase sequence, we used the InterProScan site (http://www.ebi.ac.uk/Tools/pfa/iprscan/).

Genbank accession number

The Dietrich's Hyaluronidase cDNA sequence has been submitted to the Genbank database under accession number JX402631.

Results

Cloning of a hyaluronidase from the *L. intermedia* venom gland

By screening clones of a cDNA library of the *L. intermedia* venom gland, a cDNA encoding for a hyaluronidase was obtained through a blastx search [15]. The putative protein product from this cDNA was designated Dietrich's Hyaluronidase (in honor and memoriam of Professor Carl Peter von Dietrich, born in 1936, deceased in 2005). The complete cDNA sequence of Dietrich's Hyaluronidase consist of 1200 bp with a single open reading frame (ORF) coding for 400 amino acids and a putative N terminal endoplasmic reticulum import signal of 19 residues. At least two types of post translational modification were observed: 4 putative N-glycosylation sites and 3 possible disulfide bonds (Fig. 1). The predicted molecular mass for mature Dietrich's Hyaluronidase protein was approximately 44.8 kDa, and its pI was 8.75.

Multiple alignment analysis of the cDNA-deduced amino acid sequence and the cladogram relationship of Dietrich's Hyaluronidase to other hyaluronidase family members

To explore the structural and evolutionary relationships among the newly identified glycosidase and other members of the hyaluronidase family, a BLAST GenBank database search through alignment of cDNA-deduced amino acid sequences revealed that Dietrich's Hyaluronidase has structural similarity to other hyaluronidase family members (Fig. 2A). The overall identity of hyaluronidase from *L. intermedia* venom is approximately 46% compared with the scorpion venom hyaluronidase of *Mesobuthus martensii* (gb|ACY69673.1). Dietrich's Hyaluronidase is also similar to snake venom hyaluronidases, sharing 33% sequence identity with *Echis pyramidium* (*gb|ABI33941.1*) and *Cerastes cerastes (gb|ABI33939.1)*. Interestingly, the enzyme from an arthropod venom showed approximately 30% amino acid identity with hyaluronidases from mammal species such as *Bos taurus (gb|AAP55713.1)* and *Rattus novergicus (gb|EDL77243.1)* (Fig. 2B). An InterProScan search matches Dietrich's Hyaluronidase with more than 500 proteins belonging to the glycoside hydrolase 56 family. A typical signature domain for hyaluronidases has not yet been demonstrated, and there are few studies about of the residues involved in catalysis [30,48]. However, the hyaluronidase from *L. intermedia* venom has 3 conserved amino acids (indicated in Fig. 2A at arrows: D118, E120, E259) that appear to be important for the catalytic activity of some hyaluronidases [30].

Expression, purification and refolding of Dietrich's Hyaluronidase

Recombinant hyaluronidase from *L. intermedia* venom was expressed in pET 14b in *E. coli* BL21(DE3)pLysS cells. The expression of recombinant protein was optimized when induced for 3.5–5 h with 0.1 mM of IPTG. The recombinant protein was detected only in the insoluble fraction of cell lysates and was purified under denaturing conditions by washing inclusion bodies until there were no bacterial contaminants visible in SDS-PAGE gels stained with Coomassie blue. The SDS-PAGE mobility of recombinant protein reduced by β-mercaptoethanol treatment was ~45 kDa, consistent with the calculated molecular mass (Fig. 3). After testing several refolding protocols *in vitro* (data not shown), the protocol described in the methods section, was effective in solubilizing recombinant hyaluronidase from inclusion bodies, as shown in lane 4 (Fig. 3).

Immuno cross-reactivity among native and recombinant hyaluronidases

Immunoblot analysis using antibodies against recombinant hyaluronidase (Dietrich's Hyaluronidase) and antibodies against whole venom toxins established the epitope relationship of native hyaluronidase with recombinant enzyme (Fig. 4). Antibodies against Dietrich's Hyaluronidase recognize hyaluronidase in the whole venom, as well as anti-whole venom serum reacted with recombinant glycosidase.

Hyaluronidase activity on HA and CS

To evaluate the activity of Dietrich's Hyaluronidase after refolding, purified HA was incubated at a ratio of 1:1 with recombinant hyaluronidase for 3 h, 6 h and 16 h at 37°C. The enzymatic activity was analyzed through agarose gel electrophoresis stained with toluidine blue. HA was completely degraded within 3 h (Fig. 5A, lane 3) showing that the *in vitro* refolding method was effective in adjusting hyaluronidase in an active

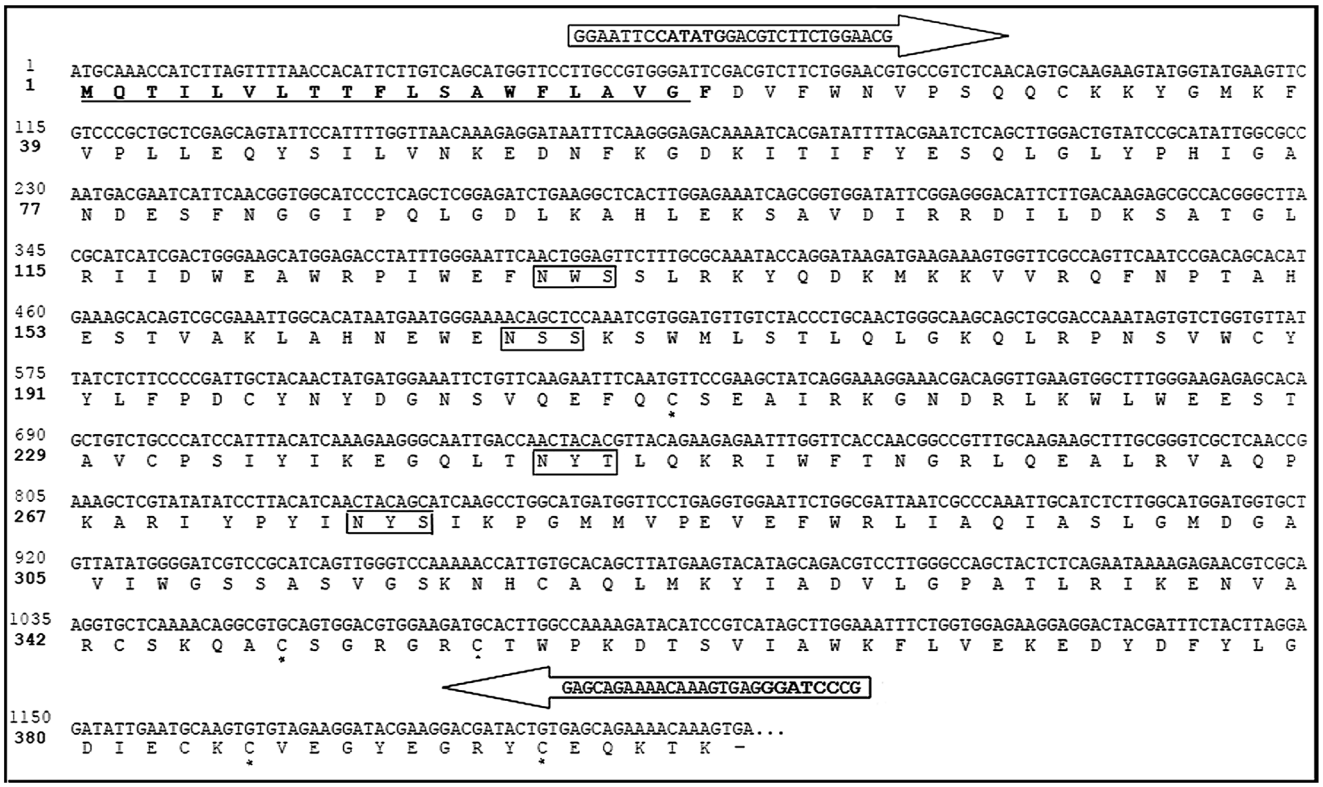

Figure 1. Molecular cloning of Dietrich's Hyaluronidase, a novel protein from *L. intermedia* venom gland. Nucleotide- and amino-acid-deduced sequences. Predicted amino acid sequence, with 400 amino acid residues and signal peptide underlined. Rectangular boxes are the predicted N-glycosylation sites (ExPASy tools parameters), and asterisks indicate cysteine residues that may constitute disulfide bonds (DiANNA web server). Arrows indicate primers with restriction sites (bold nucleotides) used for subcloning into pET 14b.
doi:10.1371/journal.pntd.0002206.g001

conformation. Through analysis with CS, DS and HS at a substrate-to-enzyme ratio of 1:1, we noted that recombinant hyaluronidase degraded CS (Fig. 5B, lane 3) and did not degrade DS and HS (data not shown), similar to the native hyaluronidases from venom.

To verify the stability of refolding *in vitro* achieved with recombinant hyaluronidase, we performed a zymogram assay using gels containing copolymerized purified HA and CS as substrates. Hydrolytic activity was found as a specific band between the 29–45 kDa regions in both substrates and strengthened the results described above (Fig. 5C).

Gravitational spreading

We sought to develop dermonecrosis experiments using rabbit skin to determine the *in vivo* involvement of brown spider venom hyaluronidase in envenomation. Moreover, we aimed to observe the relationship of hyaluronidases in the skin deleterious activities of whole venom. Injections of *L. intermedia* crude venom, recombinant dermonecrotic toxin [33] (positive controls), and dermonecrotic toxin plus Dietrich's Hyaluronidase all induced macroscopic erythema, ecchymosis and dermonecrosis in rabbit skin, which was followed by 3, 6 and 24 h of observation (Fig. 6A and Fig. 6B). On the other hand, the injection of recombinant hyaluronidase alone, PBS/BSA and a recombinant protein not related to hyaluronic acid hydrolysis (negative controls) did not show macroscopic erythema, ecchymosis or dermonecrosis (Fig. 6A and Fig.6B). The length of dermonecrosis lesions in the rabbit skin of Dietrich's Hyaluronidase concomitantly injected with dermonecrotic toxin was substantially larger than for dermonecrotic toxin alone after 24 h (Fig. 6B). The macroscopic gravitational spreading and edema induced by the two recombinant enzymes injected together were very similar to whole venom (Fig. 6C).

Histopathological findings of dermonecrosis

Light microscopic analysis of rabbit skin biopsies 24 h after of the experimentally induced dermonecrosis experiments performed above suggested that recombinant hyaluronidase was able to disorganize the extracellular matrix from rabbit skin dermis (Fig. 7B-4). Dermonecrotic toxin alone triggered typical inflammatory cell accumulation (Fig. 7B-2 and 7B-5) and edema signals (Fig. 7A, 7B-5), as well as collagen fiber disorganization (Fig. 7B-5) and presence of fibrin in connective tissue (Fig. 7B-5). Nevertheless, we noticed that these inflammatory events, developed by dermonecrotic toxin, were intensified when combined with Dietrich's Hyaluronidase (Fig. 7A; 7B-3 and 7B-6), supporting an extensive edema and spreading of lesion. By comparison, using a panoramic image under the same conditions, deleterious effects induced by dermonecrotic toxin alone were lower than those evoked by mixture of this toxin and Dietrich's Hyaluronidase (Fig. 7A). These microscopic findings corroborate the information obtained by macroscopic analysis of rabbit skin lesions.

Discussion

Hyaluronidases are present in various tissues and are involved in important biological events, including embryonic development, inflammation, fertilization, tumor cell metastasis, bacterial pathogenesis and aging [10,14]. These enzymes were described many

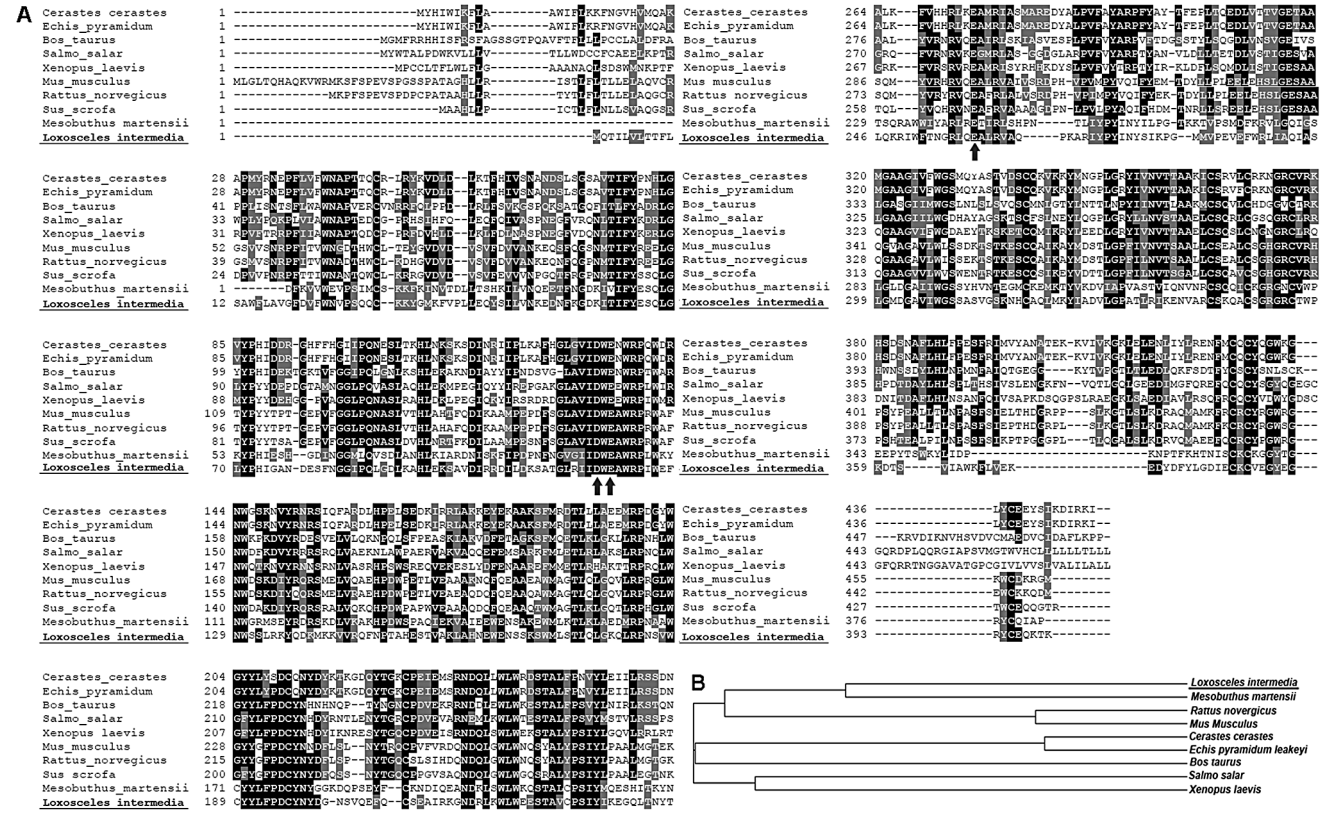

Figure 2. Multiple alignment analysis of Dietrich's Hyaluronidase sequence and several others hyaluronidases. (A) Deduced amino acid sequences compared and their GenBank accession numbers: *Cerastes cerastes* (ABI33939.1); *Echis pyramidum leakey* (ABI33941.1); *PH-20 Bos taurus* (AAP55713.1); Hyaluronidase-2 precursor *Salmo salar* (ACI33947.1); lysosomal hyaluronidase *Xenopus laevis* (AAL55823.1); hyaluronoglucosaminidase 1 *Mus musculus* (AAC15949.1); hyaluronidase 1 *Sus scrofa* (ACH56985.1); venom hyaluronidase *Mesobuthus martensii* (ACY69673.1); hyaluronoglucosaminidase 1 *Rattus norvegicus* (EDL77243.1) and *Loxosceles intermedia* (JX40263.1). Black shaded regions show amino acid identity and gray shaded regions, conservative substitutions. Arrows indicate conserved amino acids that appear to be important for catalytic hydrolysis. (B) Deduced cladogram of the cloned hyaluronidase and family members based on sequence alignment and percent identity generated by CLUSTAL W.
doi:10.1371/journal.pntd.0002206.g002

years ago in the venom of different *Loxosceles* species, featuring a conservative event and suggesting biological significance in the life cycle of these spiders [1,2,11]. A more refined understanding of brown spider venom hyaluronidase is hampered by native molecules present in low amounts in the venom and by extremely minute volume of venom obtained from spiders [2,15,49].

Here, we described the cloning, heterologous expression, purification, refolding and characterization of a novel hyaluronidase from a cDNA library of the *L. intermedia* venom gland. These results corroborate previous biochemical data that have described these enzymes in brown spider venom from different species [11,20]. The recombinant protein identified herein is designated Dietrich's Hyaluronidase (GenBank Accession no. JX402631).

The primary sequence of Dietrich's Hyaluronidase includes a hydrophobic signal sequence of 19 residues and a mature protein. The hydrophobic signal sequence probably directs its expression to the endoplasmic reticulum in venom gland epithelial cells. The molecular mass and isoelectric point calculated from the deduced amino acid sequence of mature protein were 44.8 kDa and pI 8.75, respectively. The theoretical molecular mass is within the expected range, considering the size of brown spider venom native hyaluronidases [11,20], and the isoelectric point was similar to the calculated pI of hyaluronidases from other venoms. A protein sequence analysis of brown spider venom hyaluronidase compared to hyaluronidases from different sources showed that this venom enzyme has conserved amino acids (D118, E120, E259) that seem to be important for catalytic hydrolysis [30,48]. Dietrich's Hyaluronidase was assigned to the Glycosidase 56 family; which compose a wide group of O-glycosyl-hydrolases [50]. The highest similarity to Dietrich's hyaluronidase was found in the sequences of scorpion hyaluronidase from *Mesobuthus martensii* venom (46% amino acid identity) and the snake venom of *Echis pyramidium* and *Cerastes cerastes* (33%). As might be expected, the hyaluronidase from *L. intermedia* venom was particularly similar to hyaluronidases from other venoms. However, we highlight Dietrich's Hyaluronidase's significant identity with mammalian species such as *Bos taurus* and *Rattus novergicus*. This fact, coupled with its activity at physiological pH, would be interesting for pharmaceutical use.

Dietrich's Hyaluronidase was heterogeneously expressed as a mature protein with an N-fusion His-tag using the *E. coli* BL21(DE3)pLysS strain. Isolation of the recombinant glycosidase was performed by washing inclusion bodies with denaturing buffer. The purification of recombinant proteins from inclusion bodies might be advantageous, because it is protease-resistant and is close to functional native structure [51,52,53].

Characterization of the antigenic cross-reactivity of recombinant hyaluronidase and *L. intermedia* venom showed that the venom contains proteins that have antigenic identity (sequence epitopes) with recombinant hyaluronidase because antisera raised against recombinant enzyme was able to react with native venom. Two protein bands of the whole venom were recognized by hyaluronidase antisera, corroborating with previous results that showed two

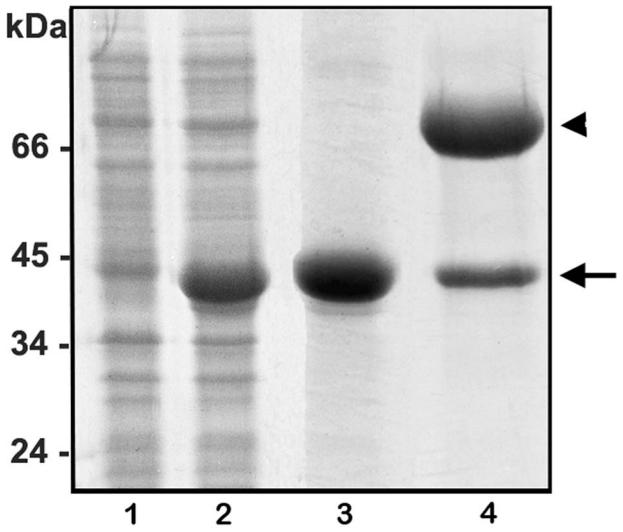

Figure 3. Heterologous expression, purification and refolding of Dietrich's Hyaluronidase. Expression of recombinant protein in *E. coli* BL21(DE3)pLysS was analyzed via 12.5% SDS-PAGE under reducing conditions and Coomassie blue staining. Lanes 1 and 2 depict *E. coli* before (0 h) and after induction (4 h) with 0.1 mM IPTG at 30°C, respectively. Lane 3 shows inclusion bodies after washing in denaturing conditions. Lane 4 shows recombinant hyaluronidase refolded *in vitro* at ~45 kDa (arrow). Band at 67 kDa is BSA used during refolding (arrowhead). Molecular mass marker positions are shown in the left of figure.
doi:10.1371/journal.pntd.0002206.g003

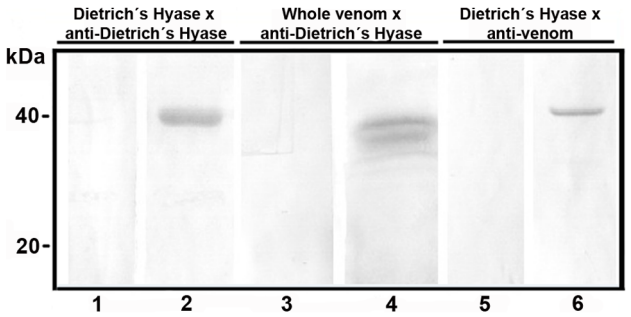

Figure 4. Immunological cross-reactivity of whole venom and Dietrich's Hyaluronidase. Purified recombinant glycosidase (2.0 μg; lanes 1, 2, 5 and 6) or whole venom (40 μg; lanes 3 and 4) were separated by 12.5% SDS-PAGE under reducing conditions, transferred onto nitrocellulose membranes and exposed to antibodies against Dietrich's Hyaluronidase (lanes 2 and 4) or whole venom toxins (lane 6). Lanes 1, 3 and 5 indicate reactions in the presence of pre-immune sera (control for antibody specificity). Molecular mass marker positions are shown in the left of figure.
doi:10.1371/journal.pntd.0002206.g004

lytic zones in zymography experiments using whole venom in a gel co-polimerized with hyaluronic acid. Those bands probably correspond to two isoforms of hyaluronidase present in *L. intermedia* whole venom [11,20]. Additionally, anti-venom cross-reacted with the recombinant hyaluronidase, suggesting that the recombinant glycosidase retains linear antigenic determinants from native hyaluronidases. In this way, the antisera to Dietrich's Hyaluronidase or purified antibodies from it could be a possible biological tool in loxoscelism therapy or for research purposes.

The functionality of refolded recombinant hyaluronidase was demonstrated through its activity upon purified hyaluronic acid and chondroitin sulfate. Dietrich's Hyaluronidase was able to directly degrade hyaluronan and chondroitin sulfate. These results are in agreement with previous data reported for native hyaluronidases from whole venom, which degrade both glycosaminoglycans [20]. The hydrolytic activity found at 29–45 kDa in zymogram assays copolymerized with hyaluronic acid and chondroitin sulfate corroborates with the degrading activity of glycosaminoglycans viewed in agarose gels, suggesting certain stability in the active folding of Dietrich's Hyaluronidase acquired after refolding *in vitro*. Again, results show that recombinant hyaluronidase can also be considered a chondroitinase, as previously reported for native hyaluronidases [20].

Regarding *in vitro* refolding it is worth mentioning that buffers with different pHs, redox agents and additives were tested [39,54] until the solubility and activity of Dietrich's Hyaluronidase was maximized (data not shown). When bovine albumin was removed from the buffer, the hyaluronidase activity was null. This result is consistent with the literature that describes how BSA may compete with hyaluronidases to form inactive electrostatic complexes with hyaluronic acid. This competition induces free hyaluronidase resulting in a large increase in the hydrolysis rate [55]. Several research groups have reported that serum proteins are able to enhance hyaluronidase activity and are sometimes required to detect the presence of hyaluronidases [55,56,57].

But what is the role of brown spider venom hyaluronidase on bite pathology? The involvement of hyaluronidase on the activity of brown spider venom is supported by the conservative phenomenon of this enzyme, which indeed is found in different species of *Loxosceles* venoms [11]. Hyaluronidases have been described for several venoms [26,55,58] and act as "spreading factors" by degrading hyaluronic acid and chondroitin sulfate. In this way, venom hyaluronidases may render surrounding regions at the bite site more permeable. Furthermore, these enzymes may facilitate the diffusion of other venoms constituents through the bodies of victims [10,58]. A hyaluronidase isolated from funnel web spider venom was able to enhance the potency of a myotoxin and a hemorrhagic toxin. This work is in accordance with the hypothesis that hyaluronidase mediates enhanced toxicity of whole venom during envenomation [22].

A typical symptom of loxoscelism is the gravitational spreading of skin lesions that appear a few hours after bites or experimental envenomation of animal models [1,2]. The mechanism by which *Loxosceles* venom causes gravitational spreading of dermonecrosis is not fully understood. Experimental inoculation of purified recombinant dermonecrotic toxins (phospholipases-D, non-proteolytic or hyaluronidase activities), evokes gravitational spreading of skin lesion on rabbits [34]. Macroscopically, Dietrich's Hyaluronidase increases the erythema, ecchymosis and dermonecrotic lesion area induced by recombinant phospholipase-D along exposure times observed. Histopathological findings for the dermonecrotic toxin exposed tissue samples revealed, as expected, the presence of a neutrophilic infiltrate, collagen fiber disorganization and signs of edema [36,46]. However, when we analyzed tissue samples treated with phospholipase-D toxin plus Dietrich's Hyaluronidase, we observed that these inflammatory evidences were much more intense, as if recombinant hyaluronidase was allowed a free diffusion of phospholipase D by rendering the connective tissue more permeable. For the first time in the literature, experimental results strongly indicate that the hyaluronidase from *Loxosceles* venom is in fact a "spreading factor" for this venom.

For brown spider venom hyaluronidase, based on the spreading property, we extrapolated that this molecule would be primarily responsible for spreading other venom toxins from the bite site into

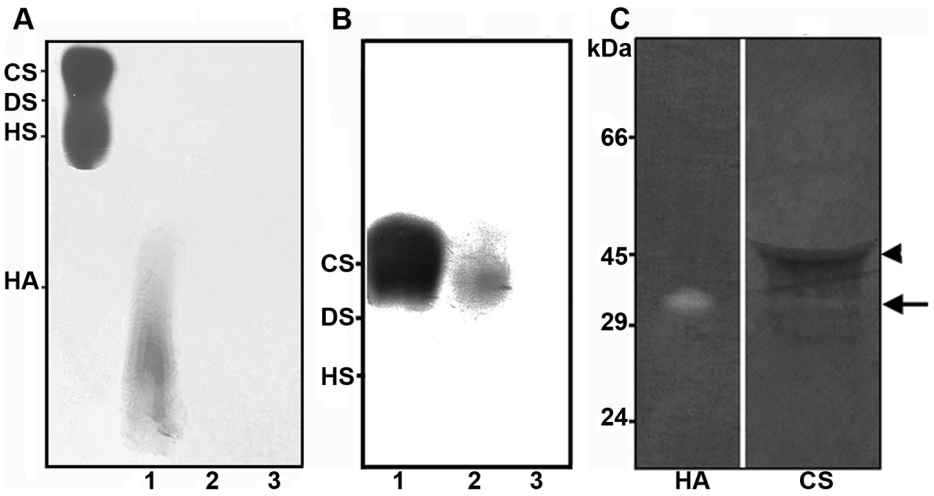

Figure 5. Detection of degradative activities of Dietrich's Hyaluronidase upon hyaluronic acid and chondroitin sulfate. (A) Purified hyaluronic acid (15 μg) was incubated with whole venom or recombinant hyaluronidase at a ratio of 1:1 for 3 h at 37°C. Degradation was assayed after agarose gel electrophoresis of the incubation mixture, followed by cetavlon precipitation and toluidine blue staining of the glycosaminoglycan sample. Chondroitin sulfate (CS), dermatan sulfate (DS) and heparan sulfate (HS) were used as molecular mass markers. Lane 1 represents the negative control (15 μg of purified hyaluronic acid), and lanes 2 and 3 show hyaluronic acid incubated with the venom and recombinant hyaluronidase, respectively. (B) Purified chondroitin sulfate (CS) was incubated with venom (lane 2) or Dietrich's Hyaluronidase (lane 3) at ratios of 1:1 for 16 h at 37°C. Chondroitin sulfate standard is shown in lane 1. (C) 5 μg of recombinant enzyme was submitted to zymography SDS-PAGE 10% impregnated with 0.17 mg/mL hyaluronic acid (HA) or 0.34 mg/mL chondroitin sulfate (CS). The zymogram was developed overnight at 37°C under pH 7.4 and the gel was stained with Alcian Blue and co-stained with Coomassie Blue. Black arrow indicates activity of recombinant hyaluronidase in zymograms. Arrowhead shows persistent BSA residue after proteolysis performed before coloration. Molecular mass marker positions are shown in the left of figure.
doi:10.1371/journal.pntd.0002206.g005

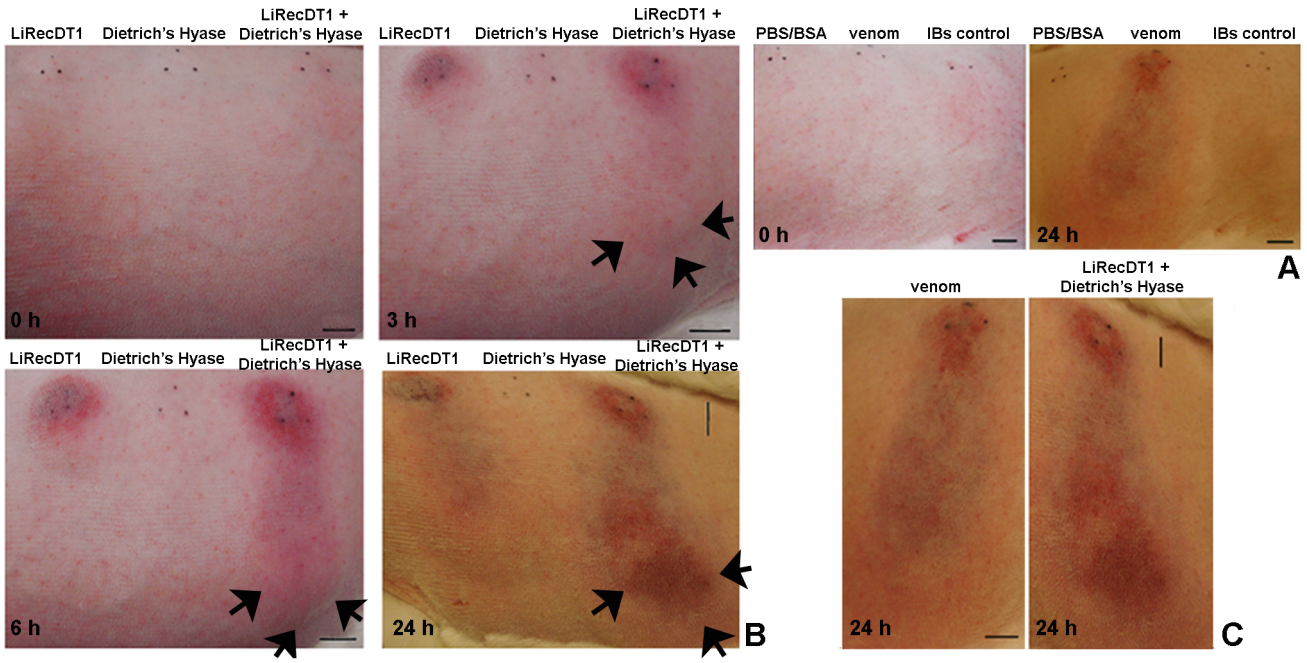

Figure 6. Macroscopic changes in rabbit skin exposed to whole venom, recombinant dermonecrotic toxin and Dietrich's Hyaluronidase. (A) Macroscopic visualization of skin injuries of rabbits intradermally injected with 10 μg of whole venom (as positive control), 10 μg of a recombinant protein not related to hyaluronic acid hydrolysis or dermonecrosis (IBs control) and PBS/BSA (negative controls). Lesions were observed 0 and 24 h following injection. (B) Macroscopic visualization of skin injuries of rabbits intradermally injected with 10 μg of dermonecrotic toxin (LiRecDT1), 10 μg of Dietrich's Hyaluronidase (Dietrich's Hyase), or both enzymes together (20 μg). Lesions were observed 0, 3, 6 and 24 h following injections. Arrows point to spreading of erythema (3 and 6 h), ecchymosis (6 and 24 h) and gravitational spreading of necrotic lesions (24 h) after injection of dermonecrotic toxin and Dietrich's Hyaluronidase, compared to lesions developed only due to dermonecrotic toxin. (C) In detail, comparison of dermonecrotic injuries developed due to venom or a mixture of recombinant hyaluronidase and phospholipase-D. Injections were applied in the center of the triangle indicated by three dots. Scale bar is shown at right of each picture and represents 1 cm.
doi:10.1371/journal.pntd.0002206.g006

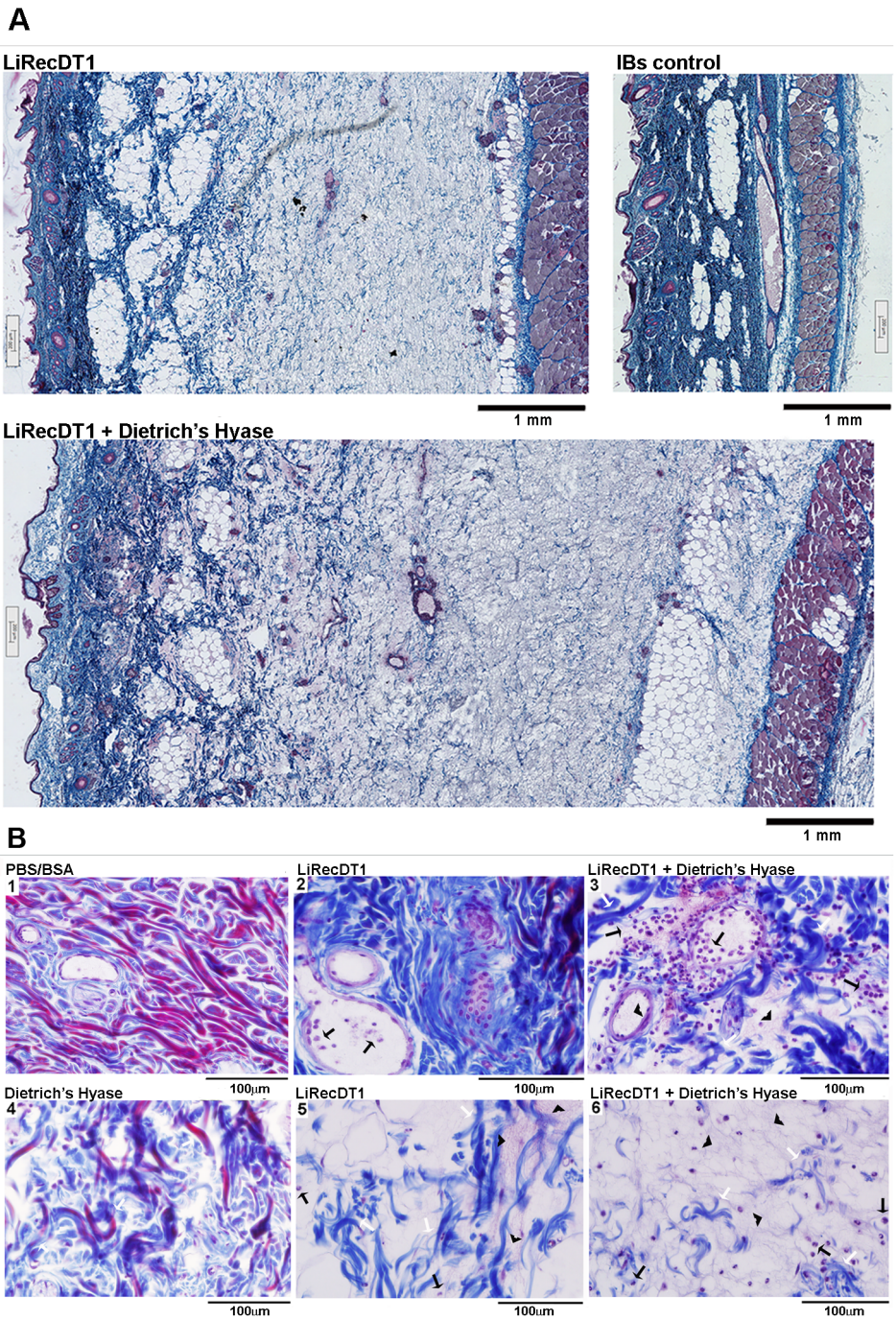

Figure 7. Histopathological changes in rabbit skin exposed to recombinant dermonecrotic toxin and Dietrich's Hyaluronidase. Light microscopic analysis of tissue sections was performed on rabbit skin after 24 h of recombinant enzymes injection. The tissue sections were stained with Massons's trichrome. The scale bar at the bottom of the figures indicates 1 mm (A) or 100 μm (B). (A) Edema triggered in rabbit skin by the combination of dermonecrotic toxin (LiRecDT1) and Dietrich's Hyaluronidase (Dietrich's Hyase), visualized by size. Comparison of the skin structures via scanning of images from epidermal (on the left of figure) to muscular tissues (on the right of figure) under the same laboratory conditions (magnification 15×). (B) Skin exposed to recombinant dermonecrotic toxin, recombinant hyaluronidase, or recombinant hyaluronidase plus recombinant dermonecrotic toxin changed the extracellular matrix in connective tissue: disorganization of collagen fibers (Fig. 7B-3, 7B-4, 7B-5 and 7B-6) (white arrows); fibrinoid exudate into the dermis (Fig. 7B-3, 7B-5 and 7B-6) (arrowheads); and intense inflammatory response with neutrophils inside blood vessels and diffusely into the dermis structures (Fig. 7B-2, 7B-3, 7B-5 and 7B-6) (black arrows) are shown (magnification 400×).
doi:10.1371/journal.pntd.0002206.g007

the systemic circulation [1,2]. Literature data have reported signs of systemic intoxication including fever, vomiting, hemolytic anemia, thrombocytopenia, disseminated intravascular coagulation, and nephrotoxicity following brown spider bites [1,2,4,31].

Moreover, brown spider venom hyaluronidase is also suggested to play a role in the cutaneous lesions following bites, as described for other venom hyaluronidases [23]. By disturbing the extracellular matrix structure, venom hyaluronidase may influence the

stability of blood vessel walls. These events may increase the spread of other venom toxins, which in turn can cause the cutaneous lesions that may follow after brown spider bites. Corroborating previous ideas, our work shows that Dietrich's Hyaluronidase is able to degrade hyaluronic acid and chondroitin sulfate *in vitro* and has increased the erythema and ecchymosis cause by phospholipase-D injected into rabbit skin. We suggest that this enzyme likely degrades both glycosaminoglycans *in vivo*. It is known that low molecular weight HA fragments are pro-inflammatory, immunostimulatory and angiogenic. Besides, HA oligosaccharides formed due to plasma HA degradation may result in hemostatic disturbances. Hence, exploring the *in vivo* fragmentation of HA and the effects on pathophysiology of envenomation might be a topic for further researches [59].

Another important feature that has been described for hyaluronidases of venoms, such as from scorpions, bees, hornets and wasps, is their classification as major allergens that can induce anaphylaxis and sometimes death [21,60]. Based on its sequence identity with other venom hyaluronidases, it is possible that the brown spider venom hyaluronidase may act as a potential allergen in susceptible individuals. This notion is strengthened by evidence observed in the course of loxoscelism, which includes itch, morbilliform erythema, cutaneous rash and petechial eruption [1,2,31,61,62]. It might also suggest the involvement of the immune system [63,64]. Cutaneous rashes respond to treatment with systemic steroids [31,63]. Thus, the hyaluronidase from *Loxosceles* genus could be further investigated as a molecule capable of inducing allergy reactions. In the same way, whether allergy's molecular mechanism is due to the enzyme molecule itself or even the HA fragments resulting from its glycosidase activity.

Besides a novel understanding of the pathogenesis of loxoscelism, Dietrich's Hyaluronidase could be an important tool for future biotechnological purposes [14,16]. Hyaluronidases are known to be involved in physiological and pathological processes such as bacterial pathogenesis, spread of toxins and venoms, fertilization, and cancer progression [65,66,67,68].

For example, hyaluronidase recombinant molecules may be developed as tools for *in vitro* fertilization [10]. On the other hand, hyaluronidase inhibitors may serve as contraceptives, because they are involved in the fertilization of eggs by mammalian sperm and could thus be used to block fertilization. Other possible applications of hyaluronidase inhibitors are as anti-tumor [58,66], anti-bacterial [67] and anti-venom/toxin agents [16,20]. Interestingly, a cloned *Buthus martensi* hyaluronidase (BmHYA1) down-regulated CD44 (a hyaluronic acid-ligand transmembrane glycoprotein involved in cell–matrix connections) in a cancer cell line, suggesting that a variant of cancer cells can be modulated by external venom hyaluronidase treatment [24].

In summary, for the first time in the literature, we have described a recombinant hyaluronidase from the venom glands of *Loxosceles* sp. We cloned, expressed, purified and refolded this enzyme, which showed degradative activity on hyaluronic acid and chondroitin sulfate. This recombinant glycosidase increased the area of dermonecrosis, gravitational spreading and edema induced by a recombinant dermonecrotic toxin, mimicking the profile of whole venom in an animal model for skin loxoscelism *in vivo*. Finally, results showed the role of this enzyme as a spreading factor in the mechanism of spreading of necrotic lesions followed by brown spider envenomation. Together, these results provide insights into loxoscelism and contribute to a further understanding of venom mechanisms and will perhaps unveil novel treatment protocols for envenomation or biotechnological applications for this venom protein.

We propose naming this novel brown spider hyaluronidase described herein as Dietrich's Hyaluronidase, in memoriam and honor of Professor Carl Peter Von Dietrich. Professor Dietrich was born in 1936 in Rio de Janeiro, Brazil, graduated in medicine from the Universidade do Estado do Rio de Janeiro, 1963, Rio de Janeiro, Brazil, specialized in biochemistry at the Instituto de Investigaciones Bioquimicas, 1963, Buenos Aires, Argentine, and earned his doctorate at the University of Saskatchewan, 1970, Saskatchewan, Canada. He was a professor and researcher in biochemistry and molecular biology at the Universidade Federal de São Paulo, São Paulo, Brazil, where he worked with macromolecules such as proteoglycans, glycosaminoglycans and heparins. Professor Dietrich died in 2005 in São Paulo, Brazil.

Acknowledgments

We would like to thank Rafael Zotz (Zoo Technician at Catholic University of Parana) for his help with rabbit manipulation, Herculano Salviano dos Reis Filho and Israel Henrique Bini (Histology Technicians at Federal University of Parana) and Thelma A.V. Ludwig (Professor, Botany Department at Federal University of Parana) for use of their light microscopy facilities.

Author Contributions

Conceived and designed the experiments: VPF LHG OMC SSV. Performed the experiments: VPF TLdM LHG DTS OMC RBdS. Analyzed the data: VPF TLdM LHG DTS OMC RBdS SSV. Contributed reagents/materials/analysis tools: HBN SSV WG ASR OMC. Wrote the paper: VPF LHG OMC SSV HBN.

References

1. Futrell JM (1992) Loxoscelism. Am J Med Sci 304: 261–267.
2. da Silva PH, da Silveira RB, Appel MH, Mangili OC, Gremski W, et al. (2004) Brown spiders and loxoscelism. Toxicon 44: 693–709.
3. Chaves-Moreira D, Chaim OM, Sade YB, Paludo KS, Gremski LH, et al. (2009) Identification of a direct hemolytic effect dependent on the catalytic activity induced by phospholipase-D (dermonecrotic toxin) from brown spider venom. J Cell Biochem 107: 655–666. doi: 10.1002/jcb.22148.
4. Kusma J, Chaim OM, Wille AC, Ferrer VP, Sade YB, et al. (2008) Nephrotoxicity caused by brown spider venom phospholipase-D (dermonecrotic toxin) depends on catalytic activity. Biochimie 90: 1722–1736. doi: 10.1016/j.biochi.2008.07.011.
5. Lucato RV, Jr., Abdulkader RC, Barbaro KC, Mendes GE, Castro I, et al. (2011) *Loxosceles gaucho* venom-induced acute kidney injury in vivo and in vitro studies. PLoS Negl Trop Dis 5: e1182. doi: 10.1371/journal.pntd.0001182.
6. Elston DM, Eggers JS, Schmidt WE, Storrow AB, Doe RH, et al. (2000) Histological findings after brown recluse spider envenomation. Am J Dermatopathol 22: 242–246.
7. Ospedal KZ, Appel MH, Fillus Neto J, Mangili OC, Veiga SS, et al. (2002) Histopathological findings in rabbits after experimental acute exposure to the *Loxosceles intermedia* (brown spider) venom. Int J Exp Pathol 83: 287–294.
8. Goncalves-de-Andrade RM, Bertani R, Nagahama RH, Barbosa MF (2012) *Loxosceles niedeguidonae* (Araneae, Sicariidae) a new species of brown spider from Brazilian semi-arid region. Zookeys 175: 27–36. doi: 10.3897/zookeys.175.2259.
9. Bjarnason JB, Fox JW (1995) Snake venom metalloendopeptidases: reprolysins. Methods Enzymol 248: 345–368.
10. Kreil G (1995) Hyaluronidases a group of neglected enzymes. Protein Sci 4: 1666–1669.
11. Barbaro KC, Knysak I, Martins R, Hogan C, Winkel K (2005) Enzymatic characterization, antigenic cross-reactivity and neutralization of dermonecrotic activity of five *Loxosceles* spider venoms of medical importance in the Americas. Toxicon 45: 489–499.
12. Baldo C, Jamora C, Yamanouye N, Zorn TM, Moura-da-Silva AM (2010) Mechanisms of vascular damage by hemorrhagic snake venom metalloproteinases: tissue distribution and in situ hydrolysis. PLoS Negl Trop Dis 4: e727. doi: 10.1371/journal.pntd.0000727.
13. de Castro CS, Silvestre FG, Araujo SC, Gabriel de MY, Mangili OC, et al. (2004) Identification and molecular cloning of insecticidal toxins from the venom of the brown spider *Loxosceles intermedia*. Toxicon 44: 273–280.
14. Senff-Ribeiro A, da Silva PH, Chaim OM, Gremski LH, Paludo KS, et al. (2008) Biotechnological applications of brown spider (*Loxosceles* genus) venom

toxins. Biotechnol Adv 26: 210–218. doi: 10.1016/j.biotechadv.2007.12.003.
15. Gremski LH, da Silveira RB, Chaim OM, Probst CM, Ferrer VP, et al. (2010) A novel expression profile of the *Loxosceles intermedia* spider venomous gland revealed by transcriptome analysis. Mol Biosyst 6: 2403–2416. doi: 10.1039/c004118a.
16. Chaim OM, Trevisan-Silva D, Chaves-Moreira D, Wille AC, Ferrer VP, et al. (2011) Brown Spider (*Loxosceles* genus) Venom Toxins: Tools for Biological Purposes. Toxins (Basel) 3: 309–344. doi: 10.3390/toxins3030309.
17. Sade YB, Boia-Ferreira M, Gremski LH, da Silveira RB, Gremski W, et al. (2012) Molecular cloning, heterologous expression and functional characterization of a novel translationally-controlled tumor protein (TCTP) family member from *Loxosceles intermedia* (brown spider) venom. Int J Biochem Cell Biol 44: 170–177. doi: 10.1016/j.biocel.2011.10.013.
18. Wright RP, Elgert KD, Campbell BJ, Barrett JT (1973) Hyaluronidase and esterase activities of the venom of the poisonous brown recluse spider. Arch Biochem Biophys 159: 415–426.
19. Young AR, Pincus SJ (2001) Comparison of enzymatic activity from three species of necrotising arachnids in Australia: *Loxosceles rufescens*, *Badumna insignis* and *Lampona cylindrata*. Toxicon 39: 391–400.
20. da Silveira RB, Chaim OM, Mangili OC, Gremski W, Dietrich CP, et al. (2007) Hyaluronidases in *Loxosceles intermedia* (Brown spider) venom are endo-beta-N-acetyl-d-hexosaminidases hydrolases. Toxicon 49: 758–768.
21. Girish KS, Kemparaju K (2005) A low molecular weight isoform of hyaluronidase: purification from Indian cobra (*Naja naja*) venom and partial characterization. Biochemistry (Mosc) 70: 708–712.
22. Nagaraju S, Devaraja S, Kemparaju K (2007) Purification and properties of hyaluronidase from *Hippasa partita* (funnel web spider) venom gland extract. Toxicon 50: 383–393.
23. Girish KS, Shashidharamurthy R, Nagaraju S, Gowda TV, Kemparaju K (2004) Isolation and characterization of hyaluronidase a ''spreading factor'' from Indian cobra (*Naja naja*) venom. Biochimie 86: 193–202.
24. Feng L, Gao R, Gopalakrishnakone P (2008) Isolation and characterization of a hyaluronidase from the venom of Chinese red scorpion *Buthus martensi*. Comp Biochem Physiol C Toxicol Pharmacol 148: 250–257. doi: 10.1016/j.cbpc.2008.06.003.
25. Kemeny DM, Dalton N, Lawrence AJ, Pearce FL, Vernon CA (1984) The purification and characterisation of hyaluronidase from the venom of the honey bee, *Apis mellifera*. Eur J Biochem 139: 217–223.
26. da C B Gouveia AI, da Silveira RB, Nader HB, Dietrich CP, Gremski W, et al. (2005) Identification and partial characterisation of hyaluronidases in *Lonomia obliqua* venom. Toxicon 45: 403–410.
27. Skov LK, Seppala U, Coen JJ, Crickmore N, King TP, et al. (2006) Structure of recombinant Ves v 2 at 2.0 Angstrom resolution: structural analysis of an allergenic hyaluronidase from wasp venom. Acta Crystallogr D Biol Crystallogr 62: 595–604.
28. Violette A, Leonardi A, Piquemal D, Terrat Y, Biass D, et al. (2012) Recruitment of Glycosyl Hydrolase Proteins in a Cone Snail Venomous Arsenal: Further Insights into Biomolecular Features of Conus Venoms. Mar Drugs 10: 258–280. doi: 10.3390/md10020258.
29. Madokoro M, Ueda A, Kiriake A, Shiomi K (2011) Properties and cDNA cloning of a hyaluronidase from the stonefish *Synanceia verrucosa* venom. Toxicon 58: 285–292. doi: 10.1016/j.toxicon.2011.07.014.
30. Markovic-Housley Z, Miglierini G, Soldatova L, Rizkallah PJ, Muller U, et al. (2000) Crystal structure of hyaluronidase, a major allergen of bee venom. Structure 8: 1025–1035.
31. Swanson DL, Vetter RS (2006) Loxoscelism. Clin Dermatol 24: 213–221.
32. Kalapothakis E, Araujo SC, de Castro CS, Mendes TM, Gomez MV, et al. (2002) Molecular cloning, expression and immunological properties of LiD1, a protein from the dermonecrotic family of *Loxosceles intermedia* spider venom. Toxicon 40: 1691–1699.
33. Chaim OM, Sade YB, da Silveira RB, Toma L, Kalapothakis E, et al. (2006) Brown spider dermonecrotic toxin directly induces nephrotoxicity. Toxicol Appl Pharmacol 211: 64–77.
34. da Silveira RB, Pigozzo RB, Chaim OM, Appel MH, Dreyfuss JL, et al. (2006) Molecular cloning and functional characterization of two isoforms of dermonecrotic toxin from *Loxosceles intermedia* (Brown spider) venom gland. Biochimie 88: 1241–1253.
35. da Silveira RB, Wille ACM, Chaim OM, Appel MH, Silva DT, et al. (2007) Identification, cloning, expression and functional characterization of an astacin-like metalloprotease toxin from *Loxosceles intermedia* (brown spider) venom. Biochem J 406: 355–363.
36. Appel MH, da Silveira RB, Chaim OM, Paludo KS, Silva DT, et al. (2008) Identification, cloning and functional characterization of a novel dermonecrotic toxin (phospholipase D) from brown spider (*Loxosceles intermedia*) venom. Biochim Biophys Acta 1780: 167–178.
37. Dietrich CP, Nader HB, Straus AH (1983) Structural differences of heparan sulfates according to the tissue and species of origin. Biochem Biophys Res Commun 111: 865–871.
38. Sambrook J, Russel DW (2001) Molecular cloning: a laboratory manual. New York, USA: Cold Spring Harbor Laboratory Press. 2100 p.
39. Burgess RR (2009) Refolding Solubilized Inclusion Body Proteins. Methods Enzymol 463: 259–282. doi: 10.1016/S0076-6879(09)63017-2.
40. Hofinger ESA, Spickenreither M, Oschmann J, Bernhardt G, Rudolph R, et al. (2007) Recombinant human hyaluronidase Hyal-1: insect cells versus *Escherichia coli* as expression system and identification of low molecular weight inhibitors. Glycobiology 17: 444–453.
41. Harlow E, Lane D (1988) Antibodies: a Laboratory Manual. New York, USA: Cold Spring Harbor Laboratory Press. 726 p.
42. Ribeiro RO, Chaim OM, da Silveira RB, Gremski LH, Sade YB, et al. (2007) Biological and structural comparison of recombinant phospholipase D toxins from *Loxosceles intermedia* (brown spider) venom. Toxicon 50: 1162–1174.
43. Bradford MM (1976) A rapid and sensitive method for the quantitation of microgram quantities of protein utilizing the principle of protein-dye binding. Anal Biochem 72: 248–254.
44. Towbin H, Staehelin T, Gordon J (1979) Electrophoretic Transfer of Proteins from Polyacrylamide Gels to Nitrocellulose Sheets - Procedure and Some Applications. Proc Natl Acad Sci U S A 76: 4350–4354.
45. Dietrich CP, Dietrich SM (1976) Electrophoretic Behavior of Acidic Mucopolysaccharides in Diamine Buffers. Anal Biochem 70: 645–647.
46. Chaim OM, da Silveira RB, Trevisan-Silva D, Ferrer VP, Sade YB, et al. (2011) Phospholipase-D activity and inflammatory response induced by brown spider dermonecrotic toxin: Endothelial cell membrane phospholipids as targets for toxicity. Biochim Biophys Acta1811: 84–96. doi: 10.1016/j.bbalip.2010.11.005.
47. Culling CFA, Allison RT, Barr WT (1985) Cellular Pathology Technique. London, England: Butterworths. 642 p.
48. Zhang L, Bharadwaj AG, Casper A, Barkley J, Barycki JJ, et al. (2009) Hyaluronidase Activity of Human Hyal1 Requires Active Site Acidic and Tyrosine Residues. J Biol Chem 284: 9433–9442. doi: 10.1074/jbc.M900210200.
49. Fernandes-Pedrosa MD, Junqueira-de-Azevedo IDM, Goncalves-de-Andrade RM, Kobashi LS, Almeida DD, et al. (2008) Transcriptome analysis of *Loxosceles laeta* (Araneae, Sicariidae) spider venomous gland using expressed sequence tags. BMC Genomics 9: 279. doi: 10.1186/1471-2164-9-279.
50. Gmachl M, Sagan S, Kreil G, Ketter S (1993) The Human Sperm Protein PH-20 has Hyaluronidase Activity. FEBS Lett 336: 545–548.
51. Ventura S, Villaverde A (2006) Protein quality in bacterial inclusion bodies. Trends Biotechnol 24: 179–185.
52. Jurgen B, Breitenstein A, Urlacher V, Buttner K, Lin HY, et al. (2010) Quality control of inclusion bodies in *Escherichia coli*. Microb Cell Fact 9: 41. doi: 10.1186/1475-2859-9-41.
53. Singh SM, Panda AK (2005) Solubilization and refolding of bacterial inclusion body proteins. J Biosci Bioeng 99: 303–310.
54. Dechavanne V, Barrillat N, Borlat F, Hermant A, Magnenat L, et al. (2011) A high-throughput protein refolding screen in 96-well format combined with design of experiments to optimize the refolding conditions. Protein Expr Purif 75: 192–203. doi: 10.1016/j.pep.2010.09.008.
55. Lenormand H, Deschrevel B, Tranchepain F, Vincent JC (2008) Electrostatic Interactions Between Hyaluronan and Proteins at pH 4: How Do They Modulate Hyaluronidase Activity. Biopolymers 89: 1088–1103. doi: 10.1002/bip.21061.
56. Rodriguez-Almazan C, Torner FJ, Costas M, Perez-Montfort R, de Gomez-Puyou MT, et al. (2007) The Stability and Formation of Native Proteins from Unfolded Monomers Is Increased through Interactions with Unrelated Proteins. PLoS One 2: e497.
57. Kumar K, Bhargava P, Roy U (2011) In Vitro Refolding of Triosephosphate Isomerase from *L. donovani*. Appl Biochem Biotechnol 164: 1207–1214. doi: 10.1007/s12010-011-9206-2.
58. Girish KS, Kemparaju K (2007) The magic glue hyaluronan and its eraser hyaluronidase: A biological overview. Life Sci 80: 1921–1943.
59. Girish KS, Kemparaju K (2011) Overlooked issues of snakebite management: time for strategic approach. Curr Top Med Chem 11: 2494–2508.
60. Kolarich D, Leonard R, Hemmer W, Altmann F (2005) The N-glycans of yellow jacket venom hyaluronidases and the protein sequence of its major isoform in *Vespula vulgaris*. FEBS J 272: 5182–5190.
61. Makris M, Spanoudaki N, Giannoula F, Chliva C, Antoniadou A, et al. (2009) Acute generalized exanthematous pustulosis (AGEP) triggered by a spider bite. Allergol Int 58: 301–303. doi: 10.2332/allergolint.08-CR-0035.
62. Pippirs U, Mehlhorn H, Antal AS, Schulte KW, Homey B (2009) Acute generalized exanthematous pustulosis following a *Loxosceles* spider bite in Great Britain. Br J Dermatol 161: 208–209. doi: 10.1111/j.1365-2133.2009.09234.x.
63. Anderson PC (1991) Loxoscelism Threatening Pregnancy - 5 Cases. American Am J Obstet Gynecol 165: 1454–1456.
64. Paludo KS, Biscaia SMP, Chaim OM, Otuki MF, Naliwaiko K, et al. (2009) Inflammatory events induced by brown spider venom and its recombinant dermonecrotic toxin: A pharmacological investigation. Comp Biochem Physiol C Toxicol Pharmacol 149: 323–333. doi: 10.1016/j.cbpc.2008.08.009.
65. Menzel EJ, Farr C (1998) Hyaluronidase and its substrate hyaluronan: biochemistry, biological activities and therapeutic uses. Cancer Lett 131: 3–11.
66. Shuster S, Frost GI, Csoka AB, Formby B, Stern R (2002) Hyaluronidase reduces human breast cancer xenografts in scid mice. Int J Cancer 102: 192–197.

67. Botzki A, Rigden DJ, Braun S, Nukui M, Salmen S, et al. (2004) L-ascorbic acid 6-hexadecanoate, a potent hyaluronidase inhibitor. X-ray structure and molecular modeling of enzyme-inhibitor complexes. J Biol Chem 279: 45990–45997.

68. Chao KL, Muthukumar L, Herzberg O (2007) Structure of human hyaluronidase-1, a hyaluronan hydrolyzing enzyme involved in tumor growth and angiogenesis. Biochemistry 46: 6911–6920.

ARTICLE
Journal of Cellular Biochemistry 114:2479–2492 (2013)

Journal of Cellular Biochemistry

Brown Spider Phospholipase-D Containing a Conservative Mutation (D233E) in the Catalytic Site: Identification and Functional Characterization

Larissa Vuitika,[1] Luiza Helena Gremski,[1,2] Matheus Regis Belisário-Ferrari,[1] Daniele Chaves-Moreira,[1,3] Valéria Pereira Ferrer,[1] Andrea Senff-Ribeiro,[1] Olga Meiri Chaim,[1] and Silvio Sanches Veiga[1]*

[1]*Department of Cell Biology, Federal University of Paraná, Curitiba, Paraná, Brazil*

[2]*Department of Clinical Pathology, Clinical Hospital, Federal University of Paraná, Curitiba, Paraná, Brazil*

[3]*Department of Biophysics and Biophysical Chemistry School of Medicine, The Jonhs Hopkins University, Baltimore, Maryland*

ABSTRACT

Brown spider (*Loxosceles* genus) bites have been reported worldwide. The venom contains a complex composition of several toxins, including phospholipases-D. Native or recombinant phospholipase-D toxins induce cutaneous and systemic loxoscelism, particularly necrotic lesions, inflammatory response, renal failure, and hematological disturbances. Herein, we describe the cloning, heterologous expression and purification of a novel phospholipase-D toxin, LiRecDT7 in reference to six other previously described in phospholipase-D toxin family. The complete cDNA sequence of this novel brown spider phospholipase-D isoform was obtained and the calculated molecular mass of the predicted mature protein is 34.4 kDa. Similarity analyses revealed that LiRecDT7 is homologous to the other dermonecrotic toxin family members particularly to LiRecDT6, sharing 71% sequence identity. LiRecDT7 possesses the conserved amino acid residues involved in catalysis except for a conservative mutation (D233E) in the catalytic site. Purified LiRecDT7 was detected as a soluble 36 kDa protein using anti-whole venom and anti-LiRecDT1 sera, indicating immunological cross-reactivity and evidencing sequence-epitopes identities similar to those of other phospholipase-D family members. Also, LiRecDT7 exhibits sphingomyelinase activity in a concentration dependent-manner and induces experimental skin lesions with swelling, erythema and dermonecrosis. In addition, LiRecDT7 induced a massive inflammatory response in rabbit skin dermis, which is a hallmark of brown spider venom phospholipase-D toxins. Moreover, LiRecDT7 induced in vitro hemolysis in human erythrocytes and increased blood vessel permeability. These features suggest that this novel member of the brown spider venom phospholipase-D family, which naturally contains a mutation (D233E) in the catalytic site, could be useful for future structural and functional studies concerning loxoscelism and lipid biochemistry. Highlights: 1- Novel brown spider phospholipase-D recombinant toxin contains a conservative mutation (D233E) on the catalytic site. 2-LiRecDT7 shares high identity level with isoforms of *Loxosceles* genus. 3-LiRecDT7 is a recombinant protein immunodetected by specific antibodies to native and recombinant phospholipase-D toxins. 4-LiRecDT7 shows sphingomyelinase-D activity in a concentration-dependent manner, but less intense than other isoforms. 5-LiRecDT7 induces dermonecrosis and inflammatory response in rabbit skin. 6-LiRecDT7 increases vascular permeability in mice. 7-LiRecDT7 triggers direct complement-independent hemolysis in erythrocytes. J. Cell. Biochem. 114: 2479–2492, 2013.

KEY WORDS: BROWN SPIDER; VENOM; DERMONECROTIC TOXIN; PHOSPHOLIPASE-D; CLONING; RECOMBINANT PROTEIN

The authors declare no conflict of interest.

GenBank data deposition information for *L. intermedia* cDNA clone: LiRecDT7, GenBank accession no. KC237286.

Grant sponsor: CAPES; Grant sponsor: CNPq; Grant sponsor: Fundação Araucária-PR; Grant sponsor: Secretaria de Estado de Ciência, Tecnologia e Ensino Superior do Paraná (SETI-PR), Brazil.

*Correspondence to: Silvio Sanches Veiga, Department of Cell Biology, Federal University of Paraná, Jardim das Américas, Curitiba, Paraná 81531-990, Brazil. E-mail: veigass@ufpr.br

Manuscript Received: 12 March 2013; Manuscript Accepted: 7 May 2013

Accepted manuscript online in Wiley Online Library (wileyonlinelibrary.com): 4 June 2013

DOI 10.1002/jcb.24594 • © 2013 Wiley Periodicals, Inc.

Spiders of the *Loxosceles* genus are commonly known as brown spiders based on their body colors that range from fawn to dark brown. At present, 103 species of spiders from the *Loxosceles* genus have been described and are distributed worldwide [Platnick, 2012]. There are 12 species of *Loxosceles* genus spiders in Brazil [Gonçalves-de-Andrade et al., 2012]. Loxoscelism is the term used to describe the lesions caused from bites by *Loxosceles* genus spiders [da Silva et al., 2004; Appel et al., 2005; Chaim et al., 2011a]. Traditionally, loxoscelism is divided in two clinical conditions: cutaneous and systemic loxoscelism. Cutaneous loxoscelism refers to the typical skin lesion with dermonecrosis, edema, erythema and gravitational spreading that appears after most accidents. Systemic loxoscelism is less common than the cutaneous form, but is responsible for complications following accidents, which might include hematological disturbances, such as thrombocytopenia, disseminated intravascular coagulation, hemolytic anemia, and renal failure [Futrell, 1992; da Silva et al., 2004; Isbister and Fan, 2011].

The volume of venom inoculated by *Loxosceles* genus spiders is typically minute (some microliters) and enriched in proteins of low molecular mass (20–45 kDa). To date, a great number of brown spider venom toxins have been identified in different *Loxosceles* species, including hyaluronidases [Young and Pincus, 2001; Barbaro et al., 2005; da Silveira et al., 2007a; dos Santos et al., 2009], metalloproteases from the astacin family [da Silveira et al., 2007b; Trevisan-Silva et al., 2010], serine proteases [Veiga et al., 2000; Gremski et al., 2010], translationally controlled tumor protein (TCTP) [Sade et al., 2012], insecticidal peptides of the ICK family [Gremski et al., 2010], serine protease inhibitors [Gremski et al., 2010], and members of the phospholipase-D family, also known as dermonecrotic toxins, based on their biological activity [Kalapothakis et al., 2007; Appel et al., 2008; Binford et al., 2009].

Previous studies using native dermonecrotic toxins purified from crude venom have biochemically characterized this toxin as a sphingomyelinase based on its ability to hydrolyze sphingomyelin into choline and ceramide-1-phosphate [Futrell, 1992]. Using recombinant isoforms of dermonecrotic toxins from different *Loxosceles* species, it has recently been postulated that these molecules are phospholipase-D enzymes based on their abilities to hydrolyze other synthetic phospholipids, such as lysophosphatidylcholine, lysophosphatidylinositol, lysobisphosphatidic acid, cyclic phosphatidic acid, and lysoplatelet-activating factor [Lee and Lynch, 2005; Chaim et al., 2011b]. The final release of lipid metabolites such as ceramide-1-phosphate (C1P) from sphingomyelin or lysophosphatidic acid from a lysophospholipid was already described for *Loxosceles* phospholipases-D [van Meeteren et al., 2004; Chalfant and Spiegel, 2005; Lee and Lynch, 2005]. These metabolites are bioactive mediators that play a major role in complex signaling pathways that control several cellular processes and also in various pathophysiologic processes [Hannun, 1994; Anliker and Chun, 2004; Moolenaar et al., 2004]. Thus, these lipid mediators could induce toxicity by activating signaling pathways involved with a variety of pathophysiologic changes [Chaim et al., 2011b].

The phospholipase-D toxins in *Loxosceles* genus spider venoms represent the most biologically and biochemically characterized brown spider venom components and various isoforms of these molecules have previously been reported for different species [Chaim et al., 2011a]. Four biochemically related isoforms of phospholipase-D in a native purified dermonecrotic toxin have been reported in *L. reclusa* venom [Futrell, 1992]. The results from N-terminal sequence studies of *L. boneti* venom have revealed three different isoforms of phospholipase-D in this species [Ramos-Cerrillo et al., 2004]. Similarly, based on proteomic analyses such as two-dimensional electrophoresis, N-terminal amino acid sequencing and mass spectrometry, the presence of at least eleven isoforms of phospholipase-D have been reported for *L. gaucho* venom [Machado et al., 2005]. Six isoforms of phospholipase-D have been identified in *L. intermedia* venom using molecular biology techniques such as cloning, heterologous expression, amino acid alignment and phylogenetic studies [Chaim et al., 2006; da Silveira et al., 2006, 2007c; Appel et al., 2008]. Additional studies have also described multiple members of the phospholipase-D family in other *Loxosceles* venoms, and these isoforms differ in various features, such as their biological activity and substrate specificity [Lee and Lynch, 2005; Kalapothakis et al., 2007; Catalán et al., 2011; Chaim et al., 2011b]. The transcriptome analysis of the venom gland of *L. intermedia* revealed that phospholipases-D represent 20.2% of the total toxin-encoding transcripts present in the gland [Gremski et al., 2010]. An inter-species family of similar phospholipase-D toxins has been postulated, and the noxious effects of *Loxosceles* spp. whole venom are due to the family synergism of these related toxins [Kalapothakis et al., 2007]. Many studies indicate that the gene family of venom phospholipase-D toxins has undergone frequent multiple duplications and occasional functional evolution [Binford et al., 2009].

Here, we describe the cloning, heterologous expression, purification, and functional evaluation of a novel phospholipase-D isoform from a cDNA library of *L. intermedia* venom gland. This novel isoform has conservative the amino acid residues involved in the catalysis and metal ion coordination that are important for phospholipase activity, as previously reported for the other members of the family [Murakami et al., 2006; de Giuseppe et al., 2011], except for a conservative mutation (D233E) in the catalytic site. Taken together, these results strengthen the concept of a gene family encoding different phospholipase-D toxins in the venom of *L. intermedia*. Here, we present evidence of a novel isoform and illustrate the features of a dermonecrotic toxin with a natural mutation in an amino acid residue in the catalytic site.

METHODS

REAGENTS

Whole venom from *L. intermedia* was extracted from spiders captured in the wild with the authorization of the Brazilian Governmental Agency "Instituto Chico Mendes de Conservação da Biodiversidade" number 29801-1, according to [Feitosa et al., 1998]. Polyclonal antibodies to *L. intermedia* crude venom toxins and phospholipase-D "dermonecrotic toxin" (LiRecDT1) were produced in rabbits as previously described [Chaim et al., 2006]. Evans Blue dye was purchased from Vetec (São Paulo, Brazil). NaCl, KCl, $CaCl_2$, Na_2HPO_4, KH_2PO_4, Na_2PO_4, NaH_2PO_4, Imidazole, Lysozyme, and Ágar XLT4 were purchased from Merck (Darmstadt, Germany). Tryptone Type I, Yeast Extract (Himedia, Mumbai, India). Chloramphenicol and

Ampicillin Trihydrate were purchased from USB Corporation (Cleveland, OH). Tris and Sucrose were purchased from Bio-Rad (Hercules, CA) and Sigma–Aldrich (St. Louis, MO), respectively. Xylasine and Ketamine were purchased from Rhobifarma (Hortolândia, São Paulo, Brazil).

cDNA CLONING

The partial cDNA sequence for the dermonecrotic toxin isoform 7 described herein was isolated from a previously constructed venom gland cDNA library [Gremski et al., 2010]. Briefly, venom gland mRNAs were purified from total RNA using a magnetic separation kit, PolyATtract mRNA Isolation System III (Promega Corporation, Madison, WI). A directional *L. intermedia* venom gland cDNA library was constructed using a Creator SMART cDNA Library Construction Kit (BD Biosciences Clontech, Mountain View, CA). The first strand of cDNA was synthesized from purified mRNA, and the second strand was obtained through long distance PCR (LD-PCR), according to the manufacturer's instructions. The cDNA was size fractionated via chromatography to avoid contaminating the library with short length sequences. Competent *Escherichia coli* DH5α cells were transformed with the cDNA library plasmids to amplify the cDNA. The transformants were selected on LB (Luria-Bertani) agar plates containing 34 μg/ml chloramphenicol, and more than 20,000 colonies were obtained.

AMPLIFICATION OF THE 5′ END OF THE cDNA

To obtain the complete 5′ end of phospholipase-D isoform 7 cDNA, a 5′RACE (Rapid Amplification of cDNA Ends) protocol was performed according to Sambrook and Russell [2001], with some modifications. Approximately 1 μg of total RNA was obtained from *L. intermedia* venom glands. The first-strand cDNA was synthesized using the gene-specific reverse primer R1 (5′-CGAACACAACTAGGGT-CAGTTCTG-3′) and Improm-II Reverse Transcriptase (Promega, Madison, WI) according to the manufacturer's instructions. The cDNA was recovered through ethanol precipitation in the presence of ammonium acetate and was subsequently poly (A)-tailed with terminal deoxynucleotidyl transferase (Fermentas, Hanover, MD) according to the manufacturer's instructions. The modified cDNA was PCR amplified with the (dT) 17-adaptor primer (5′-CGGTACCATG-GATCCTCGAGTTTTTTTTTTTTTTTT-3′) and the nested gene-specific reverse primer R2 (5′-CTTGTGACACCACCTTCTGCAATC-3′) using Pfu DNA polymerase (Fermentas). The PCR product was gel-purified using a PerfectPrep Gel Cleanup Kit (Eppendorf, Hamburg, Germany) according to the manufacturer's instructions and was sequenced on both strands using an ABI Prism BigDye Terminator Cycle Sequencing Ready Reaction Kit on a DNA 3500 Genetic Analyzer automatic sequencer (Applied Biosystems, Warrington, UK). The putative protein product from the sequenced cDNA was used to search the GenBank protein databases at NCBI.

RECOMBINANT PROTEIN EXPRESSION

The cDNAs encoding putative mature phospholipase-D isoform 7 (LiRecDT7) were PCR amplified using primers designed to contain *Nde*I (Fermentas) restriction sites at the 5′ ends (forward primers) and *Bam*HI (Fermentas) sites at the 3′ ends (reverse primers). The PCR products were digested with *Nde*I and *Bam*HI restriction enzymes and subcloned into the pET-14b plasmid (Novagen, Madison, USA) digested with the same enzymes. The recombinant construct was expressed as a fusion protein, with a 6× His-Tag at the N-terminus and a 13 amino acid linker, including a thrombin site between the 6× His-Tag and the mature protein. The expression construct was transformed into *E. coli* SHuffle T7 Express *lysY* cells (New England Biolabs, Ipswich, MA, UK) and plated on LB plates containing 100 μg/ml ampicillin. Single colonies of LiRecDT7 construct were inoculated into LB broth (100 μg/ml ampicillin) and grown overnight at 30°C. This culture was diluted 1:50 into 2 L fresh LB broth/ampicillin and incubated at 30°C until the $OD_{600\,nm} = 0.5$. Recombinant expression was induced with the addition of 0.05 mM IPTG (isopropyl β-D-thiogalactoside; Fermentas) and cells were incubated for 4 h at 30°C. The cells were harvested through centrifugation (4,000*g*, 7 min, 4°C), resuspended in 40 ml of extraction buffer (50 mM sodium phosphate pH 8.0, 500 mM NaCl, 10 mM imidazole, and 1 mg/ml lysozyme) and frozen overnight at −20°C.

PROTEIN PURIFICATION

The cells were thawed and disrupted through mechanical lysis. The lysed materials were centrifuged (9,000*g*, 30 min, 4°C), and the supernatants were incubated with 500 μl of Ni^{2+}-NTA beads for 1 h at 4°C. The suspensions were loaded onto a column and the packed gel was washed with a buffer containing 50 mM sodium phosphate, pH 8.0, 500 mM NaCl and 30 mM imidazole. The recombinant protein was eluted with 2 ml of elution buffer (50 mM sodium phosphate pH 8.0, 500 mM NaCl, and 250 mM imidazole), and the fractions were collected and analyzed using 12.5% SDS–PAGE under β-mercaptoethanol reducing conditions. The fractions were pooled and dialyzed against phosphate-buffered saline (PBS).

MOLECULAR MODELING OF THE LiRecDT7 AND STRUCTURAL ANALYSIS OF PROTEINS USING BIOINFORMATICS TOOLS

We used the SWISS-MODEL [Kiefer et al., 2009] software (http://swissmodel.expasy.org/) to construct a prediction of the three-dimensional structure of LiRecDT1 and LiRecDT7. The protein used as a model for analysis of the predictions was LiRecDT1 (PDB code: 3RLH), as this toxin has been crystallized and its 3D structure has been solved [de Giuseppe et al., 2011]. The production of the figure presented in the results was produced with the software Open Astex Viewer 3.0 (http://openastexviewer.net/web/), a program for molecular visualization.

SPHINGOMYELINASE-D ACTIVITY ASSAY

The Sphingomyelinase-D activity of purified LiRecDT7 was measured using an Amplex Red Assay Kit (Molecular Probes, Eugene, USA) through the analysis of the sphingomyelinase-D activity of recombinant toxin. In this assay, sphingomyelinase-D activity was monitored using 10-acetyl-3,7-dihydroxyphenoxazine (Amplex Red reagent), a sensitive fluorogenic probe for H_2O_2 [Chaim et al., 2011b]. First, sphingomyelinase-D hydrolyzes sphingomyelin to yield C1P and choline. Choline is then oxidized to betaine and H_2O_2 through coline oxidase. Finally, H_2O_2, in the presence of horseradish peroxidase, reacts with the Amplex reagent at 1:1 stoichiometry to generate the highly fluorescence product, resorufin. LiRecDT1 (positive control) or recombinant LiRecDT7 (5, 10, and 20 μg, in

five trials) were added to the Amplex Red reagent mixture. The reaction tubes were incubated at 37°C for 30 min, and the fluorescence was measured in a microplate fluorimeter (Tecan Infinite® M200, Männedorf, Switzerland) using excitation at 540 nm with emission detection at 570 nm.

DETERMINATION OF HEMOLYTIC ACTIVITY

The hemolysis assay was performed as previously described [Chaim et al., 2011b; Chaves-Moreira et al., 2011]. Washed red blood cells (10^8 cells) were added to each Eppendorf tube containing the appropriate concentrations of LiRecDT7 (0.025, 0.25, 2.5, and 25 μg/ml) in Tris buffer sucrose (TBS; 250 mM sucrose, 10 mM Tris/HCl, pH 7.4 and 280 mOsm\kg H_2O) containing 1 mM $CaCl_2$. For this assay, the experiments were performed in pentaplicate along with negative (in presence of the appropriate amount of TBS with 1 mM $CaCl_2$) and positive (red blood cells in 0.1% v/v Triton X-100) controls. After 24 h of incubation with gentle agitation, the controls and samples were centrifuged (refrigerated Eppendorf microfuge) for 3 min at 1,600 rpm, and the absorbance values for the supernatants were immediately measured at 550 nm (Meridian ELx 800, Auto Reader Diagnostics, Inc., USA). The absorbance values were converted to percent hemolysis using the absorbance values of the positive control as 100% lysis. Blood collection from voluntary students was authorized through agreement of the ethical committee of the Federal University of Paraná.

ANIMALS

Adult Swiss mice (25–30 g) and adult rabbits weighting approximately 3 kg from the Central Animal House of the Federal University of Parana were used for the in vivo experiments with whole venom and recombinant toxins. All procedures involving animals were performed in accordance with "Brazilian Federal Laws," following Ethical Subcommittee on Research Animal Care Agreement number 565 of the Federal University of Parana.

IN VIVO STUDIES ON RABBITS

For the evaluation of the dermonecrotic effect, 10 μg of purified recombinant LiRecDT7 diluted in PBS was injected intradermally into a shaved area of rabbit skin. Dermonecrosis was assessed at 3, 6, and 24 h after injection. For a negative control to assure that bacterium constituent contamination during purification did not influence the results, we used purified recombinant green fluorescent protein (GFP) obtained under the same conditions for LiRecDT7. Rabbits were used in experiments for dermonecrosis because this animal model reproduces skin lesions consistent with those observed in accidents with humans [da Silva et al., 2004]. The experiments were repeated twice for each sample.

HISTOLOGICAL METHODS FOR LIGHT MICROSCOPY

Rabbit skin was collected from animals anesthetized with ketamine and xylazine, and subsequently fixed in "ALFAC" (ethanol absolute 85%, formaldehyde 10%, and glacial acetic acid 5%) for 16 h at room temperature. After fixation, the samples were dehydrated in a graded series of ethanol before paraffin embedding (for 2 h at 58°C). Thin sections (4 μm) were processed for histology. The tissue sections were stained with hematoxylin and eosin (H&E) as previously described [Chaim et al., 2006; da Silveira et al., 2006]. The images were obtained using an Axio Imager Z2 microscope (Carl Zeiss, Jena, DE) equipped with a motorized scanning module VSlider (MetaSystems, Altlussheim, DE).

MEASUREMENT OF VASCULAR PERMEABILITY

The changes in capillary permeability were based on the leakage of plasma protein-bound dye into the extravascular compartment of the skin [Appel et al., 2008]. Evans Blue dye diluted in saline was administered intravenously (30 mg/kg of mice) 5 min prior to sample injections. Whole venom and the recombinant toxins LiRecDT1 and LiRecDT7 (10 μg) were injected intradermally into the dorsal skin of mice ($n = 5$ per treatment). After 30 min, the animals were anesthetized using ketamine and acepromazine, sacrificed and the dorsal skin was removed for the visualization of dye extravasation. For the negative control, animals received only a saline injection without venom toxins. Mice were used because this animal model does not develop dermonecrosis and local hemorrhage following brown spider venom exposure, an event that could mask the interpretation of vascular permeability.

GEL ELECTROPHORESIS AND IMMUNOBLOTTING

Protein content was determined using the Coomassie Blue method (BioRad, Hercules, CA). For protein analysis, 12.5% SDS–PAGE under reduced conditions. For immunoblotting, the proteins were transferred to nitrocellulose filters and immunostained polyclonal with antibodies raised against phospholipase-D isoform 1 (LiRecDT1) or against whole venom toxins. The molecular mass markers were acquired from Sigma.

STATISTICAL ANALYSIS

The statistical analyses were performed using analysis of variance (ANOVA) with a post hoc Tukey test using GraphPad InStat program version 5.00 for Windows XP. Statistical significance was considered when $P \leq 0.05$.

RESULTS

CLONING OF A NOVEL PHOSPHOLIPASE-D ISOFORM FROM *L. intermedia* VENOM GLAND

A partial cDNA encoding for a novel phospholipase-D isoform was obtained through screening clones of a cDNA library of *L. intermedia* venom gland [Gremski et al., 2010]. The complete cDNA sequence was obtained using RT-PCR in a 5′ RACE protocol. The putative protein product from this cDNA was referred to as LiRecDT7 (from *L. intermedia* recombinant dermonecrotic toxin). The other isoforms previously described were the following: LiRecDT1 [Chaim et al., 2006], LiRecDT2 and LiRecDT3 [da Silveira et al., 2006], LiRecDT4 and LiRecDT5 [da Silveira et al., 2007c], and LiRecDT6 [Appel et al., 2008]. The complete cDNA sequence of LiRecDT7 comprises 1,200 bp with a single ORF coding for 300 amino acids with a hydrophobic and putative signal peptide of 18 amino acids (Fig. 1). The calculated molecular mass of the predicted mature protein for LiRecDT7 was 34.4 kDa, with a pI of 5.94.

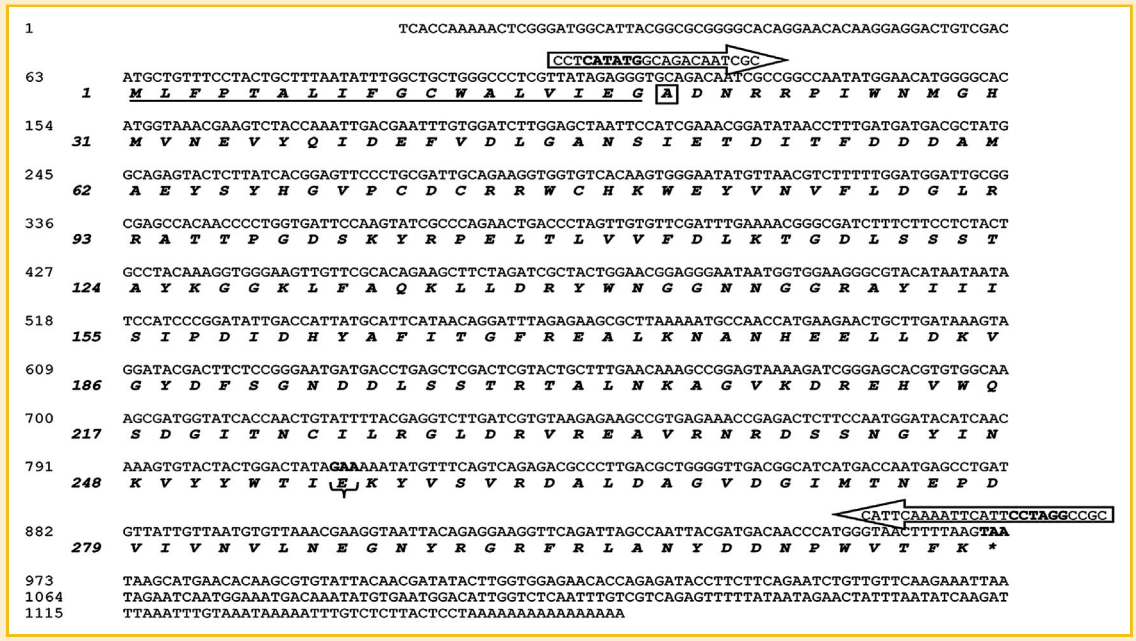

Fig. 1. Molecular cloning of a novel phospholipase-D toxin from *L. intermedia* venom gland cDNA library. Nucleotide and deduced amino acid sequences of cloned phospholipase-D. In the protein sequence, the predicted signal peptide is underlined. The arrows show the annealing positions for the primers used for subcloning into the expression vector, and the restriction sites are highlighted in bold. The alanine in the box indicates the first amino acid of the mature protein with 282 amino acids. The nucleotide and amino acid residue for the conservative substitution for LiRecDT7 (D233E) is highlighted in the bracket. The asterisk corresponds to the stop codon TAA.

MULTIPLE ALIGNMENT ANALYSIS OF THE cDNA-DEDUCED AMINO ACID SEQUENCE AND THE SIMILARITY OF LiRecDT7 WITH OTHER PHOSPHOLIPASE-D TOXIN FAMILY MEMBERS

The BLAST GenBank database search revealed that LiRecDT7 has structural similarity to other LiRecDT family members. The overall identity of LiRecDT7 is approximately 63% with LiRecDT1. From all *L. intermedia* phospholipases-D described, LiRecDT7 is more similar to LiRecDT6, sharing 71% sequence identity. When compared with the other *L. intermedia* dermonecrotic toxin isoforms, LiRecDT7 shows 64% sequence identity to LiRecDT2, 45% identity to LiRecDT3, 60% identity to LiRecDT4, and 46% identity to LiRecDT5 (Fig. 2A). LiRecDT7 also shares 58% identity with LoxTox i5 (EF535254), whose sequence has been previously described [Kalapothakis et al., 2007]. A similarity analysis (Fig. 2B) of these seven phospholipase-D isoform toxins and the cloned cDNAs of other brown spider dermonecrotic toxins revealed that LiRecDT7 was most identical to the *L. hirsuta* toxin (GenBank accession number ACN48948; 91%). These data are consistent with the idea of an intra and inter-species family of brown spider venom phospholipases-D, now containing a novel member.

EXPRESSION, PURIFICATION, AND IMMUNOLOGICAL RELATIONSHIP OF LiRecDT7 TO OTHER BROWN SPIDER MEMBERS

LiRecDT7 was expressed using the N-terminal tag of six histidine residues. Expression experiments were performed in *E. coli* SHuffle T7 Express *lysY* cells. The expression of recombinant protein was optimal when induced for 4 h with 0.05 mM of IPTG. Recombinant phospholipase-D was purified using the soluble fraction of cell lysates under native conditions using Ni^{2+} NTA agarose-chelating chromatography to obtain a 200 μg/L sample of the purified recombinant protein. The SDS–PAGE mobility of the purified recombinant protein, reduced through β-mercaptoethanol treatment, was 36 kDa (Fig. 3A). Differences between the deduced molecular mass and SDS-electrophoretic mobility of LiRecDT7 resulted from the 6× His-tag fusion peptide. Immunoblot analysis using a LiRecDT1 specific antibody and antibodies for whole venom toxins established an immunological relationship between purified recombinant LiRecDT7 and native venom phospholipases-D (dermonecrotic toxins) and LiRecDT1 (Fig. 3B). Both antibodies reacted with purified LiRecDT7, demonstrating that whole venom contains proteins similar to this recombinant toxin, and LiRecDT7 contains similar sequence/epitopes and antigenic cross-reactivity with LiRecDT1, the prototype of this family of toxins.

MOLECULAR MODELING OF LiRecDT7

To model the 3D structure of LiRecDT7, the isoform LiRecDT1 was chosen as a template because the crystallized protein in Protein Data Bank (PDB) shows more identity with the novel isoform [de Giuseppe et al., 2011]. In addition, LiRecDT1 was used as a basis for comparison in all assays performed in the present work. As the images displayed in Figure 4 demonstrate, the overall structure of the novel isoform closely resembles the LiRecDT1 general outline, despite the differences observed in the primary structure. The presence and location of the disulfide bridges (Cys51–Cys57 and Cys53–Cys201), the Mg^{2+} binding site and the two catalytic histidine residues (His12 and His47) are conserved in LiRecDT7 model, which are components of the active-site pocket of spider venom PLDs [de Giuseppe et al., 2011].

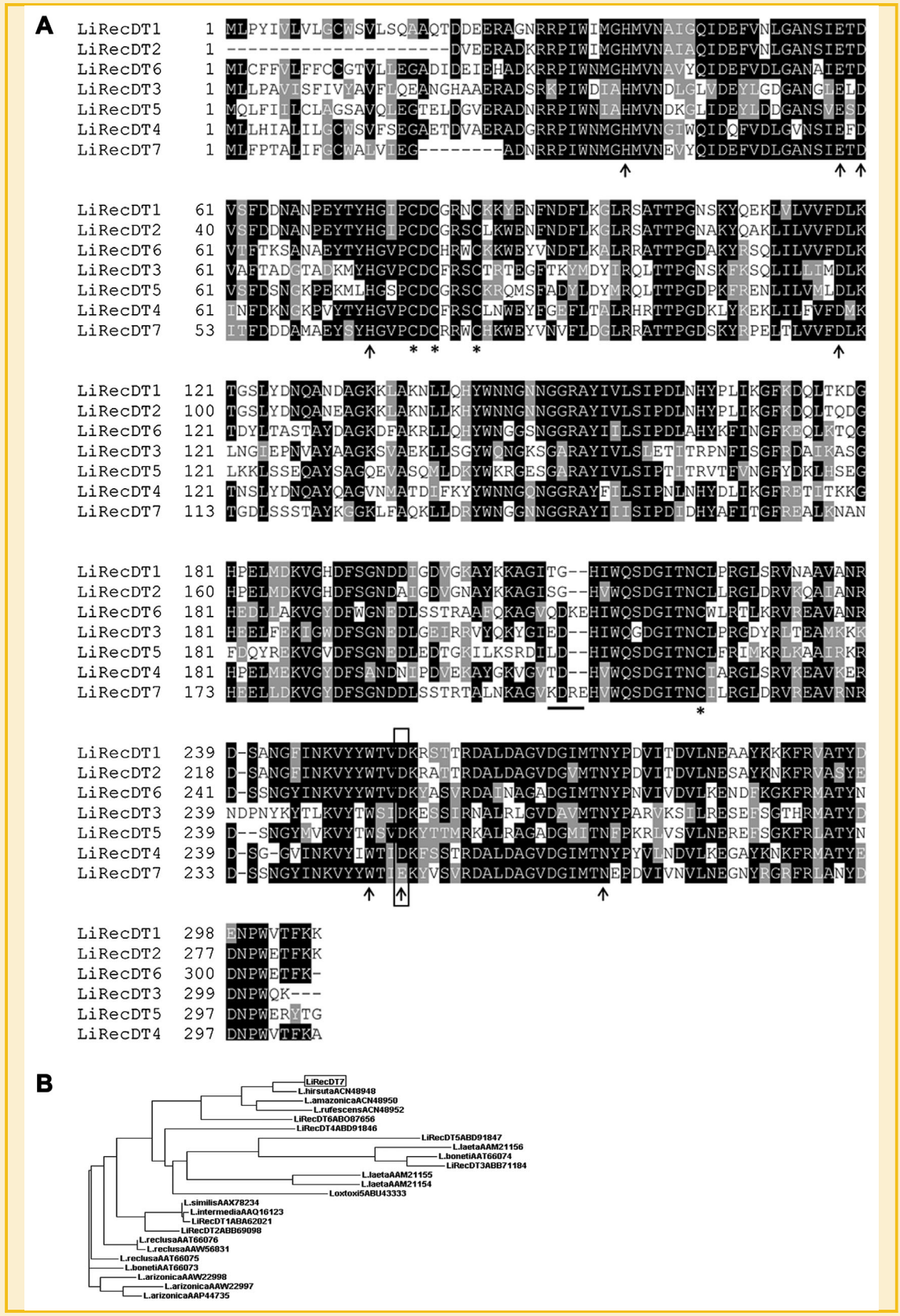

Fig. 2. Multiple alignment analysis of the cDNA-deduced amino acid sequence and the similarity relationship of described phospholipase-D with other phospholipase-D toxin family members from brown spider venoms. The sequences were aligned using the CLUSTAL W program (www.ebi.ac.uk/CLUSTAL). A: The black shaded regions show amino acid identity, the gray shaded regions show conservative substitutions, and the arrows point to amino acid residues of catalytic site of sphingomyelinases-D. The asterisks show cysteine residues. The conservative D223E substitution of LiRecDT7 is featured in the box. The line indicates the amino acids residues of the prominent loop. B: Similarity cladogram of the cloned phospholipase-D toxin members based on sequence alignment from GenBank data. The tree was constructed using the CLUSTAL program as described above. LiRecDT7 is highlighted in the box.

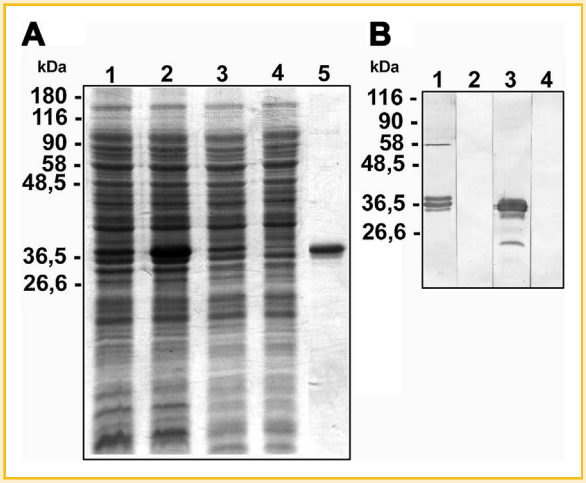

Fig. 3. Expression, purification, and immunological relationship of recombinant dermonecrotic toxin LiRecDT7 with other brown spider phospholipase-D members. A: The expression and purification of recombinant toxin was analyzed using 12.5% SDS–PAGE under reducing conditions and Coomassie blue dye staining. Lane 1 depicts *E. coli* SHuffle T7 Express *lysY* cells before 4 h of induction with 0.05 mM IPTG. Lane 2 shows the proteins of cells after induction with 0.05 mM IPTG. Lanes 3 and 4 depict the supernatant obtained through freeze, thawing and mechanical lysis in extraction buffer before and after affinity chromatography using a Ni^{2+}-NTA column, respectively. Lane 5 shows purified recombinant protein LiRecDT7. The molecular protein mass standards are shown on the left. B: Crude venom (lanes 1 and 2) and purified recombinant toxin LiRecDT7 (lanes 3 and 4; 2.5 μg) were separated using 12.5% SDS–PAGE under reducing conditions, transferred onto nitrocellulose membranes that were incubated with polyclonal antibodies against LiRecDT1 (lane 1) or polyclonal antibodies against whole venom toxins (lane 3). Lanes 2 and 4 indicate reactions in the presence of pre-immune serum (control for antibody specificity). The molecular mass markers are shown on the left.

However, it is possible to observe a significant variation in the contour of the loop located just behind the variable loop of both models. In the LiRecDT7 model, this loop is more prominent (directed toward the surface of the protein) compared with that in LiRecDT1, where this loop, although still prominent, is more positioned in the interior of the protein. As presented in Figure 4, this condition can be easily detected in LiRecDT7, as this loop follows the beginning of the near helix, while in LiRecDT1 this loop follows a different path, away from the near helix and toward the interior of the molecule.

In addition, in both models residue 233 is highlighted, illustrating the difference in the structures of aspartic acid (Asp) and glutamic acid (Glu); it is clear that Glu (LiRecDT7) has a bulkier side chain compared with to Asp (LiRecDT1), which protrudes towards the flexible loop.

SPHINGOMYELINASE AND HEMOLYTIC ACTIVITIES FOR LiRecDT7

To further assess the recombinant molecule functionality, LiRecDT7 was tested for its activity as a sphingomyelinase-D because the native brown spider dermonecrotic toxin and other LiRecDT's family members have sphingomyelinase-D activity. The sphingomyelinase activity was measured using an Amplex-R-Red Sphingomyelinase Assay Kit (as described in material and methods). LiRecDT1 (10 μg) was used as a positive control, and PBS was used as a negative control. Samples of 5, 10, and 20 μg of LiRecDT7 were tested in three subjects. As shown in Figure 5A, the recombinant LiRecDT7 toxin exhibited sphingomyelinase-D activity in a concentration-dependent manner. Nevertheless, as the graph depicts, LiRecDT7 exhibited lower sphingomyelinase-D activity than LiRecDT1.

In addition, we reported the hemolytic activity for *L. intermedia* recombinant phospholipases-D [Chaves-Moreira et al., 2009, 2011]. This hemolytic activity is attributed to the hydrolytic activity of toxins on erythrocyte membrane phospholipids, as toxins induce different degrees of hemolysis, which is proportional to sphingomyelinase-D activity. LiRecDT1H12A, a molecule without sphingomyelinase-D activity, also exhibits residual hemolytic activity [Chaves-Moreira et al., 2011]. Herein, we provide additional data suggesting the direct hemolysis activity induced though brown spider venom phospholipase-D. Figure 5B shows the hemolysis in human red blood cells incubated in serum-free medium containing different amounts of LiRecDT7 at 37°C. As observed, hemolysis occurred in a dose-dependent manner, indicating the direct hemolytic activity of LiRecDT7 in human erythrocytes.

SKIN LESIONS AND INFLAMMATORY RESPONSE EVOKED BY RECOMBINANT LiRecDT7

Because brown spider venom phospholipases-D possess dermonecrotic and inflammatory activities [da Silva et al., 2004; Appel et al., 2005; Chaim et al., 2011b], we evaluated the functionality of recombinant LiRecDT7. For this purpose, LiRecDT7 (10 μg) was injected intradermally into shaved rabbit skin. As a negative control, we used recombinant GFP (devoid of dermonecrotic activity), which was expressed and purified under the same conditions as those used for LiRecDT7. The macroscopic lesions were assessed 3, 6, and 24 h after injection, and the tissue samples were collected and histologically analyzed using a light microscope at 24 h after toxin exposure (Fig. 6). The animals that received recombinant toxin LiRecDT7 showed lesions with a deep erythema, a diffuse edema surrounding the lesion and a remarkable hemorrhage after 6 h. After 24 h, these signs were exacerbated, and an area of necrosis was observed surrounding the injection site. Gravitational spreading was not observed after the inoculation of LiRecDT7 compared with the clear spreading triggered by whole venom and LiRecDT1. The histopathological findings of skin biopsies after recombinant toxin exposure (LiRecDT7) showed a massive inflammatory response (Fig. 7C), with inflammatory cells (neutrophil leukocytes; Fig. 7D) diffusely spread within the dermis. Figure 7A,B shows panoramic views of sections of negative control and LiRecDT7, respectively, and clearly illustrate the edema triggered using the recombinant toxin, as evidenced by the length of the skin structures. As observed, the panoramic view of the tissue section after LiRecDT7 exposure is wider compared with that of the control, indicating an event induced through tissue edema. In addition, in Figure 7E it is possible to observe the disorganization of collagen fibers in the dense connective tissue inside the dermis, which also indicates edema. The images also depict areas of necrosis, including the degeneration of blood vessel walls (Fig. 7F,G). We also detected thrombus formation into dermal blood vessels after LiRecDT7 inoculation (Fig. 7H). Thus, the recombinant toxin LiRecDT7 is functional and a member of the family of dermonecrotic toxins.

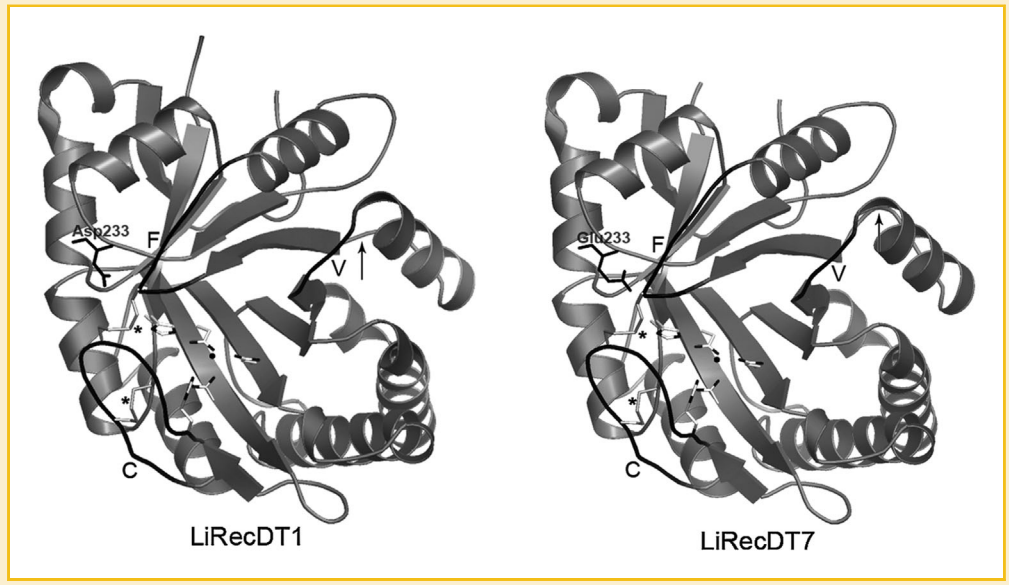

Fig. 4. Molecular modeling of LiRecDT1 and LiRecDT7. We used beta SWISS-MODEL to build a prediction of the three-dimensional structure of LiRecDT1 and LiRecDT7. Asp 233 in LiRecDT1 and Glu233 in LiRecDT7 are indicated. The black arrow indicates the significant variation of the loops in LiRecDT7 and LiRecDT1. The catalytic (C), variable (V), and flexible (F) loops are indicated. The asterisks indicate the disulfide bridges. The main amino acid residues involved in the coordination of the Mg^{2+} (represented by a sphere) in the catalytic site are highlighted (His12, Asp 32, Glu34, and His47).

RECOMBINANT TOXIN LiRecDT7 INCREASED VASCULAR PERMEABILITY

The data obtained from previous literature reported that brown spider phospholipase-D toxins increase vessel permeability [da Silveira et al., 2006, 2007c]. To examine whether LiRecDT7 could change vessel integrity and permeability in vivo, purified recombinant LiRecDT7, along with the appropriate negative control (PBS) and a positive control (LiRecDT1), was injected into the skin of mice that had been previously blue dye-perfused (Miles assay). The LiRecDT7 injection induced increased Evans blue extravasation compared with the negative control. Nevertheless, LiRecDT7 showed a lower activity compared with that of LiRecDT1 (Fig. 8).

DISCUSSION

Based on its ability to hydrolyze the phospholipid sphingomyelin into choline and C1P, previous studies have characterized brown spider venom phospholipase, also called "dermonecrotic toxin," as a sphingomyelinase-D molecule [da Silva et al., 2004]. However, the recent results obtained from lipid biochemical research have suggested that this toxin is a phospholipase-D enzyme because it degrades not only sphingophospholipids but also glycerophospholipids, generating C1P or lysophosphatidic acid (LPA) [Lee and Lynch, 2005; Chaim et al., 2011b; Chaves-Moreira et al., 2011]. It has been postulated that by degrading phospholipids and generating important lipid mediators, such as C1P or LPA, brown spider venom phospholipase-D toxin activates signaling pathways in different cells causing pathophysiological changes, such as inflammatory response, platelet aggregation, increased blood vessel permeability, hemolysis, and nephrotoxicity [Chaim et al., 2011b; Chaves-Moreira et al., 2011; Wille et al., 2013].

Currently, the idea of a family of similar molecules of phospholipase-D toxins in brown spider venom species is evident. This hypothesis was first suggested based on a biochemical characterization of *L. reclusa* venom, which contains four phospholipase-D isoforms [Futrell, 1992]. Additional studies revealed antigenic cross-reactivity for phospholipases-D from different brown spider venoms, including *L. gaucho*, *L. laeta*, and *L. intermedia* [Barbaro et al., 1996]. The biochemical and immunological analyses of *L. deserta* and *L. reclusa* venoms showed antigenic cross-reactivity and biochemical homologies (amino acid composition) for phospholipase-D toxins [Gomes et al., 2011]. Two phospholipase-D-like toxins were described in *L. gaucho* [Cunha et al., 2003] and four toxins were described in *L. boneti* venom [Ramos-Cerrillo et al., 2004]. Through proteomic analysis, several phospholipase-D isoforms were identified in *L. gaucho* venom [Machado et al., 2005], thereby confirming the idea that these molecules belong to a family of related toxins. Through molecular biology studies, the concept of an intra- and inter-species family of brown spider venom phospholipase-D was further confirmed by the cloning and expression of phospholipase-D toxins from a variety of *Loxosceles* spiders. Binford et al. [2005] reported three cDNA sequences for phospholipase-D toxins identified in *L. arizonica*. Chaim et al. [2006], da Silveira et al. [2006, 2007c], and Appel et al. [2008] cloned, expressed, and identified differential functionality for six related phospholipase-D molecules using a cDNA library obtained from the venom gland of *L. intermedia*. The transcriptional profile of the *L. intermedia* venom gland obtained through the construction of a wide cDNA library showed that members of phospholipase-D family represent 20.2% of the total

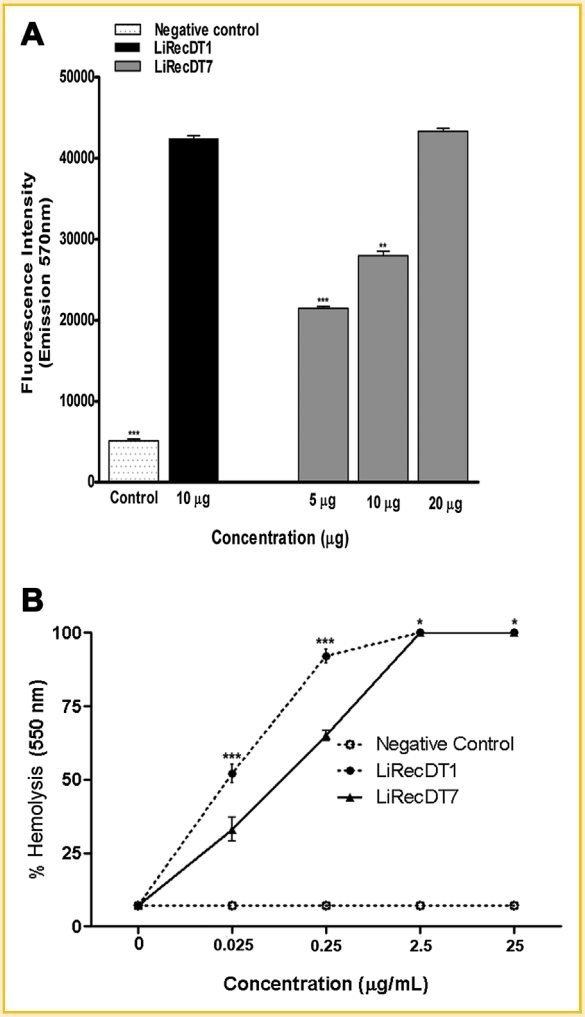

Fig. 5. Sphingomyelinase-D and hemolytic activities of LiRecDT7. A: Sphingomyelinase-D activities of recombinant dermonecrotic toxins LiRecDT1 and LiRecDT7 were evaluated using an Amplex Red Assay Kit at 37°C for 1 h, and the product of the reaction was determined at 550 nm. PBS was used as a negative control. Reactions used 5, 10, and 20 μg of LiRecDT7 and 10 μg of LiRecDT1 ($n = 5$). The means ± standard errors are shown, with significance levels $^{**}P \leq 0.01$ and $^{***}P \leq 0.001$ comparing activities of LiRecDT1 and LiRecDT7. B: Human erythrocytes suspended in TBS were incubated with different concentrations of LiRecDT7, or in the absence of toxin (negative control), for 24 h at 37°C. The absorbance values of the supernatants were measured at 550 nm, and the percentage of hemolysis was determined using the absorbance values induced with 0.1% (v/v) Triton X-100 as 100% hemolysis (positive control). The results represent the means of five experiments ± SEM. $^{*}P \leq 0.05$; $^{***}P \leq 0.001$.

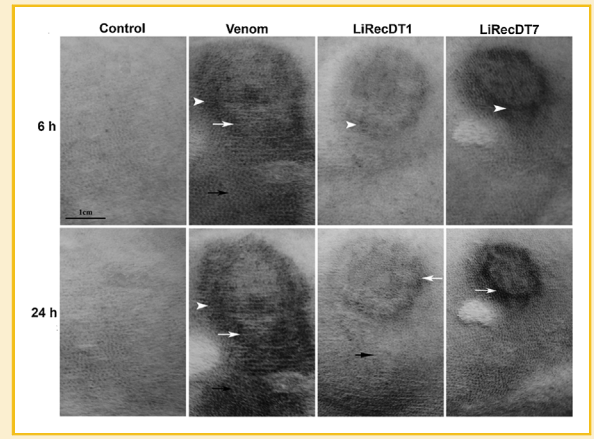

Fig. 6. Macroscopic and histological changes in rabbit skin exposed to whole venom and the recombinant toxins LiRecDT1, LiRecDT7 and negative control recombinant—Green Fluorescent Protein (GFP). Macroscopic visualization of dermonecrosis in rabbits intradermally injected with 10 μg of whole venom and the purified toxins LiRecDT1 and LiRecDT7. Lesions were observed at 6 and 24 h after the injections. The arrowhead indicates a hemorrhagic area surrounding the lesion. The white arrow indicates a necrotic area. The black arrows indicate gravitational spreading of lesions.

toxin-encoding transcripts [Gremski et al., 2010]. Brown spider venom toxins that have phospholipase-D activity are currently grouped into a family. It was postulated that the noxious effects induced by *Loxosceles* species crude venom might reflect the synergism among these related phospholipase-D toxins [Kalapothakis et al., 2007] and other components of venom, as the venom is a complex mixture containing additional constituents, such as insecticidal peptides, astacin-like metalloproteases, neurotoxins, serine proteases, venom allergen, translationally controlled tumor protein, hyaluronidases, serine protease inhibitors, and other components [Gremski et al., 2010].

Herein, we described the cloning, heterologous expression, affinity purification, and the functionality of a novel phospholipase-D "dermonecrotic toxin" family member from brown spider venom, strengthening the proteomic, immunological, and molecular biology data previously reported. The recombinant toxin identified was designated LiRecDT7 (GenBank Accession no. KC237286). The name is a reference to other previously identified brown spider (*L. intermedia*) venom phospholipase-D isoforms (LiRecDT1, LiRecDT2, LiRecDT3, LiRecDT4, LiRecDT5, and LiRecDT6) [Chaim et al., 2006; da Silveira et al., 2006, 2007c; Appel et al., 2008].

Initially, our experimental strategy for cloning this novel member of brown spider venom phospholipase-D toxin cDNA was based on the random sequence analysis obtained from a cDNA library of *L. intermedia* venom gland [Gremski et al., 2010] using a BLAST search for similarities with previous cloned phospholipase-D toxins and 5′ RACE amplification to obtain the complete cDNA sequence.

The complete sequence of this novel brown spider phospholipase-D includes a signal peptide and a mature protein with high similarity to other previously reported brown spider venom phospholipase-D molecules [Chaim et al., 2006; da Silveira et al., 2006, 2007c; Kalapothakis et al., 2007; Appel et al., 2008]. The deduced LiRecDT7 protein displayed an amino acid sequence identity of 63% compared with LiRecDT1. The similarities between LiRecDT7 and the other isoforms of *L. intermedia* varied showing the highest similarity with LiRecDT6 (71%) and the lowest similarity with LiRecDT3 (45%). Compared with phospholipase-D toxins from other *Loxosceles* species, the highest sequence similarities to LiRecDT7 were observed for sphingomyelinase-D alphaIV2 of *L. hirsuta* (ACN48948—91% amino acid identity). Binford et al. [2009] showed that recent gene duplications are apparent in groups of closely related species, which is

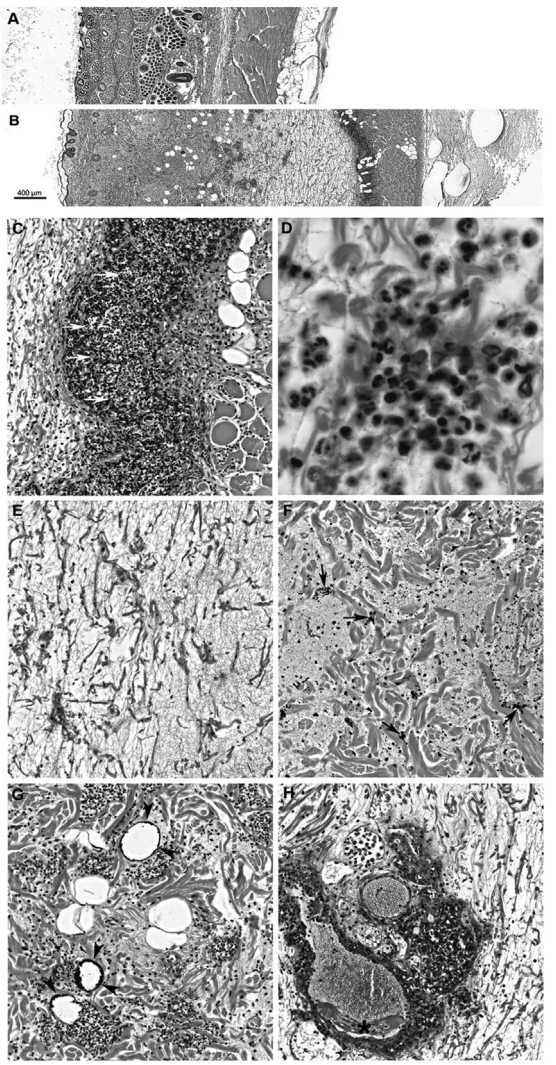

Fig. 7. Histopathology features of rabbits' skin 24 h following LiRecDT7 exposure. Light microscopy analysis of sections of dermonecrotic lesions stained with H&E. A,B: Panoramic views of sections of negative control recombinant—green fluorescent protein (GFP)—and LiRecDT7, respectively, clearly demonstrating the edema triggered by the recombinant toxin. At this stage, there was a massive inflammatory response (white arrows) (C), with the presence of neutrophils in the dermis (D), the disorganization of collagen fibers (E), areas of necrosis (black arrows; F), including the degeneration of blood vessel walls (black arrowheads; G), and thrombus formation into dermal blood vessels (asterisk; H). Magnification of panoramic views: 15×; (C,E–H) 100×; (D) 630×.

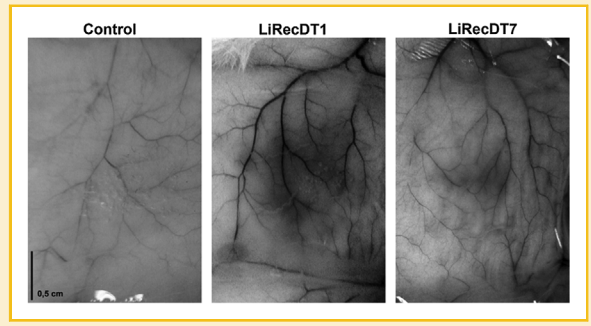

Fig. 8. Effect of LiRecDT7 on vascular permeability of skin vessels. The mice were administered with intradermal injections (10 μg) of LiRecDT7, LiRecDT1, and PBS (control for baseline permeability level; n = 5 per treatment). The photographs show increased dye leakage after recombinant toxin LiRecDT1 and LiRecDT7 exposure compared with minimal vessel permeability due to the negative control PBS.

the case for *L. intermedia* and *L. hirsuta*, members of the *spadicea* group. Thus, the high similarity observed between LiRecDT7 and sphingomyelinase-D alphaVI2 certainly reflects the closeness among the species. Some authors argue that to mantain effectiveness against preys and predators, the genes encoding venom peptides and proteins have undergone multiple duplication events. The duplicated genes, in turn, acquire related or even novel functions through adaptive evolution [Ma et al., 2012].

Moreover, LiRecDT7 contains the conserved amino acid residues involved in catalysis or metal ion coordination, which are important for phospholipase-D activity [Murakami et al., 2006], except for a punctual and conservative substitution at position 233 in the catalytic site. While all *L. intermedia* phospholipase-D isoforms contain a conserved an Asp residue in this position, LiRecDT7 has a Glu (D233E).

Structural analyses of LiRecDT1 show that the catalytic site of this enzyme is formed by two histidines at positions 12 and 47 and an Mg^{2+} ion. This catalytic site is hexacoordinated by Glu32, Asp34, and Asp91, a water molecule and two PEG4 oxygens [de Giuseppe et al., 2011]. This ion coordination is stabilized through hydrogen bonds formed by Asp34, Asp52, Trp230, Asp233, Asn252, and Gly480 [Murakami et al., 2005, 2006; de Andrade et al., 2006; de Giuseppe et al., 2011].

Asp is frequently involved in the formation of hydrogen bonds that assist in stabilizing protein structures. This residue might also be involved in active or binding sites for interactions with other proteins. Glu is also a charged amino acid. However, Asp has a less bulky side chain and is less flexible when located in the interior of a protein. These properties confer a slight preference for the inclusion of Asp in protein active sites, as is observed with the Asp233 residue in *Loxosceles* phospholipases-D, which is highly conserved. This phenomenon has also been observed in the classic example of the active site of serine proteases, whose mechanism is based in the amino acid triad Asp-His-Ser [Betts and Russell, 2003]. In this context, the substitution of Asp for Glu (Asp → Glu) is quite rare, although it is possible that Glu in the position 233 might play a similar role stabilizing the ion coordination structure of LiRecDT7, consistent with the observed biochemical and biological properties of this toxin.

Several other structural and biochemical characteristics provide confirmation of LiRecDT7 as a member of the brown spider phospholipase-D venom toxin family. First, the molecular mass of LiRecDT7 (36 kDa) and the calculated isoelectric point from the deduced amino acid sequence of the mature protein (pI 5.94) are similar to those described for other phospholipase-D members (ranging from 31 to 33 kDa and pI 5.3 to 8.7) [Kalapothakis et al., 2007]. Using immunological approaches, LiRecDT7 cross-reacted with antibodies against LiRecDT1, confirming antigenic homology

with LiRecDT1. Moreover, antibodies for crude venom toxins also cross-reacted with recombinant LiRecDT7, demonstrating that the structures of crude venom proteins are similar to LiRecDT7 and that LiRecDT7 shows sequence/epitope similarities with native venom toxins. Taken together, these results demonstrate that the phospholipase-D epitopes are strong antigenic determinants.

Full length LiRecDT7 was heterogeneously expressed in *E. coli* SHuffle T7 Express *lysY* cells and purified using single step affinity chromatography. LiRecDT7 was eluted in a pure form as visualized through SDS–PAGE. Using this approach, it was possible to obtain purified material for biochemical and functional analyses.

The native brown spider venom phospholipase-D toxins and previously described LiRecDT1 to 6 isoforms [Chaim et al., 2006; da Silveira et al., 2006, 2007c; Appel et al., 2008] exhibit sphingomyelinase-D activity. As expected, the amino acid alignment and similarity analysis demonstrated the homology of LiRecDT7 with other brown spider phospholipase-D isoforms, and LiRecDT7 demonstrated sphingomyelinase-D activity through the generation of choline in a concentration-dependent manner. The substitution of the Asp residue with Glu at position 233 in the catalytic site did not abolish the sphingomyelinase-D activity of isoform LiRecDT7, although a reduction in the enzymatic activity was observed compared with LiRecDT1. Nevertheless, these results confirm the biochemical nature of LiRecDT7 as a sphingomyelinase-D and strongly suggest functionality for this LiRecDT isoform. However, with our results, it is not possible to infer whether this novel isoform is able to hydrolyze other phospholipids as observed for other members of this family [Chaim et al., 2011b]. Further studies specifically focusing on these activities of LiRecDT7 are needed to identify such aspects. As previously reported, all pathophysiological events triggered by brown spider venom recombinant isoforms, such as nephrotoxicity, dermonecrosis, inflammatory response, mice lethality and hemolysis are dependent on phospholipase-D catalysis [Kusma et al., 2008; Paludo et al., 2009; Chaim et al., 2011a; Chaves-Moreira et al., 2011].

The data obtained from the literature have described brown spider venom phospholipases-D as remarkable inducers of necrotic skin lesions and inflammatory response. Due to these effects, brown spider venom phospholipase-D toxins are also referred to as "dermonecrotic toxins." Indeed, the hallmark of accidents following brown spider bites is dermonecrosis with gravitational spreading surrounding the bite site; thus, loxoscelism is also referred to as necrotic arachnidism or gangrenous arachnidism [da Silva et al., 2004; Senff-Ribeiro et al., 2008]. Skin lesions triggered by brown spider phospholipase-D toxins are the consequence of a massive inflammatory response observed in the epidermis and dermis. This event is histopathologically referred to as "aseptic coagulative necrosis" and is a consequence of dysregulated endothelial cell-dependent neutrophil activation [Ospedal et al., 2002]. As previously described for other LiRecDT isoforms, LiRecDT7 demonstrated necrotic and inflammatory activities, providing further evidence of the activity of this toxin. LiRecDT7 induced noxious responses upon injection in rabbit skin (a macroscopic lesion), with swelling, erythema, hemorrhage, ischemia, and necrosis. Histological studies of samples collected from macroscopic lesions at 24 h after toxin exposure provided additional evidence for LiRecDT7 as an inducer of the inflammatory response. The observed histopathological changes included diffuse dermal edema, proteinaceous exudation and a massive and diffuse aggregation of leukocytes into the dermis. In addition, LiRecDT7 induced tissue necrosis, including degeneration of blood vessel walls. The novel phospholipase-D isoform also triggered thrombus formation into dermal blood vessels. These events are consistent with the literature data and resemble the observations reported after crude venom exposure [Veiga et al., 2001; Ospedal et al., 2002; da Silva et al., 2004].

Furthermore, the functionality of LiRecDT7 was also supported through the observed increase in capillary permeability in mice after treatment with purified recombinant toxin. This event has been described in *L. intermedia* whole venom, native brown spider venom phospholipase-D toxins and other LiRecDT isoforms [da Silva et al., 2004; da Silveira et al., 2007c; Ribeiro et al., 2007; Appel et al., 2008]. Notably, the increase in blood vessel permeability triggered by LiRecDT1 was more prominent than that induced by LiRecDT7. As described for other LiRecDTs, this ability is associated with the level of enzymatic activity of the isoform, as observed for LiRecDT3 and LiRecDT5, which show lower sphingomyelinase-D activity than LiRecDT1 and also trigger a less prominent increase in blood vessel permeability [da Silveira et al., 2006, 2007c]. Apparently, through the induction of inflammatory response and leukocyte infiltration into the dermis of mice [Sunderkotter et al., 2001], phospholipase-D toxins increase vessel permeability. In addition, a direct phospholipase-D effect upon endothelia, inducing endothelial cell activation and cytotoxicity, as previously reported for brown spider crude venom [Veiga et al., 2001; Zanetti et al., 2002; Paludo et al., 2009] increases vessel permeability through a disruption of the blood vessel wall.

LiRecDT7 also induced the direct lysis of human erythrocytes. The hemolytic effect of brown spider venom has been demonstrated through the clinical and laboratory features observed in accident victims. These features include hematuria, hemoglobinuria, elevated creatine kinase levels, proteinuria and shock [Kusma et al., 2008]. We have previously described the direct hemolytic effect of LiRecDT1 upon erythrocytes of different animal sources. This activity is not dependent on the ABO or Rhesus systems, but rather is dependent on the animal species, as human, sheep, and rabbit erythrocytes were lysed, but erythrocytes from horses were less severely damaged after toxin treatment, and these results depend upon the membrane composition of the cells. This event is also dependent on the catalytic activity of the phospholipase-D, as a site-directed mutation in the catalytic site (H12A) completely abolished the hemolytic effect of the mutated isoform LiRecDT1H12A [Chaves-Moreira et al., 2009]. The results described herein using LiRecDT7, demonstrate the direct hemolytic effect of this recombinant phospholipase-D on human erythrocytes. Toxin-dependent hemolysis occurs in a concentration-dependent manner, supporting the specificity of this effect.

Based on the crystallography results obtained using recombinant phospholipase-D toxin isoforms from *L. laeta* and *L. intermedia* venom and the structural and sequence alignment comparison data [Murakami et al., 2006; de Giuseppe et al., 2011], a classification system was proposed, which considers the phospholipase-D activity of these toxins. According to the authors, brown spider venom dermonecrotic toxins can be divided into two categories: class I molecules, containing a single intrachain disulfide bond and one

extended hydrophobic loop (*L. laeta* isoform) and class II molecules, containing an additional disulfide bond linking the catalytic loop to a second flexible loop. The class II phospholipases can be subdivided into classes IIa and IIb according to their ability, or lack thereof, to hydrolyze sphingomyelin, respectively. Based on this classification, LiRecDT7 belongs to class IIa, as this isoform possesses two putative disulfide bonds (Cys51–Cys57 and Cys53–Cys201) and is able to hydrolyze sphingomyelin.

The molecular modeling data also support the classification of LiRecDT7 as a class II sphingomyelinase-D, as it revealed the presence of two disulfide bridges in the putative structure of this novel isoform, as observed in LiRecDT1 model. The 3D modeling of LiRecDT7 also demonstrated that the structural basis for Mg^{2+} ion coordination and the two catalytic histidine residues (His12 and His47), which play key roles in the active-site pocket of spider venom phospholipases-D, is maintained compared with LiRecDT1.

In LiRecDT1, these two catalytic histidine residues (His12 and His47), are supported through a network of hydrogen bonds between Asp34, Asp52, Trp230, Asp233, and Asn252. Because LiRecDT7 possesses a substitution of Asp233 to Glu233, this residue is highlighted in the 3D modeling of both isoforms (LiRecDT1 and LiRecDT7) to illustrate this natural mutation. It is clear that the side chain of Glu in LiRecDT7 is bulkier than the side chain of Asp in LiRecDT1. There is also an obvious variation in the positioning of the side chain of these residues, as Glu in LiRecDT7 protrudes toward the flexible loop. It is not possible to infer whether these differences affect the network of hydrogen bonds between this residue and the two catalytic histidine residues. Indeed, this natural mutation did not abolish the enzymatic and biological actions of this novel isoform. The molecular modeling of LiRecDT7 also revealed that one of the loops, located near the variable loop, is more prominent (directed toward the surface of the molecule) compared with the same loop in LiRecDT1. When comparing the primary structure of this specific region, we observed the presence of lysine (207), Asp (208), arginine (209) and Glu (210) residues in LiRecDT7. These amino acids generally prefer to reside on the surface of the protein. Lysine and arginine are also frequently involved in *salt-bridges* where they pair with a negatively charged Asp or Glu to stabilize hydrogen bonds that are important for protein stability [Betts and Russell, 2003]. These features might explain the prominent configuration of this loop in LiRecDT7. In addition, as shown in Figure 2, LiRecDT1 has only two amino acid residues in this region. Thus, the presence of two additional residues in this region of LiRecDT7 might also explain the presence of a longer loop in this isoform. Moreover, Figure 2 also shows that the only isoform containing the four conserved amino acid residues in this region is LiRecDT6, although it is not possible to infer a direct relation concerning their structures based on this observation.

The results presented herein, demonstrate that LiRecDT7 possesses an intermediate ability for sphingomyelin hydrolysis and biological activities compared with LiRecDT1. A putative explanation for the differences described could be inferred from a mutation in the catalytic site (D233E) that, despite involving amino acids from the same characteristics (negative charged residues), in some way could destabilize and disorganize the catalytic site, affecting enzyme/substrate interactions in the catalytic cleft as the Glu residue contains an additional CH_2 group. However, it is not possible to infer that D233E substitution alone is responsible for the observed differences, as some members of the phospholipase-D family in *L. intermedia* exhibit lower sphingomyelinase-D activity, even with all amino acids of the catalytic site conserved (e.g., LiRecDT3, LiRecDT4 and LiRecDT5) [da Silveira et al., 2006, 2007c]. As observed for these mentioned isoforms, LiRecDT7 also possesses several substitutions in the amino acid residues neighboring the catalytic site. As previously proposed [da Silveira et al., 2006] these residues might be involved in the stabilization and organization of the catalytic site or even in the synergistic domains of these toxins. Thus, in addition to the specific substitution present in LiRecDT7, these differences might also explain the variations in functionality between these isoforms.

Venom toxin molecules have recently been used to investigate molecular and cellular mechanisms, as models for the design of novel drugs or even for diagnostic or therapeutic uses [Senff-Ribeiro et al., 2008; Chaim et al., 2011a; Horta et al., 2013]. The development of a novel recombinant *Loxosceles* phospholipase-D toxin can provide an agonist molecule as an additional tool to study the inflammatory response or to design and identify antagonist molecules using co-crystallization techniques and X-ray diffraction procedures. Additionally, this novel phospholipase-D can be used as a tool in biochemical lipid research protocols or as a recombinant antigen for serum therapy applications.

In summary, we have identified a novel brown spider venom phospholipase-D "dermonecrotic toxin" family member. This molecule, referred to as LiRecDT7, was cloned, heterogeneously expressed and purified. LiRecDT7 degraded sphingomyelin to generate choline in a concentration-dependent manner, induced dermonecrosis in rabbit skin and increased inflammation in the dermis of these animals. LiRecDT7 also increased vascular permeability in mice and induced direct hemolysis in human erythrocytes. Together, these results provide new insights into loxoscelism, contribute to the understanding of venom phospholipase-D and present the possibility of applying venom toxins as biotechnological tools for lipid research.

REFERENCES

Anliker B, Chun J. 2004. Cell surface receptors in lysophospholipid signaling. Semin Cell Dev Biol 15:457–465.

Appel MH, da Silveira RB, Gremski W, Veiga SS. 2005. Insights into brown spider and loxoscelism. Invert Surviv J 2:152–158.

Appel MH, da Silveira RB, Chaim OM, Paludo KS, Silva DT, Chaves DM, da Silva PH, Mangili OC, Senff-Ribeiro A, Gremski W, Nader HB, Veiga SS. 2008. Identification, cloning and functional characterization of a novel dermonecrotic toxin (phospholipase D) from brown spider (*Loxosceles intermedia*) venom. Biochim Biophys Acta 1780:167–178.

Barbaro KC, Ferreira ML, Cardoso DF, Eickstedt VR, Mota I. 1996. Identification and neutralization of biological activities in the venoms of *Loxosceles* spiders. Braz J Med Biol Res 29:1491–1497.

Barbaro KC, Knysak I, Martins R, Hogan C, Winkel K. 2005. Enzymatic characterization, antigenic cross-reactivity and neutralization of dermonecrotic activity of five *Loxosceles* spider venoms of medical importance in the Americas. Toxicon 45:489–499.

Betts MJ, Russell RB. 2003. Amino acid and consequences of substitutions. Bioinformatics for geneticists. John Wiley & Sons, Inc. New Jersey, USA. pp 289–316.

Binford GJ, Cordes MH, Wells MA. 2005. Sphingomyelinase D from venoms of *Loxosceles* spiders: Evolutionary insights from cDNA sequences and gene structure. Toxicon 45:547–560.

Binford GJ, Bodner MR, Cordes MH, Baldwin KL, Rynerson MR, Burns SN, Zobel-Thropp PA. 2009. Molecular evolution, functional variation, and proposed nomenclature of the gene family that includes sphingomyelinase D in sicariid spider venoms. Mol Biol Evol 26:547–566.

Catalán A, Cortes W, Sagua H, González J, Araya JE. 2011. Two new phospholipase D isoforms of *Loxosceles laeta*: Cloning, heterologous expression, functional characterization, and potential biotechnological application. J Biochem Mol Toxicol 25:393–403.

Chaim OM, Sade YB, da Silveira RB, Toma L, Kalapothakis E, Chavez-Olortegui C, Mangili OC, Gremski W, von Dietrich CP, Nader HB, Sanches Veiga S. 2006. Brown spider dermonecrotic toxin directly induces nephrotoxicity. Toxicol Appl Pharmacol 211:64–77.

Chaim OM, Trevisan-Silva D, Chaves-Moreira D, Wille AC, Ferrer VP, Matsubara FH, Mangili OC, da Silveira RB, Gremski LH, Gremski W, Senff-Ribeiro A, Veiga SS. 2011a. Brown spider (*Loxosceles genus*) venom toxins: Tools for biological purposes. Toxins (Basel) 3:309–344.

Chaim OM, da Silveira RB, Trevisan-Silva D, Ferrer VP, Sade YB, Boia-Ferreira M, Gremski LH, Gremski W, Senff-Ribeiro A, Takahashi HK, Toledo MS, Nader HB, Veiga SS. 2011b. Phospholipase-D activity and inflammatory response induced by brown spider dermonecrotic toxin: Endothelial cell membrane phospholipids as targets for toxicity. Biochim Biophys Acta 1811:84–96.

Chalfant CE, Spiegel S. 2005. Sphingosine 1-phosphate and ceramide 1-phosphate: Expanding roles in cell signaling. J Cell Sci 118:4605–4612.

Chaves-Moreira D, Chaim OM, Sade YB, Paludo KS, Gremski LH, Donatti L, de Moura J, Mangili OC, Gremski W, da Silveira RB, Senff-Ribeiro A, Veiga SS. 2009. Identification of a direct hemolytic effect dependent on the catalytic activity induced by phospholipase-D (dermonecrotic toxin) from brown spider venom. J Cell Biochem 107:655–666.

Chaves-Moreira D, Souza FN, Fogaca RT, Mangili OC, Gremski W, Senff-Ribeiro A, Chaim OM, Veiga SS. 2011. The relationship between calcium and the metabolism of plasma membrane phospholipids in hemolysis induced by brown spider venom phospholipase-D toxin. J Cell Biochem 112:2529–2540.

Cunha RB, Barbaro KC, Muramatsu D, Portaro FC, Fontes W, de Sousa MV. 2003. Purification and characterization of loxnecrogin, a dermonecrotic toxin from *Loxosceles gaucho* brown spider venom. J Protein Chem 22:135–146.

da Silva PH, da Silveira RB, Appel MH, Mangili OC, Gremski W, Veiga SS. 2004. Brown spiders and loxoscelism. Toxicon 44:693–709.

da Silveira RB, Pigozzo RB, Chaim OM, Appel MH, Dreyfuss JL, Toma L, Mangili OC, Gremski W, Dietrich CP, Nader HB, Veiga SS. 2006. Molecular cloning and functional characterization of two isoforms of dermonecrotic toxin from *Loxosceles intermedia* (brown spider) venom gland. Biochimie 88:1241–1253.

da Silveira RB, Chaim OM, Mangili OC, Gremski W, Dietrich CP, Nader HB, Veiga SS. 2007a. Hyaluronidases in *Loxosceles intermedia* (Brown spider) venom are endo-beta-*N*-acetyl-D-hexosaminidases hydrolases. Toxicon 49:758–768.

da Silveira RB, Wille AC, Chaim OM, Appel MH, Silva DT, Franco CR, Toma L, Mangili OC, Gremski W, Dietrich CP, Nader HB, Veiga SS. 2007b. Identification, cloning, expression and functional characterization of an astacin-like metalloprotease toxin from *Loxosceles intermedia* (brown spider) venom. Biochem J 406:355–363.

da Silveira RB, Pigozzo RB, Chaim OM, Appel MH, Silva DT, Dreyfuss JL, Toma L, Dietrich CP, Nader HB, Veiga SS, Gremski W. 2007c. Two novel dermonecrotic toxins LiRecDT4 and LiRecDT5 from brown spider (*Loxosceles intermedia*) venom: From cloning to functional characterization. Biochimie 89:289–300.

de Andrade SA, Murakami MT, Cavalcante DP, Arni RK, Tambourgi DV. 2006. Kinetic and mechanistic characterization of the Sphingomyelinases D from *Loxosceles intermedia* spider venom. Toxicon 47:380–386.

de Giuseppe PO, Ullah A, Silva DT, Gremski LH, Wille AC, Chaves Moreira D, Ribeiro AS, Chaim OM, Murakami MT, Veiga SS, Arni RK. 2011. Structure of a novel class II phospholipase D: Catalytic cleft is modified by a disulphide bridge. Biochem Biophys Res Commun 409:622–627.

dos Santos LD, Dias NB, Roberto J, Pinto AS, Palma MS. 2009. Brown recluse spider venom: Proteomic analysis and proposal of a putative mechanism of action. Protein Pept Lett 16:933–943.

Feitosa L, Gremski W, Veiga SS, Elias MC, Graner E, Mangili OC, Brentani RR. 1998. Detection and characterization of metalloproteinases with gelatinolytic, fibronectinolytic and fibrinogenolytic activities in brown spider (*Loxosceles intermedia*) venom. Toxicon 36:1039–51.

Futrell JM. 1992. Loxoscelism. Am J Med Sci 304:261–267.

Gomes MT, Guimaraes G, Frezard F, Kalapothakis E, Minozzo JC, Chaim OM, Veiga SS, Oliveira SC, Chavez-Olortegui C. 2011. Determination of sphingomyelinase-D activity of Loxosceles venoms in sphingomyelin/cholesterol liposomes containing horseradish peroxidase. Toxicon 57:574–579.

Gonçalves-de-Andrade RM, Bertani R, Nagahama RH, Barbosa MF. 2012. *Loxosceles niedeguidonae* (Araneae, Sicariidae) a new species of brown spider from Brazilian semi-arid region. Zookeys 175:27–36.

Gremski LH, da Silveira RB, Chaim OM, Probst CM, Ferrer VP, Nowatzki J, Weinschutz HC, Madeira HM, Gremski W, Nader HB, Senff-Ribeiro A, Veiga SS. 2010. A novel expression profile of the *Loxosceles intermedia* spider venomous gland revealed by transcriptome analysis. Mol Biosyst 12:2403–2416.

Hannun YA. 1994. The sphingomyelin cycle and the second messenger function of ceramide. J Biol Chem 269:3125–3128.

Horta CC, Oliveira-Mendes BB, do Carmo AO, Siqueira FF, Barroca TM, Dos Santos Nassif Lacerda SM, de Almeida Campos PH, Jr., de Franca LR, Ferreira RL, Kalapothakis E. 2013. Lysophosphatidic acid mediates the release of cytokines and chemokines by human fibroblasts treated with *Loxosceles* spider venom. J Invest Dermatol 133:1682–1685.

Isbister GK, Fan HW. 2011. Spider bite. Lancet 378:2039–2047.

Kalapothakis E, Chatzaki M, Goncalves-Dornelas H, de Castro CS, Silvestre FG, Laborne FV, de Moura JF, Veiga SS, Chavez-Olortegui C, Granier C, Barbaro KC. 2007. The Loxtox protein family in *Loxosceles intermedia* (Mello-Leitao) venom. Toxicon 50:938–946.

Kiefer F, Arnold K, Kunzli M, Bordoli L, Schwede T. 2009. The SWISS-MODEL Repository and associated resources. Nucleic Acids Res 37:D387–D392.

Kusma J, Chaim OM, Wille AC, Ferrer VP, Sade YB, Donatti L, Gremski W, Mangili OC, Veiga SS. 2008. Nephrotoxicity caused by brown spider venom phospholipase-D (dermonecrotic toxin) depends on catalytic activity. Biochimie 90:1722–1736.

Lee S, Lynch KR. 2005. Brown recluse spider (*Loxosceles reclusa*) venom phospholipase D (PLD) generates lysophosphatidic acid (LPA). Biochem J 391:317–323.

Ma Y, He Y, Zhao R, Wu Y, Li W, Cao Z. 2012. Extreme diversity of scorpion venom peptides and proteins revealed by transcriptomic analysis: Implication for proteome evolution of scorpion venom arsenal. J Proteomics 75:1563–1576.

Machado LF, Laugesen S, Botelho ED, Ricart CA, Fontes W, Barbaro KC, Roepstorff P, Sousa MV. 2005. Proteome analysis of brown spider venom: Identification of loxnecrogin isoforms in *Loxosceles gaucho* venom. Proteomics 5:2167–2176.

Moolenaar WH, van Meeteren LA, Giepmans BN. 2004. The ins and outs of lysophosphatidic acid signaling. BioEssays 26:870–881.

Murakami MT, Fernandes-Pedrosa MF, Tambourgi DV, Arni RK. 2005. Structural basis for metal ion coordination and the catalytic mechanism of sphingomyelinases D. J Biol Chem 280:13658–13664.

Murakami MT, Fernandes-Pedrosa MF, de Andrade SA, Gabdoulkhakov A, Betzel C, Tambourgi DV, Arni RK. 2006. Structural insights into the catalytic

mechanism of sphingomyelinases D and evolutionary relationship to glycerophosphodiester phosphodiesterases. Biochem Biophys Res Commun 342:323–329.

Ospedal KZ, Appel MH, Fillus Neto J, Mangili OC, Sanches Veiga S, Gremski W. 2002. Histopathological findings in rabbits after experimental acute exposure to the *Loxosceles intermedia* (brown spider) venom. Int J Exp Pathol 83:287–294.

Paludo KS, Biscaia SM, Chaim OM, Otuki MF, Naliwaiko K, Dombrowski PA, Franco CR, Veiga SS. 2009. Inflammatory events induced by brown spider venom and its recombinant dermonecrotic toxin: A pharmacological investigation. Comp Biochem Physiol C Toxicol Pharmacol 149:323–333.

Platnick NI. 2012. The World Spider Catalog—Version 12.5. American Museum of Natural History.

Ramos-Cerrillo B, Olvera A, Odell GV, Zamudio F, Paniagua-Solis J, Alagon A, Stock RP. 2004. Genetic and enzymatic characterization of sphingomyelinase D isoforms from the North American fiddleback spiders *Loxosceles boneti* and *Loxosceles reclusa*. Toxicon 44:507–514.

Ribeiro RO, Chaim OM, da Silveira RB, Gremski LH, Sade YB, Paludo KS, Senff-Ribeiro A, de Moura J, Chavez-Olortegui C, Gremski W, Nader HB, Veiga SS. 2007. Biological and structural comparison of recombinant phospholipase D toxins from *Loxosceles intermedia* (brown spider) venom. Toxicon 50:1162–1174.

Sade YB, Boia-Ferreira M, Gremski LH, da Silveira RB, Gremski W, Senff-Ribeiro A, Chaim OM, Veiga SS. 2012. Molecular cloning, heterologous expression and functional characterization of a novel translationally-controlled tumor protein (TCTP) family member from *Loxosceles intermedia* (brown spider) venom. Int J Biochem Cell Biol 44:170–177.

Sambrook J, Russell DW. 2001. Molecular cloning: A laboratory manual. Cold Spring Harbor, NY: Cold Spring Harbor Laboratory Press.

Senff-Ribeiro A, Henrique da Silva P, Chaim OM, Gremski LH, Paludo KS, Bertoni da Silveira R, Gremski W, Mangili OC, Veiga SS. 2008. Biotechnological applications of brown spider (*Loxosceles* genus) venom toxins. Biotechnol Adv 26:210–218.

Sunderkotter C, Seeliger S, Schonlau F, Roth J, Hallmann R, Luger TA, Sorg C, Kolde G. 2001. Different pathways leading to cutaneous leukocytoclastic vasculitis in mice. Exp Dermatol 10:391–404.

Trevisan-Silva D, Gremski LH, Chaim OM, da Silveira RB, Meissner GO, Mangili OC, Barbaro KC, Gremski W, Veiga SS, Senff-Ribeiro A. 2010. Astacin-like metalloproteases are a gene family of toxins present in the venom of different species of the brown spider (genus *Loxosceles*). Biochimie 92: 21–32.

van Meeteren LA, Frederiks F, Giepmans BN, Pedrosa MF, Billington SJ, Jost BH, Tambourgi DV, Moolenaar WH. 2004. Spider and bacterial sphingomyelinases D target cellular lysophosphatidic acid receptors by hydrolyzing lysophosphatidylcholine. J Biol Chem 279:10833–10836.

Veiga SS, da Silveira RB, Dreyfus JL, Haoach J, Pereira AM, Mangili OC, Gremski W. 2000. Identification of high molecular weight serine-proteases in *Loxosceles intermedia* (brown spider) venom. Toxicon 38:825–839.

Veiga SS, Zanetti VC, Franco CR, Trindade ES, Porcionatto MA, Mangili OC, Gremski W, Dietrich CP, Nader HB. 2001. In vivo and in vitro cytotoxicity of brown spider venom for blood vessel endothelial cells. Thromb Res 102:229–237.

Wille ACM, Chaves-Moreira D, Trevisan-Silva D, Magnoni MG, Boia-Ferreira M, Gremski LH, Gremski W, Chaim OM, Senff-Ribeiro A, Veiga SS. 2013. Modulation of membrane phospholipids, the cytosolic calcium influx and cell proliferation following treatment of B16-F10 cells with recombinant phospholipase-D from *Loxosceles intermedia* (brown spider) venom. Toxicon 67:17–30.

Young AR, Pincus SJ. 2001. Comparison of enzymatic activity from three species of necrotising arachnids in Australia: *Loxosceles rufescens*, Badumna insignis and *Lampona cylindrata*. Toxicon 39:391–400.

Zanetti VC, da Silveira RB, Dreyfuss JL, Haoach J, Mangili OC, Veiga SS, Gremski W. 2002. Morphological and biochemical evidence of blood vessel damage and fibrinogenolysis triggered by brown spider venom. Blood Coagul Fibrinolysis 13:135–148.

PARECER TÉCNICO Nº 542/2006

Processo nº: 01200.000022/1997-37
Requerente: Setor de Ciências Biológicas – UFPR.
CNPJ: 000.348.003/0055-03
Endereço: Centro Politécnico da UFPR- Setor de Ciências Biológicas - 2º Piso, Sala 295 - Caixa Postal 19031 Paraná/PR.
Assunto: Solicitação de Extensão do CQB 009/97
Extrato Prévio: 350/2006 Publicado no D.O.U. de 21 de fevereiro de 2006
Reunião: 90ª Reunião Ordinária da CTNBio, ocorrida em 19 de abril de 2006
Decisão: DEFERIDO

A CTNBio, após apreciação do processo de pedido de Parecer Técnico referente à Solicitação de Extensão do CQB (Certificado de Qualidade em Biossegurança) 009/97, conclui pelo DEFERIMENTO, nos termos deste Parecer Técnico.
No âmbito das competências dispostas na Lei 11.105/05 e seu decreto 5.591/05, a Comissão concluiu que o presente pedido atende às normas da CTNBio e à legislação pertinente que visam garantir a biossegurança do meio ambiente, agricultura, saúde humana e animal.

PARECER TÉCNICO

1) Fundamentação técnica

Solicita à CTNBio Parecer Técnico para a extensão de seu CQB do Setor de Ciências Biológicas (UFPR) para a sala de número 198B e sala Preparativa, ambas do departamento de Biologia Celular do mesmo setor. Foram apresentados no processo os currículos dos pesquisadpres, a planta baixa do laboratório, o projeto a ser desenvolvido nele assim como as medidas de biossegurança.

2) Medidas de biossegurança descritas no processo.

Os microrganismos a serem manipulados no projeto (bactérias e leveduras) são da classe de segurança 1 mas, como os genes a serem expressos (toxinas de animais peçonhentos), apresentam riscos à saúde humana o laboratório que solicita a extensão de CQB tem que ser do tipo NB-2. Embora no processo não haja menção específica sobre a classe laboratorial na qual se encaixa este laboratório, todos os equipamentos apresentados são perfeitamente compatíveis com a classe NB-2, portanto, adequados para as manipulações propostas no projeto. Também foram apresentados as medidas adequadas para o transporte dos microrganismos da sala de manipulação (198B) para a sala de esterilização (sala Preparativa). Além disso, foi informado que as instalações acima mencionadas têm acesso a serviço médico emergencial no próprio setor de Ciências Biológicas da UFPR que contém um centro de atendimento médico para alunos, funcionários e professores além do Hospital Universitário.

Atendidas as recomendações e as medidas de biossegurança, recomenda-se, contudo, que sejam devidamente observadas as práticas laboratoriais compatíveis com a classe laboratorial NB-2.

Dr. Walter Colli
Presidente da CTNBio

Ministério da Educação
UNIVERSIDADE FEDERAL DO PARANÁ
Setor de Ciências Biológicas
Comitê de Ética no Uso de Animais
(CEUA)

UFPR
UNIVERSIDADE FEDERAL DO PARANÁ

Nº 553

CERTIFICADO

O Comitê de Ética no Uso de Animais (CEUA) do Setor de Ciências Biológicas da Universidade Federal do Paraná, instituído pela PORTARIA Nº 787/03-BL, de 11 de junho de 2003, com base nas normas para a constituição e funcionamento do CEUA, estabelecidas pela RESOLUÇÃO Nº 01/03-BL, de 09 de maio de 2003 e considerando o contido no Regimento Interno do CEUA, **CERTIFICA** que os procedimentos utilizando animais no projeto de pesquisa abaixo especificado, estão de acordo com os princípios éticos estabelecidos pelo Colégio Brasileiro de Experimentação Animal (COBEA) e exigências estabelecidas em "*Guide for the Care and Use of Experimental Animals (Canadian Council on Animal Care)*".

CERTIFICATION

The Ethics Animal Experiment Committee of the Setor de Ciências Biológicas of the Federal University of Paraná, established by the DECREE Nº 787/03-BL on June 11th 2003, based upon the RESOLUTION Nº 01/03-BL from May 9th 2003, and upon the CEUA internal regiment, CERTIFIES that the procedures using animals in the research project specified below are in agreement with the ethical principals established by the Experimental Animal Brazilian Council (COBEA), and with the requirements of the "Guide for the Care and Use of Experimental Animals (Canadian Council on Animal Care)".

PROCESSO: 23075.087106/2011-01 **APROVADO**: 09/08/2011 – R.O. 07/2011

TÍTULO: Expressão heteróloga e caracterização de hialuronidase e alérgeno presentes no veneno da aranha marrom (*Loxosceles intermedia*)

AUTORES: Silvio Sanches Veiga, Valéria Pereira Ferrer, Andrea Senff Ribeiro, Olga Meiri Chaim, Luiza Helena Gremski, Thiago Lopes de Mari

DEPARTAMENTO: Biologia Celular

Aleksander Zampronio
Prof. Dr. Aleksander Roberto Zampronio
Coordenador do CEUA